THESIS
5
2010
V.1

LIBRARY
Michigan State
University

This is to certify that the
dissertation entitled

ULTRASTRUCTURAL AND PHYSICOCHEMICAL MODIFICATIONS WITHIN AMMONIA TREATED LIGNOCELLULOSIC CELL WALLS AND THEIR INFLUENCE ON ENZYMATIC DIGESTIBILITY

presented by

SHISHIR PRATAP SINGH CHUNDAWAT

has been accepted towards fulfillment
of the requirements for the

Ph.D. degree in **Chemical Engineering**

Bruce T. Dale

Major Professor's Signature

Dec. 17, 2009

Date

MSU is an Affirmative Action/Equal Opportunity Employer

PLACE IN RETURN BOX to remove this checkout from your record.
TO AVOID FINES return on or before date due.
MAY BE RECALLED with earlier due date if requested.

DATE DUE	DATE DUE	DATE DUE

5/08 K:/Proj/Acc&Pres/CIRC/DateDue.indd

ULTRASTRUCTURAL AND PHYSICOCHEMICAL MODIFICATIONS WITHIN AMMONIA TREATED LIGNOCELLULOSIC CELL WALLS AND THEIR INFLUENCE ON ENZYMATIC DIGESTIBILITY

VOLUME I

By

Shishir Pratap Singh Chundawat

A DISSERTATION

Submitted to
Michigan State University
in partial fulfillment of the requirements
for the degree of

DOCTOR OF PHILOSOPHY

Chemical Engineering

2009

ABSTRACT

ULTRASTRUCTURAL AND PHYSICOCHEMICAL MODIFICATIONS WITHIN AMMONIA TREATED LIGNOCELLULOSIC CELL WALLS AND THEIR INFLUENCE ON ENZYMATIC DIGESTIBILITY

By

Shishir Pratap Singh Chundawat

The development of cellulosic ethanol based biorefineries has been largely impeded due to the native recalcitrance of plant cell walls to chemical pretreatments and enzymatic hydrolysis. Lignin-carbohydrate complex (LCC) ester linkages and cellulose crystallinity are major impediments to efficient cell wall deconstruction. Ammonia based pretreatments like AFEX (or Ammonia Fiber Expansion) are thought to overcome cell wall recalcitrance through ammonolysis of ester linkages and de-crystallization of cellulose. However, the major ammonolysis end-products and pretreatment induced cell wall based ultrastructural changes have never before been determined for AFEX treated lignocellulosics. Previous research has focused mostly on acidic pretreatments that extensively extract hemicellulose and lignin, hence minimizing the requirement for optimal cellulase and hemicellulase based enzyme cocktails. The goal of this study was to elucidate the mechanism of ammonia based pretreatments on lignocellulosic plant cell walls (e.g. corn stover, cellulose) and examine how that influences enzymatic activity.

In this study, it was found that ammonolysis of corn stover LCC ester linkages resulted in the extraction and re-deposition of decomposition products (e.g. amides, arabinoxylan oligomers, lignin phenolics) on outer cell wall surfaces. These amorphously shaped deposits were characterized by confocal fluorescence, atomic force and scanning electron based microscopic techniques. Cleavage of LCC linkages during AFEX resulted

in the formation of a nano-porous network that likely enhanced enzyme accessibility. The shape, size (e.g. pore width ranged between 10-1000 nm) and spatial distribution of the porous network was dependent on cell wall composition (e.g. middle lamella vs. secondary walls) and ammonia pretreatment conditions. Pretreated cell wall cumulative porosity (i.e. pore surface area per unit cell wall volume), estimated via analysis of transmission electron microscopy based tomograms (0.005-0.05 nm^2/nm^3), was linearly correlated to the total LCC ester linkages cleaved. Closer examination of cellulose crystal structure revealed formation of cellulose III allomorph upon treatment with anhydrous liquid ammonia (but not with ammonium hydroxide). Purified endoglucanase I (Glycosyl hydrolase or GH family 7), isolated from *T. reesei*, was found to have two-fold higher specific activity on cellulose III versus untreated cellulose. Cellulose within ammonia treated cell walls (ACW) was more readily accessible to *T. reesei* based cellobiohydrolases (GH 6, 7) compared to untreated cell walls. Further addition of endoxylanases (GH 11), β-xylosidase (GH 3) and α-arabinofuranosidase (GH 51) increased both glucan and xylan digestibility for ACW. Fourteen commercially available crude enzymes (ranging in diverse GH activities based on proteomics analysis) were optimally blended, to maximize ACW digestibility, using a high-throughput microassay. The optimal blend gave 90% total sugar conversion at 2-fold lower enzyme loading (i.e. 16.5 mg/g glucan) compared to commercial cocktails (e.g. Spezyme CP + βG rich cocktail gave 50% total sugar conversion). In summary, formation of cellulose III allomorph coupled with rationally tailored enzyme mixtures for ammonia treated lignocellulosic biomass could significantly reduce cellulosic ethanol production costs.

COPYRIGHT BY

SHISHIR P. S. CHUNDAWAT

2009

This work is dedicated to two special women in my life, my mother and my wife, who have provided me the inspiration, support and courage to be who I am.

ACKNOWLEDGEMENTS

First of all, I would like to thank my advisor, Dr. Bruce Dale, who mentored me and provided the perfect environment for me to grow as an independent researcher. I am also grateful to him for helping me advance my professional career by providing ample opportunities to present my research findings at various professional meetings. This project was funded by Michigan State Research Foundation (SPG grant) and DOE Great Lakes Bioenergy Research Center (DE-FC02-07ER64494).

I would like to thank all my committee members, especially Dr. Daniel Jones, Dr. Kenneth Keegstra and Dr. Jonathan Walton for their benevolent guidance and constructive criticisms during the course of my dissertation. Special thanks to Dr. Markus Pauly, Dr. Daniel Jones and Dr. Dennis Miller for providing access to their laboratory equipment.

I would like to gratefully acknowledge the support and access to the TEM imaging related facilities at the National Renewable Energy Laboratory (special thanks to Bryon Donohoe and Michael Himmel at Chemical and Biosciences Center). I would also like to thank the staff at the Center of Advanced Microscopy (Ewa Danielewicz, Melinda Frame, Shirley Owens) for their help and guidance while using the SEM and confocal microscopes. Special thanks to the staff at the Composite Materials and Structures Center (Per Askeland) for help with the ESEM, FTIR and ESCA instrumentation. Thanks to Thomas Elder (USDA, Louisiana), Umesh Agarwal (USDA, Wisconsin) and George Phillips/Chris Bianchetti (GLBRC, UW-Madison) for carrying out the AFM, Raman spectroscopy and X-Ray diffraction analysis, respectively. Proteomics analysis was

carried out at Pacific Northwest National Laboratory (PNNL) under the aegis of Mary Lipton and Samuel Purvine. I would also like to thank Lekh Sharma, Kevin Chambliss (Baylor University) and Ramin Vismeh for running samples on the LC-MS during the course of my dissertation. Special thanks to Paul Curran, Al French, Marcin Nowicki and Lars Peereboom for their timely help.

Last but not the least, I gratefully acknowledge all members of the Biomass Conversion Research Lab (BCRL) who provided useful insights, criticisms and technical support to my research project. I would like to especially thank Dr. Venkatesh Balan and Leonardo Sousa for being great colleagues, collaborators and mentors when it mattered most. I appreciate it very much! I would also like to extend my gratitude to Dahai Gao (for his fervent optimism), Aditya Rajagopalan (for his enthusiasm), James Humpula (for all the brewed, non-cellulosic beer among many other things), Nirmal Uppugundla (for taking special care of the devilishly unpredictable FPLC), Dr. Albert Che (for his intellectually stimulating conversations) and Christa Gunawan (for her meticulous HPLC analysis) for all the support provided to me. This work would have been incomplete without help from all of the above mentioned personnel.

I would like to finally extend my thanks to close friends and roommates (Deep C, Devesh, Madhusudhan) over the years for making my stay at MSU a truly memorable one. Finally, I would like to thank my parents (Kishan, Sunita), crazy brother (Arpit) and loving wife (Tithi) for tolerating my habitual idiosyncrasies. They were all my source of inspiration, joy and love that helped me steer through this arduous yet enjoyable journey in graduate school.

TABLE OF CONTENTS

LIST OF TABLES.....xiii

LIST OF FIGURES.....xix

ABBREVIATIONS.....xxv

CHAPTER 1: INTRODUCTION..... 1

CHAPTER 2: LITERATURE REVIEW..... 6

2.1 PLANT CELL WALLS 6

2.1.1 Major Components of Cell Wall..... 6

2.1.2 Cell Wall Architecture..... 9

2.2 THERMOCHEMICAL PRETREATMENTS 12

2.2.1 Physical Pretreatments..... 13

2.2.2 Solvent Fractionation Based Pretreatments..... 13

2.2.2.1 Organosolv process..... 13

2.2.2.2 Fractionation using phosphoric acid..... 14

2.2.2.3 Ionic liquid based fractionation 15

2.2.3 Chemical Pretreatments..... 17

2.2.3.1 Acidic pretreatments..... 17

2.2.3.2 Alkaline pretreatments..... 20

2.2.3.3 Oxidative pretreatments..... 21

2.2.4 Biological pretreatments..... 22

2.3 ENZYMATIC HYDROLYSIS 24

2.3.1 Enzyme Synergy..... 27

2.3.1.1 Endo-exo based synergy 27

2.3.1.2 Hemicellulases and accessory enzyme based synergy..... 29

2.3.1.3 Hemicellulase-cellulase based synergy..... 29

2.3.1.4 Cellulose binding domain (CBD) based synergy..... 30

2.3.1.5 Multi-catalytic domain synergy 31

2.3.1.6 Cellulosomal based synergy 31

2.3.1.7 Synergy due to non-hydrolytic additives 32

CHAPTER 3: PLANT CELL WALL SURFACE TOPOGRAPHICAL AND COMPOSITIONAL CHANGES AFTER AMMONIA BASED TREATMENTS... 33

3.1. AMMONIA PRETREATMENT SEVERITY AND SUBSTRATE PARTICLE SIZE INFLUENCE EXTENT OF CELL WALL MORPHOLOGICAL CHANGES..... 33

3.1.1 Abstract..... 33

3.1.2 Background..... 34

3.1.2.1 Gross morphology of ammonia treated cell walls 34

3.1.3 Materials and Methods..... 35

3.1.4 Results and Discussion 35

3.1.4.1 Modification of external cell wall morphology depends on ammonia pretreatment conditions..... 35

3.1.4.2 Effect of biomass particle size on extraction of ligno-phenolics during AFEX 44
3.1.4.3 Inhibition of cellulolytic enzymes by AFEX extracted ligno-phenolics .. 49
3.1.5 Conclusions *52*
3.2 CELL WALL SURFACE TOPOGRAPHY AND ATOMIC COMPOSITION AFTER CONVENTIONAL AFEX 54
3.2.1 Abstract *54*
3.2.2 Background *55*
3.2.2.1 Surface compositional analysis by X-ray photoelectron spectroscopy..... 55
3.2.2.2 Surface topographical analysis by atomic force microscopy 55
3.2.3 Materials and Methods *56*
3.2.4 Results and Discussion *56*
3.2.4.1 Outer cell wall topology visualized by AFM 56
3.2.4.2 Outer cell wall elemental composition characterized by ESCA 61
Conclusions *70*

CHAPTER 4: ULTRASTRUCTURAL MODIFICATIONS WITHIN AMMONIA TREATED CELL WALLS AND CRYSTALLINE CELLULOSE 72
4.1 FORMATION OF PORES AND DELAMINATION ZONES WITHIN AMMONIA TREATED CELL WALLS THROUGH DELOCALIZATION OF HEMICELLULOSE AND LIGNIN 72
4.1.1 Abstract *72*
4.1.2 Background *73*
4.1.2.1 Cross-linking matrix in cell walls of monocots and dicots are different .. 73
4.1.2.2 Effect of thermochemical treatment on modification of cell wall architecture 73
4.1.2.3 Cell wall porosity and electron tomography 74
4.1.3 Materials and Methods *76*
4.1.4 Results and Discussion *76*
4.1.4.1 Ultrastructural modification of cell wall depends on pretreatment severity 76
4.1.4.2 Quantifying porosity within cell walls through 3D-tomogram analysis... 92
4.1.5 Conclusions *98*
4.2 MODIFICATION OF NATIVE CELLULOSE CRYSTAL STRUCTURE BY AMMONIA BASED TREATMENTS 100
4.2.1 Abstract *100*
4.2.2 Background *101*
4.2.3 Materials and Methods *104*
4.2.4 Results and Discussion *104*
4.2.4.1 Cellulose I crystal structure is differentially altered by varying thermochemical treatments 104
4.2.4.2 Enzymatic digestibility of various cellulose allomorphs 108
4.2.4.3 Formation of cellulose III during conventional AFEX treatment..... 115
4.2.5 Conclusions *119*

CHAPTER 5: COMPARING MAJOR CELL WALL DEGRADATION PRODUCTS FORMED DURING AMMONIA AND DILUTE ACID BASED PRETREATMENTS 121

5.1.1 Abstract *121*
5.1.2 Background *122*
5.1.2.1 Degradation products formed during ammonia based pretreatments 123
5.1.2.2 Spectroscopic characterization of ammonia pretreated biomass 125
5.1.2.3 Oligosaccharides produced during ammonia based pretreatments 126
5.1.2.4 Quantitative methods for lignocellulose degradation product analysis .. 127
5.1.3 Materials and Methods *128*
5.1.4 Results and Discussion *128*
5.1.4.1 By-products of hydrolysis and ammonolysis of ester linkages during AFEX 128
5.1.4.2 Degradation products formed during dilute acid and AFEX pretreatment 137
5.1.4.3 Inhibition of glycosyl hydrolases by AFEX degradation products 141
5.1.5 Conclusions *145*

CHAPTER 6: DEVELOPMENT OF A HIGH-THROUGHPUT MICROPLATE BASED ENZYMATIC HYDROLYSIS METHODOLOGY 148
6.1.1 Abstract *148*
6.1.2 Background *149*
6.1.3 Materials and Methods *153*
6.1.4 Results and Discussion *153*
6.1.4.1 Effect of cell wall size reduction on enzymatic digestibility 153
6.1.4.2 Advantages of size reduction to high-throughput digestibility assays 154
6.1.4.3 Advantages of centrifugal milling to size reduction 156
6.1.4.4 Factors affecting microplate assay 157
6.1.4.5 Reproducibility of microplate methodology 165
6.1.4.6 Bio-enzymatic sugar assay 166
6.1.4.7 BCRL micro-assay vs. conventional macro-assay 169
6.1.4.8 Multi-pronged applicability of microplate based assays 170
6.1.5 Conclusions *171*

CHAPTER 7: MAXIMIZING TOTAL SUGAR HYDROLYTIC YIELD FOR AMMONIA PRETREATED LIGNOCELLULOSICS THROUGH CRUDE ENZYME MIXTURE OPTIMIZATION 173
7.1.1 Abstract *173*
7.1.2 Background *174*
7.1.2.1 Protein composition of crude commercial enzyme mixtures 174
7.1.2.2 Hydrolysis of pretreated biomass using commercial enzyme mixtures .. 176
7.1.3 Materials and Methods *179*
7.1.4 Results and Discussion *179*
7.1.4.1 Protein concentration determination 179
7.1.4.2 Protein composition estimated via proteomics and enzyme activity assays 181
7.1.4.3 Maximizing enzyme synergy using simplex centroid experimental designs 198
7.1.4.4 Eight-enzyme (8 ce-re) simplex centroid experimental design 201
7.1.4.5 Ten-enzyme (10 ce-re) simplex centroid experimental design 208

7.1.4.6 Five-enzyme (5 ce-re) simplex centroid experimental design 210
7.1.4.7 Protein composition and hydrolytic performance correlations 215
7.1.4.8 Role of enzyme synergy for cellulosic biorefineries 228
7.1.5 Conclusions *230*

CHAPTER 8: AMMONIA BASED PRETREATMENTS ENHANCE SYNERGISTIC HYDROLYSIS OF CRYSTALLINE CELLULOSE AND LIGNOCELLULOSIC CELL WALLS THROUGH DIFFERENT MECHANISMS **232**
8.1.1 Abstract *232*
8.1.2 Background *233*
8.1.2.1 Role of cellobiohydrolases (CBH) and endoglucanases (EG) 233
8.1.2.2 Role of endo- (EX) and exo-xylanases (βX) 237
8.1.2.3 Role of accessory hemicellulases 238
8.1.2.4 Role of xyloglucanases (XG) 238
8.1.3 Materials and Methods *240*
8.1.4 Results and Discussion *240*
8.1.4.1 Enzyme purification and activity assays 240
8.1.4.2 Comparing hydrolytic activity of core cellulases on cellulose I vs. III .. 242
8.1.4.3 Synergism between core cellulases on untreated and conventional AFEX treated corn stover 243
8.1.4.4 Effect of hemicellulase supplementation on AFEX corn stover digestibility 255
8.1.5 Conclusions *260*

CHAPTER 9: CONCLUSIONS AND RECOMMENDATIONS FOR FUTURE RESEARCH **262**

APPENDICES **269**
APPENDIX I – A (CHAPTER 3.1 - OUTER WALL MORPHOLOGY) 270
APPENDIX I – B (CHAPTER 3.2 - SURFACE TOPOGRAPHY-COMPOSITION) 275
APPENDIX II – A (CHAPTER 4.1 - CELL WALL POROSITY) 276
APPENDIX II – B (CHAPTER 4.2 - CELLULOSE III FORMATION) 281
APPENDIX III (CHAPTER 5 - DEGRADATION PRODUCTS) 283
APPENDIX IV (CHAPTER 6 - MICROPLATE METHODOLOGY) 284
APPENDIX V (CHAPTER 7 - CRUDE ENZYME OPTIMIZATION) 287
APPENDIX VI (CHAPTER 8 - PURIFIED ENZYME SYNERGY) 368
APPENDIX VII - MATERIALS AND EXPERIMENTAL METHODS 370
A-VII-1. Biomass feedstock *370*
A-VII-2. Biomass centrifugal milling *371*
A-VII-3. Particle size distribution *371*
A-VII-4. AFEX pretreatment *372*
A-VII-5. Compositional analysis of solid and liquid samples *373*
A-VII-6. Scanning electron microscopy (SEM) *373*
A-VII-7. Laser confocal scanning fluorescence microscopy (LCSM) *374*
A-VII-8. Atomic force microscopy (AFM) *374*

A-VII-9. Transmission electron microscopy (TEM) and 3D-tomography (3D-Tomo) 375
A-VII-10. Cell wall immunolabeling-electron microscopy (Immuno-EM) 376
A-VII-11. Dilute acid pretreatment 376
A-VII-12. Nitrogen physisorption analysis 377
A-VII-13. Near Infra-Red Compositional Analysis 377
A-VII-14. Electron Spectroscopy for Chemical Analysis (ESCA) 377
A-VII-15. Fourier Transform Infra-Red Spectroscopy (FTIR) 377
A-VII-16. Raman Spectroscopy 378
A-VII-17. Cellulose II, III and Amorphous Cellulose Preparation 378
A-VII-18. Powder X-Ray Diffraction (XRD) 379
A-VII-19. Solvent extraction methodologies 379
A-VII-20. Gas Chromatography Mass Spectrometry (GC-MS) 380
A-VII-21. Ammonolysis By-product Analysis by LC-MS/MS 381
A-VII-22. Other Degradation Product Analysis by LC-MS/MS 381
A-VII-23. High Performance Liquid Chromatography (HPLC) for Sugars 384
A-VII-24. Modified Prussian Blue Method (MPB) 384
A-VII-25. Robotic Dispensor Worktable Setup 385
A-VII-26. Reproducibility of Slurry Delivery 386
A-VII-27. Microplate Hydrolysis Procedure 386
A-VII-28. NREL LAP-9 Enzymatic Hydrolysis Protocol 388
A-VII-29. Bio-enzymatic Sugar Assays 388
A-VII-30. Microplate Evaporation Losses 390
A-VII-31. Commercial (CE) and Research (RE) Enzymes 391
A-VII-32. SDS-PAGE and Isoelectric Gel Electrophoresis 391
A-VII-33. Enzyme Activity Assays 392
A-VII-34. Proteomics Analysis 393
A-VII-35. Scheffé simplex-centroid CE-RE experimental design and regression .. 394
A-VII-36. Simplex-centroid design for CE-RE crude enzyme systems 395
A-VII-37. Heterologous expression of Aspergillus nidulans based β-xylosidase ... 396
A-VII-38. Enzyme purification 398

REFERENCES **399**

LIST OF TABLES

Table 3.A.1 Comparison of cell wall perimeter (L, μm), area enclosed within lumen space (A, μm^2) and isoperimetric quotient ($4\pi A/L^2$) for untreated, conventional AFEX (R-ACS) and high liquid to solid loading based AFEX (High-ACS) treated corn stover cell walls. Values with different alphabetical superscripts in an individual column were statistically different with $p < 0.05$ based on Student t-test.....38

Table 3.A.2 Composition of various particle size fractions from pre-milled corn stover.....46

Table I-3.A.3 Cell wall perimeters (L, μm), areas enclosed within lumen (A, μm^2) and isoperimetric quotients ($4\pi A/L^2$) for untreated, regular AFEX (R-ACS) and high liquid to solid loading based AFEX (High-ACS) treated corn stover cell walls.....271

Table 3.B.1 RMS (root mean square) roughness factors for untreated (U1-U10) and conventional AFEX (R-ACS; A1-A10) treated corn stover AFM amplitude images.....61

Table 3.B.2 ESCA based atomic composition of untreated (UT) and conventional AFEX treated (AT) corn stover fractions and some model compounds (Table has been partly reproduced from [1]). NA stands for 'not available'.....65

Table 3.B.3 Effect of water and solvent extraction (using NaOH, ethanol and water) on AFEX treated corn stover (ACS) surface atomic composition as compared to untreated corn stover (CS). All experiments were conducted in quadruplicates.....69

Table 4.A.1 Varying AFEX severity conditions.....77

Table 4.A.2 Surface area (SA) to volume (Vol) ratios for isosurface mesh enclosing porous regions within TEM-3D-tomograms of varying AFEX severity treated corn stover cell walls. Where; M: Middle lamella, P: Primary wall, S1/S2/S3: Secondary walls and delam: Delamination zones. See Table 4.A.1 for description of each AFEX severity.....93

Table 4.B.1 Relative change in the amount of crystalline polymorphs (with/without chemical treatment) present in Avicel (AV), cotton linters (LINT) and native cotton (COT) based on XRD spectra peak intensities ($I_{2\theta}$) at respective 2-theta angles (e.g. 2θ = 12, 18, 20, 22). Where for instance; Pk (18/22) = $1 - (I_{18}/I_{22})$; $\%\Delta\ (18/22)_{unknown} = 100 * [Pk\ (18/22)]_{unknown}/[Pk\ (18/22)]_{control}$ and control depends on substrate type (AV-I or LINT-I or COT-I).....106

Table 4.B.2 Relative change in the amount of crystalline polymorphs present in Avicel (AV), with or without AFEX treatment (N = ammonia loading and W = water loading, w/w basis) based on XRD spectra peak intensities ($I_{2\theta}$) at respective 2-theta angles (e.g. 2θ = 12, 18, 20, 22). Where for instance; Pk (18/22) = $1 - (I_{18}/I_{22})$ and $\%\Delta\ (18/22)_{unknown} = 100 * [Pk\ (18/22)]_{unknown}/[Pk\ (18/22)]_{AV\text{-}I}$.....116

Table 4.B.3 Relative change in the amount of crystalline polymorphs present in Avicel (AV), with or without AFEX treatment (N = ammonia loading and W = water loading, w/w basis) based on Raman spectral peak intensities ($I_{wavenumber}$) at respective wavenumbers (e.g. 380 and 350; cm^{-1}). Where for instance; Pk (380/350) = 1 – (I_{380}/I_{350}) and $\%\Delta\,(380/350)_{unknown}$ = 100 * [Pk (380/350)]$_{AV\text{-}unknown}$/[Pk (380/350)]$_{AV\text{-}I}$.....118

Table 5.1 Total water extractibles for untreated, AFEX and dilute acid treated corn stover compared to their respective glucan hydrolysis yields (24 hours hydrolysis time, 15 FPU Spezyme/g glucan supplemented with Novo 188). All water extractions were done using the ASE (see methods section for details) at 70 °C, 1500 psi (except Acid treated* that was extracted at 25 °C, 15 psi). See Table 4.A.1 for description of each AFEX severity.....128

Table 5.2 Six major ammonolysis and hydrolysis by-products (mg analyte per gm untreated corn stover) of acetyl, coumaroyl and feruloyl based ester linkages produced during AFEX and dilute acid pretreatment of corn stover. See Table 4.A.1 for description of each AFEX severity. NA – not applicable.....129

Table 5.3 Mass balances for major degradation products (mg analyte per gm untreated corn stover) produced during AFEX (for Regular and High-Nt severities) and dilute acid based pretreatment of corn stover based on GCMS (*), HPLC-MS/MS (ammonolysis** based) and HPLC-RI (***) analyses. See Table 4.A.1 for description of each AFEX severity. Where; ND and NA stand for not detected and not available, respectively.....132

Table III-5.4 Total nitrogen content (measured by Kjeldahl method as grams Nitrogen per 100 grams substrate) of untreated and varying AFEX severity treated cellulosic biomass. The surface atomic composition of the substrates was estimated by ESCA. Where; L (low) and H (high) stand for varying AFEX treatment severities. AFEX-L was carried in the HT-AFEX reactor at 90 °C, 1:1, 15 mins, 60% moisture. AFEX-H was carried in the HT-AFEX reactor at 130 °C, 3:1, 15 mins, 60% moisture. MetOH (methanol) extraction was carried out at 50 °C (15 psi) for 43 hours.....283

Table 6.1 Effect of mass transfer related parameters (i.e. reaction volume, solids loading, agitation speed and mixing aid) on Avicel digestibility for (A) 0.75 ml, and (B) 0.25 ml based reaction volumes. (Figure has been reproduced from [2]).....161

Table 7.1-A Protein concentration assay data for 14 crude enzyme blends using three analytical methods (Pierce BCA, Bradford and Kjeldahl Protein based assays).....180

Table 7.1-B Activity assay data for 14 crude enzyme blends on pNPG, pNPAf, pNPA, pNPX, OSX, Avicel and CMC. One unit of activity on pNP based substrates is equivalent to one nmol of pNP (p-nitrophenol) released/mg enzyme/min. One unit of activity on Avicel/Xylan/CMC is equivalent to one μM glucose equivalent released/mg enzyme/min. Where; "-" stands for no detectable activity; pNPG (pNP-β-D-glucopyranoside); pNPAf

(pNP-α-L-arabinofuranoside); pNPA (pNP-acetate); pNPX (pNP-β-D-xylopyranoside); OSX (Oat spelt xylan), CMC (Carboxymethylcellulose).....182

Table 7.2 Proteomics based protein compositional data for 14 crude enzyme blends based on total observed spectral counts.....187

Table V-7.3 Peptide ID and observed spectral counts for each family of proteins for CE 1.....295

Table 7.4 Design of experiments for range of varying crude enzyme mixture composition (based on fixed total protein loading of 16.5 mg/g glucan equivalent to 100%) that were tested on AFEX treated corn stover.....195

Table 7.5 Estimated regression coefficients for model terms (single, binary and cubic based interaction terms) predicting % glucan conversion, % xylan conversion and total sugar yield (gm sugar/kg dry weight biomass) as a function of crude enzyme mixture amount composition for 8 CE-RE based experiments. The sum of total enzyme loading is always equal to 8 mg protein/g glucan. All enzyme mixtures have a fixed loading of 8.5 mg CE6/g glucan, which is not included as a regressor in the model. Where; VIF = variance inflation factor, PRESS = prediction error sum of squares, S = first standard deviation of residuals, R-Sq(pred) = predicted R^2 (coefficient of determination); R-Sq(adj) = adjusted R^2.....202

Table V-7.6 Estimated regression coefficients for model terms (single, binary and cubic based interaction terms) predicting % glucan conversion, % xylan conversion and total sugar yield (gm sugar/kg dry weight biomass) as a function of crude enzyme mixture amount composition for 10 CE-RE based experiments. The sum of total enzyme loading is always equal to 16.5 mg protein/g glucan.....310

Table 7.7 Estimated regression coefficients for model terms (single, binary and cubic based interaction terms) predicting % glucan conversion, % xylan conversion and total sugar yield (gm sugar/kg dry weight biomass) as a function of crude enzyme mixture amount composition for 5 CE-RE (Cel x is CE 1) based experiments. The sum of total enzyme loading is always equal to 16.5 mg protein/g glucan.....211

Table V-7.8 Estimated regression coefficients for model terms (single, binary and cubic based interaction terms) predicting % glucan conversion, % xylan conversion and total sugar yield (gm sugar/kg dry weight biomass) as a function of crude enzyme mixture amount composition for 5 CE-RE (Cel x is CE 6) based experiments. The sum of total enzyme loading is always equal to 16.5 mg protein/g glucan.....316

Table V-7.9 Estimated regression coefficients for model terms (single, binary and cubic based interaction terms) predicting % glucan conversion, % xylan conversion and total sugar yield (gm sugar/kg dry weight biomass) as a function of crude enzyme mixture amount composition for 5 CE-RE (Cel x is RE 4) based experiments. The sum of total enzyme loading is always equal to 16.5 mg protein/g glucan.....317

Table V-7.10 Bivariate correlation Pearson coefficients for individual protein components of various enzyme mixtures (N = 753) with respect to their predicted % glucan, % xylan and total sugar hydrolysis yields. Values highlighted in bold signify lack of statistical significance at $p<0.05$ level.....318

Table V-7.11 Pearson correlation coefficients for individual protein components of various enzyme mixtures with respect to each other within the original 14 enzyme mixtures. Values highlighted signify statistical significance at $p<0.01$ and $p<0.05$ levels, respectively.....319

Table V-7.12 ANOVA results comparing top and bottom 25% quartile groups for individual protein components, based on varying % glucan, % xylan and total sugar hydrolysis yield. Values highlighted in bold signify statistical significance at $p<0.05$ level.....327

Table 7.13-A Descriptive statistics (minima, maxima, mean, standard deviation) comparing top and bottom 25% quartile groups for individual protein components, based on varying % glucan conversion. Values highlighted in bold signify statistical significance at $p<0.05$ level (based on Table 7.12), whereas values highlighted in red signify increase in corresponding protein component in top 25% quartile with respect to bottom quartile.....218

Table 7.13-B Descriptive statistics (minima, maxima, mean, standard deviation) comparing top and bottom 25% quartile groups for individual protein components, based on varying % xylan conversion. Values highlighted in bold signify statistical significance at $p<0.05$ level (based on Table 7.12), whereas values highlighted in red signify increase in corresponding protein component in top 25% quartile with respect to bottom quartile.....221

Table 7.13-C Descriptive statistics (minima, maxima, mean, standard deviation) comparing top and bottom 25% quartile groups for individual protein components, based on varying total sugar hydrolysis yield. Values highlighted in bold signify statistical significance at $p<0.05$ level (based on Table 7.12), whereas values highlighted in red signify increase in corresponding protein component in top 25% quartile with respect to bottom quartile.....335

Table V-7.14 Comparing individual protein composition of CE 1, CE 4 to enzyme mixtures that gave the top 5% (N = 755) response for glucan, xylan and total sugar hydrolysis yields.....338

Table V-7.15 Raw data for % glucan, % xylan and total sugar hydrolysis yield for all enzyme mixtures tested.....341

Table 8.1 Enzymatic hydrolysis of untreated (cellulose I, UAV) and liquid ammonia treated (cellulose III, AAV) Avicel by varying loadings (as mg enzyme/g glucan) of core cellulases (CBH I, CBH II, EG I, βG) resulting in the formation of glucose and cellobiose. Where; %G and $\%G_2$ stand for % glucan conversion based on glucose and

cellobiose yields, respectively. Commercial enzyme (CE) control comprised of Spezyme CP and Novo 188 at 15 mg/g glucan loading each.....244

Table 8.2 Enzymatic hydrolysis of untreated (cellulose I, UAV) and liquid ammonia treated (cellulose III, AAV) Avicel by varying loadings (as mg enzyme/g glucan) of core cellulases (CBH I, CBH II, EG I) resulting in the formation of glucose and cellobiose. Where; %G and $\%G_2$ stand for % glucan conversion based on glucose and cellobiose yields, respectively. Commercial enzyme (CE) control comprised of Spezyme CP and Novo 188 at 15 mg/g glucan loading each.....245

Table 8.3 Enzymatic hydrolysis of untreated (UCS) and conventional AFEX (ACS) treated corn stover by varying loadings (as mg enzyme/g glucan) of core cellulases (CBH I, CBH II, EG I, βG) resulting in the formation of glucose and cellobiose. Where; %G and $\%G_2$ stand for % glucan conversion based on glucose and cellobiose yields, respectively. Commercial enzyme (CE) control comprised of Spezyme CP and Novo 188 at 15 mg/g glucan loading each. 246

Table 8.4 Enzymatic hydrolysis of untreated (UCS) and conventional AFEX (ACS) treated corn stover by varying loadings (as mg enzyme/g glucan) of core cellulases (CBH I, CBH II, EG I) resulting in the formation of glucose and cellobiose. Where; %G and $\%G_2$ stand for % glucan conversion based on glucose and cellobiose yields, respectively. Commercial enzyme (CE) control comprised of Spezyme CP and Novo 188 at 15 mg/g glucan loading each.....247

Table VI-8.5 Glucan (% G) 24 hour hydrolysis yields for untreated avicel (UAV), liquid ammonia treated Avicel (AAV), untreated corn stover (UCS) and AFEX treated corn stover (ACS) by varying cellulase (CBH I, CBH II, EG I) combinations (mg enzyme/g glucan).....368

Table 8.6 Regression model predicting % glucan (% G) digestibility for untreated Avicel (UAV), liquid ammonia treated Avicel (AAV), untreated corn stover (UCS) and AFEX treated corn stover (ACS) as a function of varying cellulase loading (CBH I, CBH II and EG I; total protein loading is 15 mg/g glucan).....248

Table VI-8.7 Glucan (% G) and xylan (% X) 24 hour hydrolysis yields for AFEX treated corn stover by varying enzyme (CBH I, CBH II, EG I, EX, βX) combinations (mg enzyme/g glucan).....369

Table 8.8 Glucan and xylan saccharification yields (24 hours) for AFEX treated corn stover by cellulases (CBH I, CBH II, EG I; at fixed relative and total protein loading) and hemicellulase (α-arabinofuranosidase or ArbF, EX, β-X; varying relative protein loadings) combinations (as mg enzyme/g glucan) for fixed total protein loading of 16.5 mg/g glucan. βG loading was fixed at 1.5 mg/g glucan.....251

Table 8.9 Regression model (based on data from Table 8.8) predicting % xylan (% X) digestibility for AFEX treated corn stover (ACS) as a function of hemicellulase loading (EX, βX, ArbF as mg/g glucan).....259

LIST OF FIGURES

Images in this dissertation are presented in color

Figure 2.1 Cartoon depicting grass cell wall ultra-structural components as an intertwined matrix of cellulose, hemicellulose and lignin. Crystalline (straight, parallel lines) and amorphous cellulose (curved, wavy lines) microfibrils are composed of β-1,4 linked glucan chains. Hemicellulose (thick, short lines) with no side-chains is hydrogen-bonded to cellulose, while branches with side-chains (of arabinosyl, acetyl, glucuronyl groups shown as circles and squares) help in cross-linking cellulose microfibrils. Lignin carbohydrate complexes (between arabinose and ferulic/coumaric acids) further restrict access of enzymes to cell wall polysaccharides. Cross-linked lignin monomers (consisting of hydroxyphenyl, syringyl, guaicyl units) constitute the core-lignin fraction. (Figure has been reproduced from [3])....8

Figure 3.A.1 SEM micrographs of untreated (I), conventional AFEX treated (II) and high liquid to solid loading based AFEX treated (III) corn stover at varying degrees of magnification (Scale bars shown at the bottom of each image)....39

Figure 3.A.2 LSCM maximum intensity projection images of untreated (A) and high liquid to solid loading based AFEX treated corn stover (B) vascular bundles stained with Safranin. Sample sections were excited with 543 nm and emission was detected through LP 560 nm emission filter (fluorescence intensity shown in green). Image (A) and (B) are projection images compiled from 20 and 15 optical sections representing a thickness of 122 and 90 μms, respectively. Plan-Neofluar 10X/0.3 objective was used to obtain the images....40

Figure 3.A.3 (a) Phenolic content of AFEX treated and untreated corn stover wash streams; Untreated stover % gallic acid (empty bars), Untreated stover % ferulic acid (dot filled bars), AFEX treated stover % gallic acid (horizontal line filled bars), and AFEX treated stover % ferulic acid (slanted line filled bars). (b) Ferulic acid content of wash stream after single wash (UU-1W: Uncut corn stover => Untreated => Single Wash and UAG-1W (Uncut PM corn stover => AFEX => Ground to 0.08 mm => Single wash), multiple wash (UAG-3W: Uncut corn stover => AFEX => Ground to 0.08 mm => Washed three times) and after size reduction (GA-1W: Ground to 0.08 mm => AFEX => Single wash). (Figure has been reproduced from [1])....50

Figure 3.A.4 Effect of size reduction and water washing of AFEX treated corn stover on 72 hour glucan (left bar, black) and xylan (right bar, grey) conversions. (Abbreviations: - U-GBA: Unwashed ground before AFEX, W-GBA: Washed ground before AFEX, U-GAA: Unwashed ground after AFEX, W-GAA: Washed ground after AFEX). The standard error bars are based on duplicates. (Figure has been reproduced from [1])....51

Figure I-3.A.5 (A) Picture showing various parts of corn plant and their mass distributions are shown as pie chart in the bottom left. (B) Pictures showing various fractions for ground sample. Percent mass distributions of various particle size fractions

for pre-milled (PM*) and ground corn stover are shown as pie chart in the bottom right. (Figure has been reproduced from [1])....270

Figure 3.B.1 AFM amplitude images of untreated (A, top row) and conventional AFEX treated (B, bottom row) corn stover at varying degrees of magnification (All scale bars represent a length scale = 500 nm). Color legend (dark to light shades) depicts the amplitude current scale (V, volts)....59

Figure I-3.B.2 Untreated (U1-U10; panel I) and conventional AFEX (A1-A10; panel II) treated corn stover AFM amplitude (left) and phase (right) image dataset (image size is 2.5 x 2.5 μm^2). Box-plot of surface roughness factors (nm) along with data points scatter (N=10 per set) for untreated and AFEX treated amplitude image dataset from panels I-II....275

Figure 3.B.3 Effect of size reduction before and after AFEX pretreatment on oxygen to carbon (O/C, bars-left axis) surface atomic composition versus % phenolic acid equivalent water extractibles (line-right axis). Where; GCS: Ground corn stover (untreated), GCS-AFEX: Ground before AFEX, and AFEX-GCS: Ground after AFEX....69

Figure 4.A.1 Untreated corn stover TEM image showing cell corner, compound middle lamella (CML) and secondary wall layers (S1, S2, S3). (Scale bar shown at the bottom of the image)....78

Figure 4.A.2 AFEX treated corn stover TEM images (at varying scales of magnification) showing cell corner, compound middle lamella (CML) and secondary wall layers (S1, S2, S3). (a) Low-N, (b) Regular, (c) High-Nt, (d) Low-T, and (e) Low-W based varying AFEX severities. See Table 4.A.1 for description of each AFEX severity. (Scale bars shown at the bottom of each image)....79

Figure 4.A.3 Tomogram slices (~10 nm in thickness) depicting varying AFEX severity treated corn stover cell walls. (a) Low-N, (b) Regular, (c) High-Nt, (d) Low-T, and (e) Low-W based varying AFEX severities. See Table 4.A.1 for description of each AFEX severity. (Scale bars shown at the bottom of each image)....81

Figure 4.A.4 Iso-surface mesh enclosing porous regions within EM-tomogram for Low-N treated sample. (a) Tomogram slice (z = 10 slices), and (b) Iso-surface models enclosing porous regions within tomogram slice....84

Figure 4.A.5 Immuno-gold labeling of arabinoxylans extracted to outer cell walls (a, b) of AFEX pretreated (Regular) corn stover and water extract (c) using LM-11 based anti-body....87

Figure 4.A.6 24 hour glucan (grey bars) and xylan (white bars) digestibility, as percent conversion, for varying AFEX severity treated corn stover. Enzyme loading was 15 FPU/g glucan (Spezyme CP) and 64 p-NPGU (Novozyme 188) in 15 ml reaction volume for quadruplicates. See Table 4.A.1 for description of each AFEX severity....97

Figure II-4.A.7 AFEX treated corn stover TEM images (at varying scales of magnification) showing cell corner, compound middle lamella (CML) and secondary wall layers (S1, S2, S3) for Low-N treated AFEX corn stover.....276

Figure II-4.A.8 AFEX treated corn stover TEM images (at varying scales of magnification) showing cell corner, compound middle lamella (CML) and secondary wall layers (S1, S2, S3) for Regular treated AFEX corn stover.....277

Figure II-4.A.9 AFEX treated corn stover TEM images (at varying scales of magnification) showing cell corner, compound middle lamella (CML) and secondary wall layers (S1, S2, S3) for High-Nt treated AFEX corn stover.....278

Figure II-4.A.10 AFEX treated corn stover TEM images (at varying scales of magnification) showing cell corner, compound middle lamella (CML) and secondary wall layers (S1, S2, S3) for Low-T treated AFEX corn stover.....279

Figure II-4.A.11 AFEX treated corn stover TEM images (at varying scales of magnification) showing cell corner, compound middle lamella (CML) and secondary wall layers (S1, S2, S3) for Low-W treated AFEX corn stover.....280

Figure 4.B.1 Powder X-ray diffraction spectra of cellulose (Cellulose I) treated with liquid ammonia (Cellulose III), sodium hydroxide (Cellulose II), ammonium hydroxide and concentrated phosphoric acid (Amorphous Cellulose). Avicel was the cellulosic substrate in all cases. Y-axis and X-axis depict intensity counts and two-theta (2θ) angles, respectively.....105

Figure 4.B.2 Powder X-ray diffraction spectra of untreated (Cellulose I) and liquid ammonia (Cellulose III) treated celluloses. Avicel, cotton linters and native cotton were the cellulosic substrates used. Y-axis and X-axis depict intensity counts and two-theta (2θ) angles, respectively.....107

Figure 4.B.3 Enzymatic digestibility of untreated (Cellulose I), liquid ammonia (Cellulose III), sodium hydroxide (Cellulose II), ammonium hydroxide and concentrated phosphoric acid (Amorphous Cellulose) treated cellulose. Avicel was the cellulosic substrate in all cases. Enzyme loading was 1.5 FPU/g glucan of Spezyme CP (supplemented with Novo 188). Avicel was the cellulosic substrate in all cases. Y-axis depicts total glucan conversion after 6 or 24 hours of hydrolysis.....110

Figure 4.B.4 Enzymatic digestibility of untreated (Cellulose I) and liquid ammonia (Cellulose III) treated celluloses. Avicel, cotton linters and native cotton were the cellulosic substrates used. Enzyme loading was 1.5 or 15 FPU/g glucan of Spezyme CP (supplemented with Novo 188). Y-axis depicts total glucan conversion after 6 or 24 hours of hydrolysis.....112

Figure 4.B.5 Effect of liquid ammonia treatment temperature on the enzymatic digestibility of various cellulose III polymorphs. Enzyme loading was 1.5 FPU/g glucan of Spezyme CP (supplemented with Novo 188). Avicel was the cellulosic substrate in all cases. Y-axis depicts total glucan conversion after 24 hours of hydrolysis.....114

Figure II-4.B.6 Powder X-ray diffraction spectra of cellulose (Cellulose I) treated with liquid ammonia (Cellulose III) and varying AFEX severity. Avicel was the cellulosic substrate in all cases. The varying severity conditions are denoted by 1 or 3-NH3 (ammonia loading, w/w basis) and 0.05 or 0.6-W (water loading, w/w basis) in the figure legend. Y-axis and X-axis depict intensity counts and two-theta (2θ) angles, respectively.....281

Figure II-4.B.7 Raman spectra of cellulose (Cellulose I) treated with liquid ammonia (Cellulose III data from [4]) and varying AFEX severity. Avicel was the cellulosic substrate in all cases. The varying severity conditions are denoted by 1 or 3-NH3 (ammonia loading, w/w basis) and 0.05 or 0.6-W (water loading, w/w basis) in the figure legend. Y-axis and X-axis depict intensity counts and wavenumber (cm^{-1}), respectively.....282

Figure 5.1 Correlation between extent of enzymatic digestibility (Y, 24 hour, % Glucan conversion) and total feruloyl amide content (X, mg/gm biomass) of the varying AFEX severity treated corn stover substrates.....134

Figure 5.2 Effect of conventional AFEX corn stover degradation products (ASE extracted using hot water) on cellulase activity (hydrolyzing crystalline cellulose) as a function of hydrolysis time and total enzyme loading. Control experiment (a) was Avicel hydrolyzed by 15 FPU (or 22 mg) Spezyme CP/g glucan (supplemented with 38 mg/g glucan of Novo 188), in the absence of AFEX stover water extract, for various time points (24-168 hours). Control experiment (b) was Avicel hydrolyzed for 24 hours, in the absence of AFEX stover water, for various total enzyme loadings (12-48 mg/g glucan of Spezyme/Novo 188 in a fixed mass ratio of 37:63).....142

Figure 6.1 High-throughput BCRL microplate based saccharification methodology for lignocellulosic biomass. (Figure has been reproduced from [2]).....158

Figure 6.2 Particle size distributions for Avicel (AV) and ultra-centrifugally milled corn stover (CS). Bars indicate mean and standard errors for four replicate samples. (Figure has been reproduced from [2]).....159

Figure IV-6.3 Effect of slurry suspension solids loading (w/w) on delivery accuracy by pipetting workstation. The average amount of biomass (mg) delivered to each well is plotted on the Y-axis for varying percent slurry solids concentration (X-axis). The bars indicate standard deviations for 12 replicate experiments. (Figure has been reproduced from [2]).....284

Fig 6.4 Box plot of glucan conversions (Y) along with data points (N=48) for each set of experiments (X) performed for 0.25% glucan loading AFEX corn stover for conventional enzyme loading. (Figure has been reproduced from [2]).....166

Fig IV-6.5 (A) Hydrolysis time profile for conventional flask based assay for avicel (AV), un-ground AFEX corn stover (ACS) and milled AFEX corn stover at two different glucan loadings (0.25% and 1%). (B) Hydrolysis time profile for BCRL microplate based

assay for avicel (AV), untreated corn stover (UCS) and milled AFEX corn stover (ACS) at two different glucan loadings (0.25% and 1%). Percent glucan conversion and period of hydrolysis (hrs) are shown on the Y- and X-axis, respectively. (Figure has been reproduced from [2])....285

Figure 7.1 SDS-PAGE for 14 crude enzyme blends....185

Figure 7.2 Cox-response trace plots for % glucan conversion (A), % xylan conversion (B) and total sugar yield (C) with respect to reference blend at optimal mixture composition for 8 CE-RE experiments....207

Figure V-7.3 Cox-response trace plots for % glucan conversion (A), % xylan conversion (B) and total sugar yield (C) with respect to reference blend at optimal mixture composition for 10 CE-RE experiments....287

Figure 7.4 Cox-response trace plots for % glucan conversion (A), % xylan conversion (B) and total sugar yield (C) with respect to reference blend at optimal mixture composition for 5 CE-RE experiments (Cel x is CE 1)....212

Figure V-7.5 Cox-response trace plots for % glucan conversion (A), % xylan conversion (B) and total sugar yield (C) with respect to reference blend at optimal mixture composition for 5 CE-RE experiments (Cel x is CE 6)....289

Figure V-7.6 Cox-response trace plots for % glucan conversion (A), % xylan conversion (B) and total sugar yield (C) with respect to reference blend at optimal mixture composition for 5 CE-RE experiments (Cel x is RE 4)....290

Figure V-7.7-(A/B) Comparing protein composition of commercial enzyme (CE 1) to average composition of top 5% mixtures (N = 37), based on % glucan conversion....291

Figure V-7.7-(C/D) Comparing protein composition of commercial enzyme (CE 4) to average composition of top 5% mixtures (N = 37), based on % xylan conversion....293

Figure 7.7-(E/F) Comparing protein composition of commercial enzyme (CE 1) to average composition of top 5% mixtures (N = 37), based on % total sugar yield....226

Figure 7.8 Comparing effect of enzyme mixture composition (at fixed total protein loading of 16.5 mg/g glucan) on overall glucose (blue/bottom bar) and xylose (green/top bar) yield, with respect to dry weight untreated corn stover....229

Figure 8.1 Cox-response trace plots for % glucan conversion (AFEX corn stover) with respect to reference blend at optimal mixture composition of CBH I (34.67%), CBH II (26%) and EG I (39.33%). Sum of all three cellulase loadings is equal to 15 mg/g glucan. 1.5 mg/g glucan of βG was added to all mixtures tested (See Table VI-8.5)....250

Figure 8.2 Cox-response trace plot for % xylan conversion (AFEX corn stover or ACS) with respect to reference blend at optimal mixture composition of EX (29.07%), βX

(42.67%) and ArbF (28.27%). Sum of all three hemicellulase loadings is equal to 3.75 mg/g glucan (See Table 8.8).....260

Figure 9.1 Model for generic lignocellulosic cell walls before (A) and after ammonia based pretreatments (B). Figure depicts various lignin-carbohydrate complex (LCC) linkages between non-core lignin phenolics and hemicellulose side chains that are modified during AFEX resulting in enzyme accessible porosity. Where; Cellulose (green rods), Hemicellulose (purple strings with blue dots), Lignin (grey matrix).....264

ABBREVIATIONS

α-ArbF	α-arabinofuranosidase
α-Glu	α-glucuronidase
βG	β-glucosidase
βX	β-xylosidase
ADF	Acid Detergent Fiber
A. nidulans	*Aspergillus nidulans*
AFEX	Ammonia Fiber Expansion
AFM	Atomic Force Microscopy
ARP	Ammonia Recycle Percolation
AXE	Acetyl Xylan Esterase
CA	Coumaric Acid
C. thermocellum	*Clostridium thermocellum*
CBD	Cellulose Binding Domain
CBH	Cellobiohydrolase (or Exoglucanase)
CBM	Cellulose Binding Module
CBP	Consolidated Biological Processing
CD	Catalytic Domain
CE 1	Spezyme CP
CE 2	Novozyme 188
CE 3	Multifect xylanase
CE 4	Multifect pectinase

CE 5	Depol 670 L
CE 6	Accellerase 1000
Cip	Cellulosome Integrating Protein
CS	Corn Stover
DP	Degree of Polymerization
DRIFT	Diffusive Reflectance Infra-Red Fourier Transform Spectroscopy
DSE	Degree of Synergism
EDS	Energy Dispersive X-ray Spectrometer
EG	Endoglucanase
EM	Electron Microscopy
ESCA	Electron Spectroscopy for Chemical Analysis
EX	Endoxylanase
FA	Ferulic acid
FPLC	Fast protein liquid chromatography
FTIR	Fourier Transform Infra-Red
%G	Glucan conversion
GC	Gas Chromatography
GH	Glycosyl Hydrolase
HPLC	High Performance Liquid Chromatography
LC	Liquid Chromatography
LCC	Lignin Carbohydrate Complex
MS	Mass Spectrometry

MS/MS	Tandem Mass Spectrometry
NDF	Neutral Detergent Fiber
NREL	National Renewable Energy Laboratory
O/C	Oxygen to Carbon Ratio
OSX	Oat Spelt Xylan
PCW	Primary Cell Wall
p-NPA	p-nitrophenol-actetate
p-NPAf	p-nitrophenol-arabinofuranoside
p-NPG	p-nitrophenol-glucoside
p-NPX	p-nitrophenol-xyloside
RE 1	NS-22002
RE 2	NS-50010
RE 3	NS-50012
RE 4	NS-50013
RE 5	NS-50014
RE 6	NS-50029
RE 7	NS-50030
RE 8	NS-50053
SAXS	Small Angle X-ray Scattering
SCW	Secondary Cell Wall
SEM	Scanning Electron Microscopy
SSA	Specific Surface Area
T. reesei	*Trichoderma reesei*

TEM	Transmission Electron Microscopy
%X	Xylan conversion
XPS	X-ray Photoelectron Spectroscopy
XRD	X-Ray Diffraction

CHAPTER 1: INTRODUCTION

The economic viability of producing lignocellulosic ethanol is dependent on the cost of various thermochemical and biological processing steps involved. This is largely due to the inherent recalcitrance of lignocellulosic substrates [5,6]. Despite tremendous interest in lignocellulosic ethanol there have been few significant commercial efforts to produce it. This is predominantly due to research focus on expensive high severity, acid-based pretreatments and excessive public scrutiny of bio-fuels in recent years. A sensible approach would be to focus research efforts on sustainable, low-severity thermochemical pretreatments like AFEX [7] that could potentially co-produce pretreated feedstock for the biofuel industry as well as for animal feed. This would partly address concerns to the impending feed vs. fuel argument [8,9]. Unfortunately, the effect of AFEX pretreatment on lignocellulosic plant cell walls and enzymatic hydrolysis is insufficiently understood to successfully commercialize this technology.

The enzymatic digestibility of native and pretreated lignocellulosics depends primarily on two factors; (a) *Substrate-related* and (b) *Enzyme-related* [10,11]. Substrate related factors are typically cellulose crystallinity [12-15], hemicellulose side-chain branching [16], lignin monomer type and content [17], coumarate and ferulate cross-linking [17,18], cell wall porosity [19-22] and particle size [23]. Enzyme related characteristics that influence hydrolysis are specific activity [24], enzyme synergy [25-32], enzyme inactivation due to non-productive protein binding to lignin and cellulose during hydrolysis [33-38], and inhibition due to end-products or pretreatment degradation species [39,40].

Past studies indicate that AFEX modifies several substrate related characteristics that improve enzymatic digestibility. The improvement in hydrolysis yields after AFEX is probably due to decrystallization of cellulose [41], partial depolymerization of hemicellulose [42,43], xylan deacetylation [18], cleavage of lignin carbohydrate complex (LCC) bonds and possibly through increase in accessible surface area [44,45]. However, there are several fundamental questions that still need to be addressed for AFEX pretreatment, such as; what are the physicochemical effects of AFEX on cellulose, hemicellulose and lignin? What ultra-structural modifications are brought about within the cell wall during AFEX that enhance enzyme accessibility? What degradation products are formed during pretreatment and their potential role as biological inhibitors? What is the mathematical relationship between pretreatment thermodynamic conditions (i.e. AFEX severity) and extent of biomass digestibility for a defined enzyme cocktail?

Also in order to obtain higher cellulose and hemicellulose hydrolysis yields at commercially favorable low enzyme loadings [46,47], it becomes necessary to optimize synergistic interactions between enzymes to maximize pretreated biomass digestibility [48]. Unfortunately, cellulase and hemicellulase based synergistic hydrolysis of AFEX pretreated lignocellulosic biomass is also poorly understood. This is due to predominant focus on model substrates (like bacterial microcrystalline cellulose, avicel) and acid pretreated biomass where hemicelluloses are absent or significantly removed [26,36,49,50]. Several areas related to enzyme synergy on AFEX treated lignocellulosics that need to be explored are; what combinations of crude commercial enzymes maximize digestibility for AFEX treated biomass? What cellulases (e.g. cellobiohydrolases, endoglucanases) and hemicellulases (e.g. endoxylanases, β-xylosidases, α-

arabinofuranosidases) are critical to the hydrolysis of AFEX treated cell walls? What are the synergistic mechanisms of individual enzymes on pretreated cell walls and what role does AFEX play in modulating this? Is it possible to optimize purified enzyme combinations and reduce total protein loading (i.e. unit mass protein per unit mass pretreated biomass) to maximize digestibility? How does AFEX pretreatment severity affect synergistic enzyme activity?

The goal of this dissertation was to identify the major physicochemical modifications incorporated within lignocellulosic cell walls during various ammonia based pretreatments. The project also explores the effect of ammonia based pretreatments on synergistic interactions between cellulases, hemicellulases and various other accessory enzymes. This research should help make significant strides towards the development of mechanistic, mathematical models that help predict glucan and xylan digestibility of ammonia pretreated lignocellulosic cell walls for varying pretreatment severities and complex hydrolytic enzyme combinations.

1.1 Objectives

The mechanism by which AFEX (at lower water to solid loadings) helps enhance enzyme accessibility and ultimately improves the hydrolytic rate compared to untreated lignocellulosic biomass, like corn stover, is currently unknown. It is *hypothesized* that AFEX creates ultra-structural modifications within the plant cell wall through cleavage of certain lignin-carbohydrate based complex linkages and possibly through structural modification of cellulose microfibrils. These physicochemical modifications help

improve enzyme accessibility and enhance synergistic interactions between various enzyme components.

To test this hypothesis, it would be necessary to firstly 'visualize' the ultra-structural modifications incorporated within and outside the cell wall through various microscopic techniques (***milestone #1***); secondly, it would be necessary to obtain composition related information for chemical modifications that take place within the cell wall after AFEX pretreatment using various spectroscopic and spectrometric techniques (***milestone #2***). Lastly, the effect of pretreatment on synergistic hydrolysis of lignocellulosics would need to be studied using various cellulases, hemicellulases and accessory proteins to digest untreated and AFEX treated biomass (like avicel and corn stover) (***milestone #3***).

At the conclusion of these studies, it would be possible to identify the important substrate (e.g. cell wall porosity through TEM analysis) and enzyme (minimalist enzyme mixture that gives 90% or higher glucan and xylan conversions) related parameters that affect the ultimate digestibility of AFEX pretreated corn stover. These studies would also prove to be extremely beneficial in the eventual development of fundamental mechanistic models that accurately predict effectiveness of AFEX on biomass digestibility as a function of varying pretreatment severities and individual enzyme components.

The three over-arching objectives of this thesis project are as follows;

Objective 1: To visualize ultra-structural modifications incorporated within and outside corn stover cell walls due to varying severity ammonia based pretreatments

Objective 2: To quantify compositional changes and major degradation products formed during AFEX pretreatment of corn stover based lignocellulosic cell walls

Objective 3: To study the effect of ammonia based treatments on synergistic interactions between cellulases, hemicellulases and other accessory enzymes for maximizing cell wall polysaccharide digestibility

CHAPTER 2: LITERATURE REVIEW

2.1 Plant Cell Walls [i] [ii]

2.1.1 Major Components of Cell Wall

The primary constituents of lignocellulosic biomass are 30-50% cellulose (glucose polymer), 15-35% hemicellulose (hetero-sugar polymer), 10-30% lignin (phenyl propanoid polymer) and other minor constituents that include proteins (3-10%), lipids (1-5%), soluble sugars (1-5%) and minerals (5-10%) [51].

Cellulose is a linear homo-polysaccharide that consists of glucose (D-glucopyranose) units linked together by β-(1-4) glycosidic linkages (β-D-glucan). The degree of polymerization (DP) of cellulose varies depending on its source. Cellulose from avicel has 30-fold lower DP compared to untreated corn stover (200 vs. 7,000, respectively) [52-54]. The adjacent glucan chains form elementary microfibrils (3-5 nm diameter) of water-insoluble aggregates of varying length and width in the primary cell wall of corn stover [55]. These aggregates contain ordered (crystalline) and less-ordered (amorphous) regions of cellulose [56]. The lattice forces responsible for maintaining the crystalline regions are a result of extensive inter- and intra-molecular hydrogen bonding. The cellulose polymorph typically seen in higher plants is Cellulose I_β, which is a more tightly packed crystal structure, compared to other cellulose polymorphs (e.g. Cellulose III) due to differences in hydrogen bonding patterns [57].

---

[i] A version of this chapter was published as Chundawat, S.P.S., Balan, V., Sousa, L., Dale, B.E., 2009. Characteristics of an ideal thermochemical pretreatment for reducing recalcitrance of lignocellulosic biomass to biological processing. in: K. Waldron (Ed.) Bioalcohol production: : Biochemical conversion of lignocellulosic biomass (In Press). Woodhead Publishing, Cambridge.

[ii] A version of this chapter was published as da Costa Sousa, L., Chundawat, S.P., Balan, V., Dale, B.E., 2009. 'Cradle-to-grave' assessment of existing lignocellulose pretreatment technologies. *Curr Opin Biotechnol*, 20, 339-47.

Hemicelluloses are complex hetero-polysaccharides whose chemical composition, unlike cellulose, varies between cell tissues and plant species [58,59]. These polysaccharides are formed by a wide variety of sugar building blocks including pentoses (xylose, arabinose), hexoses (glucose, mannose, galactose) and uronic acids (4-*O*-methyl-glucuronic, galacturonic acids) [56]. Generally, hemicelluloses fall into two major classes: (a) un-branched chains such as β-(1-4)-linked xylans or mannans; and (b) branched chains such as β-(1-4)-linked galactoglucomannans and arabinoxylans (O2/O3 xylosyl linkages). The most abundant hemicelluloses found in agricultural residues like corn stover are arabinoxylans and arabino-(glucurono)-xylans [59,60]. The ratio of pentosans (xylose, arabinose) and acidic sugars (uronic acids) varies considerably between tissues, but typically corn stover cell walls contain at least 20-25% xylan, 4-5% arabinan and 3-5% uronic acids (total dry weight basis).

Lignin is a phenyl-propanoid based macromolecular network that is primarily formed through the free-radical polymerization of p-hydroxy cinnamyl alcohol units of varying methoxyl content [61]. The chemical structure of lignin is complex and is largely based on its three phenolic precursors: coniferyl alcohol, sinapyl alcohol, and p-coumaryl alcohol. The ratios and absolute amounts of these precursors vary significantly between species, phenotypes, organs (leaf, stem, sheath), tissues (xylem, sclerenchyma, parenchyma, epidermis) and hence tremendously affects the physicochemical nature of lignocellulosic cell walls [17]. Lignification of cell walls helps provide strength to plant tissues preventing collapse of water-conducting elements and provides defense against various pathogens (fungi and bacteria).

These three cell wall components are organized together in a complex matrix (schematic cartoon shown in **Figure 2.1**) depending on the plant clade (monocots vs. dicots), type of cell (sclerenchyma vs. parenchyma cells) and type of cell wall (primary vs. secondary). Several simplified models of the primary cell wall have been presented over the years [62,63], with little work on understanding the ultra-structural architecture of secondary cell walls [64,65].

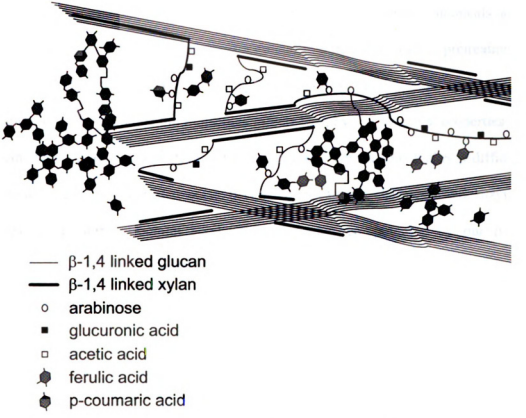

Figure 2.1 *Cartoon depicting grass cell wall ultra-structural components as an intertwined matrix of cellulose, hemicellulose and lignin. Crystalline (straight, parallel lines) and amorphous cellulose (curved, wavy lines) microfibrils are composed of β-1,4 linked glucan chains. Hemicellulose (thick, short lines) with no side-chains is hydrogen-bonded to cellulose, while branches with side-chains (of arabinosyl, acetyl, glucuronyl groups shown as circles and squares) help in cross-linking cellulose microfibrils. Lignin carbohydrate complexes (between arabinose and ferulic/coumaric acids) further restrict access of enzymes to cell wall polysaccharides. Cross-linked lignin monomers (consisting of hydroxyphenyl, syringyl, guaicyl units) constitute the core-lignin fraction. Figure has been adapted from [3].*

2.1.2 Cell Wall Architecture

There are two levels of structural arrangement within the plant cell wall that affects the rate of enzymatic hydrolysis: (1) **Macro-Structure** and (2) **Ultra-Structure**. The macro structural level is on a scale where one can identify the various types of plant cells (e.g. parenchyma, sclerenchyma), tissues and cell wall pits/pores. This is important from the point of view of recognizing the physical heterogeneity of plant biomass across the different cells and tissues. The differential transport of pretreatment chemicals and enzymes, through this super structure, plays a crucial role in understanding pretreatment and enzymatic hydrolysis [66]. The ultrastructural level is on the molecular scale where organization and orientation of the molecules affects the physico-chemical properties of the system. The complex organization of various cell wall constituents makes it difficult to understand the interactions that occur between pretreatment chemicals and enzyme complexes on an ultra structural level. This is further compounded by our poor understanding of cell wall biogenesis and ultra structural organization of the cell wall, which is a subject of ongoing research [62,67].

Several ultrastructural models have been proposed to explain the **primary cell wall** (PCW) matrix [56,63,68]. The extensive hydrogen bonds in cellulose through inter-chain (2 per anhydroglucopyranose) and intra-chain (2 to 3 per anhydroglucopyranose) interactions produces a straight, stable supramolecular fiber of great tensile strength called as an '**Elementary Microfibril**' [11]. Several glucan chains are aggregated into a single elementary fibril (4–5 nm width), and bunches of elementary fibrils are embedded in a matrix of hemicellulose ranging in thickness from 7–30 nm [57]. The natural composite that results from this close association is referred to as a **cellulose microfibril**.

Cellulose microfibril arrangements in the PCW, stabilized by hemicellulose and pectin cross-links, are randomly oriented compared to secondary cell walls [69,70]. There are proteins that can function structurally (extensin) or provide enzymatic activity (transglycolases) to help modify the structure during cell wall elongation. The major difference between primary and secondary cell walls is the inclusion of lignin and exclusion of water in the latter [71].

Secondary cell walls (SCW) can be visualized as cellulose microfibrils embedded in a matrix of hemicellulose and lignin [72]. The SCW of woody biomass are composed of three lamellae referred to as S1, S2 and S3, which vary in their helical orientation of cellulose fibrils as well as the extent of lignification [73]. Hemicelluloses are typically rod-shaped with branches folded back to the main chain by means of hydrogen bonding. This rod-like structure facilitates their interaction with cellulose, resulting in a tight association [74]. Hemicellulose monolayers can be sandwiched between crystalline cellulose domains during the synthesis of cellulose microfibrils [75]. Lignin located primarily to the exterior of cellulose microfibrils, where it is covalently linked to hemicellulose side-chains [14], is called non-core lignin. Free radical polymerization of non-core lignin to phenolic monomers results in a highly condensed core lignin. Covalent hemicellulose-lignin bonds involve ester and ether linkages that form the lignin-carbohydrate-complexes (LCC) [76]. The cleavage of these LCC bonds has been proposed to be an important factor that facilitates enzymatic hydrolysis.

No clear relationship has been identified between biomass digestibility and lignin content due to lignin quantification issues [77] and type of lignin-hemicellulose cross-linkages that are not taken into account [17,78]. Hydroxycinnamic acids (e.g. Coumaric,

Ferulic) are important LCC components that help cross-link hemicellulose to lignin in xylem & sclerenchyma tissues of grasses through carboxyl and hydroxyl groups [78]. Core lignin and hemicellulose are primarily esterified via ferulate (30-70% ester) or coumarate (90% ester) linkages [17]. Coumaric acid (CA) based esters make up to 20% of the lignin in maize tissues [79-82]. Majority of CA ester linkages (~ 80%) are with terminal hydroxy groups of core lignin that also helps build internal lignin bridges [17]. Unlike coumarate esters, ferulate esters (FA) acylated to polysaccharides have their carboxyl groups esterified to the C5-hydroxyls of arabinosyl side-chain residues of xylan [83-86]. Significantly lower amounts of arabinose units (1 in 30) were found to be esterified to CA compared to FA (1 in 15) for barley straw [17]. During SCW lignification neighboring xylans are further cross-linked through peroxidase mediated oxidation and co-polymerization of ferulate hydroxyl groups to xylan and lignin, respectively [17,87,88]. FA is deposited in the early stages of cell wall development (in the middle lamella and primary cell wall) and forms a scaffold for lignification; while CA is deposited in later stages of SCW lignification [17].

FA and CA have been found to be the predominant LCC components linked to the arabinose side-chains of xylan. However, other studies [17] have also indicated presence of uronic acid residues on the xylan backbone that may be esterified to lignin phenolics. Benzyl ether linkages to uronics should be less frequent in grasses compared to some woody species. Studies with model compounds and woody species indicate cross-linking of cell wall components with lignin-quinone methide intermediates through β-O-4 coupling of monolignols [89]. However, very few studies have actually shown the presence of benzyl ester and ether cross-linkages except some indirect studies that

showed improvement in cellulase digestibility in presence of ammoniated and hydroxypropylated model compounds attributed to suppression of quinine-methide intermediate cross-linking [90-92]. Grabber and colleagues have shown that poor degradability of DHP (dehydrogenation polymer) based cell walls is related to enhanced benzyl ester and ether cross-linking [93] Hydroxyprolines (glycoproteins) may also be cross-linked to lignin through isodityrosine bridges and with feruloylated heteroxylans in grasses [94].

2.2 Thermochemical Pretreatments

Pretreatments can be classified based on the nature of cell wall disruption (i.e. physical or chemical) into four categories [95]; (a) Physical, (b) Solvent fractionation, (c) Chemical and, (d) Biological pretreatment. Thermochemical pretreatment of lignocellulosic biomass is known to enhance the rate of enzymatic hydrolysis by 5-10 fold. Depending on the pretreatment catalyst and solvent used, it is possible to solubilize, hydrolyze and physically separate cellulose, hemicellulose and lignin [96]. Several types of pretreatment chemicals/solvents have been used, such as, concentrated acid [97], dilute acid [98], caustic soda [99], sulphur dioxide [100], hydrogen peroxide [101], steam [102], liquid ammonia [103], alkali-peroxide [104], lime [105], liquid hot water [106], carbon dioxide [7], and several organic solvents [107]. Most pretreatments physically extract lignin and hemicellulose into separate liquid process streams, hence improving cellulase accessibility [102,108-113].

However, AFEX does not physically extract lignin and hemicellulose like other pretreatments but modifies the cell wall ultra-structure through a mechanism that is currently poorly understood.

2.2.1 Physical Pretreatments

Physical pretreatments physically disrupt the lignocellulose structure with little or no chemical modifications to the individual cell wall components. Some typical methods for physical pretreatment include biomass particle size reduction through communition, including dry, wet, vibratory and compression based ball milling [114-117]. Physical treatments help increase enzyme accessibility by increasing biomass surface area to volume ratio. In some cases, extensive ball milling results in decrystallization of cellulose and reduction in degree of polymerization [118]. Particle size reduction alone is not a sufficient pretreatment to significantly enhance the rate of enzymatic hydrolysis. The cost of size reduction also increases exponentially beyond a certain size range making it economically unfeasible [119]. However, some sort of minimal particle size reduction is necessary prior to most pretreatments to improve material handling during processing.

2.2.2 Solvent Fractionation Based Pretreatments

Solvent fractionation using various solvents that can selectively solubilize cellulose, hemicellulose and lignin can also be used to pretreat lignocellulosic biomass. Cellulosic solvents like hydrazine, DMSO and concentrated mineral acids can disrupt hydrogen bonding between cellulose microfibrils to solubilize crystalline cellulose [120].

2.2.2.1 Organosolv process

Historically, the organosolv process was investigated largely from the perspective of paper production (via pulping) from hardwoods. Organosolv process includes extracting lignin from lignocellulosic biomass using organic solvents like aromatic alcohols (phenols) or aliphatic alcohols (e.g. ethylene glycol, methanol, ethanol, butanol, glycerol) typically with an acidic catalyst [121-123]. The effect of organosolv based process

parameters (e.g. solvent composition, temperature, liquid to solid loading) on fractionation of the major components in woody biomass has been extensively studied over the years [124]. Typical ethanol based organosolv pretreatment parameters have the following ranges; temperatures (90-120°C for grasses and 155-220°C for hard/soft woods), reaction times (25-100 min), acid catalyst loading (0.5-2%), and ethanol concentrations (25-75% v/v). Compared to aliphatic alcohols, aromatic alcohols were found to be more effective in solubilizing lignin from different feedstocks [125]. In addition to alcohols, various amines have been used to delignify lignocellulosic biomass, but amines also tend to solubilize substantial amounts of carbohydrates in addition to lignin. An ethanol-based organosolv process has been commercialized by Lignol Innovation Corporation (Vancouver, Canada) to separate lignin, hemicellulose and cellulose fractions from woody biomass [126]. The insoluble cellulose fraction is subjected to enzymatic hydrolysis to produce fermentable sugars, while the liquor from the organosolv step can be further processed to recover lignin, furfural, xylose, acetic acid and lipophylic extractive based fractions. Ethanol used in the process is distilled and reused. The lignin fraction recovered can be used as an additive binder among other applications. In the case of poplar, about 88% of the total cellulose is recoverable as monomeric glucose after 100 hours of enzymatic hydrolysis of the residual solid fraction.

2.2.2.2 Fractionation using phosphoric acid

Fractionation of lignocelluloses to amorphous cellulose, hemicellulose, lignin and acetic acid using concentrated phosphoric acid, acetone and water based mixtures is novel solvent fractionation based pretreatment [127]. Phosphoric acid based pretreatments may be carried out at moderate reaction conditions (i.e. 50 °C, 1 bar), which minimizes acid

catalyzed degradation of polysaccharides. The process gave 98% and 89% recovery yield for glucose and xylose, respectively, upon fractionation of corn stover. The selective fractionation of cell wall components is possible due to significant difference in solubility of cellulose, hemicellulose and lignin in phosphoric acid-acetone-water mixtures. The organic solvents are easily recoverable due to difference in volatility with respect to phosphoric acid [127-129]. Despite several advantages associated with this pretreatment method, which include enhanced rate of amorphous cellulose hydrolysis and low pretreatment utility costs (e.g. 50 °C vs. 100-200 °C for other thermochemical treatments); there are several technical challenges (e.g. solvent cost and recovery, xylose recovery and fermentation) that need to be addressed to make this process commercially viable. Other issues include phosphoric acid/sugar separation, acid recovery, and acid re-concentration.

2.2.2.3 Ionic liquid based fractionation

Ionic liquids (IL) are non-volatile solvents, under atmospheric conditions, composed exclusively of ions held together by coulombic forces. The first reported IL that could solubilize cellulose was back in 1934 using molten N-ethylpyridinium chloride, in the presence of nitrogen-containing bases [130]. However, the application of IL as lignocellulose pretreatment catalyst has gained momentum in recent years [131]. Cellulose-dissolving IL usually contains anions of chloride, formate, acetate or alkyl phosphonate, since these ions form strong hydrogen bonds with cellulose. During a typical IL pretreatment of lignocellulosics, the biomass added to ionic liquids (ratio of 1:10-15, wt/wt) is heated (50-150°C) to solubilize the cellulosic, hemicellulosic and lignin components [132]. The un-dissolved residue is filtered from solution and anti-

solvents (e.g. water/methanol/ethanol) are added to the solution to recover the solubilized cellulose (as amorphous cellulose). The mass recovery of lignin and hemicellulose is currently unknown for corn stover [132]. IL can be recovered from the anti-solvent by flash distillation and re-used in the process [131-134]. Typically, ionic liquids that incorporate anions are found to be more effective in solubilizing cellulose, due to stronger hydrogen bonding between the anion and cellulose hydroxyl groups. On the other hand, IL with non-coordinating anions and long-chain substitution are poor cellulose solvents. IL with chloride anions appear to be the most effective solvents, while IL with aromatic side chains require higher temperatures to solubilize cellulose, due to their higher melting points and viscosities [133].

While most of the reports on IL based pretreatments are on processed cellulose (e.g. Avicel, Sigmacell), there are recent publications that have pretreated woody biomass [136, 137]. The solubilization efficiency of hard woods in IL was found to vary in the following order; ball-milled wood powder > sawdust > thermomechanical pulp > wood chip. Wood flour solubilization was tested using $[Emim]^+[CH_3COO]^-$ (1-ethyl-3-methylimidazolium acetate) based IL as a function of pretreatment time and temperature. Increasing residence time and IL treatment temperature caused a significant decrease in cellulose crystallinity; while improving lignin solubility (20-60% solubilized) and enhancing regenerated biomass enzymatic digestibility. Greater than 90% glucan digestibility was achieved using commercial enzymes after 24 hours of hydrolysis. There are several concerns that need to be addressed to facilitate commercialization of IL based pretreatments. These include cost of ionic liquids, recovery of IL after pretreatment, hemicellulose recovery yield and enzyme/microbial compatibility of IL [134].

2.2.3 Chemical Pretreatments

2.2.3.1 Acidic pretreatments

Most acidic based pretreatments (like dilute acid, steam explosion and liquid hot water treatment) have very similar chemistries but vary in thermochemical severity. The acidic catalyst is either supplemented externally (as mineral acids) or is formed due to hydrolysis of hemicellulose acetyl linkages (forming acetic acid) and degradation of polysaccharides and lignin to short-chain aliphatic acids and phenolic acids, respectively. Water itself behaves as an acid at high temperatures typically employed in most pretreatments [135]. The acid is responsible for hydrolytic cleavage and removal of hemicellulose and lignin, hence improving enzymatic accessibility of cellulose. The extent of removal of hemicellulose and lignin varies considerably between various acidic pretreatments depending on the severity of pretreatment. The severity of acidic pretreatments can be quantified using a simple relationship which helps couple the effect of time (t), temperature (T) and acidity (pH) into a single factor known as the 'combined severity factor (S)' [136].

$$\log(S) = \log(\mathrm{R}) - pH$$

$$R = t \times \exp\left[{}^{(T-100)}\!/_{14.75}\right]$$

Higher acid pretreatment severities, referring to longer residence times, higher temperatures and lower pH values, result in extensive hydrolysis of hemicellulose to monomeric sugars. However, higher pretreatment severity also results in the degradation of lignin and hemicellulose derivatives to compounds like furfural, 5-hydroxymethylfurfural, levulinic acid, phenolic acids/aldehydes and other aliphatic acids that can severely inhibit downstream biological processing [137]. Most acidic based

pretreatments look to optimize severity by trading-off between enhanced cellulose enzymatic digestibility, hemicellulose hydrolysis yields and minimizing formation of biological inhibitors.

Dilute-acid pretreatment (using either sulfuric, hydrochloric or nitric acid) was one of the first pretreatment methods that was implemented to pretreat lignocellulosic biomass to produce ethanol [138]. Traditionally, dilute acid based hydrolysis of lignocellulosic biomass has been used to manufacture furfural through breakdown of hemicellulose [139]. The remaining cellulosic fraction was typically hydrolyzed to monomeric glucose using concentrated acid (10-30%) prior to fermentation [140]. However, with the development of genetically modified microbes that can co-ferment glucose and xylose it became necessary to prevent degradation of hemicellulose to furfural to improve ethanol yields. This has resulted in the development of dilute-acid based pretreatments, typically using sulfuric acid, carried out using lower acid concentrations (0.05-5%) and temperatures (160-220 °C) [141,142]. Dilute-acid pretreatment can be carried out in a stationary batch mode or flow-through continuous mode [143,144].

Steam explosion is one of the most widely implemented pretreatment methodologies to pretreat several types of lignocellulosic biomass (e.g. agricultural residues, hardwoods and softwoods). Steam explosion is typically carried out by rapidly heating lignocellulosic biomass with high pressure saturated steam with/without external chemical addition (typically acids) for certain duration of time (ranging from a few seconds to minutes), at fixed temperature (160-290 °C) prior to explosively releasing the pressure [113,145,146]. There have been several reported variants of the steam explosion

process. These variants typically incorporate pre-impregnation with an acid (like sulfuric acid, sulfur dioxide) or alkali (like sodium hydroxide, ammonia) prior to steam explosion [147-151].

Liquid hot water pretreatment (also known as hydrothermal or aquasolv treatment) is a low severity acid based pretreatment that uses water at high pressures (> 5 MPa) to maintain it in the liquid state at elevated temperatures (160-230 °C) to pretreat lignocellulosics [135,151,152]. The liquid water is contacted with the biomass in three possible modes; co-current, counter-current and flow-through [95]. Recent variants to the liquid hot water pretreatment process allow for better pH control (ranging from pH 4-7) that limits non-specific degradation of polysaccharides [152].

In addition to mineral acids (like sulfuric acid, nitric acid), organic acids (carbonic, acetic, succinic, fumaric, maleic, citric acid) have been used as catalysts (at 50 mM concentration) for pretreatment of biomass [153]. It was reported that maleic and fumaric acids had superior selectivity for the production of fermentable sugars from cellulose than sulfuric acid [154]. At high temperatures (150 °C) sulfuric acid degrades monomeric sugars to undesirable by-products, while maleic/fumaric acid does not. Corn stover, at high solids loading (150-200 g/liter), pretreated by sulfuric acid resulted in 30% degradation of xylose to furfural. While, using maleic acid preserved ~95% of monomeric xylose and resulted in greater than 90% glucose yield after enzymatic hydrolysis (15 FPU of cellulase/g of cellulose) of the xylan depleted substrate. The unconditioned hydrolyzate was fermented by recombinant *S. cerevisiae* resulting in 87% theoretical ethanol yield. Detailed economic analysis is necessary to determine the economic feasibility of this process [155,156]. In few reports carbonic acid, formed by

dissolution of carbon dioxide, was used as an organic acid to carry out pretreatment [157].

2.2.3.2 Alkaline pretreatments

Alkali based pretreatments differ in the type and thermodynamic state of the catalyst-solvent systems employed. Alkalis used for pretreatment typically include calcium hydroxide, ammonia and sodium hydroxide. Most alkali pretreatments help lower recalcitrance of lignocellulosics through cleavage of hemicellulose acetyl and lignin-carbohydrate complex linkages [16,18]. One of the other major effects is the extraction of lignin from the biomass during alkaline pretreatments that helps reduce non-specific binding of enzymes during cellulose enzymatic hydrolysis [158]. The chemical modifications and ultra-structural modifications incorporated within the biomass are poorly understood for most alkaline pretreatments, compared to their acidic counterparts.

Ammonia fiber expansion (AFEX) is a novel alkaline pretreatment method that uses concentrated liquid ammonia-water mixtures to pretreat lignocellulosics [7,103]. AFEX is a lower temperature process (60-140 Degrees Celsius) that is carried out by adding liquid ammonia (0.3-2 kg ammonia per kg dry weight biomass) to pre-wet biomass (0.05-1 kg water per kg dry weight biomass) in a pressurized reactor and cooking it for 5-45 minutes before explosively releasing the ammonia. AFEX is a dry to dry process, unlike most other pretreatments, resulting in no separate liquid stream at the end of the pretreatment. The volatility of ammonia allows for recovery and recycle for a continuous process [159]. AFEX results in de-acetylation and cleavage of lignin-carbohydrate complexes through base catalyzed hydrolysis [160]. The extent of ammonolysis of ester linkages within the biomass is currently unknown [161,162].

Ammonia is also believed to de-crystallize cellulose as shown by X-ray diffraction studies [163]. On-going research indicates significant modification of the cell wall ultra-structure during AFEX that results in enhanced enzymatic accessibility (unpublished data).

There have been several different ammonia treatment processes that have been reported in the literature; such as supercritical ammonia treatment, ammonia recycle percolation (ARP), soaking in aqueous ammonia (SAA) and ammonia-peroxide pretreatment [158,162,164-167]. Most of these pretreatments vary in the thermodynamic state of ammonia-water mixtures for varying ammonia concentrations. ARP pretreatment is carried out in a flow-through, recycle mode by percolating ammoniacal solutions (5-15% concentration) through a column reactor packed with biomass under high pressure (2-3 MPa) and at high temperatures (160-180 Degrees Celsius). A significant amount of lignin and hemicellulose is extracted to the liquid phase during ARP treatment.

2.2.3.3 Oxidative pretreatments

Ozone has also been used an oxidizing agent to break down lignin within lignocellulosic biomass to help increase enzymatic digestibility [168-170]. Traditionally, ozone had been used to bleach pulp replacing chlorine as the oxidant [171]. Ozonolysis, typically conducted at room temperature and pressure, has been used in combination with other alkaline pretreatments to help extract lignin from forage residues to help improve forage digestibility [171,172]. Ozone reacts selectively with lignin based aromatics producing several types of degradation products (primarily aromatic aldehydes and aliphatic organic acids) that have been found to inhibit biological processing of ozone treated biomass [173]. Ozonolysis based intermediate degradation products (like free radicals) are

responsible for unwanted side-reactions, like polysaccharide degradation [174-176]. There is a lack of published data on ozonolysis based pretreatments for various agricultural residues [177]. The possible inhibitory effects of various ozonolysis degradation products are also poorly understood. However, the biggest hurdle for an economically feasible ozonolysis based pretreatment is the cost of ozone.

Alkaline wet oxidative is another form of oxidative pretreatment carried out typically under alkaline conditions at high temperatures (170-220 °C) using pressurized air/oxygen or hydrogen peroxide as the oxidant [178,179]. The alkali typically employed for wet oxidation is sodium carbonate (0.02-0.05 g Na_2CO_3/g dry biomass) that partly solubilizes the hemicellulose fraction [178,180]. The advantage of an alkaline medium during treatment at elevated temperatures is in minimizing the formation of various furan based degradation products.

2.2.4 Biological pretreatments

Most chemical pretreatments are carried out at high temperature/pressure based reaction conditions, and thus require significant capital investment [181]. High thermochemical severity also results in the formation of several degradation products that are inhibitory to downstream biological processing (i.e. enzymatic hydrolysis and fermentation). Contrary to chemical based pretreatments, biological pretreatments (using enzymes or microbes as pretreatment catalysts) would consume lesser energy since they are carried out under milder reaction conditions [182-184]. However, most biological treatments are slow (reaction time ranges between several hours to months) and have low-throughput. Biological pretreatments are typically carried out by inoculating the biomass with fungal spores (e.g. white rot basidiomycetes and even certain actinomycetes) or externally

supplementing accessory enzymes (e.g. ferulic acid esterases and hemicellulases). White-rot fungi have been found to be effective to degrade lignin while minimizing polysaccharide consumption [185-188]. During microbial pretreatments, a substantial amount of delignification can take place, possibly at the expense of polysaccharide consumption depending on the microbial source [189]. White-rot microbes typically secrete lignin peroxidases, along with various types of glycosyl hydrolases, that cleave the C-C lignin backbone in the presence of hydrogen peroxide. Other enzymes involved in aerobically catalyzed lignin degradation include Mn-dependent peroxidases, laccases (monophenol oxidase) and superoxide dismutase [190]. Details about the lignin degrading microbial systems have been summarized elsewhere [190]. In recent years, the use of ferulic acid esterases and other accessory enzymes as catalysts to cleave LCC linkages within plant cell walls to help reduce thermochemical severity during subsequent pretreatment and/or to maximize recovery of valuable phenolic by-products have been explored [191].

Several articles on microbial pretreatments using solid state fermentation (SSF) have been published for both grasses and hard woods [192,193]. The effect of substrate moisture content, inorganic salt concentration, culture time on lignin degradation, solids recovery, and availability of carbohydrate on the biological pretreatment process have been explored. The solid state cultivation of cotton stalks using *Phanerochaete chrysosporium*, at 75% moisture content without salts was the preferable pretreatment condition resulting in 28% lignin degradation, 71% solids recovery and 42% availability of carbohydrates over a period of 14 days [194]. Another approach is to use minimally treated mushroom spent straw (MSS) as a feedstock for downstream thermochemical and

biological processing [185,186]. When MSS was used without any pretreatment, the glucan digestibility was around 40%, using standard commercial cellulases (15 FPU/g glucan); and 20% for untreated rice straw. Further thermochemical pretreatment is necessary for getting higher sugar yields from MSS. By using microbial pretreated biomass as a feedstock for thermochemical pretreatments; it might be possible to reduce processing costs by reducing pretreatment severity and minimizing chemical usage while obtaining higher overall hydrolysis yields. Unfortunately, there have been no detailed economic studies comparing the feasibility of scaling-up and integrating biological based pretreatments within a conventional cellulosic biorefinery.

2.3 Enzymatic Hydrolysis

All microbial enzyme systems can be broadly classified into two classes: Non-Complexed and Complexed. **Non-complexed** systems [195] are characteristic of aerobic fungi (Trichoderma), which comprise of several polysaccharide depolymerases that are secreted into the extra cellular medium. The cellulase system of *T. reesei* has been studied extensively and has become the paradigm for this group. **Complexed** systems are typical of anaerobic organisms (Clostridium) present in rumen and compost. In these systems the enzymes are uniquely assembled as a high molecular weight protein complex (held together by a scaffolding protein or Cip - Cellulosome Integrating Protein) called **Cellulosome**. Cellulosomes are exocellular macromolecular machines, designed for efficient degradation of cellulose and associated plant cell wall polysaccharides [196]. *Clostridium* species have one of the most well documented cellulosome systems that have been studied over the past two decades.

Differences in cellulolytic systems of aerobes and anaerobes may be attributed to differences in their environmental conditions and the physical size of the organisms. Aerobes excrete their enzymes in a thick aqueous film covering the plant cell wall. The absence of fluid convection allows for the enzyme to be immobilized onto the substrate in close proximity to the microbe. This allows for an efficient transport of the hydrolysis products to the microbes. Contrary to that, anaerobes inhabit large liquid volumes; where extracellular enzyme secretions would not be energetically efficient. Thus, the anaerobic cellulolytic system is efficiently packed close to the microbial cell surface to enhance the uptake flux of the hydrolysis products. Furthermore, enzymes may be organized as part of the cellulosome, or as free complexes in the culture fluid depending on specific environmental conditions (e.g., pH, temperature, distribution of carbon source) [196,197].

Glycosyl hydrolases (GH) and related carbohydrate-active enzymes have been classified based on the amino acid sequence homology of their catalytic domains [204, 205]. This has helped classify enzymes based on their structural and mechanistic features. Cellulolytic enzyme systems are comprised of several types of proteins. There are typically three classes of exogenous cellulase enzymes that have been thoroughly studied over the years:

Cellobiohydrolase or exoglucanase (CBH) which acts at the ends (reducing or non-reducing) of cellulose, processively cleaving disaccharide **cellobiose** from the glucan chain. These enzymes typically belong to GH family 6, 7 and 9.

Endoglucanase (EG) which randomly hydrolyze the interior β-1,4-glucan linkages of the cellulose chain, cleaving it into smaller units and providing more "ends"

for CBH to act on. These enzymes typically belong to GH family 5, 6, 7, 9, 12, 45 and 61.

β-Glucosidase (cellobiase, βG) which hydrolyzes cellobiose and short chain oligosaccharides into monomeric glucose units. These enzymes typically belong to GH family 1 and 3.

Complete degradation of side-chain decorated hemicelluloses requires the concerted action of several enzymes [198]. The important classes of hemicellulose degrading enzymes are:

Endoxylanases (EX) hydrolyze interior β-1,4-xylosidic linkages of the xylan backbone. These enzymes typically belong to GH family 10 (acidic pI, high molecular weight) and 11 (basic pI, low molecular weight).

β-Xylosidase (xylobiase, βX) hydrolyzes xylobiose dimers and short chain xylooligosaccharides to xylose. These enzymes typically belong to GH family 3.

α-Arabinofuranosidase (α-ArbF) hydrolyzes terminal non-reducing α-arabinofuranose from arabinoxylan side-chains. These enzymes typically belong to GH family 51, 54 and 62.

α-Glucuronidase (α-Glu) releases glucuronic acid from glucuronoxylan side-chains. These enzymes typically belong to GH family 67.

Acetyl xylan esterases (AXE) hydrolyzes acetylated ester linkages from xylan backbone. These enzymes typically belong to carbohydrate esterase family 1.

Phenolic acid esterases hydrolyze feruloyl and p-coumaroyl ester bonds in lignin-hemicellulose complexes. These enzymes typically belong to carbohydrate esterase family 1.

2.3.1 Enzyme Synergy

The structural and chemical heterogeneity of lignocellulosic substrates dictates the synergistic action of the complex enzyme systems towards its complete digestion [199]. **Synergism**, was first discovered over 50 years ago [200,201], occurs when the combined action of two or more enzymes leads to higher rate of action than the sum of their individual actions. The degree of synergism (DSE) has been found to vary with enzyme-substrate ratio (substrate site saturation), relative enzyme ratios and the form of cellulosic substrate [202,203]. There have been several types of enzyme synergy that have been studied over the past few decades.

2.3.1.1 Endo-exo based synergy

Preliminary cellulase models (Wood, 1968) sought to describe synergy as the interaction of endoglucanases (so called C_x enzymes) with C_1, a putative non-catalytic factor responsible for the disruption of hydrogen bonds in cellulose crystals [25]. But this version was abandoned to adopt a model for **'endo-exo synergy'** that describes the concerted action of endoglucanases (EG) and cellobiohydrolase (CBH). The model suggests that the action of CBH are limited by availability of cellulose chain ends; whereas EG cannot hydrolyze crystalline cellulose effectively but hydrolyzes amorphous cellulose to create chain ends for CBH to act upon. This procession of CBH helps expose deeper buried amorphous cellulose for further action by EG. **'Cross-synergy'** between EG or CBH from different microbial species has been observed where not all interactions

resulted in synergy [27]. One of the reasons for this is that it is still rather unclear which particular enzyme properties are predominantly responsible for synergistic action. Perhaps synergy requires the closely coordinated action of enzymes, similar to cellulosomal systems, which only certain EG or CBH show due to the formation of a putative enzyme complex. The synergy between endo and exo enzymes can be largely explained by the degree of accessibility of the active catalytic site to the cellulosic substrate [31].

'**Exo-exo synergy**' has been noted in some experiments [204] and a couple of plausible models to this effect have been proposed in the literature [205]. These models suggest that some exo enzymes (like CBH II) are capable of limited endo activity, while in some other cases the synergistic effect was seen largely due to endoglucanase contamination. Synergy between strictly exo acting enzymes could also be explained if each enzyme recognizes the two distinct stereo specific configurations revealed during course of hydrolysis of the cellulose chain [29,30] or due to differential binding to reducing and non-reducing ends of the cellulose chain [206-209]. Interestingly, it was found that Penicillium pinophilum exo enzymes only synergized to hydrolyze avicel but not cotton [29]. This might have to do with the lower degree of polymerization of avicel compared to cotton which results in availability of larger number of reducing ends for the exo enzymes to act upon. More recently there have been examples of other **endo-endo** synergistic cooperation among cellulases [210].

Synergy between endo-exo enzymes is strongly dependent on the nature of the substrate [10,211], relative proportion of enzyme components [30] and degree of saturation of the cellulosic substrate by the enzymes [46,47].

2.3.1.2 Hemicellulases and accessory enzyme based synergy

Many xylanases do not cleave glycosidic linkages between xylose units that have side-chain substitutions. The side chains must be removed before the xylan backbone can be completely hydrolyzed. Typically, endoxylanases have been found to synergize with accessory enzymes that remove arabinose, uronic acid and ferulic acid side-chains to enhance accessibility to the xylan backbone [32]. However, side-chains might be also necessary for some endoxylanases to help in substrate recognition by the enzyme catalytic site. There have been reported cases of anti-synergy (for in-vitro purified enzyme experiments) when an accessory enzyme removed side-chains from xylan backbone that resulted in poor activity of a certain endoxylanase on the debranched backbone [212]. Several accessory enzymes only remove side chains from xylooligosaccharides [213]. These enzymes require a partial hydrolysis of xylan before the side chains can be cleaved [214,215].

Enzymes from GH family 10 have been typically found to hydrolyze heteroxylans (with glycosidic linkages in close proximity to side-chain substitutions) to a higher degree than family 11 endoxylanases, further releasing shorter chain xylo-oligosaccharides [216-218].

2.3.1.3 Hemicellulase-cellulase based synergy

Endoglucanase-xylanase systems have been used to help boost bleaching properties of pulp and recycled paper. Removal of xylan from the pulp using cellulase-free xylanase aids in the removal of lignin [219]. Endoglucanases and hemicellulases have also been used to aid in the deinking of mixed office wastes [220-223]. Nonionic and cationic surfactants have been found to facilitate the process of deinking [224]. The cellulases

used in the paper and pulp industry have been generally low dose endoglucanases (with little or no exo activity). Synergy among xylanases and other accessory enzymes has been shown in those cases as well. However, no cellobiohydrolases have been used as they tend to detrimentally affect the strength of the fibers.

Xylanase-cellulase enzyme systems have also been used in the animal feed industry. Xylanases are used in animal feeds along with glucanases, pectinases, cellulases, proteases, amylases, galactosidases and lipases. The enzyme complex helps to break down arabinoxylans in the ingredients of the animal feed and aids in ruminant digestion, also reducing the viscosity of the feed material [225]. Xylanases are used in conjunction with cellulases, amylases and pectinases help to improve the yield of extracted juice during liquefaction of fruits and vegetables also reducing the viscosity and cloudiness in the concentrate.

2.3.1.4 Cellulose binding domain (CBD) based synergy

In addition to the catalytic domain, cellulases and hemicellulases usually contain at least one cellulose-binding domain (CBD) and other modular domains linked by sequences rich in hydroxy amino acids whose interactions are not well understood [195,226,227]. The CBD serves to direct and attach the catalytic domain to insoluble crystalline substrates. Efficient hydrolysis of crystalline substrate requires the adsorption of enzymes prior to hydrolysis, which is facilitated by the CBD. It has been found that CBD's have a stronger binding affinity to crystalline, insoluble cellulose rather than amorphous cellulose and soluble cello-oligomers [228-230].

Two main mechanisms of CBD based synergy are seen to operate: (a) increase local concentration of enzymes on cellulose surface, (b) disrupt hydrogen bonding

between packed cellulose crystals, liberating glucan chains for cleavage by the catalytic domain. Further validation of this hypothesis has been found due to sequence homology match between CBD and swollenin/expansin based non-hydrolytic proteins that swell crystalline cellulose. It might be possible to improve enzymatic activity of cellulases and hemicellulases by modifying the CBD to prevent non-productive binding to cellulose and lignin [32].

2.3.1.5 Multi-catalytic domain synergy

Some multi-domain enzymes have been found to contain multiple CBDs and/or catalytic domains. The structural linkage of two catalytic domains for these **Multifunctional Proteins** results in synergy between these catalytic domains. A multifunctional protein (Cel B in *C. saccharolyticum*) was created by gene fusion to give xylanase and cellulase catalytic domains fused together by a single CBD [231]. One particularly interesting combination of multifunctional catalytic modules that appears in the same polypeptide chain is an endoxylanase together with a feruloyl esterase [232]. Such a combination would allow the rapid cleavage of hemicellulose from lignin in natural systems. In this manner, the xylan chain would be severed by the xylanase component and the lignin-xylan association would be disconnected simultaneously by the esterase.

2.3.1.6 Cellulosomal based synergy

It is estimated that the activity of polycellulosome systems (from Clostridium) on crystalline cellulose is about 50-fold higher than extracellular enzyme systems (from Trichoderma) [233]. An important aspect of the cellulosome model proposed is that the enzyme complex hydrolyzes crystalline cellulose with remarkable efficiency because the activities of individual enzymes are highly coordinated [196]. This coordination can be

viewed as a specialized form of '**proximity synergy**' in which the spatial organization of enzymes on the cellulose chain is crucial. There has also been synergy observed between fungal (Trichoderma) and bacterial (Clostridium) enzymes [27]. Artificial mini-cellulosomes have been constructed in-vitro with xylanases and cellulase to enhance enzymatic hydrolysis of untreated lignocellulosic biomass [202].

2.3.1.7 Synergy due to non-hydrolytic additives

A frequently observed rate increase of enzymatic hydrolysis by addition of non-ionic surfactants has been typically attributed to a decreased non-specific binding of cellulases to lignin [38,234]. It was also found that the addition of bovine serum albumin (BSA) decreases the non-productive adsorption of CBH and consequently increases the conversion of lignocellulose [33]. It has been generally observed that one protein may have higher affinity for a particular surface and may even displace other proteins from the coated surface. The reduction of non-specific binding of cellulases due to addition of BSA or non-ionic surfactants is most probably due to coating of the lignin surface by the added surface active agents.

CHAPTER 3: PLANT CELL WALL SURFACE TOPOGRAPHICAL AND COMPOSITIONAL CHANGES AFTER AMMONIA BASED TREATMENTS

3.1. Ammonia pretreatment severity and substrate particle size influence extent of cell wall morphological changes

3.1.1 Abstract[iii]

The extent of plant cell wall (i.e. corn stover) morphological modification was closely related to the type of cell wall (e.g. parenchyma vs. sclerenchyma) and AFEX pretreatment conditions (e.g. water and ammonia loading) employed. Amorphously shaped deposits rich in ligno-phenolics were deposited on the outer wall regions after high-moisture/ammonia based pretreatment, as inferred from laser scanning confocal fluorescence/scanning electron microscopy (LSCM and SEM) and Prussian blue analysis of the wall extractives. There was considerable fiber disruption after high-moisture/ammonia based pretreatment as indicated by significant modification of cell morphology (i.e. cell wall length, lumen area, wall perimeter/lumen area based isoperimetric quotient). In contrast to what was seen for high-moisture/ammonia treatment, there was no major physical modification of secondary cell walls during conventional AFEX treatment (employing lower liquid to solid loading). However, despite the fact that conventional AFEX is unable to physically extract lignin and hemicellulose from within the cell walls into a separate liquid fraction, the rate of enzymatic digestibility of treated cell walls was 4-5 fold higher than that of untreated walls. This would suggest that there are certain ultrastructural modifications, currently

---

[iii] A version of this chapter was published as Chundawat S.P.S, Balan V., Dale B.E. 2006. *Effect of particle size based separation of milled corn stover on AFEX pretreatment and enzymatic digestibility*. Biotechnology and Bioengineering 96(2):219-231.

not visible through low magnification SEM and confocal microscopy, within conventional AFEX treated cell walls that enhance the accessibility of the wall polysaccharides to cellulolytic enzymes.

3.1.2 Background

3.1.2.1 Gross morphology of ammonia treated cell walls

AFEX pretreatment has been found to increase cell wall defibrillation based on scanning electron microscopic (SEM) analysis of pretreated lignocellulosics [7,235]. Ammonia based pretreatments have been typically found to disrupt woody fibers on a micrometer scale by splitting fibers parallel along the longitudinal axis [236]. Super critical ammonia treated hard wood exhibited a more '*amorphous*' surface appearance and showed a 50% increase in specific pore volume after pretreatment, with no significant change in the specific pore size [162]. Furthermore, extensive pretreatment of hardwoods by super-critical ammonia resulted in reduction of specific pore volume comparable to untreated samples.

There have been efforts in recent years to study the effect of dilute acid and steam explosion based pretreatments on ultra-structural modifications of lignocellulosic grasses using high resolution electron and atomic force microscopy (AFM) based techniques [40,111,112]. Dilute-acid and steam explosion based pretreatments have been shown to cause lignin coalescence into droplets that migrate out of corn stover cell walls. The droplets redeposit within and outside the cell walls at the end of pretreatment and range in size from 5 nm to 10 μms [112]. These spherical droplets are composed essentially of lignin and are found to severely inhibit enzymatic activity [40]. Lignin re-localization away from cellulose microfibrils helps improve cellulase accessibility, however,

complete lignin removal causes extensive collapse of microfibrils which may impede further access to enzymes (Personal communication with Bryon Donohoe at NREL; [161,162]). Alkaline extraction and delignification of spruce based softwood resulted in considerable nanostructural changes of the hemicellulose-lignin matrix surrounding cellulose microfibrils based on the severity of pretreatment [237]. Alkali pulping typically results in swelling of cellulose crystallites as seen via AFM imaging [238] and significant modification of cell wall morphology caused by extensive fiber defibrillation and extraction of lignin/hemicellulose [236].

There have been no detailed microscopic studies conducted for AFEX pretreated agricultural residues (like corn stover) to elucidate the effect of pretreatment severity on cell wall morphology and ultra-structure. A detailed analysis of these ultra-structural changes would help better understand the role of pretreatment on enhancing the physical accessibility of enzymes to cell wall polysaccharides, and might also assist in reducing any pretreatment-induced recalcitrance to enzymatic digestibility.

3.1.3 Materials and Methods

See appendix A-VII-1, 4 (a), 6, 7, 13, 15, 19 (b), 23, 24, 28 and 31.

3.1.4 Results and Discussion

3.1.4.1 Modification of external cell wall morphology depends on ammonia pretreatment conditions

Unlike AFEX, most pretreatments physically extract a significant portion of the lignin (20-85%) and hemicellulose (30-80%) from corn stover into separate liquid process streams [18,54,113,158,239-243]. This is probably due to the higher liquid to solid loading (3 to 20 gms water per gm biomass) employed during those pretreatments

compared to conventional AFEX (0.6 gm water + 1 gm liquid ammonia per gm biomass) that allows better extraction efficiency for lignin and hemicellulose [54]. In order to better understand the mechanism of AFEX, two pretreatment conditions (protocol A-VII-4 (a)) were explored to study the role of liquid to solid loading on modification of corn stover cell wall morphology. Conditions employed were; (A) Conventional (or 'Regular') AFEX (R-ACS) at 1:1 ammonia to biomass loading (w/w), 0.6:1 water to biomass loading (w/w), 15 min residence time at 100 °C; and (B) High liquid to solid loading based AFEX (High-ACS) at 2:1 ammonia to biomass loading (w/w), 2:1 water to biomass loading (w/w), 15 min residence time at 100 °C.

A modification that is immediately visible to the naked eye after AFEX treatment is the change in color of the tissue from yellow to brown, possibly indicative of the exposed lignin based components that have oxidized upon exposure to air. The stem cross-sections shriveled up immediately after removal from the reactor during the volatization of ammonia from the cell walls. SEM (protocol A-VII-6) micrographs (**Figure 3.A.1**) revealed the various cell types within the corn stalk internode cross-section comprising of epidermal cells, vascular bundles, parenchyma cells and lignified sclerenchyma cells. The secondary wall thickened vascular bundle cells are the most recalcitrant cells to enzymatic hydrolysis and contribute nearly 70-80% of the mass (along with other rind tissue cells) of the stem internode [66]. Vascular bundles are comprised of xylem and phloem based cells that allow transport of water and nutrients along the length of the stem. The xylem is composed primarily of sclerenchyma derived xylem vessels and xylem tracheid fiber cells (containing thick secondary cell walls). Hence, it was necessary to closely study cell tissue belonging to this portion of the

internode. Interestingly, conventional AFEX at lower liquid to solid loading resulted in no observable major modifications of the various types of cell wall morphologies, at various scales of magnification (**Figure 3.A.1**, Image set I vs. II). However, High-ACS samples that employed a much higher liquid to solid loading during treatment resulted in significant observable modification of the cell wall morphology. The parenchyma cells were completely disrupted resulting in the collapse and aggregation of vascular bundles (**Figure 3.A.1**, III-A). The vascular bundle cells had collapsed significantly with cell wall extractives deposited on the outer cell walls and within the empty lumen space (**Figure 3.A.1**, III-C/D). The composition of these cell wall extractives was explored in detail in chapters 3.2 and 5.

To obtain a quantitative measure of the extent of modification of the cell wall morphology, the SEM micrographs were analyzed (protocol A-VII-6) to estimate the cell wall boundary perimeter length (L) and cell lumen enclosed area (A) for various types of cells (e.g. parenchyma cells, xylem vessels, phloem and fiber cells in the vascular bundle). More than 50 images were collected per sample type from distinct tissue sections and internode region. Of these images, a dozen images per sample type were imported into the image analysis software for quantitative measure of cell wall perimeter and area enclosed within the respective perimeter space (See raw data in **Table I-3.A.3**). A summary of the average cell wall perimeter length (L) and perimeter enclosed lumen area (A) for the various sample and cell types is given in **Table 3.A.1**. The cell wall perimeter (L) could not be estimated for High-ACS parenchyma cells since they had collapsed completely. In order to estimate the circularity of the geometrical cell wall shape a dimensional number known as the isoperimetric quotient ($Q = 4\pi A/L^2$) was

calculated for each datapoint. The isoperimetric quotient of a closed curve is defined as the ratio of the curve area to the area of a circle with the same perimeter as the curve.

Table 3.A.1 *Comparison of cell wall perimeter (L, μm), area enclosed within lumen space (A, μm^2) and isoperimetric quotient ($4\pi A/L^2$) for untreated, conventional AFEX (R-ACS) and high liquid to solid loading based AFEX (High-ACS) treated corn stover cell walls. Values with different alphabetical superscripts in an individual column were statistically different with $p < 0.05$ based on Student t-test.*

	Mean value			% Standard Deviation		
Sample ID	**L**	**A**	**4 A/L^2**	**L**	**A**	**4 A/L^2**
	Parenchyma cells					
Untreated	359 ^{a}	9468 ^{aa}	0.8859 ^{aaa}	22	44	5
R-ACS	256 ^{b}	5395 ^{bb}	0.8723 ^{aaa}	44	86	7
High-ACS	-	-	-	-	-	-
	Xylem vessels					
Untreated	241 ^{c}	4403 ^{cc}	0.9450 ^{ccc}	14	27	7
R-ACS	198 ^{d}	2957 ^{dd}	0.9275 ^{ccc}	17	35	3
High-ACS	112 ^{e}	976 ^{ee}	0.9253 ^{ccc}	22	43	4
	Vascular bundle cells					
Untreated	42 ^{f}	126 ^{ff}	0.8334 ^{fff}	33	62	11
R-ACS	37 ^{f}	103 ^{ff}	0.8633 ^{fff}	34	61	6
High-ACS	22 ^{g}	33 ^{gg}	0.7855 ^{ggg}	38	83	13

Figure 3.A.1 *SEM micrographs of untreated (I), conventional AFEX treated (II) and high liquid to solid loading based AFEX treated (III) corn stover at varying degrees of magnification (Scale bars shown at the bottom of each image).*

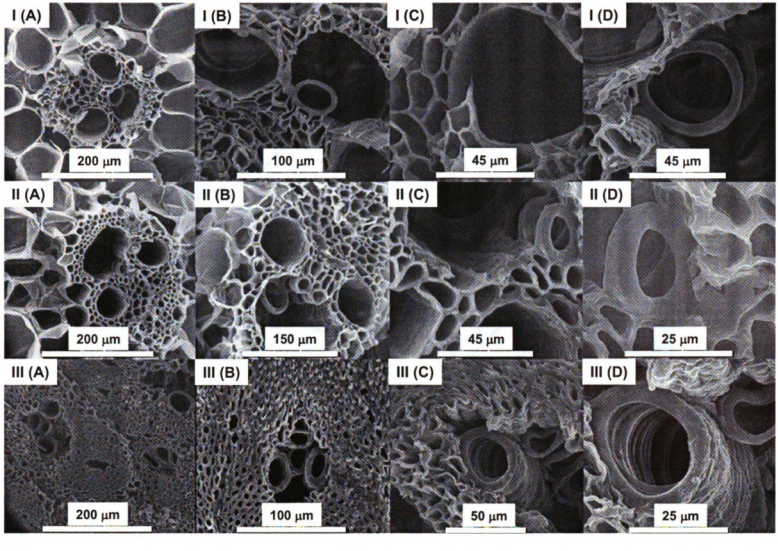

Figure 3.A.2 *LCSM maximum intensity projection images of untreated (A) and high liquid to solid loading based AFEX treated corn stover (B) vascular bundles stained with Safranin. Sample sections were excited with 543 nm and emission was detected through LP 560 nm emission filter (fluorescence intensity shown in green). Image (A) and (B) are projection images compiled from 20 and 15 optical sections representing a thickness of 122 and 90 μms, respectively. Plan-Neofluar 10X/0.3 objective was used to obtain the images.*

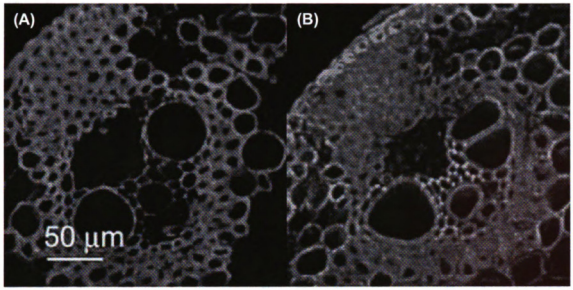

The upper limit of Q is 1 for a circle while it drops to 0.786 for a square. This dimensionless quantity (Q) helped quantify the circularity of the cell wall shape as function of cell type and pretreatment severity. Comparing L, A and Q for untreated and R-ACS parenchyma cell walls; there was significant (based on Student t-test, Degrees of freedom [DF] = 29 and $p < 0.05$) decrease in the cell wall perimeter (28% drop) and lumen area (43% drop) after conventional AFEX treatment. However, no significant change in the shape of the parenchyma cells was seen after R-ACS based on comparing the Q value to untreated stover. Comparing L, A and Q for untreated and R-ACS xylem vessels; there was significant (based on Student t-test, Degrees of freedom [DF] = 13 and $p < 0.05$) decrease in the cell wall perimeter (18% drop) and lumen area (33% drop) after conventional AFEX treatment. There was no significant change in the shape of the xylem vessels after conventional AFEX, based on the Q value. Comparing L, A and Q for untreated and High-ACS xylem vessels; there was significant (based on Student t-test, Degrees of freedom [DF] = 22 and $p < 0.05$) decrease in the cell wall perimeter (54% drop) and lumen area (78% drop) after high liquid to solid loading based AFEX treatment. There was also no significant change in the shape of the High-ACS xylem vessels compared to untreated vessels based on their Q value. Comparing L, A and Q for untreated and R-ACS vascular bundle cells; there was no significant (based on Student t-test, Degrees of freedom [DF] = 75 and $p < 0.05$) decrease in the cell wall perimeter, lumen area and shape of the cells after conventional AFEX treatment. However, upon comparing L, A and Q for untreated and High-ACS vascular bundle cells; there was a significant (based on Student t-test, Degrees of freedom [DF] = 158 and $p < 0.05$) decrease in the cell wall perimeter (48% drop), lumen area (74% drop) and shape of the

cells (6% drop in Q value) after high liquid to solid loading based AFEX treatment. It was interesting to find that R-ACS did not significantly modify the macroscopic morphology of the thickened secondary cell walls as compared to High-ACS. These results hint at certain microscopic based structural modifications that might have taken place within R-ACS treated cell walls that result in enhancing enzymatic digestibility (See Chapter 4).

The chemical composition of the cell wall extractives and their physical distribution for the High-ACS samples were studied using a ligno-phenolic selective stain (Safranin) and imaged using a laser confocal fluorescence microscope (LSCM; protocol A-VII-7). It is possible to get a more specific staining of lignin (using fluorescent O'Safranin) by using a narrow range band pass (BP) emission filter of 505-530 nm [244]. Safaranin is a cationic fluorochrome reported to stain lignin, phenolics, suberin and starch. The peak absorption and emission for Safranin has been reported to be around 530 and 590 nm, respectively [245,246]. Lignin auto fluorescence emission peaks at about 360 nm with excitation at wavelengths from 240-320 nm [247]. However, in order to avoid overlap of safranin fluorescence with lignin auto fluorescence an excitation filter of 543 nm and emission filter of 560 nm (long pass, LP) were used. No lignin auto fluorescence was seen using the 543 nm excitation filter. One of the striking differences between untreated and AFEX treated samples was the significant loss in safranin fluorescence intensity after AFEX (i.e. no perceivable difference in contrast of cell walls with respect to background), with exactly the same detector gain (Gain = 650 Volts). This suggested that lignin in AFEX treated biomass (R-ACS and High-ACS) was either delocalized from its original location and/or had been chemically modified to affect the

binding of the stain to it. In either case, it was found necessary to increase the detector gain by at least 20% (New Gain = 780 Volts) to image both the AFEX treated samples with sufficient contrast with respect to the background. There was no distinct difference in the images collected for untreated and R-ACS AFEX samples, corroborating what was seen though the SEM as well. However, for high-ACS samples, there were cell wall extractives rich in lignin-phenolics deposited within the lumen space (**Figure 3.A.2**). The deposit-like formations were noted in particular for the lignified cell walls in the vascular bundle as compared to the parenchyma cells (similar to what was seen SEM images, **Figure 3.A.1**). The wall shape was also significantly distorted for High-ACS samples as well. The LCSM imaging experiments validate the SEM findings comparing untreated and AFEX treated biomass (for both 60% and 200% moisture loadings). The resolution for confocal microscopy was limited due to difficulties in obtaining thinner sections of the sample for imaging. This prevented use of higher magnification objective oil-lens (63 X) that might have shown more interesting details for conventional AFEX treated samples. Since, it was possible to obtain higher magnification images using electron microscopy the LSCM approach was not further investigated. But there are several disadvantages associated with electron microscopy based techniques as well. Electron microscopy can be time consuming, laborious, subject to artifacts been observed due to sample preparation and sometimes fail to provide compositional dependent morphological differences.

At higher liquid to solid loadings (5:1 and greater), mass transfer regimes experienced during AFEX are similar to ammonia recycle percolation (ARP) and analogous alkali pulping processes that are effective in extracting lignin and

hemicellulose. It has been demonstrated that extraction of lignin from woody biomass by supercritical ammonia-water mixtures is diffusion limited, based on kinetic models of wood delignification [248]. However, from a commercial standpoint increasing the liquid to solid loading (through increased water usage) during AFEX would be commercially unviable due to the significant capital investment in suitable ammonia-water recovery systems [159,181]. Therefore, future work was focused on understanding the mechanism of conventional AFEX (at lower water to solid loadings).

3.1.4.2 Effect of biomass particle size on extraction of ligno-phenolics during AFEX

In order to better understand the mass transfer limitations on extraction of ligno-phenolic fragments from within cell walls to the outer wall surface, the effect of substrate particle size on the extraction efficiency of phenolics was studied.

Corn stover fractions were obtained upon laboratory blender milling (protocol A-VII-1 (b)) resulting in the following particle size ranges; a) Fraction 20-Mesh (> 850 microns), b) Fraction 35-Mesh (850-500 microns), c) Fraction 40-Mesh (500-425 microns), d) Fraction 70-Mesh (425-212 microns), e) Fraction 80-Mesh (212-180 microns), f) Fraction 100-Mesh (180-150 microns), and g) Fraction 120-Mesh (< 150 microns). The average particle size (5 replicates with variation under 1-2% from average) distribution of the milled material as compared to pre-milled (PM) corn stover is shown in **Figure I-3.A.5**. The PM stover has a more skewed particle size distribution tending towards the larger sizes. However, the particle size distribution for the milled stover fractions is approximately normally distributed centered about mid-range mesh cut (425-212 microns). Corn stover produces around 25-30% of leafy fraction (leaf-husk-sheaths) and 70-75% of fibrous and hard material (stalk and cobs), as shown in **Figure I-3.A.5**.

Compositional analysis (protocol A-VII-13) of corn stover fractions (**Table 3.A.2**) gives a good indication of the possible origin of each fraction.

Table 3.A.2 *Composition of various particle size fractions from pre-milled corn stover*

Components	Pre-milled	# 20 (> 850 μm)	# 35 (850-500 μm)	# 40 (500-425 μm)	# 70 (425-212 μm)	# 80 (212-180 μm)	# 100 (180-150 μm)	# 120 (<150 μm)
Glucan	32.6	33.5	34.4	34.4	34.0	34.0	33.3	32.3
Xylan	23.4	27.5	24.7	23.5	22.6	21.9	21.9	20.1
Galactan	1.4	1.0	1.3	1.3	1.4	1.5	1.7	1.8
Arabinan	2.7	2.4	2.7	2.5	2.6	2.7	2.9	2.9
Mannan	0.3	0.7	0.4	0.3	0.2	0.1	0.1	0.0
Lignin	12.3	12.5	12.4	12.6	12.6	12.9	12.8	12.0
Protein	3.1	1.8	2.0	2.3	2.7	2.9	3.3	4.3
Water Solubles	3.9	0.1	2.7	4.3	6.0	7.9	8.5	11.3
Alcohol Solubles	3.5	2.3	3.2	3.2	3.6	3.9	3.9	4.4

The larger particle size fractions have a higher xylan/mannan content and lower water soluble content compared to pre-milled (PM) corn stover. The finer fractions are richer in water-soluble components (i.e. proteins, soluble sugars) and have a lower hemicellulosic content. The larger fractions (# 20-80 mesh cuts) are more likely to be derived from the stem portion as compared to the finer fractions (# 100-120 mesh cuts) that are likely from the leaf, broken midrib and veins of the stover. However, the glucan and lignin content of all size fractions are largely similar (32-34% and 12-13%, respectively).

The various stover fractions were AFEX treated under identical conditions (1:1 ammonia to biomass loading w/w, 0.6:1 water to biomass loading w/w, 30 min total residence time, 90-100 Degrees °C) and extracted with distilled water based on protocol A-VII-19 (b) to remove surface bound extractives. The total phenolic content of the wash streams was quantified using suitable phenolic acid standards (protocol A-VII-24). The absorbance readings were highly reproducible due to better color stability compared to other colorimetric methods [249]. The AFEX water extracts have nearly 6-8 fold greater phenolic content than the corresponding untreated wash stream (**Figure 3.A.3-a**) for the various stover fractions. The washed ligno-phenolics are likely to be from AFEX surface deposits rather than within the cell wall ultra structure, given the short extraction time period (15 min) and mild extraction conditions (20-25 °C, 1 atm). The % phenolic acid equivalent extracted (per unit mass of substrate) from the smaller particle size based fractions was 50-100% higher than larger particle size based fractions. Particle size reduction augments extraction of ligno-phenolics and other cell wall extractives to the outer wall surfaces during AFEX. PM corn stover was AFEX treated and milled to 0.08

mm using a centrifugal mill. The ground material was water washed to obtain the UAG-1W (Uncut PM corn stover → AFEX → Ground to 0.08 mm → Single wash) wash stream. Another sample was prepared by milling the PM corn stover to 0.08 mm, followed by AFEX. The substrate was washed to obtain the GA-1W (Ground to 0.08 mm → AFEX → Single wash) wash stream. The amount of phenolics extracted in the GA-1W wash stream was found to be 30-35% higher than the UAG-1W wash stream (**Figure 3.A.3-b**). Untreated stover wash stream (UU-1W: Uncut corn stover → Untreated → Single Wash) contained 10-12 fold lesser phenolic content than AFEX treated stover wash streams (UAG-1W and GA-1W). Single step water extraction of AFEX treated substrates was found suitable to remove nearly 80-90% of the total water extractable phenolic content. The wash stream phenolic content for the triply washed substrate (UAG-3W: Uncut corn stover → AFEX → Ground to 0.08 mm → Washed three times) was 7-8 fold less than that of the unwashed substrate (UAG-1W and GA-1W). The enzymatic digestibility for the once or thrice washed substrates was found to be nearly identical (data not shown). Hence, all enzymatic hydrolysis experiments were carried out for once washed substrates. The modified Prussian blue method is a useful semi-quantitative estimate of the ligno-phenolic content of the AFEX extractives, as the method is unable to distinguish between condensed lignins and lower molecular weight phenolics. Also, since polyphenolics with varying degrees of hydroxylation patterns and degree of polymerization would react differently to the assay reagent, the results are only useful to get relative estimates of ligno-phenolic content in the water extracts. Coumaric/ferulic acid and their derivatives comprise nearly 4-6% (w/w) of corn bran cell walls [94]. A more quantitative estimate of the total p-coumaric and ferulic acid content

of the cell wall extractives were carried out in Chapter 5. In summary, biomass particle size affects the amount of ligno-phenolics extracted to outer cell wall surfaces during AFEX pretreatment. However, more detailed mass-transfer related research is necessary to elucidate the effect of substrate particle size on ammonia based pretreatment efficacy.

3.1.4.3 Inhibition of cellulolytic enzymes by AFEX extracted ligno-phenolics

Several investigators in the past have found cellulases being inhibited by lignin phenolics and other polyphenolic compounds [250-252]. It is reasonable to assume that ligno-phenolic fragments extracted from the cell wall during AFEX may inhibit cellulolytic enzymes digesting cell wall polysaccharides. Experiments were carried out to study the effect of AFEX degradation products on cellulase activity. PM corn stover was AFEX treated and milled to 0.08 mm using a centrifugal mill to prepare the GAA sample (GAA-Ground after AFEX). Another sample (GBA-Ground before AFEX) was prepared by milling the PM corn stover to 0.08 mm, followed by AFEX. The GAA and GBA samples were extracted with water to remove cell wall extractives released during AFEX. There was no significant difference in glucan hydrolysis yields for unwashed GBA and GAA samples (**Figure 3.A.4**). Enzymatic hydrolysis for all samples was carried out using 15 FPU Spezyme CP/gm glucan (supplemented with 64 p-NPGU Novozyme 188/gm glucan) in 15 ml vials for 72 hours (protocols A-VII-23, 28, 31). The unwashed GAA had slightly higher glucan conversion (1.5-2%) compared to unwashed GBA for 72 hour data. The difference in glucan hydrolytic yield was more pronounced (10-12%) at 24 hours (data not shown). The increase was found to be statistically significant ($p < 0.05$) only for 24 hour hydrolysis data.

Figure 3.A.3 *(a) Phenolic content of AFEX treated and untreated corn stover wash streams; Untreated stover % gallic acid (empty bars), Untreated stover % ferulic acid (dot filled bars), AFEX treated stover % gallic acid (horizontal line filled bars), and AFEX treated stover % ferulic acid (slanted line filled bars). (b) Ferulic acid content of wash stream after single wash (UU-1W: Uncut corn stover => Untreated => Single Wash and UAG-1W (Uncut PM corn stover => AFEX => Ground to 0.08 mm => Single wash), multiple wash (UAG-3W: Uncut corn stover => AFEX => Ground to 0.08 mm => Washed three times) and after size reduction (GA-1W: Ground to 0.08 mm => AFEX => Single wash). (Figure has been reproduced from [1]).*

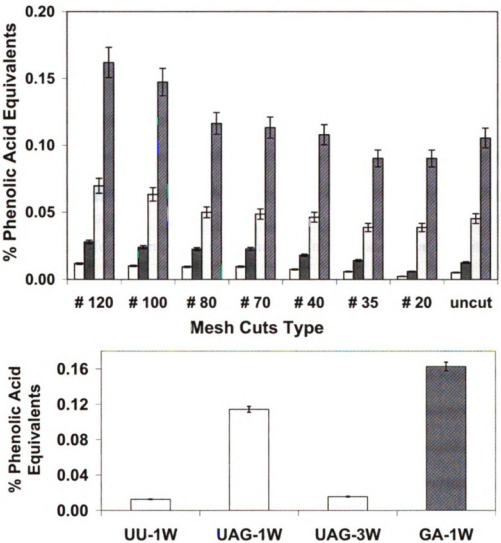

Figure 3.A.4 *Effect of size reduction and water washing of AFEX treated corn stover on 72 hour glucan (left bar, black) and xylan (right bar, grey) conversions. (Abbreviations: - U-GBA: Unwashed ground before AFEX, W-GBA: Washed ground before AFEX, U-GAA: Unwashed ground after AFEX, W-GAA: Washed ground after AFEX). The standard error bars are based on duplicates. (Figure has been reproduced from [1]).*

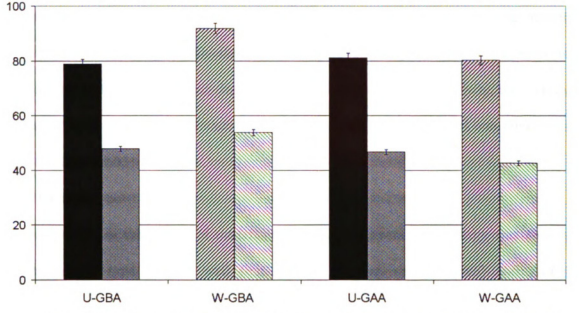

The difference in glucan conversion was more prominent at the initial hydrolysis stage, but became less significant at later stages possibly due to a two-pronged effect. Firstly, the amount of ligno-phenolics and other cell wall extractives removed from within the cell wall during AFEX were found to have a greater surface density for the unwashed GBA compared to the unwashed GAA (Figure 3.B.3; See section 3.2.4.2 for details). These AFEX extractives could play an important inhibitory role in the initial stages (24 hour data) of enzymatic hydrolysis that could explain the lower hydrolysis yield for unwashed GBA vs. GAA. Secondly, even though AFEX is probably more effective on GBA (due to reduced mass-transfer limitations for extraction of cell wall lignin and hemicellulose), the ligno-phenolic rich extractives inhibit enzymatic activity. However, extracting the GBA substrate with water (W-GBA) yielded a 10-15% increase in glucan conversion compared to the water extracted GAA substrate (W-GAA). The

enhancement in hydrolysis yield after water extraction is likely due to removal of enzyme inhibitory ligno-phenolic fragments, considering that there is a greater percentage of water extractives present within GBA based samples compared to GAA sample (**Figure 3.A.3-b**; See Chapter 3.2). However, there are several other water extractible degradation products formed during AFEX that could also inhibit enzyme activity. In order to elucidate the effect of each these degradation products on enzymatic activity, the identity of these AFEX based cell wall extractives must be established. This goal was pursued as a part of Chapter 5.

3.1.5 Conclusions

It was found that the extent of modification of the cell wall morphology was closely related to the type of cell wall (e.g. parenchyma vs. sclerenchyma) and AFEX pretreatment conditions (e.g. water and ammonia loading) employed. There were distinct amorphously shaped deposits (rich in ligno-phenolics) within the secondary cell wall lumen space along with considerable fiber disruption as indicated by the cell shape analysis (e.g. cell perimeter length, lumen area, isoperimetric quotient) for high-moisture/ammonia based AFEX cell walls. In contrast to what was expected, there was no major physical modification of secondary cell walls during conventional AFEX (low liquid to solid loading) as compared to high-moisture/ammonia based AFEX. However, despite the inability of conventional AFEX to extract lignin and hemicellulose from the cell wall, the rate of enzymatic digestibility of the treated cell walls was 4-5 fold higher than that of untreated walls. This would suggest that there are certain ultra-structural modifications (currently not visible through low magnification SEM and confocal microscopy) within conventional AFEX treated cell walls that enhance the accessibility

of the wall polysaccharides to cellulolytic enzymes. It would be of interest to explore the external cell wall surfaces after conventional AFEX using higher magnification microscopic and spectroscopic techniques to better understand the physical and chemical changes caused by conventional AFEX pretreatment that results in reduced recalcitrance of cell walls to cellulolytic enzymes.

3.2 Cell wall surface topography and atomic composition after conventional AFEX

3.2.1 Abstract[iv]

The surface chemistry and topography of untreated and conventional AFEX (R-ACS) treated corn stover (for varying cell wall particle sizes) was investigated by electron spectroscopy for chemical analysis (ESCA) and atomic force microscopy (AFM). As visualized through AFM amplitude and phase based images, the outer cell wall surfaces were found to be heterogeneously covered with amorphously shaped deposits (20-1000 nm in size) after conventional AFEX pretreatment (1:1 ammonia to biomass loading w/w, 0.6:1 water to biomass loading w/w, 30 min total residence time, 90-100 °C). These nanoscopic deposits were previously not seen through low-magnification based scanning electron and confocal fluorescence microscopy. There was a 5-30% decrease in Oxygen/Carbon (O/C) surface atomic ratio for AFEX treated corn stover fractions as compared to untreated controls. ESCA also revealed the composition of these surface deposits to be rich in lignin (1-10% increase in C1 carbon after AFEX), middle lamella based extractives (calcium surface content was 0-0.2% for untreated vs. 0.2-0.6% for AFEX corn stover) and other pretreatment based degradation products (10-65% increase in surface nitrogen content after AFEX). Hot water extraction was able to remove some of these surface deposits (based on relative change in O/C ratio after extraction). Some of these amorphously shaped surface extractives deposited on the outer wall surfaces after AFEX are thought to originate from the middle lamella. This is due to the enrichment in calcium content of wall surfaces after AFEX pretreatment, which is otherwise typically

---

[iv] A version of this chapter was published as Chundawat S.P.S, Balan V., Dale B.E. 2006. *Effect of particle size based separation of milled corn stover on AFEX pretreatment and enzymatic digestibility*. Biotechnology and Bioengineering 96(2):219-231.

found cross-linked with pectin in the compound middle lamella region of untreated cell walls. Cell wall particle size reduction prior to AFEX treatment resulted in an increased surface density of these extractives, as indicated by the greater % decrease in O/C ratio compared to un-ground substrates. This would also indicate that extraction of lignin and other wall components during conventional low liquid to solid loading based AFEX is mass transfer limited.

3.2.2 Background

3.2.2.1 Surface compositional analysis by X-ray photoelectron spectroscopy

Electron spectroscopy for chemical analysis (ESCA) or X-ray photoelectron spectroscopy (XPS) has been used in the past to analyze the surface chemical composition of wood pulp and fibers, with little focus towards agricultural residues like corn stover [253-255]. ESCA provides a true surface elemental analysis up to depths of about 20 nm, along with information about the type of chemical bonding. The chemical shifts for the carbon peak (C1s) can be deconvoluted into subpeaks providing useful quantitative information about the relative amount of each type of carbon bond and Oxygen to Carbon (O/C) ratios for the surface [255]. Based on the carbon content, the various cell wall components can be listed in a decreasing order of their theoretical O/C ratios: Cellulose (0.83) > Hemicellulose (0.8-0.82) > Lignin (0.32-0.33). It becomes apparent that it would be possible to monitor the lignin/extractive vs. carbohydrate content exclusively on the surface of AFEX pretreated biomass through relevant ESCA analysis.

3.2.2.2 Surface topographical analysis by atomic force microscopy

Atomic force microscopy (AFM) has proven to be a valuable tool for visualizing the surface of plant cell walls [55,256], with particular emphasis on cellulose fibers, woody

biomass and paper pulps [213, 236, 237]. In recent years, AFM has been used to probe the surface of plant cell walls (from corn and wheat stalks) pretreated by dilute acid and steam explosion [40,111]. Acid pretreated cell walls were found to be uniformly covered with globular shaped deposits (20-100 nm) that were essentially rich in lignin [112]. The extent of coverage of outer wall surfaces was dependent on the severity of acid pretreatment. Lignin rich globules were found to significantly inhibit cellulase activity, possibly through reducing enzyme accessibility [40]. Researchers working with woody biomass in the pulping industry have also confirmed the deposition of fiber surfaces with lignin and other cell wall extractives during the pulping process [255,257].

Characterizing pretreated biomass surface morphological (AFM) and chemical (ESCA) changes during pretreatment would yield a better insight into understanding the complex mechanism through which conventional AFEX based pretreatments (at lower liquid to solid loadings; R-ACS) helps enhance enzymatic accessibility to wall polysaccharides.

3.2.3 Materials and Methods

See appendix A-VII-1, 4, 8, 14, 19 (a) and 24.

3.2.4 Results and Discussion

3.2.4.1 Outer cell wall topology visualized by AFM

As discussed in the previous chapter (3.1), there was no significant visible modification of the plant cell walls after R-ACS (1:1 ammonia to biomass loading w/w, 0.6:1 water to biomass loading w/w, 30 min total residence time, 90-100 °C) treatment as compared to High-ACS (2:1 ammonia to biomass loading w/w, 2:1 water to biomass loading w/w, 30 min total residence time, 90-100 °C). It was thought that samples that were pretreated

under mass transfer limited AFEX conditions (R-ACS), would have cell wall extractives deposited as finer deposits (less than 1 μm in width and under 100-500 nm in thickness) on the outer cell walls. AFM amplitude and phase images (carried out in air through tapping mode) were captured simultaneously for outer cell wall regions of secondary wall thickened cells in the vascular bundles, since these were the most recalcitrant to enzymatic hydrolysis and contributed the largest mass fraction to the stem internode [66]. The AFM probe interacts with the sample surface through attractive or repulsive forces giving a three-dimensional 'chemical-map' that is dependent on the surface molecular topology and elasticity. Representative amplitude images for untreated (not air-dried prior to imaging) and conventional (or 'regular') AFEX (R-ACS, 24 hours air-dried after AFEX prior to imaging) treated corn stover cell walls, from a collection of over 50 images per sample, for varying scales of magnification are shown in **Figure 3.B.1**.

Untreated corn stover outer cell walls typically appear to be 'clean', with a fibrous network of cellulose macrofibrils visible at higher magnifications. There appears to be membrane debris, cytoplasmic residue and other cell wall remnants that were found on the outer wall surface (**Figure 3.B.1-a**; **Figure I-3.B.2**: U1, U4, U5). For some untreated cell wall surfaces there were depressions, crevices and cracks that formed part of the natural cell wall landscape (**Figure I-3.B.2**: U8, U9, U10). The cellulosic macrofibrils were clearly visible for some untreated cell walls at higher magnifications, while in others they were completely embedded in the wall matrix.

The cellulose macrofibrils ranged from 25-40 nm in thickness (depending on whether or not the samples were air-dried prior to AFM imaging), slightly larger than what has been reported for cellulose fibrils typically seen in straw based parenchyma and

epidermal based cell walls (ranging between 15-25 nm) [55,258]. The thickness of the cellulose microfibrils was closer to what has been reported for secondary cell wall thickened based cellulose fibrils (15-30 nm) [259]. The cellulose microfibrils for samples that were never air-dried prior to imaging were 42 $\pm$ 3.4 nm in thickness, while samples that were air-dried for 24 hours prior to imaging had microfibrils that were 23 $\pm$ 3.1 nm in thickness (Total number of observations = 10). Ding et al. and other researchers have reported that drying and extensive sample preparation (i.e. extraction of residual hemicellulose by alkali and other solvents or embedding/sectioning) results in modification of the morphology of cellulose microfibrils [55,238,259].

All pretreated samples were air-dried prior to imaging to remove residual ammonia from the cell walls. Roughness factor calculations were carried out for air-dried untreated and pretreated corn stover samples (**Figure I-3.B.2**). The outer cell wall surface topography and chemical composition changes significantly after conventional AFEX pretreatment, as seen through the AFM amplitude and phase images, respectively. **Figure 3.B.1-b** clearly indicates the appearance of amorphously shaped deposits (ranging in width from 20-1000 nm) that appear on the surface of outer cell walls after AFEX. These deposits seem to cover the surface non-uniformly and have no distinct shape, unlike the spherically shaped lignin rich deposits seen on fiber surfaces after acidic pretreatments [40]. AFM topography and phase images generally revealed complementary information for untreated cell walls (**Figure I-3.B.2: U1-U10**), the significance of which is explained in subsequent sections.

Figure 3.B.1 *AFM amplitude images of untreated (A, top row) and conventional AFEX treated (B, bottom row) corn stover at varying degrees of magnification (All scale bars represent a length scale = 500 nm). Color legend (dark to light shades) depicts the amplitude current scale (V, volts).*

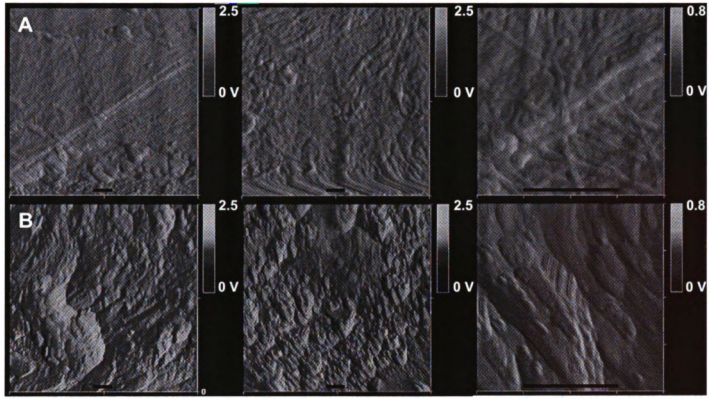

The AFM tip (silicon based) adheres more strongly to hydrophilic areas that should appear lighter in color (greater change in phase). Since all AFM imaging was performed under tapping-mode (in order to minimize sample deformation due to tip-sample friction), the phase contrast was probably due to the differences in hydrophobicity of the surface due to presence of cell wall extractives. The untreated corn stover surface was found to predominantly hydrophobic (indicated by darker phase images), however, there were hydrophilic patches (light colored) that stood out for several untreated cell wall phase images. However, this was not the case for AFEX treated cell walls where a distinct phase contrast was visible (**Figure I-3.B.2: A1-A10**).

Most of the AFEX treated cell wall phase images had several lighter patches that corresponded to hydrophilic rich regions. The morphological patterns of the phase and amplitude images matched well, indicating the deposits extracted to the surface during AFEX are *largely* hydrophilic (however, analysis by ESCA and Prussian blue also revealed presence of lignin derived components). In order to obtain a more quantitative estimate of the extent of surface modification after AFEX, surface roughness factors (RMS: root mean square based) were calculated for at least 10 images of untreated and R-ACS treated amplitude images, respectively (**Figure I-3.B.2**). The RMS surface roughness factor is a quantity typically used to assess the average variation in topography of the surface with respect to the mean height across the entire x-y coordinates of the image. The RMS roughness factor (units, nm) was found nearly 2-fold greater for AFEX treated wall surfaces compared to untreated samples (**Table 3.B.1**).

Table 3.B.1 *RMS (root mean square) roughness factors for untreated (U1-U10) and conventional AFEX (R-ACS; A1-A10) treated corn stover AFM amplitude images.*

Image ID	Untreated (U)	Image ID	AFEX treated (A)
U1	7.76	A1	38.65
U2	9.03	A2	25.25
U3	21.69	A3	33.78
U4	25.43	A4	37.52
U5	13.16	A5	11.10
U6	8.20	A6	26.88
U7	28.38	A7	27.11
U8	32.63	A8	19.36
U9	9.32	A9	33.51
U10	9.92	A10	41.88
Average	16.55	Average	29.50
% CV	57.50	% CV	32.11

The average AFM image height range for the untreated cell wall image dataset (217 $\pm$ 135 nm) was nearly half of the average height range for AFEX treated cell walls (458 $\pm$ 183 nm). Interestingly, in none of the images collected after AFEX were any cellulosic fibrils visible, indicating that most of the external wall surfaces had been covered with AFEX extractives, similar to what has been reported for acidic based pretreatments [111,112]. However, unlike the smooth, globular deposits seen after acidic pretreatments that are essentially composed of only lignin (highly hydrophobic), the amorphously shaped deposits seen after AFEX seem to be composed of lesser hydrophobic components.

3.2.4.2 Outer cell wall elemental composition characterized by ESCA

In order to gain a clearer understanding of the chemical composition of the surface deposits seen on the outer cell wall surfaces after AFEX, the samples were characterized

by ESCA. All ESCA spectra were typically collected at an optimal take-off-angle (TOA) of 45°. However, some measurements were also conducted at 15° and 75° to determine thickness of the cell wall surface extractives deposited after conventional AFEX pretreatment. The important elemental peaks obtained during analysis of all plant biomass samples were found to be carbon (C, 1s orbital), oxygen (O, 1s orbital), nitrogen (N, 1s orbital) and calcium (Ca, 2p orbital). The four carbon peaks typically obtained upon deconvoluting the ESCA carbon spectra belong to the following carbon bond classes; (i) C1 type carbon that corresponds to carbon atoms bonded to carbon or hydrogen (C-C), (ii) C2 type carbon that corresponds to carbon atoms bonded to single non-carbonyl oxygen (C-O), (iii) C3 type carbon that corresponds to carbon atoms bonded to a carbonyl or two non-carbonyls (C=O or O-C-O), and (iv) C4 type carbon that corresponds to carbon atoms bonded to a carbonyl and a non-carbonyl oxygen (O-C=O). The carbon (C1s) signal can be deconvoluted (within $\pm$ 0.3 eV) into C1 (284.7 eV), C2 (286.4 eV), C3 (288.1 eV) and C4 (289.8 eV) signals. Deconvoluting the carbon peak helps better understand the chemical structure of the extractives deposited on the biomass surface after AFEX. Cellulose contributes close to 85% of its signal to the C2 peak while lignin contributes 50% of its signal to C1 and the remaining signal to C2. Extractives contribute most of their signal to C1. Theoretical O/C values for various cell wall constituents such as cellulose, hemicellulose, lignin and other alkali extractives can be calculated based on their empirical carbon-oxygen formula. Based on the alkyl carbon content of these components, one can place these cell wall components in a decreasing order of their O/C ratios: Cellulose > Hemicellulose > Lignin > Extractives (i.e. Fatty acids, Hydrocarbons).

The effect of substrate particle size on the extraction efficiency of cell wall extractives during conventional AFEX (R-ACS) was studied using corn stover fractions, as described in Chapter 3.1. Another reason, to fractionate the biomass based on particle size, is to reduce the heterogeneity in the angular orientation of various surfaces with respect to the sample cup horizontal axis. This heterogeneity or surface roughness tends to increase the grazing angle of electron escape, but should not significantly affect the relative contributions of each component (i.e. O/C should remain unaffected) [253]. Some samples were also milled before or after AFEX pretreatment to study the effect of particle size on cell wall extractives removal during AFEX to help validate previous findings (Chapter 3.1). The atomic compositions of various corn stover fractions before and after R-ACS pretreatment are shown in **Table 3.B.2-a**. The relative increase in C1s (and its deconvoluted component peaks), O1s, N1s, Ca2p and O/C ratios are shown in **Table 3.B.2-b**. The heterogeneity of the cell wall surfaces is more clearly visible in the AFM images as compared to the ESCA measurements (which is an average representation of sample surfaces within an area of 0.25 mm x 0.25 mm). There is a consistent increase (1-28% increase) in the C1 signal on the fiber surfaces upon AFEX treatment for all fractions, along with a concomitant decrease in the C2 signal (2-40% decrease). This increase in C1/C2 ratio corresponds to the enrichment of the fiber surface with extractives rich in alkyl based carbon linkages (typically lignin, acid moieties, hydrocarbons) and/or a corresponding decrease in compounds rich in carbon-oxygen based linkages (like cellulose). There is also a consistent increase in the calcium (not detected typically for untreated samples but increased to 0.2-0.4% of total atomic surface content after AFEX) and nitrogen content (1-50% increase) on the biomass surface after

the AFEX. Calcium is thought to bind the pectin rich polysaccharides due to charged interaction with acidic side chains, typically found in the compound middle lamella [71]. The structural proteins in the cell wall (e.g. proline rich glycoproteins), functional protein (e.g. Rubisco) in leaves and other nitrogen-rich extractives contribute to the strong nitrogen atomic signal seen for untreated samples. The enhanced nitrogen signal after AFEX would be largely due to nitrogenous ammonolysis products formed during ammonia based treatments [162]. These two components might be relocated to the surface of the biomass after cleavage of the lignin carbohydrate complex (LCC) during AFEX, hence resulting in an increase in the calcium and nitrogen signals. The compound middle lamella (CML) might be partly solubilized during AFEX (and re-deposited on the outer wall surface) due to high solubility of middle lamella components in alkaline solutions [260]. The CML has been shown to be partly extracted during woody biomass delignification [261]. Further analysis of the deposited extractives and higher resolution transmission electron microscopic imaging of the collapsed middle lamella within the cell wall would add further credence to this hypothesis.

O/C atomic ratio (**Table 3.B.2-b**) is a useful indicator of the relative composition of oxygen rich versus carbon rich species present on fiber surfaces. Theoretical O/C ratios for some biomass components (e.g. cellulose = 0.83, hemicellulose = 0.82-0.8) are shown in the table. A higher O/C ratio is obtained for samples abundant in polysaccharides (e.g. Avicel O/C = 0.61), while a lower O/C ratio is noticeable for samples abundant in lignin (e.g. Kraft lignin = 0.32). After AFEX, there is a 5-30% decrease in the O/C ratio (with respect to untreated controls) indicative of deposition of carbon rich molecules on the biomass surface.

Table 3.B.2 *ESCA based atomic composition of untreated (UT) and conventional AFEX treated (AT) corn stover fractions and some model compounds (Table has been partly reproduced from [1]). NA stands for 'not available'.*

(A)

	Untreated					
Sample Notation	**% C1**	**% C2**	**% C3**	**% O**	**% N**	**% Ca**
Unground CS	77.25	17.7	5.05	17.86	1.64	n.d
Fraction # 20	68.99	24.32	6.8	19.94	2.01	n.d
Fraction # 35	71.54	22.09	6.36	19.72	1.68	n.d
Fraction # 40	73.34	21	5.66	17.66	1.49	n.d
Fraction # 70	73.81	19.86	6.32	18.49	2	n.d
Fraction # 80	68.33	24.33	7.34	20.31	2.21	n.d
Fraction # 100	71.28	21.91	6.81	19.24	2.14	n.d
Fraction # 120	65.43	26.27	8.3	21.14	2.26	n.d
Milled before AFEX	56.71	34.79	8.5	26.79	1.81	n.d
Milled after AFEX	-	-	-	-	-	-
Cellulose (Theoretical)	0	83	17	45	0	0
Avicel	27.29	59.97	12.7	37.7	0	0
Xylan	5	67	24	NA	NA	NA
Kraft Lignin	52	38	7	NA	NA	NA
	AFEX treated					
Sample Notation	**% C1**	**% C2**	**% C3**	**% O**	**% N**	**% Ca**
Unground CS	77.21	17.06	5.74	16.3	2.14	0.33
Fraction # 20	72.16	21.57	6.27	17.3	2.61	0.59
Fraction # 35	73.36	20.63	6.01	17.76	2.09	0.54
Fraction # 40	75.81	18.66	5.53	17.81	1.86	0.37
Fraction # 70	74.88	19.37	5.66	17.83	2.08	0.38
Fraction # 80	72.05	21.35	6.6	18.13	2.06	0.37
Fraction # 100	72.29	20.98	6.73	18.71	2.3	n.d
Fraction # 120	69.76	23.95	6.29	19.74	2.81	n.d
Milled before AFEX	72.5	21	6.5	20.13	1.82	0.41
Milled after AFEX	57.72	33.98	8.3	25.61	2.66	0.24
Cellulose (Theoretical)	-	-	-	-	-	-
Avicel	-	-	-	-	-	-
Xylan	-	-	-	-	-	-
Kraft Lignin	-	-	-	-	-	-

Table 3.B.2 *Contd...*

(B)

Sample Notation	Particle size (µms)	% increase after AFEX C1	C2	C3	O	N	Ca	O/C UT* (AT)	Reference
Unground CS	> 850	0	-4	14	-9	30	+	0.23* (0.20)	This study
Fraction # 20	> 850	5	-11	-8	-13	30	+	0.26* (0.22)	This study
Fraction # 35	850-500	3	-7	-6	-10	24	+	0.25* (0.22)	This study
Fraction # 40	500-425	3	-11	-2	1	25	+	0.22* (0.22)	This study
Fraction # 70	425-212	1	-2	-10	-4	4	+	0.23* (0.23)	This study
Fraction # 80	212-180	5	-12	-10	-11	-7	+	0.27* (0.23)	This study
Fraction # 100	180-150	1	-4	-1	-3	7	n.d	0.25* (0.24)	This study
Fraction # 120	<150	7	-9	-24	-7	24	n.d	0.28* (0.26)	This study
Milled before AFEX	<80	28	-40	-24	-25	1	+	0.38* (0.25)	This study
Milled after AFEX	<80	2	-2	-2	-4	47	+	(0.35)	This study
Cellulose (Theoretical)	<150	-	-	-	-	-	-	0.83*	Mjoberg (1981)
Avicel	<100	-	-	-	-	-	-	0.61*	This study
Xylan	<150	-	-	-	-	-	-	0.83*	Laine et al. (1994)
Kraft Lignin	<150	-	-	-	-	-	-	0.32*	Laine et al. (1994)

Experiments were conducted to determine the effect of cell wall size reduction before and after AFEX pretreatment on O/C ratio as compared to unground corn stover. There was a noticeably larger decrease of nearly 30% in the O/C ratio for corn stover samples that were finely ground (< 80 microns) prior to AFEX treatment ('Milled before AFEX') as compared to samples that were ground after AFEX treatment ('Milled after AFEX' samples gave only 8% decrease in O/C ratio with respect to untreated control) (**Table 3.B.2-b**). For both cases, the control sample was milled untreated corn stover that under took a similar size reduction step (< 80 microns). The extent of reduction in the O/C ratio correlates well to the water extractible phenolic content (estimated via modified Prussian blue method) for substrates that were AFEX treated after size reduction (GA-1W: Ground to 0.08 mm => AFEX => Single wash) as compared to substrates that were milled after AFEX treatment (UAW-1W: Uncut corn stover => AFEX => Ground to 0.08 mm => Single wash) (See **Figure 3.A.3, Chapter 3.1** for more details). There was an inverse correlation between the substrate O/C ratio and the total water extractible phenolic content (**Figure 3.B.3**). This would suggest that the ligno-phenolic components deposited on the outer cell wall surfaces after AFEX are likely responsible for reduction in O/C atomic ratio. The relatively larger reduction in the O/C ratio for samples AFEX pretreated after size reduction compared to unmilled samples reiterates the mass transfer limitations typically encountered during conventional AFEX (R-ACS) for efficient extraction of cell wall components (like lignin and hemicellulose).

Certain studies were conducted to elucidate the effect of simple hot water and organic solvent based extractions (using 0.1 N NaOH, 95% ethanol followed by water washing till neutral pH, See methods section for details) on the O/C ratio (**Table 3.B.3**).

The substrate was milled using a centrifugal mill (<150 μm) prior to conventional AFEX (R-ACS). There is 16% decrease in the O/C ratio after AFEX. Washing the samples with water resulted in a 10% decrease in O/C (compared to untreated stover) indicative that some of the surface deposits can be removed by extraction with water (i.e. extractives contain hydrophilic and hydrophobic components). Solvent extraction with a strong alkali, like NaOH, followed by washing with ethanol and water helped remove most of the surface extractives (along with other wall components like lignin and hemicellulose) indicated by the significantly higher O/C ratio. Interestingly, the O/C based trends are also seen by comparing the ratio of C1/C2. Some researchers have suggested C1/C2 to be a better indicator of lignin extractives on the surface compared to O/C, due to larger scatter in O/C values due to water adsorption on sample surface [257]. A similar trend is seen for C1/C2 for all corn stover fractions before and after AFEX pretreatment, comparable to information obtained from O/C ratios (data not shown).

The effect of take-off-angle (TOA) on ESCA spectra obtained was studied to get an estimated thickness of the surface deposits after AFEX. ESCA typically allows one to analyze the elemental composition of very thin surface layers (5-10 nm thickness), however, the actual sampling depth depends on the angle of emission (i.e. α: angle between sample cup and analyzer). The sampling depth is typically reduced by a factor of Sin (α), therefore, maximum analysis depth is achieved at $\alpha = \pi/2$ radians [255]. If the surface deposit layer is greater than 10 nm in thickness then there should be no effect of the emission angle on the ESCA spectral counts for each element. Interestingly, there was no significant effect found on the elemental composition and O/C ratios for both untreated and AFEX treated samples by varying angle of emission between 15-75°.

Figure 3.B.3 *Effect of size reduction before and after AFEX pretreatment on oxygen to carbon (O/C, bars-left axis) surface atomic composition versus % phenolic acid equivalent water extractibles (line-right axis). Where; GCS: Ground corn stover (untreated), GCS-AFEX: Ground before AFEX, and AFEX-GCS: Ground after AFEX.*

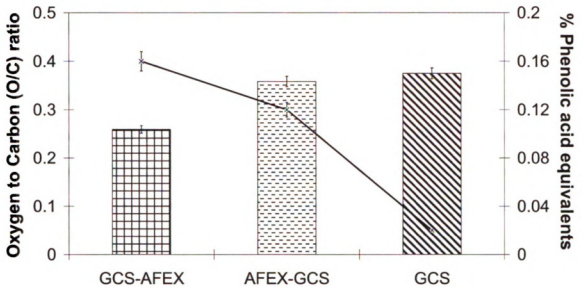

Table 3.B.3 *Effect of water and solvent extraction (using NaOH, ethanol and water) on AFEX treated corn stover (ACS) surface atomic composition as compared to untreated corn stover (CS). All experiments were conducted in quadruplicates.*

	Mean value			% CV			
Sample Notation	**% C**	**% O**	**% N**	**% C**	**% O**	**% N**	**O/C**
Untreated CS	71.3	26.6	1.7	1.0	2.7	9.3	0.37
AFEX CS	74.1	22.7	2.8	1.4	1.3	13.8	0.31
Water extracted ACS	73.4	24.1	1.7	0.6	1.0	12.2	0.33
Solvent extracted ACS	65.8	32.1	1.0	2.6	5.0	3.5	0.49
Sample Notation	**% C1**	**% C2**	**% C3**	**% C1**	**% C2**	**% C3**	**C1/C2**
Untreated CS	56.3	34.1	9.6	2.7	3.7	2.5	1.7
AFEX CS	64.5	28.3	7.1	6.7	13.1	8.3	2.3
Water extracted ACS	62.6	29.5	7.9	6.0	9.8	11.9	2.1
Solvent extracted ACS	43.2	45.0	11.7	12.3	10.2	9.0	1.0

This suggests that the layer of AFEX surface deposits are thicker than 10 nm in thickness, which also reiterates the AFM findings where the RMS roughness factor (corresponding to the modification of the surface topography due to presence of amorphously shaped deposits after AFEX) was found to be at least 2 fold larger after AFEX compared to the untreated material.

Conclusions

Combination of high-resolution AFM imaging with surface specific (5-10 nm) chemical characterization by ESCA gave valuable information regarding the mechanism of conventional AFEX (R-ACS). It was found that the external cell wall surfaces were covered with amorphously shaped deposits (20-1000 nm in size) after conventional AFEX pretreatment that had a distinct chemical composition (by phase imaging) and topography (by amplitude imaging) compared to the untreated controls. These deposits result in a two-fold increase in the root-mean-square surface roughness factor after AFEX with surface thickness ranging between 10-200 nm (based on ESCA TOA analysis and AFM height images comparing untreated to AFEX treated wall surfaces). ESCA revealed that these surface deposits were essentially composed of lignin phenolics and other cell wall extractives (some possibly extracted from the compound middle lamella region based on increased calcium surface content after AFEX). The oxygen to carbon ratio (O/C) decreased by 5-30% after AFEX, the extent of decrease was typically dependent on the particle size of the biomass substrate. The extent of decrease in O/C was inversely correlated to the ligno-phenolic content of the water extractives (based on modified Prussian blue analysis). However, water extraction only removed some of these surface deposits indicating that the surface extractives are composed of both hydrophilic and

hydrophobic components, unlike what is seen after dilute-acid based pretreatments (hydrophobic lignin rich globular deposits). It would be of interest to explore the internal cell wall region after conventional AFEX treatment using other microscopic (e.g. TEM) and spectroscopic (e.g. Raman, FT-IR) tools to help characterize the physico-chemical modifications within the cell wall that give rise to these chemically heterogenous, amorphously shaped surface deposits.

CHAPTER 4: ULTRASTRUCTURAL MODIFICATIONS WITHIN AMMONIA TREATED CELL WALLS AND CRYSTALLINE CELLULOSE

4.1 Formation of pores and delamination zones within ammonia treated cell walls through delocalization of hemicellulose and lignin

4.1.1 Abstract

The internal cell wall ultra-structure of untreated and AFEX treated corn stover (for five varying pretreatment severities) was investigated by transmission electron microscopy (TEM), dual-axis electron tomography (3D-Tomo) and immuno-electron microscopy. Three distinct ultrastructural changes take place during AFEX that were dependent on the severity of the pretreatment; (a) formation of large pores within an intact compound middle lamella (CML), (b) formation of pores within outer secondary wall layers (S3 region), and (c) delamination due to removal of lignin and hemicellulose within secondary cell walls. For conventional AFEX (R-ACS) cell walls there were amorphously shaped deposits found on the outer cell wall surfaces that were rich in hemicellulose (based on arabinoxylan immunolabeling). The extent of removal of lignin and hemicellulose was significant during low moisture ammonia treatment, resulting in extensive delamination and lignin coalescence in the outer wall regions. At higher ammonia loadings (and longer residence times) there were large pores formed in the outer S3 wall layer. Cellulose rich fibril bundles on the wall surface were exposed towards the lumen during high ammonia loading severity based AFEX. At lower pretreatment severities (low ammonia loading) the overall porosity (surface area to volume ratio, nm^{-1} or m^2/gm assuming density = 1) within the cell wall was 5-10 fold lower than at higher severities (higher ammonia/residence time or lower moisture

loading). There was a linear relationship (R^2 = 0.91) between the rate of enzymatic hydrolysis and log (porosity) for AFEX cell walls treated under different severities, indicating the importance of porosity on enzyme accessibility.

4.1.2 Background

4.1.2.1 Cross-linking matrix in cell walls of monocots and dicots are different

There has been extensive work conducted on dicots (typically woody biomass) to study the ultrastructural architecture of type I cell walls (cross-linking matrix rich in pectins and xyloglucans) using high resolution electron microscopy based techniques [62,71,237,260,262]. However, type II cell walls of commelinoid monocots (like corn stover) that have a cross-linking matrix of glucuronoarabinoxylans (GAX) and polyphenolics, are relatively poorly understood [65,262,263]. In dicots, extraction of xyloglucans and pectins (using sodium carbonate or potassium hydroxide) is typically responsible for enhancing the porosity (from <5-10 to 30-40 nm) of primary cell walls [260]. However, extensive extraction of xyloglucans results in aggregation of cellulose microfibrils with significant reduction in porosity. On the other hand, type II cell walls interstitial matrices are composed of highly branched GAX's cross-linked by phenolic residues; while unsubstituted GAX, β-glucans and glucomannans form the cellulose fibril coatings [262]. *However, the effect of liquid ammonia on type II cell walls has never before been studied.*

4.1.2.2 Effect of thermochemical treatment on modification of cell wall architecture

Recent studies on acid-treated corn stover using high resolution TEM and 3D-tomography have allowed visualization of lignin removal and delocalization within the cell wall after pretreatment [112]. The lignin seems to coalesce upon hydrolysis of

hemicellulose followed by delocalization as droplets (20-10,000 nm in size) to the outer cell wall regions, cell pits and corners. Confocal fluorescence studies have allowed visualization of hemicellulose removal and re-distribution during acid treatment of corn stover [264]. These studies reveal a dramatic loss in xylan antibody signal (due to hydrolysis and solubilization of hemicellulose to xylose and xylooligomers extracted in the liquid stream) from within the cell wall and a significant increase in xylan content on the outer wall regions possibly due to deposition of high DP xylo-oligomers and hemicellulose associated to lignin. However, unlike AFEX, dilute-acid treatments are typically conducted at higher temperatures (140-170 °C), higher liquid to solids loading (5-20 to 1, w/w) in an aqueous-acidic environment that allows near complete hydrolysis of hemicellulose to soluble monomers. Extensive hydrolysis of hemicellulose allows coalescence of lignin into hydrophobic globules (throughout the cell wall) that are extruded out of the wall significantly improving access to the embedded cellulose microfibrils. However, in an anhydrous liquid ammonia or concentrated ammonium hydroxide environment the extent of modification of the different regions of the cell wall would be very different from acid treatment. Preliminary TEM imaging work on ammonium hydroxide treated aspen wood has revealed kinking, curling and twisting of the wall due to plasticization of wood [236]. There was also partial lamellar fiber separation seen within the middle lamella and outer layers of the secondary cell wall, however, this idea was not explored in detail due to lack of high resolution images.

4.1.2.3 Cell wall porosity and electron tomography

Cell wall pore size distribution has been shown in the past to be a fundamental factor affecting enzyme accessibility and rate of hydrolysis [265,266]. Varying pretreatment

severities are believed to produce substrates of varying digestibility possibly due to varying porosities [22]. Pore volume (based on fiber saturation point) of supercritical ammonia treated woody biomass were found to be 30-60% higher than their untreated counterparts, with no significant change in maximum pore width [162,267,268]. *However, the effect of AFEX on grass cell wall pore volume and pore size distribution as a function of location within the cell wall is currently unknown.*

There are typically four methods for determining cell wall porosity; (1) ultrastructural methods like electron microscopy, (2) bulk exclusion methods like solute exclusion (SEC), (3) nitrogen physisorption based analysis (BET), and (4) functional assays using labeled tracers diffusing into the cell wall [269,270]. Bulk methods like solute exclusion and BET-Nitrogen are convenient to use compared to electron microscopy and functional tracer based assays. However, these methods are relatively insensitive and dependent on the physico-chemical properties of the probe molecule (e.g. PEG, dextrans, nitrogen). BET-nitrogen based adsorption methodologies are unable to estimate the true porosity accessible to an enzyme molecule (which is very different from what is accessible to nitrogen). Most conventional methods also fail to provide a detailed pore size distribution and shape morphology within the cell wall as a function of different cell wall layers (Middle lamella vs. Secondary cell wall).

On the other hand, dual-axis electron tomography is a powerful technique that could be used for cell wall ultra-structural characterization of architecture and structural details before and after thermochemical pretreatment [112,271]. Electron tomography allows reconstruction of the interior of a specimen through the projections collected from tilting the specimen (typically along dual orthogonal axes to minimize artefacts and

enhance resolution along specimen depth) under the electron beam. Analysis of 3D-tomograms with recently developed advanced imaging software like IMOD aid in obtaining quantitative information that has been difficult to achieve to date [272]. The high-resolution of electron microscopy coupled with tomographic reconstruction of tilt-series images should allow development of cell wall ultrastructural models. This could lay the foundation for testing 'structure-function' based hypotheses to help better understand pretreatment and enzymatic hydrolysis related phenomena (e.g. effect of porosity within middle lamella on enzyme diffusion).

4.1.3 Materials and Methods

See appendix A-VII-1, 4, 9, 10, 11, 12, 13, 23, 28 and 31.

4.1.4 Results and Discussion

4.1.4.1 Ultrastructural modification of cell wall depends on pretreatment severity

There were 5 AFEX conditions tested (protocol A-VII-4) to study the effect of pretreatment severity on extent of ultrastructural modifications (See **Table 4.A.1**). AFEX conditions employed were; (1) Low ammonia loading (**Low-N**) at 0.5:1 ammonia to biomass loading (w/w), 0.6:1 water to biomass loading (w/w), 15 min residence time at 130 °C. (2) Conventional AFEX (**Regular**) at 1:1 ammonia to biomass loading (w/w), 0.6:1 water to biomass loading (w/w), 15 min residence time at 130 °C. (3) High ammonia loading and longer residence time based AFEX (**High-Nt**) at 3:1 ammonia to biomass loading (w/w), 0.6:1 water to biomass loading (w/w), 45 min residence time at 130 °C. (4) Lower temperature based AFEX (**Low-T**) at 1:1 ammonia to biomass loading (w/w), 0.6:1 water to biomass loading (w/w), 15 min residence time at 70 °C. (5) Lower moisture based AFEX (**Low-W**) at 1:1 ammonia to biomass loading (w/w), 0.05:1 water

to biomass loading (w/w), 15 min residence time at 130 °C. All samples were embedded, sectioned and stained (with uranyl actetate and potassium permanganate). Regions of the cell wall that stained black-dark grey are typically enriched in lignin [112,273]; while regions stained dark grey-grey are typically enriched in hemicellulose [274]. The microscopic analysis was limited to vascular bundle based cells (i.e. xylem, sclerenchyma cells) due to reasons explained in previous chapters.

The various parts of the untreated plant cell wall are clearly depicted by the TEM micrograph (**Figure 4.A.1**). The compound middle lamella (CML, approx. 300-500 nm width), comprising of the middle lamella and primary cell wall, is stained black indicating that it is significantly lignified. The secondary cell walls (S1-S3) have varying amounts of lignin content indicated by the intensity of the $KMnO_4$ stain. S1 layers have been shown previously to contain lower lignin content compared to the secondary wall layers S2 and S3 [275]. There is significantly higher lignin and/or hemicellulose content in the intermediate transition zones between the secondary cell wall layers (S1-S2 and S2-S3), indicated by the darker staining of that region. TEM micrographs for the 5 AFEX severities at varying degrees of magnification are shown in **Figure 4.A.2** (and **Figures II-4.A.7 to II-4.A.11**).

Table 4.A.1 *Varying AFEX severity conditions.*

Sample ID	**Notation**	**Ammonia** gm ammonia per gm biomass	**Water** gm water per gm biomass	**Temperature** Degrees °C	**Time** Minutes	**L/S ratio** Liquid to solid (gm/gm)
1	Low-N	0.5	0.6	130	15	1.1
2	Regular	1	0.6	130	15	1.6
3	High-Nt	3	0.6	130	45	3.6
4	Low-T	1	0.6	70	15	1.6
5	Low-W	1	0.05	130	15	1.05

Figure 4.A.1 *Untreated corn stover TEM image showing cell corner, compound middle lamella (CML) and secondary wall layers (S1, S2, S3).*

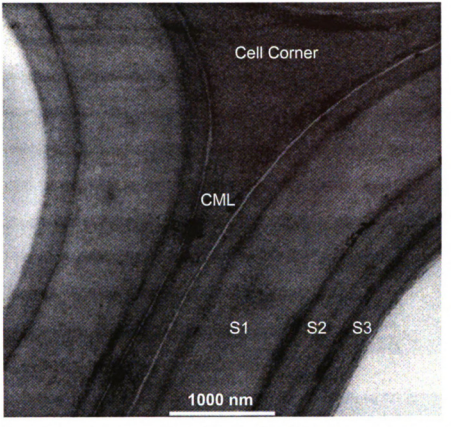

Representative tomogram slices (10 nm thickness) of the various severity AFEX treated cell walls are shown in **Figure 4.A.3**. For Low-N AFEX samples, the middle lamella is significantly modified indicated by the large pores seen within the CML, as compared to the secondary wall layers (**Figure 4.A.2 (a)** and **Figure II-4.A.7**). The pores within the middle lamella range in size from 10-500 nm. Typically, it is difficult to obtain detailed ultrastructural information about the middle lamella for native cell walls without any sort of chemical treatment due to presence of hemicellulose and lignin that obscure the under-lying cellulose microfibrils [273]. However, closer inspection of the CML after Low-N AFEX reveals a unique underlying architecture.

Figure 4.A.2 *AFEX treated corn stover TEM images (at varying scales of magnification) showing cell corner, compound middle lamella (CML) and secondary wall layers (S1, S2, S3). (a) Low-N, (b) Regular, (c) High-Nt, (d) Low-T, and (e) Low-W based varying AFEX severities. See Table 4.A.1 for description of each AFEX severity. (Scale bars shown at the bottom of each image)*

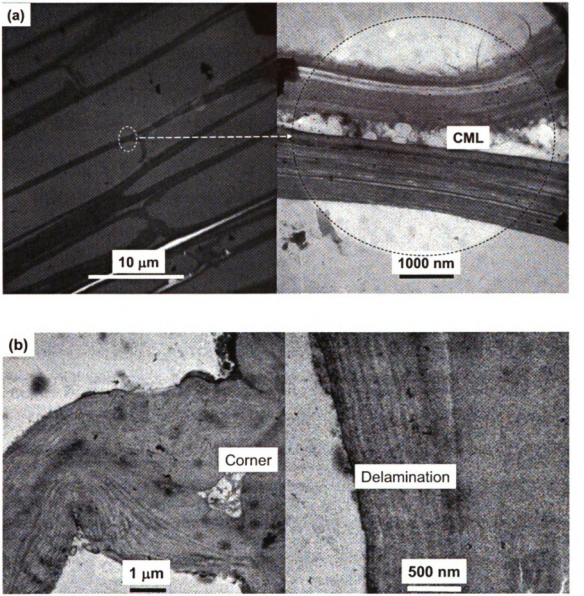

Figure 4.A.2 *Contd...*

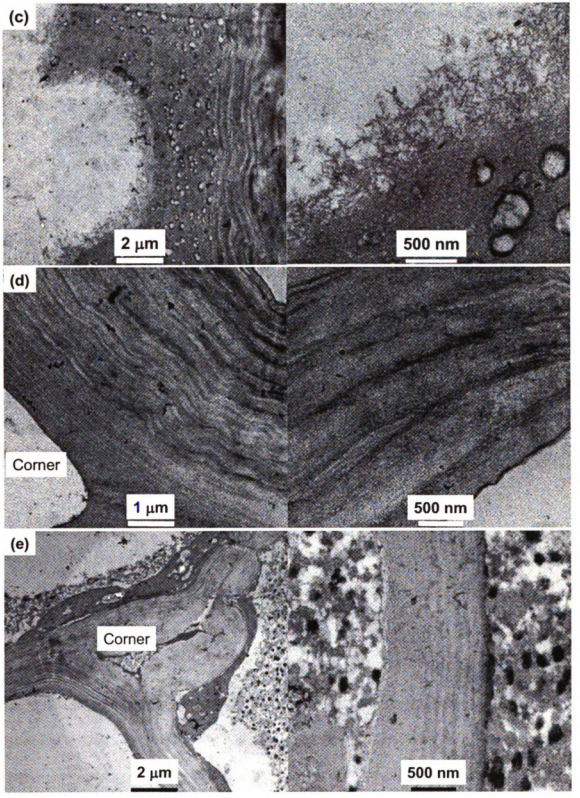

Figure 4.A.3 *Tomogram slices (~10 nm in thickness) depicting varying AFEX severity treated corn stover cell walls. (a) Low-N, (b) Regular, (c) High-Nt, (d) Low-T, and (e) Low-W based varying AFEX severities. See Table 4.A.1 for description of each AFEX severity. (Scale bars shown at the bottom of each image)*

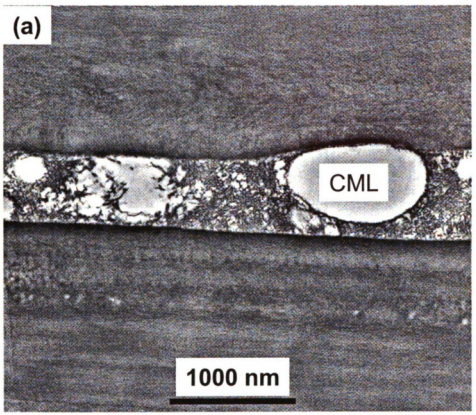

Figure 4.A.3 *Contd...*

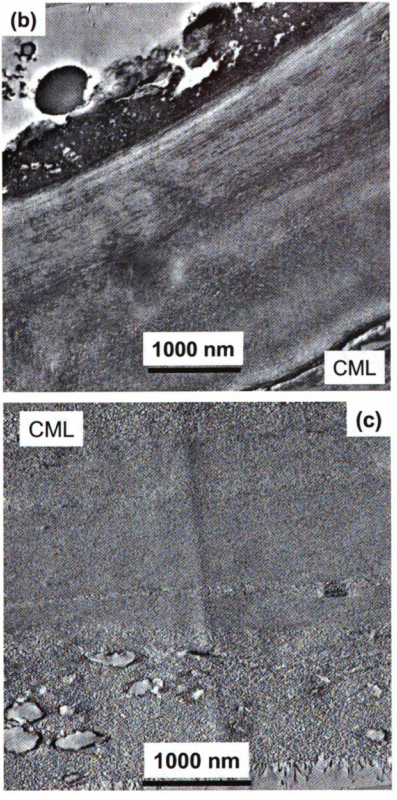

Figure 4.A.3 *Contd...*

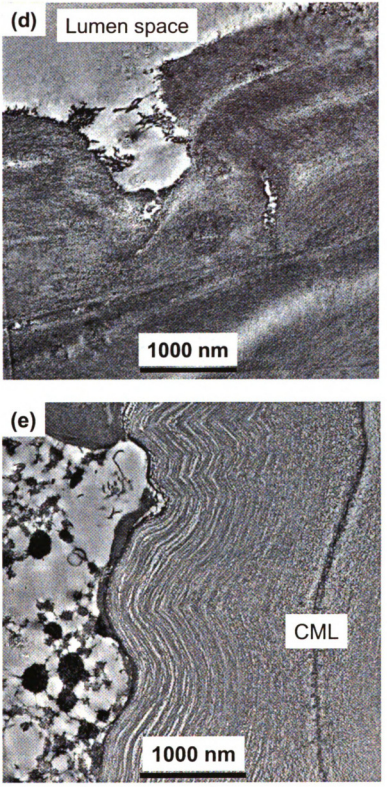

Figure 4.A.4 *Iso-surface mesh enclosing porous regions within EM-tomogram for Low-N treated sample. (a) Tomogram slice (z = 10 slices), and (b) Iso-surface models enclosing porous regions within tomogram slice.*

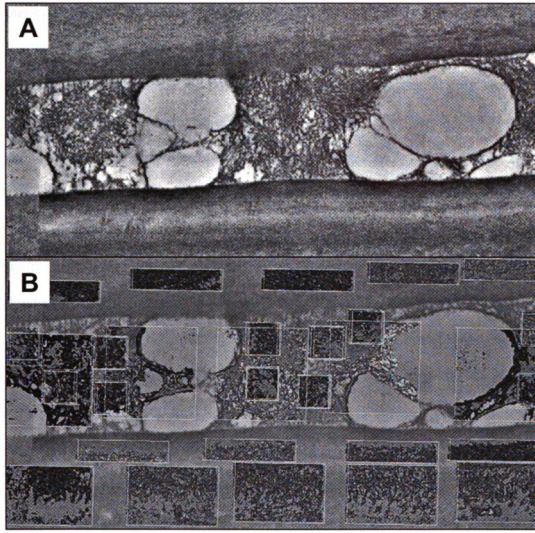

Grass cell wall based CML are known to be composed of a polysaccharide-lignin network as the matrix component, where the carbohydrate (typically GAX) and phenolic moieties are cross-linked by ferulic- or diferulic-acid bridges [94,276]. The cellulosic microfibrils are typically randomly oriented within the CML as compared to the ordered, lamellar structure seen in the secondary wall layers [55]. The degree of polymerization of cellulose in CML has a biphasic distribution, typically 500 or between 2500-4500; as compared to thicker microfibrils in secondary walls that have a DP ranging between 10,000-15,000 [277]. The presence of highly branched mesh like network that can be seen within the CML is similar to the random cellulose microfibril network typical of primary cell walls seen after extraction of hemicellulose [260]. The thickness of individual microfibrils ranges between 4-10 nm (5.8 ± 1.3 nm), which is comparable to what has been reported before [260]. These fibrils are probably coated with a thick layer of hemicelluloses, indicated by the darker stains outlining the long rod-like structures. The larger pores (100-500 nm) have been created due to the volatization of ammonia from liquid to gaseous phase during the decompression phase of AFEX, which results in creation of large pockets of empty porous spaces. Lignins found in the primary, secondary wall, middle lamella, and cell corners are different in composition and ultra-structure. There is evidence that lignification initiates in the cell corners and eventually proceeds to the middle lamella. The first type of lignin synthesized is from H-type monomers that lead to formation of condensed lignin within cell corners and the CML, eventually leading to lignification of the secondary walls towards the lumen [278,279]. Lignin particles are also known to have a globular appearance and random distribution in the CML, while they have more elongated lamellae like structure in the secondary cell

walls where the orientation of the cellulose microfibrils plays an important role in orienting lignin [279]. The orientation and ultra-structure of lignin in the cell wall is thought to play an important role on determining wall enzymatic digestibility as compared to overall lignin composition [280]. It has also been shown that lignified middle lamella/primary walls act as barriers to microbial access for degradation of maize stems [281]. Enhancing accessibility to glycosyl hydrolases through the middle lamella region would help improve overall digestibility of lignified secondary cell walls.

For conventional AFEX (or Regular-AFEX) samples, the middle lamella collapses typically and is not as distinctive as the Low-N AFEX cell walls (**Figure 4.A.2 (b)** and **Figure II-4.A.8**). Unlike the Low-N AFEX cell walls, there is significantly higher delamination within the secondary cell walls for the Regular-AFEX cell walls. There is also a heterogeneous layer of amorphously shaped deposits (rich in lignin and hemicellulose based on stain intensity and subsequent immunolabeling analysis) on the outer cell wall surfaces. These deposits are 20-150 nm in thickness and are distributed across the outermost secondary wall surface layers. This helps validates the findings in Chapter 3 that indicated that the surface of Regular-AFEX (R-ACS) is covered in lignin and hemicellulose rich deposits (10-200 nm thick) based on the AFM and ESCA data. The surface deposits might have been possibly extracted from within the outer secondary wall layers which might also explain the delamination zones typically seen adjacent to these amorphous deposits. The deposits were also shown to be rich in calcium, indicating that some of these surface deposits might be arising from the CML, which upon its collapse extruded the residual extractives into cell corners, pits and outer wall surfaces (See CML extractives within cell corner in **Figure 4.A.2 (b)**).

Immuno-gold labeling for arabinoxylan based epitope was carried out for Regular-AFEX treated cell walls using LM-11 based rat monoclonal anti-xylan antibody (primary antibody) and anti-rat antibody labeled with gold particles 15 nm in diameter (secondary antibody) [282].

Figure 4.A.5 *Immuno-gold labeling of arabinoxylans extracted to outer cell walls (a, b) of AFEX pretreated (Regular) corn stover and water extract (c) using LM-11 based anti-body.*

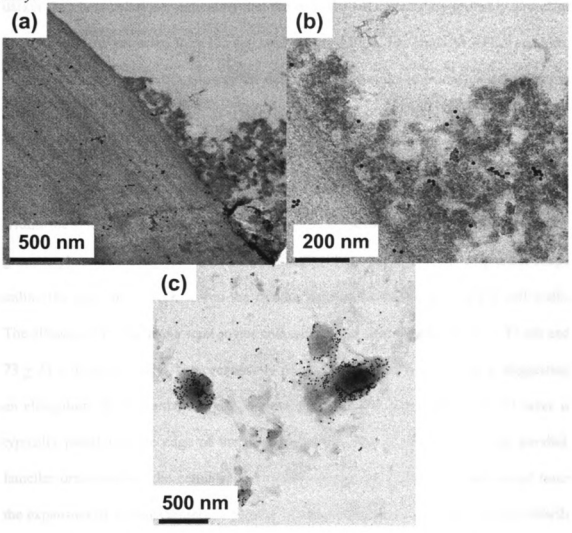

LM-11 antibody binds to both substituted arabinoxylans and unsubstituted homoxylans. Immunocytochemical analysis helps confirm the identity of the amorphously shaped deposits on the outer wall surfaces. The immuno-labeling

experiments revealed that the density of the gold particles around the amorphously shaped deposits was relatively higher (See **Figure 4.A.5 (a-b)**). Interestingly, the antibodies were also found to be localized on the amorphously shaped structures extracted into water from the cell wall (**Figure 4.A.5 (c)**). The extracts are though to be rich in lignin and hemicellulose based components. Lignin typically stains (with $KMnO_4$) darker than hemicellulose, indicating that the grey shaded extracts are probably abundant in arabinoxylans extracted from the cell wall during AFEX. For High-Nt AFEX samples, there is a distinctive modification of the cell walls that results in extensive delamination of secondary walls, collapse of CML and extrusion of CML extractives to cell corners/pits/outer wall surfaces, and formation of large pores within the S3 outer secondary wall regions (**Figure 4.A.2 (c)** and **Figure II-4.A.9**). The large pores formed within the outer wall region are probably due to volatization of liquid ammonia to the gaseous phase at the end of AFEX. Interestingly, these pores have an ellipsoidal shape unlike the large pores seen within the middle lamella for the Low-N AFEX cell walls. The ellipsoidal pores have a semi-major and semi-minor axes lengths of 162 ± 47 nm and 73 ± 21 nm, respectively. The eccentricity of the ellipse is 0.88 ± 0.05 units, suggesting an elongation about the major axis. The major axis of the pores within the S3 layer is typically parallel to the edge of the outer cell wall. This is suggestive of the parallel, lamellar orientation of the cellulose microfibrils in the outer cell walls that would force the expansion of gaseous ammonia parallel to the orientation of the cellulose microfibrils [283]. Also, upon phase transfer of liquid to the gaseous state, the cell wall extractibles (typically rich in hemicellulose and lignin) are deposited on the outer periphery of the pores as suggested by the dark stained edges. Another important structural modification

that takes place during High-Nt AFEX is on the outer periphery of the secondary cell walls facing towards the lumen. During the decompression of the liquid ammonia, the pressure drops quite significantly after AFEX within the lumen (typically from 3-5 MPa to 0.1 MPa). This sudden drop in pressure would result in the explosive decompression of liquid ammonia to the gaseous state, with the pressure drop being highest at the outer periphery of the cell wall. The sudden explosive expansion of ammonia at the periphery of the wall causes the adjacent fibrils to be blown outwards to the lumen. The thickness of the cellulose microfibrils exposed on the outer cell walls is approximately 4.1 $\pm$ 0.5 nm, based on analysis of the tomograms collected. The size of the exposed cellulose fibril corresponds to the elementary fibrils (coated with a thin layer of hemicellulose) that are thought to exist within the cell wall [50, 253, 266]. The elementary cellulosic microfibrils seen for the AFEX samples seem to be also coated with a thin layer of hemicellulose, as indicated by the grey staining of certain fibrils.

For Low-T AFEX samples, there is no major modification of the cell walls after AFEX, except minimal delamination that is seen within some of the secondary cell walls (**Figure 4.A.2 (d)** and **Figure II-4.A.10**). The compound middle lamella is largely intact after AFEX, unlike what was seen for Low-N and Regular-AFEX samples. However, there is significant delamination that is noticeable for the cell walls after AFEX, comparable to what was seen for the Low-N AFEX cell walls.

For Low-W AFEX cell walls there is significant modification that is noticeable after pretreatment (**Figure 4.A.2 (e)** and **Figure II-4.A.11**). The outer secondary wall regions seem to be disrupted quite severely, causing the outer region of the secondary cell walls to detach. There are also dark stained, globular like structures ranging in diameters

around 128 $\pm$ 22 nm. These globular like structures seem to be composed largely of lignin and/or hemicellulose based on the intensity of the $KMnO_4$ staining. Interestingly, these lignin rich globular structures have a narrow size distribution unlike what has been reported for acid treated corn stover [112]. The lignin rich globules seen within acid treated corn stover ranged in size from 5 to 10,000 nm (most abundant droplets ranging between 20-100 nm in diameter) are composed essentially of lignin and have a smooth surface texture. However, for Low-W AFEX cell walls the lignin rich globules are interspersed within a grey stained matrix (possibly rich in carbohydrates) and typically have a spiky coating of lightly stained material. The lightly stained structures are probably composed of hemicellulose and cellulose. Interestingly, in some images (**Figure 4.A.2 (e)**) it is possible to see the disintegrating secondary cell wall enveloping the lignin rich dark globules. This would suggest that the interlamellar lignin and hemicellulose matrix packed between adjacent cellulosic fibrils (typically separated by 15-70 nm, [283]) may have coalesced to result in the formation of these globular like structures. Close inspection of the globules by tomography suggests that these structures are not hollow and have a spiky, lightly stained coating on the surface (possibly rich in hemicellulose and cellulose). The CML has collapsed and the CML extractives seem to be extruded to cell corners/pits/outer wall surfaces. There is significant delamination throughout the cell wall due to removal of matrix material that results in exposure of large surface area for enhanced enzyme accessibility.

In summary, pretreatment severity played an important role in defining the ultra-structural modifications that result during AFEX. Both ammonia loading and temperature during AFEX seem to play an important role on the modification of the compound

middle lamella (CML). The CML was found to be largely intact with little or no pores being created for low temperature based AFEX (Low-T) conditions. However, at higher temperatures even at lower ammonia loadings there is significant modification of the CML. The CML is largely intact and distinctly visible (containing large pores within it) during lower ammonia loading AFEX (Low-N). However, the CML collapses and extrudes its contents into cell corners-pits-outer cell wall surfaces for all other AFEX conditions. Despite the collapse, there is significant porosity (indicated by the lack of staining by both $KMnO_4$ and uranyl acetate) seen within the CML region for all AFEX conditions. On the other hand, pressure drop across the lumen-facing secondary cell walls plays a critical role in the formation of large ellipsoidal shaped pores that are a result of decompression of liquid ammonia to its gaseous state at the end of AFEX. The orientation of the ellipsoidal shaped pores suggests the forced expansion of gaseous ammonia parallel to the orientation of the cellulose microfibrils within the S3 secondary cell walls. The relative concentration of ammonia and water seems to play an important role in the solubilization and coalescence of lignin/hemicellulose residues during AFEX. Low moisture AFEX (Low-W) treated cell walls (with 95% concentrated ammonium hydroxide), as compared to all other AFEX conditions (ranging between 45-83% concentrated ammonium hydroxide), results in the coalescence on inter-lamellar lignin from the outermost secondary cell walls into lignin rich globules enclosed within a polysaccharide rich matrix (as indicated by the relative intensity of the stain). There is significant delamination in the secondary cell walls, depending on the severity of pretreatment. In order to quantify the porosity that is created within the cell wall during AFEX, the 3D-EM-tomograms were analyzed using IMOD image analysis software.

4.1.4.2 Quantifying porosity within cell walls through 3D-tomogram analysis

The tomogram datasets for AFEX cell wall samples were created from the tilt-series TEM images based on the R-weighted back projection algorithm and then analyzed by IMOD [271,272]. The total thickness of all tomograms ranged between 150-250 nm. Representative tomogram slices (10 nm thickness) of the various severity AFEX treated cell walls are shown in **Figure 4.A.3**. For each tomogram, areas within the cell wall containing porous spaces (indicated by spaces not stained) were modeled by enclosing the empty spaces using iso-surface mesh contours based on the optimum threshold value (ranging between 130-170) using IMOD (See **Figure 4.A.4**). The tomogram dataset was opened without binning the voxels intensity; however, to generate the iso-surfaces the image bin and smooth values were set between 3-4 and 10-15, respectively. The boxes enclosing the iso-surfaces typically ranged between x-y dimensions between 100-500 nm, while the z-scale thickness was typically 80-150 nm. Each pixel is 1.08669 nm wide in the x-y plane, while it was assumed to be 1 nm in the z-plane (within the depth of the sample tomogram, assuming no beam-induced specimen thinning [271]).

Quantitative results (i.e. surface areas of iso-surfaces covering porous regions within a defined volume of the cell wall) were then obtained from the IMOD model (See **Table 4.A.2**). The total porosity within the cell wall was estimated by computing the fractional surface area to volume contributed by each region within the cell wall tomogram. The relative fractional thickness of the various regions within the cell wall (i.e. CML, S1, S2, S3, S1/S2/S3 delamination zones) was calculated based on the size of the congruous porous regions.

Table 4.A.2 *Surface area (SA) to volume (Vol) ratios for isosurface mesh enclosing porous regions within TEM-3D-tomograms of varying AFEX severity treated corn stover cell walls. Where; M: Middle lamella, P: Primary wall, S1/S2/S3: Secondary walls and delam: Delamination zones. See Table 4.A.1 for description of each AFEX severity.*

Location	Thickness	% thickness	SA/Vol	Fractional SA/Vol	% SA/Vol	Total SA/Vol
	L (nm)	$100*L/L_{total}$	P (1/nm)	$P_F = P*L/L_{total}$	$100*P_F/P_{F,\ total}$	$P_{F,\ total}$
(1) Low-N AFEX corn stover						
M+P	223	8	2.81E-02	2.37E-03	51	4.69E-03
S1	500	19	2.32E-03	4.40E-04	9	
S1 delam	125	5	3.76E-02	1.78E-03	38	
S2	865	33	1.83E-04	6.01E-05	1	
S2 delam	125	5	5.28E-04	2.50E-05	1	
S3	800	30	3.24E-05	9.83E-06	0	
(2) Regular AFEX corn stover						
M+P	260	8	4.50E-02	3.76E-03	17	2.25E-02
S1	760	24	NA	0.00E+00	0	
S1 delam	330	11	5.10E-02	5.41E-03	24	
S2	420	14	NA	0.00E+00	0	
S2 delam	670	22	3.87E-02	8.33E-03	37	
S3	670	22	2.34E-02	5.04E-03	22	

Table 4.A.2 *Contd...*

Location	Thickness	% thickness	SA/Vol	Fractional SA/Vol	% SA/Vol	Total SA/Vol
	L (nm)	$100*L/L_{total}$	P (1/nm)	$P_F = P*L/L_{total}$	$100*P_F/P_{F,\ total}$	$P_{F,\ total}$
(3) High-Nt AFEX corn stover						
M+P	220	6	4.79E-02	2.79E-03	14	1.96E-02
S1	420	11	NA	0.00E+00	0	
S1 delam	250	7	NA	0.00E+00	0	
S2	1020	27	NA	0.00E+00	0	
S2 delam	170	4	5.82E-02	2.62E-03	13	
S3	1700	45	3.16E-02	1.42E-02	72	
(4) Low-W AFEX corn stover						
M+P	330	16	4.75E-02	7.54E-03	15	4.94E-02
S1 region	780	38	5.75E-02	2.16E-02	44	
S2 region	970	47	4.35E-02	2.03E-02	41	

The ratio of the surface area of iso-surfaces enclosing the porous regions (as nm^2) to the volume of the region enclosing a defined space within the cell wall (as nm^3) is shown in **Table 4.A.2**. For Low-N treated cell walls, the largest contributions towards the overall porosity seem to from the CML (51%) and delamination zone (38%) within the S1 region. However, with increasing AFEX severity (i.e. Regular, High-Nt, Low-W) the largest contribution to overall porosity seems to shift towards the outer secondary cell wall regions with three-fold lesser contribution from the CML region (14-17% vs. 51%).

Assuming the density of the cell wall to be unity (i.e. 1 gram of cell wall occupies 1 cm^3 volume), the surface area of the porous regions per gram of biomass can be easily computed. The results indicate that Low-N, Regular, High-Nt and Low-W AFEX treated cell walls gave a total porosity of 4.69, 22.5, 19.6 and 49.4 m^2/gram of cell wall. Untreated corn stover has no discernible pores within the tomogram unlike AFEX treated cell walls. However, it was possible to estimate the porosity within the S3 region of the Low-N treated cell walls where there were no discernible pores. The porosity (as m^2/gm) for these non-porous regions ranges between 0.001-0.1 m^2/gm. This suggests that the porosity of untreated cell walls would be equal to or lesser than 0.001-0.1 m^2/gm.

Porosities typically obtained for plant cell walls with and without thermochemical pretreatments based on size exclusion based methods range between 20-100 m^2/gm [109,284]. This suggests that the porosity estimates based on the analysis of the porous regions within the tomograms is reasonably comparable to other characterization methods. Nitrogen based physisorption is another technique that was used to estimate

surface area (BET surface area) of cell walls. However, the method suffers from several issues, most notably due to the collapse of the pores during sample drying before the analysis. Secondly, since N_2 molecule is 3000-4000 times smaller than typical cellulases, the BET method estimates typically surface area that is inaccessible to enzymes. Lastly, there is a substantial difference in the measurements based on the adsorption versus desorption isotherms. Typically, specific surface area measurements have been reported to be 10-20 times lower than solute exclusion based methods [284]. Analysis of milled untreated corn stover (UCS), Regular-AFEX corn stover and High-Nt AFEX corn stover by nitrogen physisorption revealed that the BET surface areas for all three samples ranged between 1.5-2 m^2/gm. The BJH (Barret-Joyner-Halenda) adsorption based cumulative pore volume (for pore sizes ranging between 2-300 nm) for the three samples (UCS, Regular, High-Nt) were 0.005133, 0.005237 and 0.00704 cm^3/gm, respectively. While, the BJH desorption based cumulative pore volume (for pore sizes ranging between 2-300 nm) for the three samples (UCS, Regular, High-Nt) were 0.0074, 0.011633 and 0.010381 cm^3/gm, respectively. These results would suggest that characterizing porosity within ammonia treated cell walls through nitrogen adsorption would not be an ideal technique.

Enzymatic hydrolysis yields after 24 hours for various substrates using commercial enzyme mixtures (15 FPU/gm glucan of Spezyme CP, supplemented by 64 p-NPGU/g glucan of Novozyme 188) are shown in **Figure 4.A.6**. Interestingly, there is a strong correlation (R^2 = 0.97) between the 24 hour hydrolysis yield and the initial rate of hydrolysis (based on hydrolysis yield within 1-6 hrs; data not shown). The overall

variance in the hydrolysis yield for the various samples seems to have some correlation to the tomogram predicted porosity. There is observed a linear relationship between elution volume and logarithm of the molecular weight of the globular protein, indicating a retardation caused mainly by a molecular sieve action during gel filtration chromatography [285]. An analogous effect is likely to take place during enzymatic hydrolysis of porous plant cell walls by glycosyl hydrolases, indicating that there might a linear relationship between hydrolysis rate and logarithm of the pore size distribution of the cell wall [22,286].

Figure 4.A.6 *24 hour glucan (grey bars) and xylan (white bars) digestibility, as percent conversion, for varying AFEX severity treated corn stover. Enzyme loading was 15 FPU/g glucan (Spezyme CP) and 64 p-NPGU (Novozyme 188) in 15 ml reaction volume for quadruplicates. See Table 4.A.1 for description of each AFEX severity.*

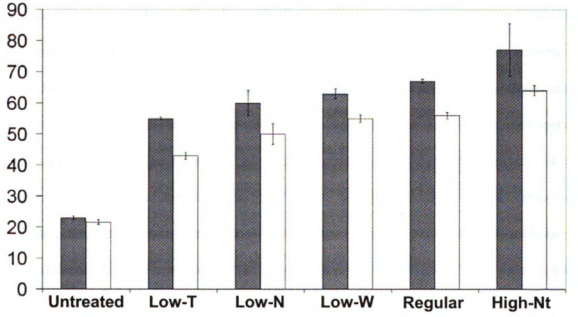

In other words, the rate at which a protein diffuses through the cell wall (and eventually hydrolyzes accessible polysaccharides) is related to the proportion of freely diffusible space available. Indeed, there is strong correlation ($R^2 = 0.91$) between the hydrolysis rate and the logarithm of porosity (based on $P_{F,total}$) for untreated (assuming

porosity = 0.01 m^2/gm) and varying severity AFEX treated corn stover samples. This would suggest that porosity plays an important role on enhancing the overall digestibility of plant cell walls, though it is one among other important factors that effect enzymatic digestibility (e.g. extent of cleavage of lignin-carbohydrate linkages, cellulose DP).

4.1.5 Conclusions

High-resolution TEM imaging allowed determination of ultrastructural modifications within the plant cell wall due to AFEX. The varying pretreatment severity had very distinct effects on the overall modifications within the wall; (a) Formation of large, pores within the compound middle lamella (CML), (b) Formation of ellipsoidal shaped pores in the lumen facing secondary cell walls, (c) Coalescence of lignin and hemicellulose from the outer most secondary cell walls, and (d) Delamination within secondary cell walls. The porosity within the cell wall is being created due to dissolution and extraction (possibly after hydrolysis of certain lignin-carbohydrate complex linkages) of lignin and hemicellulose from inter-lamellar spaces (between cellulose fibrils) to cell corners-pits-outer wall surfaces. The formation of pores within the middle lamella seems to be a critical structural modification within the cell wall that is responsible for the enhanced digestion compared to untreated walls. The deposition of hemicellulose rich amorphously shaped deposits on the outer cell walls after Regular-AFEX was confirmed by anti-xylan immuno-labeling. The morphology of the pores was characterized by constructing 3D-EM-tomograms of the cell walls, which revealed the complex network of porous tunnels formed during AFEX. The porosity was quantified by modeling iso-surfaces enclosing the porous regions in order to compute surface area to volume ratio (as nm^{-1} or m^2/gm). The difference in porosity for the lowest and highest severity pretreatment ranged

between 5-10 fold. Interestingly, there was a strong linear relationship between the porosity (log scale) of the cell wall and the extent of enzymatic hydrolysis. These studies suggested that porosity was an important determinant of the extent of hydrolysis of the cell wall. However, the role of other factors such as cellulose crystallinity, extent of ammonolysis of lignin-carbohydrate linkages, enzyme inhibition (by pretreatment induced cell wall degradation products) and enzyme synergy on the enzymatic digestion of ammonia treated cell walls is not entirely clear.

4.2 Modification of native cellulose crystal structure by ammonia based treatments

4.2.1 Abstract

The effect of cellulose crystal structure on enzymatic digestibility by glycosyl hydrolases was explored using various cellulosic substrates (Avicel, Cotton Linters, Cotton). Native cellulose I was transformed to cellulose III and cellulose II by treating the cellulosic substrates with anhydrous liquid ammonia and sodium hydroxide, respectively. However, there was no cellulose polymorph modification upon treatment with 28-30% ammonium hydroxide (at 4 °C, 1 hour reaction time). The effect of conventional AFEX parameters (ammonia/water loading, residence time, temperature) on the conversion of cellulose I to III was studied for avicel. The extent of conversion of cellulose I to its various other polymorph states was quantified using X-ray diffraction (XRD) and Raman spectroscopy. It was found that cellulose I to III formation following treatment with anhydrous liquid ammonia was largely independent of temperature. However, the extent of conversion to cellulose III during AFEX was inversely related to the water loading and directly proportional to the ammonia loading. No significant amount of cellulose III was formed during conventional AFEX pretreatment (1:1 ammonia loading, 0.6:1 water loading, 30 min, 130 °C). The extent of conversion of cellulose I to III independently measured through XRD and Raman spectroscopy showed a strong linear correlation (R^2 = 0.98). The amount of cellulose III formed during anhydrous ammonia treatment of Avicel was closely dependent on the AFEX conditions, while it seemed to be largely independent of the cellulose degree of polymerization (DP). Interestingly, the rate of enzymatic digestibility of cellulose III was found to be at least 2-fold greater than native cellulose I (1.5 FPU cellulase/g glucan enzyme loading). The extent of improvement in enzymatic

hydrolysis yield was slightly greater for higher DP cellulose (Cotton vs. Avicel), but the overall hydrolysis yield was higher for the lower DP substrates.

4.2.2 Background

There are six different reported allomorphs of cellulose that can be interconverted between certain states (I, II, III_I, III_{II}, IV_I and IV_{II}) [287,288]. Cellulose I_α and I_β are commonly found polymorphic forms of cellulose in nature, with the latter dominant in higher plants [14,289]. Cellulose I_α is thought to be less stable than I_β, as it can irreversibly be converted into the latter during hydrothermal pretreatment [290]. Treatment of native cellulose I with a suitable solvent can modify its crystal structure. Cellulose I can be converted irreversibly into cellulose II during caustic mercerization due to loss of inter-glucosyl residue hydrogen bonds and formation of new inter-sheet hydrogen bonds [291,292]. Liquid ammonia treatment is also known to modify the crystal structure of cellulose I to cellulose I-ammonia complex by accommodating ammonia molecules (which has a high hydrogen bonding potential) between hydrogen bonded sheets that cause a slip in the cellulose sheets [288,293-296]. Upon evaporation of ammonia molecules from the intermediate complex, there is relatively small slippage of the hydrogen bonded sheets in combination with a small change in chain rotation that finally results in the formation of cellulose III_I [295]. Fiber diffraction studies have provided crystallographic data for cellulose I-ammonia complex and cellulose III_I revealing lattice unit cell structural information [293,295]. These studies reveal that the unit cell dimensions of cellulose I and III_I result in distinct hydrogen bonding and van der Waals interactions that cause the latter to have a lower packing density (1.57 vs. 1.63,

respectively). There is an extended zig-zag hydrogen bonding network for chains within a sheet of cellulose III_I that reduces the distance between neighboring chains (0.82 to 0.785 nm), while increasing the intersheet separation (0.387 to 0.429 nm) as compared to cellulose I. This fundamental difference in chain packing is responsible for the lack of intersheet hydrogen bonding for cellulose III_I compared to cellulose I. Molecular dynamic simulations of cellulose III crystals have also helped further validate the crystallographic model data [297].

This difference in chain packing might be responsible for the remarkable increase in hydrolysis rate of cellulose III vs. I [292,298]. Cellulose crystal structure is known to influence cellulase accessibility and specific activity [211,292,298-301]. There have been few studies that also shown that activation of cellulose with liquid ammonia results in enhancing the rate of chemical modifications of the hydroxy groups (e.g. silylation, xanthogenation, carboxymethylation, cyanoethylation) [302-304]. It has been shown that the specific activity of cellobiohydrolase I (CBH I) is several fold higher on cellulose III than cellulose I_α (*Cladophora* based cellulose) [298]. Conversion of Cellulose I_α (isolated from *Cladophora* algae) to cellulose III by supercritical ammonium treatment has been reported recently [295]. *However, there have been no studies done using plant cell wall derived cellulose (that has a smaller crystal size compared to algal cellulose; 3-5 nm vs. 20-35 nm, respectively) to study the effect of cellulose III formation on cellulase activity.*

Cellulose III is known to revert back to I_β by heating at high temperatures in air or boiling in water [163,296]. However, the effect of AFEX (sub-critical conditions with

liquid ammonia and water) pretreatment on the conversion of cellulose I_β (major form in higher plants) to cellulose III has never before been determined. In particular, the effect of AFEX pretreatment severity on the extent of conversion is of practical importance as it probably influences cellulase activity.

X-ray diffraction (XRD) and Raman spectroscopy have been used in the past to identify significant differences between untreated and AFEX treated lignocellulosics [1,18,160,305,306]. XRD is a powerful technique used to provide crystallographic information of cellulose allomorphs due to the diffraction of incident X-rays that is dependent on the spacing between adjacent glucan sheets among other factors [307-310]. However, one of the major limitations of XRD is the unreliability of the method (to measure crystallinity using the CrI index) for samples that have a significant contribution due to their amorphous components (typically hemicellulose and lignin) [308,311]. Solid state ^{13}C nuclear magnetic resonance (NMR) is another technique that has been used in recent years to quantify the crystallinity index of cellulose after subtraction of the amorphous contribution [312]. Raman spectroscopy has several advantages over conventional infra-red (IR) spectroscopy (which provided complementary information to Raman), namely the high sensitivity of the method to the skeletal vibrations of cellulose (C-C, C-O bonds) that have high Raman scattering coefficients, with little contribution from highly polar bonds (like O-H). This allows Raman to be particularly sensitive to intra-molecular differences for polarizable covalent bonds due to slight changes in the coordinates of individual atoms, as compared to IR. The bands in Raman spectra lying between 300-400 cm^{-1} are especially sensitive to ring torsion angles [313], which is

dependent on the relative orientation of adjacent glucosyl residues in various crystalline cellulose allomorphs [295]. Closer inspection of the Raman spectra for cellulose I and III reveals a distinct difference in spectral bands around 380 and 350 cm^{-1} [4,314]. Monitoring these spectral peaks as a function of AFEX pretreatment severity would help quantify the extent of conversion of cellulose I to III, supplementing XRD data as well.

The crystallinity of the biomass (based on XRD measurements) was found to decrease after AFEX (for corn stover) but residual amorphous hemicellulose and lignin might have interfered with that analysis [18]. Laureano-Perez and colleagues reported no significant improvement in the predictive power of their regression model (predicting hydrolysis yield as a function of XRD based crystallinity, FTIR based spectral composition and Raman based lignin content) by incorporating Raman spectral data [160]. However, the authors provided no details on the effect of lignin auto-fluorescence on the analysis. Auto-fluorescence is a major detriment to the successful analysis of lignocellulosics using Raman spectroscopy [315].

4.2.3 Materials and Methods

See appendix A-VII-1, 4, 16, 17, 18, 23, 28 and 31.

4.2.4 Results and Discussion

4.2.4.1 Cellulose I crystal structure is differentially altered by varying thermochemical treatments

Avicel (97-99% glucan content) was treated with different chemicals to obtain various cellulose polymorphs to compare their XRD patterns (**Figure 4.B.1**) and enzymatic digestibility under comparable enzyme loadings. Avicel was treated with sodium hydroxide (25%, w/w) at 4 °C for 1 hour to obtain the distinct cellulose II pattern,

depicted by the relative decrease in the XRD peak at 22 degree two-theta (2θ) also accompanied by an increase the peaks at 20 and 12 degrees 2θ. However, treatment of cellulose I (Avicel) with ammonium hydroxide (28-30%, w/w) at 4 °C for 1 hour resulted in no significant modification of the crystal structure. This result is not entirely surprising, as sodium hydroxide (at concentrations greater than 10-15%, depending on source of cellulose) is a stronger base than ammonium hydroxide resulting in a much higher hydroxyl ion concentration that is responsible for disrupting the hydrogen bonding network in native cellulose I [307].

Figure 4.B.1 *Powder X-ray diffraction spectra of cellulose (Cellulose I) treated with liquid ammonia (Cellulose III), sodium hydroxide (Cellulose II), ammonium hydroxide and concentrated phosphoric acid (Amorphous Cellulose). Avicel was the cellulosic substrate in all cases. Y-axis and X-axis depict intensity counts and two-theta (2θ) angles, respectively.*

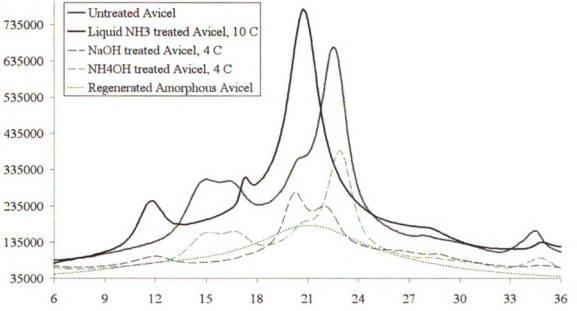

Treatment of cellulose III with ammonium hydroxide (of varying concentrations) has also been reported to cause reversion to cellulose I [316]. However, treatment with liquid ammonia (10°, 30 min) resulted in a distinct XRD pattern for cellulose, depicted by the disappearance of the peak at 22 degree 2θ accompanied by a prominent peak at 20

and 12 degrees 2θ. These results are comparable to what have been reported in literature for cellulose III from cotton [292]. Treatment of cellulose I with concentrated phosphoric acid (>81% w/w; 4°, 1 hr) resulted in complete dissolution of the solid, which was recovered as a fluffy, low-density solid by addition of excess water the solution. Dissolution of cellulose in phosphoric acid has been known to completely disrupt the super-molecular architecture of the cellulose structure, resulting in its transformation from the crystalline to amorphous state with no change in the degree of polymerization [128]. The XRD pattern for the regenerated amorphous cellulose depicts a relatively flat spectrum with no distinct peaks indicating a nearly complete loss of crystallinity.

Table 4.B.1 *Relative change in the amount of crystalline polymorphs (with/without chemical treatment) present in Avicel (AV), cotton linters (LINT) and native cotton (COT) based on XRD spectra peak intensities ($I_{2\theta}$) at respective 2-theta angles (e.g. 2θ = 12, 18, 20, 22). Where for instance; Pk (18/22) = 1 – (I_{18}/I_{22}); %Δ (18/22)$_{unknown}$ = 100 * [Pk (18/22)]$_{unknown}$/[Pk (18/22)]$_{control}$ and control depends on substrate type (AV-I or LINT-I or COT-I).*

	Pk 18/22	Pk 12/18	Pk 18/20	%Δ (18/22)	%Δ (12/18)	%Δ (18/20)
AV - I	0.65	0.44	0.36	**100**	**100**	**100**
AV - II	0.53	0.12	0.60	82	28	166
AV - III	0.16	0.16	0.62	25	37	172
AV - Amo	0.20	0.42	0.26	31	95	73
AV - NH4OH	0.67	0.41	0.32	103	94	90
LINT - I	0.75	0.43	0.35	**100**	**100**	**100**
LINT - III	0.13	0.23	0.52	17	52	148
COT - I	0.65	0.45	0.32	**100**	**100**	**100**
COT - III	0.18	0.27	0.51	28	58	160

In order to obtain more quantitative information regarding the change in the XRD spectral peaks for the various cellulosic substrates, the relative changes in peak intensity for various spectral peaks (2θ = 12°, 20°, 22°) were calculated with respect to the amorphous phase at 2θ=18°. **Table 4.B.1** summarizes this data along with % change in relative peak intensities for all substrates with respect to cellulose I (untreated Avicel as

100%). Pk 18/22 (See **Table 4.B.1** caption for details) is also commonly known as crystallinity index (CrI, [311]) that is calculated for the relative change in intensity for the peak at 22°. The CrI of untreated avicel was around 0.65, while that of ammonium hydroxide is 3% higher indicating a slightly more crystalline substrate. A similar result for ammonium hydroxide treated avicel has resulted in increased CrI possibly due to extraction/removal or residual amorphous fractions from native Avicel [317]. However, treatment with sodium hydroxide resulted in an 18% decrease in CrI (based on the 22° peak) accompanied by a 66% increase in the peak at 20°, which was a typical characteristic of cellulose II polymorphs. Treatment of native cellulose with liquid ammonia resulted in a 75% decrease in CrI, accompanied with a 72% increase in the peak at 20°. There is a similar decrease in CrI (by 70%) for amorphous cellulose, but there was no corresponding increase in the relative intensity of the peak at 20° which is due to the lack of any significant crystallinity in phosphoric acid treated cellulose [128].

Figure 4.B.2 *Powder X-ray diffraction spectra of untreated (Cellulose I) and liquid ammonia (Cellulose III) treated celluloses. Avicel, cotton linters and native cotton were the cellulosic substrates used. Y-axis and X-axis depict intensity counts and two-theta (2θ) angles, respectively.*

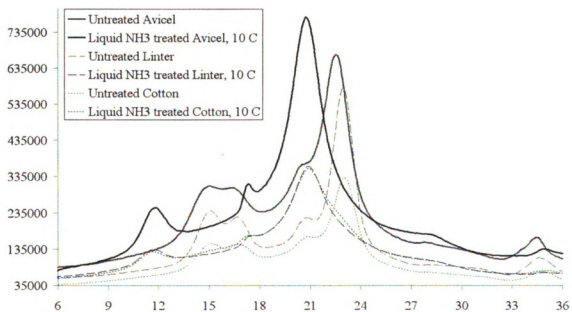

There have been conflicting reports on the exact liquid ammonia treatment conditions that are necessary to form cellulose III, due to differences in the cellulose source and method of ammonia pretreatment [163,293,296,318]. In order to study the effect of cellulose source on the extent of transformation of native cellulose I to III, three types of native cellulose I were obtained (i.e. Avicel, Cotton Linter, Cotton). Cotton linter is the short fiber of the cotton boll that grows between the cotton seeds and the long boll cotton fibers. The DP of avicel, linter and cotton has been reported to be in the range of 150-250, 750-1000 and 5000-10,000, respectively [57,302-304]. All samples were treated with liquid ammonia at 10 °C for 30 min and were dried under the hood overnight prior to further XRD analysis. The XRD spectra for the various celluloses, with and without ammonia treatment, are shown in **Figure 4.B.2**. As expected, the spectra for the untreated celluloses are independent of the cellulose sources and are typical of a cellulose I_β crystal polymorph. Treatment with liquid ammonia resulted in a similar modification of the XRD spectra for all three celluloses, as depicted by the appearance of the peak at 12° 2θ peak and disappearance of the 22° 2θ peak. **Table 4.B.1** has the quantitative data reflecting this change in relative peak intensities. CrI (or Pk 18/22) decrease by 78-83% after liquid ammonia treatment of linters and cotton cellulose, accompanied by a corresponding increase of 48-60% for Pk 18/20. This is similar to what has been noted for avicel as well.

4.2.4.2 Enzymatic digestibility of various cellulose allomorphs

There have been no studies reported in the literature rigorously comparing the relative enzymatic digestibility of plant cell wall derived cellulose allomorphs (cellulose III_I in particular). Therefore, it was found necessary to compare the effect of type of chemical

treatment (with NH_4OH, NaOH, Liquid NH_3, H_3PO_4) on the relative enzymatic hydrolysis rates of plant cell wall derived cellulose (from Avicel). The various cellulosic substrates were hydrolyzed by a crude cellulase complex (Spezyme CP supplemented with Novo 188) for 6-24 hours at a low total protein loading (6 mg/g glucan) that corresponded to 1.5 FPU cellulase loading/g glucan (**Figure 4.B.3**). There was no improvement on the glucan hydrolysis yield after ammonium hydroxide treatment, this is comparable to what has been reported earlier as well [317]. However, treatment of avicel with sodium hydroxide and liquid ammonia did significantly enhance the overall hydrolysis yield likely due to the formation of cellulose II and III, respectively. The overall improvement in the glucan hydrolysis yield after 24 hours was approximately 1.5 fold and 2 fold for the cellulose II and III, respectively, compared to the native untreated cellulose I.

Cellulose II (prepared from bacterial cellulose) has been recently reported to have 2-4 fold higher digestion yield by purified *Thermobifida fusca* cellulases, depending on the type of enzyme employed [300]. While, cellulose III (prepared from *Cladophora* algal cell wall cellulose) was reported to have 4-5 fold higher digestion yield by cellobiohydrolase I [298]. However, in either case the results are not comparable due to the differences in the substrate source and enzyme system employed. The current sets of results are more pertinent from a cellulosic biorefinery point of view where the source of cellulose would be from plant cell walls (e.g. Avicel vs. bacterial/algal cell wall cellulose).

Figure 4.B.3 *Enzymatic digestibility of untreated (Cellulose I), liquid ammonia (Cellulose III), sodium hydroxide (Cellulose II), ammonium hydroxide and concentrated phosphoric acid (Amorphous Cellulose) treated cellulose. Avicel was the cellulosic substrate in all cases. Enzyme loading was 1.5 FPU/g glucan of Spezyme CP (supplemented with Novo 188). Avicel was the cellulosic substrate in all cases. Y-axis depicts total glucan conversion after 6 or 24 hours of hydrolysis.*

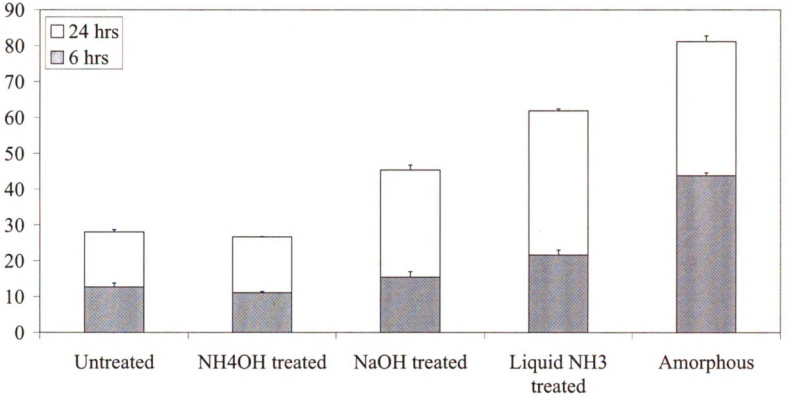

On the other hand, there was a 3-4 fold increase in the hydrolysis yield of amorphous cellulose (from phosphoric acid treated avicel), compared to native cellulose I. This result is comparable to previously reported findings on amorphous cellulose [128]. These results clearly demonstrate the differential hydrolysis kinetics for cellulose depending on its crystalline form, which proceeded in the following order; Amorphous cellulose > Cellulose III_I > Cellulose II > Cellulose I. Interestingly, similar results have been reported for digestion of cotton linters based cellulose allomorphs by ruminal bacterial systems in the following order; Amorphous cellulose > Cellulose III_I > Cellulose I > Cellulose II [292]. However, unlike the findings in that report, cellulose II was found to be more digestible than cellulose I. This is possible due to differences in the source of the substrate and the exact protocol used for preparing cellulose II. The authors also found that depending on the source of the ruminal bacterial culture (*Ruminococcus flavefaciens* vs. *Fibrobacter succinogenes*), the absolute digestion kinetics varied between the different cellulose allomorphs but the relative trends were similar [292].

The enhancement of the hydrolysis yield for cotton linters and cotton fibers after liquid ammonia treatment (10 °C, 30 min) was explored as well (**Figure 4.B.4**). The cellulosic substrates were hydrolyzed by a crude cellulase complex (Spezyme CP supplemented with Novo 188) for 6-24 hours at two different total protein loadings (6 and 60 mg/g glucan) that corresponded to 1.5 and 15 FPU cellulase loading/g glucan. The glucan hydrolysis results depict a 2-2.5 fold increase in overall yield for 6 mg/g glucan enzyme loading after 6 and 24 hours of hydrolysis for both liquid ammonia treated linter and cotton fibers as compared to their untreated counter parts.

Figure 4.B.4 *Enzymatic digestibility of untreated (Cellulose I) and liquid ammonia (Cellulose III) treated celluloses. Avicel, cotton linters and native cotton were the cellulosic substrates used. Enzyme loading was 1.5 or 15 FPU/g glucan of Spezyme CP (supplemented with Novo 188). Y-axis depicts total glucan conversion after 6 or 24 hours of hydrolysis.*

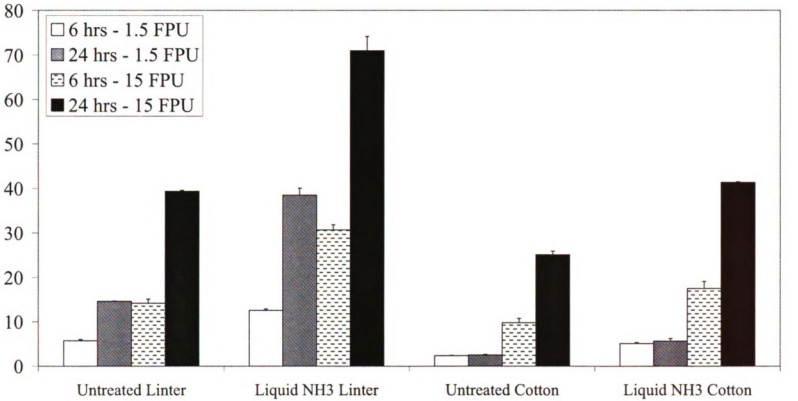

The relative increase in the glucan digestibility after liquid ammonia treatment of cotton linters and cotton fibers is sightly higher compared to avicel at the same protein loading. This is not surprising considering that cotton linters/fibers are composed of higher degree of polymerization (DP) cellulose that might possibly benefit more from the transformation of cellulose I to III to enhance activity of cellulases on it. The extent of digestion of cotton linters and fibers was significantly lower than avicel, which is also possibly due to differences in cellulose DP. However, the actual mechanism by which cellulose III is more digestible than native cellulose (for any of the celluloses) is currently unclear (See Chapter 8 for more details). Interestingly, the extent of improvement in the glucan hydrolysis yield was only 1.5-2 fold higher for liquid ammonia treated cotton linter/fibers at higher protein loading (60 mg total enzyme/g glucan or 15 FPU/g glucan) at either time points, compared to their corresponding native cellulosic substrates. This would suggest that the hydrolysis kinetics of cellulose III is closely coupled to the individual enzyme family, loading and extent of hydrolysis. Similar results, depicting dependence on enzyme source and loading, have been reported before for cellulose II based allomorphs [300].

The effect of liquid ammonia treatment temperature (i.e 10, 25, 60, 95 °C) on the formation of cellulose III was closely examined for avicel, based on comparing the enzymatic hydrolysis yields using 1.5 FPU cellulase loading per gram glucan (**Figure 4.B.5**). There was no significant difference in the enzymatic hydrolysis yield for the varying temperature liquid ammonia pretreated cellulose. In all cases, there was a 2-fold increase in the glucan yield compared to untreated cellulose I.

Figure 4.B.5 *Effect of liquid ammonia treatment temperature on the enzymatic digestibility of various cellulose III polymorphs. Enzyme loading was 1.5 FPU/g glucan of Spezyme CP (supplemented with Novo 188). Avicel was the cellulosic substrate in all cases. Y-axis depicts total glucan conversion after 24 hours of hydrolysis.*

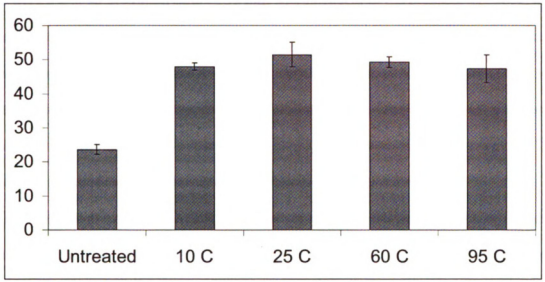

This would suggest that the formation of cellulose III is largely independent of temperature, as long as sufficient amount of liquid ammonia is present to completely swell the cellulose fibrils. However, increasing temperature above 100 degrees resulted in considerable darkening of the treated samples possibly due to Maillard based reactions of reducing aldehydic ends of cellulose (with ammonia) [319]. Maillard reactions are known to be promoted by high temperatures, low moisture and high alkalinity [319]. The enzymatic digestibility of the darkened cellulose samples after treatment with liquid ammonia was found to give significantly lower enzymatic hydrolysis yields than cellulose III prepared at temperatures below 100 °C (data not shown). In many cases, the hydrolysis yields were comparable to or significantly lower than native cellulose I (data not shown). This is not surprising as Maillard reaction products (and alkali induced peeling reaction products; [320]) are known to severely inhibit cellulases among many other enzymes [321,322]. The extent of Maillard based degradation reactions during

ammonia/AFEX treatment of crystalline cellulose was briefly explored in Chapter 5. Previous studies with liquid ammonia and celluloses (using Avicel and Linters) have reported that an activation time of 30 min was sufficient in the presence of excess liquid ammonia to completely soak the substrate [288, 289]. However, more detailed kinetics studying the diffusion of ammonia into the cellulose lattice as a function of substrate and cellulose crystal size is necessary to better understand the transformation of cellulose I to III.

4.2.4.3 Formation of cellulose III during conventional AFEX treatment

The effect of conventional AFEX parameters (ammonia loading, water loading, residence time) was studied to quantify the extent of conversion of cellulose I to III (for avicel as the cellulosic substrate). Four AFEX conditions were explored; (a) (**1-NH3, 0.6-W**) 1 gm ammonia and 0.6 gm water loading per gm of substrate at 100 °C for 15 min, (b) (**3-NH3, 0.6-W**), 3 gm ammonia and 0.6 gm water loading per gm of substrate at 100 °C for 45 min, (c) (**1-NH3, 0.05-W**) 1 gm ammonia and 0.05 gm water loading per gm of substrate at 100 °C for 15 min, and (d) (**3-NH3, 0.05-W**) 3 gm ammonia and 0.05 gm water loading per gm of substrate at 100 °C for 45 min. Liquid ammonia treated avicel (10 °C, 30 min) was the control, where the ammonia loading employed ranged between 5-7 gm ammonia per gm substrate containing 0.05 gm water/gm substrate. The XRD spectra for all cellulosic substrates are shown in **Figure II-4.B.6**. None of the four AFEX conditions gave complete conversion to cellulose III. However, the extent of conversion was closely dependent on the AFEX conditions employed.

Table 4.B.2 *Relative change in the amount of crystalline polymorphs present in Avicel (AV), with or without AFEX treatment (N = ammonia loading and W = water loading, w/w basis) based on XRD spectra peak intensities ($I_{2\theta}$) at respective 2-theta angles (e.g. 2θ = 12, 18, 20, 22). Where for instance; Pk (18/22) = 1 – (I_{18}/I_{22}) and $\%\Delta\ (18/22)_{unknown} = 100 * [Pk\ (18/22)]_{unknown}/[Pk\ (18/22)]_{AV\text{-}I}$.*

XRD	Pk 18/22	Pk 12/18	Pk 18/20	%Δ (18/22)	%Δ (12/18)	%Δ (18/20)
AV - I	0.65	0.44	0.36	**100**	**100**	**100**
1N-0.6W	0.61	0.43	0.38	94	98	105
3N-0.6W	0.63	0.44	0.34	97	100	94
1N-0.05W	0.67	0.40	0.44	103	91	123
3N-0.05W	0.57	0.36	0.44	88	82	123
AV - III	0.16	0.16	0.62	25	37	172

More quantitative information regarding the change in the XRD spectral peaks for the various cellulosic substrates, relative change in peak intensity for various spectral peaks (2θ = 12°, 20°, 22°) were calculated with respect to the amorphous phase at 2θ = 18°. **Table 4.B.2** summarizes this data along with % change in relative peak intensities for all substrates with respect to cellulose I (untreated Avicel as 100%). The CrI value for AFEX conditions containing significant moisture (1N-0.6W and 3N-0.6W) showed only a 3 and 6% decrease. However, only when AFEX was carried out in the absence of water and in presence of sufficient ammonia to completely soak the substrate (3N-0.05W) was there a significant decrease in the CrI value by 12%. As seen earlier, quantifying the extent of conversion of cellulose III through the relative increase in the spectral peak intensity at 2θ = 12° or 20° would also be possible (with respect to the amorphous peak at 18°). Comparing the change in the relative peak intensity of Pk 12/18 depicts a 9% and 18% decrease for 1N-0.05W and 3N-0.05W based AFEX conditions. For liquid ammonia treated cellulose with 100% conversion to cellulose III, there is 75% and 63% decrease in CrI and Pk 12/18, respectively. This would suggest that absence of water is critical during

ammonia treatment to prevent reversion of cellulose III back to I during conventional AFEX. Similar results have been reported earlier, where 40-100% reversion of cellulose III to I was seen in the presence of ammonium hydroxide solutions [163,296,316]. Secondly, soaking the substrate completely in liquid ammonia is critical to completing the transformation of cellulose I to III. With the current AFEX reactors used, there was no external gas addition to maintain overhead pressure. Therefore, at 100 °C a significant portion of liquid ammonia could easily undergo phase change from liquid to gas, especially in the absence of water. This could explain why the transformation of cellulose I to III was incomplete even in the absence of water (i.e. 1N-0.05W and 3N-0.05W). Future studies on cellulose III formation should be carried out using reactors with overhead pressure control to ensure ammonia is entirely in the liquid phase. This would be ideal to minimize and optimize the amount of liquid ammonia necessary to make cellulose III from a commercial stand point.

The extent of formation of cellulose III for varying AFEX severity was also confirmed by Raman spectroscopy. Raman spectroscopy is a powerful technique that has been used to study the crystal structures of various cellulosic allomorphs to provide information on their secondary and tertiary structures [314,315,323]. Raman spectra for the various cellulosic substrates are shown in **Figure II-4.B.7**. As expected, based on the XRD results, none of the four AFEX conditions resulted in complete transformation of cellulose I to III. This can be easily quantified based on the relative intensity of peaks 380/350, which has been presented in **Table 4.B.3**. The relative change in the peak ratios with respect to untreated cellulose I have also been provided in the table, depicting a 82% decrease in the ratio for cellulose III.

Table 4.B.3 *Relative change in the amount of crystalline polymorphs present in Avicel (AV), with or without AFEX treatment (N = ammonia loading and W = water loading, w/w basis) based on Raman spectral peak intensities ($I_{wavenumber}$) at respective wavenumbers (e.g. 380 and 350; cm^{-1}). Where for instance; Pk (380/350) = 1 – (I_{380}/I_{350}) and $\%\Delta\,(380/350)_{unknown}$ = 100 * [Pk (380/350)]$_{AV\text{-}unknown}$/[Pk (380/350)]$_{AV\text{-}I}$.*

Raman	Pk 380/350	%Δ (380/350)
AV - I	2.07	**100**
1N-0.6W	2.00	97
3N-0.6W	1.92	93
1N-0.05W	1.43	69
3N-0.05W	1.27	61
AV - III	0.36	18

In the case of high moisture AFEX (1N-0.6W and 3N-0.6W) there is a 3% and 6% decrease in the ratio of 380/350, respectively. However, in the absence of water (1N-0.05W and 3N-0.05W) there is 31% and 39% decrease in the ratio, respectively. These results are consistent with the XRD findings (strong correlation between overall trends), however, the absolute value of the extent of conversion to cellulose III are different (after normalizing relative peak intensity for 100% cellulose I and 100% cellulose III samples). Raman predicts nearly 1.5-2 fold higher conversion of cellulose I to III (for the four AFEX conditions) compared to XRD (based on Pk 12/18). It should be possible to get a more reliable estimate of the absolute conversion of cellulose I to III by testing several AFEX conditions (to study kinetics of cellulose III formation) to generate samples over the entire range of cellulose III formation (0-100%).

From an industrial point of view, it would seem unnecessary to transform cellulose I to III during the conventional AFEX pretreatment process (i.e. 90 °C, 1 gm ammonia loading/gm substrate, 0.6 gm water loading/gm substrate) as this would be counterproductive due to presence of water and also due to requirement of high pressure

rating reactors to maintain ammonia in the liquid phase. It would be preferential to transform AFEX treated cellulose I rich substrates (at the end of conventional AFEX pretreatment) to cellulose III by soaking in excess liquid ammonia at low temperatures (<25 °C). This would avoid investment in capital intensive higher pressure reactors for making cellulose III during AFEX, while also avoiding the reversion of cellulose III to I during conventional high-moisture AFEX. Treatment with liquid ammonia at low temperatures would also possibly prevent the coalescence of lignin (due to a glass transition temperature > 130 °C; [324]) into enzyme inhibitory globules from secondary cell walls (based on TEM findings from Chapter 4.1 for Low-W AFEX corn stover samples) [40].

4.2.5 Conclusions

Native plant cell wall cellulose I_β was transformed to cellulose III_I and cellulose II_I by treating the cellulosic substrates with anhydrous liquid ammonia and sodium hydroxide, respectively. However, there was no cellulose polymorph modification upon treatment with 28-30% ammonium hydroxide. The extent of conversion of cellulose I to its various other polymorph states was quantified using X-ray diffraction (XRD) and Raman spectroscopy. It was found that cellulose I to III_I formation following treatment with anhydrous liquid ammonia was largely independent of temperature, in presence of excess liquid ammonia and absence of water. The extent of conversion of cellulose I to III_I measured through XRD and Raman spectroscopy showed a strong correlation (R^2 = 0.98). It was found that the cellulose crystal structure played a significant role on enzymatic digestibility of various cellulosic substrates (i.e. Avicel, Cotton Linters,

Cotton). The order of enzymatic digestion rate for the various polymorphs of Avicel were found to vary as follows; Amorphous Cellulose > Cellulose III > Cellulose II > Cellulose I. The rate of enzymatic digestibility of cellulose III_I was found to be at least 1.5-2.5 fold greater than native cellulose I, which was dependent on the cellulose source (Avicel vs. Cotton), enzyme loading (1.5 vs. 15 FPU loading) and extent of hydrolysis (6 vs. 24 hours). Currently, the actual mechanism for the enhanced digestibility of cellulose III over native cellulose is unclear. Studies with purified cellulases should help reveal which glycosyl hydrolase families benefit the most due to the modification of the cellulose crystal structure. Lastly, the inhibition of cellulases due to formation of Maillard and alkali induced peeling reaction degradation products suggest a need for better understanding of the cell wall decomposition products formed during AFEX.

CHAPTER 5: COMPARING MAJOR CELL WALL DEGRADATION PRODUCTS FORMED DURING AMMONIA AND DILUTE ACID BASED PRETREATMENTS

5.1.1 Abstract

Dilute-acid pretreatment of lignocellulosic biomass has been known to produce various degradation compounds that inhibit downstream biological processing. However, similar studies have never been carried out for ammonia based pretreatments at varying treatment severities. The severity (i.e. residence time, temperature and ammonia/water loadings) of AFEX pretreatment is believed to play an important role in physicochemical modification of the Lignin-Carbohydrate-Complex (LCC). The LCC is comprised of hemicellulose side-chains (e.g. uronic acid and arabinose residues) cross-linked to phenolic aromatic moieties (e.g. ferulic, cinnamic, p-coumaric) that result in impeding enzyme accessibility. The chemistry of ammonia based treatments was better understood through identification and quantification of various degradation compounds produced during AFEX treatment of corn stover. Solvent extraction of untreated, AFEX and dilute-acid treated corn stover was carried out using an accelerated solvent extractor (ASE) for subsequent LC/GC-MS analysis. The major compounds quantified include; (1) organic acids (e.g. acetic, lactic, succinic, levulinic, formic), (2) furans (e.g. furfural, 5-HMF, 2-furoic acid), (3) nitrogenous ammnolysis by-products (e.g. acetamide, feruloyl amide, coumaroyl amide), (4) aromatic and phenolic acids (e.g. p-coumaric, ferulic acid and other cinnamyl derivatives), and (5) aromatic aldehydes (e.g. 4-hydroxy-benzadehyde, vanillin, 4-hydroxy-acetophenone). Nearly 20-25% of arabinoxylan (w/w) based oligomers released from the cell wall during AFEX were extractible by hot water. The severity of AFEX (e.g. extent of ammonolysis) was closely correlated to the enzymatic hydrolysis rate of

treated corn stover cell walls (R^2 = 0.87). Interestingly, there was significant inhibition (40-50% lower hydrolysis yield than control) of the glycosyl hydrolases by AFEX corn stover degradation products at high inhibitor concentrations. Undesirable side-reactions of ammonia with cell wall soluble sugars and polysaccharides (e.g. Maillard reactions) at higher thermochemical severity produce enzyme inhibitory products. On the other hand, it might be possible to isolate valuable co-products (e.g. phenolic amides) after AFEX to make the process more economically attractive.

5.1.2 Background

Most pretreatments have been found to generate some sort of biologically inhibitory compounds due to lignin-carbohydrate degradation [137,180]. The kind of inhibitory compounds released after a typical thermo-chemical pretreatment depends on cell wall composition and pretreatment method. Typically, the most potent inhibitory compounds released due to alkali catalyzed thermo-chemical degradation are probably lignin (e.g. Guaiacyl, Syringyl, Hydroxy Cinnamyl) and hemicellulose based [251]. Guaiacyl lignins (G-lignins) are predominantly polymerizates of coniferyl alcohol found in softwoods (gymnosperms). Guaiacyl-Syringyl lignins (GS-lignins) are made up of varying proportions of coniferyl and sinapyl alcohol, typical of hardwoods. GS lignins in addition to significant amounts of p-hydroxycinnamyl moieties (GSH-lignins) are found commonly in grasses and monocotyledons (i.e. corn stover). Lignification of xylem cells takes place by interlamellar deposition of lignin within the carbohydrate matrix of the cell wall along with formation of chemical bonds with hemicellulosic sugars. Lignification is thought to be influenced by the carbohydrate matrix ultrastructural layout [325]. For monocotyledons (i.e. corn stover) ferulic acids are deposited within the middle lamella

and cell corners during early lignification while p-coumaric and sinapic acids are deposited in the secondary walls [326-328]. However, recent results have shown ferulate deposition within corn stover internodal secondary cell walls mediates lignin-hemicellulose cross-linking [83]. These phenolic acids are invariably connected by an ester bond to arabinoxylans in grasses and by an ether bond to the lignin core. Enzymatic digestibility has been shown to be strongly dependent on ferulate cross-linking within the cell wall [79,83,276,281,329-333]. It would be of interest to determine the extent of modification of the ferulate ester linkages for varying pretreatment severities to help develop better models to predict lignocellulosic digestibility and pretreatment reaction kinetics.

5.1.2.1 Degradation products formed during ammonia based pretreatments

AFEX pretreatment has several advantages over dilute acid based pretreatments [95]. Acidic pretreatments degrade monomeric sugars to biological inhibitors (e.g. furans, levulinic acid) that decrease overall product yield and increase detoxification related processing costs [334-337]. Dilute-acid pretreatment based lignocellulosic hydrolysates and hemicellulose-rich aqueous streams have been widely studied. Several classes of potential microbial inhibitors from acid pretreated biomass have been identified, including organic acids, phenolics and aromatic aldehydes [180,334,336,338,339]. Wet-alkali oxidized pretreatment of wheat straw was shown to produce several carboxylic acid and phenolic based degradation products [180].

Although, AFEX corn stover hydrolysates are easily fermentable with no detoxification necessary [340], on-going research has indicated inhibition during xylose fermentation and reduced cellulase activity (10-30% lower activity of commercial

enzyme cocktails in presence of AFEX corn stover water extractives) by some of these unknown AFEX degradation products (unpublished data). There are a few publications that have indicated formation of potential inhibitory compounds during AFEX but did not identify them [161,162,236,341]. AFEX produced greater amounts of hot-water and ethanol-toluene extractives for several agricultural residues and forages. AFEX degradation product based extractives were also found to inhibit monomeric sugar fermentation by *Pachysolen tannophilus* [342]. Mes-Hartree and colleagues [341] found that water and methanol extraction of AFEX treated wheat straw and aspen wood gave significantly higher saccharification rates and ethanol metabolic yields. Unpublished work indicates that nearly 2-3 grams ammonia per 100 grams of dry corn stover remains with the treated biomass due to reaction of ammonia with various cell wall components. The residual nitrogenous compounds in AFEX treated biomass are believed to be a potential nitrogen source during microbial fermentations and for use as animal feed [8,340], but their chemical composition is largely unknown.

Weimer and colleagues [162] noticed a significant increase in the nitrogen content of super-critical ammonia treated hardwood possibly due to ammonolysis based reactions of LCC ester-linkages and hemicellulose acetyl groups. The major degradation compound for ammonia treated hardwoods identified so far has been acetamide [162,236]. Interestingly, even after extracting the acetamide from ammonia treated woody samples there is still some '*amide*' found associated to the insoluble hemicellulose. This is attributed possibly to amidated uronic acid side-chain residues bound to insoluble xylan [267,343]. De-esterification of LCC linkages between ferulic acid-arabinose and coumaric acid-lignin are expected to result in the formation of

phenolic acids and their corresponding amide analogs. Alkali induced degradation of polysaccharides to carboxylic acids is another important class of degradation reactions that take place during alkaline pulping of woody biomass [320,344], but have never been studied for AFEX. Overall, there has never been a detailed characterization of any of the degradation products formed during AFEX pretreatment that may have a significant inhibitory role on downstream biological processing.

5.1.2.2 Spectroscopic characterization of ammonia pretreated biomass

Several spectroscopic techniques like Fourier transform infra-red (FTIR), X-ray diffraction (XRD) and Raman spectroscopy have been used in the past to identify significant compositional differences between untreated and AFEX treated lignocellulosics [1,18,160,305,306]. Diffuse reflectance infra-red Fourier transform (DRIFT) spectroscopy has been used to quantify spectroscopic changes that take place in lignocellulosics after pretreatment, including AFEX [18,160]. Multivariate statistical analysis has been conducted to correlate changes in spectroscopic data (crystallinity indices by XRD, surface lignin content by fluorescence, chemical changes in biomass after pretreatment by DRIFT) to enzymatic digestibility for AFEX treated corn stover [18,41,160]. The authors found that initial and final rates of enzymatic hydrolysis were significantly affected by the ester-carbonyl content (determined by DRIFT) of the pretreated biomass. Cleavage of hemicellulose and hemicellulose-lignin complex based ester linkages (1720-1740 cm^{-1}) seem to be the major chemical linkages that significantly affect pretreated biomass digestibility [18,41,160,162]. The crystallinity of the biomass (based on XRD) was found to decrease after AFEX but residual hemicellulose and lignin might have interfered with that analysis. The DRIFT peak intensity for aldehydic bonds

increased after AFEX and was found to significantly influence the rate of hydrolysis. No attempt was made to determine the chemical composition of the degradation products in order to validate the spectroscopic changes detected within the biomass after AFEX. Based on multi-component regression analysis for changes in DRIFT spectral intensities it is difficult to determine the actual chemical and physical modifications that take place within the cell wall after AFEX pretreatment to accurately predict enzymatic digestibility. Laureano-Perez and colleagues reported no significant improvement in the predictive power of their regression model by incorporating Raman spectral data [160]. However, the authors provided no details on the effect of lignin auto-fluorescence on the analysis. Auto-fluorescence is a major detriment to the successful analysis of lignocellulosics using Raman spectroscopy [315].

5.1.2.3 Oligosaccharides produced during ammonia based pretreatments

AFEX treatment has been thought to degrade hemicelluloses to oligomers and significantly reduce the hemicellulose content based on crude compositional analysis conducted on untreated and AFEX treated forages (via acid/neutral detergent fiber analysis) [42,43]. The extent of hemicellulose based degradation products is unclear due to inherent disadvantages of trying to predict hemicellulose content using ADF/NDF (acid-neutral detergent fiber) based analytical methods. The xylan content of AFEX pretreated samples are typically 0-30% lower than untreated [42,43,345], depending on how compositional analysis is conducted. This discrepancy is seen if the arabinoxylan based oligomers are solvent extracted prior to acid hydrolysis based compositional analysis (NREL LAP 002, [346]), resulting in a 20-30% decrease in xylan content. Increasing ammonia loadings have been found to decrease total hemicellulose content in

sugar beet pulp and produce lower amounts of monomeric sugars (arabinose, galacturonic acid) [235]. Ammonia recycle percolation (ARP) based pretreatment is responsible for extraction of a significant amount of arabinoxylan based hemicelluloses from corn stover (indicated by decrease in xylose and arabinose content after ARP) but no detailed analysis have been conducted to identify the structural modifications of hemicellulose during ARP treatment [110,347,348]. Interestingly, it was more difficult to extract hemicellulose oligomers from poplar during ARP based pretreatments compared to corn stover, which might be due to differences in the hemicellulose and LCC organization in hardwoods compared to agricultural straw based residues [348]. There have been no detailed experiments conducted in the past to study the effect of AFEX on hemicellulose and LCC group based modifications.

5.1.2.4 Quantitative methods for lignocellulose degradation product analysis

Quantitative detection of chemical compounds in acid pretreatment hydrolysates has been performed by reversed-phase high performance liquid chromatography (HPLC) procedure developed for a variety of aliphatic and aromatic acids, aldehydes and phenolic degradation products over a wide range of concentrations (0.02-41 mM) [334]. A major advantage of this technique is simultaneous separation and quantification of aliphatic acids, multifunctional groups of aromatic and phenolic acids in a single chromatographic run. Tandem mass spectrometry coupled with UV detection allows detection and quantification of a large range of analytes compared to other analytical procedures. However, one of the major limiations of UV detection is the co-elution of compounds that can be addressed by quantifying the molecule of interest by selected reaction monitoring (SRM) using MS/MS [349].

5.1.3 Materials and Methods

See appendix A-VII-1, 4, 5, 11, 19, 20, 21, 22, 23, 28 and 31.

5.1.4 Results and Discussion

5.1.4.1 By-products of hydrolysis and ammonolysis of ester linkages during AFEX

Extracting degradation products from the AFEX treated substrate with hot water gave insight to extent of ammonolysis and hydrolysis driven reactions during AFEX. The total amount of water extractables depended on the AFEX pretreatment severity employed (**Table 5.1**). Interestingly, there seemed to be linear correlation ($R^2 = 0.89$) between the extent of enzymatic digestibility and total % water extracibles for untreated and AFEX treated substrates.

Table 5.1 *Total water extractibles for untreated, AFEX and dilute acid treated corn stover compared to their respective glucan hydrolysis yields (24 hours hydrolysis time, 15 FPU Spezyme/g glucan supplemented with Novo 188). All water extractions were done using the ASE (see methods section for details) at 70 °C, 1500 psi (except Acid treated* that was extracted at 25 °C, 15 psi). See Table 4.A.1 for description of each AFEX severity.*

	% Water Extractibles		% Glucan Conversion	
	Mean	*Std Dev*	*Mean*	*Std Dev*
Untreated	4.44	0.63	23	0.6
Low-N	19.27	2.64	60	4.1
Regular	19.34	0.17	67	0.6
High-Nt	29.05	6.78	77	8.4
Low-T	14.96	1.19	55	0.4
Low-W	16.17	0.41	63	1.6
Acid treated	42.80	2.14	-	-
Acid treated*	29.75*	4.56*	-	-

The six major ammonolysis and hydrolysis by-products formed during varying AFEX severities (See **Table 4.A.1** for description of AFEX severities) were quantified

(as mg analyte per gm original substrate) by LC-MS/MS and are depicted in **Table 5.2**. Untreated and dilute-acid treated corn stover data have been reported as well. It was found that near theoretical cleavage of the acetyl linkages to acetic acid was obtained for dilute acid treatment resulting in close to 35 mg acetic acid per gram of dilute acid treated corn stover.

Table 5.2 *Six major ammonolysis and hydrolysis by-products (mg analyte per gm untreated corn stover) of acetyl, coumaroyl and feruloyl based ester linkages produced during AFEX and dilute acid pretreatment of corn stover. See Table 4.A.1 for description of each AFEX severity. NA – not applicable*

	Acetic acid		**Coumaric acid**		**Ferulic acid**	
mg/g biomass	*Mean*	*Std Dev*	*Mean*	*Std Dev*	*Mean*	*Std Dev*
Untreated	1.61	0.02	0.44	0.03	0.117	0.004
Low-N	4.45	0.06	2.57	0.18	0.50	0.04
Regular	4.61	0.02	1.89	0.09	0.16	0.01
High-Nt	3.78	0.49	1.30	0.12	0.18	0.02
Low-T	3.03	0.19	1.82	0.11	0.14	0.01
Low-W	4.90	0.43	1.90	0.10	0.21	0.01
Acid treated	34.77	6.3	0.741	0.045	0.428	0.023
	Acetamide		**Coumaroyl amide**		**Feruloyl amide**	
mg/g biomass	*Mean*	*Std Dev*	*Mean*	*Std Dev*	*Mean*	*Std Dev*
Untreated	NA	NA	NA	NA	NA	NA
Low-N	21.89	1.79	2.96	0.04	1.58	0.06
Regular	25.04	1.10	3.91	0.14	4.70	0.39
High-Nt	32.90	2.18	6.90	0.31	7.67	0.48
Low-T	24.11	3.67	2.22	0.09	2.47	0.07
Low-W	28.02	4.18	2.44	0.08	2.53	0.17
Acid treated	NA	NA	NA	NA	NA	NA

However, only 10-15% of the total acetyl ester linkages were hydrolyzed to acetic acid during AFEX (for varying AFEX severities assuming maximum acetyl content to be 35 mg/g biomass, based on results from dilute-acid treated corn stover as shown in Table 5.2). Most of the acetyl linkages were ammonolyzed to acetamide during AFEX, which has been reported earlier for supercritical ammonia based treatments of birch wood [162].

The extent of cleavage of the acetyl linkages for Low-N, Regular, High-Nt, Low-T and Low-W, based on the average composition, was found to be around 75%, 85%, 105%, 78% and 94%, respectively. This would suggest that irrespective of the pretreatment severity, close to 80-100% of the acetyl linkages are hydrolyzed or ammonolyzed during AFEX. Higher % conversions to acetamide are noted for pretreatment conditions carried out at higher ammonia to water loadings (3:1 in presence of 0.6:1 water or 1:1 in absence of water) for longer residence times (45 min). AFEX reaction temperature (70 vs. 130 °C) does not seem to play a significant role in the cleavage of acetyl linkages, at sufficiently long residence time periods (15 mins). However, it would be of interest to carry out detailed kinetic studies to develop kinetic models for ammonolysis and hydrolysis of acetyl linkages during AFEX.

The extent of ammonolysis and hydrolysis of coumaroyl and feruloyl based ester linkages was more closely affected by AFEX pretreatment severity. The maximum amount of cleaved coumaroyl and feruloyl linkages (as acids and amides) during High-Nt AFEX were about 8.2 and 7.85 mg/g substrate, respectively. Interestingly, the total amount of phenolic acids (coumaric and ferulic) present after dilute acid treatment is significantly lower. This is most likely due to the acid catalyzed decarboxylation of the hydrolyzed phenolic acids during dilute acid pretreatment [350,351]. Some of the by-products of these acid catalyzed degradation reactions of phenolic acids are shown in **Table 5.3**. The ratio of the ammonolysis to hydrolysis products was found to be closely dependent on the AFEX pretreatment conditions employed (High-Nt vs. Low-N) and the type of ester linkage (acetyl vs. phenolic ester linkage). The ratio of coumaroyl amide (and feruloyl data in parentheses) to coumaric acid produced during Low-N, Regular,

High-Nt, Low-T and Low-W was found to be 1.15 (3.16), 2.07 (29.38), 5.31 (42.61), 1.22 (17.64) and 1.28 (12.05), respectively. The extent of ammonolysis to hydrolysis for the coumaroyl and feruloyl linkages (based on ratio of acids to amides formed) were 4.6 and 13.5 fold higher, respectively, for High-Nt versus Low-N based AFEX condition. This would suggest that the feruloyl linkages are more strongly affected by AFEX pretreatment severity. The total coumarate and ferulate content of all pretreated substrates was found to be within the range (10-20 mg phenolic acids per gram of untreated cell wall) of previously reported data for maize stalks [330,352]. It has been previously reported that the maximum amount of coumaric acid and ferulic acid based ester levels in maize internodes can reach as high as 20 and 7 mg/g biomass, respectively [81]. It is possible that the amount of total phenolic acid content would be higher considering most of the ferulic acid is ether linked and is not detected during conventional saponification based assays. Coumaric acid has been found to be extensively esterified (80-90% ester content) to lignin, as compared to ferulic acid that is extensively linked to arabinose side-chains (30-50% ester content). Ferulic acid based ester-ether linkages between lignin and hemicellulose are thought to be major impediments to enhanced enzyme digestibility [331]. Ferulate based hemicellulose esters have been known to be essential nucleation sites for lignification during grass cell wall growth [84,276,332]. There was indeed a strong linear correlation (R^2 = 0.87) found between the extent of feruloyl linkage cleavage during AFEX to the enzymatic digestion rate of cellulose as shown in **Figure 5.1**.

Table 5.3 *Mass balances for major degradation products (mg analyte per gm untreated corn stover) produced during AFEX (for Regular and High-Nt severities) and dilute acid based pretreatment of corn stover based on GCMS (*), HPLC-MS/MS (ammonolysis** based) and HPLC-RI (***) analyses. Where; ND and NA stand for not detected and not available, respectively.*

Category	Degradation products	Untreated	Regular	High-Nt	Acid treated	Untreated	Regular	High-Nt	Acid treated
	mg analyte/gm dry wt biomass	*Mean*	*Mean*	*Mean*	*Mean*	*Std Dev*	*Std Dev*	*Std Dev*	*Std Dev*
Carboxylic acids	malonic acid	0.061	0.055	0.045	0.021	0.013	0.004	0.006	0.011
	lactic acid	0.127	0.290	0.277	1.567	0.028	0.072	0.244	0.110
	maleic acid	0.004	0.006	0.016	0.019	0.002	0.005	0.020	0.007
	cis-aconitic acid	0.714	0.397	0.376	0.024	0.622	0.030	0.025	0.011
	methylmalonic acid	0.024	ND	ND	ND	0.042	-	-	-
	succinic acid	0.284	0.491	0.397	0.213	0.045	0.114	0.030	0.028
	fumaric acid	0.230	0.240	0.135	0.040	0.126	0.196	0.003	0.001
	trans-aconitic acid	0.991	1.874	1.529	0.275	0.480	0.122	0.019	0.186
	levulinic acid	0.084	0.078	0.086	3.220	0.110	0.030	0.034	2.058
	glutaric acid	0.005	0.007	0.015	0.012	0.000	0.002	0.006	0.005
	itaconic acid	0.006	0.019	0.036	0.621	0.002	0.009	0.020	0.019
	2-hydroxy-2-methylbutyric acid	0.003	0.003	0.001	0.001	0.0005	0.0004	0.0002	0.001
	gallic acid	ND	ND	ND	0.002	-	-	-	0.001
	adipic acid	0.003	0.002	0.003	0.005	0.001	0.0004	0.0003	0.003
	acetic acid*	1.61	4.61	3.78	34.77	0.02	0.02	0.49	6.3
	formic acid	0.324	0.912	NA	3.172	-	-	-	-
Amides	feruloyl amide**	ND	4.703	7.666	ND	-	0.392	0.476	-
	coumaroyl amide**	ND	3.91	6.9	ND	-	0.14	0.31	-
	acetamide*	ND	25.04	32.9	ND	-	1.1	2.18	-
Furans	2-furoic acid	0.003	0.005	0.005	0.158	0.002	0.000	0.002	0.064
	5-hydroxymethyl furfural*	0.07	0.64	NA	15.7	0.07	0.6	-	4.3
	furfural*	0.001	0.003	0.002	7.94	0.0005	0.0003	0.0004	0.74
Sugars	glucose (monomeric and oligomeric)***	27	18	NA	59	3.1	1.5	-	5.5
	xylose (monomeric and oligomeric)***	1.2	50	NA	184	0.1	10.5	-	18.9
	arabinose (monomeric and oligomeric)***	0.3	10	NA	30	0.1	2.8	-	3.3

Table 5.3 *Contd…*

Category	Degradation products	Untreated	Regular	High-Nt	Acid treated	Untreated	Regular	High-Nt	Acid treated
	mg analyte/gm dry wt biomass	*Mean*	*Mean*	*Mean*	*Mean*	*Std Dev*	*Std Dev*	*Std Dev*	*Std Dev*
Aromatics	3,4-dihydroxybenzoic acid	0.007	0.006	0.005	0.018	0.002	0.000	0.001	0.008
	3,5-dihydroxybenzoic acid	ND	ND	ND	ND	-	-	-	-
	2,5-dihydroxybenzoic acid	ND	ND	ND	0.007	-	-	-	0.003
	3,4-dihydroxybenzaldehyde	0.003	0.005	0.006	0.012	0.000	0.000	0.001	0.005
	salicylic acid	0.023	0.023	0.027	0.038	0.002	0.004	0.005	0.016
	4-hydroxybenzeldehyde	0.012	0.098	0.095	0.096	0.003	0.016	0.006	0.045
	vanillic acid	0.027	0.050	0.057	0.065	0.009	0.017	0.008	0.023
	homovanillic acid	ND	0.003	0.007	0.009		0.002	0.004	0.004
	4-hydroxyacetophenone	0.001	0.016	0.008	0.015	0.000	0.010	0.001	0.007
	caffeic acid	0.008	0.006	0.006	0.033	0.004	0.002	0.003	0.020
	syringic acid	0.012	0.019	0.027	0.115	0.003	0.001	0.001	0.064
	vanillin	0.014	0.191	0.287	0.162	0.004	0.014	0.059	0.065
	4-hydroxybenzoic acid	0.000	0.001	0.001	0.001	0.000	0.0002	-	0.001
	benzoic acid	0.010	0.007	0.005	0.010	0.008	0.001	0.001	0.004
	syringaldehyde	0.004	0.013	0.009	0.089	0.001	0.003	0.003	0.017
	p-coumaric acid*	0.440	1.890	1.300	0.741	0.030	0.090	0.120	0.045
	ferulic acid*	0.117	0.160	0.180	0.428	0.004	0.010	0.020	0.023
	sinapic acid	0.002	0.007	0.003	0.008	0.002	0.006	0.003	0.003
	4-hydroxycoumarin	ND	ND	ND	0.001	-	-	-	0.001
	ortho-toluic acid	0.001	0.001	0.001	0.001	0.001	0.0005	0.0003	0.001
	para-toluic acid	0.039	0.027	0.022	0.035	0.033	0.006	0.001	0.025
Mass Balance	**Total Identified Components (mg/g biomass)**	34	124	56	343				
	Total Extracted Water Solubles	44	193	291	428				
	Total Extracted MTBE Solubles	18	38	NA	288				
	% Mass Closure	76	64	NA	80				

Figure 5.1 *Correlation between extent of enzymatic digestibility (Y, 24 hour, % Glucan conversion) and total feruloyl amide content (X, mg/gm biomass) of the varying AFEX severity treated corn stover substrates*

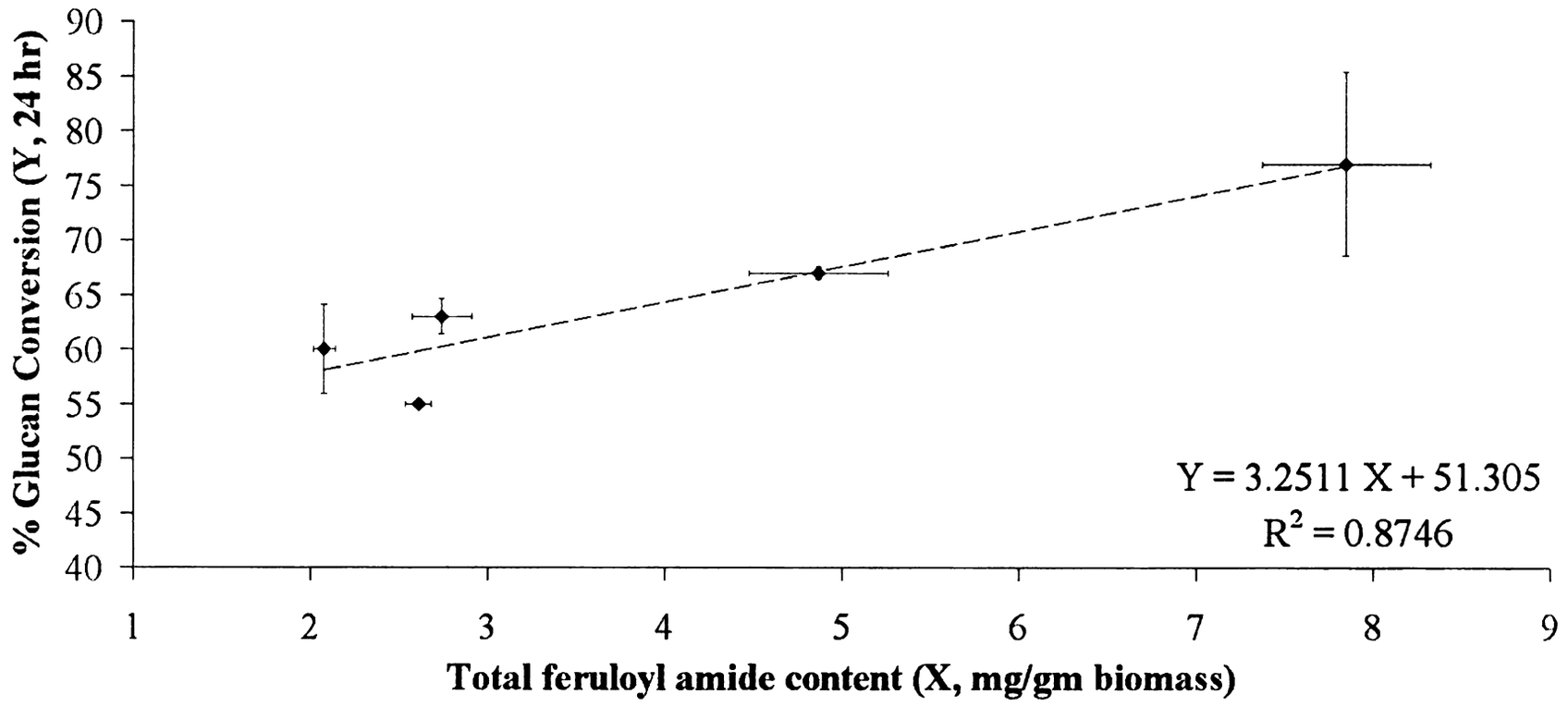

It is important to note that during conventional AFEX (or Regular) there is a significant amount of unhydrolyzed acetyl (15%), coumaroyl (30%) and feruloyl (40%) linkages. This would suggest the necessity for additional esterase activity in enzyme cocktails for efficient hydrolysis of AFEX treated corn stover (See Chapter 7).

Non-ammonolysis reactions (e.g. Maillard reactions between ammonia and reducing sugars) during AFEX pretreatment of cell walls have not been studied in the past. The extent of nitrogen incorporated within the cell wall during AFEX due to reaction of reducing sugar aldehyde end groups with ammonia was explored by carrying out AFEX on crystalline cellulose (i.e. Avicel) for two pretreatment severities (AFEX-L and AFEX-H). The amount of nitrogen incorporated within the polysaccharide was quantified by Kjeldahl method (**Table III-5.4**). There was a 280% increase in the total nitrogen content of AFEX treated corn stover compared to untreated corn stover, largely due to formation of ammonolysis by-products (acetamide, feruloyl amide, coumaroyl amide). However, the total measured ammonolysis by-products account for less than one-third of the total nitrogen incorporated within the biomass after AFEX (26 mg total Nitrogen reacted per gm corn stover based on Kjeldahl analysis). This would suggest that significant loss of ammonia during AFEX due to unwanted side-reaction of soluble saccharides and insoluble polysaccharides with ammonia that result in the formation of imidazoles and pyrazines [353]. Aromatization of soluble carbohydrates via condensation with ammonia/amines, dehydration and polymerization has been well documented over the years [319,321,322,353-356]. However, the final products of Maillard reactions have been poorly characterized due to enormous complexity in the reaction chemistry. The reaction of ammonia with insoluble polysaccharides (Avicel) was briefly explored for

two AFEX conditions (AFEX-L and AFEX-H, See **Table III-5.4** for details). Interestingly, increasing the ammonia loading by three-folds produced nearly three-fold higher nitrogen content of the treated samples. A similar stoichiometry (1:1) of nitrogenous adducts formed during reaction of sugars with amino acids has been seen for Maillard based reactions [354,356]. Analysis of the treated samples by ESCA revealed that there was a significant increase in the C1 carbon signal (representative of C-C linkages) after AFEX, especially at the higher treatment severity (AFEX-H). This would suggest significant aromatization of the insoluble polysaccharides due to condensation reactions with ammonia that would result in an increase of the C1 carbon signal (via reduction of C-O linkages driven by dehydration of sugars). Extensive extractions of the AFEX treated substrates with methanol (at 50 °C) were insufficient to completely remove the nitrogenous compounds. Nearly 35-40% of the total nitrogenous product seemed to be chemically bound to the insoluble polysaccharide. Enzymatic hydrolysis (by cellulase mixtures and purified cellulase enzymes; data not shown) of AFEX-L and AFEX-H treated avicel resulted in 10-20% and 50-60% lower glucan hydrolysis yields (compared to untreated control), respectively. Extensive hot water and methanol extractions of the treated Avicel substrate (AFEX-H) were unable to minimize enzyme inhibition, which would suggest significant modification of the insoluble polysaccharide has rendered the substrate highly indigestible. Extensive inhibition of glycosyl hydrolases by the Maillard based nitrogenous products (both insoluble and soluble) formed during high severity AFEX is likely and would need to be further explored. The extent of formation of biologically toxic nitrogenous coumpounds, like 4-methylimidazole, during AFEX is currently unknown. These studies warrant further investigation of the nitrogenous

reactions during AFEX, possibly driven due to condensation of reducing aldehyde ends of soluble and insoluble polysaccharides with ammonia.

5.1.4.2 Degradation products formed during dilute acid and AFEX pretreatment

One of the leading obstacles in comparison of degradation products generated by different pretreatment methods is the lack of a common analytical basis for comparison. These current studies help quantify and compare some of the major degradation products from two leading pretreatment technologies, AFEX and dilute-acid pretreatment. The quantification of major degradation products would allow future studies dealing with adaptation of enzymes and ethanologenic strains to various inhibitory compounds. This would be relevant for high-solids loading based hydrolysis and fermentation that is expected for industrial based biorefinery processing. A detailed mass balance for the various categories of degradation products (i.e. carboxylic acids, furans, amides, sugar oligomers, aromatics) formed during AFEX (Regular and High-Nt based severities) and dilute acid pretreatment is provided in **Table 5.3**. The degradation products chosen for quantification were based on previously published literature and ease of commercial availability. The mass balance closure is 76%, 105% and 64% (with respect to total ASE based water extractibles) for untreated, dilute acid and Regular-AFEX treated corn stover based degradation products, respectively.

Unlike AFEX, there was a significant degradation of the sugar monomers and oligomers to furan based derivatives during dilute acid pretreatment (e.g. furoic acid, furfural, 5-hydroxymethyl furfural). Nearly, 20-25 mg of furan based compounds per gm of dilute acid treated substrate was found compared to negligible amounts formed during AFEX (<1 mg/gm substrate). Furan based derivatives are known to significantly inhibit

cellulase and microbial activity during enzymatic hydrolysis and fermentation, respectively [338,357,358]. Furfural and 5-HMF are typically formed during acid catalyzed dehydration of xylose and glucose, respectively [359]. Furfural and 5-HMF further degrade to form levulinic and formic acids during acid treatment.

It was of interest to find that most of the xylan and arabinan was hydrolyzed during dilute-acid treatment to monomeric xylose and arabinose (85% and 70% of theoretical xylan and arabinan content, respectively). The remaining 15% xylan and 30% arabinan was in the oligomeric form. Unlike dilute acid treatment, most of the arabinoxylan released during AFEX from corn stover was in the oligomeric form. The total water extractible arabinoxylan content for AFEX corn stover was roughly 22% and 24% of theoretical xylan and arabinan, respectively. Previous work with sodium and ammonium hydroxide treated grasses have quantified the release of high molecular weight branched arabinoxylan oligomers [360,361]. Ammonia catalyzed cleavage of the diferulate bridges that cross-link hemicellulose oligomers would be responsible for the enhanced release of the arabinoxylan rich oligomers for AFEX versus untreated cell walls.

Alkali induced degradation of polysaccharides (typically for xylan, starch and soluble saccharides) to carboxylic acids is another important class of degradation products (via peeling reaction mechanisms, [344,362,363]) produced during alkaline pretreatments. Pretreatment temperature (150-200 °C) and base catalyst (1-3 M NaOH) loading have been found to significantly affect the formation of mono and di-carboxylic acids from cellulose and hemicellulose [344]. Typical carboxylic acids formed during alkali induced polysaccharide degradation, in order of abundance, are lactic, succinic and

other saccharinic acids [320]. Divalent cations (like calcium) are known to favor the formation of lactic acid even at lower alkaline treatment severities [362], which could explain the 2-3 fold increase in lactic and succinic acid concentration within the treated cell walls after AFEX. Alkali-induced peeling, stopping and termination reactions are expected to result in the formation of several types of carboxylic acids during biomass alkaline based pretreatments. The extent of degradation of polysaccharides to some these mono (lactic, formic) and di-carboxylic (succinic) acids have been reported here. However, the extent of polysaccharide degradation during AFEX is substantially lower than sodium hydroxide based pulping (based on total lactic acid formed per gm of original substrate). Some of the lower molecular weight carboxylic acids (glycolic, lactic) are expected to be formed for more severe pretreatment conditions (higher temperatures and/or alkalinity). Formation of di-carboxylic acids, like succinic, is typical for higher alkali concentrations [344]. Interestingly, high concentrations of trans-aconitic acid were detected after AFEX (1.5-2 fold higher than untreated control). Trans-aconitic acids have been found in high concentrations (10-20 mg/gm cell wall) in certain forage grasses in earlier studies [364], and are probably more easily extractable from the cell wall after AFEX. Despite minor alkali induced degradation of polysaccharides during AFEX, there were significantly more aliphatic carboxylic acids formed during dilute-acid (40-50 mg/g substrate) pretreatment. Saccharinic acids are expected to be the significant C6-organic acids formed at lower temperatures from cellulose and hemicellulose. However, gluco- and xylo- isosaccharinic acids were not quantified in this study. It would be necessary to determine the extent of formation of saccharinic acids during AFEX to achieve mass balance closure.

Lignin based degradation products have been quantified in the past by capillary electrophoresis and mass spectrometric based methods [334,349,365]. Several aromatic based degradation compounds (syringaldehyde, 4-hydroxyacetophenone, phenolic acids) are formed during AFEX and dilute acid based pretreatments. Phenolic aldehydes, like syringaldehyde, are likely produced under oxidative acidic conditions and are one of the major lignin degradation products formed during acid pretreatment of corn stover [137,180,366]. Some components such as 4-hydroxybenzaldehyde and 4-hydroxybenzoic acid are thought to be monomeric lignin extractives that are released during the pretreatment process, unlike other lignin cleavage products [367,368].

Compared to dilute acid pretreatment, 4-hydroxybenzaldehyde and vanillin are the only components that are produced in significant quantities during AFEX (compared to untreated control). The concentration profiles of aromatic compounds formed during Regular and High-Nt AFEX severities are largely similar, except formation of 50% higher relative concentration of vanillin for the latter severity. It is likely that the 4-hydroxybenzaldehyde produced during acid pretreatment is further degraded via hydrolytic/oxidative cleavage resulting in overall lower concentrations. Certain aromatic acids (e.g. syringic acid) are likely also formed via oxidation of their corresponding aldehydes.

It has been shown that the most inhibitory compounds, apart from the furans, found in dilute acid treated corn stover hydrolyzates appear to be lignin derived and are mostly ferulic and coumaric based based compounds [369]. There are several other lignin polyphenolics and insoluble lignin compounds that have not been identified for either dilute acid or AFEX based treatments. Previous work has shown presence of lignin

oligomers and other re-polymerization products that are difficult to identify due to the heterogeneity and complexity of their molecular structures [151,180,369,370].

5.1.4.3 Inhibition of glycosyl hydrolases by AFEX degradation products

AFEX extracted ligno-phenolic fragments and other extractives deposited on the biomass surface are preferentially removed during the ASE water extraction step. Removing these degradation products has been shown to enhance the rate of enzymatic hydrolysis, based on the hydrolysis data for washed and unwashed AFEX treated corn stover fractions [1]. The surface ligno-phenolic fragments and other degradation products might inhibit glycosyl hydrolase activity [250,251,371,372]. AFEX treated corn stover water ASE extracts were used to carry out crystalline cellulose (Avicel) hydrolysis and were found to exert a significant inhibitory effect on the cellulase complex (**Figure 5.2**). The effect of enzyme loading (12-48 mg total enzyme/g glucan) and hydrolysis time period (24-168 hrs) on the hydrolysis kinetics of crystalline cellulose were studied in the presence/absence of the degradation product extracts. The presence of AFEX corn stover degradation products resulted in a 33% lower hydrolytic rate (dY/dX) of crystalline cellulose, based on initial glucan hydrolysis rate (**Figure 5.2 (a)**, at X = 0). It was also found that the overall reduction in hydrolysis yield was largely independent of time of hydrolysis. Not surprisingly, the extent of inhibition was found to be dependent on the total enzyme loading employed during hydrolysis. There was 35% and 25% reduction in overall hydrolysis yield for cellulose in the presence of AFEX degradation products at 12 and 48 mg total enzyme loading (Spezyme CP + Novo 188 at equiprotein mass loading), respectively. Previously reported data indicates improvement in hydrolysis yields for water washed steam explosion and AFEX pretreated biomass [338,341].

Figure 5.2 *Effect of regular AFEX corn stover degradation products (ASE extracted using hot water) on cellulase activity (hydrolyzing crystalline cellulose) as a function of hydrolysis time and total enzyme loading. Control experiment (a) was Avicel hydrolyzed by 15 FPU (or 22 mg) Spezyme CP/g glucan (supplemented with 38 mg/g glucan of Novo 188), in the absence of AFEX stover water extract, for various time points (24-168 hours). Control experiment (b) was Avicel hydrolyzed for 24 hours, in the absence of AFEX stover water, for various total enzyme loadings (12-48 mg/g glucan of Spezyme/Novo 188 in a fixed mass ratio of 37:63).*

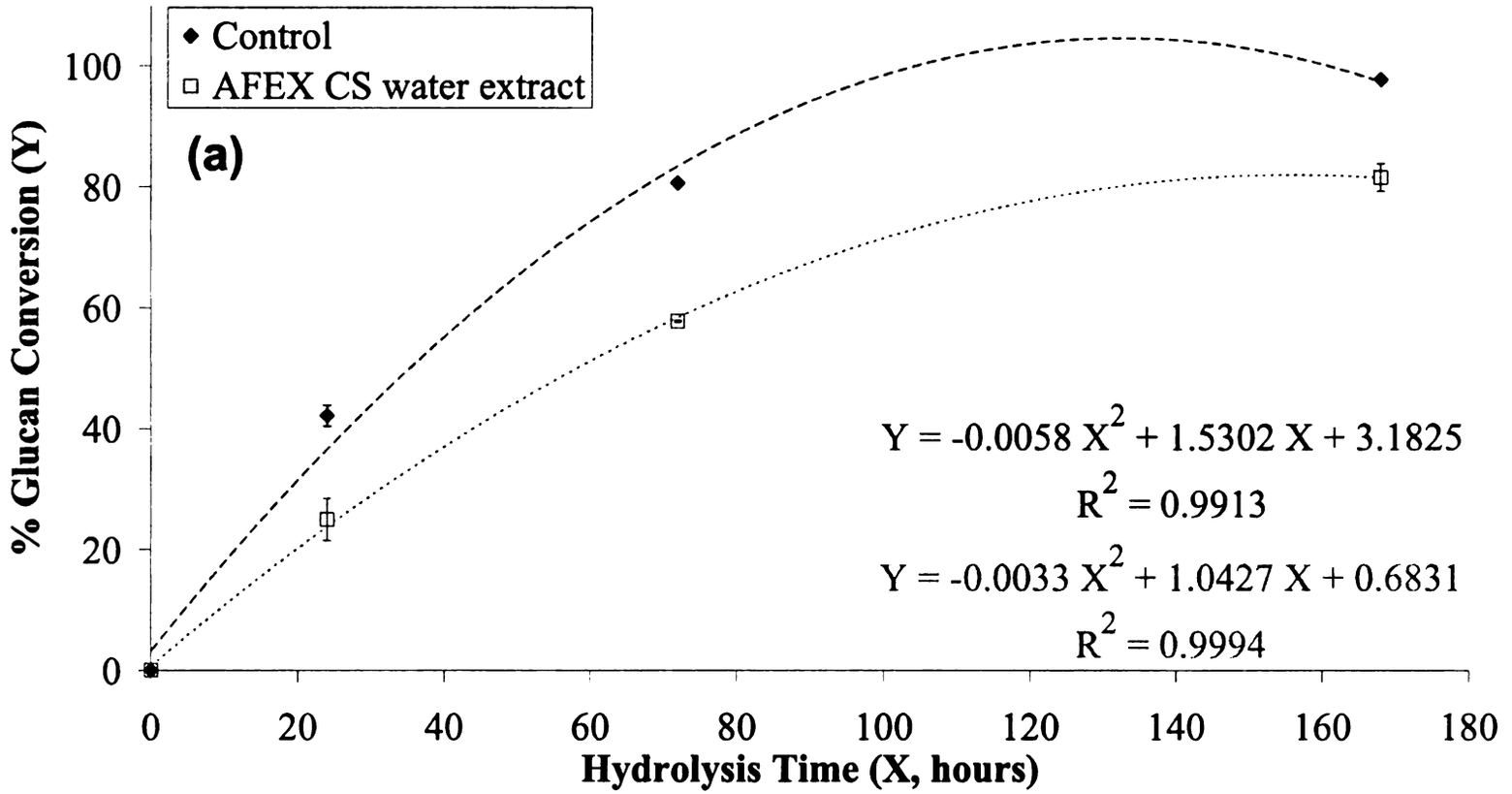

Figure 5.2 *Contd...*

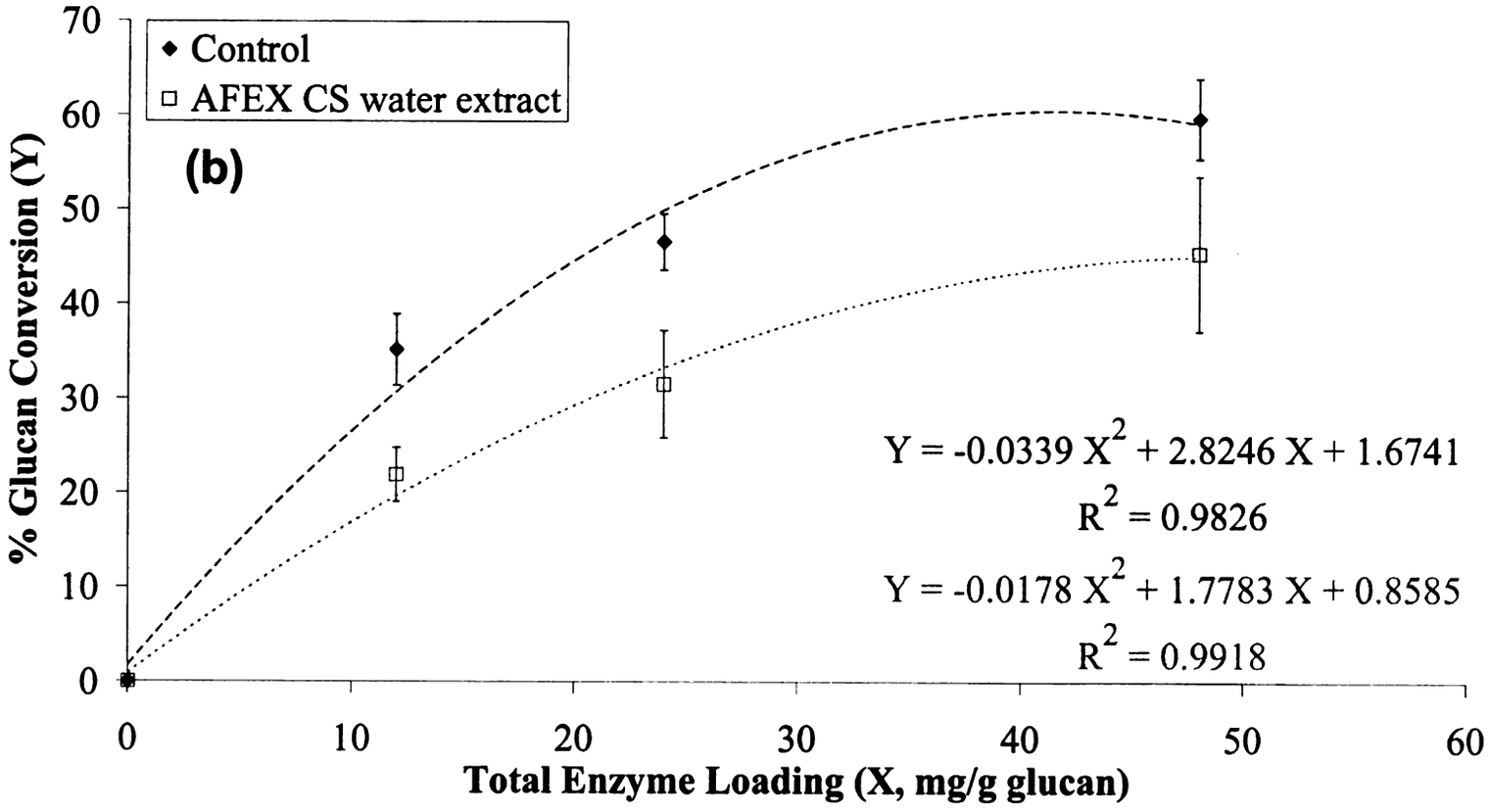

However, the nature of the inhibitory compounds produced in steam explosion is likely different from the AFEX process [339]. It would be of interest to determine the major degradation compounds (e.g. amides, oligosaccharides, lignin degradation products) formed during AFEX that inhibit the cellulases. Mixed lignin derivatives have been previously reported to be substantially detrimental to commercially available cellulase activity [91]. Literature reports show that cellulolytic enzyme systems; consisting of cellulases, β-glucosidases and xylanases, are varyingly inhibited depending on their microbial source. Phenolic compounds (p-coumaric acid, ferulic acid and vanillin) resulted in less than 10% reduction in activity of *B. ruminicola* β-glucosidase; whereas, *B. succinogenes* glucosidase activity is more severely inhibited (15-70%) depending on the concentration and type of phenolic compounds [373]. The commercial cellulase enzyme tested for hydrolysis originated from a strain of *Trichoderma reesei*, whereas the Novozym 188 β-glucosidase originated from a strain of *Aspergillus niger*. Recent research has shown that cellulases and pectinases from *T. reesei* are severely inhibited by phenolic compounds extracted from flax bast tissue [374]. Wet oxidation pretreatment of wheat straw produces large quantities of formic acid that completely deactivate cellulolytic and xylanolytic enzymes and are substantially toxic to *S. cerevisiae* fermentation [375]. Panagiotou and Olsson (2006) also reported substantial reduction (40-60%) in the xylanase activity in presence of different potentially inhibitory compounds [375]. More research is critical to evaluate the effect of potential inhibitors in AFEX hydrolyzates on individual enzyme activities. This information will be a critical determinant in developing the exact mixture of enzymes necessary for maximizing glucan and xylan digestibility in AFEX treated cell walls.

Even though acetic acid and other organic acids are potentially not inhibitory to enzymatic activity at their present concentration for AFEX corn stover extracts, these acids are ubiquitous inhibitors found in several fermentation hydrolysates [137]. The lag phase for *Saccharomyces cerevisiae* was found to be exponentially increased in presence of acetic (0.05-0.1%, w/w) and lactic acid (0.2-0.8%, w/w) in a minimal media broth, in turn reducing the specific growth rate as well [376]. Importantly, the degree of microbial inhibition due to organic acids is largely dependent on the pH of the medium, nature and concentration of the inhibitor [377]. Phenolics are also found to inhibit microbial activity through interference with soluble sugar uptake [373,378]. Despite the inhibitory components produced during the AFEX process, though in much lower concentrations compared to other thermochemical pretreatments, it was found that final AFEX corn stover enzymatic hydrolysate could be easily fermented by *E. coli* KO11 (*E. coli* fermentation data not shown) and *S. cerevisiae 424A (LNH-ST)* without any additional detoxification step [379]. However, it was found that the lag phase for microbial growth was slightly longer for the unwashed AFEX corn stover hydrolyzate compared to the washed substrate hydrolyzate (unpublished data).

5.1.5 Conclusions

A detailed mass balance for various plant cell wall (corn stover) degradation products formed during AFEX and dilute acid pretreatment, with 64% and 105% mass closure, was presented in this chapter. Unlike dilute acid treatment, ammonolysis reaction by-products (acetamide, coumaroyl amide, feruloyl amide) were the predominant cell wall degradation products formed during ammonia based pretreatments. The cleavage of the acetyl linkages during AFEX was found to be less sensitive to AFEX pretreatment

severity (ammonia/water loading, temperature, residence time) compared to ammonolysis of feruloyl/coumaroyl ester linkages. There was strong linear correlation (R^2 = 0.87) between the total ferulate ester linkages cleaved and the overall enzymatic hydrolysis rate. Formation of alkali induced peeling reaction degradation products (lactic, succinic acids) for AFEX treated corn stover was observed. However, the extent of end-group peeling catalyzed degradation reactions were significantly lower (100-200 fold lower concentrations, as mg analyte per gm substrate) than previously reported results [320]. Nearly 70-85% of the total arabinoxylan content of corn stover was acid hydrolyzed to monomeric sugars during dilute acid pretreatment, with the remaining arabinoxylan was present in the oligomeric form. However, only 25% of the total arabinoxylan content was released from the cell wall during AFEX as oligomers. Sugar degradation during dilute acid treatment resulted in 25-30 mg of furan based by-products per gm substrate, unlike AFEX where negligible formation of furans took place. Syringaldehyde, 4-hydroxybenzaldehyde, vanillin and 4-hydroxyacetophenone were the major lignin based degradation products formed during dilute acid and AFEX based treatments, in varying concentrations. It was also found that AFEX degradation products (i.e. hot water extractives from AFEX corn stover) severely inhibited cellulase activity on crystalline cellulose depending on hydrolysis time and total enzyme loading employed (25-40% lower than control). However, the exact chemical composition of these inhibitory degradation products is not known. It would be necessary to conduct more detailed kinetic studies in the future to study the effect of various AFEX pretreatment parameters on the extent of ammonolysis and hydrolysis of the LCC ester linkages. Also, the extent of Maillard based reactions due to reaction of ammonia with solubles sugars and

insoluble polysaccharides is currently unclear and needs further exploration in order to commence animal feed trial studies using AFEX treated biomass [9].

CHAPTER 6: DEVELOPMENT OF A HIGH-THROUGHPUT MICROPLATE BASED ENZYMATIC HYDROLYSIS METHODOLOGY

6.1.1 Abstract [v]

Several factors influence the viability of a biochemical platform for manufacturing lignocellulosic based fuels and chemicals (e.g. crop yield, pretreatment severity, enzyme loading). Past research on biomass conversion has focused largely on acid based pretreatment technologies that fractionate lignin and hemicellulose from cellulose. However, for alkaline based (e.g. AFEX) and other lower severity pretreatments it becomes critical to co-hydrolyze cellulose and hemicellulose using an optimized enzyme cocktail. Lignocellulosics are appropriate substrates to assess hydrolytic activity of enzyme mixtures compared to conventional unrealistic substrates (e.g. filter paper, chromogenic and fluorigenic compounds) for studying synergistic hydrolysis. However, there are few, if any, high-throughput lignocellulosic digestibility analytical platforms for optimizing biomass conversion. The "Biomass Conversion Research Lab" (BCRL) microplate method is a high-throughput, small scale assay developed to study digestibility of lignocellulosic biomass in a cost-effective manner compared to conventional methods. The most suitable method for delivering milled biomass to the microplate was through multi-pipetting slurry suspensions. Rapid bio-enzymatic, spectrophotometric based assays were developed to determine fermentable sugars. The entire procedure was automated using a robotic pipetting workstation. Several parameters that affect hydrolysis in the microplate were studied and optimized (i.e. particle size reduction, slurry solids concentration, glucan loading, mass transfer issues and time

---

[v] A version of this chapter was published as Chundawat S.P.S, Balan V., Dale B.E. 2008. *High-throughput microplate technique for enzymatic hydrolysis of lignocellulosic biomass.* Biotechnology and Bioengineering, 2008. 99(6): p. 1281-1294.

period for hydrolysis). The microplate method was optimized for crystalline cellulose (Avicel) and ammonia fiber expansion (AFEX) pretreated corn stover.

6.1.2 Background

A recent Department of Energy publication [380] envisioning biorefineries identifies several critical biological barriers that impede utilization of lignocellulosic biomass as a bio-feedstock. Identification of the primary barriers to plant cell wall hydrolysis will allow development of new crops, enzymes and microbes to facilitate bioconversion. Manipulation of cell wall synthesis regulatory pathways may allow development of a new generation of energy crops that is more easily hydrolyzable. Discovering novel extremophilic microbes and optimizing enzyme mixtures that can synergistically break down holocellulose and lignin would help greatly reduce pretreatment severity. However, each of these research initiatives would falter without a suitable high-throughput assay technique to assess biomass digestibility quickly and reproducibly.

One of the primary biofuel research agendas for 21st century according to a recent European Union EPOBIO project report identified a need for a reliable and high-throughput digestibility assay for lignocellulosics [381]. Recent developments in molecular biology and site directed mutagenesis have allowed significant advances in designing tailor-made cellulolytic enzymes and microbes [382]. However, conventional enzymatic hydrolysis protocols to screen potency of these novel enzymes and their mixtures are rather tedious and time consuming. In an effort to study biomass digestibility of diverse sources (e.g. energy crops, agricultural residues, and municipal waste) as a function of enzyme combinations (i.e. cellulases, xylanases, pectinases,

esterases, glucosidases) and pretreatment methods (i.e. AFEX, organosolv, dilute-acid), it becomes critical to conduct and analyze a large number of experiments.

In order to achieve this goal there is need for a highly automated, rapid and reliable enzyme assay to screen enzyme combinations and loadings for a variety of lignocellulosic substrates. Presently, cellulolytic enzymes are screened for their cellulase activity using the International Union of Pure and Applied Chemists (IUPAC) standard filter paper assay (FPA). However, the IUPAC FPA assay [383] utilizing filter paper as the substrate is plagued by several disadvantages for high-throughput assays. Primary disadvantages are long assay periods, high labor inputs, high sensitivity and poor reproducibility [384]. Poor reproducibility of the FPA assay is due to several factors such as filter paper properties (i.e. size, shape and folding) and accessory enzyme components (e.g. β-glucosidase). Other cellulolytic enzyme activities (e.g. xylanolytic, cellobiase) estimated using conventional substrate assays (e.g. filter paper, cellobiose, oat spelt and birch wood xylan) are not representative of their true hydrolytic efficiency on a realistic biorefinery feedstock, i.e. lignocellulosic substrates. It has been recently shown that the enzyme combination that produces the best hydrolytic yields depends on the characteristics of the substrate rather than on standard enzyme-activities measured [385]. The standard activity assays for enzymes do not correlate well with their true hydrolytic potential for different lignocellulosic substrates. Supplementary enzyme components (such as xylanases, acetyl esterase, feruloyl esterase and arabinofuranosidases) further aid synergistic hydrolysis of cellulose buried in a matrix of lignin and hemicellulose in plant cell walls. Therefore, conducting hydrolysis of lignocellulosics using enzyme mixtures

would allow better understanding of true synergistic enzyme interactions for lignocellulosic biomass.

Flow through pretreatments, such as dilute-acid, hot water, organosolv etc., typically remove most of the lignin and hemicellulose [108,109] into a separate liquid process stream. However, alkali based pretreatments such as ammonia fiber expansion (AFEX) can modify the cell wall ultra-structure without physically extracting lignin and hemicellulose into a separate liquid stream [386-388]. In general, the nature of the pretreated biomass and optimum hydrolytic enzyme combination varies depending on the cell wall composition, type and severity of thermochemical pretreatment.

There are notably two classes of substrates that are used for assaying cellulolytic enzyme activity; soluble and insoluble. Soluble substrates like cellodextrins and derivatives, nitrophenol oligosaccharides, dyed CMC and long chain cellulose derivatives are easier to adapt to high-throughput conditions. Insoluble substrates, like cellulose, cotton linters, fluorigenic and chromogenic cellulosics etc., are harder to adapt due to irreproducible solid substrate delivery, mixing and mass transfer problems. Several review articles [24,389] discuss pros and cons of available assays for cellulolytic enzymes. Little work has been done to establish a reliable and high-throughput hydrolysis assay protocol for insoluble lignocellulosic biomass. The conventional NREL (National Renewable Energy Laboratory) LAP-9 protocol [346] has been used extensively by researchers for studying biomass digestibility. However, the method is labor-intensive, low-throughput and requires a large quantity of substrate, enzyme and chemicals. Several researchers have developed high-throughput saccharification assays for crystalline cellulose and filter paper [390,391]. Decker et al. found that upon replacing filter paper

with Solka-floc, Sigmacell-20, Avicel and cotton linters one could largely automate the assay for a rather similar substrate in hydrolytic properties to filter paper [390]. Xiao et al. were successful in scaling down the reaction volume to 60 µl for filter paper based assay [391]. These assays were however not adapted to lignocellulosic biomass due to inherent variability and difficulty in delivering a suitable biomass fraction into a microplate. Recently, a high-throughput assay for lignocellulosics was developed by Berlin and colleagues [392] that utilize handsheet disks prepared from pretreated pulp biomass feedstocks. However, the handsheet preparation step requires special equipment; making it inconvenient and time consuming for utilization of small quantities of pretreated biomass from high-throughput pretreatment systems. The delivery of handsheet disks to the microplate is labor-intensive for high-throughput screening. The pulping and handsheet paper preparation process could modify the cell wall ultra structural properties; affecting its digestibility (probably making it more recalcitrant). Weimer and colleagues [393] have demonstrated good correlation between digestibility of herbaceous biomass measured by simultaneous hydrolysis and fermentation (SSF) to the amount of gas produced by ruminal inoculums. The method can be carried out in aseptic conditions and should be adaptable to high-throughput assays. Other high-throughput assays utilize fluorescent cellulosic derivatives and chromogenic substrates that are expensive and unsuitable to study digestibility of pretreated biomass [394-396].

We have scaled down the conventional test-tube (10-30 ml) saccharification method to micro-scale (100-1000 µl), carried out in 96-well plates fully adaptable to automation. Several issues have been addressed in this paper regarding solid delivery to microplates using biomass slurries, effect of particle size and mass transfer related

parameters, optimal microplate methodology, reproducibility and validity of the method compared to conventional NREL protocol. The current Biomass Conversion Research Laboratory (BCRL) microplate assay helps screen a larger gamut of variables (i.e. enzyme combinations, pretreatment severity) in a rapid, reproducible and efficient way that can provide reliable data applicable for scale-up operations (i.e. high solids loading hydrolysis and fermentation). A high-throughput hydrolysis assay is a key link in the chain of high-throughput screening efforts ranging from rapid pretreatment of several feedstocks to screening fermentation microbes for biomass conversion.

6.1.3 Materials and Methods

See appendix A-VII-1, 2, 3, 4, 23, 25, 26, 27, 28, 29, 30 and 31. An overview to the BCRL microplate based hydrolysis methodology is provided in **Figure 6.1**.

6.1.4 Results and Discussion

6.1.4.1 Effect of cell wall size reduction on enzymatic digestibility

One of the primary limitations for any high-throughput hydrolysis assay is the inherent difficulty in delivering reproducible amounts of solid substrate to a micro-reactor and overcoming mass transfer limitations during the course of the heterogeneous reaction. Size reduction of the substrate would help overcome both these limitations but at the cost of altering the tissue structure and its rate of digestion. Enzymatic digestibility of lignocellulosic biomass is dependent on several factors that can be largely classified on two levels; molecular and structural. Molecular factors include cellulose crystallinity, degree of polymerization, lignin and hemicellulose content, type of hemicelluloses, hemicellulose branching, acetyl content, syringyl to guiacyl lignin monomer ratio and lignin molecular weight etc. Structural factors include the lignin-hemicellulose physical

barrier to cellulose microfibrils, plant capillary porosity, particle size and specific surface area etc. There is overlap between these two categories on transition from a molecular to micro and eventually macro scale. Structural factors are the primary impediments to access of enzymes to the molecular substrate. Size reduction of biomass has been known to enhance digestibility of biomass due to several reasons; improvement in particle size/specific surface area being the primary factor [10]. Extensive ball milling of biomass was found to reduce cellulose crystallinity hence improving hydrolysis yield [16]. However, size reduction using a centrifugal mill for a short period of time (10-15 min) should largely allow preservation of molecular integrity on the ultra-structural level. Size reduction also influences pretreatment severity, depending on type of pretreatment [1,397,398]. Ten-fold particle size reduction of untreated corn stover (1000 μm to 100 μm) improved overall hydrolysis yield by 10-15%. AFEX pretreatment after size reduction showed a 5-10% improvement in glucan conversion if the samples were washed prior to hydrolysis [1]. These results indicate that size reduction helps increase biomass digestibility by enhancing surface area to volume ratio allowing higher enzyme and pretreatment chemical accessibility to the cell wall ultra-structure. However, when studying synergistic interaction of enzymes that co-hydrolyze lignocellulosic polymers, molecular factors are ultimately rate limiting.

6.1.4.2 Advantages of size reduction to high-throughput digestibility assays

Some of the primary advantages to size reduction for high-throughput digestibility assays are; (1) homogenization of the various biomass fractions of varying composition, (2) ease in delivery of ground substrate to microplate and (3) better mixing of biomass during hydrolysis in micro wells.

There is substantial variation in cell wall composition based on tissue type, location and structure. Corn stover fractions were found to show variability in glucan, xylan and lignin composition based on type of tissue [1]. It is important to homogenize the plant material and deliver a representative sample for digestibility assays. Size reduction allows homogenization of different plant tissues into a well mixed powder that allows delivery of truly representative samples.

Automation of digestibility assays would require rapid and reproducible delivery of solid substrate to each micro well. Size reduction of particulate biomass to a finely ground powder is a prerequisite to automation. There are two possible methods for delivery of ground biomass; solids delivery or slurry dispension. There are several advantages associated with each method; however, slurry dispension allows integration of a liquid dispensing robotic workstation to substrate delivery along with other pipetting steps. Pipetting steps involved in high-throughput digestibility assays include buffer and enzyme delivery, sampling of hydrolysate and colorimetric/spectrophotometric sugar assays. Cryogenic grinders and solid dispensing units are currently more expensive and take more time to deliver equivalent amounts of solids to microplates.

The two primary rate limiting factors of heterogeneous reactions are mass transfer (diffusion of enzyme and products to and from the substrate) and reaction rate (converting substrate to product) related. There are several stages involved in the hydrolysis of lignocellulosic biomass to monomeric sugars, namely; (1) Mass transfer of enzyme complex from liquid phase to solid substrate, (2) Adsorption of enzyme onto solid substrate active sites (and non-productive sites like lignin), (3) Hydrolytic reaction at surface and 2-dimensional surface propagation of adsorbed enzymes, (4) 3-

dimensional diffusion of free enzymes through micropores to new sites, (5) Mass transfer of reaction products (oligosaccharides, cellobiose, xylobiose) into liquid phase, (6) Homogeneous liquid phase hydrolysis of short chain oligosaccharides. The overall rate of the reaction is dependent on the rate of the slowest step of all these stages. Most enzyme kinetic studies ignore contribution of the external (mass transfer of enzyme and products through the stagnant film surrounding cellulosic solids) and internal (mass transfer of enzyme and products through lignocellulosic ultra structure) transfer resistances compared to the slower rate of hydrolysis. Van Dyke et al. found little influence of agitation on cellulose hydrolysis once the particles were completely suspended [399]. Size reduction should further help improve external and internal mass transfer of enzymes and products.

6.1.4.3 Advantages of centrifugal milling to size reduction

Ideally, one would like to conduct particle size reduction using a method that minimally alters the physical and chemical state of processed material. There are several mechanisms by which comminution can be achieved. Strain can be achieved by application of pressure (jaw crushers), impact (jet impact mills), friction (mortar mill), shear (rotor beater mill) and cutting action (shredders). Ultra centrifugal milling works on the principle of impact and shear effects between the rotor and the fixed ring sieve for particle size reduction. The pre-milled biomass (2-5 mm) is dropped onto the rotor where it is thrown by centrifugal acceleration outwards. The biomass is precrushed on impact with the wedge-shaped rotor teeth moving at high speed. The larger particles are finely ground between the rotor and the ring sieve and are collected in the downstream cyclone. The primary advantages of this process are minimal alteration of material characteristics

(i.e. crystallinity), minimum thermal damage, homogeneous comminution and high-throughput processing (< 10 min for 30-50 gm of biomass). Unlike other size reduction techniques like ball milling and cryogenic grinding that might alter the cellulosic ultra structure and induce thermal stress on the material, centrifugal milling is a rapid, reproducible and comparatively gentle methodology for size reduction.

6.1.4.4 Factors affecting microplate assay

(a) Particle size distribution

The percent standard deviation for replicate centrifugally milled corn stover samples for various particle size ranges (shown in **Figure 6.2**) is relatively small (~ 3-6 %). The particle size distribution for milled corn stover is also fairly reproducible. It is important to have reproducibility in the milling process to minimize variability in particle size distribution. Mass transfer limitations within the agglomerate particles that make up these substrates are responsible for variation in saccharification rates as a function of particle size [400]. Several models for cellulose and lignocellulose hydrolysis have been developed over the years that incorporate various parameters into the kinetic model. Earlier empirical models have shown direct correlation between hydrolysis rate and specific surface area [401]. Size reduction was also found to improve the initial rate of hydrolysis for cellulose [402].

(b) Suspension solids concentration and slurry delivery

Suspending biomass particles is a function of slurry viscosity and density, wetability, particle size, and solids concentration of the solution [403,404].

Figure 6.1 *High-throughput BCRL microplate based saccharification methodology for lignocellulosic biomass. (Figure has been reproduced from [2]).*

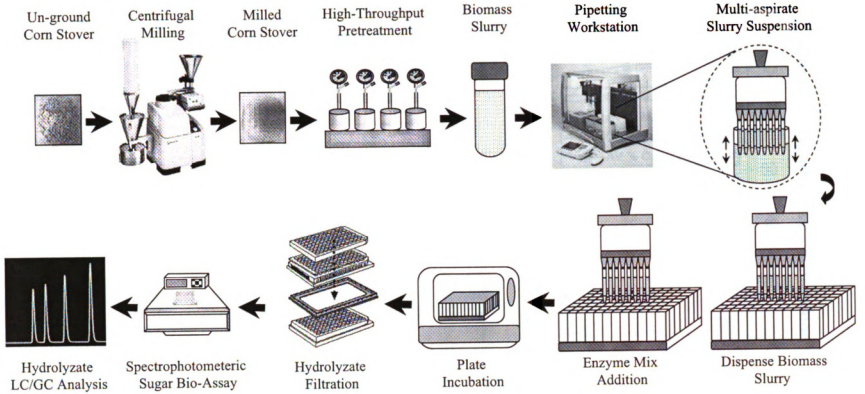

Figure 6.2 *Particle size distributions for Avicel (AV) and ultra-centrifugally milled corn stover (CS). Bars indicate mean and standard errors for four replicate samples. (Figure has been reproduced from [2]).*

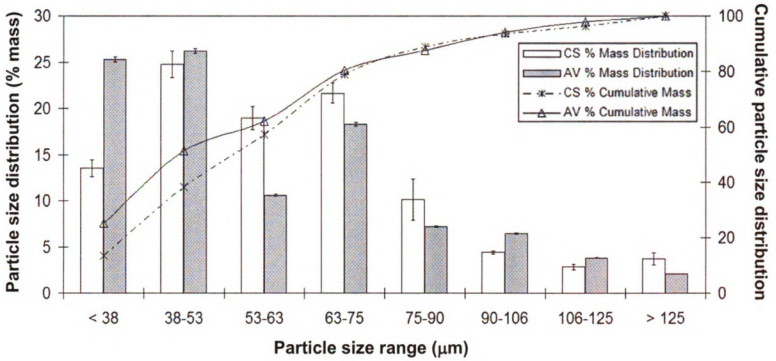

For suspension of coarser particles (20-100 μm) dispersibility is generally a problem, alleviated by use of wetting/dispersive agents and viscosity enhancers. Suspending agents, such as glycerol, can be used to increase the viscosity of water and reduce settling time of slurry particles [390]. However, there was no need to add any dispersing agent to help suspend the solids for slurries typically less than 5% solids (wt) for both Avicel and AFEX treated corn stover. The measured amount of Avicel delivered for slurry suspensions between 1 to 5 weight percent solids loading was found to be quite reproducible (**Figure IV-6.3**) with percent standard deviations within 2-5%. However, increasing the solids loading to 10 weight percent or more resulted in greater variation (i.e. larger than 10-15% standard deviation) in solids delivered to the microplate. This is largely due to difficulty in homogeneously suspending and delivering the slurry at higher solids loading for the current slurry delivery parameters (See Appendix A-VII-25, 26).

The optimal parameters (Method A-VII-25) for uniformly aspirating the slurry, prior to pipetting a pre-defined aliquot to the microplate, were based on variability in solids delivery and hydrolytic yields between wells based on preliminary experiments (data not shown). It was found that for biomass slurries under 10% (w/w, 100-150 μm or lesser particle size), 50 cycles of slurry agitation/aspiration were sufficient to uniformly suspend the biomass. The aspiration parameters may need to be adjusted based on the type of biomass and pretreatment process, which might affect the surface tension and viscosity of the slurry.

(c) Agitation and mass transfer

Minimizing interference from mass transfer limitations to a point where only reaction rate is the limiting parameter allows study of other important rate-dependent parameters (i.e.

enzyme synergy, cell wall composition and pretreatment severity). However, scale-up of lignocellulosic hydrolysis would dictate incorporation of mass transfer into the rate equation for design purposes. Previous research [399,405] indicates that intensity of agitation had little effect once the particles were completely suspended.

Table 6.1 *Effect of mass transfer related parameters (i.e. reaction volume, solids loading, agitation speed and mixing aid) on Avicel digestibility for (A) 0.75 ml, and (B) 0.25 ml based reaction volumes. (Figure has been reproduced from [2]).*

A: 0.75 ml reaction volume

Glucan Loading	**0.25%**		**1%**	
Agitation with bead	% Conversion	% Std Dev	% Conversion	% Std Dev
100 rpm	26.8	5.4	23.3	7.3
200 rpm	39.9	7.5	48.0	3.6
400 rpm	50.6	2.0	55.2	5.3
Agitation without bead				
100 rpm	1.8	1.1	11.6	5.1
200 rpm	5.8	3.3	22.3	3.8
400 rpm	32.2	5.4	39.5	2.8

B: 0.25 ml reaction volume

Glucan Loading	**0.25%**		**1%**	
Agitation with bead	% Conversion	% Std Dev	% Conversion	% Std Dev
100 rpm	41.4	6.8	41.1	3.2
200 rpm	35.3	2.5	45.6	1.7
400 rpm	56.9	3.0	60.8	6.7
Agitation without bead				
100 rpm	26.2	2.1	27.9	1.8
200 rpm	25.8	2.1	27.5	2.3
400 rpm	36.1	1.6	42.4	5.4

Enzymatic hydrolysis of Avicel at varying agitation speeds and in the presence of steel beads shows large variation in overall glucan conversion (See **Table 6.1**). Reducing reaction volume further improves glucan conversion due to ease in suspending the solids. Increasing the agitation speed invariably helps improve the glucan conversion in all

cases; especially in the absence of steel beads, at increased reaction volumes and higher glucan loadings. No significant improvement is noted upon increasing agitation speeds beyond 400 rpm (data not shown).

Adding a mixing aid like steel beads helps improve glucan conversion for all cases at varying degrees of significance depending on reaction volume, glucan loading and agitation speed. The percent drop in glucan conversion in the absence of steel beads is significant at lower versus higher agitation speeds for 0.75 ml as compared to 0.25 ml reaction volume, essentially due to inadequate mixing for larger volumes. The percent conversion decrease for 0.25 ml samples is around 30-35%. However, for 0.75 ml reaction volume the percent decrease ranges from 95% to 20%. Larger percent drops are seen at lower agitation speeds due to greater inhomogeneity in mixing.

(d) Glucan loading

It seems that 1% glucan loading has slightly higher conversions at lower agitation speeds compared to 0.25% glucan loading (**Table 6.1**) primarily due to the 4-fold higher solids loading that might assist in mixing, in the absence of a suitable mixing aid. However, there is no significant effect on glucan conversion at higher agitation speeds (i.e. 300-400 rpm) in the presence of steel beads. Increasing substrate concentration normally results in decreasing glucan yield due to several factors like substrate inhibition [406], increasing inhibitor concentrations and mass transfer issues. However, at glucan loadings under 1% there should be no significant difference in hydrolysis yields. It might be advantageous to conduct the microplate hydrolysis experiments at lower glucan/solids loading due to reduced substrate and enzyme requirements.

(e) Reaction volume

Two different reaction volumes (250 and 750 μl) were explored to study the effect on enzymatic digestibility of Avicel (**Table 6.1**). It is important that there is sufficient head space in each well when conducting the high rpm hydrolysis due to mixing and spilling issues. A larger quantity of biomass (gm of biomass per well), for corresponding larger volumes, is harder to suspend. Reactor design and process scale are known to have significant effect on biomass digestibility, primarily due to mixing problems [407,408].

The effect of reaction volume on glucan conversion is more prominent at lower agitation speeds (i.e. 100 vs. 400 rpm). Reducing reaction volume has no significant effect on glucan conversions for any RPM or glucan loading in the presence of steel beads. However, in the absence of a suitable mixing aid (e.g. steel beads) there is a significant increase in glucan conversion upon reducing the reaction volume. There is however more variability in the glucan conversions for lower reaction volumes compared to larger volumes, especially at lower agitation speeds even in the presence of steel beads.

(f) Evaporation losses

Each microplate was heated homogeneously due to close contact with aluminum slabs covering the top and bottom of the microplate. There was no significant improvement in glucan conversion for samples that were pre-incubated prior to addition of enzymes for hydrolysis carried for 6 hrs or more (data not shown). For convenience and high-throughput it might be easier to conduct the 6 hr hydrolysis assays without pre-incubating the plates. Estimated evaporative loss from the heat sealed microplate was typically under 0.1% and 0.5% at 3 and 24 hrs, respectively. The total evaporative losses for a heat sealed microplate was significantly lower compared to the 2-3% (24 hr incubation) and <7% (1

hr incubation, with heated lid) losses reported by Berlin et al. [392] and Decker et al. [390], respectively. In order to compensate for condensation losses on the foil and well walls after chilling the microplates in the freezer for 15 min, the plates should be centrifuged prior to sampling. This is more critical if the reaction volume is reduced to 100 µl or less. The losses are insignificant for larger volumes (> 500 µl) and were not considered during calculations.

(g) Other factors

It was difficult to homogenously suspend biomass slurries by simple stirring and manually dispense aliquots using multi-channel dispensers (data not shown). High-throughput and reproducible delivery of substrate and reagent requires automation. The tips used for delivery of the biomass slurry were hand-cut uniformly to prevent clogging during slurry aspiration. No significant difference was noticed for biomass delivered between individually cut tips (data not shown). The pipetting parameters (i.e. aspiration cycles) used for slurry suspension did have a significant effect on reproducibility of solids delivered which were dependent largely on the percent solids slurry concentration. It is important to multi-aspirate the slurry suspension to uniformly suspend the biomass in the reservoir vessel before pipetting aliquots into the microplate. The slurry was multi-aspirated prior to each aliquot to prevent heterogeneity in sampling. Pipetting parameters that were found to give reproducible slurry delivery are reported (See Appendix A-VII-25, 26). The volume of slurry in the reservoir vessel must not exceed 50 ml for the current delivery parameters due to incomplete mixing for higher volumes. It might be necessary to re-optimize the delivery parameters based on the surface tension properties of slurries for different pretreatments and biomass.

The biomass can be AFEX treated prior to the milling process, since AFEX is essentially a dry-to-dry pretreatment. However, for other pretreatments that result in pretreated biomass slurries (i.e. dilute-acid based treatments) it might be necessary to dry the pretreated sample prior to milling or mill the sample prior to pretreatment. The effect of particle size has been reported to be significant for most pretreatments due to easier accessibility of plant biomass by pretreatment chemicals (i.e. acid or alkali) [1,397,398,409]. It might be thus necessary to re-optimize pretreatment conditions for the finely ground biomass to prevent excessive degradation reactions. However, for screening purposes it is important to note that the current methodology can be easily adapted to other pretreatments.

6.1.4.5 Reproducibility of microplate methodology

The reproducibility of the microplate methodology was tested for 0.25% glucan loading AFEX corn stover enzymatic hydrolysis using 15 FPU cellulase/gm glucan and 64 p-NPGU β-glucosidase/gm glucan. The time period for hydrolysis was 2 hrs. **Figure 6.4** shows the box plots for glucan conversions (Y) along with the distribution of individual data points (N = 48) for two sets of experiments (X) that were conducted in separate microplates using separate slurry solutions. The average glucan conversion for experiments A and B were 33.4% (Standard Deviation = 2.22%) and 31.8% (Standard Deviation = 2.18%), respectively. Student's t-test showed no significant difference between the two data sets ($P < 0.05$).

Fig 6.4 *Box plot of glucan conversions (Y) along with data points (N = 48) for each set of experiments (X) performed for 0.25% glucan loading AFEX corn stover for conventional enzyme loading. (Figure has been reproduced from [2]).*

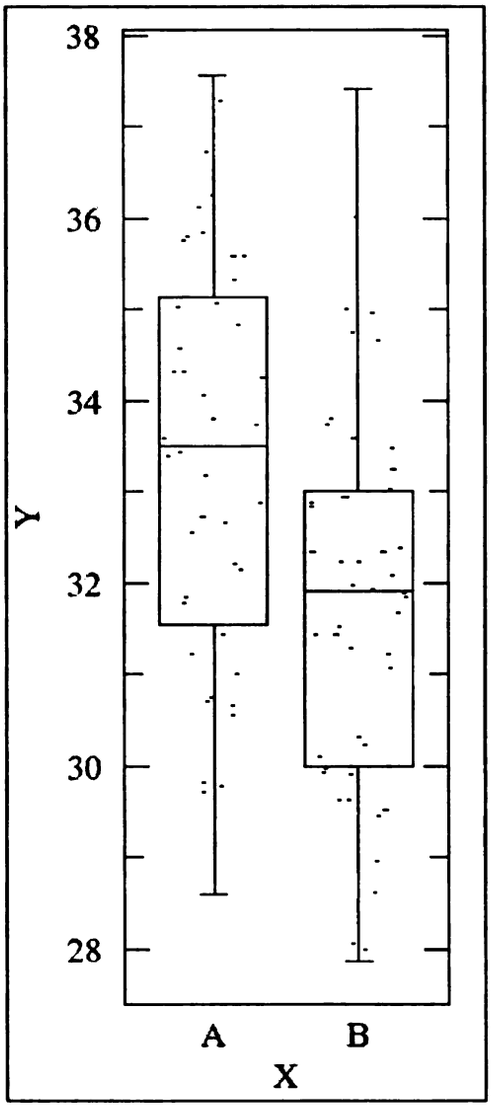

6.1.4.6 Bio-enzymatic sugar assay

One of the key limiting bottlenecks of any high-throughput assay system is composition analysis of hydrolysis products. There are several methods that can be used to assay fermentable sugars; (A) Enzyme based assay, (B) YSI glucose analyzer assay, (C) HPLC analysis and (D) Colorimetric assays. Bio-enzymatic assays are useful for rapid preliminary screening of the hydrolysate using an enzyme system to estimate glucose and

xylose. The YSI glucose analyzer can be used for rapid glucose estimation without sample dilutions at much higher detection limits (5-25 g/l) compared to conventional enzymatic assays (0.1-1 g/l). HPLC based methods are useful to quantify other monosaccharides (i.e. xylose and arabinose) and oligomeric sugars (i.e. cellobiose, xylobiose). Generally, for screening purposes there is no utility in estimating total monomeric sugar content due to high correlation between glucose and other sugars produced during biomass hydrolysis (data not shown). For rapid sugar oligosaccharide analysis for large number of samples it might be useful to couple the HPLC to a MALDI-TOF-MS system [410] or develop a rapid capillary electrophoresis based methodology. However, it is important to get sufficient preliminary data for samples prior to a more detailed analysis using more time-consuming chromatographic methods like HPLC, LCMS and Capillary Electrophoresis.

Most researchers have carried out preliminary sugar analysis through colorimetric assays such as DNS method [383,411], Nelson-Somogyi method [412,413], modified BCA method [414], phenol-sulfuric acid method [414], and anthrone-sulfuric acid method [415]. However, some of the major limitations of such colorimetric assays are poor stoichiometric correlations between the colorimetric oxidant (i.e. DNS, Cupric ions) and chain length of reducing oligosaccharidic sugar [384,416]. The colorimetric assays also suffer from non-specific interference due to protein and lignin present in the biomass hydrolysate [416,417]. Rivers and colleagues [418] found that reducing sugar data from the DNS assay correlated very poorly with more accurate HPLC and enzymatic assays for lignocellulosic hydrolysate.

Enzyme based micro-assays are rapid, reproducible, microplate-adaptable and economical compared to conventional analytical methods (i.e. HPLC). A glucose oxidase based YSI 2300 STAT analyzer (Yellow Springs Instruments, Yellow Springs, OH, USA) was used for glucose analysis for preliminary hydrolysis screening experiments. Hydrolysate samples were transferred into 1.5 ml microcentrifuge tubes for preliminary glucose assay using the automated YSI glucose analyzer. The results obtained were used to prepare suitable sample dilutions on the microplate prior to more comprehensive glucose assay using a bio-enzymatic assay system. Typical bio-enzymatic assays for sugars that result in eventual oxidation/reduction of NADH/NAD (nicotinamide adenine dinucleotide) are suitable for high-throughput absorbance based analysis. Most commercially available bio-enzymatic assays are macro scale based (1-10 ml), labor intensive and time consuming. However, adapting these assays to a micro scale (100-300 µl) in order to read the UV absorbance on a microplate helps increase throughput in an economical manner. The current hexokinase and glucose-6-phosphate dehydrogenase system was found to be suitable for detecting glucose in the hydrolysate. Glucose concentrations determined using HPLC were found to be essentially identical to the bio-enzymatic assay results for AFEX corn stover hydrolysate (data not shown). There was no significant interference of the enzymatic assay by phenolic compounds generally present in lignocellulosic hydrolysates. This is largely due to the effect of diluting the lignocellulosic hydrolysate (to less than 1 g/l glucose) to reduce degradation product (i.e. quinones, coniferyl aldehydes) concentrations, that have little or no significant UV (340 nm) absorption. Any significant absorption is also corrected for by subtracting the sample blank plate (i.e. 5 min plate) from the reaction plate (i.e. 20 min plate).

6.1.4.7 BCRL micro-assay vs. conventional macro-assay

The hydrolysis time profile for milled AFEX corn stover and Avicel for both microplate and flask assays are shown in **Figures IV-6.5**. The rate of saccharification of unground and milled AFEX corn stover vary significantly (~ 15-20%) due to improved enzyme accessibility (i.e. increased surface area to volume ratio) of the latter. The percent conversion for 1% and 0.25% glucan loading for milled AFEX corn stover is fairly comparable for both the micro and flask based assay.

It is critical to reduce the total assay time for high-throughput enzymatic hydrolysis of lignocellulosics. The conventional NREL LAP-9 protocol takes 48-72 hours to achieve 50% glucan conversion for most biomasses. The BCRL microplate assay takes under 6 hours to achieve similar conversions. There is a 7-10 fold reduction in reaction time period compared to other lignocellulosic hydrolysis assays to achieve similar yields that greatly improve throughput for screening. Sampling microplates at 1-6 and 24 hr will allow evaluation of biomass digestibility during the exponential and terminal phase of the hydrolysis reactions, respectively. Complete digestibility for optimal enzyme combinations and unground pretreated biomass could be conducted for a longer time on a larger scale.

The mixing regime in the microplate well is expected to be quite different from that of a baffled flask, at varying agitation speeds. We also expect the various surface active components in the ACS hydrolysate (e.g. organic acids, lignin phenolics and other AFEX pretreatment degradation products) would modify the surface tension and viscosity during the course of hydrolysis, allowing enhanced mass transfer compared to avicel (with little or no significant extractives, 97-99% cellulose). It is likely that mixing

is more vigorous in the microplate wells compared to the baffled flask, hence allowing ACS to achieve a slightly higher glucan conversion in the former case. The glucan conversions for ACS are also comparable for both 0.25 and 1% glucan loading in the microplate based assay. A similar trend is also noted for the flask assay for varying ACS glucan loading, indicating that the mixing regimes within the flask and microplate are sufficient and comparable to homogeneously suspend and mix the ACS substrate. However, the same trend doesn't seem to be observed for avicel. The vigorous mixing regime in the microplate gives a glucan conversion that is largely comparable for both 0.25 and 1% glucan loading, during the course of hydrolysis. However, the glucan conversions for 0.25 and 1% avicel loading in the flask assay are significantly different (and lower in overall conversions compared to microplate assay), indicating a poorer mixing regime for avicel in the flask.

There are obvious differences in the digestibility of the biomass in the microplate assay compared to the conventional flask-based (i.e. NREL LAP 9) due to several factors. Most of the differences have been pointed out in previous discussions. Some of the major differences between the two assays are biomass particle size, mass transfer differences due to agitation and reactor configuration. However, one should remember that the purpose of the microplate assay is largely to screen various parameters in a reproducible manner. The understanding gained can be easily applied for scaling up the pretreatment, hydrolysis and fermentation processes.

6.1.4.8 Multi-pronged applicability of microplate based assays

There are several applications of using a high-throughput digestibility assay, such as, (1) studying cell wall digestibility for different lignocellulosic feedstocks, (2) understanding

effect of pretreatment parameters (i.e. temperature, catalyst loading, moisture, solid loading) using small scale high-throughput pretreatment systems, (3) optimizing cellulase mixtures and synergistic additives (i.e. crude commercial and purified enzymes, novel enzymes, protein and surfactant additives), (4) studying synergistic interaction of free cellulolytic and cell-bound cellulosomal enzymes on lignocellulosic substrates, (5) screening enhanced activity for enzymes modified by site-directed mutagenesis and/or directed evolution on cellulosic substrates, (6) screening activity of novel hydrolases identified from functional metagenomic analysis, (7) preliminary and detailed screening of cell wall mutants from model plants (i.e. Arabidopsis, Populus) to identify genes responsible for cell wall recalcitrance to hydrolysis.

6.1.5 Conclusions

The 96-well BCRL microplate method was developed for conducting micro-scale digestibility studies for untreated and pretreated lignocellulosic biomass. A suitable method for delivering the biomass to the microplate was through ultra-centrifugal milling and pipetting milled biomass slurry suspensions into the microplate. A high-throughput bio-enzymatic assay was adapted to be used on a micro-scale to determine fermentable sugars in the hydrolysate. The entire procedure was automated using a robotic pipetting workstation. Reproducible particle size reduction of both untreated and AFEX pretreated stover was possible using the ultracentrifuge mill. The BCRL microplate method was optimized for crystalline cellulose (Avicel) and ammonia fiber expansion (AFEX) pretreated corn stover for varying glucan loading. The method is reproducible and comparable to larger scale flask based hydrolysis assays.

The microplate assay can be easily adapted to screening assays for multiple kinds of biomass making it a powerful analytical tool for researchers working in the field of biomass conversion. Enzyme production and thermochemical pretreatment are primary economic barriers to commercial scale-up of biorefineries that require further cost reductions through reduction in enzyme loading and pretreatment severity. Coupling high-throughput pretreatment, hydrolysis, fermentation and compositional analysis will facilitate rapid screening and identification of key bottlenecks to the biomass conversion process.

CHAPTER 7: MAXIMIZING TOTAL SUGAR HYDROLYTIC YIELD FOR AMMONIA PRETREATED LIGNOCELLULOSICS THROUGH CRUDE ENZYME MIXTURE OPTIMIZATION

7.1.1 Abstract

Commercial enzyme usage (30-100 mg protein/g glucan) necessary to achieve >90% total sugar hydrolysis yield for pretreated lignocellulosics is economically unviable. Most commercial cellulase blends lack suitable hemicellulases and other accessory enzyme activities that result in higher protein requirements. It would be ideal to optimize cellulase cocktails by supplementation of suitable hemicellulases. This would also help gain a better understanding of enzyme synergism on pretreated substrates. To this end, this paper presents a novel, extendable methodology for modeling enzyme synergies among large systems of crude enzyme mixtures to maximize biomass digestibility using a microplate based hydrolysis assay. Over 750 unique enzyme mixtures were prepared based on a simplex-centroid experimental design approach using 14 crude enzyme preparations ranging in various types of activities (e.g. cellulases, hemicellulases, pectinases, esterases). The activity of several enzyme mixtures were tested on AFEX treated corn stover to create mixture regression models predicting glucan and xylan hydrolysis yields. A detailed proteomics analysis was carried out for all 14 crude enzyme preparations to quantify individual protein components to help explain the variability in hydrolytic performance. The optimal enzyme cocktail mixtures predicted from these studies achieved substantially higher glucan (93%) and xylan (91%) conversions at lower total protein loading than conventional enzyme blends (e.g. Spezyme CP + βG rich cocktail gave 62% glucan and 39% xylan conversion, respectively). Exploiting enzyme

synergism can help minimize enzyme usage in a cellulosic biorefinery while increasing the total sugar released from pretreated biomass.

7.1.2 Background

7.1.2.1 Protein composition of crude commercial enzyme mixtures

Typically, most synergistic hydrolysis studies on pretreated lignocellulosics have been conducted using crude commercial enzyme mixtures from several sources (e.g. Novozyme, Genencor). It would be useful to determine the protein composition and specific activities of these enzyme mixtures. This would also help quantify the minimal set of enzymes necessary for hydrolyzing several types of lignocellulosic biomass for varying pretreatment conditions (acid vs. base treated). Unraveling the complex phenomena of enzyme synergy on pretreated lignocellulosics would lead to the development of optimal cellulase-hemicellulase heterologous expression systems. It would be beneficial to have controlled expression of necessary enzyme activities based on pretreatment severity and type of biomass.

Protein composition for cellulolytic and hemicellulolytic mixtures has been typically determined through the measurement of individual protein activities by model substrate assays, enzyme immunosorbent based assays, gel electrophoresis, chromatographic and capillary electrophoresis based separations. The activity assay based method is limited in its ability to distinguish between multi-functional enzymes and is inconclusive due to lack of specific model substrates [419]. Enzyme immunosorbent assays are limited due to cumbersome antibody preparation procedures for each enzyme in the mixture which may be expensive for commercial enzymes that contain more than two/three dozen glycosyl hydrolases apart from other fungal proteins [420]. Staining and

reproducibility issues of gel based electrophoresis methods limits it usage as well [421]. Chromatographic and capillary electrophoresis methods have been used to varying degrees of success. This is due to extensive method optimization limitations for each enzyme mixture, difficulties in identification of individual proteins, poor reproducibility due to protein-surface interactions, low throughput and limited separation efficiency for co-eluting proteins [50,419,422].

High-throughput proteomics analysis of enzyme mixtures (or their trypsin hydrolyzate) provides more detailed information on several protein components [423,424]. The proteomic composition might be used in a complementary manner to activity data for determining crude enzyme mixture compositions [421]. The proteomics approach is useful when comparing abundance of the same protein between different samples; however, the method has certain limitations when comparing different protein abundance within the same sample (due to varying ionization efficiencies of peptides during electro-spray ionization). Protein quantification based on spectral counts suffers from its inability to quantify low abundance proteins and is less accurate than methods based on stable isotope labeling [425]. It is nevertheless possible to quickly estimate individual protein components within a complex enzyme mixture based on some sort of identification score or extracted ion current for peptides that identify proteins of interest (e.g. spectral counts) compared to most other methods [426]. Spectral counting has been demonstrated to be powerful technique, compared to protein sequence coverage and peptide counting, to predict relative abundance of proteins within a complex mixture within two-fold (over a large linear dynamic range spanning two-orders of magnitude) of relative abundance [427-429]. Very few detailed proteomics characterization has been

performed on commercially available cellulases and hemicellulase mixtures to predict their hydrolytic potential on pretreated lignocellulosics [430].

7.1.2.2 Hydrolysis of pretreated biomass using commercial enzyme mixtures

Commercially available enzyme mixtures have been typically evaluated for their hydrolytic efficiency on model substrates like avicel (crystalline cellulose), xylan extracts (oat spelt, birch wood), p-nitrophenol based glycosides and other non-realistic substrates [32]. *However, recent work [48,385,431,432] has shown that model cellulosic and hemicellulosic substrates do not provide a reliable indication of their true hydrolytic potential on pretreated lignocellulosics.* Non-specific protein binding, variations in physicochemical properties of pretreated cell walls and synergistic interactions between enzymes are typically the cause of these substrate-specific enzyme activity based differences. For pretreated biomass with a complex cell wall ultra-structure, selecting an enzyme system that is necessary and sufficient is critical. Therefore, it is more appropriate to screen and optimize enzyme mixtures directly on pretreated lignocellulosic substrates using high-throughput digestibility assays [2,392].

Optimization of multi-enzyme systems to maximize monomeric sugar hydrolytic yields is useful from an engineering perspective, rather than determining only the degree of synergism between various enzymes. Interestingly, mixtures of enzymes that give the highest saccharification rate do not always correspond to enzyme mixtures that give the highest degree of synergy [433]. It has been found that most cellulase inducers promote the synthesis of a constant ratio of three major cellulases (CBH I, CBH II and EG I) in Trichoderma, indicating the coordinated regulation and expression of certain cellulase genes in Trichoderma [434]. The phenomenon is much more complex for hemicellulases

and varies significantly based on the substrate used for induction [32]. Most commercial enzymes (typically produced from *Trichoderma* or *Aspergillus*) do not have the correct protein ratios or sufficient type of enzyme activities necessary to hydrolyze pretreated lignocellulosic biomass. There has been no evolutionary pressure on fungi to grow on pretreated lignocellulosics to produce cellulases and hemicellulases necessary to maximize digestibility. Thus, crude protein mixtures should be optimized for total sugar hydrolysis yield as a function of varying ratios for individual proteins. This would eventually help construct multigene expression systems to produce balanced enzyme mixtures for pretreated biomass [435]. The optimum enzyme ratios can help determine critical enzyme components and rationally design heterologous expression systems for consolidated biological processing (CBP) [436,437]. However, multi-enzyme mixture optimization could get complicated without the use of suitable mathematical tools, such as factorial and mixture based statistical experimental designs [438,439].

Several studies have looked to optimize commercially available crude enzyme mixtures for acid pretreated [48], steam exploded and organosolv treated lignocellulosic biomass [431,432]. Crude enzyme mixture optimization for acid pretreated corn stover helped reduce total protein loading by two-fold for equivalent hydrolysis yields [48]. Several covalent lignin-polysaccharide bonds are not entirely cleaved during alkali pulping and require accessory enzymes to help cleave these linkages, improving pulp digestibility [440]. Studies with steam exploded wheat straw have found synergistic interactions between crude cellulases and accessory enzymes (rich in xylanases and esterases) [441]. Acid pretreated biomass has little or no residual hemicellulose compared to alkali pretreated biomass and does not require hemicellulases to significantly enhance

rate of hydrolysis [37,110]. However, significant enhancement in hydrolysis yields due to hemicellulase supplementation is expected for lower severity acid [113] and ammonia based treatments [1].

Corn fiber (containing ~ 20% starch, 20% cellulose and 30% hemicellulose), a valuable by-product of the corn-ethanol industry, is rich in heteroxylans that are not readily hydrolyzed by commercial cellulases (mixtures of amylases, cellulases, xylanases) [442]. Corn fiber xylan is heavily branched (via arabinose, uronic acids, and phenolic acids), limiting enzyme accessibility even after pretreatment. Ammonia based pretreatments have resulted in the formation of high-molecular weight arabinoxylans from corn grain husk (arabinose/xylose ratio of 0.6) [361]. These are not hydrolyzed by typical *Trichoderma* cellulase and xylanase rich mixtures, probably due to lack of significant accessory enzyme activity. Dien and colleagues [443] have been able to significantly enhance xylan digestibility of AFEX pretreated distillers grains by supplementing crude cellulase mixtures with Multifect Pectinase (from Genencor-Danisco, USA) and Depol 740 (from Biocatalysts, UK). These supplementary enzymes are rich in arabinofuranosidase, esterase based activities and were found to synergize with cellulases and xylanases. Hydrolysis of ammonia treated sugar beet by pectinases was inhibited in the absence of hemicellulase de-branching enzymes [235].

AFEX pretreatment has been found to enhance synergistic hydrolysis of sugarcane bagasse through multiple combinations of commercial cellulolytic-hemicellulolytic enzymes and xylanase rich fungal extracts at low (1%, w/v) and high (10%, w/v) glucan loadings [345]. Xylanase activity was critical in improving xylan as well as glucan conversion, depending on the source of the xylanase. However, the actual

amount and relative ratios of the enzymes used for maximizing hydrolysis yields was not systematically varied in these studies. Typically, most enzymatic hydrolysis studies for AFEX or ammonia treated lignocellulosics have been conducted using enzyme cocktails that have low xylanase and/or accessory enzyme activities (like xylosidase, esterase, arabinofuranosidase) [42,161,444]. Most commercial xylanases have applications in the paper industry where β-xylosidase activity is not critical, which has resulted in inhibition of hemicellulases by un-hydrolyzed oligosaccharides [442].

Currently, there are no suitable high-throughput enzymatic digestibility assays that can be used reliably and reproducibly for measuring the hydrolytic potential of commercially available enzymes on pretreated and native lignocellulosics. There have also been no enzyme optimization studies performed on AFEX treated lignocellulosics for varying commercial enzyme combinations rich in complementary hemicellulase activities to maximize glucan and xylan digestibility.

7.1.3 Materials and Methods

See appendix A-VII-1, 2, 3, 4, 23, 25, 27, 28, 29, 31-36.

7.1.4 Results and Discussion

7.1.4.1 Protein concentration determination

The choice of the protein concentration assay is an important decision considering the variability, accuracy and level of difficulty associated with each of these methods [445]. The protein concentration (**Table 7.1-A**; See for **Table 7.1-B** details) for the various crude enzymes was estimated by three methods (Bradford assay, Pierce BCA assay and Total crude protein by Kjeldahl nitrogen analysis). The Bradford assay (using Coomassie Blue dye) was found to predict protein concentrations several fold lower than the other

two methods. Similarly, the Bicinchonic acid assay (BCA) was found to predict significantly higher protein concentrations for most crude enzyme mixtures.

Table 7.1-A *Protein concentration assay data for 14 crude enzyme blends using three analytical methods (Pierce BCA, Bradford and Kjeldahl Protein based assays).*

Mean				*Std Dev*		
mg/ml	**Pierce BCA**	**Bradford**	**Kjeldahl**	**Pierce BCA**	**Bradford**	**Kjeldahl**
CE 1	134	31	88	6	7	1
CE 2	217	42	150	4	12	43
CE 3	47	7	35	2	3	1
CE 4	128	25	90	1	11	0
CE 5	284	36	105	3	13	1
CE 6	93	20	84	1	3	1
RE 1	22	11	20	1	2	1
RE 2	263	52	144	3	7	58
RE 3	294	16	78	1	12	0
RE 4	135	41	94	8	13	1
RE 5	5	1	5	0	1	0
RE 6	6	5	6	0	1	0
RE 7	17	11	16	1	3	2
RE 8	148	45	97	8	8	6

Several researchers in the past have indicated the interference of most colorimetric assays (i.e. Bradford and BCA) with background reducing sugars, buffers and detergents [445,446]. Binding to Coomassie blue based dyes has been found to be dependent on amino acid composition of the protein, typically skewed by presence/absence of arginine and lysine [447]. On the other hand, presence of reducing sugars causes significant interference with the reaction of copper (Cu^{2+}) with the protein during typically BCA assays. Thus, the presence of reducing sugars results in elevated BCA based protein concentration readings. The most effective method for resolving the presence of interfering substances on colorimetric assays is through protein precipitation [448]. However, there are several issues with this approach (relative efficiency of protein

precipitation, recovery and high-throughput issues) as well. Estimation of protein concentration by Kjeldahl analysis (crude protein = 6.25 x % nitrogen content) was found to be suitable for commercial enzyme blends that are more readily available in large quantities (unlike purified enzymes). The contribution by ammoniacal salts (non-protein nitrogen) typically present in commercial enzyme blends was subtracted from the total crude protein nitrogen estimate to give true protein estimate for all commercial enzymes. All protein concentrations used for further experiments are based on the Kjeldahl estimated total protein content. Interestingly, in the absence of reducing sugars and other low-molecular weight substances (removed by desalting the enzymes using size-exclusion column) the concentration predicted by BCA was comparable to the Kjeldahl method, similar to previous reports [445,446].

7.1.4.2 Protein composition estimated via proteomics and enzyme activity assays

Enzyme activity assays (See **Figure 7.1-B**) were carried out for all 14 desalted commercial enzyme blends on several model substrates (Avicel, Carboxymethylcellulose or CMC, Oat spelt xylan or OSX, p-nitrophenyl xyloside or pNPX, p-nitrophenyl arabinoside or pNPAf, p-nitrophenyl acetate or pNPA and p-nitrophenyl glycoside or pNPG).

Avicel, CMC and pNPG are model substrates that give a relative estimate of the hydrolytic performance of cellulases on crystalline cellulose, amorphous cellulose and soluble dextrans (e.g. cellobiose), respectively. Avicelase activity, in order of decreasing relative specific activity, was detected in NS-50014 (RE 4) > **Spezyme CP (CE 1)** > **Accellerase (CE 6)** = NS-50053 (RE 8) > **Depol 670L (CE 5)** > NS-22002 (RE 1) > **Multifect Pectinase (CE 4)** = NS-50012 (RE 3).

Table 7.1-B *Activity assay data for 14 crude enzyme blends on pNPG, pNPAf, pNPA, pNPX, OSX, Avicel and CMC. One unit of activity on pNP based substrates is equivalent to one nmol of pNP (p-nitrophenol) released/mg enzyme/min. One unit of activity on Avicel/Xylan/CMC is equivalent to one μM glucose equivalent released/mg enzyme/min. Where; "-" stands for no detectable activity; pNPG (pNP-β-D-glucopyranoside); pNPAf (pNP-α-L-arabinofuranoside); pNPA (pNP-acetate); pNPX (pNP-β-D-xylopyranoside); OSX (Oat spelt xylan), CMC (Carboxymethylcellulose).*

Enzyme Source	*Mean* IU/mg	Avicel	CMC	OSX	pNPX	pNPA	pNPAf	pNPG
Spezyme CP	**CE 1**	0.30	3.53	3.79	15.26	59.45	9.79	101.18
Novo 188	**CE 2**	-	0.05	0.33	94.33	6.29	21.22	402.75
Multifect Xylanase	**CE 3**	-	0.09	6.64	30.77	189.53	6.92	16.33
Multifect Pectinase	**CE 4**	0.01	0.66	3.76	52.18	40.34	413.51	163.23
Depol 670L	**CE 5**	0.08	2.08	3.42	0.86	19.32	31.67	31.54
Accellerase	**CE 6**	0.18	1.72	1.35	2.19	1.46	0.50	145.22
Novozyme NS-22002	**RE 1**	0.04	0.97	5.38	11.74	65.26	7.77	52.09
Novozyme NS-50010	**RE 2**	-	0.07	0.35	4.11	4.01	16.59	310.60
Novozyme NS-50012	**RE 3**	0.01	0.89	0.21	0.88	45.53	45.06	19.87
Novozyme NS-50013	**RE 4**	0.41	2.17	2.39	28.91	39.62	4.78	27.15
Novozyme NS-50014	**RE 5**	-	0.03	87.89	0.37	1.34	0.29	3.58
Novozyme NS-50029	**RE 6**	-	0.01	0.58	0.29	1.22	0.21	0.37
Novozyme NS-50030	**RE 7**	-	0.01	16.10	24.23	2.01	3.72	1.10
Novozyme NS-50053	**RE 8**	0.17	1.37	0.85	16.56	18.09	4.13	19.35

Enzyme Source	*Std Dev* IU/mg	Avicel	CMC	OSX	pNPX	pNPA	pNPAf	pNPG
Spezyme CP	**CE 1**	0.03	0.36	0.44	0.59	3.49	0.28	5.43
Novo 188	**CE 2**	-	0.01	0.03	25.70	0.71	0.73	9.64
Multifect Xylanase	**CE 3**	-	0.02	0.44	2.01	8.45	0.25	0.25
Multifect Pectinase	**CE 4**	-	0.02	0.20	1.61	2.37	8.68	5.28
Depol 670L	**CE 5**	0.01	0.07	0.29	0.02	5.20	0.33	5.86
Accellerase	**CE 6**	0.01	0.14	0.16	0.06	0.19	0.20	7.29
Novozyme NS-22002	**RE 1**	0.01	0.12	0.41	0.15	3.18	0.20	2.59
Novozyme NS-50010	**RE 2**	-	0.01	0.02	0.05	0.40	0.40	7.37
Novozyme NS-50012	**RE 3**	-	0.04	0.02	0.03	1.85	2.00	0.33
Novozyme NS-50013	**RE 4**	0.02	0.07	0.29	0.09	3.85	0.08	0.30
Novozyme NS-50014	**RE 5**	-	0.01	7.45	0.08	0.13	0.05	0.07
Novozyme NS-50029	**RE 6**	-	-	0.07	0.25	0.10	0.14	0.03
Novozyme NS-50030	**RE 7**	-	-	0.66	0.30	0.12	0.14	0.03
Novozyme NS-50053	**RE 8**	0.01	0.12	0.10	0.26	0.43	0.24	0.12

CMCase activity was detected in **Spezyme CP (CE 1)** > NS-50014 (RE 4) = **Depol 670L (CE 5)** > **Accellerase (CE 6)** = NS-50053 (RE 8) > NS-22002 (RE 1) = NS-

50012 (RE 3) = **Multifect Pectinase (CE 4)** > **Multifect Xylanase (CE 3)** = NS-50010 (RE 2) > NS-50014 (RE 5) = **Novozyme 188 (CE 2)** > NS50029 (RE 6) = NS-50030 (RE 7). Cellobiase activity was determined through p-NP-glucoside (p-NPG) based assays and was detected in **Novozyme 188 (CE 2)** > NS-50010 (RE 2) > **Multifect Pectinase (CE 4)** = **Accellerase (CE 6)** > **Spezyme CP (CE 1)** > NS-22002 (RE 1) = **Depol 670L (CE 5)** > **Multifect Xylanase (CE 3)** = NS-50012 (RE 3) = NS-50013 (RE 4) = NS-50053 (RE 8) > NS-50014 (RE 5) > NS50029 (RE 6) = NS-50030 (RE 7).

Oat spelt xylan, pNPX, pNPAf and pNPA are model substrates that give a relative estimate of the hydrolytic performance of hemicellulases on arabinoxylan backbone chain, soluble xylo-oligomers (e.g. xylobiose), arabinose and acetyl (or other esterase based activities) side-chains, respectively. Oat spelt xylanase activity (OSX) was detected in NS-50014 (RE 5) >> NS-50030 (RE 7) > **Multifect Xylanase (CE 3)** > NS-22002 (RE 1) > **Spezyme CP (CE 1)** = **Multifect Pectinase (CE 4)** = **Depol 670L (CE 5)** > NS-50013 (RE 4) > **Accellerase (CE 6)** = NS-50053 (RE 8) > NS50029 (RE 6) > **Novozyme 188 (CE 2)** = NS-50010 (RE 2) = NS-50012 (RE 3). NS-50014 had abnormally high activity on oat-spelt xylan compared to all other enzyme mixtures. Xylobiase activity was determined through p-NP-xyloside (p-NPX) based assays and was detected in **Novozyme 188 (CE 2)** > **Multifect Pectinase (CE 4)** > **Multifect Xylanase (CE 3)** = NS-50013 (RE 4) = NS-50030 (RE 7) > **Spezyme CP (CE 1)** = NS-50053 (RE 8) > NS-22002 (RE 1) > NS-50010 (RE 2) > **Accellerase (CE 6)** > **Depol 670L (CE 5)** = NS-50012 (RE 3) > NS-50014 (RE 5) = NS50029 (RE 6). Arabinofuranosidase activity was determined through p-NP-arabinofuranoside (p-NPAf) based assays and was detected in **Multifect Pectinase (CE 4)** >> NS-50012 (RE 3) > **Depol 670L (CE 5)** >

Novozyme 188 (CE 2) = NS-50010 (RE 2) > **Spezyme CP (CE 1)** = **Multifect Xylanase (CE 3)** = NS-22002 (RE 1) > NS-50013 (RE 4) = NS-50030 (RE 7) = NS-50053 (RE 8) > **Accellerase (CE 6)** = NS-50014 (RE 5) = NS50029 (RE 6). Multifect Pectinase had extremely high arabinofuranosidase activity compared to all other enzymes. Acetyl xylan esterase activity was determined through p-NP-acetate (p-NPA) based assays and was detected in **Multifect Xylanase (CE 3)** > NS-22002 (RE 1) = **Spezyme CP (CE 1)** > **Multifect Pectinase (CE 4)** = NS-50012 (RE 3) = NS-50013 (RE 4) > **Depol 670L (CE 5)** = NS-50053 (RE 8) > **Novozyme 188 (CE 2)** = NS-50010 (RE 2) > **Accellerase (CE 6)** = NS-50014 (RE 5) = NS50029 (RE 6) = NS-50030 (RE 7). Feruloyl esterases have also been reported to have some activity of p-NPA [214,218].

SDS-PAGE for all crude enzyme blends revealed multiple protein bands ranging from 10-120 kDa (**Figure 7.1**; where M stands for marker standards). SDS-PAGE does not reveal the compositional complexity typical of crude cellulase-hemicellulase mixtures [421]. Most glycosyl hydrolases typically range in molecular weight between 30-70 kDa, which would be overlapping each other in one-dimensional gel electrophoresis. Proteomics analysis was carried out to identify the relative abundance of key cellulolytic, hemicellulolytic and accessory enzymes present in each of the commercial blends from leading cellulolytic enzyme companies, namely, Genencor, Novozymes, and Biocatalysts (**Figure 7.2**). Peptides from enzyme tryptic digests were analyzed using high resolution reversed-phase HPLC separation coupled to an ion trap mass spectrometer (LTQ, Thermo Electron, San Jose CA) that was operated in a data-dependent MS/MS mode [423]. MS/MS spectra were analyzed using the SEQUEST algorithm [449] in conjunction with a protein collection of all fungal entries from Uniprot (i.e. Swiss-Prot and TrEMBL).

Figure 7.1 *SDS-PAGE for 14 crude enzyme blends.*

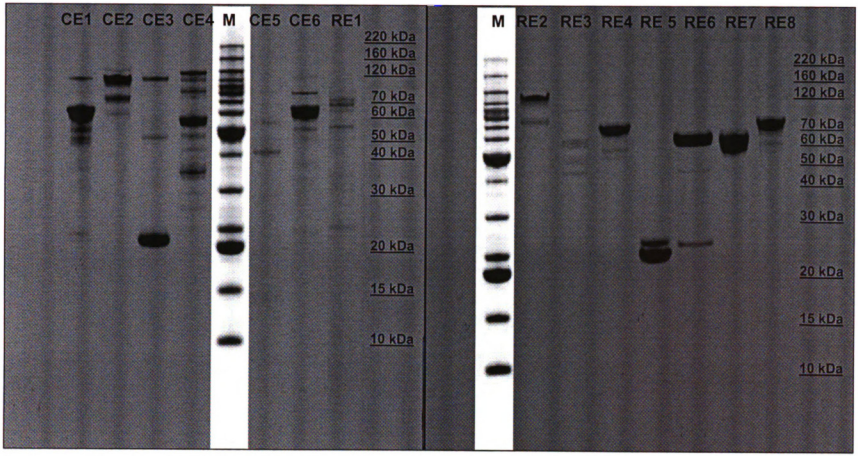

Preliminary filtering of identified peptides was performed using: a minimum cross-correlation cut-off (XCorr) of either 1.9, 3.0, or 3.2 for 1+, 2+, or 3+ charge states, respectively; partially and fully tryptic peptides (peptides that contained either an arginine or lysine at the site of cleavage); DelCn >= 0.1. Estimation of peptide False Discovery Rate (FDR) was calculated by decoy database searching techniques [450,451], resulting in values between 0.6% and 1.9%. One of the major limitations of the current approach is that minor protein components (<1%, w/w) may not be easily detected in the background of the highly abundant proteins. However, this method nevertheless proved useful to get a rough estimate of the major components in the various commercial enzyme preparations. All observation counts for peptides belonging to the same protein families were summed up to obtain relative abundance for individual enzyme families (See supplementary raw data for CE 1 crude enzyme blend in **Table-V-7.3**). Relative protein abundance within each commercial enzyme blend was determined based on an absolute basis of total observed spectral count (cumulative for all peptides detected). The classification of glycosyl hydrolases and related enzymes (polysaccharide lyases and carbohydrate esterases) into families based on amino acid sequence similarity was introduced recently [452]. It has been shown that catalytic domains for glycosyl hydrolases belonging to the same family have the same three-dimensional fold and exhibit similar stereospecificity for hydrolytic activities. Despite several limitations of this approach (e.g. possible lack of correlation between protein family and specific activity), the crude mixture protein composition was based on GH families in order to understand synergistic enzyme combinations necessary for efficient hydrolysis of pretreated cell walls.

Table 7.2 *Proteomics based protein compositional data for 14 crude enzyme blends based on total observed spectral counts.*

GH family	Enzyme Description	Acronym	RE 1	RE 2	RE 3	RE 4	RE 5	RE 6	RE 7
-	acetyl esterase	AC				1.9			
-	acetyl xylan esterase I	AXE 1				0.6			
-	acetyl xylan esterase II	AXE 2				0.1			
	Acetyl Xylan Esterases	**AXE**	-	-	-	**2.5**	-	-	-
-	feruloyl esterase	FAE		0.2	0.1				
	Feruloyl Esterases	**FAE**	-	**0.2**	**0.1**	-	-	-	-
1	β-glucosidase	BG 1	13.1						
3	β-glucosidase	BG 3	1.7	6.0	2.4	3.3	2.3		
	β-Glucosidases	**BG**	**14.8**	**6.0**	**2.4**	**3.3**	**2.3**	-	-
3	β-xylosidase	BX 3		1.0	0.3	4.9		0.2	
	β-Xylosidases	**BX**	-	**1.0**	**0.3**	**4.9**	-	**0.2**	-
6a	exocellulase II	CBH 2	5.9			13.4		0.8	0.8
7a	exocellulase I	CBH 1	17.7		1.6	34.7		2.9	
	Cellobiohydrolases	**CBH**	**23.6**	-	**1.6**	**48.1**	-	**3.7**	**0.8**
10	endoxylanase II	EX 2	15.2	1.0	0.1	0.3		0.3	10.3
11	endoxylanase I (all family 11 included)	EX 1	12.7			1.9	7.5	0.5	0.4
	Endo-xylanases	**EX**	**27.8**	**1.0**	**0.1**	**2.2**	**7.5**	**0.8**	**10.6**

Table 7.2 *Contd...*

GH family	Enzyme Description	Acronym	RE 1	RE 2	RE 3	RE 4	RE 5	RE 6	RE 7
5	endoglucanase II	EG 2	2.5	0.7	6.3	6.4	0.1	0.3	0.1
6	endoglucanase	GH 6	1.7						
7b	endoglucanase I	EG 1	2.5			6.4			
12	endoglucanase III	EG 3	2.1	0.2	2.2	0.5			
45	endoglucanase V	EG 5				0.1			
61a	endoglucanase IV	EG 4	3.4			0.6			
61b	endoglucanase VII	EG 7				0.3			
	Endo-glucanases	**EG**	**12.2**	**0.9**	**8.5**	**14.3**	**0.1**	**0.3**	**0.1**
43	arabinan arabinosidase	AA		0.3	0.9		0.1	1.8	2.0
51	α-arabinofuranosidase	ABF 1		0.8					
54	α-arabinofuranosidase	ABF 2		0.6	0.5				
62	α-arabinofuranosidase	ABF 3				0.5			
	Arabinofuranosidases	**ABF**	**-**	**1.7**	**1.4**	**0.5**	**0.1**	**1.8**	**2.0**
67	α-glucuronosidase	AGLUC				2.3			
	α-Glucuronosidase	**aGLUC**	**-**	**-**	**-**	**2.3**	**-**	**-**	**-**
74	xyloglucanase	XG			2.3	6.9			
	Xyloglucanases	**XG**	**-**	**-**	**2.3**	**6.9**	**-**	**-**	**-**

Table 7.2 *Contd...*

GH family	Enzyme Description	Acronym	RE 1	RE 2	RE 3	RE 4	RE 5	RE 6	RE 7
13	α-amylase	AMY		2.5	1.1	0.1	0.4	43.8	
15	glucoamylase	GAMY		49.3	1.7	1.8	5.5	0.4	1.6
	Amylases	**STAR**	**-**	**51.9**	**2.8**	**1.9**	**5.8**	**44.2**	**1.6**
-	pectin lyases (all PL families included)	PL			0.3			0.4	
-	pectin methyl esterase	PME			4.0		0.2		
-	rhamnogalacturonan acetyl esterase	RHAE			3.9		0.1		
-	α-rhamnosidase	ARH		0.1	1.8		0.3		0.4
28	polygalacturonases (endo/exo)	PGL		0.1	41.3		0.5		0.4
	Pectinases	**PECT**	**-**	**0.2**	**51.3**		**1.0**	**0.4**	**0.8**
-	other noncellulolytic proteins	OTHERS	21.5	23.9	10.7	2.0	76.1	26.7	69.5
-	cip protein 1	CIP 1				2.6			
-	cip protein 2	CIP 2				2.6			
-	swollenin	SWO				3.6			
2	β-mannosidase	BMANO		1.8					
5	β-mannase	BM			8.0	1.3	0.2		0.2
5	β-1,6-endogalactanase	BGAL 2				0.4			
16	GH 16 glycosyl hydrolase	GH 16		1.2	0.4		1.1	19.4	3.8
17	β-1,3-glucanase	GH 17		0.7			0.5		3.9

Table 7.2 *Contd...*

GH family	Enzyme Description	Acronym	RE 1	RE 2	RE 3	RE 4	RE 5	RE 6	RE 7
18	chitinase (endo)	CHI 1		0.1		0.4			0.4
20	chitinase (exo)	CHI 2		1.2			0.2		
27	α-galactosidase	AGAL		3.1	1.1				
30	β-1,6-glucanase, glucosylamidase, glucuronoxylanase	GH 30		0.5		0.1		1.4	
31	α-glucosidase	AG		1.0	0.3		2.2		0.7
32	β-fructofuranosidase	BFRC		1.0	1.1		0.5		
35	β-galactosidase	BGAL 1		1.2	4.7		0.1		
47	α-1,2-mannosidase (in oligomannosaccharides)	AMANO 1					0.2		0.8
53	arabinogalactan beta-galactosidase	ABGAL			3.0		0.6	1.1	2.0
55	β-1,3-glucanase (endo/exo)	GH 55		0.4		0.1			
65	trehalase	GH 65					0.1		
71	α-1,3-glucanase	GH 71							
72	glycosyl transferase	GT		0.4			1.5		2.7
76	α-1,6-mannase	AMAN							
79	β-glucuronidase	BGLUC							
81	β-1,3-1,4 endoglucanase	GH 81							
92	α-1,2-mannosidase	AMANO 2		0.7					
	Other proteins	**OTHER**	**21.5**	**37.1**	**29.2**	**13.0**	**83.2**	**48.6**	**84.0**

Table 7.2 *Contd...*

GH family	Enzyme Description	Acronym	RE 8	CE 1	CE 2	CE 3	CE 4	CE 5	CE 6
-	acetyl esterase	AC	1.9	1.2		4.4			
-	acetyl xylan esterase I	AXE 1	0.6	0.7		1.0		0.2	0.4
-	acetyl xylan esterase II	AXE 2		0.2		0.4			0.5
	Acetyl Xylan Esterases	**AXE**	**2.5**	**2.0**	**-**	**5.8**	**-**	**0.2**	**0.9**
-	feruloyl esterase	FAE			0.2		1.2		
	Feruloyl Esterases	**FAE**	**-**	**-**	**0.2**	**-**	**1.2**	**-**	**-**
1	β-glucosidase	BG 1							
3	β-glucosidase	BG 3	4.3	4.1	7.7	2.9	4.6	2.2	15.6
	β-Glucosidases	**BG**	**4.3**	**4.1**	**7.7**	**2.9**	**4.6**	**2.2**	**15.6**
3	β-xylosidase	BX 3	6.2	3.0	1.1	6.5	4.0		1.8
	β-Xylosidases	**BX**	**6.2**	**3.0**	**1.1**	**6.5**	**4.0**	**-**	**1.8**
6a	exocellulase II	CBH 2	9.6	10.4	0.1	1.0	0.3	13.0	12.7
7a	exocellulase I	CBH 1	31.8	27.5	0.3	2.0	0.8	23.0	25.1
	Cellobiohydrolases	**CBH**	**41.3**	**37.9**	**0.4**	**3.0**	**1.0**	**36.1**	**37.8**
10	endoxylanase II	EX 2	0.3	1.8	1.3	0.6	2.6	0.4	4.7
11	endoxylanase I (all family 11 included)	EX 1	2.0	2.6		35.8	1.8	4.1	1.3
	Endo-xylanases	**EX**	**2.4**	**4.4**	**1.3**	**36.4**	**4.4**	**4.5**	**6.0**

Table 7.2 *Contd...*

GH family	Enzyme Description	Acronym	RE 8	CE 1	CE 2	CE 3	CE 4	CE 5	CE 6
5	endoglucanase II	EG 2	4.5	5.3	0.6	0.2	3.1	7.6	7.1
6	endoglucanase	GH 6						0.4	
7b	endoglucanase I	EG 1	5.1	7.5		0.2		4.6	8.4
12	endoglucanase III	EG 3	0.5	2.4	0.2	0.4	1.7	2.8	2.5
45	endoglucanase V	EG 5						0.3	
61a	endoglucanase IV	EG 4	0.6	0.5		0.9	0.2	0.7	0.1
61b	endoglucanase VII	EG 7	0.2	0.2		0.1			0.5
	Endo-glucanases	**EG**	**10.9**	**15.8**	**0.8**	**1.9**	**5.1**	**16.5**	**18.6**
43	arabinan arabinosidase	AA			0.5		3.1		
51	α-arabinofuranosidase	ABF 1			0.9		3.6		
54	α-arabinofuranosidase	ABF 2	0.2	0.9	1.1	1.2	7.4	1.3	
62	α-arabinofuranosidase	ABF 3	0.4	1.0		1.2	2.8	1.4	0.4
	Arabinofuranosidases	**ABF**	**0.6**	**1.9**	**2.5**	**2.5**	**16.9**	**2.7**	**0.4**
67	α-glucuronosidase	AGLUC	3.3	2.4		2.5	1.4		0.5
	α-Glucuronosidase	**aGLUC**	**3.3**	**2.4**	**-**	**2.5**	**1.4**	**-**	**0.5**
74	xyloglucanase	XG	7.0	11.3		21.3	0.7	12.0	6.2
	Xyloglucanases	**XG**	**7.0**	**11.3**	**-**	**21.3**	**0.7**	**12.0**	**6.2**

Table 7.2 *Contd...*

GH family	Enzyme Description	Acronym	RE 8	CE 1	CE 2	CE 3	CE 4	CE 5	CE 6
13	α-amylase	AMY	1.5	0.4	3.4		1.2	0.2	0.4
15	glucoamylase	GAMY	6.6		40.2	0.2	3.3	2.0	0.2
	Amylases	**STAR**	**8.2**	**0.4**	**43.6**	**0.2**	**4.4**	**2.2**	**0.5**
-	pectin lyases (all PL families included)	PL					4.2	0.5	
-	pectin methyl esterase	PME					2.6	1.4	
-	rhamnogalacturonan acetyl esterase	RHAE					0.5	1.5	
-	α-rhamnosidase	ARH			0.2		1.5		
28	polygalacturonases (endo/exo)	PGL	0.1	0.1			6.2	6.1	
	Pectinases	**PECT**	**0.1**	**0.1**	**0.2**	-	**15.0**	**9.5**	-
-	other noncellulolytic proteins	OTHERS	4.1	2.6	27.4	5.6	20.0	3.0	2.5
-	cip protein 1	CIP 1	2.4	2.7		2.2		2.5	1.6
-	cip protein 2	CIP 2	1.8	3.0		2.1		1.1	2.2
-	swollenin	SWO	1.9	3.2				1.6	3.4
2	β-mannosidase	BMANO	0.1		1.7		2.0	0.2	
5	β-mannase	BM	1.4	1.4		0.8	0.4	3.3	1.3
5	β-1,6-endogalactanase	BGAL 2	0.2	0.7		1.5		0.4	0.8
16	GH 16 glycosyl hydrolase	GH 16	0.1		1.4		0.6		
17	β-1,3-glucanase	GH 17	0.2		1.3		0.7		

Table 7.2 *Contd...*

GH family	Enzyme Description	Acronym	RE 8	CE 1	CE 2	CE 3	CE 4	CE 5	CE 6
18	chitinase (endo)	CHI 1		0.2	0.1	0.3	0.2		0.3
20	chitinase (exo)	CHI 2	0.2	0.3	1.1	0.3	0.3		
27	α-galactosidase	AGAL	0.5	0.1	3.5	0.4	1.8	0.4	
30	β-1,6-glucanase, glucosylamidase, glucuronoxylanase	GH 30	0.1	0.2	0.4		0.1		
31	α-glucosidase	AG			1.0		2.7		
32	β-fructofuranosidase	BFRC	0.1		1.1		0.3	0.1	
35	β-galactosidase	BGAL 1		2.3	1.4	3.9	8.3	0.2	0.1
47	α-1,2-mannosidase (in oligomannosaccharides)	AMANO 1					1.4		
53	arabinogalactan beta-galactosidase	ABGAL					1.2	1.2	
55	β-1,3-glucanase (endo/exo)	GH 55			0.8		1.3		
65	trehalase	GH 65					0.4		
71	α-1,3-glucanase	GH 71					0.1		
72	glycosyl transferase	GT			0.3		0.6		
76	α-1,6-mannase	AMAN					0.1		
79	β-glucuronidase	BGLUC					0.8		
81	β-1,3-1,4 endoglucanase	GH 81					0.1		
92	α-1,2-mannosidase	AMANO 2			0.5		0.5		
	Other proteins	**OTHER**	**13.2**	**16.6**	**42.1**	**17.1**	**44.1**	**14.2**	**12.0**

Table 7.4 *Design of experiments for range of varying crude enzyme mixture composition (based on fixed total protein loading of 16.5 mg/g glucan equivalent to 100%) that were tested on AFEX treated corn stover.*

Notation	# Expts	re 1	re 2	re 3	re 4	re 5	re 6	re 7	re 8	ce 1	ce 2	ce 3	ce 4	ce 5	ce 6
8 ce-re	526	0-48%		0-48%		0-48%	0-48%	0-48%			0-48%	0-48%	0-48%		52%
10 ce-re	768	0-100%	0-100%		0-100%			0-100%	0-100%	0-100%		0-100%	0-100%	0-100%	0-100%
5 ce-re_A	72	0-100%						0-100%		0-100%			0-100%	0-100%	
5 ce-re_B	72	0-100%						0-100%					0-100%	0-100%	0-100%
5 ce-re_C	72	0-100%			0-100%			0-100%					0-100%	0-100%	

Based on **Table 7.2**, CBH I was the predominant cellulase in all major commercial enzymes ranging from 0-35%, followed by CBH II (0-14%), endoglucanase I (0-9%), endoglucanase II (0-8%), endoglucanase III (0-3%) and β-glucosidase (0-16%, GH 3). The major hemicellulases were found to be GH 11 endoxylanase (0-36%), GH 10 endoxylanase (0-15%), β-xylosidase (0-7%), GH 51 α-arabinofuranosidase (0-4%), GH 54 α-arabinofuranosidase (0-8%), GH 62 α-arabinofuranosidase (0-3%), acetyl xylan esterases (0-6%), and α-glucuronidase (0-3%). There was a significant amount of non-glycosyl hydrolytic proteins (See **Table V-7.3** for details on non-cellulolytic proteins for each CE1 based enzyme blend) present in several enzyme mixtures ranging from 2-80%. CE-4 and RE-3 had several pectin degrading enzymes (15-50%, inclusive of pectinases) that might not play a significant role in the hydrolysis of secondary cell walls. Swollenin was present in surprisingly high amounts in several cellulases (0-4%), along with cip proteins (0-3%). Starch degrading amylases were also present in relatively high concentrations in certain enzymes (0-52%). Xyloglucanases (GH 74) were also present in most crude blends in surprisingly high amounts (0-22%), indicating that the expression of these enzymes is closely coordinated with other cellulases and hemicellulases. Xyloglucanases are probably an important class of enzymes expressed by fungi growing on plant cell walls in the wild due to high amounts of xyloglucans present in the primary cell walls that the fungus must digest to get through to the secondary cell walls. However, the total amount of xyloglucanases present in most commercial enzyme mixtures is not optimized for pretreated secondary cell walls (for grasses like corn stover) that have little or no xyloglucan.

It is would be interesting to correlate specific activity data (**Table 7.1-B**) to individual protein composition (**Table 7.2**) in order to further validate the two datasets. However, this could be relatively complicated due to presence of multi-functional enzymes, synergistic interactions between enzymes and lack of correlation between activities on certain chromogenic vs. realistic substrates [385]. A strong linear correlation was seen between Avicelase and CMCase activities and total cellobiohydrolase (R^2 = 0.73; % CBH I + CBH II vs. Avicelase activity) and endoglucanase (R^2 = 0.79; % EG I + EG II + EG III + EG IV + EG V + EG VII vs. CMCase activity) content, respectively. However, there was a poorer correlation between total amounts of GH 3 β-glucosidase present vs. activity on pNPG. This is largely due to cross-activity of several other glycosyl hydrolases on pNPG [453]. NS-50014 had abnormally high activity on oat-spelt xylan compared to all other enzyme mixtures. There was no significant correlation between oat spelt xylanase activity and total endoxylanase content. This is not surprising considering that many xylanases act on only debranched xylan backbones and presence of other synergistic accessory enzymes would give variable, non-linear correlations. Multifect Pectinase had very high arabinofuranosidase activity compared to all other enzymes. There was a reasonable correlation (R^2 = 0.9) between pNPAf activity and total arabinofuranosidase content, however, this correlation might be skewed due to CE 4. Multifect xylanase (CE 3) gave the highest activity on pNPA which is not surprising considering that it contained the highest proportion of acetyl xylan esterases (6%). There was a reasonable correlation (R^2 = 0.65) between pNPA activity and total esterase content, however, this correlation might be skewed due to CE 3.

7.1.4.3 Maximizing enzyme synergy using simplex centroid experimental designs

One of the primary limitations of regular enzymatic hydrolysis assays is that they are low-throughput, time-consuming and tedious. In order to screen a larger combination of enzyme mixtures a microplate based hydrolysis assay technique was developed for lignocellulosic biomass [2,453]. The microplate methodology is automated, high-throughput and more reproducible compared to other conventional assays [392]. Low enzyme loading to produce cellulosic ethanol in an economically feasible manner lies in the range of 1-10 mg protein/gm glucan. Protein loading currently employed for AFEX treated corn stover/poplar has not been optimized and lies in the range of 30-180 mg protein/gm glucan to achieve reasonably high total sugar conversions (~ 90% glucan and 80% xylan conversion) [53,54]. Most commercial cellulase mixtures lack sufficient hemicellulase activities necessary to hydrolyze AFEX treated biomass.

In order to optimize commercial enzyme mixtures for AFEX corn stover, several mixture optimization experiments were conducted using 14 commercially available crude cellulase and hemicellulases (See **Table 7.4**). These enzyme cocktails were found to have multiple enzyme activities based on the model substrate activity assays, as discussed in the previous section. The commercial (Spezyme, Multifect Xylanase and Pectinase, Depol 670L, Accellerase, Novozyme 188; CE 1-6) and research enzymes (Novozyme NS-series; RE 1-8) were optimized for enhancing hydrolytic performance on AFEX treated corn stover using the BCRL high-throughput microplate methodology [2]. The study of synergism amongst a variety of enzymes requires the use of carefully designed experiments capable of analyzing multiple levels of synergy while fixing the sum of all mixture components; this can be achieved using the simplex-centroid experimental

design [438]. The simplex-centroid experimental design requires experiments to be performed first on single-blend "pure" mixtures, then on double-blends (that is, 50% of each of two components), and so on (thus requiring 2^n-1 trials, where n is the number of components). This allows the calculation of a multidimensional polynomial mixture regression equation, with terms representing the effect of single enzymes, binary synergies (the product of the concentration of two enzymes and a regression coefficient), ternary synergies, and so on, depending on the order of the regression equation; the magnitude of the regression coefficient indicates the relative importance of any particular enzyme or enzyme synergies (See equation below).

$$Y = \sum_{1 \le i \le q} \beta_i x_i + \sum_{1 \le i < j \le q} \beta_{ij} x_i x_j + \sum_{1 \le i < j < k \le q} \beta_{ijk} x_i x_j x_k + \cdots$$

Where; Y is the response variable (e.g. % glucan conversion); q is the number of enzymes; x_i is the proportion of the i^{th} enzyme in the mixture; and $\beta_{ij...m}$ is the coefficient of synergy for m enzymes. The magnitude of each $\beta_{ij...m}$ indicates the strength of a particular enzyme or synergistic interaction.

Three simplex centroid experiments were designed: (1) **8 CE-RE**: adding 8 mg total protein/g glucan of eight accessory enzymes – Novozyme 188, Multifect Xylanase, Multifect Pectinase, NS22002, NS50012, NS50014, NS50029, and NS50030—to fixed 8.5 mg Accellerase/gm glucan of AFEX stover; (2) **10 CE-RE**: adding 16.5 mg protein/g glucan of ten enzymes – Spezyme, Multifect Xylanase and Pectinase, Depol 670L, Accellerase, NS22002, NS50010, NS50013, NS50030, and NS50053; and (3) **5 CE-RE**: adding 16.5 mg protein/g glucan of one major cellulase (either one of Spezyme, Accellerase, or NS50013), Multifect Pectinase, Depol 670L, NS22002, and NS50030.

Hydrolysis on AFEX treated corn stover for all enzyme combinations was investigated using the high-throughput BCRL microplate methodology at pH 5, 50 °C, 270 rpm, 500 µl reaction volume and 0.2% glucan loading. The AFEX condition used for all experiments was medium severity at 1:1 ammonia loading (dry weight biomass), 15 min (total residence time), 60% moisture (dwb) and 130 Degrees °C. Details for the enzyme mixtures tested and the obtained glucan and xylan conversion are given in **Table V-7.15**.

Third-degree mixed stepwise (α-to-enter/α-to-leave: 0.15) regressions were performed on the results (% glucan conversion, % xylan conversion, total glucose and xylose released as gms sugar per kg dry weight biomass) of each experimental dataset to generate models predicting response as function of enzyme mixture composition, with the stepwise regression algorithm preserving statistically significant interaction effects [454]. The validity of the regression models obtained from stepwise special cubic regressions of all mixture experiments was confirmed by analyzing residual histograms, normal distribution curves of residuals, residuals versus fits, and residuals versus order plots (data not shown). Analysis suggested that quadratic and quaternary interaction terms based model regressions did not accurately predict the variance (low R^2 and high σ values) in the data as compared to special cubic interaction terms based regression models. The σ (sigma or S) and R^2 values were also closely analyzed for comparing models; all σ-values suggested that the first standard deviation of residuals was relatively small (<5%). The σ-values for xylan conversion were slightly higher than those for glucan conversion, suggesting possibly that the xylose assay was less precise than the glucose assay. High R^2 and R^2 (adj or adjusted) values (> 80%) indicate that the models

account for majority of the variation in the dataset and was not a result of overfitting. High R^2 (pred or predicted) (> 80%) values indicate that the models had significant predictive capabilities.

The regression equations were optimized, for response output (using Minitab response optimizer functionality), by maximizing a desirability function (weight = 1, min = 0, target = 100 for glucan and xylan conversion; 630 for total sugar hydrolytic yield) [455]. Cox response trace plots were generated to analyze the effect of varying the composition of enzyme cocktails with respect to the optimal reference blend (i.e. model-generated optimum) as a measure of relative sensitivity of output to input parameters.

7.1.4.4 Eight-enzyme (8 ce-re) simplex centroid experimental design

Table 7.5 summarizes the estimated regression coefficients (in decreasing order of magnitude for each class of terms; single-binary-ternary) for models predicting the glucan/xylan conversion and total sugar yield as a function of enzyme mixture composition. It can be inferred that NS50030 (RE 7) and NS50014 (RE 5) affected glucan conversion most significantly (based on regression coefficient for RE 7 and RE 5 based individual terms). On the other hand, Multifect Pectinase (CE 4) and Multifect Xylanase (CE 3) affected xylan conversion most significantly. Within the binary terms predicting glucan conversion, the top 4 interaction terms contain RE 7; whereas, binary terms predicting xylan conversion are dominated by CE 4 and CE 3.

Table 7.5 *Estimated regression coefficients for model terms (single, binary and cubic based interaction terms) predicting % glucan conversion, % xylan conversion and total sugar yield (gm sugar/kg dry weight biomass) as a function of crude enzyme mixture amount composition for 8 CE-RE based experiments. The sum of total enzyme loading is always equal to 8 mg protein/g glucan. All enzyme mixtures have a fixed loading of 8.5 mg CE 6/g glucan, which is not included as a regressor in the model. Where; VIF = variance inflation factor, PRESS = prediction error sum of squares, S = first standard deviation of residuals, R-Sq(pred) = predicted R^2 (coefficient of determination); R-Sq(adj) = adjusted R^2.*

Regression Terms (% Glucan conversion)				Regression Terms (% Xylan conversion)				Regression Terms (Total sugar yield, g/kg)			
Term	**Coefficient**	**P**	**VIF**	**Term**	**Coefficient**	**P**	**VIF**	**Term**	**Coefficient**	**P**	**VIF**
re 7	71.64	*	8.46	ce 4	58.8	*	8.958	ce 4	379.4	*	7.209
re 5	68.68	*	8.057	ce 3	53.2	*	8.958	ce 3	364.2	*	8.498
ce 3	63.6	*	8.368	re 7	26.6	*	3.067	re 7	321.4	*	8.556
re 1	61.08	*	7.892	ce 2	26.2	*	2.987	re 5	312.6	*	6.92
ce 4	58.44	*	5.835	re 5	22.9	*	2.763	re 1	308	*	5.006
re 3	53.22	*	4.83	re 1	20.2	*	3.037	ce 2	252.6	*	5.656
ce 2	51.89	*	5.704	re 3	15.6	*	2.763	re 3	238.6	*	4.79
re 6	47.5	*	4.83	re 6	10.8	*	2.987	re 6	220	*	4.291
ce 2*re 7	75.78	0	3.83	ce 4*re 1	119.4	0	4.639	ce 4*re 7	530.5	0	4.45
re 3*re 7	66.67	0	3.28	ce 3*re 1	116.5	0	4.639	ce 3*re 7	505.7	0	3.571
re 6*re 7	63.65	0	3.28	ce 4*re 7	104.1	0	4.111	ce 3*re 3	389.9	0	3.261
ce 4*re 7	61.77	0	4.358	ce 4*re 5	93.1	0	4.041	ce 4*re 1	381.2	0	4.225
ce 2*re 5	59.56	0	2.894	ce 3*re 7	89.9	0	4.111	ce 4*re 5	379.2	0	4.31
ce 2*re 1	59.09	0	2.145	ce 3*re 6	76.8	0	4.091	ce 2*re 7	361.3	0	3.81
ce 4*re 1	51.41	0	2.625	ce 3*re 5	69.7	0	4.041	ce 3*re 6	349.2	0	3.733

Table 7.5 *Contd...*

Regression Terms (% Glucan conversion)			
Term	**Coefficient**	**P**	**VIF**
ce 4*re 5	50.16	0	2.886
re 1*re 7	49.48	0	3.1
re 5*re 7	48.65	0	2.191
ce 3*re 7	43.45	0	3.571
re 1*re 3	42.53	0	2.186
re 1*re 6	41.36	0	2.186
ce 2*ce 3	39.24	0	3.365
re 3*re 5	36.91	0	3.28
ce 3*re 3	36.45	0	3.279
re 5*re 6	33.56	0.001	3.28
ce 3*ce 4	31.26	0.003	3.353
ce 3*re 6	29.77	0.004	3.279
ce 2*ce 4	27.54	0.003	2.564
ce 3*re 1	27.25	0.003	2.641
re 1*re 5	25.02	0.003	2.157
ce 3*re 5	23.55	0.005	2.211

Regression Terms (% Xylan conversion)			
Term	**Coefficient**	**P**	**VIF**
ce 3*re 3	68.5	0	4.041
ce 4*re 3	64.4	0	4.041
ce 4*re 6	54.4	0.003	4.091
ce 3*ce 4	47.7	0.001	2.628
ce 2*ce 3	47.4	0.01	4.091
ce 2*ce 4	42.3	0.021	4.091

Regression Terms (Total sugar yield, g/kg)			
Term	**Coefficient**	**P**	**VIF**
ce 3*re 1	346.2	0	3.783
ce 3*re 5	345.8	0	2.972
ce 2*ce 3	344.4	0	3.359
re 3*re 7	328.6	0	3.341
ce 2*re 5	271.5	0	3.313
ce 2*re 1	260.9	0	2.555
ce 3*ce 4	254.3	0	2.536
re 6*re 7	237.3	0.002	3.732
re 1*re 7	211.7	0.004	3.447
ce 4*re 3	198.2	0.014	4.202
re 5*re 6	192	0.004	2.893
re 5*re 7	189.1	0.006	3.046
re 3*re 5	154.7	0.029	3.243
ce 2*ce 4	**148.8**	**0.068**	**4.245**

Table 7.5 *Contd...*

Regression Terms (% Glucan conversion)				Regression Terms (% Xylan conversion)				Regression Terms (Total sugar yield, g/kg)			
Term	**Coefficient**	**P**	**VIF**	**Term**	**Coefficient**	**P**	**VIF**	**Term**	**Coefficient**	**P**	**VIF**
ce 2*re 6*re 7	351.52	0	1.768	ce 4*re 6*re 7	751.9	0	1.758	ce 4*re 6*re 7	3095.5	0	1.802
ce 4*re 6*re 7	279.37	0	1.77	ce 4*re 5*re 6	724.6	0	1.725	ce 4*re 5*re 6	2650.7	0	1.796
ce 2*re 3*re 7	236.41	0	1.768	ce 4*re 3*re 5	690.2	0	1.725	ce 4*re 3*re 5	2313.5	0	2.036
ce 4*re 3*re 7	203.68	0.001	1.77	ce 4*re 3*re 7	671.2	0	1.725	ce 4*re 3*re 7	2191.6	0	2.035
ce 4*re 5*re 6	195.48	0.002	1.767	ce 4*re 5*re 7	644	0	1.725	ce 4*re 3*re 6	2049.2	0	1.593
ce 2*re 3*re 5	192.74	0.002	1.793	ce 2*ce 4*re 5	623	0	1.725	ce 4*re 1*re 6	1941	0	1.593
ce 4*re 3*re 5	187.51	0.003	1.767	ce 2*ce 4*re 7	563.3	0	1.758	ce 4*re 5*re 7	1878.5	0	1.972
ce 2*re 5*re 6	182.98	0.004	1.793	ce 4*re 1*re 7	561.3	0	1.76	ce 2*ce 4*re 7	1847.4	0	1.973
ce 2*ce 3*re 6	180.79	0.004	1.762	ce 4*re 3*re 6	542.6	0	1.725	ce 2*ce 4*re 5	1846.9	0	1.996
re 3*re 6*re 7	168.37	0.008	1.774	ce 4*re 1*re 6	516.5	0	1.744	ce 4*re 1*re 7	1751.3	0	2.036
ce 4*re 3*re 6	164.89	0.004	1.461	ce 4*re 1*re 5	509.5	0	1.726	ce 2*re 6*re 7	1703	0	1.774
ce 3*re 1*re 7	151.94	0.023	2.02	ce 2*ce 4*re 1	432.5	0	1.744	ce 4*re 1*re 5	1633.6	0	1.756
ce 3*ce 4*re 6	148.25	0.018	1.762	ce 4*re 1*re 3	400.8	0	1.726	ce 2*ce 4*re 6	1410	0.001	1.606
ce 3*ce 4*re 7	131.86	0.05	2.032	ce 2*ce 4*re 3	363.5	0	1.725	ce 2*ce 4*re 1	1266	0.007	2.056
ce 2*ce 3*re 3	125.59	0.045	1.762	ce 2*ce 4*re 6	347.9	0.001	1.742	ce 2*ce 3*re 6	1235.6	0.005	1.769
ce 3*ce 4*re 3	124.37	0.047	1.762	ce 3*re 5*re 7	316.7	0.001	1.725	ce 4*re 1*re 3	1211.1	0.006	1.763
ce 2*ce 4*re 7	123.74	0.07	1.953	ce 3*re 1*re 3	310.6	0.002	1.726	ce 2*ce 4*re 3	1145.8	0.009	1.779
re 3*re 5*re 6	**115.07**	**0.067**	**1.775**	ce 3*re 1*re 5	294.7	0.003	1.726	ce 3*re 1*re 3	1142.3	0.009	1.758
ce 2*re 3*re 6	112.83	0.048	1.461	ce 3*re 3*re 7	291.3	0.003	1.725	ce 3*re 1*re 7	1126.2	0.016	2.027

Table 7.5 *Contd...*

Regression Terms (% Glucan conversion)			
Term	**Coefficient**	**P**	**VIF**
ce 4*re 1*re 7	**107.87**	**0.107**	**2.028**
ce 2*ce 3*re 7	**106.98**	**0.111**	**2.031**
ce 3*re 3*re 6	**104.49**	**0.095**	**1.774**

S = 2.77432 PRESS = 3509.79
R-Sq(pred) = 80.80% R-Sq(adj) = 89.05%

Regression Terms (% Xylan conversion)			
Term	**Coefficient**	**P**	**VIF**
ce 2*ce 3*re 7	286.4	0.004	1.758
ce 3*re 1*re 7	262.1	0.009	1.76
ce 3*re 5*re 6	254.9	0.01	1.725
ce 3*re 1*re 6	248.1	0.013	1.744
ce 2*ce 3*re 6	244.6	0.014	1.742
ce 2*ce 3*re 5	241.5	0.015	1.725
ce 3*re 6*re 7	229.9	0.022	1.758
ce 3*re 3*re 6	221.1	0.026	1.725
ce 2*ce 3*re 3	213.1	0.031	1.725
ce 2*re 6*re 7	188	0.036	1.415
ce 3*re 3*re 5	179.2	0.07	1.725
ce 2*ce 3*re 1	**154.8**	**0.119**	**1.744**
ce 2*re 1*re 7	143.2	0.11	1.415
re 1*re 6*re 7	**135.9**	**0.129**	**1.415**
ce 3*ce 4*re 1	**-174.4**	**0.104**	**2.031**

S = 4.43615 PRESS = 9019.01
R-Sq(pred) = 92.21% R-Sq(adj) = 95.55%

Regression Terms (Total sugar yield, g/kg)			
Term	**Coefficient**	**P**	**VIF**
ce 2*re 3*re 7	1054.2	0.016	1.775
ce 2*re 3*re 5	962.3	0.029	1.802
ce 2*ce 3*re 3	953.4	0.029	1.772
ce 3*re 5*re 7	947.2	0.042	2.026
ce 2*ce 3*re 7	921.9	0.048	2.032
re 3*re 6*re 7	885.6	0.042	1.757
re 1*re 3*re 5	871.7	0.034	1.569
ce 3*re 3*re 6	858.3	0.048	1.76
ce 3*re 1*re 6	840.6	0.053	1.762
ce 3*re 1*re 5	**829.9**	**0.055**	**1.744**
re 1*re 6*re 7	**754.8**	**0.082**	**1.757**
ce 2*re 5*re 6	**751.9**	**0.086**	**1.796**
ce 3*ce 4*re 6	**738.2**	**0.092**	**1.793**
re 1*re 3*re 6	**638.8**	**0.104**	**1.441**

S = 19.2908 PRESS = 161858
R-Sq(pred) = 87.54% R-Sq(adj) = 92.55%

Similar trends can be seen for the ternary terms as well, with RE 7, CE 3 and CE 4 being the predominant contributors to most synergistic interactions. Not surprisingly, the enzyme combinations that gave the highest total sugar yields were an intermediate combination of terms maximizing both glucan and xylan conversion.

The composition of the optimal enzyme cocktail giving the highest glucan, xylan and total sugar yields are shown in **Figures 7.2 A, 7.2 B** and **7.2 C**, respectively, as Cox-response trace plots (a steep slope or curvature within cox-plot due to change in input variable indicates a relatively high sensitivity of response). Each enzyme mixture is composed of 8.5 mg/g glucan of Accellerase (52% of total enzyme loading) and varying mixture ratios of other accessory enzymes (within the remaining 48% enzyme or 8 mg out of the total 16.5 mg/g glucan). For optimal glucan conversion (90.93%), the 8 mg accessory protein mixture is composed of 46.75% RE 7, 18.25% CE 2, 14.62% RE 6, 11.25 % CE 4 and 9.12% RE 3. For optimal xylan conversion (93.63%), the 8 mg accessory protein mixture is composed of 45.25% CE 4, 18.38% RE 7, 14.12% RE 5, 10.13% RE 1, 8.13% RE 6 and 4% RE 3. The glucan conversion was found to be most significantly affected by relative change in RE 6, RE 7 and CE 2 based on relative steepness of Cox-trace plot (**Figure 7.2-A**), however, maximum response was only obtained at the reference blend composition. The Cox-response plots help validate the predicted optimum solutions obtain using the desirability functions.

Figure 7.2 *Cox-response trace plots for % glucan conversion (A), % xylan conversion (B) and total sugar yield (C) with respect to reference blend at optimal mixture composition for 8 CE-RE experiments.*

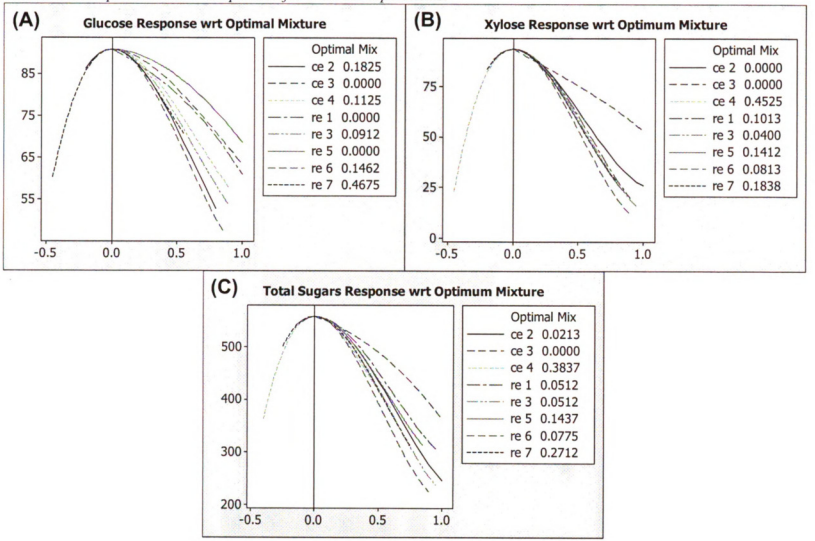

Based on the proteomics composition and activity assay analysis, it is clear that CE 6 has significant cellulase activity but lacks several hemicellulases. Supplementation of CE 6 with RE 7 and CE 2 helped increase glucan conversion, while addition of CE 4 and RE 7 significantly enhanced the xylan conversion. RE 7 and CE 2 are rich in endoxylanases and arabinofuranosidases (GH 43, 51, 54), respectively (**Table 7.2**); while, CE 4 is rich in arabinofuranosidases (GH 43, 51, 54, 62) and α-glucuronidases. This would suggest that removal of hemicellulose embedded within cell walls through addition of suitable endoxylanases helps enhance cellulose accessibility. However, in order to achieve higher xylose yield, it becomes pertinent to hydrolyze xylan side-chains through addition of suitable accessory enzymes (i.e. arabinofuranosidases, α-glucuronidases).

7.1.4.5 Ten-enzyme (10 ce-re) simplex centroid experimental design

Table V-7.6 summarizes the estimated regression coefficients (in decreasing order of magnitude for each class of terms; single-binary-ternary) for models predicting the glucan/xylan conversion and total sugar yield as a function of enzyme mixture composition. It can be inferred that RE 8, CE 6, CE 1, CE 5 and RE 4 affected glucan conversion most significantly (based on regression coefficient for individual terms). On the other hand, CE 4 and CE 3 affected xylan conversion most significantly. Within the binary terms predicting glucan conversion, the top interaction terms contain either one of the cellulase rich mixtures (i.e. CE 6, RE 4, CE 1, RE 8); whereas, binary terms predicting xylan conversion are dominated by RE 1, CE 5 or RE 7. Similar trends can be seen for the ternary terms as well, with RE 7, CE 3 and CE 4 being the predominant contributors to most synergistic interactions. As before, the enzyme combinations that

gave the highest total sugar yields were an intermediate combination of terms maximizing both glucan and xylan conversion.

The composition of the optimal enzyme cocktail giving the highest glucan, xylan and total sugar yields are shown in **Figures V-7.3 A, V-7.2 B** and **V-7.2 C**, respectively, as Cox-response trace plots (a steep slope or curvature within Cox-plot due to change in input variable indicates a relatively high sensitivity of response). Each enzyme mixture is composed of 16.5 mg/g glucan of varying mixture ratios of cellulases, hemicellulases and other accessory enzymes. For optimal glucan conversion (86.06%), the 16.5 mg protein mixture is composed of 40.18% CE 6, 16.67% RE 7, 13.15% CE 5, 11.94% RE 4, 9.09% CE 3 and 8.97% RE 1. For optimal xylan conversion (85.29%), the protein mixture is composed of 29.27% CE 5, 17.15% CE 1, 16.73% RE 7, 16% CE 3, 9.09% RE 1, 6.85% RE 4 and 4.91% CE 6. The glucan conversion was found to be most significantly affected by relative change in CE 6, RE 7 and CE 3 based on relative steepness of Cox-trace plot (**Figure V-7.3-A**), however, maximum response was only obtained at the reference blend composition.

One of the major issues with the 10 CE-RE experiments was the high multicollinearity between respective factors. Multicollinearity is a statistical phenomenon in which two or more variables in a multidimensional model have similar effects. This may affect the extrapolation of the results obtained from the model. Multicollinearity is indicated by high Variance Inflation Factor (VIF) values. VIF values greater than 5 were observed for a number of the coefficients in the 10-enzyme and 8-enzyme experiments, indicating the presence of multicollinearity. Multicollinearity in the model may have been due to the fact that several commercial and research enzymes attack similar substrates

(See **Tables 7.1 and 7.2**), but with differing effectiveness. To improve the predictive abilities of the model, another set of experiments was designed (See next section) by using a diverse set of the five most effective enzymes determined from the previous two experiments. The enzymes were selected to minimize the overlaps in their substrate specificity.

7.1.4.6 Five-enzyme (5 ce-re) simplex centroid experimental design

The 5 CE-RE experiments were setup to compare the effectiveness of three different cellulases in combination with suitable hemicellulases and accessory enzymes. The 3 cellulases chosen were based on their performance in the previous experiments (Specific activity on Avicel and performance in 8 CE-RE and 10 CE-RE experiments); namely, CE 1, CE 6 and RE 4.

Table 7.7 summarizes the estimated regression coefficients (in decreasing order of magnitude for each class of terms; single-binary-ternary) for models predicting the glucan/xylan conversion and total sugar yield as a function of enzyme mixture composition (based on CE 1 as base cellulase). It can be inferred that CE 1 and CE 5 affected glucan conversion most significantly (based on regression coefficient for individual terms). On the other hand, CE 4, RE 1 and RE 7 affected xylan conversion most significantly. Within the binary terms predicting glucan conversion, the top interaction terms contain CE 4; whereas, binary terms predicting xylan conversion are dominated by CE 4, RE 1 and RE 7. Similar trends can be seen for the ternary terms as well, with RE 7, CE 1 and CE 4 being the predominant contributors to most synergistic interactions.

Table 7.7 *Estimated regression coefficients for model terms (single, binary and cubic based interaction terms) predicting % glucan conversion, % xylan conversion and total sugar yield (gm sugar/kg dry weight biomass) as a function of crude enzyme mixture amount composition for 5 CE-RE (Cel x is CE 1) based experiments. The sum of total enzyme loading is always equal to 16.5 mg protein/g glucan.*

Regression Terms (% Glucan conversion)				Regression Terms (% Xylan conversion)				Regression Terms (Total sugar yield, g/kg)			
Term	**Coefficient**	**P**	**VIF**	**Term**	**Coefficient**	**P**	**VIF**	**Term**	**Coefficient**	**P**	**VIF**
cel x	49.99	*	2.189	ce4	39.322	*	3.203	cel x	218.13	*	1.807
ce5	27.83	*	1.809	re7	9.466	*	1.788	ce4	174.18	*	3.203
re1	21.7	*	2.189	cel x	8.475	*	1.738	ce5	114.69	*	1.807
ce4	19.68	*	2.616	re1	7.916	*	1.738	re1	108.7	*	1.807
re7	7.19	*	1.648	ce5	3.337	*	1.788	re7	48.01	*	1.845
cel x*ce4	97.94	0	2.627	cel x*ce4	104.692	0.002	2.614	cel x*ce4	621.16	0	2.635
ce4*re1	48.56	0.015	2.627	ce4*re1	102.735	0.002	2.614	ce4*re1	427.73	0.005	2.635
ce4*ce5	**28.38**	**0.142**	**2.566**	ce4*re7	96.001	0.004	2.632	ce4*ce5	299.28	0.046	2.635
cel x*re1	**27.1**	**0.143**	**2.361**	ce4*ce5	78.143	0.019	2.632	**ce4*re7**	**233.84**	**0.117**	**2.65**
cel x*ce4*re7	1151.13	0	1.445	cel x*ce4*re7	872.058	0	1.601	cel x*ce4*re7	6527.86	0	1.617
ce4*ce5*re7	666.43	0	1.446	cel x*ce4*re1	807.175	0	1.584	cel x*ce4*re1	4469.77	0	1.602
cel x*ce4*re1	586.52	0	1.848	ce4*ce5*re1	649.687	0.001	1.601	ce4*ce5*re7	4204.94	0	1.617
ce4*re1*re7	490.95	0	1.445	ce4*ce5*re7	648.034	0.002	1.617	ce4*ce5*re1	3161.02	0.001	1.602
ce4*ce5*re1	405.39	0.001	1.601	cel x*ce4*ce5	524.973	0.009	1.601	ce4*re1*re7	3079	0.001	1.617
cel x*ce4*ce5	380.06	0.002	1.601	ce4*re1*re7	498.82	0.013	1.601	cel x*ce4*ce5	2754.23	0.003	1.602
cel x*ce5*re7	333.47	0.002	1.321	**ce5*re1*re7**	**313.818**	**0.081**	**1.322**	cel x*ce5*re7	1891.78	0.021	1.326
cel x*re1*re7	303	0.008	1.444	**cel x*ce5*re7**	**269.768**	**0.132**	**1.322**	cel x*re1*re7	1642.43	0.044	1.326
ce5*re1*re7	**178.12**	**0.096**	**1.321**					**ce5*re1*re7**	**1408.13**	**0.083**	**1.326**
S = 5.82636 PRESS = 2970.91				S = 9.78623 PRESS = 7586.99				S = 44.2005 PRESS = 163717			
R-Sq(pred) = 89.01% R-Sq(adj) = 91.08%				R-Sq(pred) = 84.93% R-Sq(adj) = 86.49%				R-Sq(pred) = 86.33% R-Sq(adj) = 88.42%			

Figure 7.4 *Cox-response trace plots for % glucan conversion (A), % xylan conversion (B) and total sugar yield (C) with respect to reference blend at optimal mixture composition for 5 CE-RE experiments (Cel x is CE 1).*

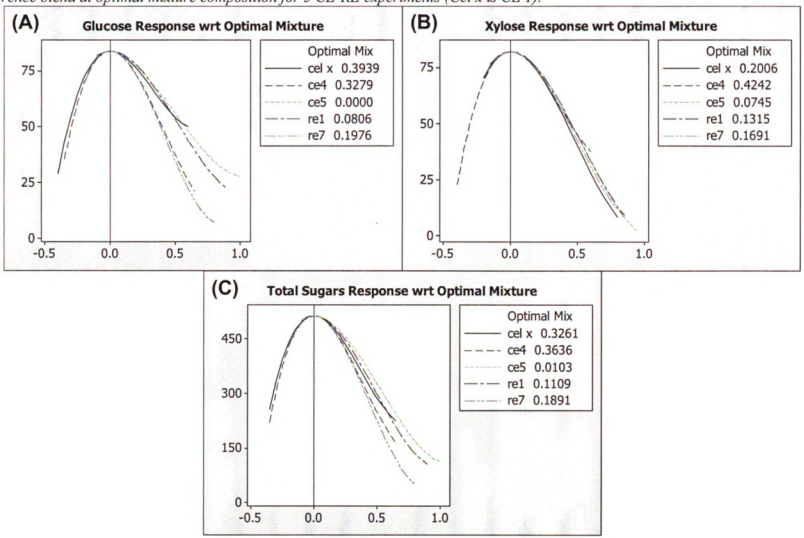

Not surprisingly, the enzyme combinations that gave the highest total sugar yields were again an intermediate combination of terms maximizing both glucan and xylan conversion. The composition of the optimal enzyme cocktail giving the highest glucan, xylan and total sugar yields are shown in **Figures 7.4 A, 7.4 B** and **7.4 C**, respectively, as Cox-response trace plots. Each enzyme mixture is composed of 16.5 mg/g glucan of varying mixture ratios of cellulases, hemicellulases and accessory enzymes. For optimal glucan conversion (84.06%), the protein mixture is composed of 39.39% CE 1, 32.79% CE 4, 19.76% RE 7 and 8.06% RE 1. For optimal xylan conversion (82.3%), the protein mixture is composed of 42.42% CE 4, 20.06% CE 1, 16.91% RE 7, 13.15% RE 1 and 7.45% CE 5. The glucan conversion was found to be most significantly affected by relative change in CE 1, CE 4 and RE7 based on relative steepness of Cox-trace plot (**Figure 7.4-A**), however, maximum response was only obtained at the reference blend composition.

Table V-7.8 summarizes the estimated regression coefficients (in decreasing order of magnitude for each class of terms; single-binary-ternary) for models predicting the glucan/xylan conversion and total sugar yield as a function of enzyme mixture composition (based on CE 6 as base cellulase). It can be inferred that RE 7 affected glucan conversion most strikingly (based on regression coefficient for individual and binary terms). On the other hand, CE 4, RE 1 and RE 7 affected xylan conversion most significantly. These results are comparable to the 8 CE-RE experiments further validating previous results. The composition of the optimal enzyme cocktail giving the highest glucan, xylan and total sugar yields are shown in **Figures V-7.5 A, V-7.5 B** and **V-7.5 C**, respectively, as Cox-response trace plots. Each enzyme mixture is composed of 16.5

mg/g glucan of varying mixture ratios of cellulases, hemicellulases and accessory enzymes. For optimal glucan conversion (77.3%), the protein mixture is composed of 51.52% CE 6, 25.82% RE 7, 20.67% CE 4 and 2% RE 1. For optimal xylan conversion (80.24%), the protein mixture is composed of 43.15% CE 4, 17.39% CE 6, 16.18% RE 1, 16.12% RE 7 and 7.15% CE 5. The glucan conversion was found to be most significantly affected by relative change in CE 6, CE 4 and RE7 based on relative steepness of Cox-trace plot (**Figure V-7.5-A**), however, maximum response was only obtained at the reference blend composition.

Table V-7.9 summarizes the estimated regression coefficients (in decreasing order of magnitude for each class of terms; single-binary-ternary) for models predicting the glucan/xylan conversion and total sugar yield as a function of enzyme mixture composition (based on RE 4 as base cellulase). It can be inferred that CE 4 affected glucan conversion most significantly (based on regression coefficient for individual and binary terms). On the other hand, CE 4, RE 1 and RE 7 affected xylan conversion most significantly. The composition of the optimal enzyme cocktail giving the highest glucan, xylan and total sugar yields are shown in **Figures V-7.6 A, V-7.6 B** and **V-7.6 C**, respectively, as Cox-response trace plots. Each enzyme mixture is composed of 16.5 mg/g glucan of varying mixture ratios of cellulases, hemicellulases and accessory enzymes. For optimal glucan conversion (83.83%), the protein mixture is composed of 38.36% RE 4, 35.09% CE 4, 23.52% RE 7 and 3.03% RE 1. For optimal xylan conversion (79.54%), the protein mixture is composed of 41.88% CE 4, 16.73% RE 7, 16.18% RE 4, 15.03% RE 1 and 10.18% CE 5. The glucan conversion was found to be most significantly affected by relative change in RE 4, CE 4 and RE7 based on relative

steepness of Cox-trace plot (**Figure V-7.6-A**), however, maximum response was only obtained at the reference blend composition.

Based on the proteomics composition and activity assay analysis, it is clear that CE 1 has significant cellulase activity but lacks several hemicellulases. Based on the response of the optimal mixtures for all three sets of 5 CE-RE experiments, CE 1 in combination with other enzymes gave the highest glucan and xylan conversions. Supplementation of CE 1 with RE 7 and CE 4 helped increase glucan conversion, while addition of CE 4 and RE 7 significantly enhanced the xylan conversion. RE 7 is rich in endoxylanases (GH 10) and certain arabinofuranosidases (GH 43) (**Table 7.2**); while, CE 4 is rich in β-xylosidase, arabinofuranosidases (GH 43, 51, 54, 62) and α-glucuronidases. CE 1 is abundant in exo/endo-cellulases but lacks in β-xylosidase, endoxylanase and arabinofuranosidase activities. These experiments again validate the hypothesis that removal of hemicellulose embedded within cell walls through addition of suitable hemicellulases helps enhance cellulose accessibility [456-458]. However, it becomes pertinent to hydrolyze xylan side-chains through addition of suitable accessory enzymes (i.e. arabinofuranosidases, α-glucuronidases), possibly avoiding end-product inhibition [456,459].

7.1.4.7 Protein composition and hydrolytic performance correlations

Despite the tremendous advantage associated with optimizing hydrolytic performance of crude enzyme mixtures through mixture optimization studies (by varying total protein loadings), there is a significant lack of fundamental understanding on the true nature of enzyme synergy that results in an optimum enzyme cocktail. It would be important to determine which individual enzyme families are truly responsible for the synergistic

improvement seen in the activity of optimal cocktails. It would also be interesting to use the proteomics compositional data (**Table 7.2**) to determine correlations with hydrolytic performance (8/10/5-CE/RE experimental data set; **Table V-7.15**) on pretreated cornstover.

The protein composition of each enzyme mixture cocktail tested was determined using the theoretical composition of the 14 crude enzymes (based on 56 individual components as listed in **Table 7.2**). All cellulolytic, hemicellulolytic, other accessory (e.g. Swollenin) and pectin degrading enzymes were included in this list. All non-hydrolytic proteins (e.g. proteases) were clubbed together in the "OTHERS" category. The total number of tested mixtures (755 unique combinations) of the 14 crude enzymes (total protein loading in all cases = 16.5 mg enzyme/g glucan), resulted in a 755 x 56 large matrix input parameter dataset. Bivariate correlations were carried out for each of the 56 input variables with respect to the three responses (% glucan/xylan conversion, total sugar yield) to determine Pearson correlation coefficients, $\mathbf{P_{CC}}$, (**Table V-7.10**) and their test of significance ($p<0.05$). One of the major concerns with bivariate correlations between response and input variables is the assumption of linear dependence. However, the correlation between hydrolytic performance and amount of enzyme loaded is most likely to be non-linear, further confounded by the synergistic action of enzymes. Nevertheless, the bivariate Pearson correlation coefficients ($\mathbf{P_{CC}}$) brings several interesting facts to light. Firstly, there seems to be a very significant 'opportunity cost' associated with individual enzymes that maximize glucan vs. xylan conversion. That is, individual enzymes that maximize only xylan conversion have a negative Pearson coefficient (upon increasing the amount added) as compared to enzymes that maximize

both glucan and xylan conversion. Therefore, it would be also useful to examine the Pearson coefficients for total sugar yield that would be maximized by enhancing both glucan and xylan conversions. Individual enzymes/proteins that give a linear relationship with respect to total sugar yield, based on a positive Pearson coefficient, include; AXE 1, AXE 2, CIP 2, SWO, BG 3, BX 3, EG 2, BM, BGAL 2, CBH 2, EG 1, EG 3, AMY, CHI 1, PGL and EG 7. However, due to significant correlation between certain enzyme components (See **Table V-7.11**), the truly significant enzymes are partly confounded in the bivariate analysis. For example, AXE I has a fairly linear correlation with AC/CIP1/CIP2/BGAL2/XG/BX3/AGLUC/EG7/AXE II (P_{CC} = 0.6-0.9). While, AXE II has a strong correlation with BGAL2 (P_{CC} = 0.88), EG 7 (P_{CC} = 0.76), AXE I (P_{CC} = 0.7), XG (P_{CC} = 0.66) and CIP2 (P_{CC} = 0.65). BG3 has a strong correlation with EG 7 (P_{CC} = 0.68) and AXE II (P_{CC} = 0.57). In order to help resolve this issue, the dataset (N = 755) was split into the bottom and top 25% quartile, based on the response variables (i.e. %glucan/xylan conversion, total sugar yield). The idea behind this split was to distinguish between the better (top 25% quartile) vs. poorer (bottom 25% quartile) performing enzyme cocktails. For example, the bottom 25% based on total sugar yield were all enzyme mixtures that yielded under 287 gms total sugar/kg biomass (<40% total sugar yield); while the top 25% were based on total sugar yield were all enzyme mixtures that yielded over 434 gms total sugar/kg biomass (>70% total sugar yield). One-way ANOVA's were carried out to compare these two datasets and the results are listed in **Table V-7.12**. Statistical mean and standard deviations for the individual enzyme components for both datasets were also computed (**Table 7.13-A, 7.13-B, V-7.13-C**).

Table 7.13-A *Descriptive statistics (minima, maxima, mean, standard deviation) comparing top and bottom 25% quartile groups for individual protein components, based on varying % glucan conversion. Values highlighted in bold signify statistical significance at p<0.05 level (based on Table 7.12), whereas values highlighted in red signify increase in corresponding protein component in top 25% quartile with respect to bottom quartile.*

Descriptive Statistics (% glucan conversion)									
	Bottom 25% (N = 185)				Top 25% (N = 191)				
Enzyme	Minimum	Maximum	Mean	Std. Deviation	Minimum	Maximum	Mean	Std. Deviation	% Increase
AC	0	4.41%	*0.63%*	0.79%	0%	2%	*0.35%*	0.40%	**-45%**
AXE 1	0	1%	*0.23%*	0.20%	0.14%	0.66%	*0.29%*	0.09%	**24%**
AXE 2	0	0.43%	*0.07%*	0.09%	0%	0.36%	*0.24%*	0.06%	**233%**
FAE	0	1.18%	*0.17%*	0.25%	0%	0.39%	*0.08%*	0.08%	**-55%**
CIP 1	0	2.67%	*1.07%*	0.74%	0.53%	2.48%	*1.05%*	0.32%	**-2%**
CIP 2	0	3.01%	*0.89%*	0.70%	0.61%	2.48%	*1.30%*	0.24%	**45%**
PL	0	4.21%	*0.64%*	0.88%	0%	1%	*0.27%*	0.28%	**-59%**
PME	0	2.64%	*0.60%*	0.60%	0%	1%	*0.35%*	0.27%	**-41%**
RHAE	0	1.89%	*0.33%*	0.36%	0%	1%	*0.23%*	0.22%	**-30%**
ARH	0	1.46%	*0.29%*	0.31%	0%	0.63%	*0.23%*	0.13%	**-20%**
SWO	0	3.60%	*0.93%*	0.85%	0.62%	2.85%	*1.72%*	0.24%	**85%**
BG 1	0	13.08%	*2.20%*	2.85%	0%	4.36%	*0.71%*	0.94%	**-68%**
BMANO	0	1.99%	*0.42%*	0.47%	0%	0.96%	*0.21%*	0.17%	**-49%**
BG 3	0	11.84%	*3.16%*	2.04%	1.84%	10.62%	*8.49%*	1.92%	**169%**
BX 3	0	6.49%	*1.93%*	1.38%	0.61%	4.07%	*1.76%*	0.60%	**-9%**
EG 2	0.14%	7.64%	*3.42%*	1.67%	1.80%	7.05%	*4.35%*	0.63%	**27%**
BM	0	4.54%	*1%*	0.73%	0.40%	2.89%	*1.17%*	0.46%	**16%**
BGAL 2	0	1.47%	*0.30%*	0.25%	0.08%	0.88%	*0.47%*	0.12%	**55%**
CBH 2	0	13.37%	*5.78%*	3.28%	2.92%	13.02%	*7.14%*	1.05%	**24%**

Table 7.13-A *Contd...*

	Descriptive Statistics (% glucan conversion)								
	Bottom 25% (N = 185)				Top 25% (N = 191)				
Enzyme	**Minimum**	**Maximum**	**Mean**	**Std. Deviation**	**Minimum**	**Maximum**	**Mean**	**Std. Deviation**	**% Increase**
GH 6	0	1.69%	*0.35%*	0.36%	0%	1%	*0.10%*	0.12%	**-71%**
CBH 1	0	34.74%	*13.18%*	7.70%	7.56%	27.63%	*14.83%*	2.54%	**13%**
EG 1	0	7.93%	*2.63%*	1.77%	1.70%	6.47%	*4.41%*	0.54%	**67%**
EX 2	0.35%	15.19%	*5.18%*	3.34%	0.77%	10.05%	*4.48%*	1.25%	**-14%**
EX 1	0	35.78%	*6.46%*	5.60%	0.54%	13.72%	*4.14%*	2.68%	**-36%**
EG 3	0	2.84%	*1.41%*	0.64%	0.22%	2.47%	*1.60%*	0.26%	**13%**
AMY	0	21.45%	*0.78%*	2.17%	0.11%	12.33%	*2.27%*	2.40%	**192%**
GAMY	0	49.31%	*4.55%*	7.11%	0.09%	19.18%	*3.42%*	3.36%	**-25%**
GH 16	0	9.39%	*0.95%*	1.16%	0%	5.61%	*1.39%*	1.06%	**47%**
GH 17	0	3.87%	*0.80%*	0.84%	0%	1.61%	*0.58%*	0.33%	**-28%**
CHI 1	0	0.38%	*0.17%*	0.09%	0.08%	0.33%	*0.20%*	0.03%	**18%**
CHI 2	0	1.20%	*0.18%*	0.19%	0%	0.55%	*0.12%*	0.09%	**-31%**
AGAL	0	3.09%	*0.57%*	0.55%	0%	1.35%	*0.38%*	0.25%	**-32%**
PGL	0	20.02%	*2.12%*	2.34%	0%	11%	*2.35%*	2.26%	11%
GH 30	0	0.70%	*0.08%*	0.10%	0%	0.41%	*0.10%*	0.08%	**26%**
AG	0	2.75%	*0.56%*	0.58%	0%	1.15%	*0.41%*	0.21%	**-27%**
BFRC	0	1.02%	*0.14%*	0.17%	0%	0.37%	*0.16%*	0.10%	15%
BGAL 1	0	8.33%	*1.75%*	1.71%	0.03%	3.92%	*1.08%*	0.62%	**-39%**
AA	0	3.11%	*0.79%*	0.73%	0%	1.69%	*0.54%*	0.25%	**-32%**
EG 5	0	0.26%	*0.05%*	0.06%	0%	0%	*0.01%*	0.02%	**-86%**
AMANO 1	0	1.43%	*0.34%*	0.34%	0%	1%	*0.19%*	0.11%	**-44%**

Table 7.13-A *Contd...*

	Descriptive Statistics (% glucan conversion)								
	Bottom 25% (N = 185)				Top 25% (N = 191)				
Enzyme	**Minimum**	**Maximum**	**Mean**	**Std. Deviation**	**Minimum**	**Maximum**	**Mean**	**Std. Deviation**	**% Increase**
ABF 1	0	3.59%	*0.54%*	0.76%	0%	1.20%	*0.25%*	0.25%	**-54%**
ABGAL	0	2.04%	*0.73%*	0.49%	0%	1%	*0.53%*	0.21%	**-27%**
ABF 2	0	7.41%	*1.42%*	1.49%	0%	2.54%	*0.60%*	0.49%	**-58%**
GH 55	0	1.26%	*0.21%*	0.26%	0%	0.46%	*0.11%*	0.09%	**-47%**
EG 4	0	3.38%	*0.89%*	0.69%	0.04%	1.41%	*0.35%*	0.25%	**-60%**
EG 7	0	0.34%	*0.07%*	0.08%	0.06%	0.28%	*0.23%*	0.05%	**229%**
ABF 3	0	2.81%	*0.83%*	0.56%	0.14%	1.25%	*0.48%*	0.22%	**-42%**
GH 65	0	0.39%	*0.05%*	0.08%	0%	0%	*0.03%*	0.03%	**-48%**
AGLUC	0	2.51%	*0.83%*	0.66%	0.17%	2.06%	*0.59%*	0.34%	**-29%**
GH 71	0	0.14%	*0.02%*	0.03%	0%	0%	*0.01%*	0.01%	**-60%**
GT	0	2.74%	*0.57%*	0.60%	0%	1.11%	*0.44%*	0.23%	**-22%**
XG	0	21.28%	*5.48%*	3.94%	2.05%	13.16%	*4.95%*	1.98%	-10%
AMAN	0	0.08%	*0.01%*	0.02%	0%	0%	*0.00%*	0.01%	**-60%**
BGLUC	0	0.81%	*0.11%*	0.17%	0%	0%	*0.04%*	0.06%	**-60%**
GH 81	0	0.14%	*0.02%*	0.03%	0%	0%	*0.01%*	0.01%	**-60%**
AMANO 2	0	0.66%	*0.11%*	0.14%	0%	0.30%	*0.06%*	0.05%	**-47%**
OTHERS	2.03%	69.50%	*21.43%*	13.88%	2.53%	36.60%	*18.84%*	5.55%	**-12%**

Table 7.13-B *Descriptive statistics (minima, maxima, mean, standard deviation) comparing top and bottom 25% quartile groups for individual protein components, based on varying % xylan conversion. Values highlighted in bold signify statistical significance at p<0.05 level (based on Table 7.12), whereas values highlighted in red signify increase in corresponding protein component in top 25% quartile with respect to bottom quartile.*

	Descriptive Statistics (% xylan conversion)								
	Bottom 25% (N = 188)				Top 25% (N = 190)				
Enzyme	**Minimum**	**Maximum**	**Mean**	**Std. Deviation**	**Minimum**	**Maximum**	**Mean**	**Std. Deviation**	**% Increase**
AC	0	2.20%	*0.35%*	0.54%	0%	2%	*0.49%*	0.51%	**39%**
AXE 1	0	1%	*0.25%*	0.16%	0.05%	0.61%	*0.29%*	0.11%	**17%**
AXE 2	0	0.46%	*0.14%*	0.11%	0%	0.36%	*0.19%*	0.10%	**41%**
FAE	0	0.46%	*0.04%*	0.10%	0%	0.39%	*0.13%*	0.11%	**201%**
CIP 1	0	2.67%	*1.15%*	0.70%	0.40%	2.52%	*1.19%*	0.43%	4%
CIP 2	0	3.01%	*1.18%*	0.64%	0.28%	2.25%	*1.25%*	0.33%	6%
PL	0	1.40%	*0.16%*	0.32%	0%	2%	*0.51%*	0.37%	**221%**
PME	0	1.92%	*0.31%*	0.38%	0%	1%	*0.53%*	0.26%	**72%**
RHAE	0	1.89%	*0.27%*	0.37%	0%	1%	*0.32%*	0.19%	16%
ARH	0	0.86%	*0.16%*	0.17%	0%	0.63%	*0.26%*	0.15%	**63%**
SWO	0	3.60%	*1.56%*	0.80%	0.40%	2.94%	*1.55%*	0.44%	0%
BG 1	0	13.08%	*1.83%*	2.74%	0%	4.36%	*1.01%*	1.30%	**-45%**
BMANO	0	1.83%	*0.21%*	0.33%	0%	1.01%	*0.31%*	0.20%	**44%**
BG 3	0	15.56%	*5.75%*	3.36%	1.29%	10.45%	*6.98%*	3.07%	**21%**
BX 3	0	6.18%	*1.53%*	1.21%	0.00%	4.42%	*2.00%*	0.71%	**31%**
EG 2	0.14%	7.64%	*4.22%*	1.53%	2.14%	6.61%	*4.40%*	0.68%	4%
BM	0	4.54%	*1%*	0.76%	0.43%	2.15%	*1.22%*	0.39%	5%
BGAL 2	0	1.11%	*0.34%*	0.19%	0.10%	0.84%	*0.45%*	0.15%	**33%**
CBH 2	0	13.37%	*7.50%*	2.80%	2.70%	12.37%	*7.21%*	1.39%	-4%

Table 7.13-B *Contd...*

	Descriptive Statistics (% xylan conversion)								
	Bottom 25% (N = 188)				Top 25% (N = 190)				
Enzyme	**Minimum**	**Maximum**	**Mean**	**Std. Deviation**	**Minimum**	**Maximum**	**Mean**	**Std. Deviation**	**% Increase**
GH 6	0	1.69%	*0.28%*	0.36%	0%	1%	*0.17%*	0.18%	**-38%**
CBH 1	0	34.74%	*16.92%*	6.91%	6.45%	29.26%	*15.29%*	3.59%	**-10%**
EG 1	0	8.39%	*4.11%*	1.64%	1.20%	6.72%	*4.06%*	0.97%	-1%
EX 2	0.33%	15.19%	*5.03%*	3.25%	0.44%	8.62%	*4.15%*	1.58%	**-18%**
EX 1	0	19.96%	*3.62%*	3.27%	0.91%	17.52%	*5.22%*	3.51%	**44%**
EG 3	0	2.84%	*1.55%*	0.61%	0.70%	2.47%	*1.67%*	0.27%	**8%**
AMY	0	21.45%	*1.69%*	2.98%	0.05%	7.53%	*1.62%*	1.97%	-4%
GAMY	0	49.31%	*4.89%*	7.31%	0.38%	17.63%	*3.09%*	3.37%	**-37%**
GH 16	0	9.39%	*1.19%*	1.42%	0%	3.83%	*1.00%*	0.89%	-16%
GH 17	0	3.87%	*0.63%*	0.79%	0%	1.53%	*0.49%*	0.38%	**-22%**
CHI 1	0	0.38%	*0.16%*	0.08%	0.00%	0.30%	*0.18%*	0.05%	**12%**
CHI 2	0	1.20%	*0.15%*	0.19%	0%	0.52%	*0.13%*	0.09%	-8%
AGAL	0	3.09%	*0.40%*	0.51%	0%	1.45%	*0.45%*	0.25%	11%
PGL	0	20.02%	*1.94%*	2.78%	0%	8%	*2.43%*	1.68%	**25%**
GH 30	0	0.70%	*0.10%*	0.12%	0%	0.25%	*0.08%*	0.07%	**-26%**
AG	0	1.48%	*0.30%*	0.31%	0%	1.19%	*0.48%*	0.28%	**59%**
BFRC	0	1.02%	*0.15%*	0.17%	0%	0.37%	*0.14%*	0.09%	-5%
BGAL 1	0	3.20%	*0.69%*	0.79%	0.05%	4.14%	*1.50%*	0.78%	**116%**
AA	0	1.97%	*0.44%*	0.46%	0%	1.69%	*0.59%*	0.34%	**36%**
EG 5	0	0.26%	*0.03%*	0.06%	0%	0%	*0.03%*	0.04%	-12%
AMANO 1	0	0.84%	*0.15%*	0.21%	0%	1%	*0.23%*	0.15%	**55%**

Table 7.13-B *Contd...*

	Descriptive Statistics (% xylan conversion)								
	Bottom 25% (N = 188)				Top 25% (N = 190)				
Enzyme	**Minimum**	**Maximum**	**Mean**	**Std. Deviation**	**Minimum**	**Maximum**	**Mean**	**Std. Deviation**	**% Increase**
ABF 1	0	1.48%	*0.15%*	0.32%	0%	1.20%	*0.41%*	0.32%	**179%**
ABGAL	0	2.04%	*0.55%*	0.47%	0%	1%	*0.56%*	0.26%	2%
ABF 2	0	2.66%	*0.46%*	0.61%	0%	3.31%	*1.09%*	0.64%	**137%**
GH 55	0	0.55%	*0.08%*	0.13%	0%	0.42%	*0.16%*	0.12%	**114%**
EG 4	0	3.38%	*0.70%*	0.68%	0.08%	1.68%	*0.52%*	0.37%	**-25%**
EG 7	0	0.46%	*0.16%*	0.10%	0.00%	0.28%	*0.18%*	0.08%	**17%**
ABF 3	0	1.39%	*0.45%*	0.33%	0.37%	1.81%	*0.73%*	0.27%	**63%**
GH 65	0	0.13%	*0.01%*	0.03%	0%	0%	*0.05%*	0.04%	**285%**
AGLUC	0	3.34%	*0.67%*	0.70%	0.00%	2.06%	*0.75%*	0.39%	13%
GH 71	0	0.05%	*0.00%*	0.01%	0%	0%	*0.01%*	0.01%	**383%**
GT	0	2.74%	*0.45%*	0.56%	0%	1.11%	*0.37%*	0.27%	-17%
XG	0	16.66%	*4.72%*	3.11%	1.72%	13.44%	*5.84%*	2.55%	**24%**
AMAN	0	0.03%	*0.00%*	0.01%	0%	0%	*0.01%*	0.01%	**383%**
BGLUC	0	0.27%	*0.02%*	0.06%	0%	0%	*0.09%*	0.07%	**383%**
GH 81	0	0.05%	*0.00%*	0.01%	0%	0%	*0.01%*	0.01%	**383%**
AMANO 2	0	0.66%	*0.06%*	0.11%	0%	0.30%	*0.08%*	0.06%	**30%**
OTHERS	2.03%	69.50%	*19.27%*	13.38%	2.54%	32.15%	*16.49%*	6.46%	**-14%**

Comparison of the ANOVA results and statistical descriptives for the top vs. bottom 25% performing enzyme cocktails along with the bivariate correlations helped reveal interesting findings. Upon closer inspection of the case for total sugar yield, the ANOVA analysis revealed a significant difference ($p<0.05$) in the protein composition of the bottom vs. top 25% quartile for AC, AXE I, AXE II, CIP 2, SWO, BG 1, BMANO, BG 3, EG 2, BM, BGAL2, CBH 2, GH 6, EG 1, EX 2, EG 3, AMY, GAMY, GH 16, GH 17, CHI 1, CHI 2, AGAL, PGL, EG 5, AMANO 1, ABGAL, ABF 2, EG 4, EG 7, AGLUC, GT, AMANO 2 and OTHERS. The statistical descriptives (i.e. mean, standard deviation) from **Table V-7.13-C** reveals the following percent increase in protein composition for the top 25% vs. bottom 25% quartile; AC (-27%), **AXE I (17%)**, **AXE II (141%)**, **CIP 2 (25%)**, **SWO (40%)**, BG 1 (-61%), BMANO (-30%), **BG 3 (97%)**, **EG 2 (20%)**, **BM (19%)**, **BGAL 2 (49%)**, **CBH 2 (13%)**, GH 6 (-59%), **EG 1 (34%)**, EX 2 (-17%), **EG 3 (17%)**, **AMY (118%)**, GAMY (-42%), GH 16 (25%), GH 17 (-34%), **CHI 1 (12%)**, CHI 2 (-31%), AGAL (-24%), **PGL (33%)**, EG 5 (-54%), AMANO 1 (-25%), ABGAL (-15%), ABF 2 (-20%), EG 4 (-48%), **EG 7 (105%)**, AGLUC (-21%), GT (-26%), AMANO 2 (-33%) and OTHERS (-15%). However, individual enzymes/proteins that give a linear relationship with respect to total sugar yield, based on a positive Pearson coefficient (**Table V-7.10**), include; AXE 1, AXE 2, CIP 2, SWO, BG 3, BX 3, EG 2, BM, BGAL 2, CBH 2, EG 1, EG 3, AMY, CHI 1, PGL and EG 7. Except BX 3, there was a significant % increase (ranging between 10-141%) in the protein composition for all other proteins/enzymes.

There are two possible ways to interpret these findings; (1) the proteins that are present in significantly ($p<0.05$) higher amounts (positive % increase) in the top 25%

quartile compared to the bottom 25% quartile are critical to enhancing the overall glucan and xylan conversion, (2) proteins that do not change significantly or drop in absolute composition for the top 25% vs. the bottom 25% quartile either have little effect on enhancing the overall hydrolysis yield or are already present in sufficient amounts to hydrolyze the pretreated cell wall. Based on (1) the enzymes/proteins that increase significantly in the top 25% quartile include AXE 1, AXE 2, CIP 2, SWO, BG 3, EG 2, BM, BGAL 2, CBH 2, EG 1, EG 3, AMY, CHI 1, PGL and EG 7. Based on (2), the remaining enzymes either do not change significantly or decrease in absolute composition with respect to the bottom 25% quartile. Another way to reflect this would be to actually compare the top 5% quartile enzyme cocktails (that result in >84% glucan, >77% xylan and >508 gm sugar/kg biomass total sugar yield) protein composition to a typical commercial enzyme blends that give significantly lower conversions at equivalent protein loadings (e.g. CE 1 and CE 4). **Figures 7.7** compares the protein compositions of commercial enzymes (CE 1 and CE 4) with respect to cocktails of top 5% quartile (N = 37 out of 755 total mixtures) based on glucan (**Figure V-7.7-A/B**), xylan (**Figure V-7.7-C/D**) and total sugar yield (**Figure 7.7-E/F**). Compared to CE 1, the top 5% cocktails contained a significantly lower amount of acetyl xylan esterases (AC + AXE 1 + AXE 2), cellobiohydrolases (CBH 1 + CBH 2), xyloglucanase, endoglucanases (EG 1 + EG 2 + EG 3 + EG 4 + EG 5 + EG 7), α-glucuronidase (AGLUC), β-xylosidase (BX 3), Cip proteins (CIP 1 + CIP 2), β-mannase (BM), swollenin (SWO), β-galactosidase (BGAL 1), chitinases (CHI 1 + CHI 2) and GH 30 (See **Table V-7.14** for quantitative comparisons).

Figure 7.7-(E/F) *Comparing protein composition of commercial enzyme (CE 1) to average composition of top 5% mixtures (N = 37), based on % total sugar yield.*

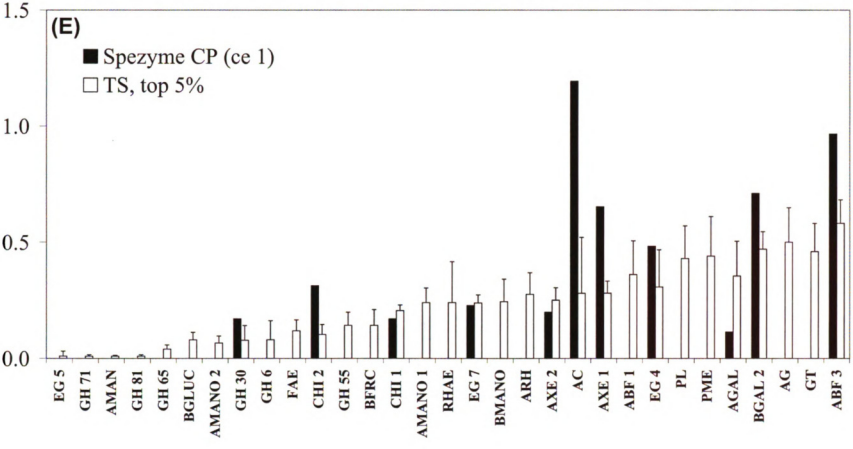

Figure 7.7-(E/F) *Contd...*

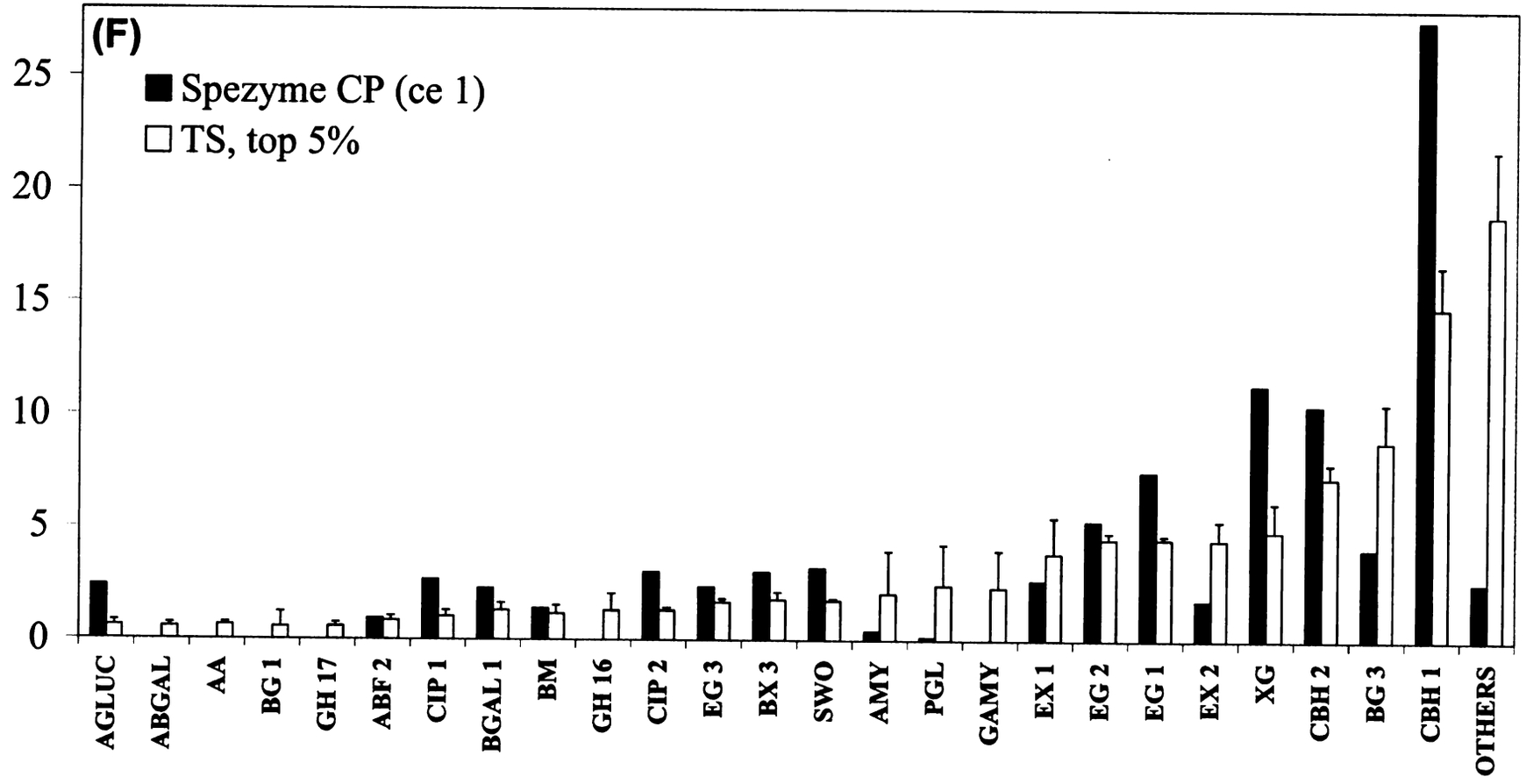

On the other hand, the top 5% cocktails had significant amounts of endoxylanases (EX 1 + EX 2), β-glucosidase (BG 3), amylases (AMY), polygalacturonases (PGL) and a-galactosidase (AGAL) compared to CE 1. Other enzymes/proteins that were present in the top 5% cocktails, but were completely absent from CE 1, included the remaining of the total 56 enzymes from **Table 7.2**. These results indicate that medium AFEX pretreatment severity stover requires several accessory enzymes to maximize glucan and xylan conversion. This mandates further experiments for higher AFEX pretreatment severities to further minimize total protein loading and type of accessory enzymes required to achieve that loading. Interestingly, the crude enzyme that had the highest oat spelt xylanase activity (RE 5) was not always seen in the optimum enzyme mixtures. This result is not surprising as it has been seen before that there is a poor correlation between the hydrolytic efficiency of enzymes on lignocellulosic substrates and model substrates like avicel and oat spelt xylan [385].

7.1.4.8 Role of enzyme synergy for cellulosic biorefineries

To illustrate the potential economic advantages of exploiting enzyme synergy, a conventional enzyme blend was compared against a number of enzyme cocktails at equivalent protein loadings (**Figure 7.8**). It is important to note from **Figure 7.8** that the theoretical sugar release from the optimum enzyme blend (mixture of 7 crude enzymes) is very close to the theoretical maximum (90% total sugar yield), compared to a conventional enzyme blends (CE 6 + CE 2) at equivalent protein loading (40% total sugar yield).

Figure 7.8 *Comparing effect of enzyme mixture composition (at fixed total protein loading of 16.5 mg/g glucan) on overall glucose (blue/bottom bar) and xylose (green/top bar) yield, with respect to dry weight untreated corn stover.*

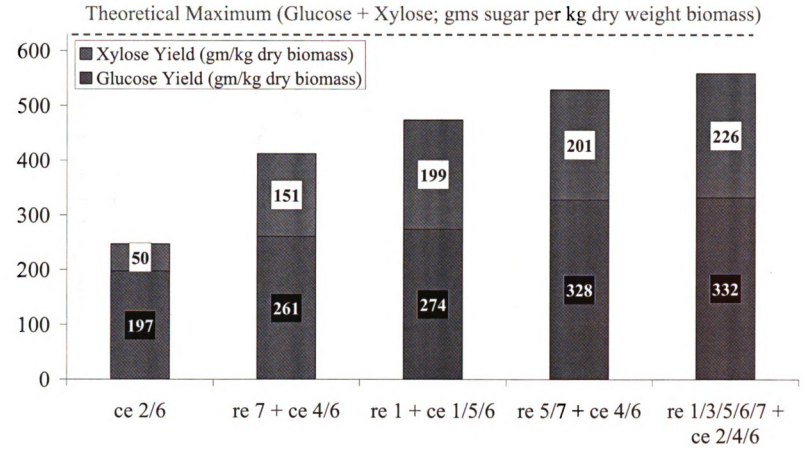

Additionally, the optimal enzyme cocktail obtained through current optimization studies achieved substantially higher glucan (>90%) and xylan (>90%) conversions than conventional enzyme cocktails at double the total enzyme loading (62% glucan and 39% xylan conversions for 16.5 mg CE 1 + 16.5 mg RE 2 per gm glucan). These results indicate that synergistic enzyme cocktails can help substantially reduce enzyme usage while increasing their specific activity to reduce overall cost of producing cellulosic ethanol.

7.1.5 Conclusions

A systematic methodology was developed to substantially reduce enzyme usage and increase specific activity of crude enzyme mixtures on AFEX pretreated lignocellulosics. It was demonstrated that simplex-centroid experimental designs can be applied to develop statistically significant models of cellulolytic-hemicellulolytic enzyme synergy for fixed total protein loadings. The models generated in this study demonstrated strong synergisms between cellulases and endoxylanases to maximize both cellulose and hemicellulose hydrolysis. There was significant synergy between endoxylanases and other debranching enzymes (e.g. β-xylosidase, arabinofuranosidase, acetyl xylan esterases etc) that result in maximizing hemicellulose hydrolysis for AFEX-treated corn stover. Optimized enzyme cocktails at a fixed protein loading of 16.5 mg protein/g glucan had significantly higher glucan (90%) and xylan (90%) conversions than conventional cellulase cocktails at equivalent or higher protein loadings (e.g. CE 1 + RE 2 gave 62% glucan and 39% xylan conversions at 33 mg/g glucan loading). Interestingly, cellulose is hydrolyzed more efficiently for fixed-protein loading mixtures in which some cellulase is replaced by endoxylanases (and other hemicellulases), possibly increasing

accessibility of cellulose embedded within hemicellulose sheaths [55]. Similarly, hemicellulose is more efficiently hydrolyzed in mixtures in which some endoxylanase is replaced with cellulases. Future studies must address to reduce the multicollinearity observed in the models generated in these experiments. This can be achieved by studying high specificity, purified enzymes to eliminate issues with high correlations between enzymes present in typical crude enzyme cocktails. This would allow development of more precise models, and potentially more active enzyme blends.

MICHIGAN STATE UNIVERSITY LIBRARIES
3 1293 03063 4665

THESIS

5
2010
v.2

LIBRARY
Michigan State
University

PLACE IN RETURN BOX to remove this checkout from your record.
TO AVOID FINES return on or before date due.
MAY BE RECALLED with earlier due date if requested.

DATE DUE	DATE DUE	DATE DUE

5/08 K:/Proj/Acc&Pres/CIRC/DateDue.indd

ULTRASTRUCTURAL AND PHYSICOCHEMICAL MODIFICATIONS WITHIN AMMONIA TREATED LIGNOCELLULOSIC CELL WALLS AND THEIR INFLUENCE ON ENZYMATIC DIGESTIBILITY

VOLUME II

By

Shishir Pratap Singh Chundawat

A DISSERTATION

Submitted to
Michigan State University
in partial fulfillment of the requirements
for the degree of

DOCTOR OF PHILOSOPHY

Chemical Engineering

2009

CHAPTER 8: AMMONIA BASED PRETREATMENTS ENHANCE SYNERGISTIC HYDROLYSIS OF CRYSTALLINE CELLULOSE AND LIGNOCELLULOSIC CELL WALLS THROUGH DIFFERENT MECHANISMS

8.1.1 Abstract[vi]

The degree of synergistic interactions between cellulases and hemicellulases was determined for native and ammonia treated cellulosic biomass (e.g. Avicel, Corn Stover). The four cellulases studied included cellobiohydrolase I (CBH I), cellobiohydrolase II (CBH II), endoglucanase I (EG I) and β-Glucosidase (βG). The hemicellulases included an endoxylanase (EX), α-arabinofuranosidase (ArbF) and β-xylosidase (βX). Synergistic interactions among the core cellulases (CBH I, CBH II, EG I) for varying protein loading (2.5-31.5 mg enzyme/g glucan) during hydrolysis of untreated (cellulose I) and liquid ammonia treated (cellulose III) Avicel were studied. Interestingly, there was a 2-fold higher specific activity detected for EG I (with or without CBH's) on cellulose III polymorph as compared to cellulose I_β. This would suggest that the overall enhancement in the hydrolytic rate of crystalline cellulose III vs. I_β is largely due to increased activity of endoglucanases. It was also found that unlike what has been reported earlier for Avicel (low DP crystalline cellulose), CBH I and CBH II had little or no synergistic interaction (degree of synergistic effect = 1) on AFEX treated corn stover. Accessibility of crystalline cellulosic microfibrils within lignocellulosic cell walls was greatly enhanced after AFEX pretreatment, which was deduced based on the difference in the hydrolysis by-products released (ratio of cellobiose to glucose) during saccharification of untreated

---

[vi] A version of this chapter was published as Gao D., Chundawat S.P.S, Krishnan C., Balan V., Dale B.E. 2009. *Mixture optimization of six core glycosyl hydrolases for maximizing saccharification of ammonia fiber expansion (AFEX) pretreated corn stover.* Bioresource Technology (Manuscript In Press). DOI: 10.1016/j.biortech.2009.10.056.

and AFEX treated corn stover by various combinations of CBH I, CBH II and EG I. Hemicellulases played a critical role in enhancing the hydrolysis of AFEX treated corn stover as well. The optimal composition (based on % total protein mass loading) of the core cellulase cocktail that maximized AFEX corn stover glucan digestibility consisted of CBH I (34.67%), CBH II (26%) and EG I (39.33%). The optimal composition (based on % total hemicellulase mass loading) of the core hemicellulase cocktail (with fixed core cellulase loading) that maximized AFEX corn stover xylan digestibility consisted of EX (29.07%), βX (42.67%) and ArbF (28.27%).

8.1.2 Background

It is impossible to study synergistic interactions between enzymes on pretreated lignocellulosics using crude commercial mixtures. Purification of individual enzyme components to high purity would help elucidate the role of synergy. There are several reported techniques for separating cellulolytic and xylanolytic enzymes from each other [419,460-462]. Typically, separation of cellobiohydrolases and endoglucanases is difficult to achieve without CBD-specific affinity based chromatography and has resulted in conflicting results over the role of CBH and EG synergy on crystalline cellulose in the literature [30,32]. The major parameters that influence enzyme synergisms are: (a) enzyme ratios and effective concentration with respect to the cellulosic substrate [29,30,46,47]; (b) substrate related physicochemical characteristics [36,463,464]; (c) competitive-synergistic adsorption of enzyme mixtures [465].

8.1.2.1 Role of cellobiohydrolases (CBH) and endoglucanases (EG)

There have been several studies carried out to optimize cellulase mixtures for hydrolyzing model cellulosic substrates like avicel and bacterial microcrystalline

cellulose [433,466-468]. Baker and colleagues [466] studied the effect of varying enzyme ratios for ternary mixtures of purified exo- and endo-cellulases (from several fungal and bacterial sources) on microcrystalline cellulose at low total protein loadings (~ 0.4 mg protein per g glucan). A ternary combination of CBH I: CBH II: EG I (native *Trichoderma* enzymes) at 60: 20: 20 (protein mass basis) gave the highest glucan conversion for crystalline cellulose (Sigmacell). The optimal ratio of individual enzyme components that gave high glucan conversions was dependent on the microbial source. Boisset and colleagues [433] studied the effect of varying exo- and endo-cellulases from *Humicola insolens* on bacterial cellulose at high total protein loadings (~ 100 mg protein per g glucan). A ternary combination of Cel7A: Cel6A: Cel 45A (native Humicola enzymes, analogous to CBH I, CBH II and EG I, respectively) at 68.75: 30: 1.25 gave the highest glucan conversion. These two findings, among many others [204,467,468], indicate the complex nature of synergy between endo- and exo-enzymes that is highly dependent on the total protein loading, substrate characteristics and individual protein binding properties to substrate active sites that give very different optimal enzyme combinations.

Few studies, if any, have been conducted using purified enzymes on pretreated lignocellulosics (most studies have focused on woody biomass). Eriksson and colleagues [34] have found that CBH I and EG I synergize to hydrolyze steam pretreated spruce wood with a degree of synergistic effect (DSE) of 1.5-2 (over the course of hydrolysis), indicating a 50-100% increase in overall digestibility in presence of both enzymes as compared to when present individually. Similar DSE values have been reported for synergistic hydrolysis of steam pretreated willow by CBH I and EG II [49]. One would

expect the DSE to decrease during the course of hydrolysis but it has been found to remain relatively constant indicating that the model of conventional endo-exo synergy is not complete. Eriksson et al. have found that endoglucanases help release non-productively bound cellobiohydrolase (bound to cellulose) which might help explain the constant DSE. In other studies on bleached softwood kraft pulp (glucomannan rich pulp), CBH was found to synergize more effectively with EG I than EG II, even though the latter had slightly higher endo-specific activity [469].

Rosgaard et al. have studied synergistic hydrolysis of acid, steam and hot-water pretreated barley straw using quaternary mixtures of purified CBH I, CBH II, EG I and EG II [26]. The optimal ratios of the four enzymes required for higher severity (acid impregnation based steam explosion) pretreated straw was different from the lower severity pretreated straws (water impregnation based steam explosion and hot water flow-through extraction). The higher severity pretreated straw, required lesser amount of EG I (and greater amount of CBH II, with nearly constant CBH I) compared to the lower severity material. The optimal ratio of CBH I: CBH II: EG I (*Trichoderma* enzymes) for high and low severity steam explosion pretreated barley straw was found to be 50: 25: 25 and 45: 20: 35, respectively (protein mass basis). This is not surprising considering that acid pretreatment possibly resulted in removal of amorphous cellulose (and hemicellulose) giving more crystalline cellulose that required lesser synergy between cellobiohydrolase (CBH I) and endoglucanases (EG I) [36]. Rosgaard et al. also found significant interaction effects between EG (EG I or EG II) with CBH I in the hydrolysis of lower severity pretreatments. Interestingly, EG II is not included in the final cocktail despite the fact that it has a higher specific activity on amorphous cellulose than EG I

[470]. This might be because EG I has significant cross-activity on xylan based substrates that would probably result in higher activity on lignocellulosic substrates rich in hemicellulose compared to EG II.

Gusakov et al. have shown that an artificial cellulase mixture comprising of cellobiohydrolases, endoglucanases, xylanase and β-glucosidase from *Chrysosporium lucknowense* was more effective than conventional crude enzyme mixtures in hydrolysis of crystalline cellulose and organosolv pretreated Douglas fir wood [471]. It was also shown that the crude enzyme mixture from *Chrysosporium* fungi was not as effective as the artificially optimized cellulase mixture, illustrating the role optimal protein ratios and activities necessary to achieve higher glucan conversions.

The extent of synergy between cellulases on pretreated lignocellulosics is probably very different from model cellulosic substrates (like avicel, bacterial and microcrystalline cellulose) due to varying degrees of non-productive binding to hemicellulose and lignin. Researchers have found that the extent of binding of CBH I and EG II to lignin extracted from pretreated softwood depends on the type of catalytic and cellulose binding domains (or CBD) [472]. Most endoglucanases have been found to be associated with a CBD (e.g. EG I, EG II) that helps improve substrate recognition unlike some endoglucanases like EG III [473]. It might be useful to select enzymes that have reduced binding to lignin (due to absence of CBD) to enhance hydrolysis of lignocellulosic biomass. However, some cellulases (like EG I) have significant hemicellulase activity that might effect their synergistic role for pretreated cell walls abundant in hemicelluloses [474].

EG I and II might both play a significant role during hydrolysis of AFEX treated corn stover due to significant amorphous cellulose and hemicellulose retained after pretreatment compared to acid/steam pretreated barley straw. Also, the synergistic interactions between CBH I and CBH II (with and without suitable endoglucanases) on AFEX treated cellulose are currently unknown.

8.1.2.2 Role of endo- (EX) and exo-xylanases (βX)

Native cellulose microfibrils are composed of a crystalline glucan core with an amorphous hemicellulose rich outer surface [55] that helps direct the self assembly of the cell wall [475,476]. The hemicellulose sheath around cellulose microfibrils (via non-covalent associations) helps effectively transmit stress applied on the cell wall. This hemicellulose sheath is not removed during alkaline pretreatments unlike dilute acid based pretreatments. This may inhibit access of cellulases to the cellulose microfibrils, necessitating the presence of hemicellulases to maximize digestibility.

There has been only one paper published so far attempting to identify endoxylanase and exo-xylanase (i.e. β-xylosidase) synergy (using purified enzymes) on AFEX pretreated corn stover [477]. Purified CBH I (50 mg/g glucan) and β-glucosidase (5 mg/g glucan) were supplemented with endoxylanase (from *Thermomyces lanuginosus*, 1.5 mg/g glucan) and β-xylosidase (from *Apsergillus awamori*, 0.5 mg/g glucan) to hydrolyze AFEX treated corn stover. Glucan conversions (to glucose) increased from 10% to 22%, while xylan conversions (to xylose) increased less than 5% to 25% in the presence of both hemicellulases. The overall conversions are low due to absence of suitable endoglucanases (like EG I and EG II) and other accessory enzymes (like arabinofuranosidases) in the enzyme mixture.

8.1.2.3 Role of accessory hemicellulases

Endoxylanases are not effective in hydrolyzing branched hemicelluloses in the absence of suitable side-chain cleaving enzymes. Some of the important accessory hemicellulases include acetyl xylan esterases, phenolic esterases, arabinofuranosidases and glucuronidases. The optimum enzyme combinations depend on the cell wall composition, type and severity of thermochemical pretreatment. Depending on the pretreatment severity, some acetyl linkages remain bound to the xylan fraction [478]. Therefore, due to incomplete cleavage of acetyl and other LCC ester linkages, it might be necessary to supplement accessory hemicellulases for some lower severity pretreated lignocellulosics.

Purified accessory hemicellulase synergy studies have been conducted for some lower severity hot-water pretreated corn stover [458,479]. It was found that the glucan conversions to cellobiose by CBH I (at 15 and 50 mg CBH I protein loading per gram glucan) increased by 13-84% in the presence of suitable acetyl xylan and feruloyl esterases (2.5 mg/g glucan). The greatest synergistic enhancements to glucan and xylan conversion were observed for lower cellobiohydrolase loading (15 mg/g glucan), probably due to lesser non-specific binding of enzymes to substrate active sites. Despite the much lower xylan content in hot-water treated corn stover, significant improvements to digestibility was observed due to accessory enzyme supplementation. One would expect a much more significant improvement in digestibility of AFEX treated biomass due to substantially higher amounts of hemicellulose retained after pretreatment.

8.1.2.4 Role of xyloglucanases (XG)

Xyloglucan is a major hemicellulose typically found in primary cell walls but the amount present varies between dicots (20-25%) and monocots (2-10%). Recent work with high-

tension woods has indicated significant presence of xyloglucans in the gelatinous layer (detached from the S2 secondary wall layer) that plays an important role in stress-transfer between the longitudinally arranged cellulose microfibrils [480]. Xyloglucan along with other hemicelluloses is tightly packed between cellulose elementary microfibrils (3 nm diameter) forming larger macrofibrils (30 nm diameter). The hemicellulose plays the role of glue that helps transfer stress between the stiff cellulose microfibrils. High-resolution imaging of untreated maize stover primary cell walls also suggests existence of hemicellulose sheaths covering cellulose microfibrils [55]. This would probably be one reason for the significant amounts of xyloglucanases secreted by fungal pathogens. These xyloglucanases (accounting close to 10-20% of total protein in commercial enzymes, [26]) may be critical to help improve accessibility of cellulases to crystalline cellulose buried under the xyloglucan and hemicellulose network. Studies conducted using purified xyloglucanases for acid pretreated wood and straws have shown slight improvement in biomass digestibility [481]. However, most of the hemicelluloses are acid hydrolyzed and extracted during the acid pretreatment thus not requiring significant amount of xyloglucanase activity to improve yields. Alkaline pretreatments should leave the hemicellulose largely unchanged. On the other hand, some endoglucanases (e.g. EG I) can also hydrolyze xyloglucans making the presence of xyloglucanase redundant in a complex cellulolytic mixture [481,482].

A lot of effort has been expended developing heterogeneous kinetic models to predict complex interactions between cellulosic substrates and purified enzymes as a function of substrate and enzyme related characteristics [11,204,467]. However, there is a need to determine critical enzymes necessary for hydrolyzing AFEX pretreated biomass

preceding the development of suitable enzymatic hydrolysis models. It will also be important to correlate ultra-structural and chemical modifications within AFEX pretreated cell walls to predict enzyme accessibility and ultimately the hydrolysis yields.

However, there have been no attempts to determine the various cellulases, hemicellulases and other accessory enzymes necessary to maximize glucan and xylan digestibility of AFEX treated corn stover.

8.1.3 Materials and Methods

See appendix A-VII-1, 2, 3, 4, 17, 23, 25, 27, 28, 29, 31-36 and 38.

8.1.4 Results and Discussion

8.1.4.1 Enzyme purification and activity assays

All cellulases and hemicellulases (except β-xylosidase, which was heterologously expressed) were purified from crude commercial enzyme blends (e.g. Spezyme CP, Multifect Xylanase, Novozyme 188), with details on the purification and heterologous expression methodology provided elsewhere [453]. α-Arabinofuranosidase (GH 51, E-AFASE) was procured from Megazyme (Bray, Ireland). Spezyme CP has high specific activity on cellulosic biomass (Chapter 7; **Table 7.1-B**) and was thus the source of CBH I, CBH II and EG I obtained using suitable chromatographic purification steps (i.e. ion-exchange, hydrophobic interaction chromatography). CBH I and CBH II were further polished using p-aminophenyl-1-thio-β-D-cellobioside (APTC) based affinity chromatography to remove trace endoglucanase contaminants [462,483,484]. Typically, crude cellulase mixtures are supplemented with Novozyme 188 to prevent inhibition of cellobiohydrolase by cellobiose [485,486]. Novozyme 188 was chosen as the source for purification of β-glucosidase, based on previous findings (**Table 7.1-B, 7.2**). Multifect®

Xylanase was the source to purify endo-xylanases based on previously reported findings (**Table 7.1-B, 7.2**). Several recombinant enzymes have been successfully expressed using the *Pichia pastoris* expression system [487,488]. In recombinant *P. pastoris* the gene of interest is integrated into its genome under methanol inducible alcohol oxidase promoter (*AOX1*p). The *P. pastoris* expression system was used for expression of β-xylosidase encoded via gene from *Aspergillus nidulans* [489]. Enzyme identity and glycosyl hydrolase family for all six purified proteins was confirmed through proteomics ([453]). The six purified enzymes were evaluated for their specific activity on several substrates (e.g. Avicel, Oat Spelt Xylan or OSX, Carboxymethyl cellulose or CMC, cellobiose, xylobiose) using a modified BCRL microplate method (see methods section for details). One unit of specific activity (U) was defined as 1 μmol (glucose equivalents) reducing sugars released based on DNS assay (for Avicel, CMC and cellobiose) per mg protein per min. For oat spelt xylan and xylobiose, specific activity was defined based on xylose equivalents. EG I was found to have high specific activity on CMC (6.69 U) and OSX (5.08 U). Interestingly, EG I and EX had comparable activity of oat spelt xylan (5.08 vs. 8.24 U, respectively). Endoxylanase (and xylo-oligomerase) activity for EG I has been reported earlier [474], suggesting that this enzyme could play a dual role in hydrolyzing glucan and xylan in pretreated cell walls, unlike other endoglucanases. CBH I and CBH II had significant activity on Avicel (0.019 and 0.027 U, respectively), compared to EG I (0.011 U). EG I activity on Avicel is not surprising, considering that Avicel is composed of a significant proportion of nearly 20-30% amorphous cellulose [312]. It was also found that if the CBH's were not extensively polished (by affinity chromatography), they had detectable CMC activity. Therefore, extensive polishing is critical to obtain high purity

cellobiohydrolases. βG and βX had significant activity on cellobiose (124.9 U) and xylobiose (52.2 U), respectively.

8.1.4.2 Comparing hydrolytic activity of core cellulases on cellulose I vs. III

Enzymatic hydrolysis (for 24 hours) using the core cellulases (CBH I, CBH II, EG I, βG) was carried out on untreated and ammonia treated cellulosic biomass. The first sets of experiments were conducted on untreated and liquid ammonia treated crystalline cellulose (i.e. Avicel). These experiments (**Table 8.1-8.2**) revealed the nature of synergistic interactions between the various cellulases that are responsible for the higher rate of glucan hydrolysis for cellulose III vs I_β (Chapter 4.2, **Figure 4.B.3**). The core cellulases (CBH I, CBH II, EG I) were added in various relative and total protein loadings (with/without βG supplementation at fixed loading). Interestingly, unlike the previous report on cellulose III [298], there was no improvement in specific activity for cellobiohydrolase I or II at low and high total protein loadings (2.5-10 mg/g glucan). On the contrary, there was a 25-50% lower activity for both CBH I or II detected on cellulose III vs. I. This would suggest that the nature of the cellulosic microfibril (e.g. Algal vs. Plant cell wall based cellulose) also plays an important role on the hydrolysis yield of cellulose III. On the other hand, endoglucanase I resulted in a two-fold increase in specific activity on cellulose III compared to native cellulose (with or without βG loading). There seemed to be a slight decrease in the rate enhancement for EG I at higher protein loadings (10 vs. 2.5 mg/g glucan). In binary enzyme systems, where EG I was supplemented with CBH I or CBH II, there was a significant enhancement in the overall hydrolysis yield for both cellulose I and III. However, the rate of hydrolysis of cellulose III ranged between 1.5-2 fold, compared to cellulose I, for binary systems incorporating

EG I (in the presence of βG) (**Table 8.1**; Expt# 5-6, 12-13, 19-20). Whereas, the rate of hydrolysis of cellulose III was always nearly 2-fold, compared to cellulose I, in the absence of βG (**Table 8.2**; Expt# 26-27, 33-34, 40-41).

In the absence of βG, the cellobiohydrolases are more severely inhibited by cellobiose compared to EG [490]. This could explain the greater improvement in the rate of hydrolysis for cellulose III vs I for binary enzyme systems incorporating EG I, in the absence of βG. For ternary enzyme systems, incorporating CBH I, CBH II and EG I, there was nearly a two-fold increase in activity seen on cellulose III compared to I (**Table 8.1**; Expt # 7, 14). These results validate previous findings of improved hydrolysis characteristics of cellulose III vs. I crystal structure (Chapter 4.2). However, an important discovery made through these series of experiments was the significant improvement in hydrolytic activity detected only for endoglucanase I on plant cell wall derived cellulose III.

8.1.4.3 Synergism between core cellulases on untreated and conventional AFEX treated corn stover

Enzymatic hydrolysis (for 24 hours) using the core cellulases (CBH I, CBH II, EG I, βG) was carried out on untreated and conventional AFEX treated corn stover. These experiments (**Table 8.3-8.4**) revealed the nature of synergistic interactions between the various cellulases that is responsible for the higher rate of glucan hydrolysis for pretreated cell walls. The core cellulases (CBH I, CBH II, EG I) were added in various relative and total protein loadings (with/without βG supplementation at fixed loading). Addition of single enzymes (with or without βG supplementation) typically resulted in less than 5-6% glucan conversion, irrespective of the total protein loading.

Table 8.1 *Enzymatic hydrolysis of untreated (cellulose I, UAV) and liquid ammonia treated (cellulose III, AAV) Avicel by varying loadings (as mg enzyme/g glucan) of core cellulases (CBH I, CBH II, EG I, βG) resulting in the formation of glucose and cellobiose. Where; %G and $\%G_2$ stand for % glucan conversion based on glucose and cellobiose yields, respectively. Commercial enzyme (CE) control comprised of Spezyme CP and Novo 188 at 15 mg/g glucan loading each.*

					Untreated Avicel					**Cellulose III Avicel**				
					Glucose		**Cellobiose**		**Total**	**Glucose**		**Cellobiose**		**Total**
					Mean	*Std Dev*	*Mean*	*Std Dev*		*Mean*	*Std Dev*	*Mean*	*Std Dev*	
Expt #	**CBH I**	**CBH II**	**EG I**	**βG**	**% G**	**% G**	**% G_2**	**% G_2**	**% G+G_2**	**% G**	**% G**	**% G_2**	**% G_2**	**% G+G_2**
1	2.5	0	0	0.125	3.3	0.4			3.3	1.9	0.3			1.9
2	0	2.5	0	0.125	3.7	0.3			3.7	2.8	0.5			2.8
3	0	0	2.5	0.125	1.8	0.0			1.8	3.5	0.4			3.5
4	2.5	2.5	0	0.25	12.5	1.0			12.5	12.5	2.1			12.5
5	0	2.5	2.5	0.25	8.5	0.1			8.5	13.1	1.7			13.1
6	2.5	0	2.5	0.25	10.4	1.4			10.4	15.9	0.4			15.9
7	2.5	2.5	2.5	0.375	31.3	2.6			31.3	64.6	3.6			64.6
8	5	0	0	0.25	5.7	1.4			5.7	3.3	0.5			3.3
9	0	5	0	0.25	5.8	0.3			5.8	3.1	3.1			3.1
10	0	0	5	0.25	2.0	0.1			2.0	5.1	1.1			5.1
11	5	5	0	0.5	19.0	0.2			19.0	19.6	1.0			19.6
12	0	5	5	0.5	14.9	1.4			14.9	14.3	2.4			14.3
13	5	0	5	0.5	15.5	0.2			15.5	26.1	1.2			26.1
14	5	5	5	0.75	39.9	0.6			39.9	78.3	6.0			78.3
15	10	0	0	0.5	7.0	0.3			7.0	4.5	1.3			4.5
16	0	10	0	0.5	6.8	0.9			6.8	3.7	0.2			3.7
17	0	0	10	0.5	2.7	0.3			2.7	4.8	0.3			4.8
18	10	10	0	1	22.9	4.6			22.9	28.5	0.2			28.5
19	0	10	10	1	17.3	1.0			17.3	22.3	2.0			22.3
20	10	0	10	1	25.9	1.2			25.9	47.8	8.6			47.8
21	10	10	10	1.5	52.0	4.6			52.0	90.2	0.5			90.2
CE control (30 mg/g glucan)					52.7	2.8			52.7	82.3	4.6			82.3

Table 8.2 *Enzymatic hydrolysis of untreated (cellulose I, UAV) and liquid ammonia treated (cellulose III, AAV) Avicel by varying loadings (as mg enzyme/g glucan) of core cellulases (CBH I, CBH II, EG I) resulting in the formation of glucose and cellobiose. Where; %G and %G_2 stand for % glucan conversion based on glucose and cellobiose yields, respectively. Commercial enzyme (CE) control comprised of Spezyme CP and Novo 188 at 15 mg/g glucan loading each.*

					Untreated Avicel					Cellulose III Avicel				
					Glucose		Cellobiose		Total	Glucose		Cellobiose		Total
					Mean	*Std Dev*	*Mean*	*Std Dev*		*Mean*	*Std Dev*	*Mean*	*Std Dev*	
Expt #	CBH I	CBH II	EG I	βG	% G	% G	% G_2	% G_2	% G+G_2	% G	% G	% G_2	% G_2	% G+G_2
22	2.5	0	0	0	0.1	0.0	1.7	0.4	1.8	0.1	0.0	0.9	0.1	1.0
23	0	2.5	0	0	0.1	0.0	2.1	0.4	2.2	0.2	0.0	1.0	0.2	1.2
24	0	0	2.5	0	0.3	0.1	0.8	0.2	1.1	0.6	0.0	1.9	0.0	2.5
25	2.5	2.5	0	0	0.4	0.0	5.9	0.9	6.3	0.5	0.0	6.2	0.3	6.7
26	0	2.5	2.5	0	0.8	0.1	4.2	0.6	5.0	1.4	0.2	7.3	0.3	8.7
27	2.5	0	2.5	0	0.7	0.1	4.0	0.3	4.7	1.6	0.1	9.1	2.4	10.7
28	2.5	2.5	2.5	0	1.4	0.0	14.2	0.1	15.6	3.8	0.1	20.5	0.3	24.3
29	5	0	0	0	0.3	0.1	2.7	0.1	2.9	0.2	0.1	2.0	0.2	2.2
30	0	5	0	0	0.1	0.0	2.9	0.4	3.0	0.1	0.1	1.9	0.1	2.0
31	0	0	5	0	0.3	0.0	1.1	0.1	1.5	0.7	0.0	2.3	0.2	3.0
32	5	5	0	0	0.6	0.1	10.7	0.1	11.4	0.8	0.0	11.9	0.1	12.6
33	0	5	5	0	0.9	0.0	6.6	0.2	7.5	1.7	0.1	10.8	0.0	12.5
34	5	0	5	0	1.1	0.0	6.8	0.4	7.9	2.3	0.3	14.0	1.0	16.4
35	5	5	5	0	2.6	0.0	16.9	0.1	19.5	5.5	0.3	24.8	0.1	30.3
36	10	0	0	0	0.4	0.1	3.4	0.4	3.8	0.4	0.2	2.6		3.0
37	0	10	0	0	0.4	0.0	3.9	0.2	4.3	0.2	0.1	2.3	0.4	2.5
38	0	0	10	0	0.4	0.1	1.5	0.3	1.9	0.8	0.0	2.9	0.3	3.7
39	10	10	0	0	0.9	0.1	13.5	0.9	14.5	1.2	0.1	14.4	0.1	15.6
40	0	10	10	0	1.3	0.1	10.8	0.6	12.1	2.5	0.1	13.4	0.6	15.9
41	10	0	10	0	1.5	0.1	11.2	0.3	12.8	3.1	0.1	14.6	0.4	17.7
42	10	10	10	0	3.1	0.1	18.0	0.2	21.1	6.5	0.3	26.8	1.7	33.3
CE control (30 mg/g glucan)					52.7	2.8			52.7	82.3	4.6			82.3

Table 8.3 *Enzymatic hydrolysis of untreated (UCS) and conventional AFEX (ACS) treated corn stover by varying loadings (as mg enzyme/g glucan) of core cellulases (CBH I, CBH II, EG I, βG) resulting in the formation of glucose and cellobiose. Where; %G and %G_2 stand for % glucan conversion based on glucose and cellobiose yields, respectively. Commercial enzyme (CE) control comprised of Spezyme CP and Novo 188 at 15 mg/g glucan loading each.*

					Untreated Corn Stover					**Regular AFEX-treated Corn Stover**				
					Glucose		**Cellobiose**		**Total**	**Glucose**		**Cellobiose**		**Total**
					Mean	*Std Dev*	*Mean*	*Std Dev*		*Mean*	*Std Dev*	*Mean*	*Std Dev*	
Expt #	**CBH I**	**CBH II**	**EG I**	**βG**	**% G**	**% G**	**% G_2**	**% G_2**	**% G+G_2**	**% G**	**% G**	**% G_2**	**% G_2**	**% G+G_2**
1	2.5	0	0	0.125	0.6	0.0			0.6	1.9	0.2			1.9
2	0	2.5	0	0.125	1.4	0.9			1.4	3.2	0.1			3.2
3	0	0	2.5	0.125	2.9	0.9			2.9	4.9	1.4			4.9
4	2.5	2.5	0	0.25	2.5	1.2			2.5	3.7	1.1			3.7
5	0	2.5	2.5	0.25	5.0	0.3			5.0	13.9	0.7			13.9
6	2.5	0	2.5	0.25	8.1	0.2			8.1	19.3	1.1			19.3
7	2.5	2.5	2.5	0.375	10.4	2.1			10.4	35.3	1.1			35.3
8	5	0	0	0.25	1.5	0.0			1.5	2.2	2.6			2.2
9	0	5	0	0.25	1.7	1.1			1.7	3.9	0.2			3.9
10	0	0	5	0.25	3.6	1.4			3.6	6.5	0.3			6.5
11	5	5	0	0.5	4.7	0.2			4.7	5.0	0.1			5.0
12	0	5	5	0.5	8.6	0.3			8.6	20.7	1.7			20.7
13	5	0	5	0.5	8.8	1.6			8.8	27.7	2.0			27.7
14	5	5	5	0.75	13.1	0.8			13.1	47.3	1.9			47.3
15	10	0	0	0.5	2.5	0.2			2.5	3.6	0.1			3.6
16	0	10	0	0.5	2.8	0.0			2.8	4.2	0.3			4.2
17	0	0	10	0.5	3.7	1.5			3.7	6.8	0.1			6.8
18	10	10	0	1	4.6	0.6			4.6	5.8	0.7			5.8
19	0	10	10	1	8.0	0.9			8.0	26.9	0.3			26.9
20	10	0	10	1	10.8	1.2			10.8	47.9	1.7			47.9
21	10	10	10	1.5	16.0	1.1			16.0	61.5	1.5			61.5
CE control (30 mg/g glucan)					26.1	2.4			26.1	73.6	2.8			73.6

Table 8.4 *Enzymatic hydrolysis of untreated (UCS) and conventional AFEX (ACS) treated corn stover by varying loadings (as mg enzyme/g glucan) of core cellulases (CBH I, CBH II, EG I) resulting in the formation of glucose and cellobiose. Where; %G and $\%G_2$ stand for % glucan conversion based on glucose and cellobiose yields, respectively. Commercial enzyme (CE) control comprised of Spezyme CP and Novo 188 at 15 mg/g glucan loading each.*

					Untreated Corn Stover					Regular AFEX-treated Corn Stover				
					Glucose		Cellobiose		Total	Glucose		Cellobiose		Total
					Mean	*Std Dev*	*Mean*	*Std Dev*		*Mean*	*Std Dev*	*Mean*	*Std Dev*	
Expt #	CBH I	CBH II	EG I	βG	% G	% G	$\%G_2$	$\%G_2$	$\%G+G_2$	% G	% G	$\%G_2$	$\%G_2$	$\%G+G_2$
22	2.5	0	0	0	3.0	1.6	0.1	0.0	3.2	0.1	0.1	2.6	0.0	2.7
23	0	2.5	0	0	2.0	0.5	0.3	0.0	2.3	0.1	0.0	2.7	0.1	2.8
24	0	0	2.5	0	3.5	1.0	0.4	0.1	3.9	2.1	0.0	4.4	0.0	6.4
25	2.5	2.5	0	0	2.6	1.4	0.2	0.1	2.8	0.0	0.0	2.9	0.1	2.9
26	0	2.5	2.5	0	6.0	1.1	0.5	0.0	6.5	3.3	0.1	4.1	5.6	7.4
27	2.5	0	2.5	0	5.6	0.7	0.8	0.2	6.4	4.5	0.1	12.1	0.3	16.7
28	2.5	2.5	2.5	0	8.3	0.2	0.9	0.1	9.2	7.4	0.3	15.2	0.1	22.6
29	5	0	0	0	1.0	0.1	0.3	0.3	1.3	0.0	0.0	2.9	0.0	2.9
30	0	5	0	0	1.5	0.9	0.3	0.2	1.8	0.0	0.1	2.8	0.3	2.8
31	0	0	5	0	2.6	0.0	0.4	0.1	3.0	2.5	0.1	5.1	0.0	7.5
32	5	5	0	0	3.7	0.5	0.4	0.1	4.1	0.2	0.0	3.3	0.3	3.5
33	0	5	5	0	5.7	0.1	0.9	0.2	6.7	5.5	0.0	11.7	0.2	17.2
34	5	0	5	0	7.7	1.5	1.0	0.4	8.8	8.3	0.1	14.0	0.0	22.3
35	5	5	5	0	11.2	0.9	1.2	0.3	12.3	14.9	1.8	17.3	0.1	32.2
36	10	0	0	0	3.9	0.2	0.2		4.0	0.5	0.2	2.7		3.1
37	0	10	0	0	2.5	0.3	0.2	0.0	2.7	0.0	0.1	2.7	0.0	2.6
38	0	0	10	0	4.6	1.7	0.2	0.1	4.8	3.2	0.2	5.3	0.3	8.5
39	10	10	0	0	4.0	1.0	0.3	0.2	4.2	0.3	0.1	4.4	0.1	4.8
40	0	10	10	0	8.0	0.1	0.9	0.1	8.9	7.7	0.6	13.9	0.0	21.6
41	10	0	10	0	9.2	0.7	0.9	0.1	10.0	13.4	0.6	16.1	0.2	29.5
42	10	10	10	0	13.2	0.3	1.5	0.3	14.6	21.7	0.4	18.7	0.4	40.5
CE control (30 mg/g glucan)					26.1	2.4			26.1	73.6	2.8			73.6

Table 8.6 *Regression model (based on Table VI-8.5) predicting % glucan (% G) digestibility for untreated Avicel (UAV), liquid ammonia treated Avicel (AAV), untreated corn stover (UCS) and AFEX treated corn stover (ACS) as a function of varying cellulase loading (CBH I, CBH II and EG I; total protein loading is 16.5 mg/g glucan inclusive of 1.5 mg/g glucan βG).*

Regression Terms (UAV %G)				**Regression Terms (AAV %G)**			
Term	**Coefficient**	**P**	**VIF**	**Term**	**Coefficient**	**P**	**VIF**
CBH I	13.702	*	1.973	CBH II	8.3	*	1.973
CBH II	10.978	*	1.973	EG I	7.55	*	1.973
EG I	4.531	*	1.973	CBH I	4.65	*	1.973
CBH I*EG I	75.965	0	2.375	CBH I*EG I	152.69	0	2.375
CBH I*CBH II	58.127	0	2.375	CBH I*CBH II	106.91	0.003	2.375
CBH II*EG I	37.113	0.009	2.375	CBH II*EG I	85.3	0.013	2.375
CBH I*CBH II*EG I	555.773	0	2.471	CBH I*CBH II*EG I	1439.95	0	2.471

S = 4.64474 PRESS = 701.100
R-Sq(pred) = 87.42% R-Sq(adj) = 88.77%

S = 11.2883 PRESS = 4228.84
R-Sq(pred) = 84.94% R-Sq(adj) = 86.84%

Table 8.6 *Contd...*

Regression Terms (UCS %G)				Regression Terms (ACS %G)			
Term	**Coefficient**	**P**	**VIF**	**Term**	**Coefficient**	**P**	**VIF**
EG I	4.485	*	1.973	EG I	7.541	*	1.972
CBH I	2.202	*	1.973	CBH II	7.433	*	1.587
CBH II	1.277	*	1.973	CBH I	6.786	*	1.587
CBH I*EG I	25.59	0	2.375	CBH I*EG I	134.387	0	2.306
CBH II*EG I	17.019	0	2.375	CBH II*EG I	73.565	0	2.306
CBH I*CBH II	11.396	0.006	2.375				
CBH I*CBH II*EG I	101.904	0	2.471	CBH I*CBH II*EG I	756.827	0	2.061

S = 1.33175 PRESS = 65.6442
R-Sq(pred) = 83.77% R-Sq(adj) = 87.29%

S = 5.21775 PRESS = 899.527
R-Sq(pred) = 91.25% R-Sq(adj) = 92.32%

Figure 8.1 *Cox-response trace plot for % glucan conversion (AFEX corn stover or ACS) with respect to reference blend at optimal mixture composition of CBH I (34.67%), CBH II (26%) and EG I (39.33%). Sum of all three cellulase loadings is equal to 15 mg/g glucan. 1.5 mg/g glucan of βG was added to all mixtures tested (See Table VI-8.5 for details).*

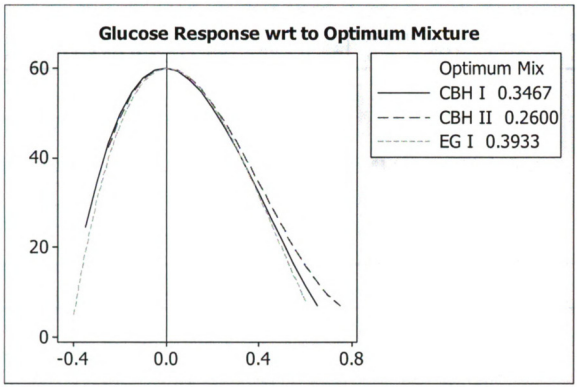

Table 8.8 *Glucan and xylan saccharification yields (24 hours) for AFEX treated corn stover by cellulases (CBH I, CBH II, EG I; at fixed relative and total protein loading) and hemicellulase (α-arabinofuranosidase or ArbF, EX, βX; varying relative protein loadings) combinations (as mg enzyme/g glucan) for fixed total protein loading of 16.5 mg/g glucan. βG loading was fixed at 1.5 mg/g glucan.*

	Relative protein loading						% Glucose yield		% Xylose yield	
Expt #	**CBH I**	**CBH II**	**EG I**	**EX**	**βX**	**ArbF**	*Mean*	*Std Dev*	*Mean*	*Std Dev*
1	3.75	3.75	3.75	3.75	0	0	66.5	0.7	9.7	1.2
2	3.75	3.75	3.75	0	3.75	0	53.6	0.4	37.9	1.5
3	3.75	3.75	3.75	0	0	3.75	50.7	1.7	6.4	1.0
4	3.75	3.75	3.75	1.875	0	1.875	64.2	0.9	9.8	1.3
5	3.75	3.75	3.75	0	1.875	1.875	53.1	1.2	48.6	1.7
6	3.75	3.75	3.75	1.25	1.25	1.25	63.9	2.5	63.0	2.7
7	3.75	3.75	3.75	2.5	0.625	0.625	65.3	0.9	64.2	1.7
8	3.75	3.75	3.75	0.625	2.5	0.625	63.8	1.4	64.2	5.2
9	3.75	3.75	3.75	0.625	0.625	2.5	61.9	0.9	60.2	1.0
Control H	3.75	3.75	3.75	1.875	1.875	0	65.6	2.8	49.0	2.3
Control C	5	5	5	0	0	0	55.8	1.0	5.6	1.9

However, the activity of the single enzymes (with βG supplementation) was significantly higher (50-200% increase; depending on type of enzyme and total protein loading) on AFEX treated vs. untreated corn stover (**Table 8.3**). In the absence of βG, the activity of the single enzymes was even higher (900-2000% increase based on cellobiose release) on AFEX treated vs. untreated corn stover (**Table 8.3**). The difference in the activity of purified enzymes on untreated and AFEX treated corn stover is likely dependent on enzyme accessibility. AFEX pretreatment has been shown to create pores within the cell wall that would substantially enhance cellulase accessibility to embedded cellulose microfibrils (Chapter 4.1). The cellulose microfibrils are embedded within the cell wall surrounded by hemicellulose and lignin. It was of interest to note that the products of hydrolysis for untreated vs. AFEX treated corn stover (in the absence of βG) were very different. There was a significantly higher amount of cellobiose released by CBH I and/or CBH II acting on AFEX treated corn stover. This would suggest that cellobiohydrolases are more easily able to act on cellulose microfibrils within AFEX treated cell walls, as compared to untreated cell walls, possibly due to enhanced porosity. Interestingly, it was found that the major product of hydrolysis for untreated corn stover was glucose (8.3% glucan conversion; Expt # 28 Table 8.4). On the other hand, the major product of hydrolysis for AFEX corn stover was cellobiose (15.2% glucan conversion; Expt # 28 Table 8.4). For binary enzyme systems (with or without βG), the highest activity was obtained only for CBH I + EG I or CBH II + EG I based combinations for both AFEX and untreated corn stover. These results were unlike what was seen for Avicel, where CBH I + CBH II gave the highest activity compared to EG I based binary combinations. These results are not surprising considering Avicel and plant cell walls

have differing compositions (e.g. Avicel has lower DP cellulose with 30 fold higher concentration of available reducing ends for CBH I and CBH II to act upon) and ultra-structural organization of those components (e.g. corn stover has hemicellulose interlaced between cellulose microfibrils that EG I could act upon). For ternary enzyme systems, including all three core cellulases (CBH I + CBH II + EG I), the activity was 3-4 fold higher (with βG supplementation) for AFEX treated vs. untreated corn stover. The improvement in % glucan conversion was 2.5-3 fold for AFEX corn stover, in the absence of βG. The major product of hydrolysis for all ternary enzyme combinations (at 7.5, 15 and 30 mg total enzyme/g glucan) was mostly glucose for untreated corn stover. On the other hand, cellobiose was the major end-product of hydrolysis for AFEX treated corn stover. These results are an indication of the enhanced accessibility of crystalline cellulose microfibrils to cellobiohydrolases for AFEX treated cell walls as compared to untreated corn stover.

The degree of synergistic effect (DSE) between CBH I and CBH II on untreated avicel and corn stover ranges between 1.8-2.1 and 0.6-1.2, respectively. Interestingly, formation of cellulose III (liquid ammonia treated Avicel) results in significant enhancement of DSE between CBH I-CBH II to 2.7-3.5 from 1.7-2.1 for native cellulose I. This improvement in hydrolysis yield is likely due to the partial endo-activity of CBH II [207,491], which may result in enhanced synergy with CBH I. It is likely that the overall rate enhancement for CBH I-CBH II mixture on cellulose III is through a currently unknown mechanism. However, unlike cellulose III Avicel, there is no significant change in the DSE values between untreated and AFEX treated corn stover for CBH I-CBH II. This result is not surprising, since there is no significant modification of

cellulose crystal structure (i.e. formation of cellulose III) during conventional AFEX pretreatment (Chapter 4.2). The DSE between CBH I and EG I is typically greater than CBH II and EG I (DSE absolute value depends on supplementation of βG, due to inhibition of CBH by residual cellobiose). It was also found that the difference in DSE between CBH I-EG I and CBH II-EG I is greater on ammonia treated cellulosic biomass compared to native, untreated cellulose for both Avicel and corn stover. This is largely due to the formation of cellulose III and enhanced cellulose microfibril accessibility during ammonia based pretreatment of Avicel and corn stover, respectively.

The enzyme mixture composition and % glucan conversion data (**Table VI-8.5**) were analyzed as fixed amount (i.e. total enzyme loading is constant) mixture regression to develop a statistically based predictive model for hydrolysis of Avicel and corn stover. The regression model terms and coefficients are given in **Table 8.6**. The model coefficients are representative of the degree of importance of each individual enzyme and its synergistic interactions with other cellulases depending on the substrate. Though CBH I had the highest single term regression coefficient for untreated Avicel; EG I and CBH II had higher regression coefficients for ammonia treated Avicel. This is not surprising considering CBH II is known to have a partial endo-activity that would see a significant enhancement in hydrolysis rate due to formation of cellulose III. The optimized mixture composition (comprised of CBH I, CBH II and EG I) and predicted responses for AFEX corn stover are shown in **Figure 8.1** (as a function of relative enzyme loading with respect to reference optimal blend to depict sensitivity of yield to mixture composition). The optimal composition (based on % protein mass loading) of the core cellulase cocktail (at 16.5 mg/g glucan; inclusive of 1.5 mg/g glucan of βG) that maximized AFEX corn

stover glucan digestibility consisted of CBH I (34.67%), CBH II (26%) and EG I (39.33%). Interestingly, the relative ratios of the three cellulases are comparable to the predicted optimum cocktail comprising of cellulases and hemicellulases hydrolyzing AFEX treated corn stover [453]. The inclusion of hemicellulases results in slightly higher glucan conversion, possibly through minimizing xylo-oligomers end-product inhibition and maximizing cellulose accessibility by hydrolysis of insoluble hemicellulose.

8.1.4.4 Effect of hemicellulase supplementation on AFEX corn stover digestibility

The effect of supplementation of hemicellulases (i.e. endoxylanase, β-xylosidase, α-arabinofuranosidase) on AFEX treated corn stover was tested at a fixed total protein loading (comparable to previous experiments in Chapter 7). The total protein loading was fixed at 16.5 mg/g glucan with βG loaded at 1.5 mg/g glucan to prevent cellobiose inhibition. The individual ratios of the other enzymes (CBH I, CBH II, EG I, EX, βX, ArbF) were varied to study synergistic interactions between the various glycosyl hydrolases.

From **Table VI-8.7** (Experimental data #1-31 from [453]) **and Table 8.8** (Experiments #1-9), the mixture of enzymes that gave the highest glucan and xylan hydrolysis yield contained all glycosyl hydrolases (Table VI-8.7 #31 and Table 8.8 #7). Replacing the cellulase mass fraction with hemicellulases (Table VI-8.7 #29) helped increase xylan conversion by 500-1000% (with respect to Table VI 8.7 #7) without significantly affecting the glucan yield. On the contrary, there was a 20% increase in glucan conversion upon addition of an endoxylanase (Table 8.8 Control C vs. #1). Selig et al. reported 80-150% increase in xylan conversion (to xylobiose) due to supplementation of CBH I with an endoxylanase (from *Thermomyces lanuginosus*) and a

corresponding 15-20% increase in glucan conversion (to cellobiose) during hydrolysis of hot water treated corn stover [458,477]. However, in those experiments the total protein loading was 5-15% higher for the endoxylanase supplementation mixture unlike the current set of experiments where the total protein loading is constant. These experiments suggest that endoxylanases help enhance cellulose accessibility based on the improvement seen in glucan digestibility upon supplementation of endoxylanase to CBH I.

Individual enzymes (supplemented along with βG) resulted in poor glucan and xylan hydrolytic yields (Table VI-8.7 #1 vs. #5). Significant xylan conversion was obtained by only EG I (Table VI-8.7 #3), which is not unexpected based on its significant oat spelt xylan activity. It may be possible that bi-functional enzymes like EG I have an advantage over endoglucanases from other GH families (e.g. GH 5, GH 12, GH 61). This is because cellulose microfibrils are thought to be enclosed within hemicellulose rich sheaths [55] that would hinder the activity of mono-functional endoglucanases.

For binary enzyme combinations (Table VI-8.7 #6 to #15), CBH I/EG I mixture (#7) gave the highest glucose yield (47.9%) and EX/βX mixture (#15) gave the highest xylose yield (49.6%) followed by EG I/βX (#14, 36%) likely due to EG I's xylan cross-activity. Interestingly, it was possible to achieve close to 50% xylan conversion in the absence of any cellulases (< 2 % glucan conversion, #15). This suggests that the cell wall ultra-structure is significantly modified during AFEX pretreatment (Chapter 4.1) that allowed significant enhanced enzymatic accessibility to both glucan and xylan fractions, unlike untreated cell walls (Table 8.2 and 8.3) [492]. Interestingly, even though CBH II had significantly higher activity (42% higher) on crystalline cellulose than CBH I, the

latter resulted in significantly higher conversions (45-50% higher) in binary/ternary/quartenary mixtures that had either one of the CBH's (Compare #7 vs. 10; 19 vs. 22; 29 vs. 30). This result reiterates the importance of optimizing enzyme cocktails on pretreated lignocellulosic biomass and not artificial cellulosic substrates like Avicel [385]. For ternary enzyme combinations (#16 to #25), CBH I/CBH II/EG I mixture (#16) gave the highest glucose yield but very low xylose yield. Binary mixtures of CBH I + EG I synergized together to give higher combined glucan and xylan conversion (1.5–2.5 fold, #7) compared to CBH I + EX, CBH II + EG I and CBH II + EX. However, for ternary systems that included CBH II the combined glucan and xylan conversions for CBH I + CBH II with either EG I or EX are remarkably similar. This suggests that presence of CBH II reduces the advantage of EG I over EX when synergizing with CBH I alone, possibly due to the minor endo-activity typically seen for CBH II [491]. In order to get higher xylose yields, either a EG I-βX or EX-βX combination is necessary. For quarternary enzyme combinations (#26 to #30), without βX, xylan conversion dropped dramatically (#26) and without CBH I, glucan conversion decreased as well (#30).

TEM imaging results from previous chapters along with other published work seem to suggest that elementary cellulose fibrils are coated with a thin layer of hemicellulose (probably unbranched hemicelluloses to allow stronger hydrogen bonding with cellulosic fibrils) [55,493]. Hydrolysis of cellulose would be impeded by steric inhibition due to the hemicellulose coating that must be hydrolyzed in order to enhance cellulase accessibility. This would result in strong synergy between cellulases and hemicellulases (Table VI-8.7 Experiments # 26, 31 vs. 16). This could also explain the significant cross-activity of EG I on hemicellulose that would enhance accessibility of

cellulases to the underlying cellulose fibrils. Hydrolysis of hemicellulose wrapped around glucan microfibrils would help increase cellulose accessibility [464] and prevent cellulase inhibition via hemicellulose oligomers [459].

From **Table VI-8.7 and Table 8.8**, it is not surprising to find that CBH I, CBH II and EG I are critical for glucan hydrolysis; while EG I, EX, βX and ArbF are important for xylan hydrolysis. The highest xylose yield was below 50% in the absence of ArbF (Control H, Table 8.8). This is probably due to the lack of other accessory enzyme activities such as α-arabinofuranosidase, feruloyl/acetyl xylan esterases, pectinases and α-glucuronidase. Supplementation of CBH I, CBH II, EG I, EX, βX and βG cocktail with purified α-arabinofuranosidase resulted in 30% increase in xylan hydrolysis yields (**Table 8.8**, Expt #6-8 vs. Control H). These results (Control C vs. H, Table 8.8) also validate earlier findings that hemicellulase supplementation can help reduce cellulase loading while giving higher overall hydrolysis yields [48,458,477,479,494,495]. These results also suggest that other accessory enzymes would be critical in further enhancing the hemicellulose hydrolysis yield in order to minimize total protein loading and maximize hydrolysis yields.

The enzyme mixture composition and % glucan conversion data (**Table 8.8**) were analyzed as fixed amount (i.e. total enzyme loading is constant) mixture regression to develop a statistically based predictive model for xylan hydrolysis (AFEX corn stover). The regression model terms and coefficients are given in **Table 8.9**. The model coefficients indicate that EX, βX and ArbF work synergistically to help increase xylan hydrolysis yields. Interestingly, though βX had the highest single term regression

coefficient; EX and ArbF had significant synergistic interactions contributing to binary and ternary term coefficients.

Table 8.9 *Regression model (based on data from Table 8.8) predicting % xylan (% X) digestibility for AFEX treated corn stover (ACS) as a function of hemicellulase loading (EX, βX, ArbF as mg/g glucan).*

Regression Terms (ACS %X)			
Term	**Coefficient**	**P**	**VIF**
βX	35.51	*	1.972
EX	15.23	*	1.587
ArbF	11.17	*	1.587
βX*ArbF	103.58	0	2.306
EX*βX	99.91	0	2.306
EX*βX*ArbF	890.14	0	2.061

S = 9.24827 PRESS = 3634.26
R-Sq(pred) = 82.69% R-Sq(adj) = 84.11%

The optimized mixture compositions (comprising of EX, βX and ArbF) and predicted responses for AFEX corn stover are shown in **Figure 8.2** (as a function of relative enzyme loading with respect to reference optimal blend to depict sensitivity of yield to mixture composition). The optimal composition (based on % protein mass loading) of the core cellulase cocktail (at 16.5 mg/g glucan; inclusive of 1.5 mg/g glucan of βG) that maximized AFEX corn stover glucan digestibility consisted of CBH I (34.67%), CBH II (26%) and EG I (39.33%). It is interesting to note that the relative ratio of CBH I to CBH II based on the current purified enzyme optimal mixture is about 1.3 (based on Figure 8.1); whereas, this ratio was about 2 based on the proteomics compositional analysis of the top 5% CE-RE mixtures that gave the highest glucan conversions (**Figure 7.7**). The relative ratio of CBH I to CBH II ranges between 2.6-3 for RE 1, RE 4, RE 8 and CE 1 (based on proteomics based composition; **Table 7.2**). It is

likely that inclusion of other purified enzymes to maximize both glucan and xylan conversion would result in a different optimal enzyme composition.

Figure 8.2 *Cox-response trace plot for % xylan conversion (AFEX corn stover or ACS) with respect to reference blend at optimal mixture composition of EX (29.07%), βX (42.67%) and ArbF (28.27%). Sum of all three hemicellulase loadings is equal to 3.75 mg/g glucan (See Table 8.8). Cellulase loading (CBH I, CBH II, EG I) was fixed at 11.25 mg/g glucan along with 1.5 mg/g glucan βG.*

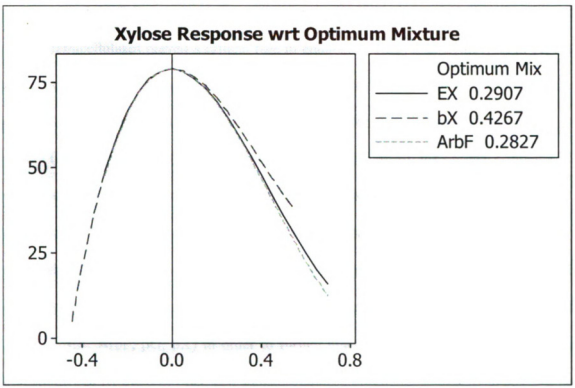

8.1.5 Conclusions

Synergistic interactions amongst core cellulases (CBH I, CBH II, EG I, βG) for varying total protein loading (2.5-31.5 mg enzyme/g glucan) during hydrolysis of untreated (cellulose I) and liquid ammonia treated cellulose (cellulose III) resulted in a 2-fold higher specific activity for EG I (with or without CBH's) on ammonia treated cellulose compared to native cellulose. This would suggest that the overall enhancement in the hydrolytic rate of crystalline cellulose III vs. I_β is largely due to increased activity of

endoglucanases. It was also found that unlike what has been reported earlier for Avicel, CBH I and CBH II had very little synergistic interaction (DSE ~ 1) on AFEX treated corn stover. Accessibility of crystalline cellulosic microfibrils within lignocellulosic cell walls was greatly enhanced after AFEX. This observation is based on the difference in the hydrolysis by-products released (ratio of cellobiose to glucose) during saccharification of untreated and AFEX treated corn stover by various combinations of CBH I, CBH II and EG I. Hemicellulases played a critical role in enhancing the glucan hydrolysis of AFEX treated corn stover. The optimal composition (based on % protein mass loading) of the core cellulase cocktail that maximized AFEX corn stover glucan digestibility consisted of CBH I (34.67%), CBH II (26%) and EG I (39.33%). In contrast, the optimal composition of the core hemicellulase cocktail (with fixed equimass core cellulase loading) that maximized AFEX corn stover xylan digestibility consisted of EX (29.07%), βX (42.67%) and ArbF (28.27%). Current results suggest inclusion of hemicellulases and other cellulolytic enzymes to produce an optimum enzyme cocktail (comprised of CBH I, CBH II, EG I, EX, ArbF, βG, βX) in order to further enhance the overall glucan and xylan digestibility of AFEX pretreated cell walls.

CHAPTER 9: CONCLUSIONS AND RECOMMENDATIONS FOR FUTURE RESEARCH

The effect of ammonia based treatments (e.g. AFEX) on corn stover cell wall ultra-structure and chemical composition was explored through several spectroscopic, spectrometric and microscopic techniques. This is an important step towards bridging the gap of limited understanding of the role of ammonia based treatments on plant cell wall physicochemical characteristics that ultimately affect their rate of enzymatic hydrolysis.

Conventional AFEX (at 1:1 and 0.6:1 ammonia and water loading, respectively) is not a high liquid-to-solids loading based flow-through pretreatment (unlike dilute acid and ammonia recycle percolation) that continually leach the cell wall, physically extracting lignin and hemicellulose into a separate liquid process stream. The ultra-structural modifications within ammonia treated cell walls (**Figure 9.1**) are very different from conventional acidic treatments and are closely dependent on pretreatment conditions (ammonia/water loading, temperature, reaction time). Liquid ammonia is responsible for swelling crystalline cellulose I_β crystal polymorphs in native plant cell walls to cellulose III_I, which has a nearly two-fold higher enzymatic digestion rate than native cellulose. However, presence of water during conventional AFEX results in near complete reversion of cellulose III to I. The extent of enzymatic digestibility for the various polymorphs of cellulose were found to vary in the following order; Amorphous Cellulose > Cellulose III > Cellulose II > Cellulose I. Ammonia was also found to chemically modify the lignin-carbohydrate complexes via cleavage of ester linkages through ammonolysis (by NH_3) or hydrolysis (by OH^-). The various cell wall decomposition products and alkali extractives like arabinoxylan oligomers, ammonolysis byproducts

(acetamide, phenolic amides), peeling reaction products (lactic acid), middle lamella components (possibly bound to calcium) and other lignin rich residues are extracted from within the cell wall and deposited on the the outer wall surfaces, cell pits and corners. The cell wall extractives are deposited on the outer cell wall surface due to the rapid decompression of ammonia at end of AFEX pretreatment. These degradation products deposited on the surface are responsible for the drop in O/C atomic ratio and result in amorphously shaped smear like formations as confirmed via ESCA, SEM and AFM based analysis. Several degradation products formed during conventional AFEX and dilute-acid based pretreatments (e.g. carboxylic acids, furans, aromatics, amides, arabinoxylan oligomers) were quantified and compared by LC-MS/MS and GC-MS based methodologies. The extraction of these AFEX cell wall components results in the formation of a unique semi-continuous, nano-pore (10-500 nm width) based network that is probably responsible for minimizing diffusional resistance and enhancing enzyme accessibility to within ammonia pretreated cell walls. The nano-pores were visualized through TEM and 3D-TEM based tomography to estimate cell wall porosity for varying AFEX treatment severities (as nm^{-1} or m^2/gm). Enzymatic digestion results indicated a linear dependence between rate of hydrolysis and the logarithm of pretreated cell wall porosity. The extent of porosity was also found to be strongly correlated to the ammonolysis of ferulate ester bridges within the cell wall. Interestingly, the extent and type of pore formation (e.g. ellipsoidal vs. spherical) depended on the location within the cell wall and AFEX pretreatment severity (e.g. Low temperature vs. No-moisture AFEX).

Figure 9.1 *Model for generic lignocellulosic cell walls before (A) and after ammonia based pretreatments (B). Figure depicts various lignin-carbohydrate complex (LCC) linkages between non-core lignin phenolics and hemicellulose side chains that are modified during AFEX resulting in enzyme accessible porosity. Where; Cellulose (green rods), Hemicellulose (purple strings with blue dots), Lignin (grey matrix).*

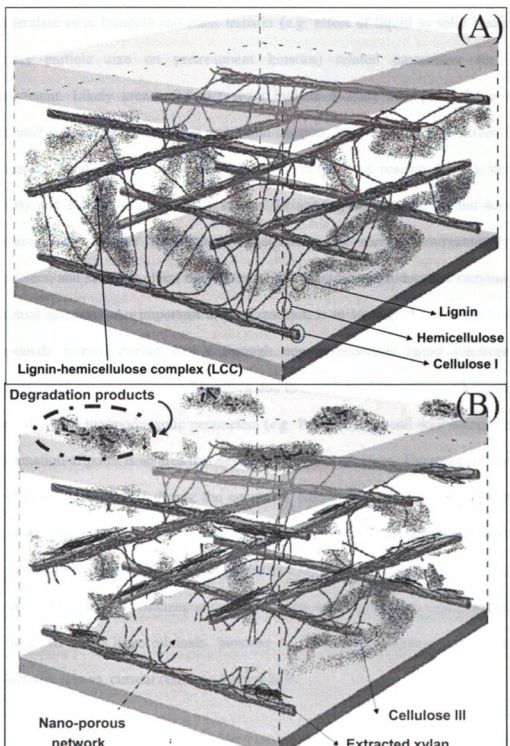

The current research project identified the major ultra-structural and chemical modifications incorporated within lignocellulosic cell walls during AFEX. The long-term goal should be to determine the various kinetic (e.g. rate of ammonolysis vs. hydrolysis of diferulate ester bridges) and mass transfer (e.g. effect of liquid to solid loading and biomass particle size on pretreatment kinetics) related parameters for AFEX pretreatment. Likely areas of future work include enzyme adsorption for ammonia pretreated cellulose, hemicellulose and lignin fractions isolated from corn stover; kinetic studies for ammonolysis based reactions (for pretreatment reactor design); cell wall porosity and enzymatic digestibility studies for varying AFEX pretreatment severities; formation of cellulose III through modification of current pretreatment/process parameters; and studying effect of various AFEX degradation products on enzymatic and microbial activities. An important area of research is to identify the major nitrogenous compounds formed during AFEX through non-ammonolysis based reactions (e.g. Maillard reactions, amine/imine formation due to reaction of ammonia with lignin). The effect of AFEX thermodynamic parameters (e.g. Pressure) and cell wall composition on the formation of pores is an area that needs to be further explored. The extent of reversion of cellulose III back to I during the course of enzymatic hydrolysis as a function of process parameters (e.g. solids loading, temperature, impeller agitation speed) needs to be understood to maximize the benefit of improved digestibility of the former. It would be interesting to conduct simultaneous saccharification and fermentation (SSF) studies using cellulose III rich lignocellulosic biomass to determine enhancement in ethanol productivity rate vs. current cellulose I based SSF.

Optimized crude enzyme cocktails, using the BCRL high-throughput microplate based hydrolysis assay, at a fixed protein loading of 16.5 mg protein/g glucan had significantly higher glucan and xylan (~ 90%) conversions than commercially available cellulase blends at equivalent or higher protein loadings (e.g. CE 1 + RE 2 gave 62% glucan and 39% xylan conversions at 33 mg/g glucan loading). Interestingly, cellulose is hydrolyzed more efficiently for fixed-protein loading mixtures in which certain amount of the cellulase was replaced by endoxylanases (and other hemicellulases), possibly increasing accessibility of cellulose embedded between hemicellulose sheaths [55]. Similarly, hemicellulose is more efficiently hydrolyzed in mixtures in which some endoxylanase is replaced with cellulases. Synergistic interactions amongst purified core cellulases (CBH I, CBH II, EG I, βG) for varying total protein loading (2.5-31.5 mg enzyme/g glucan) during hydrolysis of untreated (cellulose I) and liquid ammonia treated cellulose (cellulose III) indicated a 2-fold higher specific activity for EG I (with or without CBH's) on the ammonia treated substrate compared to native cellulose. This is an important discovery that could lead to modification in the way conventional AFEX is currently being conducted. Formation of cellulose III within pretreated plant cell walls could potentially result in 2-fold increase in the overall enzymatic digestibility rate at equivalent protein loading. Also the optimal enzyme cocktail mixture composition might skew more towards the endoglucanases based on significantly higher activity of EG I vs. CBH's on cellulose III. It was also found that unlike what has been reported earlier for Avicel, CBH I and CBH II had little or no synergistic interaction on untreated and AFEX treated corn stover. This is likely due to the high cellulose degree of polymerization (and hence lower number of available reducing ends) and presence of residual hemicellulose

that results in poor exo-cellulase activity on native and pretreated plant cell walls. The optimal composition (based on % protein mass loading) of the core cellulase cocktail that maximized AFEX corn stover glucan digestibility consisted of CBH I (34.67%), CBH II (26%) and EG I (39.33%). Preliminary experiments with supplementation of α-arabinofuranosidase along with core cellulases, EX and βX (at fixed total protein loading of 15.75 mg/g glucan) resulted in significantly higher xylan conversions (65%). The optimal composition of the hemicellulase cocktail (with fixed equimass core cellulase loading) that maximized AFEX corn stover xylan digestibility consisted of EX (29.07%), βX (42.67%) and ArbF (28.27%). These results suggests the lack of critical hemicellulases and other cellulolytic enzymes/proteins (e.g. Mannanases, Galactanases, Pectinases, Swollenin, Esterase, Glucuronidase) from the current core enzyme cocktail that would need to be included to further enhance the overall glucan and xylan digestibility of AFEX pretreated cell walls. Recent results suggest inclusion of cellulases and hemicellulases to develop an optimum enzyme cocktail (comprising of six major enzymes, like, CBH I, CBH II, EG I, EX, βG, βX) is necessary to maximize both glucan and xylan digestibility of AFEX pretreated cell walls [453]. The synergistic enzyme cocktail composition for cellulose III rich lignocellulosic biomass is currently unknown. The effect of pretreatment severity is known to modify the cell wall ultra-structure differentially. However, the effect of varying pretreatment severity on optimum enzyme cocktail composition is relatively unknown. It is likely that for lower severity (and economically viable pretreatment conditions) AFEX conditions, the cleavage of LCC esters would be incomplete after pretreatment. Therefore, an optimal enzyme cocktail for

lower severity AFEX treated lignocelluloses would probably need to include various esterases (acetyl xylan esterase, phenolic esterases), among other accessory enzymes.

In summary, a fundamental understanding of physicochemical modifications incorporated within lignocellulosic cell walls during ammonia based pretreatments and its effect on enzyme synergy should help 'engineer' biomass feedstock, hydrolytic enzymes and ethanologenic microbes suitable for cellulosic biorefineries. This research should aid in the development of mechanistic models for pretreated cell walls that are dependent on cell wall ultra-structural properties and individual enzyme component characteristics.

APPENDICES

APPENDIX I – A (Chapter 3.1 - Outer wall morphology)

Figure I-3.A.5 *(A) Picture showing various parts of corn plant and their mass distributions are shown as pie chart in the bottom left. (B) Pictures showing various fractions for ground sample. Percent mass distributions of various particle size fractions for pre-milled (PM*) and ground corn stover are shown as pie chart in the bottom right. (Figure has been reproduced from [1]).*

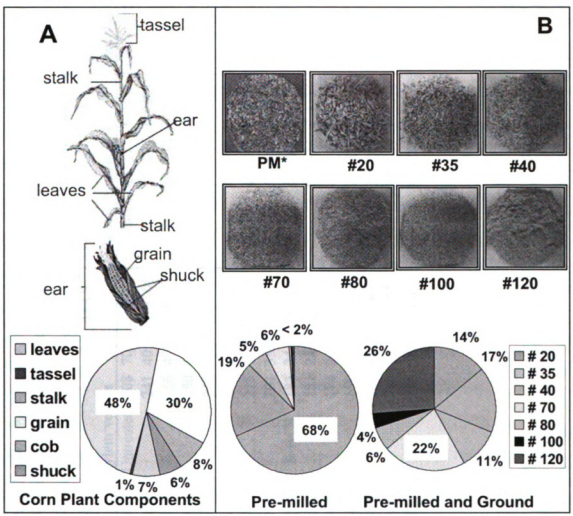

Table I-3.A.3 *Cell wall perimeters (L, μm), areas enclosed within lumen (A, μm^2) and isoperimetric quotients ($4\pi A/L^2$) for untreated, regular AFEX (R-ACS) and high liquid to solid loading based AFEX (High-ACS) treated corn stover cell walls.*

	L	A	$4\pi A/L^2$		L	A	$4\pi A/L^2$		L	A	$4\pi A/L^2$		L	A	$4\pi A/L^2$
Parenchyma cells				**Xylem vessels**				**Vascular bundle cells**				**Vascular bundle cells**			
Untreated	440	14264	0.9279	Untreated	308	7050	0.9367	Untreated	40	117	0.9157	Untreated	59	179	0.6387
	439	12874	0.8391		241	4055	0.8805		52	194	0.9009		42	101	0.7063
	351	8629	0.8798		256	4768	0.9138		56	230	0.9365		50	156	0.7793
	305	6816	0.9188		250	4548	0.9156		42	133	0.9347		49	144	0.7395
	249	4377	0.8848		248	4461	0.9097		43	129	0.8880		28	57	0.9090
	471	16532	0.9378		209	3297	0.9449		49	172	0.9029		32	74	0.9045
	278	5690	0.9259		215	3520	0.9566		45	113	0.6912		35	86	0.8782
	307	6805	0.9104		201	3528	1.1022		53	182	0.8040		30	63	0.8819
	281	5698	0.9089	R-ACS	183	2447	0.9192		62	265	0.8566		30	67	0.9065
	269	4763	0.8303		181	2430	0.9342		51	194	0.9314		34	81	0.8831
	421	12796	0.9066		174	2209	0.9124		45	144	0.9068		35	93	0.9338
	301	6666	0.9265		150	1664	0.9293		20	29	0.9392		22	35	0.8928
	363	8362	0.7969		226	3898	0.9601		56	204	0.8099		33	70	0.8154
	470	15123	0.8604		242	4459	0.9536		57	209	0.8091		34	74	0.8023
	436	12624	0.8342		226	3594	0.8839		48	175	0.9536		23	39	0.9112

Table I-3.A.3 *Contd...*

	L	A	$4\pi A/L^2$		L	A	$4\pi A/L^2$		L	A	$4\pi A/L^2$		L	A	$4\pi A/L^2$
Parenchyma cells				**Xylem vessels**				**Vascular bundle cells**				**Vascular bundle cells**			
R-ACS	444	14630	0.9324	High-ACS	115	1015	0.9563	Untreated	57	239	0.9208	Untreated	21	29	0.7857
	294	6243	0.9057		118	1070	0.9667		48	155	0.8407		28	56	0.9157
	411	12443	0.9249		116	1002	0.9384		44	124	0.8168		18	20	0.7857
	183	2081	0.7787		105	762	0.8707		64	280	0.8512		22	23	0.5833
	136	1349	0.9172		115	939	0.8880		48	143	0.7760		38	94	0.8023
	242	4195	0.8968		129	1171	0.8857		39	105	0.8571		31	60	0.7697
	181	2364	0.9116		97	717	0.9586		57	219	0.8604		30	56	0.7612
	419	13124	0.9411		127	1179	0.9204		53	173	0.7750		27	52	0.9076
	196	2855	0.9317		155	1802	0.9433		45	112	0.6860		21	33	0.9149
	279	4973	0.8024		137	1402	0.9412		60	171	0.6030		27	47	0.8271
	244	3788	0.7982		135	1394	0.9609		55	131	0.5365		16	19	0.9209
	419	10451	0.7494		137	1407	0.9445		35	73	0.7491				
	124	1091	0.8853		69	327	0.8632		56	218	0.8692				
	129	1114	0.8450		81	468	0.8937		49	164	0.8713				
	143	1390	0.8569		76	435	0.9529		76	414	0.9029				
	246	4228	0.8804		84	522	0.9197		47	149	0.8479				

Table I-3.A.3 *Contd...*

	L	A	$4\pi A/L^2$		L	A	$4\pi A/L^2$		L	A	$4\pi A/L^2$		L	A	$4\pi A/L^2$
Vascular bundle cells				**Vascular bundle cells**				**Vascular bundle cells**				**Vascular bundle cells**			
R-ACS	44	136	0.8920	High-ACS	20	26	0.8258	High-ACS	21	28	0.8254	High-ACS	15	15	0.8221
	41	112	0.8256		16	14	0.6953		16	18	0.9220		13	11	0.8113
	27	53	0.8990		22	26	0.6868		31	54	0.6849		24	36	0.7797
	30	67	0.9094		10	7	0.9300		12	8	0.7516		13	12	0.9075
	41	108	0.8251		9	4	0.6839		15	15	0.8510		16	18	0.8765
	56	226	0.9116		12	7	0.5872		17	19	0.8144		18	21	0.8438
	41	107	0.7967		14	12	0.7464		16	16	0.7925		15	15	0.8040
	47	161	0.9097		20	27	0.8739		19	21	0.6874		21	21	0.5841
	39	103	0.8643		11	5	0.5102		16	14	0.6547		14	13	0.8600
	35	91	0.9210		10	5	0.7415		26	52	0.9538		25	24	0.4889
	26	43	0.8073		14	13	0.8077		17	19	0.8458		12	8	0.7103
	26	45	0.8403		13	13	0.8967		13	12	0.9183		14	11	0.7473
	55	208	0.8543		20	25	0.7977		35	79	0.8257		15	14	0.8265
	50	182	0.9050		15	14	0.7911		37	82	0.7548		24	43	0.8976
	46	140	0.8507		17	15	0.6829		30	64	0.8873		23	35	0.8328
	54	174	0.7454		25	37	0.7432		29	48	0.7346		23	33	0.7875
	22	35	0.9092		16	15	0.7512		26	43	0.8100		20	24	0.7421
	23	37	0.8926		32	62	0.7714		14	14	0.8721		16	14	0.6773

Table I-3.A.3 *Contd...*

Vascular bundle cells	L	A	$4\pi A/L^2$	Vascular bundle cells	L	A	$4\pi A/L^2$	Vascular bundle cells	L	A	$4\pi A/L^2$	Vascular bundle cells	L	A	$4\pi A/L^2$
R-ACS	17	21	0.8800	High-ACS	29	33	0.4836	High-ACS	20	26	0.7777	High-ACS	34	73	0.8131
	18	22	0.8267		19	24	0.8277		18	22	0.8849		14	11	0.7477
					14	12	0.7779		36	76	0.7442		17	17	0.7651
					16	18	0.9416		39	67	0.5545		21	29	0.8202
					25	42	0.8646		25	36	0.7209		16	15	0.7035
					26	43	0.8044		21	21	0.6241		16	17	0.7974
					42	124	0.8842		20	23	0.7481		18	16	0.6477
					26	42	0.7714		25	40	0.8159		35	83	0.8724
					31	66	0.8604		21	21	0.5887		27	39	0.6708
					21	28	0.7677		40	118	0.9351		35	87	0.9004
					17	21	0.9087		55	175	0.7196		22	38	0.9436
					18	17	0.6503		33	66	0.7760		25	49	0.9700
					16	17	0.8811		37	85	0.7703		25	40	0.8233
					18	20	0.8021		23	40	0.9176		25	47	0.9560
					15	16	0.9047		20	28	0.8541		20	26	0.7994
					24	30	0.6563		24	37	0.8082				
					31	52	0.6918		23	35	0.8443				

APPENDIX I – B (Chapter 3.2 - Surface topography-composition)

Figure I-3.B.2 *Untreated (U1-U10; panel I) and conventional AFEX (A1-A10; panel II) treated corn stover AFM amplitude (left) and phase (right) image dataset (image size is 2.5 x 2.5 μm^2). Box-plot of surface roughness factors (nm) along with data points scatter (N=10 per set) for untreated and AFEX treated amplitude image dataset from panels I-II.*

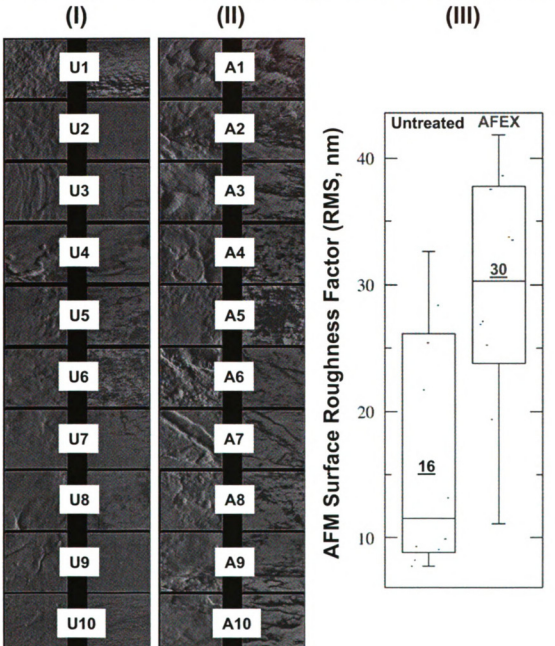

APPENDIX II – A (Chapter 4.1 - Cell wall porosity)

Figure II-4.A.7 *AFEX treated corn stover TEM images (at varying scales of magnification) showing cell corner, compound middle lamella (CML) and secondary wall layers (S1, S2, S3) for Low-N treated AFEX corn stover.*

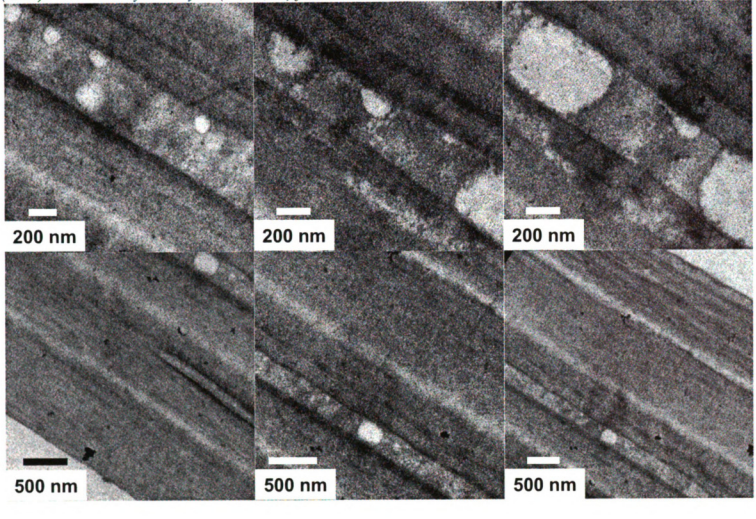

Figure II-4.A.8 *AFEX treated corn stover TEM images (at varying scales of magnification) showing cell corner, compound middle lamella (CML) and secondary wall layers (S1, S2, S3) for Regular treated AFEX corn stover.*

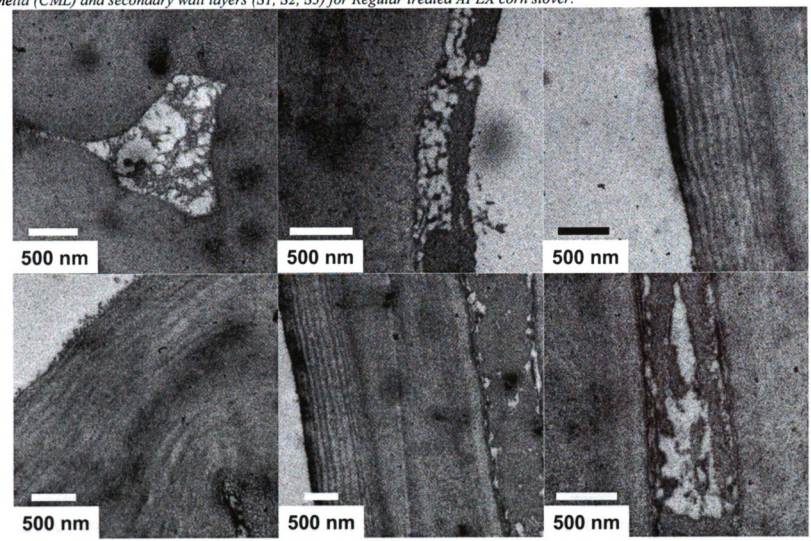

Figure II-4.A.9 *AFEX treated corn stover TEM images (at varying scales of magnification) showing cell corner, compound* ***middle*** *lamella (CML) and secondary wall layers (S1, S2, S3) for High-Nt treated AFEX corn stover.*

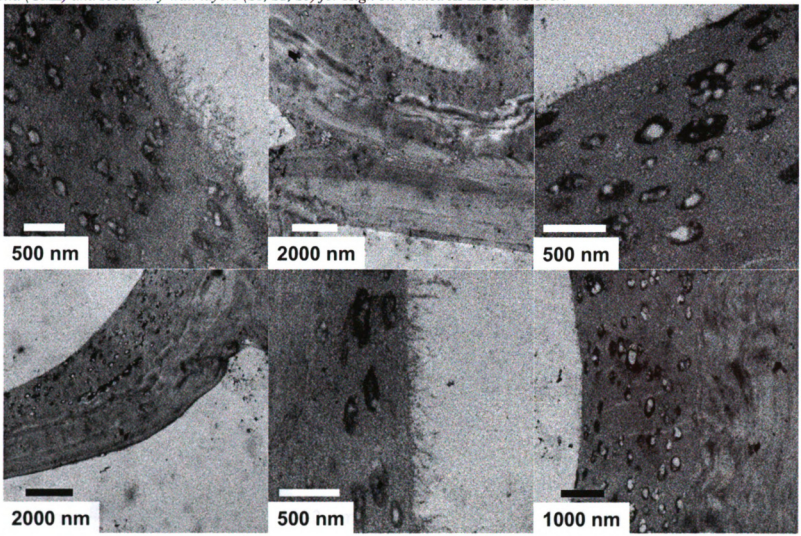

Figure II-4.A.10 *AFEX treated corn stover TEM images (at varying scales of magnification) showing cell corner, compound middle lamella (CML) and secondary wall layers (S1, S2, S3) for Low-T treated AFEX corn stover.*

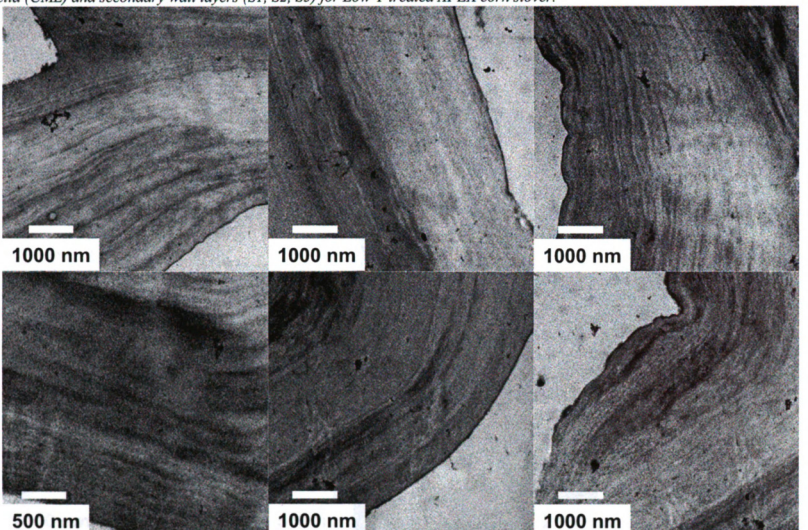

Figure II-4.A.11 *AFEX treated corn stover TEM images (at varying scales of magnification) showing cell corner, compound middle lamella (CML) and secondary wall layers (S1, S2, S3) for Low-W treated AFEX corn stover.*

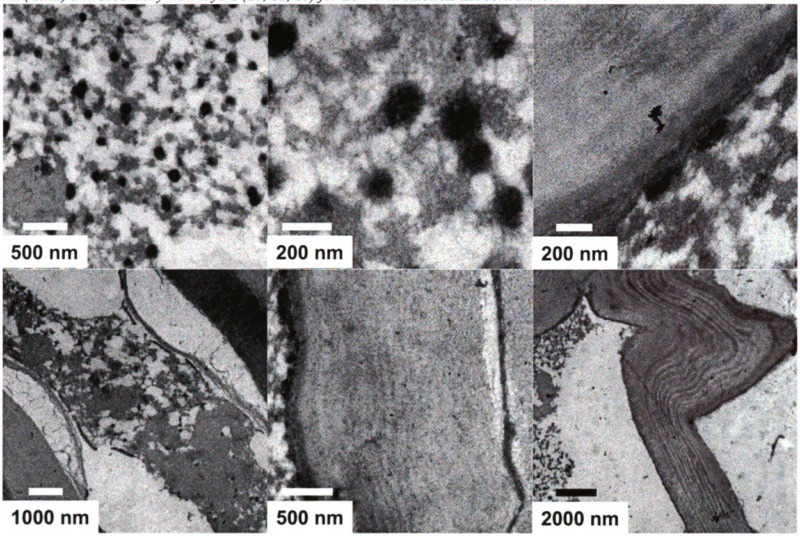

APPENDIX II – B (Chapter 4.2 - Cellulose III formation)

Figure II-4.B.6 *Powder X-ray diffraction spectra of cellulose (Cellulose I) treated with liquid ammonia (Cellulose III) and varying AFEX severity. Avicel was the cellulosic substrate in all cases. The varying severity conditions are denoted by 1 or 3-NH3 (ammonia loading, w/w basis) and 0.05 or 0.6-W (water loading, w/w basis) in the figure legend. Y-axis and X-axis depict intensity counts and two-theta (2θ) angles, respectively.*

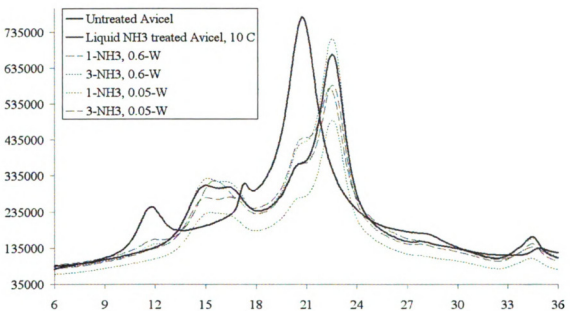

Figure II-4.B.7 *Raman spectra of cellulose (Cellulose I) treated with liquid ammonia (Cellulose III data from [4]) and varying AFEX severity. Avicel was the cellulosic substrate in all cases. The varying severity conditions are denoted by 1 or 3-NH3 (ammonia loading, w/w basis) and 0.05 or 0.6-W (water loading, w/w basis) in the figure legend. Y-axis and X-axis depict intensity counts and wavenumber (cm^{-1}), respectively.*

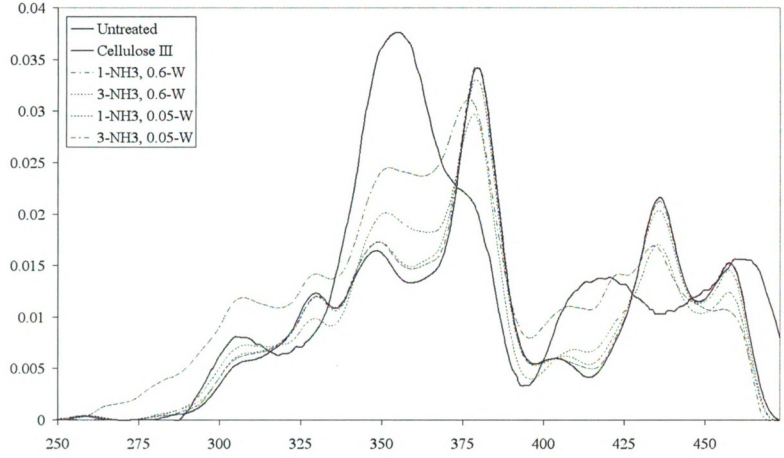

APPENDIX III (Chapter 5 - Degradation products)

Table III-5.4 *Total nitrogen content (measured by Kjeldahl method as grams Nitrogen per 100 grams substrate) of untreated and varying AFEX severity treated cellulosic biomass. The surface atomic composition of the substrates was estimated by ESCA. Where; L (low) and H (high) stand for varying AFEX treatment severities. AFEX-L was carried in the HT-AFEX reactor at 90 °C, 1:1, 15 mins, 60% moisture. AFEX-H was carried in the HT-AFEX reactor at 130 °C, 3:1, 15 mins, 60% moisture. MetOH (methanol) extraction was carried out at 50 °C (15 psi) for 43 hours.*

Substrate	**% Nitrogen content**		**Surface Atomic Composition by ESCA**			**Type of Elemental Carbon**		
gms N per 100 gms biomass	*Mean*	*Std Dev*	*% Carbon*	*% Oxygen*	*% Nitrogen*	*% C1*	*% C2*	*% C3*
Untreated Stover	0.93	0.16	71.35	26.59	1.75	56.31	34.07	9.65
Regular AFEX Stover	3.54	0.2	74.09	22.75	2.85	64.51	28.33	7.11
Untreated (Unt) Avicel	0.06	0.01	62.27	37.73	0.00	27.29	59.97	12.70
AFEX Avicel (L)	0.57	0.31	61.68	37.76	0.56	25.27	61.80	12.90
AFEX Avicel (H)	1.46	0.18	67.41	27.84	4.76	48.30	45.40	6.30
MetOH Extracted Unt Avicel	0.02	0.01	-	-	-	-	-	-
MetOH Extracted AFEX AV (L)	0.2	0.04	-	-	-	-	-	-
MetOH Extracted AFEX AV (H)	0.57	0.09	-	-	-	-	-	-

Figure IV-6.3 *Effect of slurry suspension solids loading (w/w) on delivery accuracy by pipetting workstation. The average amount of biomass (mg) delivered to each well is plotted on the Y-axis for varying percent slurry solids concentration (X-axis). The bars indicate standard deviations for 12 replicate experiments. (Figure has been reproduced from [2]).*

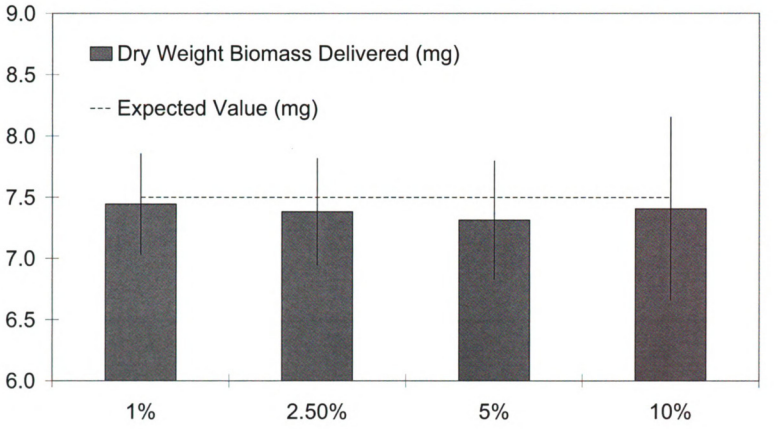

Fig IV-6.5 *(A) Hydrolysis time profile for conventional flask based assay for avicel (AV), un-ground AFEX corn stover (ACS) and milled AFEX corn stover at two different glucan loadings (0.25% and 1%). (B) Hydrolysis time profile for BCRL microplate based assay for avicel (AV), untreated corn stover (UCS) and milled AFEX corn stover (ACS) at two different glucan loadings (0.25% and 1%). Percent glucan conversion and period of hydrolysis (hrs) are shown on the Y- and X-axis, respectively. (Figure has been reproduced from [2]).*

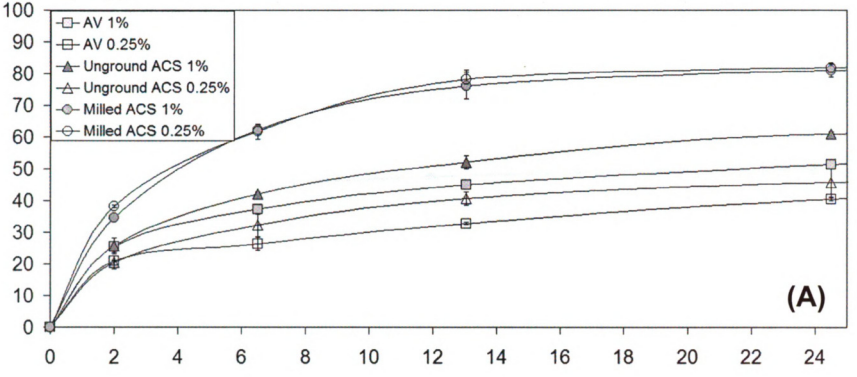

Fig IV-6.5 *Contd...*

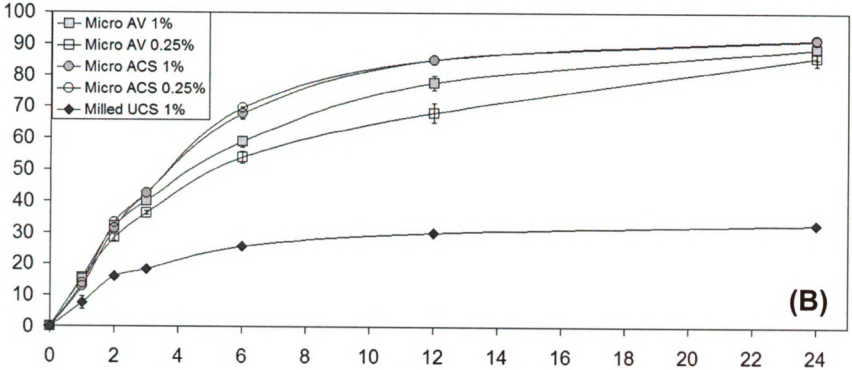

APPENDIX V (Chapter 7 - Crude enzyme optimization)

Figure V-7.3 *Cox-response trace plots for % glucan conversion (A), % xylan conversion (B) and total sugar yield (C) with respect to reference blend at optimal mixture composition for 10 CE-RE experiments.*

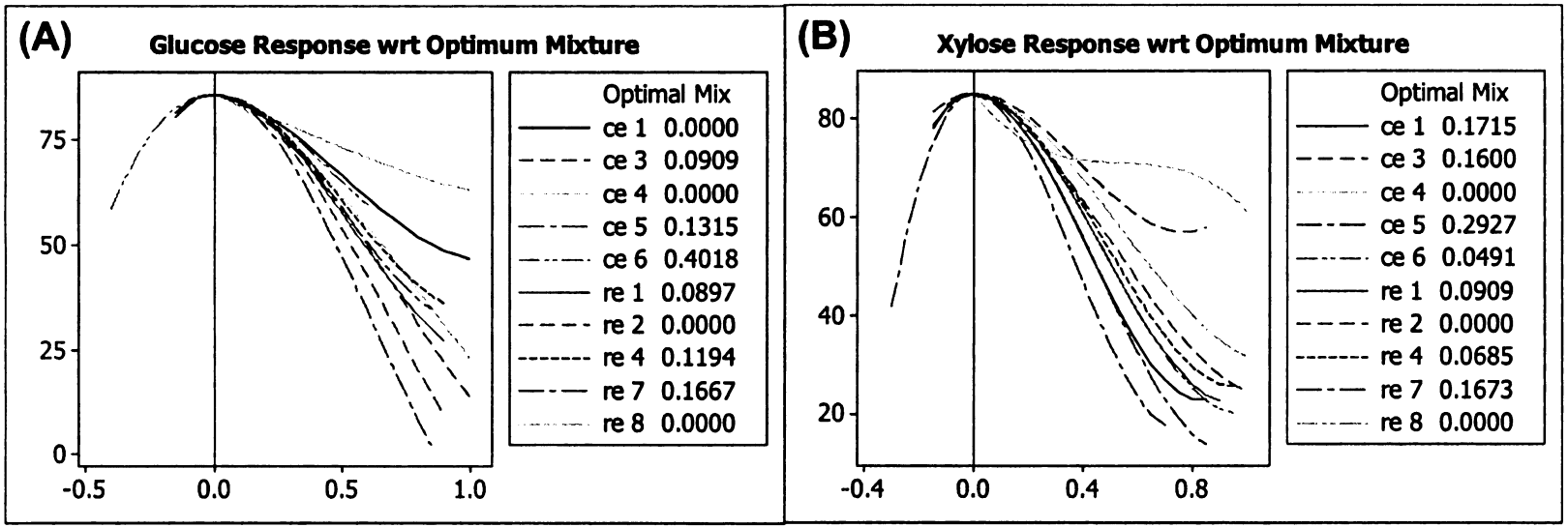

Figure V-7.3 *Contd...*

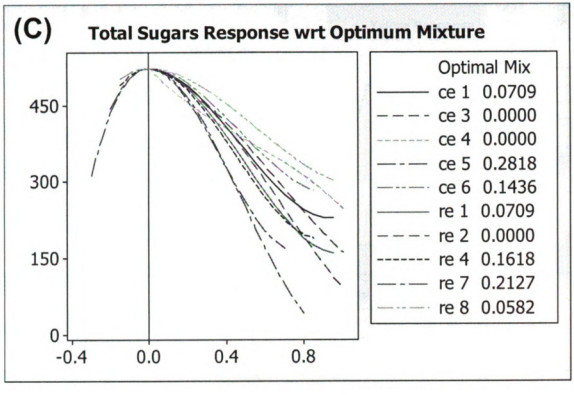

Figure V-7.5 *Cox-response trace plots for % glucan conversion (A), % xylan conversion (B) and total sugar yield (C) with respect to reference blend at optimal mixture composition for 5 CE-RE experiments (Cel x is CE 6).*

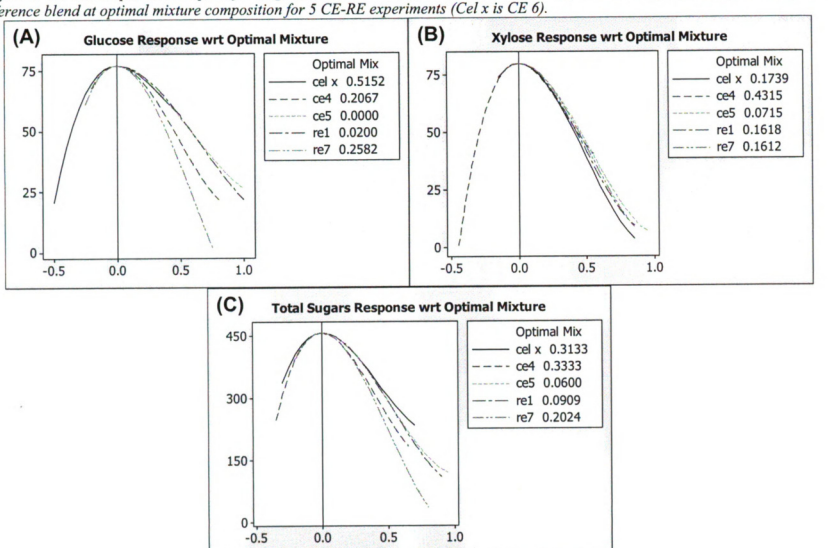

Figure V-7.6 *Cox-response trace plots for % glucan conversion (A), % xylan conversion (B) and total sugar yield (C) with respect to reference blend at optimal mixture composition for 5 CE-RE experiments (Cel x is RE 4).*

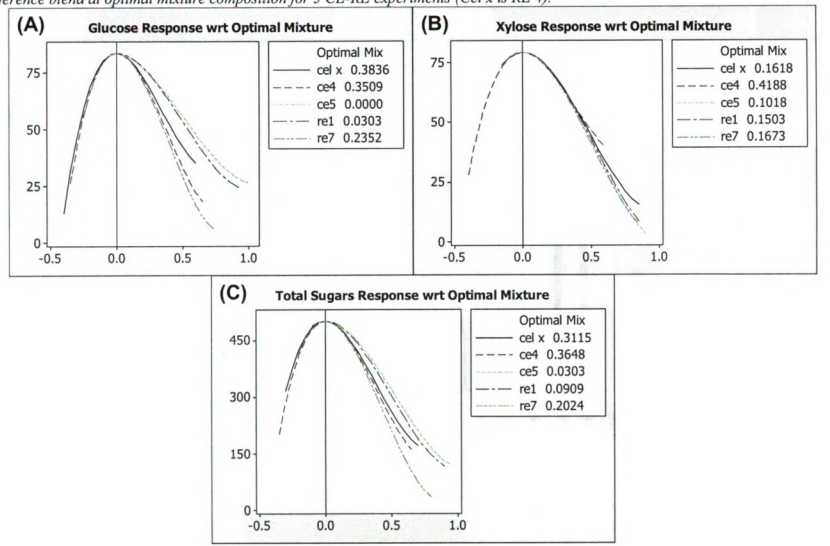

Figure V-7.7-(A/B) *Comparing protein composition of commercial enzyme (CE 1) to average composition of top 5% mixtures (N = 37), based on % glucan conversion.*

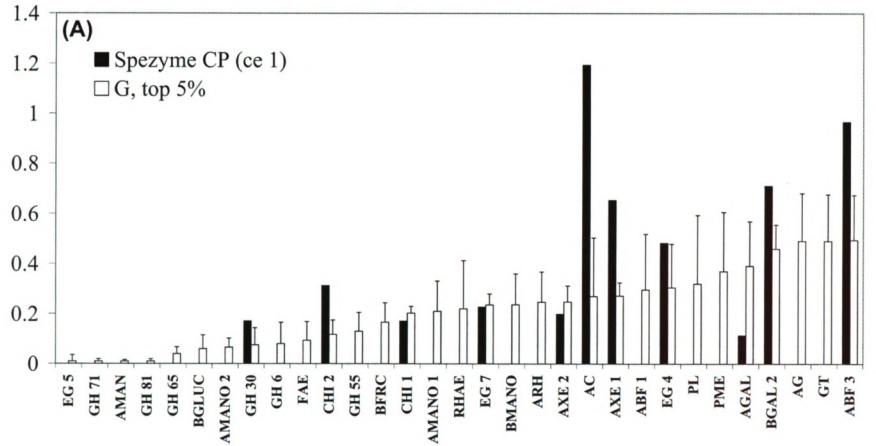

Figure V-7.7-(A/B) *Contd...*

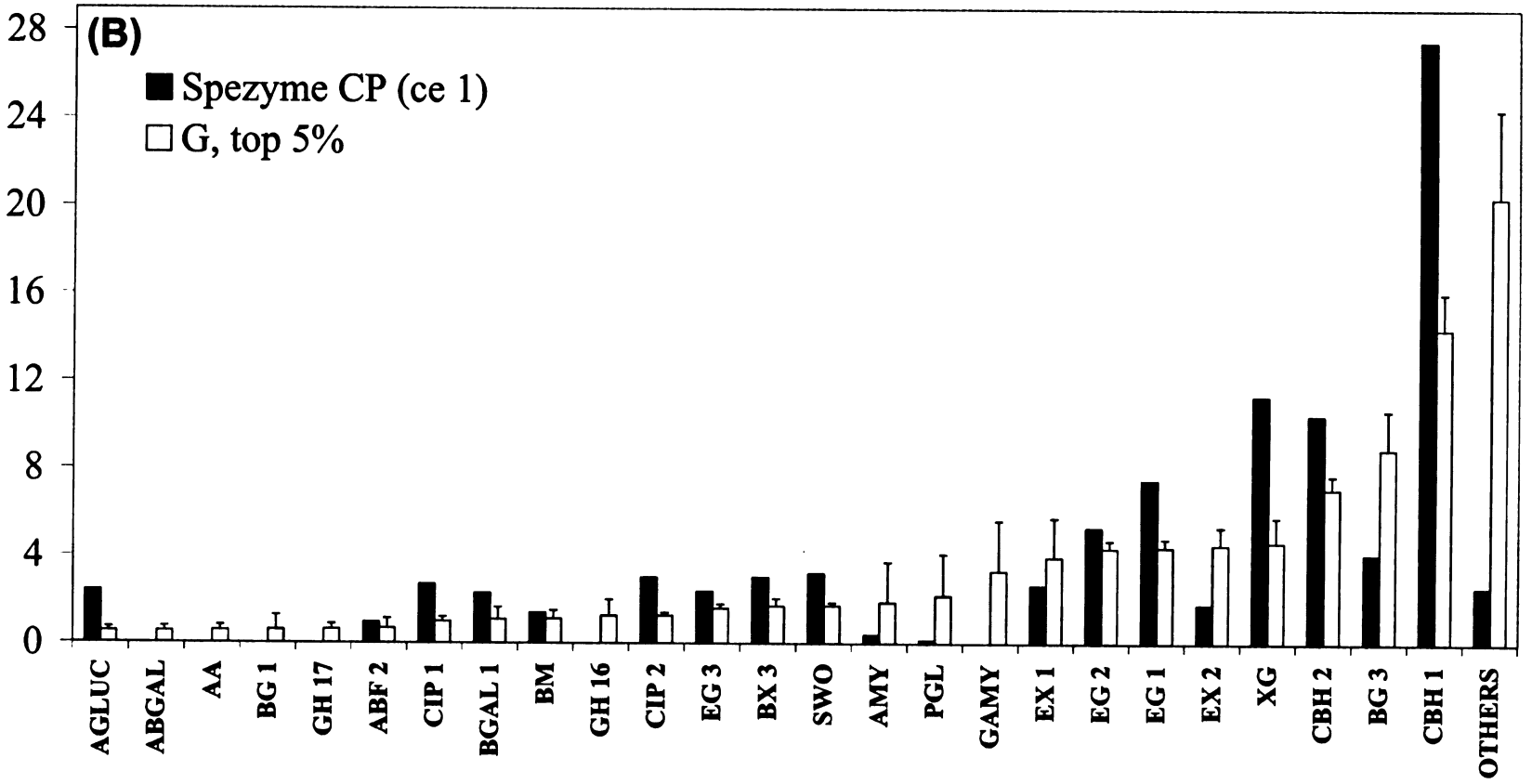

Figure V-7.7-(C/D) *Comparing protein composition of commercial enzyme (CE 4) to average composition of top 5% mixtures (N = 37), based on % xylan conversion.*

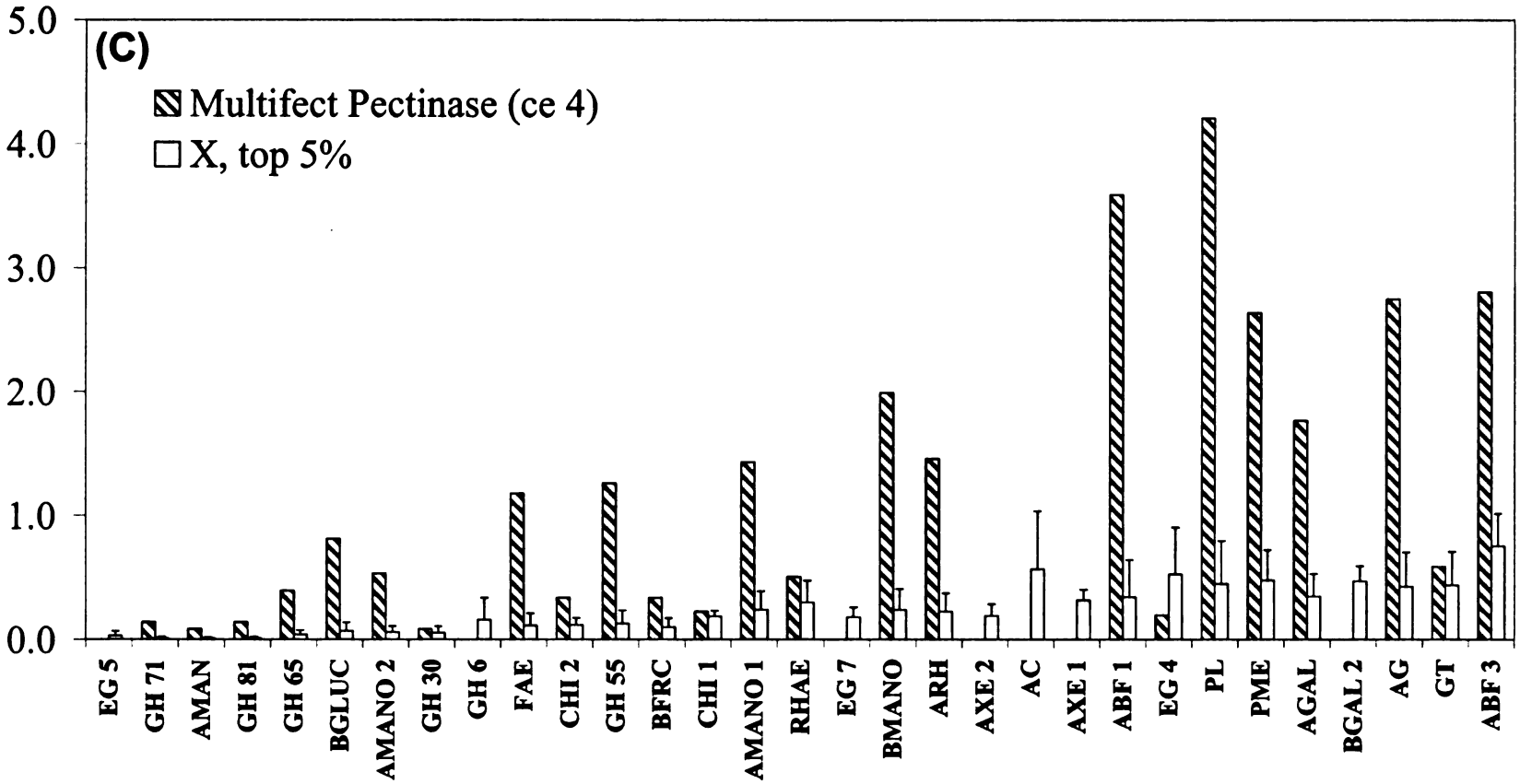

Figure V-7.7-(C/D) *Contd...*

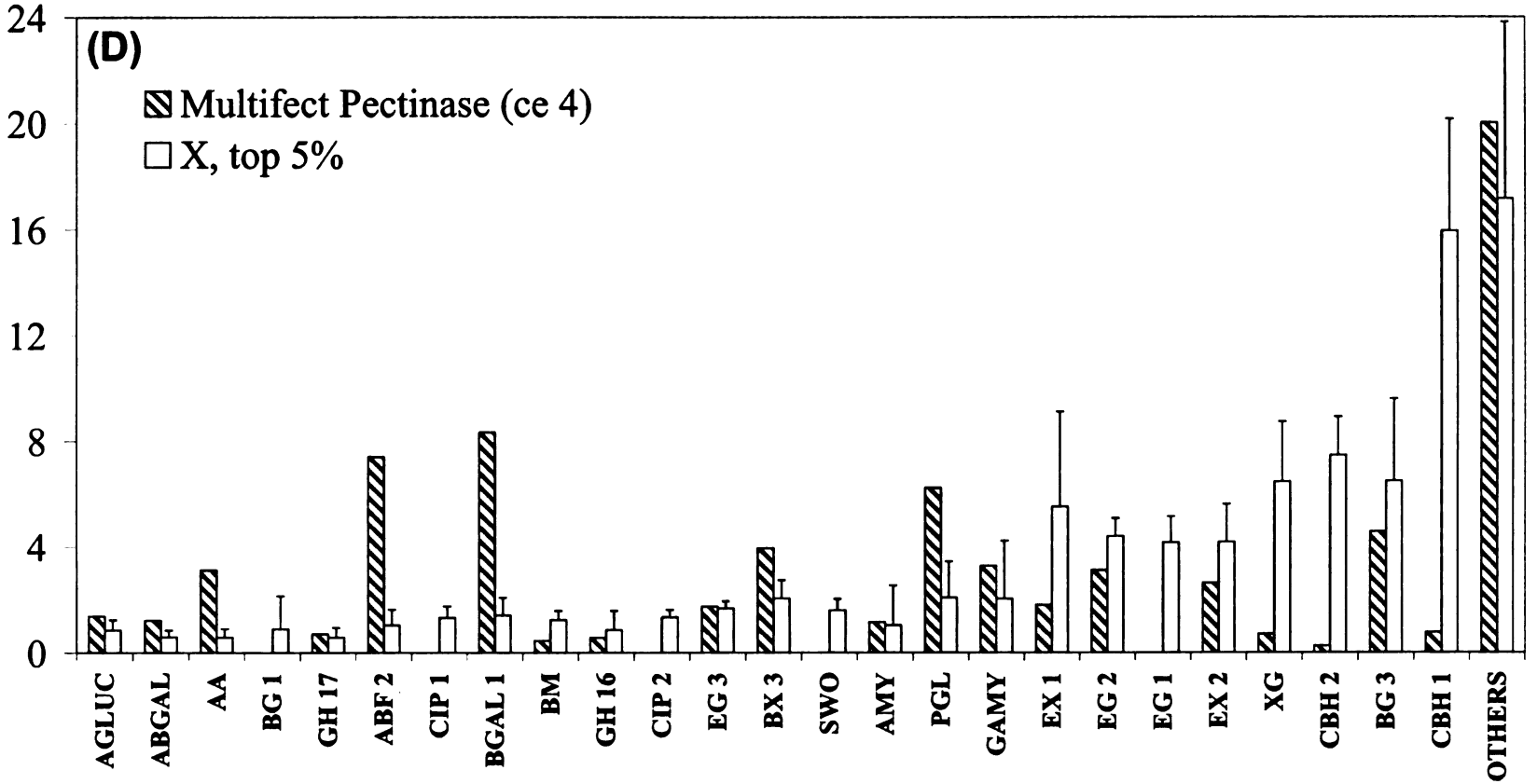

Table V-7.3 *Peptide ID and observed spectral counts for each family of proteins for CE 1.*

Observation Count	Peptide	Reference	GH Family
12	R.YAVAPLTSGPALTVGSSISLR.A	sp|Q92455|ABF1_TRIRE	GH 54, α-Arabinofuranosidase 1
5	K.AYGVFVSPGTGYR.N	sp|Q92455|ABF1_TRIRE	
5	R.HSNFGLVLNANDGSK.L	sp|Q92455|ABF1_TRIRE	
4	R.YIAHSGSTVNTQVVSSSSATALK.Q	sp|Q92455|ABF1_TRIRE	
3	R.AGLANNACFSFESR.D	sp|Q92455|ABF1_TRIRE	
2	R.GGNAASGSLSTFYSGARPQVSGYNPMSK.E	sp|Q92455|ABF1_TRIRE	
1	K.GPWIMADLENGLFSGSSPGNNAGDPSISYR.F	sp|Q92455|ABF1_TRIRE	
1	K.LFAEDATFCTQAGINGQGSSIR.S	sp|Q92455|ABF1_TRIRE	
6	K.M*TPGTVAPTVFYFAPK.N	tr|Q7Z9N0|Q7Z9N0_TRIRE	GH 62, α-Arabinofuranosidase 2
6	R.SFTATNLGGTWTPQATSESQPFAGK.A	tr|Q7Z9N0|Q7Z9N0_TRIRE	
4	R.NNLFEAVQVYTVSGQK.Q	tr|Q7Z9N0|Q7Z9N0_TRIRE	
3	K.ANSGATWTNDISHGDLIR.S	tr|Q7Z9N0|Q7Z9N0_TRIRE	
3	K.MTPGTVAPTVFYFAPK.N	tr|Q7Z9N0|Q7Z9N0_TRIRE	
3	R.ATNSGGDYGLLPYRPGLLTLQR.-	tr|Q7Z9N0|Q7Z9N0_TRIRE	
3	R.SNPDQTM*TIDPCNLQFLYQGR.A	tr|Q7Z9N0|Q7Z9N0_TRIRE	
2	R.ASMPIGNFPGSFGSTSTVVLSDER.N	tr|Q7Z9N0|Q7Z9N0_TRIRE	
2	R.SNPDQTMTIDPCNLQFLYQGR.A	tr|Q7Z9N0|Q7Z9N0_TRIRE	
1	R.ASM*PIGNFPGSFGSTSTVVLSDERNNLFEAVQVYTVSGQK.Q	tr|Q7Z9N0|Q7Z9N0_TRIRE	
1	R.ASMPIGNFPGSFGSTSTVVLSDERNNLFEAVQVYTVSGQK.Q	tr|Q7Z9N0|Q7Z9N0_TRIRE	
8	K.VAVYDIHSLIMDIYNQPSR.Y	tr|A7J2C6|A7J2C6_TRIRE	Acetyl esterase
8	R.WAAFMNANYPSIITDEIPSFK.A	tr|A7J2C6|A7J2C6_TRIRE	
6	R.SKYGTYWEHW.-	tr|A7J2C6|A7J2C6_TRIRE	
5	K.MLEYTTSSNTMIDYGVPFHLLVK.N	tr|A7J2C6|A7J2C6_TRIRE	
5	K.YLITFGDSYTDNGR.L	tr|A7J2C6|A7J2C6_TRIRE	
4	R.WAAFM*NANYPSIITDEIPSFK.A	tr|A7J2C6|A7J2C6_TRIRE	
3	R.EFLNVVSGR.S	tr|A7J2C6|A7J2C6_TRIRE	
2	R.GVTSANTVYALWIGTNDLSYTGILSDSQVK.G	tr|A7J2C6|A7J2C6_TRIRE	
1	K.VAVYDIHSLIM*DIYNQPSR.Y	tr|A7J2C6|A7J2C6_TRIRE	
14	K.AAIFM*GDPR.N	sp|Q99034|AXE1_TRIRE	Acetylxylan esterase 1
6	K.AAIFMGDPR.N	sp|Q99034|AXE1_TRIRE	
2	R.PAGFVCPSASK.I	sp|Q99034|AXE1_TRIRE	

Table V-7.3 *Contd...*

1	R.NIHGLPYNVGTCTTQGFDARPAGFVCPSASK.I	sp|Q99034|AXE1_TRIRE	
5	R.YGDEIVDFVVSQFEK.S	tr|Q7Z9M3|Q7Z9M3_TRIRE	Acetylxylan esterase 2
1	K.GLYMVVAR.G	tr|Q7Z9M3|Q7Z9M3_TRIRE	
1	R.QLLNSYAEACPGNK.I	tr|Q7Z9M3|Q7Z9M3_TRIRE	
5	K.WHWYHFDGADWDESR.K	AMY_BACAM	GH 13, α-amylase
3	K.WGIWYANELSLDGFR.I	AMY_BACAM	
3	R.KEYAYGPQHDYIDHPDVIGWTR.E	AMY_BACAM	
1	A.KNTGIVSSFFTYTGPTEGTPWDEIDIEFLGK.D	GUB_BACAM	
2	K.WHWYHFDGADWDESRK.I	AMY_BACAM	
3	R.VTGSYSAWLTEGESQLLR.L	tr|Q92451|Q92451_TRIRE	GH 27, α-Galactosidase
1	K.LDFLTPGSPSNGANLACDSSDAVR.A	tr|Q92451|Q92451_TRIRE	
10	R.GALYGAFQYLSYLGQGDFSGK.A	sp|Q99024|AGUA_TRIRE	GH 67, α-glucuronidase
6	K.AFASNPSAPVR.W	sp|Q99024|AGUA_TRIRE	
6	K.LNLKEDGYWLSTK.G	sp|Q99024|AGUA_TRIRE	
6	R.LTFGLDRDVVSTIADMSLK.S	sp|Q99024|AGUA_TRIRE	
5	K.GILGLDLDVSSR.G	sp|Q99024|AGUA_TRIRE	
5	R.GYGGPSIFFENGLIK.E	sp|Q99024|AGUA_TRIRE	
5	R.WSNQWDNLNAATAAHGSIER.G	sp|Q99024|AGUA_TRIRE	
4	K.AVQPHGGIVVFR.A	sp|Q99024|AGUA_TRIRE	
4	K.LQYQTGHSLVWR.D	sp|Q99024|AGUA_TRIRE	
4	K.SIVISTLDTYQSACGK.L	sp|Q99024|AGUA_TRIRE	
4	K.SLDGQFDDNVLVQIK.Y	sp|Q99024|AGUA_TRIRE	
3	K.GGSVQIIGQNER.G	sp|Q99024|AGUA_TRIRE	
3	R.IYQLVPDLAGYLVK.A	sp|Q99024|AGUA_TRIRE	
3	R.TLAEGANLFAK.A	sp|Q99024|AGUA_TRIRE	
2	K.SVIQHFYDAHYTGAATVQR.F	sp|Q99024|AGUA_TRIRE	
2	R.DIISGEVFGHK.L	sp|Q99024|AGUA_TRIRE	
2	R.LTFGLDRDVVSTIADM*SLK.S	sp|Q99024|AGUA_TRIRE	
1	K.LGGYAGVINVGMDDTWLGSHLAMSNMFAYGR.L	sp|Q99024|AGUA_TRIRE	
1	K.NGPLASASSELHK.G	sp|Q99024|AGUA_TRIRE	
1	K.WKGDSETHLGHDFSTFLDCHSAIR.I	sp|Q99024|AGUA_TRIRE	
1	K.YGPIDFQVR.E	sp|Q99024|AGUA_TRIRE	
1	K.YGPIDFQVREPASPLFANLPK.T	sp|Q99024|AGUA_TRIRE	
1	R.ANAAVDFFK.S	sp|Q99024|AGUA_TRIRE	

Table V-7.3 *Contd...*

1	R.EPASPLFANLPK.T	sp|Q99024|AGUA_TRIRE	
1	R.GHLTSFPDR.I	sp|Q99024|AGUA_TRIRE	
1	R.GTGNAQEQAAIDYVSILPQGVVD.-	sp|Q99024|AGUA_TRIRE	
1	R.GYGGPSIFFENGLIKEDLSR.V	sp|Q99024|AGUA_TRIRE	
13	R.IVSGGSDSFSEGLFIDYK.H	tr|Q12715|Q12715_TRIRE	GH 3, β-glucosidase
13	R.LWGPALTNAVNSNQVPTSR.V	tr|Q12715|Q12715_TRIRE	
12	K.LNLTPGQSGTATFNIR.R	tr|Q12715|Q12715_TRIRE	
12	K.NDANILPLKKPASIAVVGSAAIIGNHAR.N	tr|Q12715|Q12715_TRIRE	
9	R.DGIVLLKNDANILPLKKPASIAVVGSAAIIGNHAR.N	tr|Q12715|Q12715_TRIRE	
8	K.ASGIHVILGPVAGPLGK.T	tr|Q12715|Q12715_TRIRE	
8	K.WVVPSGSFGISVGASSR.D	tr|Q12715|Q12715_TRIRE	
7	R.NWEGFGVDPYLTGIAMGQTINGIQSVGVQATAK.H	tr|Q12715|Q12715_TRIRE	
7	R.VDDM*VTR.I	tr|Q12715|Q12715_TRIRE	
7	R.YSTGSTAFTPGVQAASTWDVNLIR.E	tr|Q12715|Q12715_TRIRE	
5	K.AVVWAGLPSQESGNALVDVLWGDVSPSGK.L	tr|Q12715|Q12715_TRIRE	
5	R.DLSYWDTASQK.W	tr|Q12715|Q12715_TRIRE	
4	K.VGIVSGVGWNGGPCVGNTSPASK.I	tr|Q12715|Q12715_TRIRE	
4	R.NWEGFGVDPYLTGIAM*GQTINGIQSVGVQATAK.H	tr|Q12715|Q12715_TRIRE	
3	A.ISYPSLCLQDGPLGVR.Y	tr|Q12715|Q12715_TRIRE	
3	K.HFDDANITPR.Y	tr|Q12715|Q12715_TRIRE	
3	R.IVSGGSDSFSEGLFIDYKHFDDANITPR.Y	tr|Q12715|Q12715_TRIRE	
2	K.HYILNEQELNRETISSNPDDR.T	tr|Q12715|Q12715_TRIRE	
2	N.LTPGQSGTATFNIR.R	tr|Q12715|Q12715_TRIRE	
2	R.NSPSCNDKGCDDGALGMGWGSGAVNYPYFVAPYDAINTR.A	tr|Q12715|Q12715_TRIRE	
1	K.GCDDGALGMGWGSGAVNYPYFVAPYDAINTR.A	tr|Q12715|Q12715_TRIRE	
1	K.HYILNEQELNR.E	tr|Q12715|Q12715_TRIRE	
1	K.SPNDYNTR.I	tr|Q12715|Q12715_TRIRE	
1	L.NLTPGQSGTATFNIR.R	tr|Q12715|Q12715_TRIRE	
1	R.DGIVLLKNDANILPLK.K	tr|Q12715|Q12715_TRIRE	
1	R.ETISSNPDDR.T	tr|Q12715|Q12715_TRIRE	
1	R.NVQGNHKTNVR.A	tr|Q12715|Q12715_TRIRE	
1	R.TLHELYTWPFADAVQANVASVMCSYNK.V	tr|Q12715|Q12715_TRIRE	
1	N.TIVVIHNAGIR.L	tr|Q12653|Q12653_9SACH	
4	K.HYLLNEQELNR.N	tr|A4R3K4|A4R3K4_MAGGR	

Table V-7.3 *Contd...*

1	R.VDDMVTR.I	tr|Q12715|Q12715_TRIRE	
7	R.QVVQLGSLVIYMVDR.N	tr|Q70SY0|Q70SY0_TRIRE	GH 35, β-galactosidase
6	K.LPTSAGDLTIPQLGGSLTLTGR.D	tr|Q70SY0|Q70SY0_TRIRE	
6	R.FRADGIFSLEPFFEAATK.A	tr|Q70SY0|Q70SY0_TRIRE	
6	R.VVIFSGEVHPFR.L	tr|Q70SY0|Q70SY0_TRIRE	
5	K.LRTDAPDYLHATDNYVAHIASIIAK.A	tr|Q70SY0|Q70SY0_TRIRE	
5	R.TDAPDYLHATDNYVAHIASIIAK.A	tr|Q70SY0|Q70SY0_TRIRE	
4	K.ALGFNTVSFYVDWALLEGKPGR.F	tr|Q70SY0|Q70SY0_TRIRE	
4	K.TPVSLYGSDYGFHAGTLLFR.G	tr|Q70SY0|Q70SY0_TRIRE	
4	R.LPVPSLYLDVFHK.I	tr|Q70SY0|Q70SY0_TRIRE	
3	K.LKWYKVDSLPEIR.S	tr|Q70SY0|Q70SY0_TRIRE	
3	K.QSAYGSSLMNPDSVIINGGYLIR.S	tr|Q70SY0|Q70SY0_TRIRE	
3	K.TVLVLYGGAQELHEFAVK.N	tr|Q70SY0|Q70SY0_TRIRE	
3	R.ADGIFSLEPFFEAATK.A	tr|Q70SY0|Q70SY0_TRIRE	
3	R.GPLNEGGLFFER.Q	tr|Q70SY0|Q70SY0_TRIRE	
3	R.SNYDDSRWPLANLR.T	tr|Q70SY0|Q70SY0_TRIRE	
2	K.ELGYSVSELGDWIAHPAIEIPHVQVPELTK.L	tr|Q70SY0|Q70SY0_TRIRE	
2	R.ALLYVNGFQYGK.Y	tr|Q70SY0|Q70SY0_TRIRE	
2	R.ERVEVVKGPHFK.K	tr|Q70SY0|Q70SY0_TRIRE	
2	R.VVIFSGEVHPFRLPVPSLYLDVFHK.I	tr|Q70SY0|Q70SY0_TRIRE	
1	K.AQITNGGPVILYQPENEYSGAAEGVLFPNKPYMQYVIDQAR.N	tr|Q70SY0|Q70SY0_TRIRE	
1	K.GPLQNIVTWDEHSLFVHGER.V	tr|Q70SY0|Q70SY0_TRIRE	
1	K.WYKVDSLPEIR.S	tr|Q70SY0|Q70SY0_TRIRE	
1	K.YSELKLQGQFLK.V	tr|Q70SY0|Q70SY0_TRIRE	
1	R.NSAYNYWVPTLPGSGK.Q	tr|Q70SY0|Q70SY0_TRIRE	
1	R.QVVQLGSLVIYM*VDR.N	tr|Q70SY0|Q70SY0_TRIRE	
1	R.VEVVKGPHFK.K	tr|Q70SY0|Q70SY0_TRIRE	
13	R.CNGCSTDVIVQWATSVSQYVK.S	tr|Q99036|Q99036_TRIRE	GH 5, β-mannase
10	R.VWGFNDVNTQPSPGQIWFQK.L	tr|Q99036|Q99036_TRIRE	
6	K.LSATGSTINTGADGLQTLDYVVQSAEQHNLK.L	tr|Q99036|Q99036_TRIRE	
6	K.SLDSNHLVTLGDEGLGLSTGDGAYPYTYGEGTDFAK.N	tr|Q99036|Q99036_TRIRE	
6	R.ASSFVTISGTQFNIDGK.V	tr|Q99036|Q99036_TRIRE	
4	R.KYVQAVVSR.Y	tr|Q99036|Q99036_TRIRE	
3	K.VGYFAGTNCYWCSFLTNHADVDSTFSHISSSGLK.V	tr|Q99036|Q99036_TRIRE	

Table V-7.3 *Contd...*

1	S.YVQAVVSR.E	tr|Q99036|Q99036_TRIRE	
2	R.LGLPQYQVWNEALHGLDR.A	tr|Q8X212|Q8X212_TALEM	GH 3, β-xylosidase
14	K.VNSLVWGGYPGQSGGVALFDILSGK.R	tr|Q92458|Q92458_TRIRE	
8	R.TLIHQIADIISTQAR.A	tr|Q92458|Q92458_TRIRE	
7	K.TESPYTAMLFVR.T	tr|Q92458|Q92458_TRIRE	
7	R.LGFDAIITQQDLSEYYTPQFLAAAR.Y	tr|Q92458|Q92458_TRIRE	
6	K.KVNSLVWGGYPGQSGGVALFDILSGK.R	tr|Q92458|Q92458_TRIRE	
6	R.AQALISLFTLEELILNTQNSGPGVPR.L	tr|Q92458|Q92458_TRIRE	
6	R.LGLPNYQVWNEALHGLDR.A	tr|Q92458|Q92458_TRIRE	
6	R.TSNAGPAPYPNK.W	tr|Q92458|Q92458_TRIRE	
5	K.KSDAIIYLGGIDNTIEQEGADRTDIAWPGNQLDLIK.Q	tr|Q92458|Q92458_TRIRE	
5	K.NSGKTESPYTAMLFVR.T	tr|Q92458|Q92458_TRIRE	
5	K.VNSLVWGGYPGQSGGVALFDILSGKR.A	tr|Q92458|Q92458_TRIRE	
5	R.GQETPGEDAFFLSSAYTYEYITGIQGGVDPEHLK.V	tr|Q92458|Q92458_TRIRE	
4	K.SNPGQTYIWYTGKPVYEFGSGLFYTTFK.E	tr|Q92458|Q92458_TRIRE	
3	K.KVNSLVWGGYPGQSGGVALFDILSGKR.A	tr|Q92458|Q92458_TRIRE	
3	K.SNPGQTYIWYTGKPVYEFGSGLFYTTFKETLASHPK.S	tr|Q92458|Q92458_TRIRE	
3	R.YGLDVYAPNVNGFR.S	tr|Q92458|Q92458_TRIRE	
2	K.LSIPIPVSALAR.V	tr|Q92458|Q92458_TRIRE	
2	K.NNLVCDSSAGYVER.A	tr|Q92458|Q92458_TRIRE	
2	K.QLSEVGKPLVVLQMGGGQVDSSSLK.S	tr|Q92458|Q92458_TRIRE	
2	R.LVTTQYPAEYVHQFPQNDMNLRPDGK.S	tr|Q92458|Q92458_TRIRE	
1	R.LADIKPGHSSK.L	tr|Q92458|Q92458_TRIRE	
1	R.SLM*CAYNSVNGVPSCANSFFLQTLLR.E	tr|Q92458|Q92458_TRIRE	
1	R.SLMCAYNSVNGVPSCANSFFLQTLLR.E	tr|Q92458|Q92458_TRIRE	
68	K.VAGSGSTAGQVYVGTNGR.G	tr|Q7Z9M8|Q7Z9M8_TRIRE	GH 74, xyloglucanase
43	K.TNSVFYAGSGSTFYVSK.D	tr|Q7Z9M8|Q7Z9M8_TRIRE	
26	K.LGGGGGFVPGIIFHPK.T	tr|Q7Z9M8|Q7Z9M8_TRIRE	
25	R.SQFQGSFASVSSLPAGAVIASDKK.T	tr|Q7Z9M8|Q7Z9M8_TRIRE	
24	K.ALYLTYSDGTGPYDGTLGSVWR.Y	tr|Q7Z9M8|Q7Z9M8_TRIRE	
24	R.DIAAHPTTAGTLYVSTDVGIFR.S	tr|Q7Z9M8|Q7Z9M8_TRIRE	
17	R.LYASGDSGASWTDIQGSQGFGSIDSTK.V	tr|Q7Z9M8|Q7Z9M8_TRIRE	
14	R.NDLGTSPQTVWATPTWATSTSVDYAGNSVK.S	tr|Q7Z9M8|Q7Z9M8_TRIRE	
14	R.SQFQGSFASVSSLPAGAVIASDK.K	tr|Q7Z9M8|Q7Z9M8_TRIRE	

Table V-7.3 *Contd...*

11	R.STDSGTTWSPIWAWASYPTETYYYSISTPK.A	tr|Q7Z9M8|Q7Z9M8_TRIRE	
10	K.DITPVSGSDLYFGFGGLGLDLQKPGTLVVASLNSWWPDAQLFR.S	tr|Q7Z9M8|Q7Z9M8_TRIRE	
10	K.NNFIDVTSESPSDGLIK.R	tr|Q7Z9M8|Q7Z9M8_TRIRE	
10	K.NNFIDVTSESPSDGLIKR.L	tr|Q7Z9M8|Q7Z9M8_TRIRE	
8	K.VYAAVGMYTNSWDPSNGAIIR.S	tr|Q7Z9M8|Q7Z9M8_TRIRE	
8	R.SSDRGATWSFTNLPFK.V	tr|Q7Z9M8|Q7Z9M8_TRIRE	
7	K.LGSAGTIRDIAAHPTTAGTLYVSTDVGIFR.S	tr|Q7Z9M8|Q7Z9M8_TRIRE	
7	K.STDGGVTFSK.V	tr|Q7Z9M8|Q7Z9M8_TRIRE	
7	R.LGWMIESLEIDPTDSNHWLYGTGMTIFGGHDLTNWDTR.H	tr|Q7Z9M8|Q7Z9M8_TRIRE	
7	R.STDSGTTFGQVSTALTNTYQIALGVGSGSNWNLYAFGTGPSGAR.L	tr|Q7Z9M8|Q7Z9M8_TRIRE	
6	K.VSSFTATGTYIPDPSDSNGYNSDK.Q	tr|Q7Z9M8|Q7Z9M8_TRIRE	
6	R.LAVDPANSNIIYFGAR.S	tr|Q7Z9M8|Q7Z9M8_TRIRE	
6	R.LNADDSWTAVTDGIADNAGWHNWGIDAVALDPQDDQK.V	tr|Q7Z9M8|Q7Z9M8_TRIRE	
5	R.YDIAGGTWK.D	tr|Q7Z9M8|Q7Z9M8_TRIRE	
4	K.QGLMWVTFDSTSSTTGGATSR.I	tr|Q7Z9M8|Q7Z9M8_TRIRE	
4	K.RLGWMIESLEIDPTDSNHWLYGTGMTIFGGHDLTNWDTR.H	tr|Q7Z9M8|Q7Z9M8_TRIRE	
4	K.VSSFTATGTYIPDPSDSNGYNSDKQGLMWVTFDSTSSTTGGATSR.I	tr|Q7Z9M8|Q7Z9M8_TRIRE	
3	K.VYAAVGM*YTNSWDPSNGAIIR.S	tr|Q7Z9M8|Q7Z9M8_TRIRE	
2	K.KTNSVFYAGSGSTFYVSK.D	tr|Q7Z9M8|Q7Z9M8_TRIRE	
2	R.GATWSFTNLPFK.V	tr|Q7Z9M8|Q7Z9M8_TRIRE	
1	K.APWIKNNFIDVTSESPSDGLIKR.L	tr|Q7Z9M8|Q7Z9M8_TRIRE	
1	K.LGGGGGFVPGIIFHPKTK.G	tr|Q7Z9M8|Q7Z9M8_TRIRE	
1	K.RLGWMIESLEIDPTDSNHWLYGTGM*TIFGGHDLTNWDTR.H	tr|Q7Z9M8|Q7Z9M8_TRIRE	
1	R.LGWM*IESLEIDPTDSNHWLYGTGMTIFGGHDLTNWDTR.H	tr|Q7Z9M8|Q7Z9M8_TRIRE	
1	R.LGWMIESLEIDPTDSNHWLYGTGM*TIFGGHDLTNWDTR.H	tr|Q7Z9M8|Q7Z9M8_TRIRE	
1	S.SLPAGAVIASDKK.T	tr|Q7Z9M8|Q7Z9M8_TRIRE	
9	R.LAVDPANSDILYFGAR.S	tr|Q2GSJ3|Q2GSJ3_CHAGB	
1	T.FDSTSSTTGGATSR.I	tr|Q7Z9M8|Q7Z9M8_TRIRE	
3	K.DRPHFGGLSLWDLSR.G	tr|A2VEC7|A2VEC7_TRIRE	GH 18, Chitinase
2	K.LYIGLPAIQEPNESGYIDPIAMK.N	tr|A2VEC7|A2VEC7_TRIRE	
1	R.LVLGMPLYGR.A	tr|Q5VHW8|Q5VHW8_COCPO	
24	R.LQTALGSNHVTFIIM*PDTAQGGK.H	tr|Q7Z9M9|Q7Z9M9_TRIRE	Cip 1

Table V-7.3 *Contd...*

19	R.LQTALGSNHVTFIIMPDTAQGGK.H	tr|Q7Z9M9|Q7Z9M9_TRIRE	
15	K.VVGGPNGYCGHIFFGTTQVPTGDVYVR.A	tr|Q7Z9M9|Q7Z9M9_TRIRE	
14	R.ASYIPEITGVNFGWEAYSGDVNTVWFDDISIASTR.V	tr|Q7Z9M9|Q7Z9M9_TRIRE	
9	R.IGGQSQVLDYNR.E	tr|Q7Z9M9|Q7Z9M9_TRIRE	
4	K.WPISAPDCNQGGTVSLDTTVAHSGSNSMK.V	tr|Q7Z9M9|Q7Z9M9_TRIRE	
4	R.AWIRLQTALGSNHVTFIIMPDTAQGGK.H	tr|Q7Z9M9|Q7Z9M9_TRIRE	
2	H.IFFGTTQVPTGDVYVR.A	tr|Q7Z9M9|Q7Z9M9_TRIRE	
2	K.WPISAPDCNQGGTVSLDTTVAHSGSNSM*K.V	tr|Q7Z9M9|Q7Z9M9_TRIRE	
1	R.LQTALGSNHVTF.I	tr|Q7Z9M9|Q7Z9M9_TRIRE	
12	K.FYDLYGSSHSAGAMTAWAWGVSR.V	tr|Q7Z9N1|Q7Z9N1_TRIRE	Cip 2
11	K.LNDLFTM*FNGDKVTTK.D	tr|Q7Z9N1|Q7Z9N1_TRIRE	
11	R.VIDALELVPGAR.I	tr|Q7Z9N1|Q7Z9N1_TRIRE	
10	R.NGKGAMVAGAFEKR.I	tr|Q7Z9N1|Q7Z9N1_TRIRE	
9	R.IVLTLPQESGAGGSACWR.I	tr|Q7Z9N1|Q7Z9N1_TRIRE	
8	K.GAMVAGAFEKR.I	tr|Q7Z9N1|Q7Z9N1_TRIRE	
6	K.RIVLTLPQESGAGGSACWR.I	tr|Q7Z9N1|Q7Z9N1_TRIRE	
5	R.QAEMSELIQR.Y	tr|Q7Z9N1|Q7Z9N1_TRIRE	
4	K.LNDLFTM*FNGDK.V	tr|Q7Z9N1|Q7Z9N1_TRIRE	
4	K.LNDLFTMFNGDK.V	tr|Q7Z9N1|Q7Z9N1_TRIRE	
4	K.LNDLFTMFNGDKVTTK.D	tr|Q7Z9N1|Q7Z9N1_TRIRE	
4	R.NGKGAMVAGAFEK.R	tr|Q7Z9N1|Q7Z9N1_TRIRE	
3	R.NGKGAM*VAGAFEKR.I	tr|Q7Z9N1|Q7Z9N1_TRIRE	
3	R.QAEM*SELIQR.Y	tr|Q7Z9N1|Q7Z9N1_TRIRE	
3	R.YELGTLPGRPSTLTASFSGNTLTINCGEAGK.S	tr|Q7Z9N1|Q7Z9N1_TRIRE	
2	K.FYDLYGSSHSAGAM*TAWAWGVSR.V	tr|Q7Z9N1|Q7Z9N1_TRIRE	
2	K.LNDLFTMFNGDKVTTKDK.F	tr|Q7Z9N1|Q7Z9N1_TRIRE	
1	K.GAM*VAGAFEKR.I	tr|Q7Z9N1|Q7Z9N1_TRIRE	
1	K.GAMVAGAFEK.R	tr|Q7Z9N1|Q7Z9N1_TRIRE	
1	K.IGVTGCSRNGKGAMVAGAFEKR.I	tr|Q7Z9N1|Q7Z9N1_TRIRE	
1	R.GQGKFYDLYGSSHSAGAMTAWAWGVSR.V	tr|Q7Z9N1|Q7Z9N1_TRIRE	
1	R.NGKGAM*VAGAFEK.R	tr|Q7Z9N1|Q7Z9N1_TRIRE	
27	R.VNQPSIIGTATFYQYWSVR.R	sp|P36217|XYN2_TRIRE	GH 11, endoxylanase II
22	R.NPLIEYYIVENFGTYNPSTGATK.L	sp|P36217|XYN2_TRIRE	
14	K.VINFSGSYNPNGNSYLSVYGWSR.N	sp|P36217|XYN2_TRIRE	

Table V-7.3 *Contd...*

11	K.LGEVTSDGSVYDIYR.T	sp|P36217|XYN2_TRIRE	
9	K.NKVINFSGSYNPNGNSYLSVYGWSR.N	sp|P36217|XYN2_TRIRE	
2	R.VNQPSIIGTATFY.Q	sp|P36217|XYN2_TRIRE	
1	A.TFYQYWSVR.R	sp|P36217|XYN2_TRIRE	
1	R.VNQPSIIGTAT.F	sp|P36217|XYN2_TRIRE	
2	R.VNQPSIDGTATFYQYWSVR.Q	tr|Q1K5S8|Q1K5S8_NEUCR	
1	R.TQRVNQPSIDGTATFYQYWSVR.Q	tr|Q1K5S8|Q1K5S8_NEUCR	
2	K.VINFSGSYNPNGNSYLSIYGWSR.N	sp|P48793|XYN_TRIHA	
1	K.NKVINFSGSYNPNGNSYLSIYGWSR.N	sp|P48793|XYN_TRIHA	
22	R.TVNSISSMPTTASWSYSGSNIR.A	tr|O00095|O00095_TRIRE	GH 12, endoglucanase
17	R.ANVAYDLFTAANPNHVTYSGDYELMIWLGK.Y	tr|O00095|O00095_TRIRE	
15	R.TVNSISSM*PTTASWSYSGSNIR.A	tr|O00095|O00095_TRIRE	
7	K.SYQNSQIAIPQKR.T	tr|O00095|O00095_TRIRE	
7	R.ANVAYDLFTAANPNHVTYSGDYELM*IWLGK.Y	tr|O00095|O00095_TRIRE	
5	K.SYQNSQIAIPQK.R	tr|O00095|O00095_TRIRE	
1	R.ADVAYDLFTASNPNHVTYSGDYELMIWLGK.Y	tr|Q8NJY4|Q8NJY4_TRIVI	
6	R.TVNSISSMPTTASWSYTGSDIR.A	tr|Q8NJY5|Q8NJY5_TRIKO	
2	R.TVNSISSM*PTTASWSYTGSDIR.A	tr|Q8NJY5|Q8NJY5_TRIKO	
1	K.RTVNSISSMPTTASWSYSGSNIR.A	tr|O00095|O00095_TRIRE	
6	K.AFGNRDDLASVFFSR.N	tr|Q76FP5|Q76FP5_TRIVI	GH 5, β-1,6-endogalactanase
4	R.DTLYSLASQAGK.R	tr|Q76FP5|Q76FP5_TRIVI	
4	R.RDTLYSLASQAGK.R	tr|Q76FP5|Q76FP5_TRIVI	
3	R.TAGSNGATVPR.W	tr|Q76FP5|Q76FP5_TRIVI	
3	R.WSTQTGGGDQYR.S	tr|Q76FP5|Q76FP5_TRIVI	
2	R.DDLASVFFSR.N	tr|Q76FP5|Q76FP5_TRIVI	
1	K.YFVLAQLTR.H	tr|Q76FP5|Q76FP5_TRIVI	
1	R.DTLYSLASQAGKR.L	tr|Q76FP5|Q76FP5_TRIVI	
1	R.RDTLYSLASQAGKR.L	tr|Q76FP5|Q76FP5_TRIVI	
59	R.LYLLDSDGEYVMLK.L	sp|P07981|GUN1_TRIRE	GH 7B, endoglucanase I
48	K.TFTIITQFNTDNGSPSGNLVSITR.K	sp|P07981|GUN1_TRIRE	
45	R.LYLLDSDGEYVM*LK.L	sp|P07981|GUN1_TRIRE	
15	R.ANALTPHSCTATACDSAGCGFNPYGSGYK.S	sp|P07981|GUN1_TRIRE	
13	K.SYYGPGDTVDTSK.T	sp|P07981|GUN1_TRIRE	
13	K.TFTIITQFNTDNGSPSGNLVSITRK.Y	sp|P07981|GUN1_TRIRE	

Table V-7.3 *Contd...*

11	R.KYQQNGVDIPSAQPGGDTISSCPSASAYGGLATMGK.A	sp|P07981|GUN1_TRIRE	
8	R.KYQQNGVDIPSAQPGGDTISSCPSASAYGGLATM*GK.A	sp|P07981|GUN1_TRIRE	
5	K.SYYGPGDTVDTSKTFTIITQFNTDNGSPSGNLVSITR.K	sp|P07981|GUN1_TRIRE	
5	K.YQQNGVDIPSAQPGGDTISSCPSASAYGGLATMGK.A	sp|P07981|GUN1_TRIRE	
5	T.SGGCVAQDTSVVLDWNYR.W	sp|P07981|GUN1_TRIRE	
4	A.NNPNTHVVFSNIR.W	sp|P07981|GUN1_TRIRE	
4	K.YQQNGVDIPSAQPGGDTISSCPSASAYGGLATM*GK.A	sp|P07981|GUN1_TRIRE	
4	N.ILANNPNTHVVFSNIR.W	sp|P07981|GUN1_TRIRE	
3	L.ANNPNTHVVFSNIR.W	sp|P07981|GUN1_TRIRE	
2	F.GPGDTVDTSK.T	sp|P07981|GUN1_TRIRE	
2	F.NTDNGSPSGNLVSITR.K	sp|P07981|GUN1_TRIRE	
2	K.NCFIEGVDYAASGVTTSGSSLTMNQYMPSSSGGYSSVSPR.L	sp|P07981|GUN1_TRIRE	
2	N.GSPSGNLVSITR.K	sp|P07981|GUN1_TRIRE	
2	N.PNTHVVFSNIR.W	sp|P07981|GUN1_TRIRE	
2	N.PSNILANNPNTHVVFSNIR.W	sp|P07981|GUN1_TRIRE	
2	N.TDNGSPSGNLVSITR.K	sp|P07981|GUN1_TRIRE	
2	Y.YGPGDTVDTSK.T	sp|P07981|GUN1_TRIRE	
1	K.TCTSGTTCQYSNDYYSQCL.-	sp|P07981|GUN1_TRIRE	
1	N.QYMPSSSGGYSSVSPR.L	sp|P07981|GUN1_TRIRE	
1	R.NGTLNTSHQGFCCNEMDILEGNSR.A	sp|P07981|GUN1_TRIRE	
1	Q.NPDTHVVFSNIR.W	tr|B6ZBT2|B6ZBT2_9EURO	
1	S.YYGPGDTVDTSK.T	sp|P07981|GUN1_TRIRE	
50	R.FAGVNIAGFDFGCTTDGTCVTSK.V	sp|P07982|GUN2_TRIRE	GH 5, endoglucanase II
34	R.WNGGIIGQGGPTNAQFTSLWSQLASK.Y	sp|P07982|GUN2_TRIRE	
23	R.VWFGIM*NEPHDVNINTWAATVQEVVTAIR.N	sp|P07982|GUN2_TRIRE	
23	R.VWFGIMNEPHDVNINTWAATVQEVVTAIR.N	sp|P07982|GUN2_TRIRE	
16	K.YLDSDNSGTHAECTTNNIDGAFSPLATWLR.Q	sp|P07982|GUN2_TRIRE	
15	R.LPVGWQYLVNNNLGGNLDSTSISK.Y	sp|P07982|GUN2_TRIRE	
9	K.YDQLVQGCLSLGAYCIVDIHNYAR.W	sp|P07982|GUN2_TRIRE	
6	R.WNGGIIGQGGPTNAQFTSLWSQLASKYASQSR.V	sp|P07982|GUN2_TRIRE	
4	N.NIDGAFSPLATWLR.Q	sp|P07982|GUN2_TRIRE	
2	W.AATVQEVVTAIR.N	sp|P07982|GUN2_TRIRE	
1	H.KYLDSDNSGTHAECTTNNIDGAFSPLATWLR.Q	sp|P07982|GUN2_TRIRE	
1	N.AQFTSLWSQLASK.Y	sp|P07982|GUN2_TRIRE	

Table V-7.3 *Contd...*

1	N.GGIIGQGGPTNAQFTSLWSQLASK.Y	sp|P07982|GUN2_TRIRE	
1	N.TWAATVQEVVTAIR.N	sp|P07982|GUN2_TRIRE	
8	K.AGDTILFQWVPVPWPHPGPIVDYLANCNGDCETVDKTTLEFFK.I	sp|O14405|GUN4_TRIRE	GH 61, endoglucanase IV, Cel61a
8	K.IPDNLAPGNYVLR.H	sp|O14405|GUN4_TRIRE	
1	K.AGDTILFQWVPVPWPHPGPIVDYLANCNGDCETVDK.T	sp|O14405|GUN4_TRIRE	
3	K.IQEAGINYNTQVWAQQDLINQGNKWTVK.I	sp|Q7Z9M7|GUN7_TRIRE	GH 61, endoglucanase VII, Cel61b
2	K.ALPAGTPATQLYKPTDPGILFNPYTTITSYTIPGPALWQG.-	sp|Q7Z9M7|GUN7_TRIRE	
1	K.IQEAGINYNTQVWAQQDLINQGNK.W	sp|Q7Z9M7|GUN7_TRIRE	
1	K.QNTGHFPNVAGWYAEDLDLGFISPDQYTTPDIVCHK.N	sp|Q7Z9M7|GUN7_TRIRE	
1	R.HELLAAHGASSANGM*QNYPQCVNIAVTGSGTK.A	sp|Q7Z9M7|GUN7_TRIRE	
3	K.SSTGVLHALETFSQLFYK.H	tr|P78738|P78738_TRIHA	GH 20, Chitinase
2	K.LSQAGAYHPSLVYTPADLAGIFQYGVAR.G	tr|P78738|P78738_TRIHA	
2	K.VIDTDYNFYYLDCGR.G	tr|P78738|P78738_TRIHA	
4	R.GLETFSQLFFK.H	tr|P78739|P78739_TRIHA	
1	G.SVVLDANWR.W	sp|Q9P8P3|GUX1_TRIHA	GH 7A, Cellobiohydrolase I
1	K.CTAAGSCTDQKGSVVIDANWR.W	tr|A1CE97|A1CE97_ASPCL	
1	R.YGGTCDPDGCDWDPYR.L	tr|Q6UJY1|Q6UJY1_TRIVI	
3	K.FGPIGSTGNPSGGNPPGGNPP.G	tr|B5TWC6|B5TWC6_9HYPO	
1	R.GSCSTSSGVPAQLESQSPNAK.V	tr|B5TWC6|B5TWC6_9HYPO	
411	K.KLTVVTQFETSGAINR.Y	sp|P62694|GUX1_TRIRE	
282	K.LTVVTQFETSGAINR.Y	sp|P62694|GUX1_TRIRE	
96	K.NCCLDGAAYASTYGVTTSGNSLSIGFVTQSAQK.N	sp|P62694|GUX1_TRIRE	
50	K.CSSGGTCTQQTGSVVIDANWR.W	sp|P62694|GUX1_TRIRE	
33	R.GSCSTSSGVPAQVESQSPNAK.V	sp|P62694|GUX1_TRIRE	
32	K.YGTGYCDSQCPR.D	sp|P62694|GUX1_TRIRE	
5	N.SLSIGFVTQSAQK.N	sp|P62694|GUX1_TRIRE	
5	R.LGNTSFYGPGSSFTLDTTK.K	sp|P62694|GUX1_TRIRE	
3	C.TLQSETHPPLTWQK.C	sp|P62694|GUX1_TRIRE	
3	K.NCCLDGAAYASTYGVTTSGNSLSIGFVTQSAQKNVGAR.L	sp|P62694|GUX1_TRIRE	
3	R.LGNTSFYGPGSSFTLDTTKK.L	sp|P62694|GUX1_TRIRE	
3	S.SFSDKGGLTQFKK.A	sp|P62694|GUX1_TRIRE	
2	C.STSSGVPAQVESQSPNAK.V	sp|P62694|GUX1_TRIRE	
2	K.FGPIGSTGNPSGGN.P	sp|P62694|GUX1_TRIRE	
2	K.YPTNTAGAK.Y	sp|P62694|GUX1_TRIRE	

Table V-7.3 *Contd...*

2	L.SIGFVTQSAQK.N	sp|P62694|GUX1_TRIRE	
2	N.GALYFVSMDADGGVSKYPTNTAGAK.Y	sp|P62694|GUX1_TRIRE	
2	R.YGGTCDPDGCDWNPYR.L	sp|P62694|GUX1_TRIRE	
2	R.YYVQNGVTFQQPNAELGSYSGNELNDDYCTAEEAEFGGSSFSDK.G	sp|P62694|GUX1_TRIRE	
2	S.SFSDKGGLTQFK.K	sp|P62694|GUX1_TRIRE	
2	S.SGVPAQVESQSPNAK.V	sp|P62694|GUX1_TRIRE	
2	S.TYGVTTSGNSLSIGFVTQSAQK.N	sp|P62694|GUX1_TRIRE	
2	Y.GVTTSGNSLSIGFVTQSAQK.N	sp|P62694|GUX1_TRIRE	
1	C.GLNGALYFVSMDADGGVSKYPTNTAGAK.Y	sp|P62694|GUX1_TRIRE	
1	F.VSMDADGGVSKYPTNTAGAK.Y	sp|P62694|GUX1_TRIRE	
1	R.YYVQNGVTFQQPN.A	sp|P62694|GUX1_TRIRE	
1	S.LSIGFVTQSAQK.N	sp|P62694|GUX1_TRIRE	
1	S.MDADGGVSKYPTNTAGAK.Y	sp|P62694|GUX1_TRIRE	
1	T.QFETSGAINR.Y	sp|P62694|GUX1_TRIRE	
1	Y.FVSMDADGGVSKYPTNTAGAK.Y	sp|P62694|GUX1_TRIRE	
1	Y.GPGSSFTLDTTK.K	sp|P62694|GUX1_TRIRE	
1	Y.YANM*LWLDSTYPTNETSSTPGAVRGSCSTSSGVPAQVESQSPNAK.V	sp|P62694|GUX1_TRIRE	
4	K.NCCLDGAAYASTYGVTTSADSLSIGFVTQSAQK.N	sp|P19355|GUX1_TRIVI	
33	K.LYIHAIGPLLANHGWSNAFFITDQGR.S	sp|P07987|GUX2_TRIRE	GH 6A, Cellobiohydrolase II
33	K.VPSFMWLDTLDKTPLMEQTLADIR.T	sp|P07987|GUX2_TRIRE	
31	R.TLLVIEPDSLANLVTNLGTPK.C	sp|P07987|GUX2_TRIRE	
24	K.VPSFM*WLDTLDKTPLMEQTLADIR.T	sp|P07987|GUX2_TRIRE	
23	K.VPSFM*WLDTLDKTPLM*EQTLADIR.T	sp|P07987|GUX2_TRIRE	
17	K.NGGNYAGQFVVYDLPDRDCAALASNGEYSIADGGVAK.Y	sp|P07987|GUX2_TRIRE	
17	R.QIVVEYSDIR.T	sp|P07987|GUX2_TRIRE	
14	K.NGGNYAGQFVVYDLPDR.D	sp|P07987|GUX2_TRIRE	
14	K.YKNYIDTIR.Q	sp|P07987|GUX2_TRIRE	
12	K.TPLM*EQTLADIR.T	sp|P07987|GUX2_TRIRE	
12	K.VPSFMWLDTLDKTPLM*EQTLADIR.T	sp|P07987|GUX2_TRIRE	
11	R.DCAALASNGEYSIADGGVAK.Y	sp|P07987|GUX2_TRIRE	
11	R.FDSHCALPDALQPAPQAGAWFQAYFVQLLTNANPSFL.-	sp|P07987|GUX2_TRIRE	
9	K.TPLMEQTLADIR.T	sp|P07987|GUX2_TRIRE	
7	K.VPSFMWLDTLDK.T	sp|P07987|GUX2_TRIRE	

Table V-7.3 *Contd...*

6	K.VPSFM*WLDTLDK.T	sp|P07987|GUX2_TRIRE	
5	K.YKNYIDTIRQIVVEYSDIR.T	sp|P07987|GUX2_TRIRE	
4	M.YLDAGHAGWLGWPANQDPAAQLFANVYK.N	sp|P07987|GUX2_TRIRE	
4	R.TANKNGGNYAGQFVVYDLPDRDCAALASNGEYSIADGGVAK.Y	sp|P07987|GUX2_TRIRE	
3	H.AIGPLLANHGWSNAFFITDQGR.S	sp|P07987|GUX2_TRIRE	
2	K.LYIHAIGPLLANHGWSNAF.F	sp|P07987|GUX2_TRIRE	
2	N.GEYSIADGGVAK.Y	sp|P07987|GUX2_TRIRE	
2	R.TANKNGGNYAGQFVVYDLPDR.D	sp|P07987|GUX2_TRIRE	
1	D.SLANLVTNLGTPK.C	sp|P07987|GUX2_TRIRE	
1	K.LYIHAIGPL.L	sp|P07987|GUX2_TRIRE	
1	K.LYIHAIGPLLANH.G	sp|P07987|GUX2_TRIRE	
1	K.NYIDTIRQIVVEYSDIR.T	sp|P07987|GUX2_TRIRE	
1	K.NYIDTIRQIVVEYSDIRTLLVIEPDSLANLVTNLGTPK.C	sp|P07987|GUX2_TRIRE	
1	K.YKNYIDTIRQIVVEYSDIRTLLVIEPDSLANLVTNLGTPK.C	sp|P07987|GUX2_TRIRE	
1	L.LVIEPDSLANLVTNLGTPK.C	sp|P07987|GUX2_TRIRE	
1	M.WLDTLDKTPLMEQTLADIR.T	sp|P07987|GUX2_TRIRE	
1	N.AFFITDQGR.S	sp|P07987|GUX2_TRIRE	
1	N.LVTNLGTPK.C	sp|P07987|GUX2_TRIRE	
1	N.VAMYLDAGHAGWLGWPANQDPAAQLFANVYK.N	sp|P07987|GUX2_TRIRE	
1	R.FDSHCALPDALQPAPQAGAWFQAY.F	sp|P07987|GUX2_TRIRE	
1	R.PSANTGDSLLDSFVWVKPGGECDGTSDSSAPR.F	sp|P07987|GUX2_TRIRE	
1	R.QIVVEYSDIRTLLVIEPDSLANLVTNLGTPK.C	sp|P07987|GUX2_TRIRE	
1	R.TLLVIEPDSLANL.V	sp|P07987|GUX2_TRIRE	
1	R.TLLVIEPDSLANLVTN.L	sp|P07987|GUX2_TRIRE	
37	R.TILVIEPDSLANLVTNLGTPK.C	tr|Q66PN1|Q66PN1_9HYPO	
3	R.QIVVEYSDIRTILVIEPDSLANLVTNLGTPK.C	tr|Q66PN1|Q66PN1_9HYPO	
1	K.VPSFM*WLDTFDKTPLMEQTLADIR.T	tr|Q1HCL5|Q1HCL5_TRIKO	
1	K.LYIHAIGRLLANHGWSNAFFITDQGR.S	tr|Q9HEY8|Q9HEY8_TRIRE	
6	K.VPSFM*WLDTFDKTPLM*EQTLADIR.T	tr|B5TWC7|B5TWC7_9HYPO	
4	K.VPSFMWLDTFDKTPLMEQTLADIR.T	tr|B5TWC7|B5TWC7_9HYPO	
2	K.VPSFMWLDTFDKTPLM*EQTLADIR.T	tr|B5TWC7|B5TWC7_9HYPO	
1	K.VPSFM*WLDTFDKTPLMEQTLADIR.T	tr|B5TWC7|B5TWC7_9HYPO	
3	K.IVNSPVQVFSVAGSDYLTLK.D	sp|O74213|PGLR1_ASPAC	GH 28, polygalacturonase
2	K.FFAAHSLTNSVISGLK.I	sp|O74213|PGLR1_ASPAC	

Table V-7.3 *Contd...*

29	R.YGSWVIPQGSGPFNLPVGIR.L	tr|Q9P8D0|Q9P8D0_TRIRE	Swollenin
13	R.NGGGPYYFALTAVNTNGPGSVTK.I	tr|Q9P8D0|Q9P8D0_TRIRE	
11	K.YGCPLPADSIHLDLSDIAM*GR.L	tr|Q9P8D0|Q9P8D0_TRIRE	
8	K.TFTPPATGDPNFYYIDIGVQFSQN.-	tr|Q9P8D0|Q9P8D0_TRIRE	
8	R.LTSPTGEQIVNEQAIK.T	tr|Q9P8D0|Q9P8D0_TRIRE	
8	R.STHFGLTSGGACGFGLYGLCTK.N	tr|Q9P8D0|Q9P8D0_TRIRE	
7	K.VGNAYIWLR.S	tr|Q9P8D0|Q9P8D0_TRIRE	
6	K.YGCPLPADSIHLDLSDIAMGR.L	tr|Q9P8D0|Q9P8D0_TRIRE	
5	K.GSVTASWTDPMLGATCDAFCTAYPLLCK.D	tr|Q9P8D0|Q9P8D0_TRIRE	
4	K.GADTDNWVALVHDPNYTSSRPQER.Y	tr|Q9P8D0|Q9P8D0_TRIRE	
4	K.GSVTASWTDPM*LGATCDAFCTAYPLLCK.D	tr|Q9P8D0|Q9P8D0_TRIRE	
4	K.GSVTASWTDPMLGATCDAFCTAYPLLCKDPTGTTLR.G	tr|Q9P8D0|Q9P8D0_TRIRE	
2	K.IEIKGADTDNWVALVHDPNYTSSRPQER.Y	tr|Q9P8D0|Q9P8D0_TRIRE	
1	F.ALTAVNTNGPGSVTK.I	tr|Q9P8D0|Q9P8D0_TRIRE	
1	K.VGNAYIWLRNGGGPYYFALTAVNTNGPGSVTK.I	tr|Q9P8D0|Q9P8D0_TRIRE	
1	R.NGGGPYYFALTAVNTNGPGSVTKIEIK.G	tr|Q9P8D0|Q9P8D0_TRIRE	
11	R.LLGEEFVSIAFR.A	tr|Q9P973|Q9P973_TRIRE	GH 10, endoxylanase III
8	R.ASTNPLLFDANFNPKPAYNSIVGILQ.-	tr|Q9P973|Q9P973_TRIRE	
7	K.NAAIIQADLGQVTPENSM*K.W	tr|Q9P973|Q9P973_TRIRE	
7	K.WQSLENNQGQLNWGDADYLVNFAQQNGK.S	tr|Q9P973|Q9P973_TRIRE	
4	K.IRAWDVVNEIFNEDGTLR.S	tr|Q9P973|Q9P973_TRIRE	
4	K.LYINDYNLDR.P	tr|Q9P973|Q9P973_TRIRE	
3	R.GHTLIWHSQLPAWVNNINNADTLR.Q	tr|Q9P973|Q9P973_TRIRE	
3	R.THVSTVVGR.Y	tr|Q9P973|Q9P973_TRIRE	
2	K.NAAIIQADLGQVTPENSMK.W	tr|Q9P973|Q9P973_TRIRE	
2	R.EKNAAIIQADLGQVTPENSM*K.W	tr|Q9P973|Q9P973_TRIRE	
2	R.EKNAAIIQADLGQVTPENSMK.W	tr|Q9P973|Q9P973_TRIRE	
2	R.GKLYFGTATDR.G	tr|Q9P973|Q9P973_TRIRE	
1	R.ASTNPLLFDANFNPK.P	tr|Q9P973|Q9P973_TRIRE	
1	R.QVIRTHVSTVVGR.Y	tr|Q9P973|Q9P973_TRIRE	
3	K.GDVIADLADANGQYLR.C	tr|Q5AWC9|Q5AWC9_EMENI	
1	K.WDSTEPSQGTFSFTKGDVIADLADANGQYLR.C	tr|Q5AWC9|Q5AWC9_EMENI	
1	Y.AWDVVNEIFDEDGTLR.D	tr|O94163|O94163_ASPOR	

Table V-7.3 *Contd...*

4	K.VQNQWYSQCLP.-	sp|P43317|GUN5_TRIRE	GH 45, endoglucanase V
2	K.QGSLEVTDVSLDFFK.A	tr|Q870G8|Q870G8_ASPNG	GH 15, Glucoamylase
1	R.AGDVDESYSLTVSK.N	tr|P87258|P87258_TRIHA	GH 2, Glucoaminidase
1	K.LGTWVAGRK.D	tr|B2ARI3|B2ARI3_PODAN	GH 16
1	K.QAFANYLVQYVK.F	tr|B2ALJ0|B2ALJ0_PODAN	GH 30, glucosylamidase
1	R.TSGAGFSILR.N	tr|Q873Z0|Q873Z0_LEPMC	
3	E.VTKILFDENIGGLSIVR.N	tr|B6QTH8|B6QTH8_PENMA	
1	K.TVGTENDGGQICGVR.G	tr|B6QTH8|B6QTH8_PENMA	
1	R.TFVVAGGR.F	tr|B2A9W9|B2A9W9_PODAN	GH 37
1	K.VLQFAAANNK.I	tr|Q8TG99|Q8TG99_TRIVE	GH 55, β-1,3-glucanase
1	K.GTVTSDGATYTIWENTR.V	sp|P36218|XYN1_TRIRE	endoxylanase I, GH 11
1	K.FAADAVTLK.E	tr|A2QMZ4|A2QMZ4_ASPNC	Non-cellulolytic & others
3	K.FAADAVTLKDILR.E	tr|B2VRY5|B2VRY5_PYRTR	
1	R.SYLVQCPGVPV.-	tr|Q2U068|Q2U068_ASPOR	
1	K.LLFDLWDRDVSSGSK.Q	tr|Q2UB67|Q2UB67_ASPOR	
1	K.SVMEM*QSMQKTKQKK.S	tr|B0D8R1|B0D8R1_LACBS	
1	R.EVERHSHPVAAVAISAEFFR.L	tr|B8NZ90|B8NZ90_9APHY	
1	K.QIVVETM*M*NR.K	tr|A7EBF5|A7EBF5_SCLS1	
1	R.AIQQLLSQLNAETANIADICAK.L	tr|B8NX08|B8NX08_ASPFL	
1	G.KGGKGGKSGKNNK.G	tr|B9WHL8|B9WHL8_CANDU	
1	-.MHFTTSLALFGTLVAASQAVEPIR.G	tr|Q1E4M1|Q1E4M1_COCIM	
6	R.MVTAHLYNQDAYNK.G	tr|Q5B7G2|Q5B7G2_EMENI	
1	V.GLACLSPGFHTQDPTM*REQLQRSLDVRER.Q	tr|Q0V391|Q0V391_PHANO	
2	K.GIIAIEAMSR.I	tr|A7EU82|A7EU82_SCLS1	
1	A.TFNTMAIR.L	tr|Q4P714|Q4P714_USTMA	
2	D.FRNEYDTLR.L	tr|A7TQH6|A7TQH6_VANPO	
2	K.LTGLTTLTTLSFAALTK.V	tr|B8NA16|B8NA16_ASPFL	
1	R.RSPSYSSYGYSSRSRSPDR.N	tr|B6H2V9|B6H2V9_PENCH	
2	R.SSTSALTQESAGGVLR.G	tr|A2QTC8|A2QTC8_ASPNC	
1	R.AREREAIQGQTQMPPSNEITALNSVILP.A	tr|A2R1E1|A2R1E1_ASPNC	
1	K.FKVWLPDGLAPVQNDNEWAM*ALVSASNVDWMDGDLR.V	tr|A2R8Q5|A2R8Q5_ASPNC	
1	D.ADLTALYEAIELGR.D	tr|B6HUF9|B6HUF9_PENCH	
1	R.RPTWRKLISLVSSLLM*CAMTQRK.I	tr|B5VQF3|B5VQF3_YEAS6	

Table V-7.3 *Contd...*

1	K.CYQLHYAAGNVDK.S	tr|B8NHG5|B8NHG5_ASPFL
1	D.VFSGGIVYM*YFEEDNDYGLVK.V	tr|Q872H7|Q872H7_NEUCR
1	R.IPGIGVGGFATGGGITFASR.E	tr|B8NE86|B8NE86_ASPFL
1	R.MALFLDNIISSDGESVKNRLADPEVVAFLAR.E	tr|Q2HI66|Q2HI66_CHAGB
3	K.TLPTYQWLADAGITPDGSK.S	sp|P24657|RNTR_TRIVI
1	L.VDRLISCM*PDLKEPLGYWETAFDR.K	tr|B2ALK1|B2ALK1_PODAN
1	G.KM*SKSKGNVVDPVM*IIDRYGLDALR.Y	SYM_BACST
1	K.IDDQILTTAIKYIPEYGFQSQCITK.A	tr|Q59NL3|Q59NL3_CANAL
1	K.VNVFLADMKDFQ.D	tr|Q5AXE0|Q5AXE0_EMENI
1	K.GSLQDGQFVAAEPDGAK.S	sp|P24657|RNTR_TRIVI
2	K.GSVANMSLGGGK.S	tr|A4V8W2|A4V8W2_TRIHA
5	R.GSNPFDILGDVFLK.S	tr|A0SZ74|A0SZ74_TRIHA
1	R.AGIPAGGIATGAEGIK.S	tr|A4R6Z8|A4R6Z8_MAGGR
1	K.YLVTNAKK.I	A0RKJ7_BACAH
4	K.TSFLGTIVLSR.A	tr|Q157R5|Q157R5_TRIRE
3	K.GLSLDTFYAK.A	tr|Q157R5|Q157R5_TRIRE
3	R.AFDHYFGTMAGVR.G	tr|Q157R5|Q157R5_TRIRE
3	R.HLVLEANGFALTQK.T	tr|Q157R5|Q157R5_TRIRE
3	R.LPFYIISPWTR.N	tr|Q157R5|Q157R5_TRIRE
3	R.WAVDNSPYSIGFYK.R	tr|Q157R5|Q157R5_TRIRE
2	R.FQQFQDAEPGSSLYER.G	tr|Q157R5|Q157R5_TRIRE
1	K.AVVFTVGYK.S	tr|Q157R5|Q157R5_TRIRE
2	R.GFDNAGFVMGTSSSLFNQFILR.L	sp|Q6U819|PLB3_ASPFU
1	R.GFADANLQMNDGVPVWK.Q	tr|Q157R5|Q157R5_TRIRE

Table V-7.6 *Estimated regression coefficients for model terms (single, binary and cubic based interaction terms) predicting % glucan conversion, % xylan conversion and total sugar yield (gm sugar/kg dry weight biomass) as a function of crude enzyme mixture amount composition for 10 CE-RE based experiments. The sum of total enzyme loading is always equal to 16.5 mg protein/g glucan.*

Regression Terms (% Glucan conversion)				Regression Terms (% Xylan conversion)				Regression Terms (Total sugar yield, g/kg)			
Term	**Coefficient**	**P**	**VIF**	**Term**	**Coefficient**	**P**	**VIF**	**Term**	**Coefficient**	**P**	**VIF**
Block 4	10.2	0	1.312	Block 5	12	0	1.69	Block 4	55	0	1.319
Block 3	4.2	0	1.309	Block 6	10	0	1.682	Block 5	40	0	1.682
Block 1	2.6	0	2.002	Block 4	7	0	1.325	Block 6	30	0	1.661
Block 5	2.4	0	1.643	**Block 7**	**2**	**0.056**	**1.617**	Block 3	16	0	1.325
Block 6	**0.8**	**0.226**	**1.623**	**Block 8**	**1**	**0.315**	**1.616**	**Block 9**	**-10**	**0.181**	**1.763**
Block 2	**-0.9**	**0.193**	**2.017**	**Block 3**	**0**	**0.784**	**1.333**	Block 7	-15	0	1.763
Block 9	**-1.9**	**0.109**	**1.743**	**Block 9**	**-1**	**0.58**	**1.683**	Block 1	-24	0	2.093
Block 7	-4.7	0	1.78	Block 1	-14	0	1.724	Block 8	-28	0	1.761
Block 8	-7.7	0	1.785	Block 2	-16	0	1.727	Block 2	-42	0	2.093
re 8	63.3	*	7.753	ce 4	61	*	7.542	re 8	305	*	8.036
ce 6	59.8	*	7.761	ce 3	58	*	4.908	ce 6	283	*	7.802
ce 1	47	*	5.826	re 8	32	*	3.773	ce 4	247	*	8.874
re 4	37	*	6.536	re 4	26	*	4.091	ce 1	230	*	6.229
ce 5	34.1	*	6.917	re 2	25	*	2.935	re 4	191	*	6.532

Table V-7.6 *Contd...*

Regression Terms (% Glucan conversion)				Regression Terms (% Xylan conversion)				Regression Terms (Total sugar yield, g/kg)			
Term	**Coefficient**	**P**	**VIF**	**Term**	**Coefficient**	**P**	**VIF**	**Term**	**Coefficient**	**P**	**VIF**
re 1	26.9	*	6.262	ce 1	23	*	3.92	ce 5	167	*	7.096
ce 4	23.1	*	8.878	re 1	22	*	3.603	ce 3	162	*	9.88
re 2	13.9	*	7.096	ce 6	20	*	2.504	re 1	162	*	6.327
ce 3	8.5	*	8.165	ce 5	18	*	5.378	re 2	91	*	8.091
re 7	4.2	*	6.636	re 7	14	*	6.538	re 7	49	*	9.366
ce 6*re 7	147.5	0	4.5	ce 4*re 1	131	0	3.539	ce 4*re 4	663	0	4.129
ce 4*re 4	141.9	0	3.285	ce 4*ce 5	118	0	3.121	re 7*re 8	658	0	3.379
re 2*re 4	130.2	0	3.921	ce 4*re 7	115	0	4.139	ce 1*ce 4	622	0	2.996
ce 1*ce 4	125.7	0	2.711	ce 4*ce 6	88	0	3.002	ce 6*re 7	553	0	4.12
re 7*re 8	119.1	0	3.519	ce 1*ce 4	79	0	2.668	re 2*re 4	543	0	4.233
ce 3*ce 6	113.3	0	4.697	re 7*re 8	71	0	2.968	ce 3*ce 6	537	0	3.885
ce 1*re 2	106.5	0	3.888	re 2*re 7	62	0	2.658	ce 3*re 4	508	0	2.986
re 2*re 8	83.4	0	3.192	re 4*re 7	57	0.001	2.947	ce 4*re 7	472	0	3.443
ce 1*ce 3	79.5	0	2.593	re 1*re 8	52	0.001	2.895	ce 1*re 2	463	0	4.025
ce 6*re 1	76	0	3.375	ce 3*re 1	50	0.001	2.722	re 2*re 8	454	0	3.474
re 1*re 2	75.2	0	3.749	ce 4*re 4	50	0.011	3.895	ce 1*ce 3	424	0	2.434
ce 3*re 8	73	0	3.693	ce 3*ce 4	45	0.011	3.486	ce 3*re 8	422	0	3.862
ce 3*re 4	69.3	0	3.198	ce 5*re 8	44	0.021	4.029	re 1*re 8	422	0	3.014
re 1*re 8	69.3	0	2.989	**ce 5*re 7**	**41**	**0.055**	**4.551**	ce 4*re 1	412	0	3.137
ce 6*re 2	65.4	0	3.518	ce 3*re 4	39	0.009	2.437	ce 4*ce 5	376	0	4.214
ce 4*re 8	61.3	0	3.752	ce 3*re 7	37	0.022	2.94	ce 4*ce 6	363	0	3.554
ce 1*re 7	60.8	0	4.112	**ce 5*re 2**	**32**	**0.087**	**3.769**	ce 5*re 2	334	0	3.546
ce 4*ce 6	58.6	0	3.13	ce 1*re 4	-50	0.015	4.518	re 4*re 7	307	0	3.588

Table V-7.6 *Contd...*

Regression Terms (% Glucan conversion)			
Term	**Coefficient**	**P**	**VIF**
ce 4*re 7	58.6	0	4.805
ce 3*ce 5	55.6	0	4.328
ce 3*ce 4	52.9	0	3.569
ce 6*re 4	52.7	0	3.926
ce 4*re 1	51.4	0.001	3.722
ce 5*ce 6	50.4	0	3.663
ce 4*ce 5	46.1	0	3.337
ce 5*re 2	45	0	3.473
ce 1*re 1	37.1	0.001	2.613
re 4*re 8	34.4	0.004	3.174
ce 5*re 7	**28**	**0.066**	**4.699**
ce 3*re 1	26.6	0.024	3.108
re 4*re 7	**25.7**	**0.055**	**3.833**
ce 5*re 8	22	0.07	3.266

Regression Terms (% Xylan conversion)			
Term	**Coefficient**	**P**	**VIF**

Regression Terms (Total sugar yield, g/kg)			
Term	**Coefficient**	**P**	**VIF**
ce 4*re 8	296	0	3.495
re 1*re 2	291	0	3.583
ce 6*re 1	290	0	3.385
ce 3*ce 4	285	0	3.265
re 2*re 7	276	0.002	4.651
ce 3*ce 5	270	0.001	4.009
re 4*re 8	265	0.001	3.606
ce 6*re 2	255	0	2.974
ce 5*re 7	242	0.007	4.289
ce 5*re 8	239	0.003	3.92
ce 1*re 7	232	0.008	4.202
ce 1*re 1	184	0.008	2.668
ce 6*re 4	172	0.025	3.429
ce 3*re 7	168	0.029	3.461
ce 3*re 1	164	0.028	3.353
ce 5*ce 6	**153**	**0.103**	**4.876**

Table V-7.6 *Contd...*

Regression Terms (% Glucan conversion)				Regression Terms (% Xylan conversion)				Regression Terms (Total sugar yield, g/kg)			
Term	Coefficient	P	VIF	Term	Coefficient	P	VIF	Term	Coefficient	P	VIF
ce 5*re 4*re 7	1295.3	0	1.625	ce 1*ce 5*re 7	1212	0	1.341	ce 5*re 4*re 7	7224	0	1.606
re 2*re 4*re 7	981	0	1.492	ce 5*ce 6*re 7	1206	0	1.378	ce 1*ce 5*re 7	6318	0	1.384
ce 1*re 2*re 7	968.4	0	1.603	ce 1*ce 5*re 1	1087	0	1.278	ce 5*re 1*re 4	5942	0	1.338
ce 1*ce 5*re 7	914.3	0	1.387	ce 1*ce 3*ce 5	1068	0	1.357	ce 1*ce 5*re 1	5254	0	1.358
ce 5*re 1*re 4	855.2	0	1.336	ce 5*re 1*re 4	1043	0	1.251	ce 1*ce 3*ce 5	4683	0	1.45
ce 3*re 2*re 4	728.9	0	1.579	ce 5*ce 6*re 1	998	0	1.25	ce 5*re 7*re 8	4312	0	1.733
ce 3*ce 5*re 4	698.8	0	1.552	ce 5*ce 6*re 4	957	0	1.226	ce 5*ce 6*re 7	4066	0	1.809
ce 1*ce 5*re 1	687.3	0	1.353	ce 5*re 1*re 7	950	0	1.428	ce 1*re 2*re 7	4041	0	1.839
ce 5*re 7*re 8	667.8	0	1.735	ce 5*re 4*re 7	900	0	1.541	ce 5*re 1*re 7	3959	0	1.473
re 2*re 7*re 8	639	0	1.487	ce 5*ce 6*re 2	881	0	1.343	ce 5*ce 6*re 1	3884	0	1.615
ce 3*ce 6*re 7	620.7	0	1.603	ce 5*re 1*re 2	808	0	1.391	ce 3*ce 5*re 4	3808	0	1.537
ce 4*re 2*re 7	601	0	1.504	ce 5*re 2*re 7	799	0	1.724	re 2*re 4*re 7	3760	0	1.734
ce 1*ce 3*ce 5	596	0	1.415	ce 5*re 7*re 8	730	0	1.755	ce 5*ce 6*re 4	3352	0	1.563
ce 1*ce 3*re 2	485.4	0	1.498	ce 1*ce 5*ce 6	693	0	1.275	ce 5*ce 6*re 2	3282	0	1.72
ce 6*re 1*re 7	477.8	0	1.605	ce 5*re 1*re 8	653	0	1.533	ce 5*re 1*re 8	2924	0	1.537
re 1*re 2*re 4	475.6	0	1.607	ce 3*ce 5*ce 6	605	0	1.287	ce 3*re 2*re 4	2770	0	1.586
ce 4*ce 6*re 7	451.2	0	1.824	ce 5*ce 6*re 8	603	0	1.365	ce 3*ce 6*re 7	2742	0	1.734
ce 3*re 2*re 8	449.9	0	1.512	ce 5*re 4*re 8	596	0	1.395	ce 3*ce 5*ce 6	2555	0	1.871
ce 6*re 2*re 7	449.2	0	1.561	ce 3*ce 5*re 1	587	0	1.358	ce 3*ce 5*re 8	2467	0	1.744
ce 5*re 1*re 7	413.3	0	1.484	ce 1*ce 5*re 4	569	0	1.469	ce 5*re 4*re 8	2360	0	1.553
re 1*re 2*re 7	408.5	0	1.444	ce 3*ce 5*re 7	560	0	1.514	ce 4*ce 5*re 7	2255	0	1.798
ce 4*re 1*re 2	403.6	0	1.665	ce 3*ce 5*re 4	543	0	1.339	ce 3*ce 4*ce 5	2228	0	1.788
ce 3*ce 6*re 2	399.7	0	1.565	ce 5*re 2*re 4	511	0	1.306	ce 1*ce 5*re 4	2120	0	1.321
ce 3*ce 5*re 8	390	0	1.74	ce 3*ce 5*re 8	492	0	1.4	ce 1*ce 3*re 2	2107	0	1.498
ce 3*ce 4*ce 5	368.9	0	1.776	ce 3*ce 5*re 2	415	0	1.408	re 2*re 7*re 8	2091	0	1.706

Table V-7.6 *Contd...*

Regression Terms (% Glucan conversion)				Regression Terms (% Xylan conversion)				Regression Terms (Total sugar yield, g/kg)			
Term	**Coefficient**	**P**	**VIF**	**Term**	**Coefficient**	**P**	**VIF**	**Term**	**Coefficient**	**P**	**VIF**
ce 5*ce 6*re 1	358.9	0	1.567	ce 1*ce 5*re 2	390	0	1.404	ce 1*ce 6*re 4	1854	0	1.395
ce 5*re 1*re 8	352.1	0	1.507	ce 1*re 4*re 7	387	0.001	1.57	ce 3*ce 6*re 2	1852	0	1.519
ce 3*ce 6*re 1	349.1	0	1.737	ce 1*ce 3*re 4	364	0.001	1.548	ce 3*ce 4*re 2	1840	0	1.38
ce 4*ce 5*re 7	344	0	1.856	ce 1*re 2*re 4	338	0.001	1.442	re 1*re 2*re 4	1825	0	1.618
ce 1*ce 6*re 4	325.3	0	1.395	ce 5*re 2*re 8	326	0.003	1.572	ce 5*re 2*re 4	1785	0.002	1.42
ce 3*ce 5*ce 6	322.9	0	1.862	ce 1*re 4*re 8	324	0.002	1.441	ce 3*ce 5*re 1	1763	0	1.558
ce 3*re 7*re 8	321.3	0	1.522	ce 3*ce 4*re 2	314	0.003	1.315	ce 5*ce 6*re 8	1753	0	1.617
ce 4*ce 6*re 2	313.2	0	1.507	ce 1*re 2*re 8	294	0.003	1.239	ce 3*re 2*re 8	1740	0	1.533
ce 1*ce 4*re 7	291.4	0.001	1.73	ce 4*ce 5*re 7	292	0.014	1.81	ce 4*ce 5*re 4	1664	0.001	1.625
ce 1*ce 6*re 8	283.7	0	1.341	ce 3*ce 6*re 8	288	0.003	1.242	ce 1*ce 5*ce 6	1656	0.005	1.337
ce 1*re 1*re 2	278.4	0.001	1.757	ce 3*ce 4*ce 5	282	0.009	1.512	ce 1*ce 5*re 2	1511	0.002	1.563
ce 6*re 1*re 4	276.8	0.001	1.528	ce 1*ce 6*re 4	280	0.008	1.414	ce 1*ce 6*re 7	1468	0.002	1.595
ce 5*re 4*re 8	269	0	1.509	ce 1*re 7*re 8	255	0.013	1.354	ce 6*re 1*re 7	1449	0.003	1.589
ce 5*ce 6*re 7	264.2	0.003	1.777	re 4*re 7*re 8	251	0.022	1.422	ce 6*re 2*re 7	1443	0.006	1.746
ce 5*ce 6*re 2	263.8	0.003	1.713	ce 1*ce 3*re 7	245	0.021	1.331	ce 5*re 1*re 2	1413	0.003	1.558
ce 4*ce 5*re 4	250.7	0.001	1.549	ce 3*re 1*re 8	238	0.025	1.459	ce 1*re 7*re 8	1407	0.004	1.591
ce 3*re 2*re 7	248.5	0.001	1.328	ce 1*re 1*re 4	230	0.03	1.445	ce 1*re 4*re 7	1402	0.004	1.579
ce 3*re 1*re 2	246.8	0.002	1.586	ce 1*re 2*re 7	218	0.034	1.357	ce 3*re 1*re 2	1379	0.005	1.602
ce 1*ce 6*re 7	245.7	0.002	1.606	ce 1*ce 3*re 8	217	0.027	1.246	ce 3*ce 6*re 1	1377	0.006	1.72
ce 3*ce 4*re 2	241.5	0.002	1.392	ce 3*ce 6*re 7	217	0.032	1.323	ce 1*ce 4*re 7	1335	0.012	1.708
ce 6*re 4*re 7	236.7	0.005	1.793	**ce 4*ce 5*re 4**	**194**	**0.077**	**1.554**	ce 1*ce 6*re 8	1310	0.003	1.344
ce 1*ce 5*re 4	229.7	0.001	1.315	**ce 1*ce 5*re 8**	**186**	**0.073**	**1.384**	ce 3*re 1*re 8	1283	0.01	1.696
ce 3*re 4*re 7	214.1	0.006	1.557	**ce 1*re 1*re 7**	**184**	**0.073**	**1.249**	ce 1*re 2*re 4	1258	0.009	1.598
ce 4*ce 6*re 1	212	0.039	1.568	**ce 1*ce 6*re 7**	**173**	**0.08**	**1.258**	ce 6*re 1*re 4	1207	0.015	1.555
ce 3*ce 4*ce 6	210.4	0.012	1.785	**ce 3*ce 6*re 2**	**158**	**0.104**	**1.225**	ce 1*re 1*re 2	1189	0.019	1.752
ce 3*re 1*re 8	197.8	0.015	1.689	**ce 1*ce 3*re 2**	**156**	**0.116**	**1.221**	ce 1*re 1*re 7	1165	0.019	1.539
ce 1*re 2*re 4	192.4	0.014	1.578	**ce 1*re 1*re 8**	**153**	**0.139**	**1.371**	re 1*re 2*re 7	1143	0.018	1.589

Table V-7.6 *Contd...*

Regression Terms (% Glucan conversion)			
Term	Coefficient	P	VIF
ce 1*re 1*re 7	190	0.018	1.526
ce 5*ce 6*re 4	183.9	0.024	1.571
ce 1*ce 3*ce 6	180	0.02	1.537
ce 1*ce 5*re 2	177	0.024	1.568
ce 1*re 7*re 8	175.4	0.026	1.592
ce 1*re 4*re 7	173.3	0.03	1.577
ce 1*re 4*re 8	163.6	0.027	1.394
ce 3*ce 4*re 8	**163.3**	**0.051**	**1.728**
ce 4*re 7*re 8	**134.3**	**0.109**	**1.801**
ce 1*re 2*re 8	**132.8**	**0.087**	**1.548**
ce 3*ce 6*re 4	**131.2**	**0.113**	**1.759**
ce 4*ce 5*re 1	**125.7**	**0.124**	**1.717**
ce 5*re 1*re 2	**-137.8**	**0.078**	**1.569**
ce 6*re 2*re 4	**-148.4**	**0.083**	**1.733**
ce 4*re 1*re 8	-164	0.061	1.809
ce 5*re 2*re 7	-174.4	0.04	1.564
ce 1*ce 4*re 8	-202.7	0.009	1.518
ce 3*ce 5*re 7	-228.5	0.006	1.573
ce 3*ce 4*re 7	-229	0.004	1.651
ce 4*re 4*re 8	-256.1	0.002	1.727
re 2*re 4*re 8	-265.7	0.002	1.691
ce 3*ce 5*re 2	-273.1	0.001	1.586
ce 4*re 4*re 7	-320.2	0	1.705
ce 4*re 1*re 4	-353.9	0	1.451
ce 1*ce 4*re 4	-569.4	0	1.374

S = 4.89170 PRESS = 21460.8
R-Sq(pred) = 88.60% R-Sq(adj) = 90.76%

Regression Terms (% Xylan conversion)			
Term	Coefficient	P	VIF
ce 6*re 1*re 7	**-169**	**0.091**	**1.284**
ce 1*ce 3*ce 4	**-201**	**0.076**	**1.583**
ce 1*ce 4*re 8	-222	0.029	1.337
ce 3*ce 4*re 1	-243	0.044	1.875
ce 4*re 2*re 8	-266	0.011	1.241
ce 4*re 4*re 8	-282	0.007	1.427
ce 4*ce 6*re 8	-292	0.005	1.362
ce 4*re 2*re 4	-321	0.002	1.419
ce 4*re 7*re 8	-395	0	1.561
ce 1*ce 4*re 4	-555	0	1.464
ce 4*ce 6*re 4	-566	0	1.557
ce 3*ce 4*re 7	-667	0	1.788
ce 4*ce 6*re 2	-699	0	1.347
ce 4*re 1*re 8	-709	0	1.622
ce 4*re 4*re 7	-762	0	1.693
ce 4*re 2*re 7	-784	0	1.544
ce 4*ce 6*re 7	-807	0	1.565
ce 4*re 1*re 4	-887	0	1.46
ce 4*re 1*re 2	-940	0	1.481
ce 4*ce 6*re 1	-1092	0	1.453

S = 6.89826 PRESS = 42630.5
R-Sq(pred) = 87.37% R-Sq(adj) = 89.75%

Regression Terms (Total sugar yield, g/kg)			
Term	Coefficient	P	VIF
ce 1*re 4*re 8	1132	0.013	1.408
ce 5*re 2*re 7	1129	0.044	1.803
ce 1*re 2*re 8	1071	0.025	1.562
ce 4*ce 5*re 1	1024	0.04	1.691
ce 6*re 4*re 7	1006	0.047	1.743
ce 3*re 2*re 7	963	0.044	1.563
ce 4*ce 5*ce 6	**924**	**0.074**	**1.823**
ce 1*ce 4*ce 5	**852**	**0.075**	**1.565**
ce 3*re 7*re 8	**845**	**0.096**	**1.686**
ce 1*ce 5*re 8	**820**	**0.072**	**1.415**
ce 3*ce 4*ce 6	**778**	**0.126**	**1.767**
ce 4*ce 6*re 8	**-733**	**0.124**	**1.55**
ce 4*re 2*re 4	**-746**	**0.13**	**1.658**
ce 4*re 2*re 8	**-749**	**0.133**	**1.494**
ce 3*re 4*re 8	**-918**	**0.067**	**1.716**
ce 4*ce 6*re 4	-1128	0.034	1.777
ce 1*ce 4*re 8	-1311	0.006	1.536
re 2*re 4*re 8	-1571	0.003	1.725
ce 4*ce 6*re 1	-1602	0.01	1.518
ce 4*re 4*re 8	-1935	0	1.786
ce 4*re 1*re 8	-2252	0	1.75
ce 3*ce 4*re 7	-2460	0	1.753
ce 4*re 4*re 7	-3100	0	1.682
ce 4*re 1*re 4	-3320	0	1.479
ce 1*ce 4*re 4	-3604	0	1.381

S = 30.0078 PRESS = 810085
R-Sq(pred) = 86.49% R-Sq(adj) = 89.08%

Table V-7.8 *Estimated regression coefficients for model terms (single, binary and cubic based interaction terms) predicting % glucan conversion, % xylan conversion and total sugar yield (gm sugar/kg dry weight biomass) as a function of crude enzyme mixture amount composition for 5 CE-RE (Cel x is CE 6) based experiments. The sum of total enzyme loading is always equal to 16.5 mg protein/g glucan.*

Regression Terms (% Glucan conversion)				Regression Terms (% Xylan conversion)				Regression Terms (Total sugar yield, g/l		
Term	**Coefficient**	**P**	**VIF**	**Term**	**Coefficient**	**P**	**VIF**	**Term**	**Coefficient**	**P**
cel x	57.491	*	3.18	ce4	39.597	*	3.203	cel x	238.82	*
ce5	26.312	*	2.615	re1	10.063	*	1.65	ce4	178.43	*
re1	22.921	*	2.239	re7	9.795	*	1.65	ce5	121.16	*
ce4	22.204	*	2.615	ce5	7.636	*	1.65	re1	107.7	*
re7	3.189	*	2.239	cel x	5.352	*	1.65	re7	36.56	*
cel x*re7	125.705	0	2.702	ce4*re7	109.65	0.004	2.589	cel x*re7	448.71	0.001
cel x*re1	66.985	0	2.702	cel x*ce4	84.452	0.025	2.589	cel x*ce4	408.78	0.003
cel x*ce4	54.552	0	2.423	ce4*re1	77.892	0.038	2.589	ce4*re1	342.17	0.012
ce4*ce5	44.063	0	2.35	**ce4*ce5**	**64.002**	**0.087**	**2.589**	ce4*ce5	332.8	0.014
ce4*re1	33.124	0.009	2.651					ce4*re7	329.37	0.016
cel x*ce5	26.591	0.026	2.423					cel x*re1	271.54	0.033
ce5*re7	**19.348**	**0.116**	**2.651**							
cel x*ce4*re7	618.697	0	1.628	cel x*ce4*re1	856.162	0	1.584	cel x*ce4*re7	4224.67	0
ce4*ce5*re7	507.577	0	1.628	cel x*ce4*re7	779.505	0.001	1.584	ce4*ce5*re7	3229.02	0
ce4*re1*re7	437.86	0	1.472	ce4*ce5*re1	759.92	0.001	1.584	cel x*ce4*re1	3183.36	0
cel x*ce5*re7	351.903	0	1.848	cel x*ce4*ce5	650.025	0.005	1.584	ce4*re1*re7	3133.18	0
ce4*ce5*re1	343.498	0	1.628	ce4*re1*re7	637	0.006	1.584	ce4*ce5*re1	3055.33	0
cel x*ce4*re1	283.87	0.001	1.848	ce4*ce5*re7	564.172	0.013	1.584	cel x*ce5*re7	2276.5	0.004
cel x*ce5*re1	177.449	0.019	1.628					cel x*ce4*ce5	1901.36	0.02
cel x*re1*re7	**147.133**	**0.049**	**1.624**	S = 11.2048 PRESS = 9930.93				**cel x*ce5*re1**	**1118.21**	**0.141**
ce5*re1*re7	**103.266**	**0.143**	**1.472**	R-Sq(pred) = 80.62% R-Sq(adj) = 82.61%				**ce5*re1*re7**	**1087.96**	**0.134**

S = 3.65086 PRESS = 1110.40
R-Sq(pred) = 95.29% R-Sq(adj) = 95.98%

S = 39.4779 PRESS = 124329
R-Sq(pred) = 86.14% R-Sq(adj) = 87.66%

Table V-7.9 *Estimated regression coefficients for model terms (single, binary and cubic based interaction terms) predicting % glucan conversion, % xylan conversion and total sugar yield (gm sugar/kg dry weight biomass) as a function of crude enzyme mixture amount composition for 5 CE-RE (Cel x is RE 4) based experiments. The sum of total enzyme loading is always equal to 16.5 mg protein/g glucan.*

Regression Terms (% Glucan conversion)				Regression Terms (% Xylan conversion)				Regression Terms (Total sugar yield,		
Term	Coefficient	P	VIF	Term	Coefficient	P	VIF	Term	Coefficient	P
cel x	34.47	*	1.866	ce4	40.957	*	3.203	cel x	175.48	*
ce5	26.65	*	1.866	cel x	15.997	*	1.807	ce4	167.38	*
re1	23.66	*	1.866	re1	8.472	*	1.807	re1	115.47	*
ce4	18.31	*	2.616	re7	8.372	*	1.845	ce5	114.2	*
re7	5.11	*	1.642	ce5	3.369	*	1.807	re7	35.24	*
cel x*ce4	109.78	0	2.588	ce4*re1	108.962	0.001	2.635	cel x*ce4	607.3	0
ce4*ce5	53.75	0.018	2.588	ce4*re7	95.269	0.004	2.65	ce4*re1	410.64	0.012
ce4*re1	**37.45**	**0.094**	**2.588**	ce4*ce5	81.111	0.012	2.635	ce4*ce5	403.62	0.013
				cel x*ce4	76.976	0.017	2.635	**ce4*re7**	**291.91**	**0.07**
cel x*ce4*re7	1337.87	0	1.444	cel x*ce4*re7	713.264	0	1.617	cel x*ce4*re7	6770.5	0
cel x*ce4*re1	707.18	0	1.617	ce4*ce5*re7	702.813	0	1.617	cel x*ce4*re1	4442.63	0
ce4*ce5*re7	617.97	0	1.444	cel x*ce4*re1	671.094	0.001	1.602	ce4*ce5*re7	3995.65	0
ce4*re1*re7	463.6	0.001	1.444	ce4*ce5*re1	605.005	0.002	1.602	cel x*ce4*ce5	2899.7	0.003
cel x*ce4*ce5	433.78	0.002	1.617	ce4*re1*re7	471.052	0.016	1.617	ce4*ce5*re1	2896.16	0.003
ce4*ce5*re1	345.21	0.012	1.617	cel x*ce4*ce5	470.4	0.015	1.602	ce4*re1*re7	2829.96	0.004
cel x*ce5*re7	263.82	0.033	1.321	**ce5*re1*re7**	**287.222**	**0.098**	**1.326**	cel x*ce5*re7	1753.64	0.046
cel x*re1*re7	253.56	0.04	1.321	**cel x*ce5*re7**	**275.251**	**0.113**	**1.326**	**cel x*re1*re7**	**1679.8**	**0.056**
cel x*ce5*re1	**191.95**	**0.118**	**1.328**	**cel x*re1*re7**	**261.305**	**0.132**	**1.326**	**ce5*re1*re7**	**1501.97**	**0.086**
ce5*re1*re7	**190.12**	**0.121**	**1.321**							

S = 6.69457 PRESS = 3807.21
R-Sq(pred) = 86.52% R-Sq(adj) = 88.74%

S = 9.45854 PRESS = 7047.39
R-Sq(pred) = 84.11% R-Sq(adj) = 85.68%

S = 47.6015 PRESS = 186009
R-Sq(pred) = 84.65% R-Sq(adj) = 86.73%

Table V-7.10 *Bivariate correlation Pearson coefficients for individual protein components of various enzyme mixtures (N = 753) with respect to their predicted % glucan, % xylan and total sugar hydrolysis yields. Values highlighted in bold signify lack of statistical significance at p<0.05 level.*

Enzyme	% Glucan	% Xylan	Total Sugars	Enzyme	% Glucan	% Xylan	Total Sugars
AC	-.106**	**0.056**	**-0.038**	**GH 17**	-.281**	-.099**	-.235**
AXE 1	.220**	.078*	.184**	**CHI 1**	.121**	.109**	.136**
AXE 2	.595**	.213**	.498**	**CHI 2**	-.102**	**-0.029**	-.080*
FAE	-.198**	.216**	**-0.013**	**AGAL**	-.150**	**0.063**	**-0.063**
CIP 1	.080*	**-0.02**	**0.041**	**PGL**	**0.041**	.132**	.096**
CIP 2	.393**	**0.017**	.264**	**GH 30**	.126**	-.082*	**0.039**
PL	-.218**	.231**	**-0.018**	**AG**	-.170**	.194**	**-0.007**
PME	-.198**	.219**	**-0.013**	**BFRC**	**0.064**	**0.018**	**0.052**
RHAE	-.127**	.083*	**-0.04**	**BGAL 1**	-.177**	.268**	**0.028**
ARH	-.135**	.206**	**0.022**	**AA**	-.256**	.143**	-.090*
SWO	.527**	**-0.032**	.324**	**EG 5**	-.345**	**-0.062**	-.258**
BG 1	-.286**	-.162**	-.271**	**AMANO 1**	-.299**	.143**	-.118**
BMANO	-.218**	.124**	-.075*	**ABF 1**	-.200**	.211**	**-0.017**
BG 3	.667**	.181**	.528**	**ABGAL**	-.306**	**0.032**	-.182**
BX 3	**0.021**	.137**	.088*	**ABF 2**	-.260**	.233**	**-0.044**
EG 2	.365**	**0.04**	.257**	**GH 55**	-.185**	.200**	**-0.013**
BM	.158**	**0.047**	.126**	**EG 4**	-.374**	-.151**	-.322**
BGAL 2	.359**	.201**	.339**	**EG 7**	.685**	.116**	.505**
CBH 2	.300**	-.088*	.147**	**ABF 3**	-.258**	.247**	**-0.036**
GH 6	-.356**	-.162**	-.316**	**GH 65**	-.159**	.242**	**0.026**
CBH 1	.210**	-.159**	**0.052**	**AGLUC**	**-0.057**	**0.017**	**-0.027**
EG 1	.543**	**-0.041**	.329**	**GH 71**	-.197**	.230**	**-0.006**
EX 2	-.198**	-.143**	-.204**	**GT**	-.251**	-.073*	-.202**
EX 1	-.183**	.142**	**-0.043**	**XG**	**0.007**	.117**	**0.066**
EG 3	.194**	.095**	.175**	**AMAN**	-.197**	.230**	**-0.006**
AMY	.270**	**0.041**	.197**	**BGLUC**	-.197**	.230**	**-0.006**
GAMY	**-0.069**	-.116**	-.105**	**GH 81**	-.197**	.230**	**-0.006**
GH 16	.099**	**-0.023**	**0.052**	**AMANO 2**	-.187**	.086*	-.074*
OTHERS	-.239**	-.094**	-.205**				

Correlation significant at 0.01** or 0.05* level (2-tailed), N = 753

Table V-7.11 *Pearson correlation coefficients for individual protein components of various enzyme mixtures with respect to each other within the original 14 enzyme mixtures. Values highlighted signify statistical significance at p<0.01 and p<0.05 levels, respectively.*

1 - A	AC	AXE 1	AXE 2	FAE	CIP 1	CIP 2	PL	PME	RHAE	ARH	SWO	BG 1	BMANO	BG 3	BX 3	EG 2
AC		0.896	0.535		0.637	0.634									0.837	
AXE 1	0.896		0.704		0.865	0.897					0.571				0.814	
AXE 2	0.535	0.704				0.648								0.572		
FAE							0.96			0.629			0.728			
CIP 1	0.637	0.865				0.932					0.787				0.629	0.592
CIP 2	0.634	0.897	0.648		0.932						0.867				0.658	0.547
PL				0.96				0.554		0.609			0.548			
PME							0.554		0.886	0.914						
RHAE								0.886		0.723						
ARH				0.629			0.609	0.914	0.723							
SWO		0.571			0.787	0.867										0.742
BG 1																
BMANO				0.728			0.548									
BG 3			0.572													
BX 3	0.837	0.814			0.629	0.658										
EG 2					0.592	0.547					0.742					
BM								0.784	0.955	0.593						0.612
BGAL 2	0.794	0.896	0.881		0.723	0.766									0.598	
CBH 2					0.806	0.767					0.907					0.799
GH 6												0.97				
CBH 1		0.542			0.797	0.779					0.891					0.741
EG 1		0.545			0.771	0.831					0.961					0.765
EX 2												0.793				
EX 1	0.758	0.571														
EG 3																0.777
AMY																
GAMY													0.752			

Table V-7.11 *Contd...*

1 - B	AC	AXE 1	AXE 2	FAE	CIP 1	CIP 2	PL	PME	RHAE	ARH	SWO	BG 1	BMANO	BG 3	BX 3	EG 2
GH 16																
GH 17																
CHI 1																
CHI 2													0.798			
AGAL													0.901			
PGL								0.888	0.97	0.806						
GH 30																
AG				0.744	-0.557	-0.534	0.665						0.634			
BFRC					-0.542	-0.541							0.613			
BGAL 1				0.809			0.781	0.703		0.768						
AA				0.719	-0.551		0.759			0.608						
EG 5																0.542
AMANO 1				0.8			0.818			0.545						
ABF 1				0.986			0.921			0.535			0.812			
ABGAL								0.76	0.775	0.751						
ABF 2				0.958			0.962			0.553			0.633			
GH 55				0.897			0.783						0.905			
EG 4												0.927				
EG 7		0.671	0.761		0.651	0.837					0.853			0.68		
ABF 3				0.721			0.803									
GH 65				0.911			0.926			0.553						
AGLUC	0.789	0.842			0.737	0.761									0.942	
GH 71				0.974			0.988			0.577			0.579			
GT																
XG	0.816	0.893	0.664		0.83	0.755									0.615	
AMAN				0.974			0.988			0.577			0.579			
BGLUC				0.974			0.988			0.577			0.579			
GH 81				0.974			0.988			0.577			0.579			
AMANO 2				0.647									0.987			
OTHERS		-0.573			-0.655	-0.632					-0.557					-0.681

Table V-7.11 *Contd...*

2 - A	BM	BGAL 2	CBH 2	GH 6	CBH 1	EG 1	EX 2	EX 1	EG 3	AMY	GAMY	GH 16	GH 17	CHI 1	CHI 2	AGAL	PGL
AC		0.794						0.758									
AXE 1		0.896			0.542	0.545		0.571									
AXE 2		0.881															
FAE																	
CIP 1		0.723	0.806		0.797	0.771											
CIP 2		0.766	0.767		0.779	0.831											
PL																	
PME	0.784																0.888
RHAE	0.955																0.97
ARH	0.593																0.806
SWO			0.907		0.891	0.961											
BG 1				0.97			0.793										
BMANO											0.752				0.798	0.901	
BG 3																	
BX 3		0.598															
EG 2	0.612		0.799		0.741	0.765			0.777								
BM																	0.927
BGAL 2								0.709									
CBH 2					0.958	0.951											
GH 6							0.748										
CBH 1			0.958			0.933											
EG 1			0.951		0.933												
EX 2				0.748													
EX 1		0.709															
EG 3																	
AMY												0.978					
GAMY															0.941	0.895	

Table V-7.11 *Contd...*

2 - B	BM	BGAL 2	CBH 2	GH 6	CBH 1	EG 1	EX 2	EX 1	EG 3	AMY	GAMY	GH 16	GH 17	CHI 1	CHI 2	AGAL	PGL
GH 16										0.978							
GH 17																	
CHI 1																	
CHI 2											0.941					0.897	
AGAL											0.895				0.897		
PGL	0.927																
GH 30										0.929		0.897					
AG			-0.562		-0.573												
BFRC			-0.563		-0.553						0.748				0.687	0.822	
BGAL 1																	
AA					-0.534												
EG 5			0.573														
AMANO 1																	
ABF 1																0.533	
ABGAL	0.658																0.772
ABF 2																	
GH 55															0.535	0.709	
EG 4				0.934			0.667										
EG 7		0.614	0.695		0.68	0.832											
ABF 3																	
GH 65																	
AGLUC		0.559			0.557												
GH 71																	
GT													0.887				
XG		0.93						0.673									
AMAN																	
BGLUC																	
GH 81																	
AMANO 2											0.825				0.858	0.921	
OTHERS			-0.596		-0.611	-0.587			-0.548				0.676				

Table V-7.11 *Contd...*

3 - A	GH 30	AG	BFRC	BGAL 1	AA	EG 5	AMANO 1	ABF 1	ABGAL	ABF 2	GH 55	EG 4	EG 7	ABF 3	GH 65	AGLUC
AC																0.789
AXE 1													0.671			0.842
AXE 2													0.761			
FAE		0.744		0.809	0.719		0.8	0.986		0.958	0.897			0.721	0.911	
CIP 1		-0.557	-0.542		-0.551								0.651			0.737
CIP 2		-0.534	-0.541										0.837			0.761
PL		0.665		0.781	0.759		0.818	0.921		0.962	0.783			0.803	0.926	
PME				0.703					0.76							
RHAE									0.775							
ARH				0.768	0.608		0.545	0.535	0.751	0.553					0.553	
SWO													0.853			
BG 1												0.927				
BMANO		0.634	0.613					0.812		0.633	0.905					
BG 3													0.68			
BX 3																0.942
EG 2						0.542										
BM									0.658							
BGAL 2													0.614			0.559
CBH 2		-0.562	-0.563			0.573							0.695			
GH 6												0.934				
CBH 1		-0.573	-0.553		-0.534								0.68			0.557
EG 1													0.832			
EX 2												0.667				
EX 1																
EG 3																
AMY	0.929															
GAMY			0.748													

Table V-7.11 *Contd...*

3 - B	GH 30	AG	BFRC	BGAL 1	AA	EG 5	AMANO 1	ABF 1	ABGAL	ABF 2	GH 55	EG 4	EG 7	ABF 3	GH 65	AGLUC
GH 16	0.897															
GH 17																
CHI 1																
CHI 2			0.687								0.535					
AGAL			0.822					0.533			0.709					
PGL									0.772							
GH 30																
AG					0.547		0.729	0.76		0.657	0.723				0.851	
BFRC																
BGAL 1							0.578	0.751		0.844	0.652			0.701	0.701	
AA		0.547		0.551			0.839	0.686	0.559	0.652	0.588				0.656	
EG 5																
AMANO 1		0.729		0.578	0.839			0.771		0.772	0.639			0.583	0.832	
ABF 1		0.76		0.751	0.686		0.771			0.94	0.95			0.688	0.881	
ABGAL					0.559											
ABF 2		0.657		0.844	0.652		0.772	0.94			0.837			0.874	0.892	
GH 55		0.723		0.652	0.588		0.639	0.95		0.837				0.544	0.747	
EG 4																
EG 7																
ABF 3				0.701			0.583	0.688		0.874	0.544				0.711	
GH 65		0.851		0.701	0.656		0.832	0.881		0.892	0.747			0.711		
AGLUC																
GH 71		0.704		0.781	0.729		0.845	0.945		0.966	0.815			0.797	0.946	
GT							0.571									
XG																0.619
AMAN		0.704		0.781	0.729		0.845	0.945		0.966	0.815			0.797	0.946	
BGLUC		0.704		0.781	0.729		0.845	0.945		0.966	0.815			0.797	0.946	
GH 81		0.704		0.781	0.729		0.845	0.945		0.966	0.815			0.797	0.946	
AMANO 2		0.589	0.655					0.737			0.84					
OTHERS		0.561														

Table V-7.11 *Contd...*

4 - A	GH 71	GT	XG	AMAN	BGLUC	GH 81	AMANO 2	OTHERS
AC			0.816					
AXE 1			0.893					-0.573
AXE 2			0.664					
FAE	0.974			0.974	0.974	0.974	0.647	
CIP 1			0.83					-0.655
CIP 2			0.755					-0.632
PL	0.988			0.988	0.988	0.988		
PME								
RHAE								
ARH	0.577			0.577	0.577	0.577		
SWO								-0.557
BG 1								
BMANO	0.579			0.579	0.579	0.579	0.987	
BG 3								
BX 3			0.615					
EG 2								-0.681
BM								
BGAL 2			0.93					
CBH 2								-0.596
GH 6								
CBH 1								-0.611
EG 1								-0.587
EX 2								
EX 1			0.673					
EG 3								-0.548
AMY								
GAMY							0.825	

Table V-7.11 *Contd...*

4 - B	GH 71	GT	XG	AMAN	BGLUC	GH 81	AMANO 2	OTHERS
GH 16								
GH 17		0.887						0.676
CHI 1								
CHI 2							0.858	
AGAL							0.921	
PGL								
GH 30								
AG	0.704			0.704	0.704	0.704	0.589	0.561
BFRC							0.655	
BGAL 1	0.781			0.781	0.781	0.781		
AA	0.729			0.729	0.729	0.729		
EG 5								
AMANO 1	0.845	0.571		0.845	0.845	0.845		
ABF 1	0.945			0.945	0.945	0.945	0.737	
ABGAL								
ABF 2	0.966			0.966	0.966	0.966		
GH 55	0.815			0.815	0.815	0.815	0.84	
EG 4								
EG 7								
ABF 3	0.797			0.797	0.797	0.797		
GH 65	0.946			0.946	0.946	0.946		
AGLUC			0.619					
GH 71				1	1	1		
GT								0.882
XG								-0.572
AMAN	1				1	1		
BGLUC	1			1		1		
GH 81	1			1	1			
AMANO 2								
OTHERS		0.882	-0.572					

Table V-7.12 *ANOVA results comparing top and bottom 25% quartile groups for individual protein components, based on varying % glucan, % xylan and total sugar hydrolysis yield. Values highlighted in bold signify statistical significance at p<0.05 level.*

		ANOVA (% glucan conversion)					ANOVA (% xylan conversion)					ANOVA (Total Sugars)				
		Sum of Squares	**df**	**Mean Square**	**F**	**Sig.**	**Sum of Squares**	**df**	**Mean Square**	**F**	**Sig.**	**Sum of Squares**	**df**	**Mean Square**	**F**	**Sig.**
AC	B/w groups	7.47	1	7.475	19.28	**.000**	1.78	1	1.785	6.46	**.011**	2.47	1	2.469	6.29	**.013**
	Within groups	144.99	374	.388			103.81	376	.276			146.84	374	.393		
	Total	152.46	375				105.59	377				149.31	375			
AXE 1	B/w groups	0.28	1	.283	12.26	**.001**	0.18	1	.177	10.04	**.002**	0.19	1	.188	7.61	**.006**
	Within groups	8.64	374	.023			6.64	376	.018			9.27	374	.025		
	Total	8.92	375				6.82	377				9.45	375			
AXE 2	B/w groups	2.69	1	2.688	476.37	**.000**	0.30	1	.295	27.70	**.000**	1.62	1	1.622	187.60	**.000**
	Within groups	2.11	374	.006			4.01	376	.011			3.23	374	.009		
	Total	4.80	375				4.30	377				4.86	375			
FAE	B/w groups	0.84	1	.843	25.14	**.000**	0.76	1	.759	71.53	**.000**	0.05	1	.054	1.60	.207
	Within groups	12.54	374	.034			3.99	376	.011			12.50	374	.033		
	Total	13.38	375				4.75	377				12.56	375			
CIP 1	B/w groups	0.07	1	.066	0.20	.652	0.16	1	.159	0.47	.493	0.00	1	.002	0.01	.944
	Within groups	120.03	374	.321			127.11	376	.338			151.85	374	.406		
	Total	120.10	375				127.27	377				151.85	375			
CIP 2	B/w groups	15.47	1	15.468	56.76	**.000**	0.50	1	.502	1.96	.163	6.65	1	6.646	20.27	**.000**
	Within groups	101.92	374	.273			96.57	376	.257			122.64	374	.328		
	Total	117.38	375				97.07	377				129.29	375			
PL	B/w groups	13.39	1	13.393	31.75	**.000**	11.55	1	11.554	96.33	**.000**	0.54	1	.542	1.31	.253
	Within groups	157.76	374	.422			45.10	376	.120			154.68	374	.414		
	Total	171.15	375				56.65	377				155.22	375			

Table V-7.12 *Contd...*

		ANOVA (% glucan conversion)					ANOVA (% xylan conversion)					ANOVA (Total Sugars)				
		Sum of Squares	df	Mean Square	F	Sig.	Sum of Squares	df	Mean Square	F	Sig.	Sum of Squares	df	Mean Square	F	Sig.
PME	B/w groups	5.67	1	5.666	26.35	**.000**	4.63	1	4.626	43.91	**.000**	0.02	1	.022	0.11	.746
	Within groups	80.43	374	.215			39.61	376	.105			77.80	374	.208		
	Total	86.10	375				44.24	377				77.82	375			
RHAE	B/w groups	0.96	1	.960	10.66	**.001**	0.18	1	.179	2.03	.155	0.00	1	.001	0.01	.912
	Within groups	33.67	374	.090			33.10	376	.088			33.84	374	.090		
	Total	34.63	375				33.28	377				33.84	375			
ARH	B/w groups	0.33	1	.325	5.83	**.016**	0.91	1	.910	34.32	**.000**	0.00	1	.002	0.04	.838
	Within groups	20.85	374	.056			9.97	376	.027			21.96	374	.059		
	Total	21.17	375				10.88	377				21.96	375			
SWO	B/w groups	58.40	1	58.402	152.03	**.000**	0.01	1	.006	0.01	.907	21.68	1	21.679	42.25	**.000**
	Within groups	143.67	374	.384			155.98	376	.415			191.92	374	.513		
	Total	202.08	375				155.99	377				213.60	375			
BG 1	B/w groups	210.20	1	210.198	47.19	**.000**	63.45	1	63.450	13.81	**.000**	143.27	1	143.273	30.39	**.000**
	Within groups	1666.04	374	4.455			1727.36	376	4.594			1763.37	374	4.715		
	Total	1876.24	375				1790.81	377				1906.64	375			
BMANO	B/w groups	4.07	1	4.066	32.23	**.000**	0.83	1	.833	11.06	**.001**	1.07	1	1.074	8.28	**.004**
	Within groups	47.19	374	.126			28.32	376	.075			48.51	374	.130		
	Total	51.25	375				29.16	377				49.58	375			
BG 3	B/w groups	2665.72	1	2666	679.79	**.000**	142.71	1	142.715	13.80	**.000**	1411.25	1	1411	192.55	**.000**
	Within groups	1466.60	374	3.921			3889.37	376	10.344			2741.12	374	7.329		
	Total	4132.32	375				4032.09	377				4152.36	375			

Table V-7.12 *Contd...*

		ANOVA (% glucan conversion)					ANOVA (% xylan conversion)					ANOVA (Total Sugars)				
		Sum of Squares	df	Mean Square	F	Sig.	Sum of Squares	df	Mean Square	F	Sig.	Sum of Squares	df	Mean Square	F	Sig.
BX 3	B/w groups	2.88	1	2.876	2.56	.110	21.04	1	21.036	21.48	**.000**	0.19	1	.185	0.15	.697
	Within groups	420.20	374	1.124			368.17	376	.979			456.31	374	1.220		
	Total	423.08	375				389.20	377				456.49	375			
EG 2	B/w groups	81.33	1	81.329	51.81	**.000**	2.83	1	2.831	2.03	.155	54.77	1	54.769	30.30	**.000**
	Within groups	587.08	374	1.570			523.60	376	1.393			676.11	374	1.808		
	Total	668.40	375				526.43	377				730.88	375			
BM	B/w groups	2.56	1	2.560	6.97	**.009**	0.36	1	.355	0.99	.321	3.77	1	3.769	9.87	**.002**
	Within groups	137.25	374	.367			135.41	376	.360			142.80	374	.382		
	Total	139.81	375				135.76	377				146.57	375			
BGAL 2	B/w groups	2.60	1	2.595	67.28	**.000**	1.17	1	1.166	40.94	**.000**	2.32	1	2.317	57.23	**.000**
	Within groups	14.43	374	.039			10.71	376	.028			15.14	374	.040		
	Total	17.02	375				11.88	377				17.46	375			
CBH 2	B/w groups	174.02	1	174.021	29.80	**.000**	8.14	1	8.136	1.67	.198	67.67	1	67.666	9.28	**.002**
	Within groups	2184.27	374	5.840			1837.27	376	4.886			2727.32	374	7.292		
	Total	2358.29	375				1845.41	377				2794.98	375			
GH 6	B/w groups	5.85	1	5.848	80.00	**.000**	1.04	1	1.044	12.92	**.000**	3.20	1	3.199	40.90	**.000**
	Within groups	27.34	374	.073			30.38	376	.081			29.25	374	.078		
	Total	33.19	375				31.42	377				32.45	375			
CBH 1	B/w groups	255.18	1	255.175	7.86	**.005**	250.21	1	250.210	8.27	**.004**	7.42	1	7.418	0.17	.678
	Within groups	12139.8	374	32.459			11369.4	376	30.238			16061.5	374	42.945		
	Total	12395.0	375				11619.6	377				16068.9	375			

Table V-7.12 *Contd...*

		ANOVA (% glucan conversion)					ANOVA (% xylan conversion)					ANOVA (Total Sugars)				
		Sum of Squares	**df**	**Mean Square**	**F**	**Sig.**	**Sum of Squares**	**df**	**Mean Square**	**F**	**Sig.**	**Sum of Squares**	**df**	**Mean Square**	**F**	**Sig.**
EG 1	B/w groups	296.50	1	296.503	175.27	**.000**	0.26	1	.255	0.14	.708	114.11	1	114.113	47.05	**.000**
	Within groups	632.68	374	1.692			683.16	376	1.817			907.10	374	2.425		
	Total	929.19	375				683.42	377				1021.21	375			
EX 2	B/w groups	46.03	1	46.026	7.32	**.007**	74.35	1	74.351	11.45	**.001**	69.34	1	69.343	10.10	**.002**
	Within groups	2352.72	374	6.291			2441.74	376	6.494			2567.88	374	6.866		
	Total	2398.75	375				2516.09	377				2637.23	375			
EX 1	B/w groups	504.57	1	504.569	26.50	**.000**	241.52	1	241.523	20.98	**.000**	32.36	1	32.362	1.72	.191
	Within groups	7120.20	374	19.038			4329.07	376	11.513			7046.65	374	18.841		
	Total	7624.77	375				4570.59	377				7079.01	375			
EG 3	B/w groups	3.27	1	3.269	13.77	**.000**	1.36	1	1.356	6.18	**.013**	5.37	1	5.370	21.29	**.000**
	Within groups	88.77	374	.237			82.52	376	.219			94.32	374	.252		
	Total	92.04	375				83.87	377				99.69	375			
AMY	B/w groups	208.54	1	208.538	39.87	**.000**	0.44	1	.442	0.07	.793	101.70	1	101.703	21.02	**.000**
	Within groups	1956.33	374	5.231			2401.95	376	6.388			1809.18	374	4.837		
	Total	2164.87	375				2402.39	377				1910.88	375			
GAMY	B/w groups	119.35	1	119.354	3.90	**.049**	306.30	1	306.302	9.50	**.002**	398.65	1	398.646	12.52	**.000**
	Within groups	11434.7	374	30.574			12121.8	376	32.239			11911.2	374	31.848		
	Total	11554.1	375				12428.1	377				12309.9	375			
GH 16	B/w groups	18.63	1	18.634	15.03	**.000**	3.39	1	3.391	2.44	.119	4.88	1	4.878	4.19	**.041**
	Within groups	463.67	374	1.240			523.20	376	1.391			435.08	374	1.163		
	Total	482.30	375				526.59	377				439.96	375			

Table V-7.12 *Contd...*

		ANOVA (% glucan conversion)					ANOVA (% xylan conversion)					ANOVA (Total Sugars)				
		Sum of Squares	**df**	**Mean Square**	**F**	**Sig.**	**Sum of Squares**	**df**	**Mean Square**	**F**	**Sig.**	**Sum of Squares**	**df**	**Mean Square**	**F**	**Sig.**
GH 17	B/w groups	4.62	1	4.623	11.51	**.001**	1.89	1	1.887	4.94	**.027**	5.76	1	5.759	13.94	**.000**
	Within groups	150.18	374	.402			143.75	376	.382			154.55	374	.413		
	Total	154.80	375				145.64	377				160.30	375			
CHI 1	B/w groups	0.09	1	.086	20.14	**.000**	0.03	1	.033	7.74	**.006**	0.04	1	.040	8.62	**.004**
	Within groups	1.60	374	.004			1.59	376	.004			1.74	374	.005		
	Total	1.69	375				1.63	377				1.78	375			
CHI 2	B/w groups	0.28	1	.279	13.07	**.000**	0.01	1	.013	0.57	.451	0.29	1	.287	13.00	**.000**
	Within groups	7.98	374	.021			8.73	376	.023			8.27	374	.022		
	Total	8.26	375				8.74	377				8.55	375			
AGAL	B/w groups	3.22	1	3.221	17.70	**.000**	0.19	1	.186	1.17	.281	1.43	1	1.434	7.68	**.006**
	Within groups	68.05	374	.182			59.86	376	.159			69.82	374	.187		
	Total	71.27	375				60.05	377				71.25	375			
PGL	B/w groups	4.88	1	4.880	0.92	.337	22.67	1	22.673	4.31	**.039**	34.33	1	34.326	6.94	**.009**
	Within groups	1978.25	374	5.289			1978.53	376	5.262			1849.08	374	4.944		
	Total	1983.13	375				2001.20	377				1883.40	375			
GH 30	B/w groups	0.04	1	.037	4.53	**.034**	0.07	1	.067	7.20	**.008**	0.00	1	.000	0.04	.851
	Within groups	3.06	374	.008			3.51	376	.009			3.05	374	.008		
	Total	3.10	375				3.58	377				3.05	375			
AG	B/w groups	2.11	1	2.111	11.21	**.001**	2.96	1	2.963	34.80	**.000**	0.04	1	.036	0.18	.674
	Within groups	70.41	374	.188			32.01	376	.085			75.95	374	.203		
	Total	72.52	375				34.98	377				75.98	375			

Table V-7.12 *Contd...*

		ANOVA (% glucan conversion)					ANOVA (% xylan conversion)					ANOVA (Total Sugars)				
		Sum of Squares	df	Mean Square	F	Sig.	Sum of Squares	df	Mean Square	F	Sig.	Sum of Squares	df	Mean Square	F	Sig.
BFRC	B/w groups	0.04	1	.040	2.18	.141	0.01	1	.006	0.31	.578	0.01	1	.006	0.30	.583
	Within groups	6.81	374	.018			7.09	376	.019			7.14	374	.019		
	Total	6.85	375				7.09	377				7.14	375			
BGAL 1	B/w groups	42.80	1	42.796	26.32	.000	60.78	1	60.782	98.07	.000	0.74	1	.740	0.45	.501
	Within groups	608.01	374	1.626			233.05	376	.620			610.16	374	1.631		
	Total	650.81	375				293.83	377				610.90	375			
AA	B/w groups	6.01	1	6.006	20.65	.000	2.35	1	2.353	14.50	.000	1.07	1	1.068	3.35	.068
	Within groups	108.75	374	.291			61.01	376	.162			119.11	374	.318		
	Total	114.76	375				63.36	377				120.18	375			
EG 5	B/w groups	0.17	1	.170	93.76	.000	0.00	1	.001	0.62	.431	0.05	1	.049	21.36	.000
	Within groups	0.68	374	.002			0.90	376	.002			0.86	374	.002		
	Total	0.85	375				0.90	377				0.91	375			
AMANO 1	B/w groups	2.09	1	2.091	33.91	.000	0.65	1	.649	19.86	.000	0.42	1	.416	6.21	.013
	Within groups	23.06	374	.062			12.29	376	.033			25.03	374	.067		
	Total	25.15	375				12.94	377				25.44	375			
ABF 1	B/w groups	8.11	1	8.112	25.86	.000	6.69	1	6.685	64.08	.000	0.62	1	.617	1.97	.162
	Within groups	117.32	374	.314			39.22	376	.104			117.39	374	.314		
	Total	125.43	375				45.91	377				118.01	375			
ABGAL	B/w groups	3.69	1	3.686	25.93	.000	0.01	1	.015	0.10	.747	0.86	1	.856	5.41	.021
	Within groups	53.17	374	.142			53.43	376	.142			59.22	374	.158		
	Total	56.85	375				53.44	377				60.08	375			

Table V-7.12 *Contd...*

		ANOVA (% glucan conversion)					ANOVA (% xylan conversion)					ANOVA (Total Sugars)				
		Sum of Squares	**df**	**Mean Square**	**F**	**Sig.**	**Sum of Squares**	**df**	**Mean Square**	**F**	**Sig.**	**Sum of Squares**	**df**	**Mean Square**	**F**	**Sig.**
ABF 2	B/w groups	62.30	1	62.298	51.33	**.000**	37.66	1	37.664	96.05	**.000**	4.71	1	4.707	3.90	**.049**
	Within groups	453.94	374	1.214			147.44	376	.392			451.29	374	1.207		
	Total	516.24	375				185.11	377				456.00	375			
GH 55	B/w groups	0.90	1	.896	23.15	**.000**	0.70	1	.700	48.10	**.000**	0.08	1	.076	1.93	.166
	Within groups	14.48	374	.039			5.47	376	.015			14.65	374	.039		
	Total	15.37	375				6.17	377				14.72	375			
EG 4	B/w groups	27.01	1	27.008	102.75	**.000**	2.91	1	2.906	9.59	**.002**	14.66	1	14.656	51.23	**.000**
	Within groups	98.31	374	.263			113.88	376	.303			106.99	374	.286		
	Total	125.32	375				116.79	377				121.65	375			
EG 7	B/w groups	2.41	1	2.413	599.02	**.000**	0.07	1	.068	7.86	**.005**	1.12	1	1.123	159.65	**.000**
	Within groups	1.51	374	.004			3.26	376	.009			2.63	374	.007		
	Total	3.92	375				3.33	377				3.75	375			
ABF 3	B/w groups	11.47	1	11.473	63.74	**.000**	7.61	1	7.605	81.62	**.000**	0.57	1	.570	3.15	.077
	Within groups	67.32	374	.180			35.04	376	.093			67.72	374	.181		
	Total	78.79	375				42.64	377				68.29	375			
GH 65	B/w groups	0.06	1	.060	15.91	**.000**	0.11	1	.108	94.31	**.000**	0.00	1	.000	0.01	.921
	Within groups	1.42	374	.004			0.43	376	.001			1.41	374	.004		
	Total	1.48	375				0.54	377				1.41	375			
AGLUC	B/w groups	5.27	1	5.267	19.20	**.000**	0.70	1	.701	2.18	.141	3.26	1	3.257	9.52	**.002**
	Within groups	102.57	374	.274			121.16	376	.322			128.01	374	.342		
	Total	107.84	375				121.86	377				131.27	375			

Table V-7.12 *Contd...*

		ANOVA (% glucan conversion)					ANOVA (% xylan conversion)					ANOVA (Total Sugars)				
		Sum of Squares	**df**	**Mean Square**	**F**	**Sig.**	**Sum of Squares**	**df**	**Mean Square**	**F**	**Sig.**	**Sum of Squares**	**df**	**Mean Square**	**F**	**Sig.**
GH 71	B/w groups	0.01	1	.012	25.21	**.000**	0.01	1	.013	91.79	**.000**	0.00	1	.000	0.98	.323
	Within groups	0.18	374	.000			0.05	376	.000			0.18	374	.000		
	Total	0.19	375				0.07	377				0.18	375			
GT	B/w groups	1.42	1	1.418	6.99	**.009**	0.54	1	.539	2.79	.096	1.63	1	1.633	7.69	**.006**
	Within groups	75.90	374	.203			72.62	376	.193			79.43	374	.212		
	Total	77.32	375				73.16	377				81.06	375			
XG	B/w groups	25.88	1	25.884	2.69	.102	119.96	1	119.964	14.82	**.000**	7.63	1	7.631	0.72	.397
	Within groups	3596.30	374	9.616			3043.77	376	8.095			3970.55	374	10.616		
	Total	3622.19	375				3163.73	377				3978.19	375			
AMAN	B/w groups	0.00	1	.004	25.21	**.000**	0.00	1	.005	91.79	**.000**	0.00	1	.000	0.98	.323
	Within groups	0.06	374	.000			0.02	376	.000			0.06	374	.000		
	Total	0.07	375				0.02	377				0.06	375			
BGLUC	B/w groups	0.41	1	.408	25.21	**.000**	0.43	1	.432	91.79	**.000**	0.02	1	.016	0.98	.323
	Within groups	6.05	374	.016			1.77	376	.005			5.96	374	.016		
	Total	6.46	375				2.20	377				5.98	375			
GH 81	B/w groups	0.01	1	.012	25.21	**.000**	0.01	1	.013	91.79	**.000**	0.00	1	.000	0.98	.323
	Within groups	0.18	374	.000			0.05	376	.000			0.18	374	.000		
	Total	0.19	375				0.07	377				0.18	375			
AMANO 2	B/w groups	0.27	1	.271	23.76	**.000**	0.03	1	.032	3.90	**.049**	0.11	1	.105	8.79	**.003**
	Within groups	4.26	374	.011			3.11	376	.008			4.49	374	.012		
	Total	4.53	375				3.14	377				4.60	375			
OTHERS	B/w groups	627.65	1	627.651	5.68	**.018**	730.40	1	730.402	6.64	**.010**	838.95	1	838.954	6.88	**.009**
	Within groups	41309.6	374	110.453			41376.0	376	110.042			45589.0	374	121.896		
	Total	41937.2	375				42106.4	377				46427.9	375			

Table 7.13-C *Descriptive statistics (minima, maxima, mean, standard deviation) comparing top and bottom 25% quartile groups for individual protein components, based on varying total sugar hydrolysis yield. Values highlighted in bold signify statistical significance at p<0.05 level (based on Table 7.12), whereas values highlighted in red signify increase in corresponding protein component in top 25% quartile with respect to bottom quartile.*

Descriptive Statistics (Total Sugars)

	Bottom 25% (N = 188)				Top 25% (N = 188)				
Enzyme	**Minimum**	**Maximum**	**Mean**	**Std. Deviation**	**Minimum**	**Maximum**	**Mean**	**Std. Deviation**	**% Increase**
AC	0	4.41%	*0.61%*	0.77%	0%	**2%**	*0.45%*	**0.44%**	**-27%**
AXE 1	0	1%	*0.26%*	0.20%	0.14%	0.61%	*0.30%*	0.09%	**17%**
AXE 2	0	0.46%	*0.09%*	0.10%	0%	0.36%	*0.22%*	0.08%	**141%**
FAE	0	1.18%	*0.13%*	0.24%	0%	0.39%	*0.11%*	0.09%	**-18%**
CIP 1	0	2.67%	*1.17%*	0.80%	0.64%	2.52%	*1.17%*	0.42%	**0%**
CIP 2	0	3.01%	*1.06%*	0.77%	0.65%	2.25%	*1.33%*	0.25%	**25%**
PL	0	4.21%	*0.48%*	0.85%	0%	1%	*0.41%*	0.32%	**-16%**
PME	0	2.64%	*0.47%*	0.59%	0%	1%	*0.46%*	0.25%	**-3%**
RHAE	0	1.89%	*0.28%*	0.37%	0%	1%	*0.28%*	0.20%	**1%**
ARH	0	1.46%	*0.24%*	0.31%	0%	0.63%	*0.24%*	0.15%	**2%**
SWO	0	3.60%	*1.21%*	0.97%	0.80%	2.94%	*1.69%*	0.28%	**40%**
BG 1	0	13.08%	*2.03%*	2.88%	0%	4.36%	*0.80%*	1.06%	**-61%**
BMANO	0	1.99%	*0.36%*	0.48%	0%	0.66%	*0.25%*	0.16%	**-30%**
BG 3	0	15.56%	*4.01%*	2.78%	1.84%	10.62%	*7.88%*	2.63%	**97%**
BX 3	0	6.49%	*2.00%*	1.45%	0.46%	4.23%	*1.96%*	0.59%	**-2%**
EG 2	0.14%	7.64%	*3.74%*	1.81%	2.67%	7.05%	*4.50%*	0.59%	**20%**
BM	0	4.54%	*1%*	0.76%	0.48%	2.89%	*1.23%*	0.42%	**19%**
BGAL 2	0	1.47%	*0.32%*	0.25%	0.09%	0.88%	*0.48%*	0.13%	**49%**
CBH 2	0	13.37%	*6.54%*	3.61%	3.84%	13.02%	*7.39%*	1.24%	**13%**

Table 7.13-C *Contd...*

	Descriptive Statistics (Total Sugars)								
	Bottom 25% (N = 188)				Top 25% (N = 188)				
Enzyme	**Minimum**	**Maximum**	**Mean**	**Std. Deviation**	**Minimum**	**Maximum**	**Mean**	**Std. Deviation**	**% Increase**
GH 6	0	1.69%	*0.31%*	0.37%	0%	1%	*0.13%*	0.15%	**-59%**
CBH 1	0	34.74%	*15.24%*	8.69%	9.42%	29.26%	*15.52%*	3.23%	2%
EG 1	0	8.39%	*3.27%*	2.10%	2.14%	6.72%	*4.37%*	0.66%	**34%**
EX 2	0.33%	15.19%	*5.00%*	3.45%	0.44%	7.64%	*4.14%*	1.36%	**-17%**
EX 1	0	35.78%	*5.42%*	5.36%	0.91%	13.98%	*4.83%*	2.98%	-11%
EG 3	0	2.84%	*1.44%*	0.67%	0.74%	2.47%	*1.68%*	0.25%	**17%**
AMY	0	21.45%	*0.88%*	2.23%	0.08%	12.33%	*1.92%*	2.17%	**118%**
GAMY	0	49.31%	*4.87%*	7.59%	0.35%	14.39%	*2.81%*	2.47%	**-42%**
GH 16	0	9.39%	*0.90%*	1.18%	0%	5.50%	*1.12%*	0.96%	**25%**
GH 17	0	3.87%	*0.72%*	0.84%	0%	1.52%	*0.47%*	0.35%	**-34%**
CHI 1	0	0.38%	*0.17%*	0.09%	0.00%	0.32%	*0.19%*	0.04%	**12%**
CHI 2	0	1.20%	*0.18%*	0.20%	0%	0.46%	*0.12%*	0.07%	**-31%**
AGAL	0	3.09%	*0.52%*	0.58%	0%	1.06%	*0.40%*	0.20%	**-24%**
PGL	0	20.02%	*1.82%*	2.47%	0%	11%	*2.43%*	1.95%	**33%**
GH 30	0	0.70%	*0.08%*	0.11%	0%	0.41%	*0.08%*	0.07%	-2%
AG	0	2.75%	*0.45%*	0.58%	0%	1.19%	*0.44%*	0.26%	-4%
BFRC	0	1.02%	*0.13%*	0.18%	0%	0.37%	*0.14%*	0.09%	6%
BGAL 1	0	8.33%	*1.43%*	1.68%	0.05%	3.67%	*1.34%*	0.66%	-6%
AA	0	3.11%	*0.65%*	0.74%	0%	1.69%	*0.55%*	0.31%	-16%
EG 5	0	0.26%	*0.04%*	0.06%	0%	0%	*0.02%*	0.04%	**-54%**
AMANO 1	0	1.43%	*0.27%*	0.34%	0%	1%	*0.20%*	0.14%	**-25%**

Table 7.13-C *Contd...*

	Descriptive Statistics (Total Sugars)								
	Bottom 25% (N = 188)				Top 25% (N = 188)				
Enzyme	**Minimum**	**Maximum**	**Mean**	**Std. Deviation**	**Minimum**	**Maximum**	**Mean**	**Std. Deviation**	**% Increase**
ABF 1	0	3.59%	*0.42%*	0.74%	0%	1.20%	*0.34%*	0.28%	-19%
ABGAL	0	2.04%	*0.62%*	0.52%	0%	1%	*0.52%*	0.22%	**-15%**
ABF 2	0	7.41%	*1.11%*	1.46%	0%	2.78%	*0.89%*	0.54%	**-20%**
GH 55	0	1.26%	*0.17%*	0.26%	0%	0.46%	*0.14%*	0.10%	-17%
EG 4	0	3.38%	*0.83%*	0.69%	0.08%	1.58%	*0.43%*	0.31%	**-48%**
EG 7	0	0.46%	*0.10%*	0.10%	0.04%	0.28%	*0.21%*	0.06%	**105%**
ABF 3	0	2.81%	*0.72%*	0.55%	0.30%	1.60%	*0.64%*	0.24%	-11%
GH 65	0	0.39%	*0.04%*	0.08%	0%	0%	*0.04%*	0.03%	-2%
AGLUC	0	3.34%	*0.90%*	0.74%	0.13%	2.06%	*0.71%*	0.36%	**-21%**
GH 71	0	0.14%	*0.01%*	0.03%	0%	0%	*0.01%*	0.01%	-16%
GT	0	2.74%	*0.50%*	0.60%	0%	1.11%	*0.37%*	0.24%	**-26%**
XG	0	21.28%	*5.38%*	3.94%	1.89%	13.44%	*5.66%*	2.38%	5%
AMAN	0	0.08%	*0.01%*	0.02%	0%	0%	*0.01%*	0.01%	-16%
BGLUC	0	0.81%	*0.08%*	0.17%	0%	0%	*0.07%*	0.06%	-16%
GH 81	0	0.14%	*0.01%*	0.03%	0%	0%	*0.01%*	0.01%	-16%
AMANO 2	0	0.66%	*0.10%*	0.15%	0%	0.18%	*0.07%*	0.05%	**-33%**
OTHERS	2.03%	69.50%	*19.49%*	14.41%	2.53%	30.69%	*16.50%*	6.01%	**-15%**

Table V-7.14 *Comparing individual protein composition of CE 1, CE 4 to enzyme mixtures that gave the top 5% (N = 755) response for glucan, xylan and total sugar hydrolysis yields.*

				Mean			*Std Dev*						
Enzyme	**ce 1**	**ce 4**	**ce 1 + ce 4**	**G, top 5%**	**X, top 5%**	**TS, top 5%**	**G, top 5%**	**X, top 5%**	**TS, top 5%**	**% difference (G-top 5%) - (ce 1)**	**% difference (X-top 5%) - (ce 4)**	**% difference (TS-top 5%) - (ce 1)**	**% difference (TS-top 5%) - (ce1+ce4)**
AC	1.19	0	0.60	0.27	0.57	0.28	0.23	0.47	0.24	-342	**100**	-326	-113
AXE 1	0.65	0	0.33	0.27	0.32	0.28	0.05	0.09	0.05	-140	**100**	-133	-16
AXE 2	0.20	0	0.10	0.25	0.19	0.25	0.06	0.10	0.05	**20**	**100**	**21**	**60**
FAE	0	1.18	0.59	0.09	0.11	0.12	0.08	0.10	0.05	100	-947	**100**	-397
CIP 1	2.67	0	1.34	0.98	1.32	1.03	0.21	0.44	0.27	-171	**100**	-160	-30
CIP 2	3.01	0	1.51	1.25	1.34	1.30	0.14	0.28	0.13	-140	**100**	-131	-16
PL	0	4.21	2.10	0.32	0.45	0.43	0.27	0.35	0.14	100	-835	**100**	-389
PME	0	2.64	1.32	0.37	0.48	0.44	0.24	0.24	0.17	100	-449	**100**	-200
RHAE	0	0.51	0.25	0.22	0.30	0.24	0.19	0.18	0.18	100	-68	**100**	-5
ARH	0	1.46	0.73	0.25	0.23	0.28	0.12	0.15	0.09	100	-546	**100**	-165
SWO	3.18	0	1.59	1.71	1.60	1.76	0.14	0.43	0.08	-86	**100**	-81	10
BG 1	0	0	0	0.60	0.89	0.56	0.67	1.25	0.66	**100**	**100**	**100**	**100**
BMANO	0	1.99	1.00	0.24	0.24	0.24	0.12	0.17	0.10	100	-731	**100**	-308
BG 3	4.06	4.57	4.32	8.91	6.50	8.84	1.76	3.10	1.68	**54**	**30**	**54**	**51**
BX 3	3.01	3.96	3.48	1.70	2.06	1.79	0.34	0.68	0.34	-77	-93	-68	-94
EG 2	5.29	3.11	4.20	4.35	4.41	4.50	0.35	0.68	0.29	-21	**29**	-17	7
BM	1.39	0.45	0.92	1.11	1.24	1.16	0.38	0.34	0.37	-25	**64**	-20	21
BGAL 2	0.71	0	0.36	0.46	0.47	0.47	0.10	0.12	0.08	-55	**100**	-51	24

Table V-7.14 *Contd...*

				Mean			*Std Dev*						
Enzyme	**ce 1**	**ce 4**	**ce 1 + ce 4**	**G, top 5%**	**X, top 5%**	**TS, top 5%**	**G, top 5%**	**X, top 5%**	**TS, top 5%**	**% difference (G-top 5%) - (ce 1)**	**% difference (X-top 5%) - (ce 4)**	**% difference (TS-top 5%) - (ce 1)**	**% difference (TS-top 5%) - (ce1+ce4)**
CBH 2	10.43	0.25	5.34	7.08	7.47	7.22	0.61	1.45	0.62	-47	97	-44	26
GH 6	0	0	0	0.08	0.16	0.08	0.09	0.18	0.08	**100**	**100**	**100**	**100**
CBH 1	27.51	0.76	14.13	14.38	15.92	14.76	1.64	4.22	1.87	-91	95	-86	4
EG 1	7.47	0	3.74	4.40	4.17	4.51	0.38	0.98	0.16	-70	**100**	-66	17
EX 2	1.76	2.64	2.20	4.51	4.20	4.46	0.81	1.43	0.85	**61**	37	**61**	**51**
EX 1	2.64	1.80	2.22	3.94	5.53	3.86	1.80	3.59	1.61	**33**	**68**	**31**	**42**
EG 3	2.36	1.74	2.05	1.60	1.67	1.68	0.19	0.27	0.14	-48	-4	-40	-22
AMY	0.40	1.15	0.77	1.87	1.03	2.06	1.85	1.51	1.89	79	-11	**81**	62
GAMY	0	3.28	1.64	3.31	2.04	2.33	2.31	2.19	1.66	100	-61	**100**	30
GH 16	0	0.56	0.28	1.25	0.85	1.30	0.74	0.72	0.76	**100**	34	**100**	**78**
GH 17	0	0.70	0.35	0.62	0.57	0.57	0.26	0.37	0.17	100	-22	**100**	39
CHI 1	0.17	0.22	0.20	0.20	0.19	0.21	0.03	0.05	0.02	16	-20	**17**	4
CHI 2	0.31	0.34	0.32	0.12	0.12	0.10	0.06	0.06	0.04	-166	-192	-204	-216
AGAL	0.11	1.77	0.94	0.39	0.35	0.35	0.18	0.18	0.15	71	-407	**68**	-166
PGL	0.14	6.23	3.19	2.18	2.08	2.44	1.90	1.37	1.81	93	-199	**94**	-31
GH 30	0.17	0.08	0.13	0.08	0.05	0.08	0.07	0.05	0.06	-126	-59	-119	-63
AG	0	2.75	1.37	0.49	0.43	0.50	0.19	0.28	0.15	100	-542	**100**	-175
BFRC	0	0.34	0.17	0.17	0.10	0.14	0.08	0.07	0.07	100	-239	**100**	-18

Table V-7.14 *Contd...*

				Mean			*Std Dev*						
Enzyme	**ce 1**	**ce 4**	**ce 1 + ce 4**	**G, top 5%**	**X, top 5%**	**TS, top 5%**	**G, top 5%**	**X, top 5%**	**TS, top 5%**	**% difference (G-top 5%) - (ce 1)**	**% difference (X-top 5%) - (ce 4)**	**% difference (TS-top 5%) - (ce 1)**	**% difference (TS-top 5%) - (ce1+ce4)**
BGAL 1	2.27	8.33	5.30	1.09	1.41	1.31	0.55	0.67	0.34	-110	-490	-74	-306
AA	0	3.11	1.56	0.57	0.57	0.63	0.24	0.33	0.12	100	-445	**100**	-147
EG 5	0	0	0	0.01	0.03	0.01	0.03	0.04	0.02	**100**	**100**	**100**	**100**
AMANO 1	0	1.43	0.72	0.21	0.24	0.24	0.12	0.15	0.06	100	-496	**100**	-198
ABF 1	0	3.59	1.80	0.30	0.34	0.36	0.22	0.30	0.15	100	-947	**100**	-397
ABGAL	0	1.21	0.60	0.53	0.59	0.56	0.22	0.25	0.15	100	-104	**100**	-8
ABF 2	0.94	7.41	4.17	0.67	1.04	0.85	0.45	0.59	0.21	-39	-615	-10	-391
GH 55	0	1.26	0.63	0.13	0.13	0.14	0.08	0.11	0.06	100	-878	**100**	-345
EG 4	0.48	0.20	0.34	0.30	0.53	0.31	0.17	0.38	0.16	-58	**63**	-57	-11
EG 7	0.23	0	0.11	0.24	0.18	0.24	0.04	0.08	0.03	**4**	**100**	**5**	**52**
ABF 3	0.97	2.81	1.89	0.50	0.76	0.58	0.18	0.26	0.10	-95	-271	-66	-224
GH 65	0	0.39	0.20	0.04	0.04	0.04	0.03	0.04	0.02	100	-882	**100**	-391
AGLUC	2.39	1.37	1.88	0.52	0.84	0.59	0.18	0.39	0.22	-355	-63	-304	-219
GH 71	0	0.14	0.07	0.01	0.01	0.01	0.01	0.01	0.01	100	-1303	**100**	-601
GT	0	0.59	0.29	0.49	0.44	0.46	0.19	0.27	0.12	100	-34	**100**	36
XG	11.31	0.70	6.01	4.63	6.48	4.84	1.14	2.26	1.28	-144	**89**	-134	-24
AMAN	0	0.08	0.04	0.01	0.01	0.01	0.01	0.01	0.00	100	-742	**100**	-321
BGLUC	0	0.81	0.41	0.06	0.07	0.08	0.06	0.07	0.03	100	-1062	**100**	-409
GH 81	0	0.14	0.07	0.01	0.01	0.01	0.01	0.01	0.01	100	-1303	**100**	-601
AMANO 2	0	0.53	0.27	0.07	0.06	0.07	0.04	0.05	0.03	100	-809	**100**	-304
OTHERS	2.56	20.01	11.28	20.39	17.15	18.87	4.00	6.67	2.90	87	-17	**86**	40

Table V-7.15 *Raw data for % glucan, % xylan and total sugar hydrolysis yield for all enzyme mixtures tested.*

Mix #	re 1	re 2	re 3	re 4	re 5	re 6	re 7	re 8	ce 1	ce 2	ce 3	ce 4	ce 5	ce 6	% G	% X	TS
1	0%		0%		0%	0%	0%			48%	0%	0%		52%	51.7	20.0	247.0
2	0%		0%		0%	0%	0%			0%	48%	0%		52%	64.2	54.5	380.5
3	0%		0%		0%	0%	0%			0%	0%	48%		52%	59.2	60.0	375.0
4	48%		0%		0%	0%	0%			0%	0%	0%		52%	63.8	17.7	287.6
5	0%		48%		0%	0%	0%			0%	0%	0%		52%	50.1	11.9	221.1
6	0%		0%		48%	0%	0%			0%	0%	0%		52%	70.2	17.0	310.4
7	0%		0%		0%	48%	0%			0%	0%	0%		52%	45.7	9.4	198.0
8	0%		0%		0%	0%	48%			0%	0%	0%		52%	74.8	19.6	334.4
9	0%		0%		0%	0%	0%			24%	24%	0%		52%	67.3	52.3	387.0
10	0%		0%		0%	0%	0%			24%	0%	24%		52%	57.2	57.1	360.2
11	24%		0%		0%	0%	0%			24%	0%	0%		52%	67.4	21.9	311.6
12	0%		24%		0%	0%	0%			24%	0%	0%		52%	52.0	18.7	245.1
13	0%		0%		24%	0%	0%			24%	0%	0%		52%	70.2	23.1	325.6
14	0%		0%		0%	24%	0%			24%	0%	0%		52%	48.4	14.9	222.0
15	0%		0%		0%	0%	24%			24%	0%	0%		52%	79.2	26.5	368.2
16	0%		0%		0%	0%	0%			0%	24%	24%		52%	68.3	67.6	429.1
17	24%		0%		0%	0%	0%			0%	24%	0%		52%	67.4	63.3	414.9
18	0%		24%		0%	0%	0%			0%	24%	0%		52%	66.7	50.4	380.0
19	0%		0%		24%	0%	0%			0%	24%	0%		52%	70.5	55.7	407.7
20	0%		0%		0%	24%	0%			0%	24%	0%		52%	64.7	51.4	374.8
21	0%		0%		0%	0%	24%			0%	24%	0%		52%	78.0	62.2	452.6
22	24%		0%		0%	0%	0%			0%	0%	24%		52%	70.9	72.0	449.8
23	0%		24%		0%	0%	0%			0%	0%	24%		52%	58.9	58.4	370.2
24	0%		0%		24%	0%	0%			0%	0%	24%		52%	72.6	68.5	447.7
25	0%		0%		0%	24%	0%			0%	0%	24%		52%	52.0	52.6	329.4
26	0%		0%		0%	0%	24%			0%	0%	24%		52%	81.3	73.6	493.6
27	24%		24%		0%	0%	0%			0%	0%	0%		52%	65.3	13.3	282.4
28	24%		0%		24%	0%	0%			0%	0%	0%		52%	70.3	19.2	316.1
29	24%		0%		0%	24%	0%			0%	0%	0%		52%	62.6	13.6	273.1

Table V-7.15 *Contd...*

Mix #	re 1	re 2	re 3	re 4	re 5	re 6	re 7	re 8	ce 1	ce 2	ce 3	ce 4	ce 5	ce 6	% G	% X	TS
30	24%		0%		0%	0%	24%			0%	0%	0%		52%	78.2	23.4	356.9
31	0%		24%		24%	0%	0%			0%	0%	0%		52%	70.9	16.9	312.9
32	0%		24%		0%	24%	0%			0%	0%	0%		52%	51.4	10.7	222.8
33	0%		24%		0%	0%	24%			0%	0%	0%		52%	80.0	20.8	356.9
34	0%		0%		24%	24%	0%			0%	0%	0%		52%	68.2	15.9	299.8
35	0%		0%		24%	0%	24%			0%	0%	0%		52%	80.9	21.9	363.3
36	0%		0%		0%	24%	24%			0%	0%	0%		52%	76.8	18.5	339.1
37	0%		0%		0%	0%	0%			16%	16%	16%		52%	66.2	64.0	412.1
38	16%		0%		0%	0%	0%			16%	16%	0%		52%	71.1	58.2	416.1
39	0%		16%		0%	0%	0%			16%	16%	0%		52%	68.9	50.0	387.4
40	0%		0%		16%	0%	0%			16%	16%	0%		52%	75.8	56.1	429.0
41	0%		0%		0%	16%	0%			16%	16%	0%		52%	66.9	50.5	381.1
42	0%		0%		0%	0%	16%			16%	16%	0%		52%	83.4	61.9	472.4
43	16%		0%		0%	0%	0%			16%	0%	16%		52%	71.4	66.2	437.3
44	0%		16%		0%	0%	0%			16%	0%	16%		52%	59.2	55.4	363.7
45	0%		0%		16%	0%	0%			16%	0%	16%		52%	76.9	73.2	475.9
46	0%		0%		0%	16%	0%			16%	0%	16%		52%	56.8	52.7	347.9
47	0%		0%		0%	0%	16%			16%	0%	16%		52%	84.5	74.3	507.6
48	16%		16%		0%	0%	0%			16%	0%	0%		52%	67.8	19.3	306.7
49	16%		0%		16%	0%	0%			16%	0%	0%		52%			
50	16%		0%		0%	16%	0%			16%	0%	0%		52%	63.7	21.5	296.8
51	16%		0%		0%	0%	16%			16%	0%	0%		52%	83.2	32.0	397.3
52	0%		16%		16%	0%	0%			16%	0%	0%		52%	73.9	21.6	336.0
53	0%		16%		0%	16%	0%			16%	0%	0%		52%	51.9	16.7	239.8
54	0%		16%		0%	0%	16%			16%	0%	0%		52%	82.3	24.8	375.9
55	0%		0%		16%	16%	0%			16%	0%	0%		52%	74.6	21.8	339.0
56	0%		0%		16%	0%	16%			16%	0%	0%		52%	86.3	28.8	401.3
57	0%		0%		0%	16%	16%			16%	0%	0%		52%	82.3	25.0	376.4
58	16%		0%		0%	0%	0%			0%	16%	16%		52%	74.3	77.7	477.0

Table V-7.15 *Contd...*

Mix #	re 1	re 2	re 3	re 4	re 5	re 6	re 7	re 8	ce 1	ce 2	ce 3	ce 4	ce 5	ce 6	% G	% X	TS
59	0%		16%		0%	0%	0%			0%	16%	16%		52%	69.7	67.5	433.7
60	0%		0%		16%	0%	0%			0%	16%	16%		52%	75.2	72.6	467.6
61	0%		0%		0%	16%	0%			0%	16%	16%		52%	63.4	61.1	394.0
62	0%		0%		0%	0%	16%			0%	16%	16%		52%	83.6	76.2	508.7
63	16%		16%		0%	0%	0%			0%	16%	0%		52%	71.1	60.5	422.1
64	16%		0%		16%	0%	0%			0%	16%	0%		52%	72.6	62.4	432.5
65	16%		0%		0%	16%	0%			0%	16%	0%		52%	67.3	58.0	401.3
66	16%		0%		0%	0%	16%			0%	16%	0%		52%	82.7	66.7	481.8
67	0%		16%		16%	0%	0%			0%	16%	0%		52%	72.6	53.0	408.9
68	0%		16%		0%	16%	0%			0%	16%	0%		52%	66.2	49.4	375.6
69	0%		16%		0%	0%	16%			0%	16%	0%		52%	82.2	62.1	468.5
70	0%		0%		16%	16%	0%			0%	16%	0%		52%	68.6	54.0	396.2
71	0%		0%		16%	0%	16%			0%	16%	0%		52%	82.2	64.1	473.1
72	0%		0%		0%	16%	16%			0%	16%	0%		52%	76.0	55.1	427.2
73	16%		16%		0%	0%	0%			0%	0%	16%		52%	63.7	61.2	395.2
74	16%		0%		16%	0%	0%			0%	0%	16%		52%	74.5	73.3	466.7
75	16%		0%		0%	16%	0%			0%	0%	16%		52%	65.3	66.3	414.1
76	16%		0%		0%	0%	16%			0%	0%	16%		52%	82.1	78.6	508.9
77	0%		16%		16%	0%	0%			0%	0%	16%		52%	73.9	70.1	456.4
78	0%		16%		0%	16%	0%			0%	0%	16%		52%	56.7	56.5	357.0
79	0%		16%		0%	0%	16%			0%	0%	16%		52%	81.2	72.7	491.0
80	0%		0%		16%	16%	0%			0%	0%	16%		52%	73.6	72.2	460.7
81	0%		0%		16%	0%	16%			0%	0%	16%		52%	85.9	80.7	528.7
82	0%		0%		0%	16%	16%			0%	0%	16%		52%	83.4	74.0	502.5
83	16%		16%		16%	0%	0%			0%	0%	0%		52%	71.8	17.8	318.4
84	16%		16%		0%	16%	0%			0%	0%	0%		52%	61.5	13.8	268.9
85	16%		16%		0%	0%	16%			0%	0%	0%		52%	77.1	20.7	345.9
86	16%		0%		16%	16%	0%			0%	0%	0%		52%	69.1	18.0	308.5
87	16%		0%		16%	0%	16%			0%	0%	0%		52%	78.5	22.7	356.2

Table V-7.15 *Contd...*

Mix #	re 1	re 2	re 3	re 4	re 5	re 6	re 7	re 8	ce 1	ce 2	ce 3	ce 4	ce 5	ce 6	% G	% X	TS
88	16%		0%		0%	16%	16%			0%	0%	0%		52%	77.8	22.5	352.9
89	0%		16%		16%	16%	0%			0%	0%	0%		52%	70.6	14.9	306.7
90	0%		16%		16%	0%	16%			0%	0%	0%		52%	82.1	19.4	361.9
91	0%		16%		0%	16%	16%			0%	0%	0%		52%	77.8	18.0	341.9
92	0%		0%		16%	16%	16%			0%	0%	0%		52%	79.8	19.1	352.2
93	12%		0%		0%	0%	0%			12%	12%	12%		52%	75.0	68.6	456.7
94	0%		12%		0%	0%	0%			12%	12%	12%		52%	66.8	63.7	413.4
95	0%		0%		12%	0%	0%			12%	12%	12%		52%	75.9	68.3	459.6
96	0%		0%		0%	12%	0%			12%	12%	12%		52%	70.7	63.6	427.9
97	0%		0%		0%	0%	12%			12%	12%	12%		52%	80.4	70.7	482.8
98	12%		12%		0%	0%	0%			12%	12%	0%		52%	70.9	52.8	401.8
99	12%		0%		12%	0%	0%			12%	12%	0%		52%	76.4	56.6	432.3
100	12%		0%		0%	12%	0%			12%	12%	0%		52%	72.5	55.0	413.4
101	12%		0%		0%	0%	12%			12%	12%	0%		52%	85.4	58.1	470.6
102	0%		12%		12%	0%	0%			12%	12%	0%		52%	76.2	52.3	420.9
103	0%		12%		0%	12%	0%			12%	12%	0%		52%	71.6	48.7	394.5
104	0%		12%		0%	0%	12%			12%	12%	0%		52%	83.4	59.0	465.0
105	0%		0%		12%	12%	0%			12%	12%	0%		52%	74.5	52.8	416.0
106	0%		0%		12%	0%	12%			12%	12%	0%		52%	87.3	60.8	484.6
107	0%		0%		0%	12%	12%			12%	12%	0%		52%	82.8	57.6	459.5
108	12%		12%		0%	0%	0%			12%	0%	12%		52%	67.6	61.7	411.7
109	12%		0%		12%	0%	0%			12%	0%	12%		52%	78.9	72.4	481.2
110	12%		0%		0%	12%	0%			12%	0%	12%		52%	65.9	62.0	405.9
111	12%		0%		0%	0%	12%			12%	0%	12%		52%	83.8	73.5	502.9
112	0%		12%		12%	0%	0%			12%	0%	12%		52%	75.6	69.5	461.7
113	0%		12%		0%	12%	0%			12%	0%	12%		52%	58.2	52.2	351.9
114	0%		12%		0%	0%	12%			12%	0%	12%		52%	82.4	68.8	486.0
115	0%		0%		12%	12%	0%			12%	0%	12%		52%	74.7	67.1	452.1

Table V-7.15 *Contd...*

Mix #	re 1	re 2	re 3	re 4	re 5	re 6	re 7	re 8	ce 1	ce 2	ce 3	ce 4	ce 5	ce 6	% G	% X	TS
116	0%		0%		12%	0%	12%			12%	0%	12%		52%			
117	0%		0%		0%	12%	12%			12%	0%	12%		52%	83.3	70.1	492.4
118	12%		12%		12%	0%	0%			12%	0%	0%		52%	78.5	20.3	350.2
119	12%		12%		0%	12%	0%			12%	0%	0%		52%	63.2	16.2	281.7
120	12%		12%		0%	0%	12%			12%	0%	0%		52%	80.5	22.7	364.0
121	12%		0%		12%	12%	0%			12%	0%	0%		52%	71.8	19.3	322.4
122	12%		0%		12%	0%	12%			12%	0%	0%		52%	82.8	24.6	377.3
123	12%		0%		0%	12%	12%			12%	0%	0%		52%	82.7	23.3	373.7
124	0%		12%		12%	12%	0%			12%	0%	0%		52%	73.4	18.8	327.1
125	0%		12%		12%	0%	12%			12%	0%	0%		52%	86.3	23.5	388.1
126	0%		12%		0%	12%	12%			12%	0%	0%		52%	84.2	21.6	375.3
127	0%		0%		12%	12%	12%			12%	0%	0%		52%	84.7	23.1	380.6
128	12%		12%		0%	0%	0%			0%	12%	12%		52%	74.5	70.8	460.5
129	12%		0%		12%	0%	0%			0%	12%	12%		52%	77.0	74.9	480.1
130	12%		0%		0%	12%	0%			0%	12%	12%		52%	73.3	71.1	456.8
131	12%		0%		0%	0%	12%			0%	12%	12%		52%	85.1	79.2	521.9
132	0%		12%		12%	0%	0%			0%	12%	12%		52%	76.4	70.5	466.9
133	0%		12%		0%	12%	0%			0%	12%	12%		52%	71.0	70.8	447.0
134	0%		12%		0%	0%	12%			0%	12%	12%		52%	83.5	74.8	505.0
135	0%		0%		12%	12%	0%			0%	12%	12%		52%	77.8	74.9	483.5
136	0%		0%		12%	0%	12%			0%	12%	12%		52%	85.4	80.8	527.2
137	0%		0%		0%	12%	12%			0%	12%	12%		52%	85.2	80.4	525.3
138	12%		12%		12%	0%	0%			0%	12%	0%		52%	75.3	62.2	442.2
139	12%		12%		0%	12%	0%			0%	12%	0%		52%	73.1	57.0	420.8
140	12%		12%		0%	0%	12%			0%	12%	0%		52%	85.1	66.0	489.0
141	12%		0%		12%	12%	0%			0%	12%	0%		52%	71.4	59.2	419.9
142	12%		0%		12%	0%	12%			0%	12%	0%		52%	84.8	68.7	494.4
143	12%		0%		0%	12%	12%			0%	12%	0%		52%	81.2	62.7	465.9

Table V-7.15 *Contd...*

Mix #	re 1	re 2	re 3	re 4	re 5	re 6	re 7	re 8	ce 1	ce 2	ce 3	ce 4	ce 5	ce 6	% G	% X	TS
144	0%		12%		12%	12%	0%			0%	12%	0%		52%	68.5	49.3	384.3
145	0%		12%		12%	0%	12%			0%	12%	0%		52%	76.8	50.9	419.8
146	0%		12%		0%	12%	12%			0%	12%	0%		52%	75.8	52.5	420.1
147	0%		0%		12%	12%	12%			0%	12%	0%		52%	76.8	54.9	429.9
148	12%		12%		12%	0%	0%			0%	0%	12%		52%	78.7	73.8	484.0
149	12%		12%		0%	12%	0%			0%	0%	12%		52%	66.9	62.6	411.0
150	12%		12%		0%	0%	12%			0%	0%	12%		52%	86.8	74.2	516.1
151	12%		0%		12%	12%	0%			0%	0%	12%		52%	78.4	73.1	481.3
152	12%		0%		12%	0%	12%			0%	0%	12%		52%	88.0	79.8	534.4
153	12%		0%		0%	12%	12%			0%	0%	12%		52%	82.7	72.7	496.7
154	0%		12%		12%	12%	0%			0%	0%	12%		52%	76.6	69.7	465.5
155	0%		12%		12%	0%	12%			0%	0%	12%		52%	85.7	76.8	518.2
156	0%		12%		0%	12%	12%			0%	0%	12%		52%	81.7	70.2	486.6
157	0%		0%		12%	12%	12%			0%	0%	12%		52%	78.6	72.4	480.0
158	12%		12%		12%	12%	0%			0%	0%	0%		52%	69.1	16.8	305.7
159	12%		12%		12%	0%	12%			0%	0%	0%		52%	79.2	23.8	361.5
160	12%		12%		0%	12%	12%			0%	0%	0%		52%	79.1	21.6	355.7
161	12%		0%		12%	12%	12%			0%	0%	0%		52%	76.1	21.9	345.0
162	0%		12%		12%	12%	12%			0%	0%	0%		52%	78.1	21.4	351.5
163	10%		10%		0%	0%	0%			10%	10%	10%		52%	75.7	72.9	470.4
164	10%		0%		10%	0%	0%			10%	10%	10%		52%	76.3	71.6	469.4
165	10%		0%		0%	10%	0%			10%	10%	10%		52%	74.4	71.4	461.7
166	10%		0%		0%	0%	10%			10%	10%	10%		52%	86.8	76.5	521.6
167	0%		10%		10%	0%	0%			10%	10%	10%		52%	79.1	70.9	478.5
168	0%		10%		0%	10%	0%			10%	10%	10%		52%	71.3	63.2	429.4
169	0%		10%		0%	0%	10%			10%	10%	10%		52%	81.2	69.1	482.0
170	0%		0%		10%	10%	0%			10%	10%	10%		52%	75.4	69.3	460.0
171	0%		0%		10%	0%	10%			10%	10%	10%		52%	85.4	74.7	511.7

Table V-7.15 *Contd...*

Mix #	re 1	re 2	re 3	re 4	re 5	re 6	re 7	re 8	ce 1	ce 2	ce 3	ce 4	ce 5	ce 6	% G	% X	TS
172	0%		0%		0%	10%	10%			10%	10%	10%		52%	83.5	72.6	499.4
173	10%		10%		10%	0%	0%			10%	10%	0%		52%	75.9	53.0	421.5
174	10%		10%		0%	10%	0%			10%	10%	0%		52%	66.7	45.4	367.5
175	10%		10%		0%	0%	10%			10%	10%	0%		52%	80.9	51.4	436.8
176	10%		0%		10%	10%	0%			10%	10%	0%		52%	71.0	49.4	393.7
177	10%		0%		10%	0%	10%			10%	10%	0%		52%	82.8	53.6	449.4
178	10%		0%		0%	10%	10%			10%	10%	0%		52%	79.8	53.9	438.7
179	0%		10%		10%	10%	0%			10%	10%	0%		52%	72.1	44.6	386.0
180	0%		10%		10%	0%	10%			10%	10%	0%		52%	83.8	53.2	452.3
181	0%		10%		0%	10%	10%			10%	10%	0%		52%	82.5	52.3	445.3
182	0%		0%		10%	10%	10%			10%	10%	0%		52%	85.4	54.4	461.1
183	10%		10%		10%	0%	0%			10%	0%	10%		52%	76.5	68.3	462.1
184	10%		10%		0%	10%	0%			10%	0%	10%		52%	67.0	57.8	399.8
185	10%		10%		0%	0%	10%			10%	0%	10%		52%	79.8	67.6	472.8
186	10%		0%		10%	10%	0%			10%	0%	10%		52%	71.3	65.4	434.9
187	10%		0%		10%	0%	10%			10%	0%	10%		52%	83.3	72.6	498.6
188	10%		0%		0%	10%	10%			10%	0%	10%		52%	81.8	72.0	491.1
189	0%		10%		10%	10%	0%			10%	0%	10%		52%	72.2	64.1	435.0
190	0%		10%		10%	0%	10%			10%	0%	10%		52%	81.7	70.8	488.1
191	0%		10%		0%	10%	10%			10%	0%	10%		52%	81.3	68.1	479.8
192	0%		0%		10%	10%	10%			10%	0%	10%		52%	83.7	72.8	500.7
193	10%		10%		10%	10%	0%			10%	0%	0%		52%	73.6	18.7	327.4
194	10%		10%		10%	0%	10%			10%	0%	0%		52%	84.9	24.8	385.8
195	10%		10%		0%	10%	10%			10%	0%	0%		52%	82.2	20.9	366.0
196	10%		0%		10%	10%	10%			10%	0%	0%		52%	85.9	22.1	383.0
197	0%		10%		10%	10%	10%			10%	0%	0%		52%	81.7	21.0	364.1
198	10%		10%		10%	0%	0%			0%	10%	10%		52%	72.9	69.8	451.8
199	10%		10%		0%	10%	0%			0%	10%	10%		52%	68.1	64.6	420.8

Table V-7.15 *Contd...*

Mix #	re 1	re 2	re 3	re 4	re 5	re 6	re 7	re 8	ce 1	ce 2	ce 3	ce 4	ce 5	ce 6	% G	% X	TS
200	10%		10%		0%	0%	10%			0%	10%	10%		52%	80.0	71.4	483.3
201	10%		0%		10%	10%	0%			0%	10%	10%		52%	73.6	70.4	455.8
202	10%		0%		10%	0%	10%			0%	10%	10%		52%	85.2	77.6	518.4
203	10%		0%		0%	10%	10%			0%	10%	10%		52%	82.7	73.9	499.6
204	0%		10%		10%	10%	0%			0%	10%	10%		52%	76.2	71.0	467.6
205	0%		10%		10%	0%	10%			0%	10%	10%		52%	85.4	77.6	518.9
206	0%		10%		0%	10%	10%			0%	10%	10%		52%	81.6	72.5	491.7
207	0%		0%		10%	10%	10%			0%	10%	10%		52%	85.6	77.1	518.7
208	10%		10%		10%	10%	0%			0%	10%	0%		52%	74.1	48.9	404.4
209	10%		10%		10%	0%	10%			0%	10%	0%		52%	78.6	51.4	428.1
210	10%		10%		0%	10%	10%			0%	10%	0%		52%	75.7	47.9	408.0
211	10%		0%		10%	10%	10%			0%	10%	0%		52%	75.7	52.0	418.3
212	0%		10%		10%	10%	10%			0%	10%	0%		52%	79.8	53.0	436.7
213	10%		10%		10%	10%	0%			0%	0%	10%		52%	74.9	68.6	456.6
214	10%		10%		10%	0%	10%			0%	0%	10%		52%	85.4	77.0	517.5
215	10%		10%		0%	10%	10%			0%	0%	10%		52%	81.7	78.7	507.6
216	10%		0%		10%	10%	10%			0%	0%	10%		52%	83.8	74.3	504.7
217	0%		10%		10%	10%	10%			0%	0%	10%		52%	83.3	74.8	504.0
218	10%		10%		10%	10%	10%			0%	0%	0%		52%	79.8	18.7	351.3
219	8%		8%		8%	0%	0%			8%	8%	8%		52%	75.9	69.0	461.3
220	8%		8%		0%	8%	0%			8%	8%	8%		52%	70.5	63.4	427.0
221	8%		8%		0%	0%	8%			8%	8%	8%		52%	83.1	71.7	495.4
222	8%		0%		8%	8%	0%			8%	8%	8%		52%	70.6	63.8	428.0
223	8%		0%		8%	0%	8%			8%	8%	8%		52%	82.6	74.1	499.7
224	8%		0%		0%	8%	8%			8%	8%	8%		52%	83.2	74.2	502.1
225	0%		8%		8%	8%	0%			8%	8%	8%		52%	73.5	67.5	448.4
226	0%		8%		8%	0%	8%			8%	8%	8%		52%	86.2	76.9	520.5
227	0%		8%		0%	8%	8%			8%	8%	8%		52%	85.7	74.6	512.6

Table V-7.15 *Contd...*

Mix #	re 1	re 2	re 3	re 4	re 5	re 6	re 7	re 8	ce 1	ce 2	ce 3	ce 4	ce 5	ce 6	% G	% X	TS
228	0%		0%		8%	8%	8%			8%	8%	8%		52%	85.7	77.3	519.5
229	8%		8%		8%	8%	0%			8%	8%	0%		52%	74.7	47.7	403.7
230	8%		8%		8%	0%	8%			8%	8%	0%		52%	82.6	47.8	434.3
231	8%		8%		0%	8%	8%			8%	8%	0%		52%	83.2	49.2	440.2
232	8%		0%		8%	8%	8%			8%	8%	0%		52%	85.6	54.5	462.3
233	0%		8%		8%	8%	8%			8%	8%	0%		52%	78.2	45.1	410.7
234	8%		8%		8%	8%	0%			8%	0%	8%		52%	71.2	62.7	427.9
235	8%		8%		8%	0%	8%			8%	0%	8%		52%	83.3	71.4	495.7
236	8%		8%		0%	8%	8%			8%	0%	8%		52%	82.0	67.8	481.8
237	8%		0%		8%	8%	8%			8%	0%	8%		52%	85.2	72.4	505.3
238	0%		8%		8%	8%	8%			8%	0%	8%		52%	85.5	71.4	504.1
239	8%		8%		8%	8%	8%			8%	0%	0%		52%	85.1	21.4	378.2
240	8%		8%		8%	8%	0%			0%	8%	8%		52%	75.5	70.6	463.7
241	8%		8%		8%	0%	8%			0%	8%	8%		52%	86.6	75.1	517.4
242	8%		8%		0%	8%	8%			0%	8%	8%		52%	81.4	73.4	493.2
243	8%		0%		8%	8%	8%			0%	8%	8%		52%	83.4	75.6	506.5
244	0%		8%		8%	8%	8%			0%	8%	8%		52%	84.2	73.4	504.0
245	8%		8%		8%	8%	8%			0%	8%	0%		52%	77.6	45.2	408.6
246	8%		8%		8%	8%	8%			0%	0%	8%		52%	81.4	72.0	489.8
247	7%		7%		7%	7%	0%			7%	7%	7%		52%	74.6	68.4	454.9
248	7%		7%		7%	0%	7%			7%	7%	7%		52%	84.3	75.6	509.8
249	7%		7%		0%	7%	7%			7%	7%	7%		52%	84.7	73.4	505.9
250	7%		0%		7%	7%	7%			7%	7%	7%		52%	84.6	75.6	511.2
251	0%		7%		7%	7%	7%			7%	7%	7%		52%	85.8	76.0	516.5
252	7%		7%		7%	7%	7%			7%	7%	0%		52%	83.3	49.0	439.8
253	7%		7%		7%	7%	7%			7%	0%	7%		52%	88.0	73.5	519.0
254	7%		7%		7%	7%	7%			0%	7%	7%		52%	81.7	74.4	497.0
255	6%		6%		6%	6%	6%			6%	6%	6%		52%	87.6	76.1	523.7

Table V-7.15 *Contd...*

Mix #	re 1	re 2	re 3	re 4	re 5	re 6	re 7	re 8	ce 1	ce 2	ce 3	ce 4	ce 5	ce 6	% G	% X	TS
256	3%		3%		3%	3%	3%			27%	3%	3%		52%	86.4	64.9	491.2
257	3%		3%		3%	3%	3%			3%	27%	3%		52%	79.9	67.5	472.8
258	3%		3%		3%	3%	3%			3%	3%	27%		52%	79.2	73.2	484.4
259	27%		3%		3%	3%	3%			3%	3%	3%		52%	79.2	61.3	454.5
260	3%		27%		3%	3%	3%			3%	3%	3%		52%	79.4	59.6	451.3
261	3%		3%		27%	3%	3%			3%	3%	3%		52%	82.3	60.8	465.4
262	3%		3%		3%	27%	3%			3%	3%	3%		52%	77.8	57.3	439.2
263	3%		3%		3%	3%	27%			3%	3%	3%		52%	79.9	63.2	462.1
ce1.A1.a1	0%						0%		100%			0%	0%		46.4	6.8	194.3
ce1.A1.a2	0%						0%		0%			100%	0%		19.4	43.2	181.4
ce1.A1.a3	0%						0%		0%			0%	100%		24.5		
ce1.A1.a4	100%						0%		0%			0%	0%		20.4	3.2	85.9
ce1.A1.a5	0%						100%		0%			0%	0%		3.6	5.4	27.0
ce1.A1.a6	0%						0%		50%			50%	0%		60.8	52.5	362.7
ce1.A1.a7	0%						0%		50%			0%	50%		37.0	1.3	144.5
ce1.A1.a8	50%						0%		50%			0%	0%		41.7	3.1	167.0
ce1.A1.a9	0%						50%		50%			0%	0%		34.7	3.9	142.3
ce1.A1.a10	0%						0%		0%			50%	50%		31.7	44.3	231.3
ce1.A1.a11	50%						0%		0%			50%	0%		34.4	52.8	262.6
ce1.A1.a12	0%						50%		0%			50%	0%		14.5	51.8	184.1
ce1.A1.b1	50%						0%		0%			0%	50%		25.2	5.3	109.4
ce1.A1.b2	0%						50%		0%			0%	50%		18.8	7.7	90.8
ce1.A1.b3	50%						50%		0%			0%	0%		14.4	11.2	82.8
ce1.A1.b4	0%						0%		33%			33%	33%		56.3	50.8	341.5
ce1.A1.b5	33%						0%		33%			33%	0%		66.8	66.0	419.1
ce1.A1.b6	0%						33%		33%			33%	0%		73.5	68.0	449.7
ce1.A1.b7	33%						0%		33%			0%	33%		36.7	3.5	148.9
ce1.A1.b8	0%						33%		33%			0%	33%		36.2	8.2	158.8

Table V-7.15 *Contd...*

Mix #	re 1	re 2	re 3	re 4	re 5	re 6	re 7	re 8	ce 1	ce 2	ce 3	ce 4	ce 5	ce 6	% G	% X	TS
ce1.A1.b9	33%						33%		33%			0%	0%		35.7	5.3	149.4
ce1.A1.b10	33%						0%		0%			33%	33%		42.4	54.6	297.7
ce1.A1.b11	0%						33%		0%			33%	33%		40.9	54.1	290.8
ce1.A1.b12	33%						33%		0%			33%	0%		34.2	53.3	263.2
ce1.A1.c1	33%						33%		0%			0%	33%		21.1	9.2	103.5
ce1.A1.c2	25%						0%		25%			25%	25%		61.1	62.8	389.4
ce1.A1.c3	0%						25%		25%			25%	25%		72.8	68.0	446.9
ce1.A1.c4	25%						25%		25%			25%	0%		76.7	67.9	461.8
ce1.A1.c5	25%						25%		25%			0%	25%		37.4	12.9	174.8
ce1.A1.c6	25%						25%		0%			25%	25%		50.5	68.0	361.8
ce1.A1.c7	20%						20%		20%			20%	20%		71.3	65.0	433.8
ce1.A1.c8	10%						10%		60%			10%	10%		74.3	63.2	440.8
ce1.A1.c9	10%						10%		10%			60%	10%		62.1	63.4	394.7
ce1.A1.c10	10%						10%		10%			10%	60%		58.2	52.9	353.8
ce1.A1.c11	60%						10%		10%			10%	10%		52.6	54.2	335.8
ce1.A1.c12	10%						60%		10%			10%	10%		48.4	57.5	327.7
ce6.A1.a1	0%						0%					0%	0%	100%	57.6	2.3	225.5
ce6.A1.a2	0%						0%					100%	0%	0%	20.8	44.7	190.4
ce6.A1.a3	0%						0%					0%	100%	0%	24.2		
ce6.A1.a4	100%						0%					0%	0%	0%	21.1	7.5	99.3
ce6.A1.a5	0%						100%					0%	0%	0%		3.1	
ce6.A1.a6	0%						0%					50%	0%	50%	53.7	47.4	323.0
ce6.A1.a7	0%						0%					0%	50%	50%	47.5	0.9	183.7
ce6.A1.a8	50%						0%					0%	0%	50%	57.1	4.4	229.2
ce6.A1.a9	0%						50%					0%	0%	50%	62.1		
ce6.A1.a10	0%						0%					50%	50%	0%	34.7	43.1	239.9
ce6.A1.a11	50%						0%					50%	0%	0%	31.5	49.0	242.3

Table V-7.15 *Contd...*

Mix #	re 1	re 2	re 3	re 4	re 5	re 6	re 7	re 8	ce 1	ce 2	ce 3	ce 4	ce 5	ce 6	% G	% X	TS
ce6.A1.a12	0%						50%					50%	0%	0%	16.4	56.4	202.9
ce6.A1.b1	50%						0%					0%	50%	0%	25.0	2.8	102.5
ce6.A1.b2	0%						50%					0%	50%	0%	19.2	7.7	92.5
ce6.A1.b3	50%						50%					0%	0%	0%	13.7	9.6	76.3
ce6.A1.b4	0%						0%					33%	33%	33%	48.9	50.3	311.8
ce6.A1.b5	33%						0%					33%	0%	33%	59.7	62.6	383.5
ce6.A1.b6	0%						33%					33%	0%	33%	68.4	60.8	412.4
ce6.A1.b7	33%						0%					0%	33%	33%	51.6	2.4	203.0
ce6.A1.b8	0%						33%					0%	33%	33%	60.2	3.1	237.6
ce6.A1.b9	33%						33%					0%	0%	33%	53.6	1.1	207.4
ce6.A1.b10	33%						0%					33%	33%	0%	42.3	57.4	304.5
ce6.A1.b11	0%						33%					33%	33%	0%	40.4	51.2	281.6
ce6.A1.b12	33%						33%					33%	0%	0%	33.1	58.6	272.1
ce6.A1.c1	33%						33%					0%	33%	0%	21.8	7.2	101.2
ce6.A1.c2	25%						0%					25%	25%	25%	57.8	62.3	375.6
ce6.A1.c3	0%						25%					25%	25%	25%	66.5	62.8	410.0
ce6.A1.c4	25%						25%					25%	0%	25%	68.1	68.2	429.4
ce6.A1.c5	25%						25%					0%	25%	25%	50.1	8.3	212.0
ce6.A1.c6	25%						25%					25%	25%	0%	46.2	61.7	329.8
ce6.A1.c7	20%						20%					20%	20%	20%	65.1	67.9	417.4
ce6.A1.c8	10%						10%					10%	10%	60%	72.8	60.2	427.8
ce6.A1.c9	10%						10%					60%	10%	10%	51.3	57.2	338.2
ce6.A1.c10	10%						10%					10%	60%	10%	54.9	62.1	364.0
ce6.A1.c11	60%						10%					10%	10%	10%	50.3	49.4	315.0
ce6.A1.c12	10%						60%					10%	10%	10%	44.5	58.6	315.5
re4.A1.a1	0%			100%			0%					0%	0%		30.7	11.9	146.9
re4.A1.a2	0%			0%			0%					100%	0%		16.8	44.1	173.8

Table V-7.15 *Contd...*

Mix #	re 1	re 2	re 3	re 4	re 5	re 6	re 7	re 8	ce 1	ce 2	ce 3	ce 4	ce 5	ce 6	% G	% X	TS
re4.A1.a3	0%			0%			0%					0%	100%		24.2		
re4.A1.a4	100%			0%			0%					0%	0%		20.4	3.0	85.1
re4.A1.a5	0%			0%			100%					0%	0%		1.8	4.9	19.1
re4.A1.a6	0%			50%			0%					50%	0%		55.4	50.0	335.9
re4.A1.a7	0%			50%			0%					0%	50%		29.5	4.3	123.6
re4.A1.a8	50%			50%			0%					0%	0%		32.9	11.4	153.8
re4.A1.a9	0%			50%			50%					0%	0%		20.6	14.0	113.6
re4.A1.a10	0%			0%			0%					50%	50%		37.2	44.9	253.8
re4.A1.a11	50%			0%			0%					50%	0%		31.9	54.2	256.6
re4.A1.a12	0%			0%			50%					50%	0%		15.9	51.4	188.6
re4.A1.b1	50%			0%			0%					0%	50%		25.1	4.3	106.6
re4.A1.b2	0%			0%			50%					0%	50%		17.7	6.1	82.6
re4.A1.b3	50%			0%			50%					0%	0%		14.0	10.4	79.3
re4.A1.b4	0%			33%			0%					33%	33%		55.4	47.8	330.6
re4.A1.b5	33%			33%			0%					33%	0%		62.2	63.1	394.4
re4.A1.b6	0%			33%			33%					33%	0%		74.8	63.7	444.1
re4.A1.b7	33%			33%			0%					0%	33%		31.0	6.5	134.6
re4.A1.b8	0%			33%			33%					0%	33%		27.2	11.4	132.1
re4.A1.b9	33%			33%			33%					0%	0%		25.2	15.7	135.3
re4.A1.b10	33%			0%			0%					33%	33%		41.0	54.9	293.2
re4.A1.b11	0%			0%			33%					33%	33%		40.4	57.5	297.4
re4.A1.b12	33%			0%			33%					33%	0%		31.3	56.8	260.9
re4.A1.c1	33%			0%			33%					0%	33%		21.4	10.4	107.5
re4.A1.c2	25%			25%			0%					25%	25%		62.6	60.7	389.8
re4.A1.c3	0%			25%			25%					25%	25%		72.1	67.3	442.7
re4.A1.c4	25%			25%			25%					25%	0%		73.7	64.0	440.5
re4.A1.c5	25%			25%			25%					0%	25%		31.1	16.7	160.5

Table V-7.15 *Contd...*

Mix #	re 1	re 2	re 3	re 4	re 5	re 6	re 7	re 8	ce 1	ce 2	ce 3	ce 4	ce 5	ce 6	% G	% X	TS
re4.A1.c6	25%			0%			25%					25%	25%		47.9	64.0	342.1
re4.A1.c7	20%			20%			20%					20%	20%		68.5	66.3	426.5
re4.A1.c8	10%			60%			10%					10%	10%		71.1	61.1	423.4
re4.A1.c9	10%			10%			10%					60%	10%		62.2	64.8	398.5
re4.A1.c10	10%			10%			10%					10%	60%		58.0	58.2	366.3
re4.A1.c11	60%			10%			10%					10%	10%		55.5	56.4	352.2
re4.A1.c12	10%			10%			60%					10%	10%		47.8	50.8	308.6
A1.a1	0%	0%		0%			0%	0%	100%		0%	0%	0%	0%	51.4	12.2	226.8
A1.a2	0%	0%		0%			0%	0%	0%		100%	0%	0%	0%	10.4	41.7	143.3
A1.a3	0%	0%		0%			0%	0%	0%		0%	100%	0%	0%	25.1	41.6	199.4
A1.a4	0%	0%		0%			0%	0%	0%		0%	0%	100%	0%	34.3		
A1.a5	0%	0%		0%			0%	0%	0%		0%	0%	0%	100%	63.3	3.9	251.4
A1.a6	100%	0%		0%			0%	0%	0%		0%	0%	0%	0%	26.2	3.6	108.8
A1.a7	0%	100%		0%			0%	0%	0%		0%	0%	0%	0%	13.0	2.3	55.3
A1.a8	0%	0%		100%			0%	0%	0%		0%	0%	0%	0%	36.9	5.4	154.5
A1.a9	0%	0%		0%			100%	0%	0%		0%	0%	0%	0%	3.3		
A1.a10	0%	0%		0%			0%	100%	0%		0%	0%	0%	0%	62.8	10.4	265.8
A1.a11	0%	0%		0%			0%	0%	50%		50%	0%	0%	0%	48.8	26.2	251.5
A1.a12	0%	0%		0%			0%	0%	50%		0%	50%	0%	0%	58.1	32.1	301.7
A1.b1	0%	0%		0%			0%	0%	50%		0%	0%	50%	0%	42.3	6.5	177.4
A1.b2	0%	0%		0%			0%	0%	50%		0%	0%	0%	50%	51.8	0.2	198.5
A1.b3	50%	0%		0%			0%	0%	50%		0%	0%	0%	0%	43.4	0.7	167.5
A1.b4	0%	50%		0%			0%	0%	50%		0%	0%	0%	0%	55.5	7.1	229.7
A1.b5	0%	0%		50%			0%	0%	50%		0%	0%	0%	0%	42.6	1.9	167.3
A1.b6	0%	0%		0%			50%	0%	50%		0%	0%	0%	0%	41.7		
A1.b7	0%	0%		0%			0%	50%	50%		0%	0%	0%	0%	56.3	7.6	233.9
A1.b8	0%	0%		0%			0%	0%	0%		50%	50%	0%	0%	23.5	52.7	220.6
A1.b9	0%	0%		0%			0%	0%	0%		50%	0%	50%	0%	36.1	19.5	186.5

Table V-7.15 *Contd...*

Mix #	re 1	re 2	re 3	re 4	re 5	re 6	re 7	re 8	ce 1	ce 2	ce 3	ce 4	ce 5	ce 6	% G	% X	TS
A1.b10	0%	0%		0%			0%	0%	0%		50%	0%	0%	50%	63.2	19.7	290.4
A1.b11	50%	0%		0%			0%	0%	0%		50%	0%	0%	0%	26.8	30.5	178.0
A1.b12	0%	50%		0%			0%	0%	0%		50%	0%	0%	0%	14.6	18.9	102.6
A1.c1	0%	0%		50%			0%	0%	0%		50%	0%	0%	0%	42.7	36.3	253.3
A1.c2	0%	0%		0%			50%	0%	0%		50%	0%	0%	0%	8.7	32.9	115.1
A1.c3	0%	0%		0%			0%	50%	0%		50%	0%	0%	0%	57.9	33.0	303.4
A1.c4	0%	0%		0%			0%	0%	0%		0%	50%	50%	0%	39.6	47.1	268.2
A1.c5	0%	0%		0%			0%	0%	0%		0%	50%	0%	50%	54.7	47.7	327.3
A1.c6	50%	0%		0%			0%	0%	0%		0%	50%	0%	0%	35.4	54.5	270.9
A1.c7	0%	50%		0%			0%	0%	0%		0%	50%	0%	0%	20.6	32.0	158.1
A1.c8	0%	0%		50%			0%	0%	0%		0%	50%	0%	0%	65.4	45.8	363.6
A1.c9	0%	0%		0%			50%	0%	0%		0%	50%	0%	0%	27.6	54.1	239.9
A1.c10	0%	0%		0%			0%	50%	0%		0%	50%	0%	0%	59.6	40.7	328.9
A1.c11	0%	0%		0%			0%	0%	0%		0%	0%	50%	50%	55.0		
A1.c12	50%	0%		0%			0%	0%	0%		0%	0%	50%	0%	29.8		
A1.d1	0%	50%		0%			0%	0%	0%		0%	0%	50%	0%	36.3	11.5	167.4
A1.d2	0%	0%		50%			0%	0%	0%		0%	0%	50%	0%	37.1	6.5	157.7
A1.d3	0%	0%		0%			50%	0%	0%		0%	0%	50%	0%	26.7	8.7	123.7
A1.d4	0%	0%		0%			0%	50%	0%		0%	0%	50%	0%	52.7	16.3	241.8
A1.d5	50%	0%		0%			0%	0%	0%		0%	0%	0%	50%	58.9	5.0	237.5
A1.d6	0%	50%		0%			0%	0%	0%		0%	0%	0%	50%	50.8	3.6	202.8
A1.d7	0%	0%		50%			0%	0%	0%		0%	0%	0%	50%	58.8	3.8	233.8
A1.d8	0%	0%		0%			50%	0%	0%		0%	0%	0%	50%	68.0		
A1.d9	0%	0%		0%			0%	50%	0%		0%	0%	0%	50%	64.0	10.0	269.3
A1.d10	50%	50%		0%			0%	0%	0%		0%	0%	0%	0%	37.1	11.4	170.0
A1.d11	50%	0%		50%			0%	0%	0%		0%	0%	0%	0%	37.7	6.7	160.4
A1.d12	50%	0%		0%			50%	0%	0%		0%	0%	0%	0%	19.8	6.9	92.6

Table V-7.15 *Contd...*

Mix #	re 1	re 2	re 3	re 4	re 5	re 6	re 7	re 8	ce 1	ce 2	ce 3	ce 4	ce 5	ce 6	% G	% X	TS
A1.e1	50%	0%		0%			0%	50%	0%		0%	0%	0%	0%	58.7	24.7	285.5
A1.e2	0%	50%		50%			0%	0%	0%		0%	0%	0%	0%	57.3	14.3	254.2
A1.e3	0%	50%		0%			50%	0%	0%		0%	0%	0%	0%	15.0	19.7	106.2
A1.e4	0%	50%		0%			0%	50%	0%		0%	0%	0%	0%	59.2	16.6	267.4
A1.e5	0%	0%		50%			50%	0%	0%		0%	0%	0%	0%	26.5	16.9	143.3
A1.e6	0%	0%		50%			0%	50%	0%		0%	0%	0%	0%	57.7	14.8	257.1
A1.e7	0%	0%		0%			50%	50%	0%		0%	0%	0%	0%	62.6	23.0	296.4
A1.e8	0%	0%		0%			0%	0%	33%		33%	33%	0%	0%	68.8	58.5	408.2
A1.e9	0%	0%		0%			0%	0%	33%		33%	0%	33%	0%	46.5	26.5	243.6
A1.e10	0%	0%		0%			0%	0%	33%		33%	0%	0%	33%	65.1	18.8	295.3
A1.e11	33%	0%		0%			0%	0%	33%		33%	0%	0%	0%	47.2	26.5	245.9
A1.e12	0%	33%		0%			0%	0%	33%		33%	0%	0%	0%	64.5	20.9	298.2
A1.f1	0%	0%		33%			0%	0%	33%		33%	0%	0%	0%	47.0	31.1	256.6
A1.f2	0%	0%		0%			33%	0%	33%		33%	0%	0%	0%	35.9	27.5	205.3
A1.f3	0%	0%		0%			0%	33%	33%		33%	0%	0%	0%	55.9	29.4	286.3
A1.f4	0%	0%		0%			0%	0%	33%		0%	33%	33%	0%	59.2	51.2	353.1
A1.f5	0%	0%		0%			0%	0%	33%		0%	33%	0%	33%	61.6	47.6	353.4
A1.f6	33%	0%		0%			0%	0%	33%		0%	33%	0%	0%	64.3	59.9	394.3
A1.f7	0%	33%		0%			0%	0%	33%		0%	33%	0%	0%	56.8	46.2	332.0
A1.f8	0%	0%		33%			0%	0%	33%		0%	33%	0%	0%	70.6	46.1	384.2
A1.f9	0%	0%		0%			33%	0%	33%		0%	33%	0%	0%	71.7	57.4	416.6
A1.f10	0%	0%		0%			0%	33%	33%		0%	33%	0%	0%	62.8	42.0	344.1
A1.f11	0%	0%		0%			0%	0%	33%		0%	0%	33%	33%	60.3		
A1.f12	33%	0%		0%			0%	0%	33%		0%	0%	33%	0%	39.5		
A1.g1	0%	33%		0%			0%	0%	33%		0%	0%	33%	0%	58.2	15.3	260.4
A1.g2	0%	0%		33%			0%	0%	33%		0%	0%	33%	0%	38.3	8.2	166.4

Table V-7.15 *Contd...*

Mix #	re 1	re 2	re 3	re 4	re 5	re 6	re 7	re 8	ce 1	ce 2	ce 3	ce 4	ce 5	ce 6	% G	% X	TS
A1.g3	0%	0%		0%			33%	0%	33%		0%	0%	33%	0%	40.8	11.0	183.2
A1.g4	0%	0%		0%			0%	33%	33%		0%	0%	33%	0%	52.7	11.8	230.6
A1.g5	33%	0%		0%			0%	0%	33%		0%	0%	0%	33%	57.5	8.7	241.1
A1.g6	0%	33%		0%			0%	0%	33%		0%	0%	0%	33%	58.8	9.0	247.1
A1.g7	0%	0%		33%			0%	0%	33%		0%	0%	0%	33%	61.8	11.5	264.3
A1.g8	0%	0%		0%			33%	0%	33%		0%	0%	0%	33%	67.8	5.8	273.4
A1.g9	0%	0%		0%			0%	33%	33%		0%	0%	0%	33%	64.3	11.3	273.7
A1.g10	33%	33%		0%			0%	0%	33%		0%	0%	0%	0%	67.7	13.2	291.4
A1.g11	33%	0%		33%			0%	0%	33%		0%	0%	0%	0%	43.8	7.2	185.1
A1.g12	33%	0%		0%			33%	0%	33%		0%	0%	0%	0%	41.0	8.0	176.6
A1.h1	33%	0%		0%			0%	33%	33%		0%	0%	0%	0%	57.7	16.0	260.0
A1.h2	0%	33%		33%			0%	0%	33%		0%	0%	0%	0%	68.4	15.0	298.4
A1.h3	0%	33%		0%			33%	0%	33%		0%	0%	0%	0%	83.2	23.0	375.1
A1.h4	0%	33%		0%			0%	33%	33%		0%	0%	0%	0%	74.1	19.1	330.6
A1.h5	0%	0%		33%			33%	0%	33%		0%	0%	0%	0%	46.3	14.6	213.0
A1.h6	0%	0%		33%			0%	33%	33%		0%	0%	0%	0%	58.6	10.8	250.7
A1.h7	0%	0%		0%			33%	33%	33%		0%	0%	0%	0%	66.4	19.2	301.3
A1.h8	0%	0%		0%			0%	0%	0%		33%	33%	33%	0%	52.7	66.2	366.0
A1.h9	0%	0%		0%			0%	0%	0%		33%	33%	0%	33%	66.3	63.5	411.1
A1.h10	33%	0%		0%			0%	0%	0%		33%	33%	0%	0%	40.6	57.9	298.9
A1.h11	0%	33%		0%			0%	0%	0%		33%	33%	0%	0%	27.5	50.7	231.0
A1.h12	0%	0%		33%			0%	0%	0%		33%	33%	0%	0%	64.9	50.1	372.3
A2.a1	0%	0%		0%			33%	0%	0%		33%	33%	0%	0%	27.0	40.7	204.2
A2.a2	0%	0%		0%			0%	33%	0%		33%	33%	0%	0%	68.8	53.2	395.0
A2.a3	0%	0%		0%			0%	0%	0%		33%	0%	33%	33%	76.5	63.6	450.4
A2.a4	33%	0%		0%			0%	0%	0%		33%	0%	33%	0%	39.6	68.7	322.0
A2.a5	0%	33%		0%			0%	0%	0%		33%	0%	33%	0%	21.4	61.4	234.5

Table V-7.15 *Contd...*

Mix #	re 1	re 2	re 3	re 4	re 5	re 6	re 7	re 8	ce 1	ce 2	ce 3	ce 4	ce 5	ce 6	% G	% X	TS
A2.a6	0%	0%		33%			0%	0%	0%		33%	0%	33%	0%	73.6	66.6	446.7
A2.a7	0%	0%		0%			33%	0%	0%		33%	0%	33%	0%	21.5	69.7	255.4
A2.a8	0%	0%		0%			0%	33%	0%		33%	0%	33%	0%	73.2	66.7	445.3
A2.a9	33%	0%		0%			0%	0%	0%		33%	0%	0%	33%	75.1	45.8	400.5
A2.a10	0%	33%		0%			0%	0%	0%		33%	0%	0%	33%	74.7	46.9	401.7
A2.a11	0%	0%		33%			0%	0%	0%		33%	0%	0%	33%	74.1	45.3	395.4
A2.a12	0%	0%		0%			33%	0%	0%		33%	0%	0%	33%	77.8	48.7	418.2
A2.b1	0%	0%		0%			0%	33%	0%		33%	0%	0%	33%	74.4	48.0	403.5
A2.b2	33%	33%		0%			0%	0%	0%		33%	0%	0%	0%	38.4	42.4	252.1
A2.b3	33%	0%		33%			0%	0%	0%		33%	0%	0%	0%	37.6	46.8	260.0
A2.b4	33%	0%		0%			33%	0%	0%		33%	0%	0%	0%	18.0	39.1	166.1
A2.b5	33%	0%		0%			0%	33%	0%		33%	0%	0%	0%	62.8	56.5	380.1
A2.b6	0%	33%		33%			0%	0%	0%		33%	0%	0%	0%	74.6	42.5	390.5
A2.b7	0%	33%		0%			33%	0%	0%		33%	0%	0%	0%	14.4	41.8	159.1
A2.b8	0%	33%		0%			0%	33%	0%		33%	0%	0%	0%	67.7	40.0	357.9
A2.b9	0%	0%		33%			33%	0%	0%		33%	0%	0%	0%	38.5	48.7	268.3
A2.b10	0%	0%		33%			0%	33%	0%		33%	0%	0%	0%	66.8	45.7	368.6
A2.b11	0%	0%		0%			33%	33%	0%		33%	0%	0%	0%	62.3	45.9	352.0
A2.b12	0%	0%		0%			0%	0%	0%		0%	33%	33%	33%	65.6	53.7	383.9
A2.c1	33%	0%		0%			0%	0%	0%		0%	33%	33%	0%	53.4	67.2	370.8
A2.c2	0%	33%		0%			0%	0%	0%		0%	33%	33%	0%	40.9	52.7	287.2
A2.c3	0%	0%		33%			0%	0%	0%		0%	33%	33%	0%	64.3	61.2	397.6
A2.c4	0%	0%		0%			33%	0%	0%		0%	33%	33%	0%	54.8	68.2	379.1
A2.c5	0%	0%		0%			0%	33%	0%		0%	33%	33%	0%	60.8	52.7	363.4
A2.c6	33%	0%		0%			0%	0%	0%		0%	33%	0%	33%	69.4	11.8	294.3
A2.c7	0%	33%		0%			0%	0%	0%		0%	33%	0%	33%	68.1	21.3	312.9
A2.c8	0%	0%		33%			0%	0%	0%		0%	33%	0%	33%	76.6	28.9	364.5

Table V-7.15 *Contd...*

Mix #	re 1	re 2	re 3	re 4	re 5	re 6	re 7	re 8	ce 1	ce 2	ce 3	ce 4	ce 5	ce 6	% G	% X	TS
A2.c9	0%	0%		0%			33%	0%	0%		0%	33%	0%	33%	85.1	22.1	379.7
A2.c10	0%	0%		0%			0%	33%	0%		0%	33%	0%	33%	68.8	32.7	343.9
A2.c11	33%	33%		0%			0%	0%	0%		0%	33%	0%	0%	55.4	16.7	253.1
A2.c12	33%	0%		33%			0%	0%	0%		0%	33%	0%	0%	41.9	9.7	184.1
A2.d1	33%	0%		0%			33%	0%	0%		0%	33%	0%	0%	28.8	13.5	143.4
A2.d2	33%	0%		0%			0%	33%	0%		0%	33%	0%	0%	61.0	37.4	326.0
A2.d3	0%	33%		33%			0%	0%	0%		0%	33%	0%	0%	62.2	28.4	308.2
A2.d4	0%	33%		0%			33%	0%	0%		0%	33%	0%	0%	52.8	23.2	259.1
A2.d5	0%	33%		0%			0%	33%	0%		0%	33%	0%	0%	56.5	32.0	295.3
A2.d6	0%	0%		33%			33%	0%	0%		0%	33%	0%	0%	38.9	27.9	218.1
A2.d7	0%	0%		33%			0%	33%	0%		0%	33%	0%	0%	60.9	38.2	327.5
A2.d8	0%	0%		0%			33%	33%	0%		0%	33%	0%	0%	67.4	40.8	358.8
A2.d9	33%	0%		0%			0%	0%	0%		0%	0%	33%	33%	75.6	67.6	456.6
A2.d10	0%	33%		0%			0%	0%	0%		0%	0%	33%	33%	69.9	59.9	415.9
A2.d11	0%	0%		33%			0%	0%	0%		0%	0%	33%	33%	77.4	63.5	453.2
A2.d12	0%	0%		0%			33%	0%	0%		0%	0%	33%	33%	82.9	68.5	487.0
A2.e1	0%	0%		0%			0%	33%	0%		0%	0%	33%	33%	74.2	65.3	445.6
A2.e2	33%	33%		0%			0%	0%	0%		0%	0%	33%	0%	39.8	62.6	307.7
A2.e3	33%	0%		33%			0%	0%	0%		0%	0%	33%	0%	73.4	72.7	461.0
A2.e4	33%	0%		0%			33%	0%	0%		0%	0%	33%	0%	43.9	71.3	344.9
A2.e5	33%	0%		0%			0%	33%	0%		0%	0%	33%	0%	72.2	72.3	455.3
A2.e6	0%	33%		33%			0%	0%	0%		0%	0%	33%	0%	63.9	57.6	387.2
A2.e7	0%	33%		0%			33%	0%	0%		0%	0%	33%	0%	26.9	70.8	278.5
A2.e8	0%	33%		0%			0%	33%	0%		0%	0%	33%	0%	58.9	54.6	360.7
A2.e9	0%	0%		33%			33%	0%	0%		0%	0%	33%	0%	85.6	70.4	502.2
A2.e10	0%	0%		33%			0%	33%	0%		0%	0%	33%	0%	70.6	62.7	425.5
A2.e11	0%	0%		0%			33%	33%	0%		0%	0%	33%	0%	85.9	69.1	499.6
A2.e12	33%	33%		0%			0%	0%	0%		0%	0%	0%	33%	72.7	30.4	353.0

Table V-7.15 *Contd...*

Mix #	re 1	re 2	re 3	re 4	re 5	re 6	re 7	re 8	ce 1	ce 2	ce 3	ce 4	ce 5	ce 6	% G	% X	TS
A2.f1	33%	0%		33%			0%	0%	0%		0%	0%	0%	33%	76.1	29.2	362.9
A2.f2	33%	0%		0%			33%	0%	0%		0%	0%	0%	33%	76.8	19.0	340.3
A2.f3	33%	0%		0%			0%	33%	0%		0%	0%	0%	33%	72.8	32.6	359.0
A2.f4	0%	33%		33%			0%	0%	0%		0%	0%	0%	33%	67.8	28.8	330.6
A2.f5	0%	33%		0%			33%	0%	0%		0%	0%	0%	33%	81.9	27.6	381.5
A2.f6	0%	33%		0%			0%	33%	0%		0%	0%	0%	33%	70.3	34.0	352.9
A2.f7	0%	0%		33%			33%	0%	0%		0%	0%	0%	33%	79.6	27.5	372.5
A2.f8	0%	0%		33%			0%	33%	0%		0%	0%	0%	33%	73.1	29.7	353.1
A2.f9	0%	0%		0%			33%	33%	0%		0%	0%	0%	33%	82.1	32.7	394.8
A2.f10	33%	33%		33%			0%	0%	0%		0%	0%	0%	0%	73.1	19.6	327.9
A2.f11	33%	33%		0%			33%	0%	0%		0%	0%	0%	0%	42.5	27.5	230.7
A2.f12	33%	33%		0%			0%	33%	0%		0%	0%	0%	0%	70.4	31.1	346.1
A2.g1	33%	0%		33%			33%	0%	0%		0%	0%	0%	0%	34.4	36.3	221.7
A2.g2	33%	0%		33%			0%	33%	0%		0%	0%	0%	0%	63.9	44.6	355.1
A2.g3	33%	0%		0%			33%	33%	0%		0%	0%	0%	0%	60.9	47.6	350.6
A2.g4	0%	33%		33%			33%	0%	0%		0%	0%	0%	0%	74.3	41.1	385.8
A2.g5	0%	33%		33%			0%	33%	0%		0%	0%	0%	0%	63.0	35.0	327.6
A2.g6	0%	33%		0%			33%	33%	0%		0%	0%	0%	0%	78.4	44.4	409.8
A2.g7	0%	0%		33%			33%	33%	0%		0%	0%	0%	0%	66.3	54.5	388.7
A2.g8	0%	0%		0%			0%	0%	25%		25%	25%	25%	0%	73.1	71.3	456.4
A2.g9	0%	0%		0%			0%	0%	25%		25%	25%	0%	25%	75.0	40.4	387.0
A2.g10	25%	0%		0%			0%	0%	25%		25%	25%	0%	0%	51.2	45.3	308.2
A2.g11	0%	25%		0%			0%	0%	25%		25%	25%	0%	0%	76.5	48.9	413.7
A2.g12	0%	0%		25%			0%	0%	25%		25%	25%	0%	0%	52.7	44.7	312.3
A2.h1	0%	0%		0%			25%	0%	25%		25%	25%	0%	0%	43.7	50.8	293.3
A2.h2	0%	0%		0%			0%	25%	25%		25%	25%	0%	0%	62.1	44.5	347.8
A2.h3	0%	0%		0%			0%	0%	25%		25%	0%	25%	25%	74.7	68.5	455.5
A2.h4	25%	0%		0%			0%	0%	25%		25%	0%	25%	0%	67.7	78.2	453.0

Table V-7.15 *Contd...*

Mix #	re 1	re 2	re 3	re 4	re 5	re 6	re 7	re 8	ce 1	ce 2	ce 3	ce 4	ce 5	ce 6	% G	% X	TS
A2.h5	0%	25%		0%			0%	0%	25%		25%	0%	25%	0%	70.8	73.8	453.9
A2.h6	0%	0%		25%			0%	0%	25%		25%	0%	25%	0%	76.7	73.4	475.2
A2.h7	0%	0%		0%			25%	0%	25%		25%	0%	25%	0%	79.3	75.0	489.5
A2.h8	0%	0%		0%			0%	25%	25%		25%	0%	25%	0%	76.1	71.5	468.4
A2.h9	25%	0%		0%			0%	0%	25%		25%	0%	0%	25%	77.5	45.0	407.7
A2.h10	0%	25%		0%			0%	0%	25%		25%	0%	0%	25%	77.3	44.7	406.2
A2.h11	0%	0%		25%			0%	0%	25%		25%	0%	0%	25%	79.4	42.4	408.5
A2.h12	0%	0%		0%			25%	0%	25%		25%	0%	0%	25%	79.3	36.7	394.2
A12.a1	0%	0%		0%			0%	25%	25%		25%	0%	0%	25%	66.6	46.1	368.7
A3.a2	25%	25%		0%			0%	0%	25%		25%	0%	0%	0%	63.2	46.9	357.9
A3.a3	25%	0%		25%			0%	0%	25%		25%	0%	0%	0%	44.6	59.7	318.9
A3.a4	25%	0%		0%			25%	0%	25%		25%	0%	0%	0%	36.7	53.4	272.9
A3.a5	25%	0%		0%			0%	25%	25%		25%	0%	0%	0%	61.4	63.8	393.2
A3.a6	0%	25%		25%			0%	0%	25%		25%	0%	0%	0%	71.0	59.2	418.3
A3.a7	0%	25%		0%			25%	0%	25%		25%	0%	0%	0%	64.6	59.6	394.8
A3.a8	0%	25%		0%			0%	25%	25%		25%	0%	0%	0%	68.4	57.6	404.2
A3.a9	0%	0%		25%			25%	0%	25%		25%	0%	0%	0%	47.6	70.0	356.0
A3.a10	0%	0%		25%			0%	25%	25%		25%	0%	0%	0%	54.2	54.3	342.0
A3.a11	0%	0%		0%			25%	25%	25%		25%	0%	0%	0%	60.4	62.0	384.6
A3.a12	0%	0%		0%			0%	0%	25%		0%	25%	25%	25%	64.3	76.4	435.5
A12.b1	25%	0%		0%			0%	0%	25%		0%	25%	25%	0%	56.8	66.2	381.7
A3.b2	0%	25%		0%			0%	0%	25%		0%	25%	25%	0%	48.3	58.1	328.9
A3.b3	0%	0%		25%			0%	0%	25%		0%	25%	25%	0%	61.2	67.9	402.3
A3.b4	0%	0%		0%			25%	0%	25%		0%	25%	25%	0%	72.4	77.3	468.9
A3.b5	0%	0%		0%			0%	25%	25%		0%	25%	25%	0%	54.4	59.0	354.6
A3.b6	25%	0%		0%			0%	0%	25%		0%	25%	0%	25%	65.2	24.7	310.4
A3.b7	0%	25%		0%			0%	0%	25%		0%	25%	0%	25%	67.2	34.8	343.2
A3.b8	0%	0%		25%			0%	0%	25%		0%	25%	0%	25%	63.9	37.5	337.3
A3.b9	0%	0%		0%			25%	0%	25%		0%	25%	0%	25%	79.6	42.0	408.5

Table V-7.15 *Contd...*

Mix #	re 1	re 2	re 3	re 4	re 5	re 6	re 7	re 8	ce 1	ce 2	ce 3	ce 4	ce 5	ce 6	% G	% X	TS
A3.b10	0%	0%		0%			0%	25%	25%		0%	25%	0%	25%	63.7	42.1	347.8
A3.b11	25%	25%		0%			0%	0%	25%		0%	25%	0%	0%	64.8	35.0	334.3
A3.b12	25%	0%		25%			0%	0%	25%		0%	25%	0%	0%	40.0	42.8	259.1
A12.c1	25%	0%		0%			25%	0%	25%		0%	25%	0%	0%	68.3	72.3	440.5
A3.c2	25%	0%		0%			0%	25%	25%		0%	25%	0%	0%	57.2	37.7	312.1
A3.c3	0%	25%		25%			0%	0%	25%		0%	25%	0%	0%	60.9	35.5	320.8
A3.c4	0%	25%		0%			25%	0%	25%		0%	25%	0%	0%	71.0	34.3	356.5
A3.c5	0%	25%		0%			0%	25%	25%		0%	25%	0%	0%	63.2	37.9	335.7
A3.c6	0%	0%		25%			25%	0%	25%		0%	25%	0%	0%	40.4	40.9	255.8
A3.c7	0%	0%		25%			0%	25%	25%		0%	25%	0%	0%	53.8	41.9	309.8
A3.c8	0%	0%		0%			25%	25%	25%		0%	25%	0%	0%	65.8	45.4	364.1
A3.c9	25%	0%		0%			0%	0%	25%		0%	0%	25%	25%	71.9	80.1	473.6
A3.c10	0%	25%		0%			0%	0%	25%		0%	0%	25%	25%	63.4	71.0	418.8
A3.c11	0%	0%		25%			0%	0%	25%		0%	0%	25%	25%	68.6	70.2	436.6
A3.c12	0%	0%		0%			25%	0%	25%		0%	0%	25%	25%	73.1	91.5	506.8
A12.d1	0%	0%		0%			0%	25%	25%		0%	0%	25%	25%	55.7	27.8	281.9
A3.d2	25%	25%		0%			0%	0%	25%		0%	0%	25%	0%	60.9	70.5	407.9
A3.d3	25%	0%		25%			0%	0%	25%		0%	0%	25%	0%	67.8	74.5	444.2
A3.d4	25%	0%		0%			25%	0%	25%		0%	0%	25%	0%	75.7	81.3	491.2
A3.d5	25%	0%		0%			0%	25%	25%		0%	0%	25%	0%	69.3	78.9	460.7
A3.d6	0%	25%		25%			0%	0%	25%		0%	0%	25%	0%	63.1	67.4	408.5
A3.d7	0%	25%		0%			25%	0%	25%		0%	0%	25%	0%	68.2	78.8	456.6
A3.d8	0%	25%		0%			0%	25%	25%		0%	0%	25%	0%	63.1	70.2	415.5
A3.d9	0%	0%		25%			25%	0%	25%		0%	0%	25%	0%	83.6	87.8	537.5
A3.d10	0%	0%		25%			0%	25%	25%		0%	0%	25%	0%	69.0	76.1	452.7
A3.d11	0%	0%		0%			25%	25%	25%		0%	0%	25%	0%	81.6	88.0	530.3
A3.d12	25%	25%		0%			0%	0%	25%		0%	0%	0%	25%	66.0	34.6	338.1
A12.e1	25%	0%		25%			0%	0%	25%		0%	0%	0%	25%	55.8	27.2	280.8

Table V-7.15 *Contd...*

Mix #	re 1	re 2	re 3	re 4	re 5	re 6	re 7	re 8	ce 1	ce 2	ce 3	ce 4	ce 5	ce 6	% G	% X	TS
A3.e2	25%	0%		0%			25%	0%	25%		0%	0%	0%	25%	70.7	37.8	363.9
A3.e3	25%	0%		0%			0%	25%	25%		0%	0%	0%	25%	74.4	46.7	400.1
A3.e4	0%	25%		25%			0%	0%	25%		0%	0%	0%	25%	69.1	41.6	367.1
A3.e5	0%	25%		0%			25%	0%	25%		0%	0%	0%	25%	78.6	49.5	423.3
A3.e6	0%	25%		0%			0%	25%	25%		0%	0%	0%	25%	67.9	47.2	376.6
A3.e7	0%	0%		25%			25%	0%	25%		0%	0%	0%	25%	78.0	49.5	420.8
A3.e8	0%	0%		25%			0%	25%	25%		0%	0%	0%	25%	69.9	44.7	378.3
A3.e9	0%	0%		0%			25%	25%	25%		0%	0%	0%	25%	83.2	50.5	443.3
A3.e10	25%	25%		25%			0%	0%	25%		0%	0%	0%	0%	66.5	43.3	361.5
A3.e11	25%	25%		0%			25%	0%	25%		0%	0%	0%	0%	78.5	46.2	414.7
A3.e12	25%	25%		0%			0%	25%	25%		0%	0%	0%	0%	63.6	49.5	365.8
A12.f1	25%	0%		25%			25%	0%	25%		0%	0%	0%	0%	36.9	31.6	219.5
A3.f2	25%	0%		25%			0%	25%	25%		0%	0%	0%	0%	55.9	50.0	337.5
A3.f3	25%	0%		0%			25%	25%	25%		0%	0%	0%	0%	62.3	58.7	383.7
A3.f4	0%	25%		25%			25%	0%	25%		0%	0%	0%	0%	79.6	51.3	431.5
A3.f5	0%	25%		25%			0%	25%	25%		0%	0%	0%	0%	69.3	47.4	382.3
A3.f6	0%	25%		0%			25%	25%	25%		0%	0%	0%	0%	80.1	52.2	435.6
A3.f7	0%	0%		25%			25%	25%	25%		0%	0%	0%	0%	61.5	62.3	389.8
A3.f8	0%	0%		0%			0%	0%	0%		25%	25%	25%	25%	69.3	75.7	452.9
A3.f9	25%	0%		0%			0%	0%	0%		25%	25%	25%	0%	46.4	73.8	360.7
A3.f10	0%	25%		0%			0%	0%	0%		25%	25%	25%	0%	41.1	70.2	331.4
A3.f11	0%	0%		25%			0%	0%	0%		25%	25%	25%	0%	69.1	84.8	474.7
A3.f12	0%	0%		0%			25%	0%	0%		25%	25%	25%	0%	39.4	84.0	359.4
A12.g1	0%	0%		0%			0%	25%	0%		25%	25%	25%	0%	65.0	69.8	421.8
A3.g2	25%	0%		0%			0%	0%	0%		25%	25%	0%	25%	66.1	48.0	371.7
A3.g3	0%	25%		0%			0%	0%	0%		25%	25%	0%	25%	60.9	45.0	344.6
A3.g4	0%	0%		25%			0%	0%	0%		25%	25%	0%	25%	66.9	53.9	389.5
A3.g5	0%	0%		0%			25%	0%	0%		25%	25%	0%	25%	73.7	47.8	400.1
A3.g6	0%	0%		0%			0%	25%	0%		25%	25%	0%	25%	66.4	56.7	394.8

Table V-7.15 *Contd...*

Mix #	re 1	re 2	re 3	re 4	re 5	re 6	re 7	re 8	ce 1	ce 2	ce 3	ce 4	ce 5	ce 6	% G	% X	TS
A3.g7	25%	25%		0%			0%	0%	0%		25%	25%	0%	0%	47.5	55.7	320.0
A3.g8	25%	0%		25%			0%	0%	0%		25%	25%	0%	0%	34.8	55.2	270.1
A3.g9	25%	0%		0%			25%	0%	0%		25%	25%	0%	0%	25.5	57.6	240.6
A3.g10	25%	0%		0%			0%	25%	0%		25%	25%	0%	0%	49.2	58.4	333.2
A3.g11	0%	25%		25%			0%	0%	0%		25%	25%	0%	0%	61.7	63.7	394.1
A3.g12	0%	25%		0%			25%	0%	0%		25%	25%	0%	0%	36.6	62.0	294.0
A12.h1	0%	25%		0%			0%	25%	0%		25%	25%	0%	0%	65.1	66.5	414.1
A3.h2	0%	0%		25%			25%	0%	0%		25%	25%	0%	0%	29.0	41.7	214.6
A3.h3	0%	0%		25%			0%	25%	0%		25%	25%	0%	0%	59.9	53.4	361.3
A3.h4	0%	0%		0%			25%	25%	0%		25%	25%	0%	0%	54.0	54.3	341.3
A3.h5	25%	0%		0%			0%	0%	0%		25%	0%	25%	25%	70.8	75.1	457.1
A3.h6	0%	25%		0%			0%	0%	0%		25%	0%	25%	25%	65.6	73.7	433.6
A3.h7	0%	0%		25%			0%	0%	0%		25%	0%	25%	25%	74.9	74.3	470.7
A3.h8	0%	0%		0%			25%	0%	0%		25%	0%	25%	25%	73.0	83.4	486.2
A3.h9	0%	0%		0%			0%	25%	0%		25%	0%	25%	25%	78.6	76.7	490.9
A3.h10	25%	25%		0%			0%	0%	0%		25%	0%	25%	0%	39.5	74.5	335.8
A3.h11	25%	0%		25%			0%	0%	0%		25%	0%	25%	0%	66.1	83.6	460.2
A3.h12	25%	0%		0%			25%	0%	0%		25%	0%	25%	0%	26.8	82.0	306.2
A4.a1	25%	0%		0%			0%	25%	0%		25%	0%	25%	0%	60.9	70.1	406.9
A4.a2	0%	25%		25%			0%	0%	0%		25%	0%	25%	0%	52.9	58.3	346.8
A4.a3	0%	25%		0%			25%	0%	0%		25%	0%	25%	0%	8.1	61.9	184.9
A4.a4	0%	25%		0%			0%	25%	0%		25%	0%	25%	0%	50.5	59.4	340.4
A4.a5	0%	0%		25%			25%	0%	0%		25%	0%	25%	0%	65.0	65.7	411.6
A4.a6	0%	0%		25%			0%	25%	0%		25%	0%	25%	0%	59.2	61.4	378.7
A12.a2	0%	0%		0%			25%	25%	0%		25%	0%	25%	0%	49.6	45.6	302.8
A12.b2	25%	25%		0%			0%	0%	0%		25%	0%	0%	25%	55.8	37.1	305.2
A4.a9	25%	0%		25%			0%	0%	0%		25%	0%	0%	25%	63.7	40.5	344.1
A4.a10	25%	0%		0%			25%	0%	0%		25%	0%	0%	25%	67.3	31.3	334.8
A4.a11	25%	0%		0%			0%	25%	0%		25%	0%	0%	25%	59.3	46.6	342.2

Table V-7.15 *Contd...*

Mix #	re 1	re 2	re 3	re 4	re 5	re 6	re 7	re 8	ce 1	ce 2	ce 3	ce 4	ce 5	ce 6	% G	% X	TS
A4.a12	0%	25%		25%			0%	0%	0%		25%	0%	0%	25%	67.0	36.6	346.9
A4.b1	0%	25%		0%			25%	0%	0%		25%	0%	0%	25%	66.5	44.0	363.4
A4.b2	0%	25%		0%			0%	25%	0%		25%	0%	0%	25%	56.3	42.0	319.4
A4.b3	0%	0%		25%			25%	0%	0%		25%	0%	0%	25%	61.1	41.5	336.4
A4.b4	0%	0%		25%			0%	25%	0%		25%	0%	0%	25%	60.8	42.5	337.9
A4.b5	0%	0%		0%			25%	25%	0%		25%	0%	0%	25%	71.7	54.6	409.5
A4.b6	25%	25%		25%			0%	0%	0%		25%	0%	0%	0%	58.0	41.4	324.3
A12.c2	25%	25%		0%			25%	0%	0%		25%	0%	0%	0%	35.5	43.6	244.1
A12.d2	25%	25%		0%			0%	25%	0%		25%	0%	0%	0%	67.7	50.9	385.1
A4.b9	25%	0%		25%			25%	0%	0%		25%	0%	0%	0%	26.3	49.8	224.3
A4.b10	25%	0%		25%			0%	25%	0%		25%	0%	0%	0%	43.8	52.0	296.3
A4.b11	25%	0%		0%			25%	25%	0%		25%	0%	0%	0%	54.7	53.4	341.6
A4.b12	0%	25%		25%			25%	0%	0%		25%	0%	0%	0%	67.3	50.5	382.6
A4.c1	0%	25%		25%			0%	25%	0%		25%	0%	0%	0%	61.7	41.1	337.8
A4.c2	0%	25%		0%			25%	25%	0%		25%	0%	0%	0%	64.1	44.0	354.3
A4.c3	0%	0%		25%			25%	25%	0%		25%	0%	0%	0%	49.6	46.2	304.5
A4.c4	25%	0%		0%			0%	0%	0%		0%	25%	25%	25%	57.6	59.7	368.4
A4.c5	0%	25%		0%			0%	0%	0%		0%	25%	25%	25%	56.5	60.4	365.9
A4.c6	0%	0%		25%			0%	0%	0%		0%	25%	25%	25%	61.9	56.0	375.8
A12.e2	0%	0%		0%			25%	0%	0%		0%	25%	25%	25%	62.5	65.1	400.7
A12.f2	0%	0%		0%			0%	25%	0%		0%	25%	25%	25%	60.5	61.0	382.7
A4.c9	25%	25%		0%			0%	0%	0%		0%	25%	25%	0%	38.6	58.3	292.2
A4.c10	25%	0%		25%			0%	0%	0%		0%	25%	25%	0%	54.2	55.7	345.6
A4.c11	25%	0%		0%			25%	0%	0%		0%	25%	25%	0%	40.3	72.9	335.0
A4.c12	25%	0%		0%			0%	25%	0%		0%	25%	25%	0%	46.8	55.0	315.3
A4.d1	0%	25%		25%			0%	0%	0%		0%	25%	25%	0%	45.4	53.3	306.0
A4.d2	0%	25%		0%			25%	0%	0%		0%	25%	25%	0%	33.1	64.1	285.9
A4.d3	0%	25%		0%			0%	25%	0%		0%	25%	25%	0%	39.5	47.1	268.1
A4.d4	0%	0%		25%			25%	0%	0%		0%	25%	25%	0%	68.8	68.1	432.0
A4.d5	0%	0%		25%			0%	25%	0%		0%	25%	25%	0%	55.2	51.9	339.7

Table V-7.15 *Contd...*

Mix #	re 1	re 2	re 3	re 4	re 5	re 6	re 7	re 8	ce 1	ce 2	ce 3	ce 4	ce 5	ce 6	% G	% X	TS
A4.d6	0%	0%		0%			25%	25%	0%		0%	25%	25%	0%	65.6	76.5	440.4
A12.g2	25%	25%		0%			0%	0%	0%		0%	25%	0%	25%	56.7	65.3	378.8
A12.h2	25%	0%		25%			0%	0%	0%		0%	25%	0%	25%	68.0	69.9	433.4
A4.d9	25%	0%		0%			25%	0%	0%		0%	25%	0%	25%	66.4	22.1	308.7
A4.d10	25%	0%		0%			0%	25%	0%		0%	25%	0%	25%	57.5	27.2	287.0
A4.d11	0%	25%		25%			0%	0%	0%		0%	25%	0%	25%	54.9	24.6	270.7
A4.d12	0%	25%		0%			25%	0%	0%		0%	25%	0%	25%	59.2	13.5	259.3
A4.e1	0%	25%		0%			0%	25%	0%		0%	25%	0%	25%	56.5	27.2	283.2
A4.e2	0%	0%		25%			25%	0%	0%		0%	25%	0%	25%	63.4	27.4	310.1
A4.e3	0%	0%		25%			0%	25%	0%		0%	25%	0%	25%	58.1	30.2	297.0
A4.e4	0%	0%		0%			25%	25%	0%		0%	25%	0%	25%	67.3	30.3	332.4
A4.e5	25%	25%		25%			0%	0%	0%		0%	25%	0%	0%	56.5	18.7	262.1
A4.e6	25%	25%		0%			25%	0%	0%		0%	25%	0%	0%	43.7	19.5	215.5
A12.a3	25%	25%		0%			0%	25%	0%		0%	25%	0%	0%	56.8	61.4	369.5
A12.b3	25%	0%		25%			25%	0%	0%		0%	25%	0%	0%	64.5	62.7	402.1
A4.e9	25%	0%		25%			0%	25%	0%		0%	25%	0%	0%	50.8	26.9	260.8
A4.e10	25%	0%		0%			25%	25%	0%		0%	25%	0%	0%	43.3	38.1	260.1
A4.e11	0%	25%		25%			25%	0%	0%		0%	25%	0%	0%	58.4	28.7	294.2
A4.e12	0%	25%		25%			0%	25%	0%		0%	25%	0%	0%	44.1	23.7	227.6
A4.f1	0%	25%		0%			25%	25%	0%		0%	25%	0%	0%	65.3	30.6	325.6
A4.f2	0%	0%		25%			25%	25%	0%		0%	25%	0%	0%	51.9	37.2	290.7
A4.f3	25%	25%		0%			0%	0%	0%		0%	0%	25%	25%	55.4	58.0	355.7
A4.f4	25%	0%		25%			0%	0%	0%		0%	0%	25%	25%	62.9	64.0	399.3
A4.f5	25%	0%		0%			25%	0%	0%		0%	0%	25%	25%	73.7	67.1	448.2
A4.f6	25%	0%		0%			0%	25%	0%		0%	0%	25%	25%	61.9	55.2	373.4
A12.c3	0%	25%		25%			0%	0%	0%		0%	0%	25%	25%	50.5	18.6	239.2

Table V-7.15 *Contd...*

Mix #	re 1	re 2	re 3	re 4	re 5	re 6	re 7	re 8	ce 1	ce 2	ce 3	ce 4	ce 5	ce 6	% G	% X	TS
A12.d3	0%	25%		0%			25%	0%	0%		0%	0%	25%	25%	59.6	17.6	271.2
A4.f9	0%	25%		0%			0%	25%	0%		0%	0%	25%	25%	51.7	53.6	330.8
A4.f10	0%	0%		25%			25%	0%	0%		0%	0%	25%	25%	65.5	74.5	435.5
A4.f11	0%	0%		25%			0%	25%	0%		0%	0%	25%	25%	57.8	62.4	375.6
A4.f12	0%	0%		0%			25%	25%	0%		0%	0%	25%	25%	55.6	70.0	386.2
A4.g1	25%	25%		25%			0%	0%	0%		0%	0%	25%	0%	56.0	63.3	371.1
A4.g2	25%	25%		0%			25%	0%	0%		0%	0%	25%	0%	28.2	64.1	267.3
A4.g3	25%	25%		0%			0%	25%	0%		0%	0%	25%	0%	49.4	56.7	329.6
A4.g4	25%	0%		25%			25%	0%	0%		0%	0%	25%	0%	62.9	65.7	403.3
A4.g5	25%	0%		25%			0%	25%	0%		0%	0%	25%	0%	62.7	60.4	389.5
A4.g6	25%	0%		0%			25%	25%	0%		0%	0%	25%	0%	68.1	68.7	430.7
A12.e3	0%	25%		25%			25%	0%	0%		0%	0%	25%	0%	58.2	28.3	292.7
A12.f3	0%	25%		25%			0%	25%	0%		0%	0%	25%	0%	56.9	35.8	306.2
A4.g9	0%	25%		0%			25%	25%	0%		0%	0%	25%	0%	67.8	67.0	425.5
A4.g10	0%	0%		25%			25%	25%	0%		0%	0%	25%	0%	72.8	74.0	462.0
A4.g11	25%	25%		25%			0%	0%	0%		0%	0%	0%	25%	60.4	28.2	300.8
A4.g12	25%	25%		0%			25%	0%	0%		0%	0%	0%	25%	58.6	15.7	262.6
A4.h1	25%	25%		0%			0%	25%	0%		0%	0%	0%	25%	63.3	25.5	305.0
A4.h2	25%	0%		25%			25%	0%	0%		0%	0%	0%	25%	62.4	24.2	298.4
A4.h3	25%	0%		25%			0%	25%	0%		0%	0%	0%	25%	59.1	22.8	282.1
A4.h4	25%	0%		0%			25%	25%	0%		0%	0%	0%	25%	64.8	28.9	319.4
A4.h5	0%	25%		25%			25%	0%	0%		0%	0%	0%	25%	70.6	24.2	329.8
A4.h6	0%	25%		25%			0%	25%	0%		0%	0%	0%	25%	57.9	27.2	288.6
A12.g3	0%	25%		0%			25%	25%	0%		0%	0%	0%	25%	71.0	32.5	351.8
A12.h3	0%	0%		25%			25%	25%	0%		0%	0%	0%	25%	61.0	37.4	325.9
A4.h9	25%	25%		25%			25%	0%	0%		0%	0%	0%	0%	62.9	33.6	323.7
A4.h10	25%	25%		25%			0%	25%	0%		0%	0%	0%	0%	52.8	31.2	279.2
A4.h11	25%	25%		0%			25%	25%	0%		0%	0%	0%	0%	57.2	31.3	296.3
A4.h12	25%	0%		25%			25%	25%	0%		0%	0%	0%	0%	39.9	27.5	220.8

APPENDIX VI (Chapter 8 - Purified enzyme synergy)

Table VI-8.5 *Glucan (% G) 24 hour hydrolysis yields for untreated avicel (UAV), liquid ammonia treated Avicel (AAV), untreated corn stover (UCS) and AFEX treated corn stover (ACS) by varying cellulase (CBH I, CBH II, EG I) combinations (mg enzyme/g glucan).*

#	Protein loading (mg/g glucan)				UAV	AAV	UCS	ACS
	CBH I	CBH II	EG I	βG	% G	% G	% G	% G
1	15	0	0	0.75	13.4	4.5	1.7	5.0
2	0	15	0	0.75	9.7	4.2	1.0	5.2
3	0	0	15	0.75	3.7	5.9	4.7	7.8
4	7.5	7.5	0	0.75	25.2	28.9	3.9	4.9
5	7.5	0	7.5	0.75	26.9	42.5	9.5	39.6
6	0	7.5	7.5	0.75	14.9	23.5	7.1	24.3
7	5	5	5	0.75	41.8	80.9	10.9	49.7
8	10	2.5	2.5	0.75	41.5	70.0	10.9	45.0
9	2.5	10	2.5	0.75	39.7	78.0	8.9	41.5
10	2.5	2.5	10	0.75	36.7	74.0	10.3	46.7

Table VI-8.7 *Glucan (% G) and xylan (% X) 24 hour hydrolysis yields for AFEX treated corn stover by varying enzyme (CBH I, CBH II, EG I, EX, βX) combinations (mg enzyme/g glucan).*

	Protein loading (mg/g glucan)							
#	CBH I	CBH II	EG I	EX	βX	βG	% G	% X
1	15	0	0	0	0	1.5	5.4	1.3
2	0	15	0	0	0	1.5	6.1	0.2
3	0	0	15	0	0	1.5	12.1	6.5
4	0	0	0	15	0	1.5	2.2	16.0
5	0	0	0	0	15	1.5	1.8	8.2
6	7.5	7.5	0	0	0	1.5	9.7	0.3
7	7.5	0	7.5	0	0	1.5	47.9	5.8
8	7.5	0	0	7.5	0	1.5	11.6	13.5
9	7.5	0	0	0	7.5	1.5	5.1	9.6
10	0	7.5	7.5	0	0	1.5	30.5	5.3
11	0	7.5	0	7.5	0	1.5	14.9	13.3
12	0	7.5	0	0	7.5	1.5	5.4	6.8
13	0	0	7.5	7.5	0	1.5	12.3	12.7
14	0	0	7.5	0	7.5	1.5	11.3	36.0
15	0	0	0	7.5	7.5	1.5	1.7	49.6
	Protein loading (mg/g glucan)							
#	CBH I	CBH II	EG I	EX	βX	βG	% G	% X
16	4.95	4.95	4.95	0	0	1.5	56.8	5.4
17	4.95	4.95	0	4.95	0	1.5	36.7	10.5
18	4.95	4.95	0	0	4.95	1.5	9.3	8.2
19	4.95	0	4.95	4.95	0	1.5	52.1	9.8
20	4.95	0	4.95	0	4.95	1.5	42.9	37.4
21	4.95	0	0	4.95	4.95	1.5	12.3	47.1
22	0	4.95	4.95	4.95	0	1.5	35.1	10.7
23	0	4.95	4.95	0	4.95	1.5	28.0	35.5
24	0	4.95	0	4.95	4.95	1.5	12.5	47.9
25	0	0	4.95	4.95	4.95	1.5	11.8	47.5
26	3.75	3.75	3.75	3.75	0	1.5	65.3	9.1
27	3.75	3.75	3.75	0	3.75	1.5	53.7	37.8
28	3.75	3.75	0	3.75	3.75	1.5	30.5	48.1
29	3.75	0	3.75	3.75	3.75	1.5	48.4	50.5
30	0	3.75	3.75	3.75	3.75	1.5	31.2	47.8
31	3	3	3	3	3	1.5	64.1	51.4

APPENDIX VII - Materials and Experimental Methods

A-VII-1. Biomass feedstock

(a) Pre-milled (PM) corn stover, passed through a 10 mm screen, was generously provided by the National Renewable Energy Laboratory (NREL), Golden (Colorado). The corn stover feedstock was grown from Pioneer Hybrid seed variety (33A14) and harvested in 2002 from the Kramer farm in Wray, CO. NREL corn stover was used for most experiments, except in some cases where other sources of biomass were utilized.

(b) NREL pre-milled corn stover was further milled in a conventional laboratory blender for a period of ten minutes, followed by sieving for twenty minutes in a Ro-Tap testing sieve shaker (Model B, Tyler) to obtain various corn stover mesh cut fractions. The PM corn stover was also milled down to a desired particle size range using a centrifugal mill (Model ZM 200, Retsch) fitted with various ring sieve attachments.

(c) Corn stover was also freshly harvested from MSU farms (2 harvest time points: early and late corresponding to late July and early September, respectively) and used for certain microscopy experiments (e.g. AFM, SEM, and LSCM). The MSU corn stems were sectioned into thin slices (slice thickness ranging from 100 μm to 1 mm) using a blade prior to AFEX pretreatment.

(d) Avicel (PH-101, Sigma-Aldrich, St-Louis), cotton linters (Long fibers, Sigma-Aldrich, St-Louis), oat spelt xylan (Sigma-Aldrich, St-Louis) and regular cotton balls (scoured and bleached; Courtesy Dr. Al French, USDA) were procured from respective sources.

A-VII-2. Biomass centrifugal milling

The pre-milled corn stover (before or after AFEX pretreatment) was sieved in a Ro-Tap testing sieve shaker (Model B, Tyler) to separate corn stover fractions larger than 100 μms. The larger stover fractions were milled using a centrifugal mill (Model ZM 200, Retsch, Newtown, PA) fitted with a 250 μm ring sieve attachment followed by sieving to separate stover residual fraction larger than 100 μms. The milled fractions were sieved to remove finer particles and help speed up the milling process. This also avoided excessive heating of the biomass due to accumulation of fines within the mill. The residual fraction (larger than 100 μms) was centrifugally milled with an 80 μm ring sieve attachment. The milled fraction was again sieved to ensure particle size was less than 100 μms. No fraction of the original substrate was left out during the milling process and milled fractions (particle size < 100 μms) were mixed at the end to give a homogeneous, representative sample. Revolution speed for grinding was set at 18,000 rpm with the biomass fed continuously (feed rate ~ 10 gm/min) using a vibratory feeder (DR 100, Retsch). The ground material was removed continuously from the cassette using a cyclone separator to avoid heat build up during the milling operation.

A-VII-3. Particle size distribution

Particle size distribution for centrifugally milled corn stover was determined using a sieve shaker (AS 200, Retsch, Newtown, PA) using standard sieves with mesh sizes ranging from 0.038 to 0.125 mm (sieve diameter 8" x 2" according to ASTM E11-01) at amplitude 1.2 mm, interval time of 10 sec and sieving duration of 5 min. A fixed amount of corn stover (25-30 gms) was milled in 4 replicate batches and particle size distribution determined for the entire quantity of milled sample. The particle size for crystalline

cellulose (Avicel) was also determined in duplicate. The particle size distribution results are reported in Chapter 5.1.

A-VII-4. AFEX pretreatment

(a) AFEX pretreatment on corn stem cross-sections for certain microscopy experiments (SEM, LSCM, AFM) was carried out in a small 22 ml bench-top reactor (316 SS, PARR Instrument Co, IL) due to limited availability of sample. The vessel was loaded with feedstock containing the appropriate moisture content (60% or 200%, dwb). The reactor was clamped shut and the required amount of ammonia (1:1 or 2:1 ammonia to biomass loading, w/w) was injected using a pre-weighed delivery vessel. The reactor was heated using a custom made aluminium block on a Vela hot plate and was maintained at the desired temperature for the necessary residence time. It took approximately 30-45 minutes to complete a typical AFEX reaction. At the end of the residence time, the pressure was explosively released using a half inch National pipe threat (NPT) stainless steel ball valve and biomass was removed from the reactor and left in the hood overnight to remove residual ammonia.

(b) Varying AFEX severity pretreatments were carried out in a 2 liter or 300 ml Parr reactor (PARR Instrument Co, IL). The protocol was modified from the conventional AFEX pretreatment approach for better control over residence time. The reactor vessel was preheated to the desired pretreatment temperature using a suitably modified heating mantle. The biomass (at suitable moisture content) was added to the preheated reactor and clamped shut. The ammonia delivery vessel was filled with the necessary amount of ammonia (preheated in advance) to deliver to the reactor. The rate of heating was empirically optimized through a trial and error approach by measuring pressure and

temperature of the ammonia delivery vessel during the heating process. Upon addition of the heated ammonia to the biomass the contents of the reactor instantaneously achieved the desired temperature (within ± 10 °C) in the reactor upon delivery. The actual residence time for the pretreatment was clocked from the time of delivery of ammonia to the reactor. All experiments in Chapter 6 were performed on samples that were AFEX treated (1:1 ammonia loading, 60% moisture, 90 °C, 30 min) after the milling process. Whereas, experiments in Chapters 7-8 were carried out on samples that were milled after the AFEX process.

A-VII-5. Compositional analysis of solid and liquid samples

(a) Compositional analyses of lignocellulosic biomass were performed according to NREL Laboratory Analytical Procedures (LAPs): (i) Preparation of samples for compositional analysis, (ii) Determination of structural carbohydrates and lignin in biomass [346]. The polysaccharide composition of untreated NREL corn stover was determined (at NREL) to be 34.4% glucan, 22.4% xylan, 4.2% arabinan, 0.6% mannan, 1.4% galactan, 11% lignin, 2.3% protein, 5.6% acetyl, 6.1% ash, 3.8% uronic acids and 2.2% sucrose.

(b) Oligosaccharides in the water extracts were quantified by acid hydrolysis based on the NREL LAP protocol (Determination of Sugars, Byproducts, and Degradation Products in Liquid Fraction Process Samples) [346].

A-VII-6. Scanning electron microscopy (SEM)

Scanning electron microscopy was carried out on a JEOL (Japan Electron Optics Laboratories) 6400V SEM with a LaB6 emitter. The biomass samples were gold sputter coated without critical point drying (CPD), to avoid possible extraction of AFEX surface

deposits during CPD, and imaged at accelerating voltages between 10-20 kV to prevent electron beam induced damage to the specimens. Cell wall lumen perimeter and enclosed area were calculated using Zeiss LSM Image Browser (Version 3.0, Carl Zeiss International, Jena, Germany).

A-VII-7. Laser confocal scanning fluorescence microscopy (LCSM)

Untreated and AFEX pretreated MSU corn stems sections (slice thickness ranging from 100 μm to 1 mm) were stained with 1% O' Safranin (Sigma, St Louis, MO) in distilled water for 15 minutes. After staining, the sections were thoroughly rinsed in fresh distilled water. The stained and rinsed samples were carefully mounted in distilled water with a coverslip and observed using a Zeiss Pascal LSCM. Several objective lenses (10 X/0.3 NA and 20 X/0.5 NA Carl Zeiss Plan-Neofluar lenses; NA- numerical aperture) were used to image the thicker samples that required a larger working distance. Excitation from a 543 nm laser line and emission passing through a long pass (LP) 560 nm filter was used for observing fluorescence (digitally colored in green). Sections of the tissue were also observed for auto-fluorescence without staining the samples. Stacks of confocal optical sections were taken throughout the z-depth of the observed plant stem section. Several individual cross-sections were observed and extended focus images of the stacks were compiled using the maximum intensity algorithm software (LSM 5 Pascal Version 3, Carl Zeiss International, Jena, Germany).

A-VII-8. Atomic force microscopy (AFM)

AFM imaging was conducted using a Dimension Nanoscope 3100 Scanning Probe Microscope (Digital Instruments) with a Nanoscope IIIa controller. Both amplitude and phase images were collected simultaneously in tapping mode with an MPP-11100, etched

silicon probe with a nominal frequency of 300 kHz and a nominal spring constant of 40 N/m. Some samples were extracted three times, at room temperature, with (1:10 biomass to solvent loading, w/w) 0.1 N sodium hydroxide, followed by 75% ethanol and D/I water prior to imaging. RMS roughness factors were estimated after image flattening and plane fitting of the height images using the software that came along with the instrument. The width of the cell wall microfibrils and AFEX deposits were calculated using Zeiss LSM Image Browser (Version 3.0, Carl Zeiss International, Jena, Germany).

A-VII-9. Transmission electron microscopy (TEM) and 3D-tomography (3D-Tomo)

Corn stover samples were processed using the microwave Electron Microscopy (EM) processing methodology [112]. The biomass was fixed twice for 6 min in 2.5% gluteraldehyde solution buffered in 0.1 M sodium cacodylate buffer (EMS, Hatfield, PS) under vacuum. Dehydration was carried out in graded ethanol series for 1 min each (15%, 30%, 60%, 90%, twice for 100% ethanol). Samples were infiltrated with LR White (or Epon) resin in the microwave under vacuum and incubated overnight at room temperature for increasing concentrations of the resin (15%, 30%, 60%, 90%, thrice for 100% resin, diluted in ethanol). The samples were then transferred to gelatin capsules and the resin was polymerized by heating to 60 °C overnight. LR White embedded samples were sectioned to ~ 100-250 nm with a Diatome diamond knife on a Leica EM UTC ultramicrotome (Leica, Wetzlar, Germany). The sectioned samples were collected on Formvar coated copper or nickel slot grids (SPI Supplies, West Chester, PA). Grids were post-stained for 6 min with 2% aqueous uranyl acetate. The grids were also stained with 1% $KMnO_4$ for 10 min to selectively stain for lignin. Images were taken with a Gatan UltraScan 1000 camera (Gatan, Pleasanton, CA) on a FEI Tecnai G220 Twin 200 kV

LaB6 TEM (FEI, Hilsboro, OR). Tomograms were created by capturing dual-axis +/– 60–65° tilt series using Serial EM (http://bio3d.colorado.edu/). Tomograms were constructed using an R-weighted back projection algorithm within the IMOD software package (http://bio3d.colorado.edu/). Single-axis tomograms were then combined to yield dual-axis tomograms using a warping algorithm within IMOD [496]. Tomograms were displayed and analyzed using the IMOD software package [272].

A-VII-10. Cell wall immunolabeling-electron microscopy (Immuno-EM)

Anti-arabinoxylan LM-11 antibody was obtained from Plant probes (Leeds, UK). The epitope for LM-11 has four xylose residues that are able to accommodate un-substituted and substituted xylan backbones [282]. For anti-xylan immuno-EM, sample grids were placed on 15 μL drops of 1.5% BSA (bovine serum albumin) in 1X PBS-0.1% Tween (PBST) for 30 min, blotted, then directly placed on 15 μL drops of respective primary antibodies diluted 1:10 in 1% BSA-PBST for 90 min. Following 3 x 1 min rinses, the grids were then placed on 15 μL drops of anti-rat (IgG) secondary antibody conjugated to a 15 nm gold particle (British BioCell, Ted Pella) diluted 1:100 in PBST. Samples were then rinsed 3 x 1 min with PBST and again in H2O. The grids were post-stained with Uranyl acetate and $KMnO_4$ for better contrast, if necessary.

A-VII-11. Dilute acid pretreatment

Dilute acid pretreated corn stover was procured from NREL. Dilute acid pretreatment was carried out as described elsewhere [497]. Pretreatment was conducted at 190°C at a biomass solids and sulfuric acid loading of 30% (w/w) and 0.048 g/g dry corn stover, respectively. The whole slurry from the reactor was used in this study.

A-VII-12. Nitrogen physisorption analysis

The Brunauer-Emmett-Teller (BET) surface area and pore size distribution were measured by nitrogen adsorption at 77 K using a Micromeritics ASAP 2700 instrument. At least 2-3 gms of sample was used for each run and were degassed at 60 °C overnight.

A-VII-13. Near Infra-Red Compositional Analysis

The compositional analysis of the corn stover fractions was performed by the Near-IR spectroscopic analysis (courtesy of Dr. Bonnie Hames) at the National Renewable Energy Laboratory (NREL), Golden (Colorado) [498].

A-VII-14. Electron Spectroscopy for Chemical Analysis (ESCA)

Surface chemical characterization was carried out using a Physical Electronics PHI5400 ESCA electron spectrometer equipped with a non-monochromatic Mg Kα (15 V, 300W) X-ray source. An area of 250 x 250 square microns with a take off angle of 45 degrees was analyzed. Peak intensities were determined by peak area integration. Curve fitting to the C1s and O1s peaks was carried out with a Lorentzian-Gaussian curve-fitting program. Calcium and nitrogen peaks were deconvoluted and fitted by the software as well. Some samples were extracted three times, at room temperature, with (1:10 biomass to solvent loading, w/w) 0.1 N sodium hydroxide, followed by 75% ethanol and D/I water prior to analysis.

A-VII-15. Fourier Transform Infra-Red Spectroscopy (FTIR)

Spectrum One FTIR system (Perkin Elmer) with a universal ATR (Attenuated Total Reflection) accessory was used to qualitatively monitor chemical changes in AFEX pretreated biomass. The sample (milled to 100 μms) was pressed uniformly and tightly against the diamond surface using a spring-loaded anvil. Mid-IR spectra were obtained

by averaging 16 scans from 4000 to 400 cm^{-1} at 2 cm^{-1} resolution. The region between 1900 and 2200 cm^{-1} was avoided because of the strong diamond IR absorption. Baseline and ATR corrections for penetration depth and frequency variations were carried out using the Spectrum One software supplied with the equipment.

A-VII-16. Raman Spectroscopy

Raman spectra of untreated and AFEX treated samples were obtained using a near-IR FT-Raman based spectroscope. The problem of laser-induced fluorescence was minimized using the near IR (1064 nm Nd:YAG diode) laser for sample excitation. Some samples were delignified using acid chlorite and then bleached with sodium borohydride to minimize fluorescence interference.

A-VII-17. Cellulose II, III and Amorphous Cellulose Preparation

Cellulose III (from Avicel, Cotton Linter, Cotton) was prepared by soaking dry biomass in excess anhydrous liquid ammonia (> 5:1 gms ammonia per gm biomass) at the required temperature (ranging from 4 to 130 °C) for a total treatment time of 30 min. The samples were dried in the hood overnight to remove residual ammonia and then stored in the fridge.

Cellulose II (Avicel) was prepared by mixing Avicel with 25% NaOH at 4 °C, at a loading of 1:10 (gm substrate per ml of sodium hydroxide solution) for 60 min. The slurry was then centrifuged, filtered and washed with DI water till neutral pH. Avicel was also soaked in 28-30% ammonium hydroxide solutions for 60 mins at 4 °C prior to filtration and washing till neutral pH. Regenerated amorphous cellulose from Avicel was prepared using 83% phosphoric acid (at 4 °C for 60 min) based on a previously published protocol [128].

A-VII-18. Powder X-Ray Diffraction (XRD)

Dried samples were packed into 1.5 mm diameter quartz capillaries (Charles supply company, Natick MA) and mounted on a Bruker AXS three circle goniometer. The quartz capillaries are for all practical purposes transparent to CuK_α X-rays and did not contribute any appreciable background signal. All X-ray diffraction patterns were collected on a Smart6000 CCD area detector that was positioned 50 mm from the sample with an exposure time of 90 seconds. CuK_α radiation was generated by a Microstar rotating Cu anode generator at 45 kV and 45 mA (Bruker AXS, Madison, WI) with a source size of approximately 0.3 mm in diameter. Each diffraction pattern image contained data ranging from 1 to 37 degrees 2θ. The images were unwarped and converted using the Apex2 v2009.3-0 (Bruker AXS, Madison WI) software package. The converted images were integrated from 3 to 37 degrees 2θ in 0.04 degrees steps using the XRD^2Eval module in Apex2 v2009.3-0 (Bruker AXS, Madison, WI).

A-VII-19. Solvent extraction methodologies

(a) The degradation products from the solid samples were extracted using a Dionex ASE 200 extractor (Dionex Corporation, Sunnyvale, CA) at 70 °C using DI water (or acetone). The pretreated samples used for each extraction ranged between 0.5-1 gm (for a 11 ml cell) at 70 °C, 2 extraction cycles, 1500 psi cell pressure, static time of 10 mins and purge time of 60 seconds. The ASE extracted samples were kept at room temperature overnight prior to further analysis by LC-MS/MS and GC-MS. The extracted samples were analyzed the next day after extraction to prevent irreversible precipitation of certain degradation products upon long-term storage (especially at lower temperatures). All

samples in chapter 3.1 were extracted for degradation product analysis using this protocol.

(b) Untreated and AFEX treated biomass were presoaked and washed in distilled (de-ionized) water with a substrate to water loading of 1:10 (w/w). The slurry was mixed for 15 minutes. The wash liquid was removed from the substrate by squeezing the slurry through a filtration cloth (Calbiochem, CA). All samples in chapter 3.1 were washed using this protocol for analysis of ligno-phenolics in the water extract.

A-VII-20. Gas Chromatography Mass Spectrometry (GC-MS)

Certain degradation products that could not be quantified by LC-MS/MS (e.g. acetic acid, furfural, 5-HMF, and acetamide) were analyzed by GC-MS. The lignocellulosic samples were extracted with acetone at 70 °C using the automated solvent extractor, as mentioned earlier, and were analyzed directly. The instrumentation consisted of an Agilent 6890N GC-MS system equipped with an Agilent 7683 ALS. Chromatographic separation was achieved using a 30 m J&W DBWAX column (0.25 mm I.D., 0.25 μm film thickness). The injection volume was 1 μL in splitless mode with 240 °C injector temperature. The injector sleeve was replaced at regular intervals (due to deposition of non-volatile components of the plant extracts) to improve reproducibility of the analysis. The oven temperature profile was varied as follows: temperature held initially at 50 °C for 1 min and then increased by 30 °C/ min to 100 °C, to be held at 100 °C for 1 min. The column temperature was finally increased at 38 °C/ min to 240 °C and held at 240 °C for 2 min. Data was collected by the MS in EI mode using selected ion monitoring (SIM), focusing on the primary and secondary masses of the compounds of interest. The data was exported and analyzed using Mass-Lynx software.

A-VII-21. Ammonolysis By-product Analysis by LC-MS/MS

The LC-MS system utilized for quantification of phenolic acids (ferulic and coumaric acid) and their corresponding amides consisted of an Acquity UPLC® connected to a Waters Quattro Premier triple quadrupole mass spectrometer (with ESI or electro-spray ionization). Samples (ASE water extracts) were analyzed by LC-MS using an Ascentis Express C18 (5 cm × 2.1 mm × 2.7 μm) reversed phase column (Supelco, USA). Gradient elution was carried out using aqueous 0.1% formic acid (v/v; solvent A) and methanol (solvent B) under the following conditions; (1) Initial gradient of 95%-A/5%-B held for 1 min, (2) linear gradient to 70%-A/30%-B at 10 min and then to 65%-A/35%B at 12 min, (3) gradient is changed immediately to 10%-A/90%-B at 12.01, held for 2 min, (4) followed by a linear gradient back to the initial condition at 14.01 min and held for 3 min. Injection volume, column temperature and flow rates employed were 3 μL, 50 °C and 0.25 ml/min, respectively. Standard curves were generated based on the areas under the peak ($[M-H]^-$ peak in negative ESI mode) for each compound.

A-VII-22. Other Degradation Product Analysis by LC-MS/MS

Details of the LC-MS/MS analytical methodology (for non-ammonolysis products) have been reported elsewhere [334,349] and are summarized below. AFEX degradation products in the pretreated biomass were extracted with hot water (70 °C) using the accelerated solvent extraction apparatus, as mentioned earlier. The pH of the AFEX stover water extract solution was found to be slightly alkaline and was acidified to pH 2 before processing according to a previously published protocol [334]. A 5-ml aliquot of each aqueous extract was then extracted two times with methyl *tertiary*-butyl ether (MTBE). The resulting MTBE extracts were combined and the solvent was removed by

purging under a gentle stream of nitrogen at 55 °C. All samples were reconstituted in 5 ml water prior to analysis.

Instrumentation employed for analysis consisted of a Varian (Palo Alto, CA, USA) ProStar Model 210 binary pump system, Model 410 auto sampler, and Model 1200L triple-quadrapole mass analyzer. A binary solvent gradient consisting of two solvents A and B. Solvent A consists of aqueous formic acid (0.025% (v/v) formic acid in water) and solvent B consists of 10% aqueous formic acid and 90% acetonitrile was used to achieve chromatographic separation on a 150 mm × 4.6 mm (S 03 μm, 99) YMC Carotenoid column (Waters, Milford, MA, USA) connected in series to a 1 mm RP C18 OPTI-Guard column (Altech, Deerfield, IL, USA). Additional chromatographic parameters were as follows: injection volume, 50 μL; column temperature, 30 °C; flow rate, 750 μL/min. It is important to note that these chromatographic conditions are similar to those reported in previous work. The only major difference was the substitution of formic acid for phosphoric acid. This change was implemented to improve mobile phase compatibility with MS detection. Upon exiting the column, the mobile phase was directed to both a UV-visible photodiode array (PDA) detector and the mass analyzer, which was operated exclusively in negative electrospray ionization (–ve ESI) mode. The majority of target analytes were assessed by monitoring an optimized MS/MS for each compound, with parent ion $[M-H]^-$ selected in the first quadrapole. A flow-splitter was inserted between the PDA detector and the mass spectrometer such that the volume of liquid passing through the flow-splitter was diverted 50:50 between the mass analyzer and the waste line. Mass spectrometry parameters were held constant during all experiments and were as follows: nebulizing gas, O_2 at 60 psi; drying gas, N_2 at 20 psi; drying gas

temperature, 400 °C; needle voltage, 4500 V; collision gas, Ar at 2.0 mTorr. Exceptions include acetic acid, furfural, and 5-hydroxymethylfurfural (5-HMF) which were not amenable to mass spectral monitoring under these conditions and were instead detected via GC-MS.

Quantitation of target analytes by LC-MS/MS was accomplished using a multipoint, internal-standard calibration curve. Calibration standards were prepared by successive dilutions of stock solutions in water. Aliquots of each calibration standard were extracted with MTBE prior to analysis (as described earlier). Response factors were determined for each analyte by dividing the peak area of the analyte by the peak area of the internal standard, and calibration curves were constructed by plotting a linear regression ($R^2 \geq 0.99$) of response factor versus analyte concentration. It has been previously demonstrated [334] that this approach to quantitation does not require independent knowledge of MTBE extraction efficiencies in order to assess analyte concentrations. However, this approach does not take into account potential matrix effects of co-extracted components on electro spray ionization efficiency.

In order to characterize the matrix effects for various degradation product quantified by the LC-MS/MS method, matrix spike analysis was conducted. Calculated spike recoveries revealed negligible matrix influence in samples derived from untreated lignocellulosic biomass (i.e. spike recoveries were essentially quantitative in these samples). More significant matrix interference was identified for some analytes in samples derived from pretreated (AFEX and dilute acid treated) biomass. The matrix effects were most pronounced for acid pretreated corn stover samples. Spike recoveries for all analyte concentrations derived from calibration curves were accurate within a

factor of 1-3, independent of sample source, which was deemed sufficient to support the goals of the present study.

A-VII-23. High Performance Liquid Chromatography (HPLC) for Sugars

A high performance liquid chromatography (HPLC) system was used for analyzing monomeric and oligomeric sugars. The HPLC system consisted of Waters (Milford, MA) Pump and Waters 410 refractive index detector. An Aminex HPX-87P carbohydrate analysis column (BioRad, Hercules, CA) equipped with a deashing guard cartridge (BioRad) was used for quantifying monomeric sugars. Degassed HPLC grade water was used as the mobile phase at 0.6 ml/min at a column temperature of 85 °C. The injection volume was 10 µl with a run time of 20 min. Mixed sugar standards were used to quantify cellobiose and other monosaccharides (glucose, xylose, galactose, arabinose and mannose). The monomeric sugars produced after acid hydrolysis were quantified by using a Bio-Rad Aminex HPX-87H ion exclusion column (60°C; 5 mM H_2SO_4; flow rate, 0.6 ml min^{-1}; injection volume, 10 µl) and differential refractive index detector.

A-VII-24. Modified Prussian Blue Method (MPB)

Phenolic compounds content of the degradation product extracts was quantified by the MPB method [249]. The water extract was centrifuged to remove suspended solids and filtered through a 0.2-micron nylon membrane filter before carrying out the MPB analysis. Phosphoric acid (85%), Gum Arabic, Gallic acid, Ferulic acid, $K_3Fe(CN)_6$ and $FeCl_3$, were purchased from the Sigma Chemical Co. (St. Louis, MO). MPB stabilizer reagent was prepared by mixing 6 parts of distilled water with 2 parts of 85% phosphoric acid and 2 parts of 1% gum arabic solution. One hundred micro liters of the undiluted

wash extract was placed in duplicate sets of large (150 x 25 mm) falcon tubes. Three milliliters of distilled (deionized) water was added to the tubes and mixed well with the wash extract. 1 ml of 0.016 M $K_3Fe(CN)_6$ was added followed immediately by 1 ml of 0.02 M $FeCl_3$ in 0.1 N HCl. The mixture was vortex mixed and allowed to stand at room temperature. After 15 min, 5 ml of the MPB stabilizer reagent was added to the contents of the tube and vortexed again. The intensity of the Prussian blue color developed was measured at 700 nm against a reagent blank using a digital spectrophotometer (Barnstead/Thermolyne Series SP-800). Gallic and ferulic acids were used as standards to determine equivalent phenolic concentration.

A-VII-25. Robotic Dispensor Worktable Setup

Liquid Handling Workstation epMotion 5070 (Eppendorf, Hamburg, Germany) was used to deliver biomass slurries and reagents to deep well microplates. The workstation worktable was equipped with 1000 µL hand cut filter tips (epT.I.P.S.), a reservoir rack with 100 mL epMotion reagent reservoirs (slurry suspension and buffer-antibiotic mixture), 96 deep-well reaction microplate with 2 ml cavities (Greiner Bio-one, Monroe, NC) and corresponding 96-well enzyme mixture microplate. A slurry suspension of suitable solids loading was prepared in a 50 ml falcon tube and transferred to a 100 ml reservoir. All slurry dispensing steps were carried out with the epMotion multi-channel dispensing tool (1000 µL). All reagent liquid levels were determined via the optical sensor on the Workstation. The labware, total number of tips and type of tip rack were checked via the sensor. The optimal slurry dispension epMotion parameters are as follows; slurry aspiration cycles (50), agitation speed (60 mm/s), agitation volume (0.6-

0.8 ml/tip), aspiration speed (15-25 mm/s), dispension speed (15-30 mm/s), delay blow (1 s) and speed blow (30-90 mm/s).

A-VII-26. Reproducibility of Slurry Delivery

Reproducibility and accuracy of the slurry delivery to the microplate was determined by collecting the slurry delivered, for varying avicel solids loading (1-10 %, w/w), in a pre-weighed plastic trough and then evaporated in an oven set at 60 °C until constant weight was obtained. A slurry of suitable solids loading (e.g. 1%, w/w) was prepared in a 50 ml falcon tube and transferred to the reservoir vessel on the worktable. A 1000 µl, 8-channel multi-dispensing tool was used to deliver necessary volume of slurry (e.g. 750 µl for 1% slurry to deliver 7.5 mgs of solids to each well) to each column in the microplate. The volume of slurry dispensed was calculated based on the solids loading in order to deliver 7.5 mg of solids in each well. Slurry volume equivalent to 16 microwell volumes was collected in a suitable collection vessel (e.g. trough). Three replicate batches (16 well volumes each) of slurry were delivered for each 50 ml starting reservoir volume. The reservoir slurry was replaced with a freshly prepared solution after delivery of 48 well volumes. The tips were renewed automatically for each new batch of reservoir slurry. Twelve replicate experiments were carried out for each solids loading. The total solids loaded per well is based on the average amount of solids dispensed in each trough (i.e. total amount of dry solids/16).

A-VII-27. Microplate Hydrolysis Procedure

The ground biomass was suspended as solid slurry in deionized water. The solids concentration (typically 0.727%, wt solids/wt slurry) was dependent on several experimental parameters; glucan loading (0.25-1%), pipetting volume, reaction volume

(250-1500 µl) and remaining free volume for delivery of other reagents and enzymes. The slurry was prepared in a 50 ml falcon tube that was mixed well and transferred to the epMotion 100 ml reagent reservoir. The slurry was aspirated multiple times by the robotic dispensor (dispension parameters listed earlier) to ensure homogeneous solid suspension for pipetting slurry to a 2 ml 96 deep-well reaction microplate. One steel bead (2 mm diameter) was added to each well prior to addition of slurry to promote mass transfer during hydrolysis. The slurry was multi-aspirated each time before pipetting required volume to the microplate. After addition of the slurry a buffer-antibiotic chemical and suitable enzyme mixtures were added using the robotic dispensor. The buffer-antibiotic mixture contained citrate buffer (pH 4.5-5.0, 1 M), cycloheximide (0.5 g/l) and tetracycline (0.7 g/l). A fixed amount (e.g. 5.7% of total reaction volume) of buffer-antibiotic mixture was added to each well. The substrates were hydrolyzed at desired glucan loadings ranging from 0.2-1% (w/v) in a 0.05 M citrate buffer solution for given enzyme mixtures. Suitable enzyme mixtures were prepared fresh before the start of each experiment using epMotion. A thermoblock was used to facilitate heat sealing the plate with an aluminum foil using the Eppendorf Heat Sealer to minimize evaporation losses during hydrolysis. The sealed microplate was incubated in a benchtop incubator (C24, New Brunswick, Edison, NJ) with a microplate holder at required rpm (typical rpm used was 250) for a defined time period (1-24 hrs) at 50 °C. For determining the rate of hydrolysis, separate replicate plates were used for each time point (i.e. 1, 2, 3, 6, 12, 24 h). At the end of the hydrolysis, the microplate was rapidly cooled down by transferring to a freezer (at - 20 °C) for 15 min before transferring the liquid hydrolysate to a filtration assembly (Multiscreen solvinert hydrophilic deep well filter plate, Millipore, Billerica,

MA). Alternatively, at the end of the hydrolysis the 2 ml deep well microplates (Reaction plate) were centrifuged at 3000 rpm (at 4 °C) for 15 minutes. 100 µL of the hydrolysate supernatant was then transferred and mixed with 100 µL of Na_2CO_3 buffer (pH 11, 200 mM), in a 0.3 mL Greiner microplate (Stop plate) using JANUS (Perkin Elmer, Waltham) 96-channel pipetting system, to arrest the reaction. Glucose and xylose in the stop plate solution was estimated using suitable bio-enzymatic assays, as mentioned later.

A-VII-28. NREL LAP-9 Enzymatic Hydrolysis Protocol

The NREL standard protocol (LAP-009) was followed for the conventional hydrolysis method. The substrate was hydrolyzed at desired glucan loading (typically 1%, w:v) in a 0.05 M citrate buffer solution (pH 4.5-5) at the necessary enzyme loading. Samples were hydrolyzed at 50 °C in a baffled 250 ml (100 ml reaction volume) conical flask at 200 rpm for a period of 24 hours (100 ml reaction volume). Alternatively, the reaction was also carried out in a 15 ml glass vial (for smaller reaction volumes). The hydrolysate sample was boiled to denature the enzymes and filtered through a 0.2 µm nylon membrane filter at predetermined time periods (i.e. 2, 6, 12 and 24 h). The samples were frozen for subsequent sugar analysis by the HPLC.

A-VII-29. Bio-enzymatic Sugar Assays

High-throughput bio-analytical methods were used to estimate the fermentable sugars in the hydrolysate since HPLC based methods were found to be time consuming and expensive for large number of samples obtained after microplate based hydrolysis. All pipetting steps were conducted using the epMotion/JANUS robotic systems to automate the high-throughput sugar assay. Glucose bio-enzymatic assays, utilizing hexokinase and glucose-6-phosphate dehydrogenase, was adapted to micro-liter scale based on a

modified method previously described [499]. Enzyme kit for determining glucose was purchased from R-Biopharm (R-Biopharm Inc., Marshall, MI). The basic principle of the assay is to use an enzyme system that uses NAD/NADH reduction/oxidation stoichiometric to the amount of glucose. D-glucose is phosphorylated to glucose-6-phosphate by hexokinase (HK) in the presence of adenosine triphosphate (ATP). The glucose-6-phosphate is then oxidized by nicotinamide adenine dinucleotide phosphate (NADP) to D-gluconate-6-phosphate along with formation of reduced nicotinamide adenine dinucleotide phosphate (NADPH). The increase in the amount of NADPH formed is measured by UV absorbance at 340 nm.

The enzyme assay was adapted for microscale reaction volume carried out in a 110 µl, 384 well microplate (Fisherbrand). The substrate solution containing triethanolamine buffer (pH 7.6), NADP, ATP and magnesium sulfate was prepared from the powder mixture provided in the assay kit. The enzyme solution containing hexokinase and glucose-6-phosphate dehydrogenase was prepared by 20-fold dilution of the enzyme suspension provided in the assay kit. The contents of buffer substrate solution are stable for 2-4 weeks at 4 °C; however, the diluted enzyme solution was prepared fresh before each assay. The hydrolyzate supernatant 'stop plate' solution (see A-VII-27) was diluted by 20 fold in 100 mM sodium phosphate buffer (pH 7.5) to prepare 'dilution plates'. 25 µl of triethanoamine containing substrate solution was added along with 50 µl of 'dilution plate' sample in to the wells. The plates were incubated at 25 °C for 5 min before measuring the absorbance at 340 nm ($[ABS]_1$). 10 µl of the diluted enzyme solution was then added to each well followed by 20 min incubation prior to measuring the absorbance again ($[ABS]_2$). Differences in absorbance between the two time periods

was calculated as dA (where, dA = $[ABS]_2$ - $[ABS]_1$). Blanks were subtracted from sample dA to obtain DA (where, DA = dA_{sample} - dA_{blank}). Suitably diluted standards (concentration ranging between 0.1 to 2 g/l) were added to each 384 well microplate and were used to obtain the standard curve (i.e. DA vs. Sugar concentration).

The xylose bio-assay (Megazyme, Bray, Ireland) is based on analogous two-step reactions to the glucose assay that were scaled down to be carried out in a 384 well microplate. α-D-xylose is converted to isomeric β-D-xylose by xylose mutarotase. β-D-xylose is then reacted with NAD^+ to form D-xylonic acid and NADH. The corresponding increase of NADH is measured at 340 nm to determine the xylose concentration. The specificity of the assays for glucose and xylose was analyzed in the presence of lignin based components and other monomeric hydrolysate sugars such as xylose and arabinose.

Quality control standards (mixed glucose-xylose standards) were included in all assays that showed less than 3-5 percent deviation from target values. Enzyme and substrate blank readings were subtracted from sample readings before estimating hydrolysis yields.

A-VII-30. Microplate Evaporation Losses

The total evaporation losses from the sealed microplate were estimated under standard microplate assay conditions. To estimate the evaporative loss during the course of hydrolysis the microplates were weighed before and after hydrolysis for two time periods (i.e. 3 and 24 hrs). All incubations were carried out at 50 °C and 375 rpm.

A-VII-31. Commercial (CE) and Research (RE) Enzymes

The following commercial enzyme (CE) preparations were provided by Genencor Intl. (Rochester, NY): Spezyme CP (CE 1), Multifect Xylanase (CE 3), Multifect Pectinase (CE 4), and Accellerase 1000 (CE 6). The commercial enzyme Depol 670L (CE 5) was provided by Biocatalysts Inc. (Cardiff, UK). The commercial enzyme Novozyme 188 (Novo188, CE 2) was procured from Sigma. The following eight research enzymes (RE) preparations were provided by Novozyme (Davis, CA): NS22002 (RE 1), NS50010 (RE 2), NS50012 (RE 3), NS50013 (RE 4), NS50014 (RE 5), NS50029 (RE 6), NS50030 (RE 7), and NS50053 (RE 8). Protein concentration for all CE and RE was determined using the Kjeldahl nitrogen analysis method (in triplicates by Dairy One Cooperative Inc, Ithaca, NY), BCA (bicinchoninic acid) and Bradford based assays (Thermo Fisher Scientific, Rockford, IL) with bovine serum albumin (BSA) as the standard. The non-protein protein equivalents (e.g. Urea and Ammonium salts estimated by AOAC Method 941.04) was subtracted from the Kjeldahl total crude protein equivalents (estimated by AOAC Method 2001.11) to estimate actual protein content (6.25 x % Nitrogen). All experiments in Chapter 3.1, 4.1 and 6 were conducted using CE 1 (123 mg/ml, 59 filter paper units/ml) and CE 2 (165 mg/ml, 250 p-nitrophenylglycoside units/ml). In all other chapters, the protein concentration was based on the results from Kjeldahl analysis (See Chapter 7 for protein concentrations).

A-VII-32. SDS-PAGE and Isoelectric Gel Electrophoresis

SDS-PAGE and Isoelectric gel based electrophoresis were run on the Novex XCell SureLock Mini-Cell system (Invitrogen, Carlsbad, CA, USA) using pre-cast gels from NuPAGE Novex 4-12% Bis-Tris Gel and Novex pH 3–10 IEF Gels, respectively. After

completion of the electrophoresis run, the gels were fixed with 50% methanol/7% acetic acid for 15 min and stained with GelCode Blue Stain Reagent (Thermo Fisher Scientific, Rockford, IL, USA) to visualize protein bands. The gel was photographed using the UVP BioDoc-It Imaging System (Upland, CA, USA). Protein purity was estimated using the UN-SCAN-IT gel software (Version 6.1, Orem, Utah, USA).

A-VII-33. Enzyme Activity Assays

The enzyme activity assays were based on a high-throughput microplate based method as described earlier. A 2.2 ml deep-well microplate (Greiner, Monroe, NC) was used to add 250 µl of 1% (w/v) stock substrate (CMC, Avicel, oat spelt xylan, cellobiose, xylobiose), 50 µl of 0.5 M citrate buffer (pH 5.0) and 200 µl of appropriately diluted enzyme samples (20 ng to 100 µg/well). The microplates were incubated at 50 °C with shaking at 200 rpm for 10 min (cellobiose), 60 min (CMC, xylan) or 300 min (Avicel). The amount of glucose and xylose was estimated using previously defined enzyme assays. One unit of cellobiase was defined as one micromole of glucose released per milligram enzyme per minute under the assay conditions. For CMC, Avicel and xylan based substrates the reducing sugars released were estimated using 3,5-dinitrosalicylic acid (DNS) reagent [411]. One unit of CMCase, Avicelase and xylanase activity was defined as one micromole of reducing sugars (as glucose equivalents) released per milligram enzyme per minute under the respective assay conditions.

The *para*-nitrophenyl (*p*NP) based chromogenic substrates used were 4-nitrophenyl-β-D-cellobioside (*p*NPC), 4-nitrophenyl-β-D-glucopyranoside (*p*NPG), 4-nitrophenyl-β-D-xylopyranoside (*p*NPX), 4-nitrophenyl-acetate (*p*NPA) and 4-nitrophenyl-β-D-arabinofuranoside (*p*NPAf) (Sigma-Aldrich, St. Louis, MO). The assay

mixtures containing 80 µl of 1 mM *p*NP substrate, 10 µl of 0.5 M citrate buffer (pH 5.0) and 10 µl of diluted enzymes (20 ng to 16 ug/well) in 350 µl micro plates were incubated at 50 °C with shaking at 200 rpm. After 15 min reaction time, 200 µl of 1M Na_2CO_3 (Note: pH 7.5 phosphate buffer was used for *p*NPA assays only to prevent substrate hydrolysis under alkaline conditions) was added to assay mixtures to arrest the hydrolytic reaction. The amount of *p*NP released was measured at OD 420 nm. One unit of enzyme activity was defined as one nanomole of *p*-nitrophenol released per milligram enzyme per minute under the assay conditions.

A-VII-34. Proteomics Analysis

Proteins of interest were denatured and reduced by adding urea and thiourea to a final concentration of 7 M and 2 M, respectively. Fresh dithiothreitol was added to a final concentration of 5mM, and samples were incubated at 60 °C for 30 min. Following incubation, the protein sample was diluted 10-fold with 100 mM NH_4HCO_3, pH 8.4, to reduce salt concentration. A volume of 1 M $CaCl_2$ was added to the diluted sample to a final concentration of 1 mM, and the sample was digested at 37 °C using sequencing grade trypsin (Promega, Madison, WI) at a ratio of 1 unit/50 units of protein (1 unit =< 1 µg of protein) for 4 h. Following incubation, digested samples were desalted using an appropriately sized C-18 SPE column (Supelco, St. Louis, MO) and vacuum manifold. Three column volumes of methanol were passed through the column followed by 2 column volumes of nanopure water. After passing the sample through the column, the column was washed with 4 volumes of a 95% acetonitrile (ACN), 0.1% trifluoroacetic acid (TFA) solution. Peptides were eluted using one column volume of an 80% ACN,

0.1% TFA solution. The collected peptides were concentrated to a final volume of 150 µl and measured using the BCA assay (Pierce Biotechnology, Rockfort, IL) according to the manufacturer's instructions. Peptides from enzyme tryptic digests were analyzed using high resolution reversed-phase HPLC separation coupled to an ion trap mass spectrometer (LTQ, Thermo Electron, San Jose CA) that was operated in a data-dependent MS/MS mode [423]. MS/MS spectra were analyzed using the SEQUEST algorithm [449] in conjunction with a protein collection of all fungal entries from Uniprot (Swiss-Prot and TrEMBL). Preliminary filtering of identified peptides was performed using: a minimum cross-correlation cut-off (XCorr) of either 1.9, 3.0, or 3.2 for 1+, 2+, or 3+ charge states, respectively; partially and fully tryptic peptides (peptides that contained either an arginine or lysine at the site of cleavage); DelCn >= 0.1. Estimation of peptide False Discovery Rate (FDR) was calculated by decoy database searching techniques [444, 445], resulting in values between 0.5% and 2%.

A-VII-35. Scheffé simplex-centroid CE-RE experimental design and regression

The simplex-centroid experimental design [438] used in this research requires experiments to be performed first on single-blend "pure" mixtures, then on double-blends (50% of each of two components), then on triple-blends, and so on (thus requiring 2^n-1 trials, where n is the number of components). This allows for the calculation of a polynomial mixture regression equation, with terms representing the effect of single enzymes, binary synergies (the product of the concentration of two enzymes and a regression coefficient), ternary synergies, and so on, depending on the order of the regression equation, as shown below:

$$\eta = \sum_{1 \le i \le q} \beta_i x_i + \sum_{1 \le i < j \le q} \beta_{ij} x_i x_j + \sum_{1 \le i < j < k \le q} \beta_{ijk} x_i x_j x_k + \cdots$$

Where; η is the response variable; q is the number of enzymes; x_i is the proportion of the i^{th} enzyme in the mixture; and $\beta_{ij...m}$ is a coefficient of synergy for m enzymes. The magnitude of each $\beta_{ij...m}$ indicates the strength of a particular enzyme or synergistic interaction.

Glucan conversion, xylan conversion, and total sugars released (gm sugars per kg biomass) were analyzed to generate suitable statistically based regression models using Minitab (Version 15.0, Minitab Inc, State College, PA). Third-degree mixed stepwise (α-to-enter/α-to-leave: 0.15) regression was performed on the results of each of the experiments to generate models of the interactions amongst the studied enzymes, with the stepwise step preserving only statistically significant interaction effects. Residuals were analyzed against order, fit, normal probability, and distribution to ensure quality-of-fit. Analysis suggested that quadratic and quaternary regressions (low R^2 and high σ values) did not model as accurately as the special cubic regressions. The regression equations were optimized by maximizing a desirability function (weight = 1, min = 0, target = theoretical maximum sugar conversion). Cox response trace plots were generated to analyze the effect of varying the composition of the enzyme cocktails (reference blend = model-generated optimum).

A-VII-36. Simplex-centroid design for CE-RE crude enzyme systems

Three simplex centroid experiments were designed: (1) adding mixtures of 8 mg protein/g glucan of eight accessory enzymes (Novozyme 188, Multifect Xylanase, Multifect Pectinase, NS22002, NS50012, NS50014, NS50029, and NS50030) to fixed 8.5 mg Accellerase/gm glucan of AFEX stover; (2) mixtures of 10 enzymes (Spezyme,

Multifect Xylanase and Pectinase, Depol 670 L, Accellerase, NS22002, NS50010, NS50013, NS50030, and NS50053) at a loading of 16.5 mg protein/g glucan of AFEX stover; and (3) mixtures of 5 enzymes at 16.5 mg protein/g glucan consisting of atleast one major crude cellulase preparation (either Spezyme CP, Accellerase, or NS50013), Multifect Pectinase, Depol 670L, NS22002, and NS50030. For all experiments, glucose and xylose released was determined for each unique enzyme mixture employed as specified by the simplex-centroid experimental design. All experiments were conducted using the microplate hydrolysis method outlined earlier for 4 and 24 hours in triplicates. All protein concentrations were estimated based on the Kjeldahl method.

A-VII-37. Heterologous expression of *Aspergillus nidulans* based β-xylosidase

Recombinant *Pichia pastoris* strains containing suitable cellulase and xylanase genes were obtained from the Fungal Genetics Stock Center (FGSC) at the University of Missouri (Kansas City, MO). The genes encoding cell wall degrading enzymes were isolated from *Aspergillus nidulans* and integrated into the genome of *P. pastoris* X-33 by Bauer et al. (2006) [489]. The recombinant strain FGSC #10077 expressing β-xylosidase was used for all heterologous expression experiments. The protocols employed followed for culture media composition, seed culture preparation and expression in shake flasks were based on methods obtained from Dr Chris Somerville (Personal Communication).

The recombinant strain was maintained on YPD plates containing yeast extract (1 % w/v), peptone (2 % w/v), dextrose (2 % w/v) and agar (2 % w/v). Plate cultures were stored at 4 °C for routine use. Culture stocks were stored in 40 % glycerol at -80 °C for long term use. For *preparation of seed culture* BMGY medium was used. The BMGY medium contained (in 1L) 10 g of yeast extract, 20 g of peptone, 100 ml of yeast nitrogen

base (YNB) (20.4 g of yeast nitrogen base without ammonium sulfate and amino acids and 60 g of ammonium sulfate in 600 ml water), 100 ml of 1M potassium phosphate buffer at pH 6.0, 100 ml of 10 % (v/v) glycerol and 2 ml of 0.02% (w/v) biotin. YNB and biotin was filter sterilized and added to the sterile medium containing other components. For *high cell density fermentation* rich medium BMMY was used. The BMMY medium was composed of yeast extract, peptone, yeast nitrogen base, phosphate buffer and biotin at concentrations similar to BMGY medium. Instead of glycerol, methanol was added as the carbon source. The expression of recombinant enzymes was tested by the cultivation of *P. pastoris* in BMMY medium in shake flasks. Baffled Erlenmeyer flasks (250 ml) with 50 ml of media was inoculated with the seed culture to an initial OD 600 of approximately 1.0 and incubated at 28 °C with agitation at 225 rpm. The cultures were supplemented with 0.6% methanol every 24 h for 3-5 days. A lab scale 1 liter BIOSTAT B plus fermentor (Sartorius) was used for fed-batch fermentation. High cell-density was achieved by cultivation of *P. pastoris* in batch phase for 24 h in glycerol medium. After seed culture growth to high OD, fed-batch fermentation was initiated with automated feeding of methanol (which was dependent on dissolved oxygen spikes indicating substrate depletion) to induce expression of the recombinant enzyme. The batch fermentation phase was carried out using rich BMMY medium with 4% (w/v) glycerol. The culture pH and temperature were maintained at pH 6 and 30 °C. After removing the cells by centrifugation the supernatant was analyzed for expression of β-xylosidase by *p*NP-xyloside based activity assays and SDS-PAGE. The fermentation broth was concentrated and partially desalted using a 10 kDa tangential flow ultra-filtration membrane (Sartorius) at 4 °C prior to FPLC polishing.

A-VII-38. Enzyme purification

Enzyme purification (See [453] for details) was performed using a fast protein liquid chromatography (FPLC) system (GE Healthcare, Buckinghamshire, United Kingdom) at room temperature, while the fraction collector was kept at 4°C. The following pre-packed FPLC columns (GE Healthcare, Buckinghamshire, United Kingdom) were used: 51 ml HisPrep 26/10 desalting column, 6 ml Resource Q anion exchange column, 1.7 ml Mono S cation exchange column, 1.7 ml Mono Q anion exchange column and 1 ml PHE hydrophobic interaction column. The crude enzyme samples were filtered (using 0.2 μm filter) and buffer exchanged to initial buffer (buffer A) using HisPrep 26/10 desalting column before injecting onto respective columns. Protein samples were concentrated using a tangential flow-filtration system (10 kDa Vivaflow membrane, Sartorius, Bohemia, NY). Milli-Q water was used to prepare buffers. Elution buffers were filtered through 0.2 μm PES membrane and degassed under vacuum prior to use.

REFERENCES

1. Chundawat S, Balan V, Dale B: **Effect of particle size based separation of milled corn stover on AFEX pretreatment and enzymatic digestibility**. *Biotech Bioeng* 2006, **96**:219 – 231.

2. Chundawat SPS, Balan V, Dale BE: **High-throughput microplate technique for enzymatic hydrolysis of lignocellulosic biomass**. *Biotechnology and Bioengineering* 2008, **99**:1281-1294.

3. Chundawat SPS, Balan V, Sousa L, Dale BE: **Characteristics of an ideal thermochemical pretreatment for reducing recalcitrance of lignocellulosic biomass to biological processing**. In *Bioalcohol production: : Biochemical conversion of lignocellulosic biomass (In Press)*. Edited by Waldron K: Woodhead Publishing; 2009.

4. Zhbankov R, Firsov S, Grinshpan D, Baran J, Marchewka M, Ratajczak H: **Vibrational spectra and noncovalent interactions of carbohydrates molecules**. *J Mol Struc* 2003, **645**:9–16.

5. Kamm B, Kamm M: **Biorefinery - Systems**. *Chemical & Biochemical Engineering Quarterly* 2004, **18**:1-6.

6. Himmel M, Ding S, Johnson D, Adney W, Nimlos M, Brady J, Foust T: **Biomass recalcitrance: engineering plants and enzymes for biofuels production**. *Science* 2007, **315**:804–807.

7. Dale B, Moreira M: **A freeze-explosion technique for increasing cellulose hydrolysis**. *Biotechnol Bioeng Symp* 1982, **12**:31–43.

8. Bals B, Teachworth L, Dale B, Balan V: **Extraction of Proteins from Switchgrass Using Aqueous Ammonia within an Integrated Biorefinery**. *Appl Biochem Biotechnol* 2007, **143**:187–198.

9. Carolan J, Joshi S, Dale B: **Technical and Financial Feasibility Analysis of Distributed Bioprocessing Using Regional Biomass Pre-Processing Centers**. *J Agri Food Ind Org* 2007, **5**:10.

10. Mansfield SD, Mooney C., Saddler JN: **Substrate and enzyme characteristics that limit cellulose hydrolysis**. *Biotech Prog* 1999, **15**:804.

11. Zhang P, Lynd R: **Towards an aggregated understanding of enzymatic hydrolysis of cellulose: Noncomplexed cellulase systems**. *Biotech Bioeng* 2004, **88**:797-824.

12. Fan LT, Lee Y, Beardmore DR: **The influence of major structural features of cellulose on rate of enzymatic hydrolysis**. *Biotech Bioeng* 1980, **22**:177-190.

13. Stalbrand H, Mansfield S, Saddler J, Kilburn D, Warren R, Gilkes N: **Analysis of molecular size distributions of cellulose molecules during hydrolysis of cellulose by**

recombinant Cellulomonas fimi beta-1,4-Glucanases. *Appl Environ Microbiol* 1998, **64**:2374-2379.

14. Klein G, Snodgrass W: *Cellulose.* Edited by Macrae R, Robinson R, Saddler M. London: Academic Press; 1993.

15. Ramos L, Nazhad M, Saddler JN: **Effect of enzymatic hydrolysis on the morphology and fine structure of pretreated cellulosic residues.** *Enzyme Microb Technol* 1993, **15**:821-831.

16. Chang V, Holtzapple M: **Fundamental factors affecting biomass enzymatic reactivity.** *Appl Biochem Biotechnol* 2000, **84-86**:5-37.

17. Besle J, Cornu A, Jouany J: **Roles of structural phenylpropanoids in forage cell wall digestion.** *J Sci Food Agric* 1994, **64**:171–190.

18. Laureano-Perez L, Teymouri F, Alizadeh H, Dale B: **Understanding factors that limit enzymatic hydrolysis of biomass: Characterization of pretreated corn stover.** *Appl Biochem Biotechnol* 2005, **124**:1081-1099.

19. Stone JE, Scallan AM: **The effect of component removal upon the porous structure of the cell wall of wood. Part III. A Comparision between sulphite and kraft processes.** *Pap Mag Can* 1969, **69**:T219-T240.

20. White A, Brown M: **Enzymatic hydrolysis of cellulose: Visual characterization of the process.** *Proc Natl Acad Sci USA* 1981, **78**:1047-1051.

21. Thompson D, Chen H, Grethlein H: **Comparison of pretreatment methods on the basis of available surface area.** *Bioresour Technol* 1992, **39**:155-163.

22. Ishizawa CI, Davis MF, Schell DF, Johnson DK: **Porosity and its effect on the digestibility of dilute sulfuric acid pretreated corn stover.** *J Agric Food Chem* 2007, **55**:2575-2581.

23. Zadrazil F, Puniya A: **Studies on the effect of particle size on solid-state fermentation of sugarcane bagasse into animal feed using white-rot fungi.** *Bioresour Technol* 1995, **54**:85-87.

24. Zhang P, Himmel M, Mielenz J: **Outlook for cellulase improvement: screening and selection strategies.** *Biotechnol Adv* 2006, **24**:452-481.

25. Reese E, Siu R, Levinson H: **Biological degradation of soluble derivatives and its relationship to the mechanism of cellulose hydrolysis.** *J Bacteriol* 1950, **59**:485-497.

26. Rosgaard L, Pedersen S, Langston J, Akerhielm D, Cherry J, Meyer A: **Evaluation of Minimal Trichoderma reesei Cellulase Mixtures on Differently Pretreated Barley Straw Substrates.** *Biotechnol Prog* 2007, **23**:1270-1276.

27. Gow L, Wood T: **Breakdown of crystalline cellulose by synergistic action between cellulase components from Clostridium thermocellum and Trichoderma koningii.** *FEMS Microbiology Letters* 1988, **50**:247-252.

28. Wood T: **Cellulolytic enzymes system of Trichoderma koningii. Separation of components attacking native cotton.** *Biochem J* 1968, **109**:217-229.

29. Wood T, McCrae S: **The cellulase of Penicillium pinophilum. Synergism between enzyme components in solubilizing cellulose with special reference to the involvement of two immunologically distinct cellobiohydrolases.** *Biochem J* 1986, **234**:93-99.

30. Wood T, Mcrae S, Bhat K: **The mechanism of fungal cellulase action. Synergism between enzyme components of Penicillium pinophilum cellulase in solubilizing hydrogen-bond ordered cellulose.** *Biochem J* 1989, **260**:37-43.

31. Bhat M, Bhat S: **Cellulose degrading enzymes and their potential industrial applications.** *Biotechnology Advances* 1997, **15**:583-620.

32. Bhat MK, Hazlewood GP: **Enzymology and Other Characteristics of Cellulases and Xylanases.** In *Enzymes in Farm Animal Nutrition.* Edited by Bedford MR, Partridge GG: CABI Publishing; 2001:11-60.

33. Eriksson T, Borjesson J, Tjerneld F: **Mechanism of surfactant effect in enzymatic hydrolysis of lignocellulose.** *Enzyme Microb Technol* 2002, **31**:353–364.

34. Eriksson T, Karlsson J, Tjerneld F: **A model explaining declining rate in hydrolysis of lignocellulose substrates with cellobiohydrolase I (Cel7A) and endoglucanase I (Cel7B) of Trichoderma reesei.** *Appl Biochem Biotechnol* 2002, **101**:41-60.

35. Yang B, Willies D, Wyman C: **Changes in the enzymatic hydrolysis rate of avicel cellulose with conversion.** *Biotech Bioeng* 2006, **94**:1122-1128.

36. Väljamäe P, Sild V, Nutt A, Pettersson G, Johansson G: **Acid hydrolysis of bacterial cellulose reveals different modes of synergistic action between cellobiohydrolase I and endoglucanase I.** *Eur J Biochem* 1999, **266**:327-334.

37. Holtzapple MT, Ripley EP, Nikolaou M: **Saccharification, fermentation, and protein recovery from low-temperature AFEX-treated coastal Bermuda grass.** *Appl Biochem Biotech* 1994, **44**:1122-1131.

38. De La Rosa L, Reshamwala S, Latimer V, Shawky B, Dale B, Stuart E: **Integrated production of ethanol fuel and protein from coastal Bermuda grass.** *Appl Biochem Biotech* 1994, **45-46**:483-497.

39. Gusakov A, Sinitsyn A: **A theoretical analysis of cellulase product inhibition: effect of cellulase binding constant, enzyme/substrate ratio, and beta-glucosidase activity on the inhibition pattern.** *Biotech Bioeng* 1992, **40**:663-671.

40. Selig M, Viamajala S, Decker S, Tucker M, Himmel M, Vinzant T: **Deposition of Lignin Droplets Produced During Dilute Acid Pretreatment of Maize Stems Retards Enzymatic Hydrolysis of Cellulose.** *Biotechnol Prog* 2007, **23**:1333-1339.

41. Gollapalli L, Dale B, Rivers D: **Predicting digestibility of ammonia fiber explosion (AFEX) treated rice straw.** *Appl Biochem Biotechnol* 2002, **98-100**:23-35.

42. Ferrer A, Byers F, Sulbarán-de-Ferrer B, Dale B, Aiello C: **Optimizing ammonia pressurization/depressurization processing conditions to enhance enzymatic susceptibility of dwarf elephant grass.** *Appl Biochem Biotechnol* 2000, **84-86**:163-179.

43. Ferrer A, Byers F, Sulbarán-de-Ferrer B, Dale B, Aiello C: **Optimizing Ammonia Processing Conditions to Enhance Susceptibility of Legumes to Fiber Hydrolysis.** *Appl Biochem Biotechnol* 2002, **98**:123-134.

44. Turner N, McDonough C, Byers F, Holtzapple M, Dale B, Jun J, Greene L: **Disruption of forage structure with an ammonia fiber explosion process.** In *Proceedings for American Society of Animal Sciences (Western Section)*: American Society of Animal Sciences: 1990.

45. Sulbaran de Ferrer B, Ferrer A, Byers F, Dale B, Aristiguieta M: *Arch Latinoam Prod Anim* 1997, **5**:112-114

46. Woodward J, Hayes M, Lee N: **Hydrolysis of cellulose by saturating and non-saturating concentrations of cellulase: implications for synergism.** *Bio/Technology* 1988, **6**:301-304.

47. Woodward J, Lima M, Lee N: **The role of cellulase concentration in determining the degree of synergism in the hydrolysis of microcrystalline cellulose.** *Biochem J* 1988, **255**:895-899.

48. Berlin A, Maximenko V, Gilkes N, Saddler J: **Optimization of Enzyme Complexes for Lignocellulose Hydrolysis.** *Biotechnology and Bioengineering* 2007, **97**:287-296.

49. Karlsson J, Medve J, Tjerneld F: **Hydrolysis of steam pretreated lignocellulose: Synergism and adsorption for CBH I and EG II of Trichoderma reesei.** *Appl Biochem Biotechnol* 1999, **82**:243–258.

50. Medve J, Lee D, Tjerneld F: **Ion-exchange chromatographic purification and quantitative analysis of Trichoderma reesei cellulases cellobiohydrolase I, II and endoglucanase II by fast protein liquid chromatography.** *J Chromat A* 1998, **808**:153–165.

51. Pauly M, Keegstra K: **Cell Wall Carbohydrates and their Modifications as a Resource for Biofuels.** *The Plant Journal* 2008, **54**:559-568.

52. Goring D, Timmel T: *Tappi* 1962, **45**:454.

53. Wyman CE, Dale BE, Elander RT, Holtzapple M, Ladisch MR, Lee YY, Mitchinson C, Saddler JN: **Comparative sugar recovery and fermentation data following pretreatment of poplar wood by leading technologies**. *Biotechnology Progress* 2009, **25**:333-339.

54. Wyman CE, Dale BE, Elander RT, Holtzapple MT, Ladisch MR, Lee YY: **Comparative sugar recovery data from laboratory scale application of leading pretreatment technologies to corn stover**. *Bioresource Technology* 2005, **96**:2026-2032.

55. Ding S, Himmel M: **The maize primary cell wall microfibril: a new model derived from direct visualization**. *J Agric Food Chem* 2006, **54**:597-606.

56. Fengel D, Wegener G: *Wood: chemistry, ultrastructure and reactions*. Berlin: Walter de Gruyter; 1989.

57. O'Sullivan A: **Cellulose: the structure slowly unravels**. *Cellulose* 1997, **4**:173–207.

58. Ebringerova A: **Structural Diversity and Application Potential of Hemicelluloses**. *Macromolecular Symposia* 2006, **232**:1-12.

59. Ebringerova A, Heinze T: **Xylan and xylan derivatives – biopolymers with valuable properties: Naturally occurring xylans structures, isolation procedures and properties**. *Macromol Rapid Commun* 2000, **21**:542–556.

60. Buranov A, Mazza G: **Lignin in straw of herbaceous crops**. *Ind Crops Prod* 2008, **28**:237-259.

61. Palonen H: **Role of lignin in the enzymatic hydrolysis of lignocellulose [Dissertation]**. Espoo: Helsinki University of Technology: 2004.

62. McCann M, Carpita N: **Designing the deconstruction of plant cell walls**. *Curr Opin Plant Biol* 2008, **11**:314-320.

63. Carpita N, Gibeaut D: **Structural models of primary-cell walls in flowering plants – Consistency of molecular-structure with the physical properties of the walls during growth**. *Plant J* 1993, **3**:1-30.

64. Ruel K, Chevalier-billosta V, Guillemin F, Sierra JB, Joseleau J-P: **The Wood Cell Wall at the Ultrastructural Scale - Formation and Topochemical Organization**. *Maderas: Ciencia y Technologia* 2006, **8**:107-116.

65. Bidlack J, Malone M, Benson R: **Molecular Structure and Component Integration of Secondary Cell Walls in Plants**. *Proceedings of the Oklahoma Academy of Science* 1992, **72**:51-56.

66. Viamajala S, Selig M, Vinzant T, Tucker M, Himmel M, McMillan J, Decker S: **Catalyst Transport in Corn Stover Internodes Elucidating Transport Mechanisms Using Direct Blue-1.** *Appl Biochem Biotech* 2006, **130**:509 – 527.

67. Ye Z, York W, Darvill A: **Important new players in secondary wall synthesis.** *Trends Plant Sci* 2006, **11**:162-164.

68. Carpita N, McCann M: *The cell wall.* Edited by Buchanan B, Gruissem W, Jones R. Rockville, MD: American Society of Plant Physiologists; 2000.

69. Esau K: *Cell Wall.* New York: John Wiley & Sons; 1977.

70. Hatfield R: **Structural Polysaccharides in Forages and Their Digestibility.** *Agron J* 1989, **18**:39-46.

71. Buchanan B, Gruissem W, Jones R: *Biochemistry and Molecular Biology of Plants* edn 3rd: Courier Companies Inc; 2001.

72. Salisbury F, Ross C: *Plant Physiology and Plant Cells.* Belmont, CA: Wadsworth Inc; 1992.

73. Goodwin T, Mercer E: *The Plant Cell Wall.* New York: Pergamon Press; 1983.

74. McNeil M, Albersheim P, Taiz L, Jones R: *Plant physiol* 1975, **55**:64.

75. Atalla R, Hackney J, Uhlin I, Thompson N: **Hemicelluloses as structural regulators in the aggregation of native cellulose.** *Intl J Biol Macromol* 1993, **15**:109-112.

76. Koshijima T, Watanabe T, Yaku F: *Structure and properties of the lignin carbohydrate complex polymer as an amphipathic substance*, vol ACS Symposium Series 397: American Chemical Society; 1989.

77. Van Soest PJ: **Lignin.** In *Nutritional Ecology of the Ruminant.* Edited by: Comstock Publishing; 1994:177-194.

78. Lam T, Iiyama K, Stone B: *Primary and secondary walls of grasses and other forage plants, taxonomic and structural considerations.* Edited by Akin DE, Ljungdahl LG, Wilson JR, Harris PJ. New York: Elservier; 1990.

79. Hatfield RD, Ralph J, Grabber JH: **Cell wall cross-linking by ferulates and diferulates in grasses.** *Journal of the Science of Food and Agriculture* 1999, **79**:403-407.

80. Hatfield R, Wilson J, Mertens D: **Composition of cell walls isolated from cell types of grain sorghum stems.** *J Sci Food Agric* 1999, **79**:891–899.

81. Morrison T, Jung H, Buxton D, Hatfield R: **Cell-wall composition of maize internodes of varying maturity.** *Crop Sci* 1998, **38**:455–460.

82. Ralph J, Hatfield R, Quideau S, Helm R, Grabber J, Jung H: **Pathway of p-coumaric acid incorporation into maize lignin as revealed by NMR.** *J Am Chem Soc* 1994, **116**:9448–9456.

83. Jung H: **Maize stem tissues: Ferulate deposition in developing internode cell walls.** *Phytochemistry* 2003, **63**:543–549.

84. MacAdam J, Grabber J: **Relationship of growth cessation with the formation of diferulate cross-links and p-coumaroylated lignins in tall fescue.** *Planta* 2002, **215**:785–793.

85. Migne C, Prensier G, Utille J, Angibeaud P, Cornu A, Grenet E: **Immunocytochemical localisation of p-coumaric acid and feruloyl-arabinose in the cell walls of maize stem.** *J Sci Food Agric* 1998, **78**:373–381.

86. Myton K, Fry S: **Intraprotoplasmic feruloylation of arabinoxylans in Festuca arundinacea cell cultures.** *Planta* 1994, **193**:326–330.

87. Fry S: **Cross-linking of matrix polymers in the growing cell walls of angiosperms.** *Annu Rev Plant Physiol* 1986, **37**:165–186.

88. Grabber J, Ralph J, Lapierre C, Barrière Y: **Genetic and molecular basis of grass cell wall degradability. (I) Lignin-cell wall matrix interactions.** *Comptes Rendus Biol* 2004, **327**:455–465.

89. Koshijima T, Watanabe T: **Preparation and Characterization of Lignin-Carbohydrate Complexes.** In *Association between Lignin and Carbohydrates in Wood and Other Plant Tissues*. Edited by; 2003:1-5. Springer Series in Wood Science

90. Sewalt V, De Olivera W, Glasser W, Fontenot J: **Lignin impact on fiber degradation. (2) A model study using cellulose hydrogels.** *J Sci Food Agric* 1996, **71**:204-208.

91. Sewalt V, Fontenot J, Allen V, Glasser W: **Fiber composition and in Vitro digestibility of corn stover fractions in response to ammonia treatment.** *J Agric Food Chem* 1996, **44**:3136-3142.

92. Sewalt V, Glasser W, Beauchemin K: **Lignin impact on fiber degradation. 3. Reversal of inhibition of enzymatic hydrolysis by chemical modification of lignin and additives.** *J Agric Food Chem* 1997, **45**:1823–1828.

93. Grabber J, Hatfield R, Ralph J: **Apoplastic pH and monolignol addition rate effects on lignin formation and cell wall degradability in maize.** *J Agric Food Chem* 2003, **51**:4984–4989.

94. Saulnier L, Thibault J: **Ferulic acid and diferulic acids as components of sugar-beet pectins and maize bran heteroxylans.** *J Sci Food Agric* 1999, **79**:396–402.

95. Mosier N, Wyman C, Dale B, Elander R, Lee YY, Holtzapple M, Ladisch M: **Features of promising technologies for pretreatment of lignocellulosic biomass.** *Bioresource Technology* 2005, **96**:673-686.

96. Weil J, Westgate P, Kohlmann K, Ladisch M: **Cellulose pretreatments of lignocellulosic substrates.** *Enzyme Microb Technol* 1994, **16**:1002–1004.

97. Goldstein I, Easter J: **An improved process for converting cellulose to ethanol.** *Tappi* 1992, **75**:135–140.

98. Saha B, Bothast R: **Pretreatment and enzymatic saccharification of corn fiber.** *Appl Biochem Biotechnol* 1999, **76**:65–77.

99. Koullas D, Christakopoulos P, Kekos D, Koukios E, Macris B: **Effect of alkali delignification on wheat straw saccharification by Fusarium oxysporum cellulases.** *Biomass Bioenergy* 1993, **4**:9–13.

100. Clark D, Mackie K: **Steam explosion of the softwood Pinus radiata with sulphur dioxide addition: (1) Process optimization.** *J Wood Chem Technol* 1987, **7**:373–403.

101. Gould J: **Alkaline peroxide delignification of agricultural residues to enhance enzymatic saccharification.** *Biotech Bioeng* 1984, **26**:46–52.

102. Fernández-Bolaños J, Felizón B, Heredia A, Rodríguez R, Guillén R, Jiménez A: **Steam-explosion of olive stones: hemicellulose solubilization and enhancement of enzymatic hydrolysis of cellulose.** *Bioresource Technology* 2001, **79**:53-61.

103. Dale B, Leong C, Pham T, Esquivel V, Rios I, Latimer V: **Hydrolysis at low enzyme levels: application of the AFEX process.** *Bioresour Technol* 1996, **56**:111–116.

104. Schmidt A, Thomsen A: **Optimization of wet oxidation pretreatment of wheat straw.** *Bioresour Technol* 1998, **64**:139–151.

105. Kaar W, Holtzaple M: **Using lime pretreatment to facilitate the enzymatic hydrolysis of corn stover.** *Biomass Bioenergy* 2000, **18**:189–199.

106. Laser M, Schulman D, Allen SG, Lichwa J, Antal MJ, Lynd LR: **A comparison of liquid hot water and steam pretreatments of sugar cane bagasse for bioconversion to ethanol.** *Bioresource Technology* 2002, **81**:33-44.

107. Chum H, Johnson D, Black S, Baker J, Grohmann K, Sarkanen K, Wallace K, Schroeder H: **Organosolv pretreatment for enzymatic hydrolysis of poplars: (1) enzyme hydrolysis of cellulosic residues.** *Biotechnol Bioeng* 1988, **31**:643– 649.

108. Liu C, Wyman C: **Partial flow of compressed-hot water through corn stover to enhance hemicellulose sugar recovery and enzymatic digestibility of cellulose.** *Bioresour Technol* 2005, **96**:1978-1985.

109. Chandra R, Bura R, Mabee W, Berlin A, Pan X, Saddler J: **Substrate Pretreatment: The Key to Effective Enzymatic Hydrolysis of Lignocellulosics?** *Adv Biochem Eng Biotechnol* 2007, **108**:67-93.

110. Wu Z, Lee Y: **Ammonia recycled percolation as a complementary pretreatment to the dilute-acid process.** *Applied Biochemistry and Biotechnology* 1997, **63-65**:21-34.

111. Kristensen J, Thygesen L, Felby C, Jørgensen H, Elder T: **Cell-wall structural changes in wheat straw pretreated for bioethanol production.** *Biotechnology for Biofuels* 2008, **1**:5.

112. Donohoe B, Decker S, Tucker M, Himmel M, Vinzant T: **Visualizing lignin coalescence and migration through maize cell walls following thermochemical pretreatment.** *Biotechnol Bioeng* 2008, **101**:913-925.

113. Öhgren K, Bura R, Saddler J, Zacchi G: **Effect of hemicellulose and lignin removal on enzymatic hydrolysis of steam pretreated corn stover.** *Bioresource Technology* 2007, **98**:2503-2510.

114. Millett MA, Baker AJ, Satter LD: **Pretreatments to Enhance Chemical, Enzymatic, and Microbiological Attack of Cellulosic Materials.** *Biotechnology and Bioengineering* 1975:193-219.

115. Sidiras D, Koukios E: **Acid saccharification of ball milled straw.** *Biomass* 1989, **19**:289-306.

116. Tassinari T, Macy C, Spano L: **Energy requirements and process design considerations in compression-milling pretreatment of cellulosic wastes for enzymatic hydrolysis.** *Biotech Bioeng* 1980, **22**:1689-1705.

117. Alvo P, Belkacemi K: **Enzymatic saccharification of milled timothy (*Phleum pratense* l.) and alfalfa (*Medicago sativa* L.).** *Bioresource Technology* 1997, **61**:185-198.

118. Fan LT, Lee YH, Beardmore DR: **The Influence of Major Structural Features of Cellulose on Rate of Enzymatic Hydrolysis.** *Biotechnology and Bioengineering* 1981, **23**:419-424.

119. McMillan JD: **Pretreatment of lignocellulosic biomass.** In *ACS Symp. Ser. 566*Edited by Himmel ME, Baker JO, Overend RP: 1994:292-324.

120. Heinze T, Koschella A: **Solvents applied in the field of cellulose chemistry: a mini review.** *Polímeros* 2005, **15**:84-90.

121. Sidiras D, Koukios E: **Simulation of acid-catalysed organosolv fractionation of wheat straw.** *Bioresour Technol* 2004, **94**:91-98.

122. Pan X, Gilkes N, Kadla J, Pye K, Saka S, Gregg D, Ehara K, Xie D, Lam D, Saddler J: **Bioconversion of Hybrid Poplar to Ethanol and Co-products Using an Organosolv Fractionation Process: Optimization of Process Yields.** *Biotechnology and Bioengineering* 2006, **94**:851-861.

123. Sun F, Chen H: **Organosolv pretreatment by crude glycerol from oleochemicals industry for enzymatic hydrolysis of wheat straw.** *Bioresour Technol* 2008, **99**:5474-5479.

124. Zhao X, Cheng K, Liu D: **Organosolv pretreatment of lignocellulosic biomass for enzymatic hydrolysis.** *Appl Microbiol Biotechnol* 2009, **82**:815-827.

125. Lee YH, Robinson CW, Moo-Young M: **Evaluation of Organosolv process for the fraction and modification of corn stover for bioconversion.** *Biotechnol Bioeng* 1987, **29**:572-581.

126. Arato C, Pye E, Gjennestad G: **The lignol approach to biorefining of woody biomass to produce ethanol and chemicals.** *Applied Biochemistry and Biotechnology* 2005, **123**:871-882.

127. Zhang Y-HP, Ding S-Y, Mielenz JR, Cui J-B, Elander RT, Laser M, Himmel ME, McMillan JR, Lynd LR: **Fractionating recalcitrant lignocellulose at modest reaction conditions.** *Biotechnology and Bioengineering* 2007, **97**:214-223.

128. Zhang YHP, Cui J, Lynd LR, Kuang LR: **A Transition from Cellulose Swelling to Cellulose Dissolution by o-Phosphoric Acid: Evidence from Enzymatic Hydrolysis and Supramolecular Structure.** *Biomacromolecules* 2006, **7**:644-648.

129. Moxley G, Zhu Z, Zhang YHP: **Efficient Sugar Release by the Cellulose Solvent-Based Lignocellulose Fractionation Technology and Enzymatic Cellulose Hydrolysis.** *Journal of Agricultural and Food Chemistry* 2008, **56**:7885-7890.

130. Graenacher C: **Cellulose Solution (U.S. Patent No. 1,943,176).** US Patent 1934.

131. Swatloski RP, Spear SK, Holbrey JD, Rogers RD: **Dissolution of cellulose with ionic liquids.** *Journal of the American Chemical Society* 2002, **124**:4974-4975.

132. Singh S, Simmons BA, Vogel KP: **Visualization of biomass solubilization and cellulose regeneration during ionic liquid pretreatment of switchgrass.** *Biotechnology and Bioengineering* 2009, **104**:68-75.

133. Zhao H, Jones CL, Baker GA, Xia S, Olubajo O, Person VN: **Regenerating cellulose from ionic liquids for an accelerated enzymatic hydrolysis.** *Journal of Biotechnology* 2009, **139**:47-54.

134. Turner MB, Spear SK, Huddleston JG, Holbrey JD, Rogers RD: **Ionic liquid salt-induced inactivation and unfolding of cellulase from Trichoderma reesei.** *Green Chemistry* 2003, **5**:443-447.

135. Weil JR, Sarikaya A, Rau S-L, Goetz J, Ladisch CM, Brewer M, Hendrickson R, Ladisch MR: **Pretreatment of corn fiber by pressure cooking in water.** *Applied Biochemistry and Biotechnology* 1998, **73**:1-17.

136. Chum HL, Johnson DK, Black SK, Overend RP: **Pretreatment-catalyst effects and the combined severity parameter.** *Appl Biochem Biotechnol* 1990, **24/25**:1-14.

137. Klinke HB, Thomsen AB, Ahring BK: **Inhibition of ethanol-producing yeast and bacteria by degradation products produced during pre-treatment of biomass.** *Applied Microbiology and Biotechnology* 2004, **66**:10-26.

138. Ruttan RF: **Ethyl alcohol from sawdust and other wood waste.** *Society of Chemical Industries* 1909, **28**:1290-1294.

139. Zeitsch KJ: *The chemistry and technology of furfural and its many by-products*, vol 13. New York: Elsevier; 2000.

140. Harris EE, Begliner E: **Hydrolysis of wood. Treatment with sulfuric acid in a stationary digester.** *Industrial Engineering Chemistry* 1946, **37**:12-23.

141. Kim JS, Lee YY, Torget RW: **Cellulose hydrolysis under extremely low sulfuric acid and high-temperature conditions.** *Applied Biochemistry and Biotechnology* 2001, **91-93**:331-340.

142. Torget R, Himmel M, Grohmann K: **Dilute acid pretreatment of two short rotation herbaceous crops.** *Applied Biochemistry and Biotechnology* 1992, **34/35**:115-123.

143. Lloyd TA, Wyman CE: **Combined sugar yields for dilute sulfuric acid pretreatment of corn stover followed by enzymatic hydrolysis of the remaining solids.** *Bioresource Technology* 2005, **96**:1967-1977.

144. Lee YY, Iyer P, Torget RW: **Dilute acid hydrolysis of lignocellulosic biomass.** *Advances in Biochemical Engineering and Biotechnology* 1999, **65**:93.

145. Ballesteros I, Oliva JM, Navarro AA, González A, Carrasco J, Ballesteros M: **Effect of chip size on steam explosion pretreatment of softwood.** *Applied Biochemistry and Biotechnology* 2000, **84-86**:97-110.

146. Ballesteros I, Negro MJ, Oliva JM, Cabanas A, Manzanares P, Ballesteros M: **Ethanol production from steam-explosion pretreated wheat straw.** *Applied Biochemistry and Biotechnology* 2006, **130**:496-508.

147. Chen H, Liu L, Yang X, Li Z: **New process of maize stalk amination treatment by steam explosion.** *Biomass & Bioenergy* 2005, **28**:411-417.

148. Playne MJ: **Increased digestibility of bagasses by pretreatment with alkalis and steam explosion.** *Biotechnology and Bioengineering* 1984, **26**:426-433.

149. Brownell HH, Saddler JN: **Steam explosion pretreatment for enzymatic hydrolysis.** In *Biotechnology and Bioengineering Symposium 14*. Edited by; 1984:55-68.

150. Hsu TA: **Pretreatment of biomass.** In *Handbook on bioethanol, production and utilization*. Edited by Wyman CE: Taylor and Francis; 1996.

151. Bobleter O, Binder H, Concin R, Burtscher E: **The conversion of biomass to fuel raw material by hydrothermal pretreatment.** In *Energy from biomass*. Edited by Palz W, Chartier P, Hall DO: Applied science publishers; 1981:554-562.

152. Mosier NS, Hendrickson R, Brewer M, Ho N, Sedlak M, Dreshel R, Welch G, Dien BS, Aden A, Ladisch MR: **Industrial scale-up of pH-controlled liquid hot water pretreatment of corn fiber for fuel ethanol production.** *Applied Biochemistry and Biotechnology* 2005, **125**:77-97.

153. Mosier NS, Ladisch CM, Ladisch MR: **Characterization of acid catalytic domains for cellulose hydrolysis and glucose degradation.** *Biotechnology and Bioengineering* 2002, **79**:610-618.

154. Kootstra AM, Mosier NS, Scott EL, Beeftink HH: **Differential effects of mineral and organic acids on the kinetics of arabinose degradation under lignocellulose pretreatment conditions.** *Biochem. Eng. J.* 2009, **43**:92-97.

155. Lu Y, Mosier NS: **Biomimetic Catalysis for Hemicellulose Hydrolysis in Corn Stover.** *Biotechnology Progress* 2007, **23**:116-123.

156. Lu Y, Mosier NS: **Kinetic modeling analysis of maleic acid-catalyzed hemicellulose hydrolysis in corn stover.** *Biotechnology and Bioengineering* 2008, **101**:1170-1181.

157. Peter Van Walsum G, Garcia-Gil M, Chen S-F, Chambliss K: **Effect of dissolved carbon dioxide on accumulation of organic acids in liquid hot water pretreated biomass hydrolyzates.** *Applied Biochemistry and Biotechnology* 2007, **137-140**:301-311.

158. Kim TH, Lee YY: **Pretreatment and fractionation of corn stover by ammonia recycle percolation process.** *Bioresource Technology* 2005, **96**:2007-2013.

159. Sendich E, Laser M, Kim S, Alizadeh H, Laureano-Perez L, Dale B, Lynd L: **Recent process improvements for the ammonia fiber expansion (AFEX) process and resulting reductions in minimum ethanol selling price.** *Bioresource Technology* 2008, **99**:8429-8435.

160. Laureano-Perez L, Dale B, O'Dwyer J, Holtzapple M: **Statistical Correlation of Spectroscopic Analysis and Enzymatic Hydrolysis of Poplar Samples.** *Biotechnol Prog* 2006, **22**:835-841.

161. Chou Y: **Supercritical ammonia pretreatment of lignocellulosic materials.** *Biotechnol Bioeng Symp* 1986, **17**:19-32.

162. Weimer P, Chou Y, Weston W, Chase D: **Effect of supercritical ammonia on the physical and chemical structure of ground wood.** *Biotechnol Bioeng Symp* 1986, **17**:5-18.

163. Lewin M, Roldan LG: **The Effect of Liquid Anhydrous Ammonia in the Structure and Morphology of Cotton Cellulose.** *Journal of Polymer Science Part C-Polymer Symposium* 1971:213-229.

164. Kim SB, Lee YY: **Fractionation of Herbaceous Biomass by Ammonia-Hydrogen Peroxide Percolation Treatment.** *Applied Biochemistry and Biotechnology* 1996, **57/58**:147-156.

165. Kim TH, Kim JS, Sunwoo C, Lee YY: **Pretreatment of corn stover by aqueous ammonia.** *Bioresource Technology* 2003, **90**:39-47.

166. Kim TH, Lee YY: **Pretreatment of corn stover by soaking in aqueous ammonia.** *Applied Biochemistry and Biotechnology* 2005, **124**:1119-1131.

167. Hennessey SM, Friend J, Dunson JB, Tucker MP, Elander RT, Hames B: **Integration of alternative feedstreams for biomass treatment and utilization.** US Patent 2007, US20070037259 A1.

168. Puri VP: **Ozone pretreatment to increase digestibility of lignocellulose.** *Biotechnol Lett* 1983, **5**:773-776.

169. Quesada J, Rubio M, GÇümez D: **Ozonation of Lignin Rich Solid Fractions from Corn Stalks.** *Journal of Wood Chemistry and Technology* 1999, **19**:115 - 137-115 - 137.

170. Garcia-Cubero MT, Gonzalez-Benito G, Indacoechea I, Coca M, Bolado S: **Effect of ozonolysis pretreatment on enzymatic digestibility of wheat and rye straw.** *Bioresource Technology* 2009, **100**:1608-1613.

171. Roncero MB, Torres AL, Colom JF, Vidal T: **TCF bleaching of wheat straw pulp using ozone and xylanase. Part A: paper quality assessment.** *Bioresource Technology* 2003, **87**:305-314.

172. Akin DE, Morrison WH: **Ozone treatment of forage: Structure and digestibility of different lignified cell walls.** *Crop Science* 1988, **28**:337-342.

173. Quesada J, Rubio M, Gomez D: **Chemical characterization of ozonated lignin solutions from corn (Zea mays) stalk and poplar (Populus deltoides) wood by capillary gas chromatography.** *Journal of high resolution chromatography* 1997, **20**:565-568.

174. Jablonský M, Vrška M, Katuščák S: **Cellulose protectors for improving ozone bleaching - Review.** *Wood Research* 2004, **49**:71-86.

175. Ragnar M, Tord E, Torbjörn R: **Radical formation in ozone reactions with lignin and carbohydrate model compounds.** *Holzforschung* 1999, **53**:292-298.

176. Shatalov AA, Pereira H: **Polysaccharide degradation during ozone-based TCF bleaching of non-wood organosolv pulps.** *Carbohydrate Polymers* 2007, **67**:275-281.

177. Silverstein RA, Chen Y, Sharma-Shivappa RR, Boyette MD, Osborne J: **A comparison of chemical pretreatment methods for improving saccharification of cotton stalks.** *Bioresource Technology* 2007, **98**:3000-3011.

178. Martin C, Thomsen AB: **Wet oxidation pretreatment of lignocellulosic residues of sugarcane, rice, cassava and peanuts for ethanol production.** *Journal of Chemical Technology & Biotechnology* 2007, **82**:174-181.

179. Varga E, Schmidt A, Réczey K, Thomsen A: **Pretreatment of corn stover using wet oxidation to enhance enzymatic digestibility.** *Applied Biochemistry and Biotechnology* 2003, **104**:37-50.

180. Klinke H, Ahring B, Schmidt A, Thomsen A: **Characterization of degradation products from alkaline wet oxidation of wheat straw.** *Bioresour Technol* 2002, **82**:15–26.

181. Eggeman T, Elander RT: **Process and economic analysis of pretreatment technologies.** *Bioresource Technology* 2005, **96**:2019-2025.

182. Lee J: **Biological conversion of lignocellulosic biomass to ethanol.** *Journal of Biotechnology* 1997, **56**:1-24.

183. Lee J-W, Gwak K-S, Park J-Y, Park M-J, Choi D-H, Kwon M, Choi I-G: **Biological Pretreatment of Softwood Pinus densiflora by Three White Rot Fungi.** *J. Microbiol.* 2007, **45**:455-491.

184. Keller FA, Hamilton JE, Nguyen QA: **Microbial pretreatment of biomass: Potential for reducing severity of thermochemical biomass pretreatment.** *Applied Biochemistry and Biotechnology* 2003, **105**:27-41.

185. Balan V, da Costa Sousa L, Chundawat SPS, Vismeh R, Jones AD, Dale BE: **Mushroom spent straw: a potential substrate for an ethanol-based biorefinery.** *Journal of Industrial Microbiology & Biotechnology* 2008, **35**:293-301.

186. Taniguchi M, Suzuki H, Watanabe D, Sakai K, Hoshino K, Tanaka T: **Evaluation of pretreatment with *Pleurotus ostreatus* for enzymatic hydrolysis of rice straw.** *Journal of Bioscience and Bioengineering* 2005, **100**:637-643.

187. Zadrazil F: **Is conversion of lignocellulosics into feed with white rot fungi realizable? Practical problems of scale-up and technology transfer.** In *Science and Cultivation of Edible Fungi*. Edited by Van Griensven LJLD; 2000:919-928.

188. Karunanandaa K, Varga GA, Akin DE, Rigsby LL, Royse DJ: **Botanical fractions of rice straw colonized by white-rot fungi: changes in chemical composition and structure.** *Animal Feed Science and Technology* 1995, **55**:179-199.

189. Kerem Z, Friesem D, Hadar Y: **Lignocellulose Degradation during Solid-State Fermentation: *Pleurotus ostreatus* versus *Phanerochaete chrysosporium*.** *Applied and Environmental Microbiology* 1992, **58**:1121-1127.

190. Leonowicz A, Matuszewska A, Luterek J, Ziegenhagen D, Wojtaś-Wasilewska M, Nam-Seok C, Hofrichter M, Rogalski J: **Biodegradation of lignin by white rot fungi.** *Fungal Genetics and Biology* 1999, **27**:175-185.

191. Akin DE, Morrison WH, III, Rigsby LL, Barton FE, II, Himmelsbach DS, Hicks KB: **Corn Stover Fractions and Bioenergy: Chemical Composition, Structure, and Response to Enzyme Pretreatment.** *Applied Biochemistry and Biotechnology* 2006, **129**:104-116.

192. Mendonça R, Jara J, González V, Elissetche J, Freer J: **Evaluation of the white-rot fungi Ganoderma australe and Ceriporiopsis subvermispora in biotechnological applications.** *Journal of Industrial Microbiology and Biotechnology* 2008, **35**:1323-1330.

193. Lee J-W, Kim H-Y, Koo B-W, Choi D-H, Kwon M, Choi I-G: **Enzymatic saccharification of biologically pretreated Pinus densiflora using enzymes from brown rot fungi.** *Journal of Bioscience and Bioengineering* 2008, **106**:162-167.

194. Shi J, Chinn MS, Sharma-Shivappa RR: **Microbial pretreatment of cotton stalks by solid state cultivation of Phanerochaete chrysosporium.** *Bioresource Technology* 2008, **99**:6556-6564.

195. Tomme P, Warren R, Gilkes N: **Cellulose Hydrolysis by bacteria and fungi.** *Adv Microb Physiol* 1995, **37**:1-81.

196. Bayer E, Chanzy H, Lamed R, Shoham Y: **Cellulose, cellulases and cellulosomes.** *Curr Opin Struct Biol* 1998, **8**:548–557.

197. Bayer EA, Shimon LJW, Shoham Y, Lamed R: **Cellulosomes - Structure and ultrastructure.** *Journal of Structural Biology* 1998, **124**:221-234.

198. Saha B: **Hemicellulose bioconversion.** *J Ind Microb Biotech* 2003, **30**:279 - 291.

199. Teeri T: **Trichoderma reesei cellobiohydrolase I with an endoglucanase cellulose-binding domain: action on bacterial microcrystalline cellulose.** *J Biotechnol* 1997, **57**:49-57.

200. Giligan W, Reese E: **Evidence for multiple components in microbial cellulases.** *Canadian Journal of Microbiology* 1954, **1**:90-107.

201. Mandels M, Reese E: *Dev Ind Microb* 1964, **5**:5-16.

202. Murashima K, Kosugi A, Doi RH: **Synergistic effects of cellulosomal xylanase and cellulases from *Clostridium cellulovorans* on plant cell wall degradation.** *Journal of Bacteriology* 2003, **185**:1518-1524.

203. Henrissat B: **Cellulases and their interaction with cellulose.** *Cellulose* 1994, **1**:169-196.

204. Nidetzky B: **Synergism of Trichoderma reesei cellulases while degrading different celluloses.** *Biotech Lett* 1993, **15**:71-76.

205. Ståhlberg J: **Trichoderma reesei has no true exo-cellulase: all intact and truncated cellulases produce new reducing end groups on cellulose.** *Biochim Biophys Acta* 1993, **1157**:107-113.

206. Divne C, Stahlberg J, Reinikainen T, Ruohonen L, Pettersson G, Knowles J, Teeri T, Jones T: **The three-dimensional crystal structure of the catalytic core of cellobiohydrolase I from Trichoderma reesei.** *Science* 1994, **265**:524-528.

207. Rouvinen J, Bergfors T, Teeri T, Knowles J, Jones T: **Three-dimensional structure of cellobiohydrolase II from Trichoderma reesei.** *Science* 1990, **249**:380-386.

208. Barr B, Hsieh Y, Ganem B, Wilson D: **Identification of two functionally different classes of exocellulases.** *Biochemistry* 1996, **35**:586-592.

209. Imai T, Boisset C, Samejima M, Igarashi K, Sugiyama J: **Unidirectional processive action of cellobiohydrolase Cel7A on Valonia cellulose microcrystals.** *FEBS Letters* 1998, **432**:113-116.

210. Mansfield SD, Saddler JN, Gübitz GM: **Characterization of endoglucanases from the brown rot fungi Gloeophyllum sepiarium and Gloeophyllum trabeum.** *Enzyme and Microbial Technology* 1998, **23**:133-140.

211. Amano Y, Nozaki K, Araki T, Shibasaki H, Kuga S, Kanda T: **Reactivities of cellulases from fungi towards ribbon-type bacterial cellulose and band-shaped bacterial cellulose.** *Cellulose* 2002, **8**:267-274.

212. Coughlan M, Hazelwood G: *Hemicellulose and hemicellulases*. London: Portland Press; 1993.

213. De Vries R, Kester H, Poulsen C, Benen J, Visser J: **Synergy between enzymes from Aspergillus involved in the degradation of plant cell wall polysaccharides.** *Carbohydr Res* 2000, **327**:401-410.

214. Poutanen K, Tenkanen M, Korte H, Puls J: *Accessory enzymes involved in the hydrolysis of xylans*, vol 460. Edited by Leatham G, Himmel, ME. Washington DC: American Chemical Society; 1991.

215. Poutanen K, Puls J: *The xylanolytic enzyme system of Trichoderma reesei*, vol 399. Edited by Lewis G, Paice M. Washington DC: American Chemical Society; 1989.

216. Biely P, Vrsanska M, Claeyssens M: **The endo-1,4-beta-glucanase I from Trichoderma reesei.** *European Journal of Biochemistry* 1991, **200**:157-163.

217. Biely P, Vranskáa M, Tenkanen M, Kluepfel D: **Endo-β-1,4-xylanase families: differences in catalytic properties.** *J Biotechnol* 1997, **57**:151-166.

218. Biely P, Puchart V: **Recent progress in the assays of xylanolytic enzymes.** *Journal of the Science of Food and Agriculture* 2006, **86**:1636-1647.

219. Kenealy W, Jeffries T: *Enzyme processes for pulp and paper: a review of recent developments. Wood deterioration and preservation: advances in our changing world*, vol ACS symposium series 845. Washington, DC: American Chemical Society: Oxford University Press; 2003.

220. Gübitz GM, Stebbing DW, Johansson CI, Saddler JN: **Lignin-hemicellulose complexes restrict enzymatic solubilization of mannan and xylan from dissolving pulp.** *Applied Microbiology and Biotechnology* 1998, **50**:390-395.

221. Gübitz GM, Mansfield SD, Böhm D, Saddler JN: **Effect of endoglucanases and hemicellulases in magnetic and flotation deinking of xerographic and laser-printed papers.** *Journal of Biotechnology* 1998, **65**:209-215.

222. Gübitz GM, Lischnig T, Stebbing D, Saddler JN: **Enzymatic removal of hemicellulose from dissolving pulps.** *Biotechnology Letters* 1997, **19**:491-495.

223. Gübitz GM, Haltrich D, Latal B, Steiner W: **Mode of depolymerisation of hemicellulose by various mannanases and xylanases in relation to their ability to bleach softwood pulp.** *Applied Microbiology and Biotechnology* 1997, **47**:658-662.

224. Kaya F, Heitmann JA, Joyce TW: **Influence of Surfactants on the Enzymatic Hydrolysis of Xylan and Cellulose.** *Tappi Journal* 1995, **78**:150-157.

225. Morgavi D, Beauchemin K, Nsereko V, Rode L, Iwaasa A, Yang W, McAllister T, Wang Y: **Synergy between ruminal fibrolytic enzymes and enzymes from Trichoderma longibrachiatum.** *J Dairy Sci* 2000, **83**:1310-1321.

226. Ferreira L, Wood T, Williamson G, Faulds C, Hazlewood G, Black G, Gilbert H: **A modular esterase from Pseudomonas fluorescens subsp. cellulosa contains a non-catalytic cellulose-binding domain.** *Biochem J* 1993, **294**:349–355.

227. Davies G, Henrissat B: **Structures and mechanisms of glycosyl hydrolases.** *Structure* 1995, **3**:853–859.

228. Bolam DN, Ciruela A, McQueen-Mason S, Simpson P, Williamson MP, Rixon JE, Boraston A, Hazlewood GP, Gilbert HJ: ***Pseudomonas* cellulose-binding domains**

mediate their effects by increasing enzyme substrate proximity. *Biochemical Journal* 1998, **331**:775-781.

229. Carrard G, Linder M: **Widely different off rates of two closely related cellulose-binding domains from *Trichoderma reesei***. *European Journal of Biochemistry* 1999, **262**:637-643.

230. Linder M, Teeri TT: **The roles and function of cellulose-binding domains**. *Journal of Biotechnology* 1997, **57**:15-28.

231. Saul D, Williams L, Grayling R, Chamley L, Love D, Bergquist P: **CelB, a gene coding for a bifunctional cellulase from the extreme thermophile "Caldocellum saccharolyticum"**. *Appl Environ Microb* 1990, **56**:3117.

232. Flint HJ, Martin J, McPherson CA, Daniel AS, Jun-Xian Z: **A bifunctional enzyme, with separate xylanase and β(1,3-1,4)-glucanase domains, encoded by the xynD gene of Ruminococcus flavefaciens**. *J Bacteriol* 1993, **175**:2943–2951.

233. Demain AL, Newcomb M, Wu JHD: **Cellulase, Clostridia, and Ethanol**. *Microbiology and Molecular Biology Reviews* 2005, **69**:124-154.

234. Holtzapple MT, Ripley EP, Nikolaou M: **Saccharification, Fermentation, and Protein Recovery from Low-Temperature Afex-Treated Coastal Bermudagrass**. *Biotechnology and Bioengineering* 1994, **44**:1122-1131.

235. Foster B, Dale B, Doran-Peterson J: **Enzymatic hydrolysis of ammonia-treated sugar beet pulp**. *Appl Biochem Biotech* 2001, **91**:269-282.

236. O'Connor J: **Ammonia explosion pulping: A new fiber separation process**. *Tappi* 1972, **55**:353-358.

237. Jungnikl K, Paris O, Fratzl P, Burgert I: **The implication of chemical extraction treatments on the cell wall nanostructure of softwood**. *Cellulose* 2008, **15**:407-418.

238. Fahlen J, Salmen L: **Cross-sectional structure of the secondary wall of fibers as affected by processing**. *J Mat Sci* 2003, **38**:119-126.

239. Öhgren K, Galbe M, Zacchi G: **Optimization of steam pretreatment of SO_2-impregnated corn stover for fuel ethanol production**. *Applied Biochemistry and Biotechnology* 2005, **124**:1055-1067.

240. Teymouri F, Laureano-Perez L, Alizadeh H, Dale BE: **Optimization of the ammonia fiber explosion (AFEX) treatment parameters for enzymatic hydrolysis of corn stover**. *Bioresource Technology* 2005, **96**:2014-2018.

241. Kim S, Holtzapple MT: **Lime pretreatment and enzymatic hydrolysis of corn stover**. *Bioresource Technology* 2005, **96**:1994-2006.

242. Kim S, Holtzapple MT: **Delignification kinetics of corn stover in lime pretreatment.** *Bioresource Technology* 2006, **97**:778-785.

243. Mosier N, Hendrickson R, Ho N, Sedlak M, Ladisch MR: **Optimization of pH controlled liquid hot water pretreatment of corn stover.** *Bioresource Technology* 2005, **96**:1986-1993.

244. Angeles G, Owens S, Ewers F: **Fluoresence shell: A novel view of sclereid morphology with the confocal laser scanning microscope.** *Microscopy Research and Techniques* 2004, **63**:282-288.

245. Lillie R: *HJ Conn's Biological stains* edn 9th. Baltimore: The Williams and Wilkins Co; 1977.

246. Kasten F: *The origins of modern fluorescent microscopy and fluorescent probes.* Edited by Kohen E, Hirschberg J. San Diego: Academic Press; 1989.

247. Albinsson B, Li S, Lundquist K, Stomberg R: **The origin of lignin fluorescence.** *J Mol Structure* 1999, **508**:19-27.

248. Bludworth J, Carl Knopf F: **Reactive extraction of lignin from wood using supercritical ammonia-water mixtures.** *The Journal of Supercritical Fluids* 1993, **6**:249-254.

249. Graham HD: **Stabilization of the Prussian Blue Color in the Determination of Polyphenols.** *Journal of Agricultural and Food Chemistry* 1992, **40**:801-805.

250. Hartley RD, Jones EC: **Phenolic Components and Degradability of the Cell Walls of the Brown Midrib Mutant, bm_3, of Zea mays.** *Journal of the Science of Food and Agriculture* 1978, **29**:777-782.

251. Hartley RD: ***p*-Coumaric and Ferulic Acid Components of Cell Walls of Ryegrass and their Relationships with Lignin and Digestibility.** *Journal of the Science of Food and Agriculture* 1972, **23**:1347-1354.

252. Berlin A, Balakshin M, Gilkes N, Kadla J, Maximenko V, Kubo S, Saddler J: **Inhibition of cellulase, xylanase and beta-glucosidase activities by softwood lignin preparations.** *Journal of Biotechnology* 2006, **125**:198-209.

253. Dorris G, Gray D: **The surface analysis of paper and wood fibers by ESCA, II. Surface composition of mechanical pulps.** *Cellul Chem Technol* 1978, **12**:721-734.

254. Mjoberg P: **Chemical surface analysis of wood fibers by means of ESCA.** *Cellul Chem Technol* 1981, **15**:481-486.

255. Laine J, Stenius P, Carlsson G, Strom G: **Surface characterization of unbleached kraft pulps by means of ESCA.** *Cellulose* 1994, **1**:145-160.

256. Yan L, Li W, Yang J, Zhu Q: **Direct visualizaton of straw cell walls by AFM.** *Macromol Biosci* 2004, **4**:112-118.

257. Koljonen K, Osterberg M, Johansson L, Stenius P: **Surface chemistry and morphology of different mechanical pulps determined by ESCA and AFM.** *Colloids and Surfaces A: Physicochemical and Engineering Aspects* 2003, **228**:143-158.

258. Yu H, Liu R, Shen D, Wu Z, Huang Y: **Arrangement of cellulose microfibrils in the wheat straw cell wall.** *Carbohydrate polymers* 2008, **72**:122-127.

259. Zimmermann T, Thommen V, Reimann P, Hug H: **Ultrastructural appearance of embedded and polished wood cell walls as revealed by AFM.** *J Struc Biol* 2006, **156**:363-369.

260. McCann MC, Wells B, Roberts K: **Direct visualization of cross-links in the primary plant cell wall.** *J Cell Sci* 1990, **96**:323-334.

261. Hafren J, Fujino T, Itoh T, Westermark U, Terashima N: **Ultrastructural Changes in the Compound Middle Lamella of Pinus thunbergii During Lignification and Lignin Removal.** *Holzforschung* 2005, **54**:234-240.

262. Carpita NC, Defernez M, Findlay K, Wells B, Shoue DA, Catchpole G, Wilson RH, McCann MC: **Cell Wall Architecture of the Elongating Maize Coleoptile.** *Plant Physiology* 2001, **127**:551-565.

263. Carpita NC: **Structure and biogenesis of the cell walls of grasses.** *Annual Review of Plant Physiology and Plant Molecular Biology* 1996, **47**:445-476.

264. Brunecky R, Vinzant TB, Porter SE, Donohoe BS, Johnson DK, Himmel ME: **Redistribution of xylan in maize cell walls during dilute acid pretreatment.** *Biotechnology and Bioengineering* 2009, **102**:1537-1543.

265. Grethlein HE: **The Effect of Pore Size Distribution on the Rate of Enzymatic Hydrolysis of Cellulose Substrates** *Bio/Technology* 1985, **3**:155-160.

266. Stone JE, Scallan AM, Donefer E, Ahlgren E: **Digestibility as a Simple Function of a Molecule of Similar Size to a Cellulase Enzyme.** In *Cellulases and Their Applications.* Edited by: AMERICAN CHEMICAL SOCIETY; 2009:219-241. Advances in Chemistry

267. Rosca I, Puhringer R, Schmidt H, Tanczos I: *New Aspects in studying and applications of ammonia treatment of softwood.* Edited by Kudela J, Kurjatko S. Zvolen, Slovakia: Arbora Publishers; 2002.

268. Tarkow H, Feist WC: **A Mechanism for Improving the Digestibility of Lignocellulosic Materials with Dilute Alkali and Liquid Ammonia.** *Advances in Chemistry Series* 1969:197-217.

269. Read SM, Bacic A: **Cell wall porosity and its determination.** In *Modern Methods of Plant Analysis. 17: Plant Cell Wall Analysis.* Edited by Linskens HF, Jackson JF: Springer Verlag; 1996:63-80. vol 17.]

270. Chesson A, Gardner PT, Wood TJ: **Cell wall porosity and available surface area of wheat straw and wheat grain fractions.** *Journal of the Science of Food and Agriculture* 1997, **75**:289-295.

271. Xu P, Donaldson L, Gergely Z, Staehelin L: **Dual-axis electron tomography: a new approach for investigating the spatial organization of wood cellulose microfibrils.** *Wood Science and Technology* 2007, **41**:101-116.

272. Kremer J, Mastronarde D, McIntosh J: **Computer visualization of three-dimensional image data using IMOD.** *J Struct Biol* 1996, **116**:71–76.

273. Wi SG, Singh AP, Le KH, Kim YS: **The Pattern of Distribution of Pectin, Peroxidase and Lignin in the Middle Lamella of Secondary Xylem Fibres in Alfalfa (Medicago sativa).** *Ann Bot* 2005, **95**:863-868.

274. Singh A, Daniel G, Nilsson T: **Ultrastructure of the S2 layer in relation to lignin distribution in Pinus radiata tracheids.** *Journal of Wood Science* 2002, **48**:95-98.

275. Fromm J, Rockel B, Lautner S, Windeisen E, Wanner G: **Lignin distribution in wood cell walls determined by TEM and backscattered SEM techniques.** *Journal of Structural Biology* 2003, **143**:77-84.

276. Lapierre C, Pollet B, Ralet M-C, Saulnier L: **The phenolic fraction of maize bran: evidence for lignin-heteroxylan association.** *Phytochemistry* 2001, **57**:765-772.

277. McNeil M, Darvill AG, Fry SC, Albersheim P: **Structure and Function of the Primary Cell Walls of Plants.** *Annual Review of Biochemistry* 1984, **53**:625-663.

278. Joseleau JP, Ruel K: **Study of Lignification by Noninvasive Techniques in Growing Maize Internodes (An Investigation by Fourier Transform Infrared Cross-Polarization-Magic Angle Spinning 13C-Nuclear Magnetic Resonance Spectroscopy and Immunocytochemical Transmission Electron Microscopy).** *Plant Physiol.* 1997, **114**:1123-1133.

279. Donaldson LA: **Lignification and lignin topochemistry - an ultrastructural view.** *Phytochemistry* 2001, **57**:859-873.

280. Grabber JH, Ralph J, Hatfield RD, Quideau S: ***p*-Hydroxyphenyl, Guaiacyl, and Syringyl Lignins Have Similar Inhibitory Effects on Wall Degradability.** *Journal of Agricultural and Food Chemistry* 1997, **45**:2530-2532.

281. Jung H-JG, Jorgensen MA, Linn JG, Engels FM: **Impact of accessibility and chemical composition on cell wall polysaccharide degradability of maize and lucerne stems.** *Journal of the Science of Food and Agriculture* 2000, **80**:419-427.

282. McCartney L, Marcus SE, Knox JP: **Monoclonal antibodies to plant cell wall xylans and arabinoxylans.** *Journal of Histochemistry & Cytochemistry* 2005, **53**:543-546.

283. Crow E, Murphy RJ: **Microfibril orientation in differentiating and maturing fibre and parenchyma cell walls in culms of bamboo (Phyllostachys viridi-glaucescens (Garr.) Riv. & Riv.).** *Botanical Journal of the Linnean Society* 2000, **134**:339-359.

284. Chandra RP, Esteghlalian AR, Saddler JN: **Assessing substrate accessibility to enzymatic hydrolysis by cellulases.** In *Characterization of Lignocellulosic Materials.* Edited by Hu T: Blackwell; 2008:60-80.

285. Andrews P: **Estimation of the molecular weights of proteins by Sephadex gel-filtration.** *Biochem J* 1964, **91**:222-233.

286. Tepfer M, Taylor IEP: **The Permeability of Plant Cell Walls as Measured by Gel Filtration Chromatography.** *Science* 1981, **213**:761-763.

287. O'Sullivan AC: **Cellulose: the structure slowly unravels.** *Cellulose* 1997, **4**:173-207.

288. Wada M, Nishiyama Y, Chanzy H, Forsyth T, Langan P: **The structure of celluloses.** *Powder Diffraction* 2008, **23**:92-95.

289. Vincent J: **From cellulose to cell.** *J Exp Biol* 1999, **202**:3263-3268.

290. Yamamoto H, Horii F, Odani H: **Structural changes of native cellulose crystals induced by annealing in aqueous alkaline and acidic solutions at high temperatures.** *Macromolecules* 1989, **22**:4130-4132.

291. Zugenmaier P: **Conformation and packing of various crystalline cellulose fibers.** *Progress in Polymer Science* 2001, **26**:1341-1417.

292. Weimer PJ, French AD, Calamari TA, Jr.: **Differential Fermentation of Cellulose Allomorphs by Ruminal Cellulolytic Bacteria.** *Appl. Environ. Microbiol.* 1991, **57**:3101-3106.

293. Wada M, Heux L, Isogai A, Nishiyama Y, Chanzy H, Sugiyama J: **Improved Structural Data of Cellulose IIII Prepared in Supercritical Ammonia.** *Macromolecules* 2001, **34**:1237-1243.

294. Chanzy H, Henrissat B, Vincendon M, Tanner S, Belton P: **Solid-state carbon-13 NMR and electron microscopy study on the reversible cellulose I to cellulose III transformation in Valonia.** *Carbohydr Res* 1987, **160**:1-11.

295. Wada M, Nishiyama Y, Langan P: **X-ray Structure of Ammonia-Cellulose I: New Insights into the Conversion of Cellulose I to Cellulose III.** *Macromolecules* 2006, **39**:2947 -2952.

296. Clark GL, Parker EA: **An X-ray diffraction study of the action of liquid ammonia on cellulose and its derivatives.** *Journal of Physical Chemistry* 1937, **41**:777-786.

297. Yui T, Hayashi S: **Structural stability of the solvated cellulose IIII crystal models: a molecular dynamics study.** *Cellulose* 2009, **16**:151-165.

298. Igarashi K, Wada M, Samejima M: **Activation of crystalline cellulose to cellulose III results in efficient hydrolysis by cellobiohydrolase.** *FEBS Journal* 2007, **274** 1785-1792.

299. Weimer PJ, Lopez-Guisa JM, French AD: **Effect of cellulose fine structure on kinetics of its digestion by mixed ruminal microorganisms in vitro.** *Appl. Environ. Microbiol.* 1990, **56**:2421-2429.

300. Chen Y, Stipanovic A, Winter W, Wilson D, Kim Y-J: **Effect of digestion by pure cellulases on crystallinity and average chain length for bacterial and microcrystalline celluloses.** *Cellulose* 2007, **14**:283-293.

301. Sasaki T, Tanaka T, Nanbu N, Sato Y, Kainuma K: **Correlation between X-ray diffraction measurements of cellulose crystalline structure and the susceptibility to microbial cellulase.** *Biotechnology and Bioengineering* 1979, **21**:1031-1042.

302. Schleicher H, Daniels C, Philipp B: **Changes of Cellulose Accessibility to Reactions in Alkaline Medium by Activation with Ammonia.** *Journal of Polymer Science Part C-Polymer Symposium* 1974:251-260.

303. Mormann W: **Silylation of cellulose with hexamethyldisilazane in ammonia-activation, catalysis, mechanism, properties.** *Cellulose* 2003, **10**:271-281.

304. Mormann W, Michel U: **Hydrocelluloses with low degree of polymerisation from liquid ammonia treated cellulose.** *Carbohydrate Polymers* 2002, **50**:349-353.

305. Michell A: **Usefulness of Fourier-transform infrared difference spectroscopy for studying the reactions of wood during pulping.** *Cellul Chem Technol* 1988, **22**:105-113.

306. Stewart D, Wilson H, Hendra P, Morrison I: **Fourier-Transform Infrared and Raman Spectroscopic Study of Biochemical and Chemical Treatments of Oak Wood (Quercus rubru) and Barley (Hordeum vulgare) Straw.** *J Agric Food Chem* 1995, **43**:2219-2225.

307. Okano T, Sarko A: **Mercerization of cellulose. I. X-ray diffraction evidence for intermediate structures.** *Journal of Applied Polymer Science* 1984, **29**:4175-4182.

308. Thygesen A, Oddershede J, Lilholt H, Thomsen AB, Ståhl K: **On the determination of crystallinity and cellulose content in plant fibres.** *Cellulose* 2005, **12**:563-576.

309. Segal L, Loeb L, Creely JJ: **An X-ray Study of the Decomposition Product of the Ethylamine-Cellulose Complex.** *Journal of Polymer Science* 1954, **13**:193-206.

310. Segal L, Nelson ML, Conrad CM: **Further Studies on Cotton Cellulose with Reduced Crystallinity.** *Textile Research Journal* 1953, **23**:428-435.

311. Segal L, Creely JJ, Martin AE, Conrad CM: **An Empirical Method for Estimating the Degree of Crystallinity of Native Cellulose Using the X-Ray Diffractometer.** *Textile Research Journal* 1959, **29**:786-794.

312. Park S, Johnson D, Ishizawa C, Parilla P, Davis M: **Measuring the crystallinity index of cellulose by solid state 13C nuclear magnetic resonance.** *Cellulose* 2009, **16**:641-647.

313. Atalla RH, Isogai A: **Recent developments in spectroscopic and chemical characterization of cellulose.** In *Polysaccharides: Structural Diversity and Functional Versatility.* Edited by Dumitriu S: Marcel Dekker; 1998.

314. Atalla R, Vanderhart D: **Studies on the structure of cellulose using Raman spectroscopy and solid state 13C-NMR.** In *Institute for Paper Chemistry (IPC Technical Paper Series 217).* Edited by chemistry Ifp; 1987. vol IPC Technical Paper Series 217.]

315. Agarwal U, Ralph S: **FT-Raman Spectroscopy of Wood: Identifying Contributions of Lignin and Carbohydrate Polymers in the Spectrum of Black Spruce (Picea mariana).** *Applied Spectroscopy* 1997, **51**:1648–1655.

316. Barry AJ, Peterson FC, King AJ: **X-Ray Studies of Reactions of Cellulose in Non-Aqueous Systems. I. Interaction of Cellulose and Liquid Ammonia.** *Journal of the American Chemical Society* 1936, **58**:333-337.

317. Bommarius AS, Katona A, Cheben SE, Patel AS, Ragauskas AJ, Knudson K, Pu Y: **Cellulase kinetics as a function of cellulose pretreatment.** *Metabolic Engineering* 2008, **10**:370-381.

318. Hess K, Gundermann J: **The effect of liquid ammonia on cellulose fibers (Formation from ammonia-cellulose I, ammonia-gellulose II and cellulose III).** *Berichte Der Deutschen Chemischen Gesellschaft* 1937, **70**:1788-1799.

319. Nursten H: **The Maillard Reaction.** In *The Maillard Reaction: Chemistry, Biochemistry and Implications.* Edited by: The Royal Society of Chemistry; 2005:1-4.

320. Sjöström E: **Carbohydrate degradation products from alkaline pretreatment of biomass.** *Biomass Bioenergy* 1991, **1**:61–64.

321. Marounek M, Kostyukovsky V, Hodrová B, Fliegerová K: **Effect of soluble maillard reaction products on rumen microorganisms.** *Folia Microbiologica* 1995, **40**:267-270.

322. Schumacher D, Kroh LW: **The Effect of Maillard Reaction Products on Enzyme Reactions.** *Zeitschrift Fur Ernahrungswissenschaft* 1996, **35**:213-225.

323. Schenzel K, Fischer S: **NIR FT Raman Spectroscopy–a Rapid Analytical Tool for Detecting the Transformation of Cellulose Polymorphs.** *Cellulose* 2001, **8**:49-57.

324. Irvine GM: **The significance of the glass transition of lignin in thermomechanical pulping.** *Wood Science and Technology* 1985, **19**:139-149.

325. Houtman CJ, Atalla RH: **Cellulose-lignin interactions.** *Plant Physiol* 1995, **107**:977-984.

326. He L, Terashima N: **Formation and structure of lignin in monocotyledons I. Selective labeling of the structural units of lignin in rice plant (*Oryza sativa*) with ^{3}H and visualization of their distribution in the tissue by microautoradiography.** *Mokuzai Gakkaishi* 1989, **35**:116-122.

327. He LT, N.: **Formation and structure of lignin in monocotyledons II. Deposition and distribution of phenolic acids and their association with cell wall polymers in rice plants (Oryza sativa).** *Mokuzai Gakkaishi* 1989, **35**:123-129.

328. He L, Terashima N: **Formation and structure of lignin in monocotyledons. III. Heterogeneity of sugarcane (Saccharum officinarum L.) lignin with respect to the composition of structural units in different morphological regions.** *J. Wood Chem. Technol* 1990, **10**:435-459.

329. Jung HG, Casler MD: **Maize Stem Tissues: Impact of Development on Cell Wall Degradability.** *Crop Science* 2006, **46**:1801-1809.

330. Jung HG, Casler MD: **Maize Stem Tissues: Cell Wall Concentration and Composition during Development.** *Crop Science* 2006, **46**:1793-1800.

331. Grabber JH, Hatfield RD, Ralph J: **Diferulate Cross-Links Impede the Enzymatic Degradation of Non-Lignified Maize Walls.** *Journal of the Science of Food and Agriculture* 1998, **77**:193-200.

332. Grabber JH, Ralph J, Lapierre C, Barrière Y: **Genetic and molecular basis of grass cell-wall degradability. I. Lignin-cell wall matrix interactions.** *Comptes Rendus Biologies* 2004, **327**:455-465.

333. Bunzel M, Allerdings E, Ralph J, Steinhart H: **Cross-linking of arabinoxylans via 8-8-coupled diferulates as demonstrated by isolation and identification of diarabinosyl 8-8 (cyclic)-dehydrodiferulate from maize bran.** *Journal of Cereal Science* 2008, **47**:29-40.

334. Chen S, Mowery R, Castleberry V, van Walsum G, Chambliss C: **High performance liquid chromatography method for simultaneous determination of aliphatic acid, aromatic acid and neutral degradation products in biomass pretreatment hydrolysates.** *J Chromat A* 2006, **1104**:54-61.

335. Hodge D, Karim M, Schell D, McMillan J: **Soluble and insoluble solids contributions to high-solids enzymatic hydrolysis of lignocellulose.** *Bioresource Technology* 2008, **99**:8940–8948.

336. Luo C, Brink D, Blanch H: **Identification of potential fermentation inhibitors in conversion of hybrid poplar hydrolyzate to ethanol.** *Biomass Bioenergy* 2002, **22**:125-138.

337. Palmqvist E, Hahn-Hägerdal B: **Fermentation of lignocellulosic hydrolysates. (I) Inhibition and detoxification.** *Bioresour Technol* 2000, **74**:17–24.

338. Cantarella M, Cantarella L, Gallifuoco A, Spera A, Alfani F: **Effect of inhibitors released during steam-explosion treatment of poplar wood on subsquent enzymatic hydrolysis and SSF.** *Biotechnol Prog* 2004, **20**:200-206.

339. Garcia-Aparicio M, Ballesteros I, Gonzalez A, Oliva J, Ballesteros M, Negro M: **Effect of inhibitors released during steam pretreatment of barley straw on enzymatic hydrolysis.** *Appl Biochem Biotechnol* 2006, **129-132**:278-288.

340. Lau M, Dale B, Balan V: **Ethanolic fermentation of hydrolysates from ammonia fiber expansion (AFEX) treated corn stover and distillers grain without detoxification and external nutrient supplementation.** *Biotechnol Bioeng* 2008, **99**:529–539.

341. Mes-Hartree M, Dale B, Craig W: **Comparison of steam and ammonia pretreatment for enzymatic hydrolysis of cellulose.** *Appl Microbiol Biotechnol* 1988, **29**:462-468.

342. Belkacemi K, Turcotte G, Halleux D, Savoie P: **Ethanol Production from AFEX-Treated Forages and Agricultural Residues.** *Appl Biochem Biotechnol* 1998, **70-72**:441-462.

343. Wang P, Bolker H, Purves C: **Ammonolysis of uronic ester groups in birch xylan.** *Canadian Journal of Chemistry* 1964, **42**:2434-2439.

344. Niemelä K: **Conversion of xylan, starch, and chitin into carboxylic acids by treatment with alkali.** *Carbohydr Res* 1990, **204**:37-49.

345. Prior B, Day D: **Hydrolysis of Ammonia-pretreated Sugar Cane Bagasse with Cellulase, β-Glucosidase, and Hemicellulase Preparations.** *Appl Biochem Biotechnol* 2008, **146**:151-164.

346. Standard Biomass Analytical Procedures on World Wide Web URL: http://www.nrel.gov/biomass/analytical_procedures.html

347. Zhu Y, Kim T, Lee Y, Che R, Elander R: **Enzymatic production of xylooligosaccharides from corn stover and corn cobs treated with aqueous ammonia.** *Appl Biochem Biotechnol* 2006, **129-132**:586-598.

348. Gupta R, Kim T, Lee Y: **Substrate Dependency and Effect of Xylanase Supplementation on Enzymatic Hydrolysis of Ammonia-Treated Biomass.** *Appl Biochem Biotechnol* 2008, **148**:59–70.

349. Sharma LN, Becker C, Chambliss CK: **Analytical Characterization of Fermentation Inhibitors in Biomass Pretreatment Samples Using Liquid Chromatography, UV-Visible Spectroscopy, and Tandem Mass Spectrometry.** In *Biofuels*. Edited by; 2009:125-143.

350. Herrera F, Pulgarin C, Nadtochenko V, Kiwi J: **Accelerated photo-oxidation of concentrated p-coumaric acid in homogeneous solution. Mechanistic studies, intermediates and precursors formed in the dark.** *Applied Catalysis B: Environmental* 1998, **17**:141-156.

351. Mantzavinos D, Hellenbrand R, Livingston AG, Metcalfe IS: **Catalytic wet oxidation of p-coumaric acid: Partial oxidation intermediates, reaction pathways and catalyst leaching.** *Applied Catalysis B: Environmental* 1996, **7**:379-396.

352. Sun R, Sun XF, Wang SQ, Zhu W, Wang XY: **Ester and ether linkages between hydroxycinnamic acids and lignins from wheat, rice, rye, and barley straws, maize stems, and fast-growing poplar wood.** *Industrial Crops and Products* 2002, **15**:179-188.

353. Agyei-Aye K, Chian MX, Lauterbach JH, Moldoveanu SC: **The role of the anion in the reaction of reducing sugars with ammonium salts.** *Carbohydrate Research* 2002, **337**:2273-2277.

354. Van Soest PJ: **Carbohydrates.** In *Nutritional Ecology of the Ruminant*. Edited by: Comstock Publishers; 1994:156-176.

355. Thornalley PJ: **Dicarbonyl intermediates in the Maillard reaction.** In *Maillard Reaction: Chemistry at the Interface of Nutrition, Aging, and Disease*. Edited by: Annals of the New York Academy of Sciences; 2005:111-117. Annals of the New York Academy of Sciences, vol 1043.]

356. Van Soest PJ, Mason VC: **The influence of the Maillard reaction upon the nutritive value of fibrous feeds.** *Animal Feed Science and Technology* 1991, **32**:45-53.

357. Jing X, Zhang X, Bao J: **Inhibition Performance of Lignocellulose Degradation Products on Industrial Cellulase Enzymes During Cellulose Hydrolysis.** *Applied Biochemistry and Biotechnology* 2009, **159**:696-707.

358. Taherzadeh MJ, Eklund R, Gustafsson L, Niklasson C, Liden G: **Characterization and Fermentation of Dilute-Acid Hydrolyzates from Wood.** *Industrial & Engineering Chemistry Research* 1997, **36**:4659-4665.

359. Dunlop AP: **Furfural Formation and Behavior.** *Industrial & Engineering Chemistry* 1948, **40**:204-209.

360. Xu F, Sun JX, Geng ZC, Liu CF, Ren JL, Sun RC, Fowler P, Baird MS: **Comparative Study of Water-Soluble and Alkali-Soluble Hemicelluloses from Perennial Ryegrass Leaves (*Lolium peree*).** *Carbohydrate Polymers* 2007, **67**:56-65.

361. Kurakake M, Kisaka W, Kazuya Ouchi K, Komaki T: **Pretreatment with ammonia water for enzymatic hydrolysis of corn husk, bagasse, and switchgrass.** *Appl Biochem Biotechnol* 2001, **90**.

362. Knill C, Kennedy J: **Degradation of cellulose under alkaline conditions.** *Carbohydrate Polymers* 2003, **51**:281-300.

363. Pavasars I, Hagberg J, Boren H, Allard B: **Alkaline Degradation of Cellulose: Mechanisms and Kinetics.** *Journal of Polymers and the Environment* 2003, **11**:39-47.

364. Burau R, Stout P: **Trans-Aconitic Acid in Range Grasses in Early Spring.** *Science* 1965, **150**:766-767.

365. Masselter S, Zemann A, Bobleter O: **Analysis of lignin degradation products by capillary electrophoresis.** *Chromatographia* 1995, **40**:51-57.

366. Klinke HB, Olsson L, Thomsen AB, Ahring BK: **Potential inhibitors from wet oxidation of wheat straw and their effect on ethanol production of *Saccharomyces cerevisiae*: Wet oxidation and fermentation by yeast.** *Biotechnology and Bioengineering* 2003, **81**:738-747.

367. Baeza J, Freer J: *Chemical characterization of wood and its components*. Edited by Hon DNS, Shirashi N. New York: Dekker; 1997.

368. Jönsson LJ, Palmqvist E, Nilvebrant NO, Hahn-Hägerdal B: **Detoxification of wood hydrolysates with laccase and peroxidase from the white-rot fungus *Trametes versicolor*.** *Appl Microbiol Biotechnol* 1998, **49**:691-697.

369. Agblevor FA, Fu J, Hames B, McMillan JD: **Identification of Microbial Inhibitory Functional Groups in Corn Stover Hydrolysate by Carbon-13 Nuclear Magnetic Resonance Spectroscopy.** *Applied Biochemistry and Biotechnology* 2004, **119**:97-120.

370. Fenske JJ, Griffin DA, Penner MH: **Comparison of aromatic monomers in lignocellulosic biomass prehydrolysates.** *Journal of Industrial Microbiology & Biotechnology* 1998, **20**:364-368.

371. Chesson A: **Effect of sodium hydroxide on cereal straws in relation to enhanced degradation of structural polysaccharides by rumen microorganisms.** *J Sci Food Agri* 1981, **32**:745-758.

372. Theodorou MK, Gascoyne DJ, Akin DE, Hartley RD: **Effect of Phenolic-Acids and Phenolics from Plant-Cell Walls on Rumenlike Fermentation in Consecutive Batch Culture.** *Applied and Environmental Microbiology* 1987, **53**:1046-1050.

373. Martin SA, Akin DE: **Effect of Phenolic Monomers on the Growth and Beta-Glucosidase Activity of *Bacteroides Ruminicola* and on the Carboxymethylcellulase, Beta-Glucosidase, and Xylanase Activities of *Bacteroides Succinogenes*.** *Applied and Environmental Microbiology* 1988, **54**:3019-3022.

374. Gamble GR, Snook ME, Henriksson G, Akin DE: **Phenolic constituents in flax bast tissue and inhibition of cellulase and pectinase.** *Biotechnology Letters* 2000, **22**:741-746.

375. Panagiotou G, Olsson L: **Effect of compounds released during pretreatment of wheat straw on microbial growth and enzymatic hydrolysis rates.** *Biotechnology and Bioengineering* 2007, **96**:250-258.

376. Narendranath NV, Thomas KC, Ingledew WM: **Effects of acetic acid and lactic acid on the growth of *Saccharomyces cerevisiae* in a minimal medium.** *Journal of Industrial Microbiology & Biotechnology* 2001, **26**:171-177.

377. Zaldivar J, Martinez A, Ingram LO: **Effect of alcohol compounds found in hemicellulose hydrolysate on the growth and fermentation of ethanologenic *Escherichia coli*.** *Biotechnology and Bioengineering* 2000, **68**:524-530.

378. Martin SA: **Effect of Phenolic Compounds on Fiber-Degrading Enzymes from Rumen Bacteria.** Edited by Akin DE; 1990:289-300.

379. Lau MW, Dale BE: **Cellulosic ethanol production from AFEX-treated corn stover using Saccharomyces cerevisiae 424A(LNH-ST).** *Proceedings of the National Academy of Sciences* 2009, **106**:1368-1373.

380. Houghton J, Weathermax S, Ferrell J: **Breaking the Biological Barriers to Cellulosic Ethanol: A Joint Research Agenda.** In *Department of Energy*. Edited by Energy Do; 2006.

381. EPOBIO: **Cell wall saccharification. Outputs from the EPOBIO project - November 2006.** *http://www.epobio.net/pdfs/0611CellWallSaccharificationReport_c.pdf*.

382. Turner P, Mamo G, Karlsson EN: **Potential and utilization of thermophiles and thermostable enzymes in biorefining.** *Microbial cell factories* 2007, **6**:9.

383. Ghose T: **Measurement of cellulase activity.** In *Commission on Biotechnology, International Union of Pure and Applied Chemistry, New Delhi, India,* 1984.

384. Coward-Kelly G, Aiello-Mazzari C, Kim S, Granda C, Holtzapple MT: **Suggested improvements to the standard filter paper assay used to measure cellulase activity.** *Biotechnol Bioeng* 2003, **82**:745-749.

385. Kabel M, van der Maarel M, Klip G, Voragen A, Schols H: **Standard assays do not predict the efficiency of commercial cellulase preparations towards plant materials.** *Biotechnology and Bioengineering* 2006, **93**:56-63.

386. Alizadeh H, Teymouri F, Gilbert TI, Dale BE: **Pretreatment of switchgrass by ammonia fiber explosion (AFEX).** *Applied Biochemistry and Biotechnology* 2005, **124**:1133-1141.

387. Murnen HK, Balan V, Chundawat SPS, Bals B, Sousa LD, Dale BE: **Optimization of ammonia fiber expansion (AFEX) pretreatment and enzymatic hydrolysis of Miscanthus x giganteus to fermentable sugars.** *Biotechnology Progress* 2007, **23**:846-850.

388. Teymouri F, Laureano-Perez L, Alizadeh H, Dale BE: **Ammonia fiber explosion treatment of corn stover.** *Applied Biochemistry and Biotechnology* 2004, **113-16**:951-963.

389. Sharrock KR: **Cellulase assay methods: a review.** *Journal of Biochemical and Biophysical Methods* 1988, **17**:81-105.

390. Decker SR, Adney WS, Jennings E, Vinzant TB, Himmel ME: **Automated filter paper assay for determination of cellulase activity.** *Applied Biochemistry and Biotechnology* 2003, **105**:689-703.

391. Xiao Z, Storms R, Tsang A: **Microplate-based filter paper assay to measure total cellulase activity.** *Biotechnology and Bioengineering* 2004, **88**:832-837.

392. Berlin A, Maximenko V, Bura R, Kang K, Gilkes N, Saddler J: **A rapid microassay to evaluate enzymatic hydrolysis of lignocellulosic substrates.** *Biotech Bioeng* 2006, **93**:880–886.

393. Weimer PJ, Dien BS, Springer TL, Vogel KP: **In vitro gas production as a surrogate measurement of the fermentability of cellulosic biomass.** *Appl Microbiol Biotechnol* 2005, **67**:52-58.

394. Boyer V, Fort S, Frandsen TP, Schülein M, Cottaz S, Driguez H: **Chemoenzymatic synthesis of a bifunctionalized cellohexaoside as a specific substrate for the sensitive assay of cellulase by fluorescence quenching.** *Chemistry (Weinheim an der Bergstrasse, Germany)* 2002, **8**:1389-1394.

395. Helbert W, Chanzy H, Husum T, Schulein M, Ernst S: **Fluorescent Cellulose Microfibrils As Substrate for the Detection of Cellulase Activity.** *Biomacromolecules* 2003, **4**:481-487.

396. Goddard J, Reymond J: **Enzyme assays for high-throughput screening.** *Curr Opin Biotechnol* 2004, **15**:314-322.

397. Cullis IF, Saddler JN, Mansfield SD: **Effect of initial moisture content and chip size on the bioconversion efficiency of softwood lignocellulosics.** *Biotechnology and Bioengineering* 2004, **85**:413-421.

398. Zeng M, Mosier NS, Huang C-P, Sherman DM, Ladisch MR: **Microscopic examination of changes of plant cell structure in corn stover due to hot water pretreatment and enzymatic hydrolysis.** *Biotechnology and Bioengineering* 2007, **97**:265-278.

399. Van dyke Jr HH: **Enzymatic hydrolysis of cellulose: a kinetic study [Ph.D. Thesis].** Boston: MIT: 1972.

400. Sangseethong K, Meunier-Goddik L, Tantasucharit U, Liaw E, Penner MH: **Rationale for particle size effect on rates of enzymatic saccharification of microcrystalline cellulose.** *J Food Biochem* 1998, **22**:321-330.

401. Gharpuray MM, Lee Y, Fan LT: **Structural modification of lignocellulosics by pretreatments to enhance enzymatic hydrolysis.** *Biotechnol Bioeng* 1983, **25**:157-172.

402. Gan Q, Allen SJ, Taylor G: **Kinetic dynamics in heterogeneous enzymatic hydrolysis of cellulose: an overview, an experimental study and mathematical modeling.** *Proc Biochem* 2003, **38**:1003-1018.

403. Coulson JM, Richardson JF: *Chemical Engineering - Particle Technology & Separation Processes*, vol 2 edn 5. Oxford: Butterworth-Heinemann; 2002.

404. Perry RH, Green DW: *Perry's Chemical Engineers' Handbook* edn 7. New York: McGraw-Hill; 1997.

405. Huang AA: **Kinetic studies on insoluble cellulose/cellulase system.** *Biotech Bioeng* 1975, **17**:1421-1433.

406. Penner MH, Liaw ET: **Kinetic consequences of high ratios of substrate to enzyme saccharification systems based on *Trichoderma* cellulase.** In *Enzymatic Conversion of Biomass for Fuels Production*; *Washington, DC*,Edited by Himmel ME, Baker JO, Overend RP: American Chemical Society: 1994:363-371.

407. Gusakov AV, Sinitsyn AP, Davydkin IY, Davydkin VY, Protas OV: **Enhancement of enzymatic cellulose hydrolysis using a novel type of bioreactor with intensive stirring induced by electromagnetic field.** *Appl Biochem Biotech* 1996, **56**:141-153.

408. Gut'erres B, Sinitsyn AP, Kastel'yanos OF, Berlin AK, Kovalev GV, Okunev ON: **Enzymatic saccharification of cellulose-based materials by the cellulase complex of *Penicillium verruculosum* in various typres of stirred reactors.** *Appl Biochem Microbiol* 1998, **34**:564-568.

409. Elshafei AM, Vega JL, Klasson KT, Clausen EC, Gaddy JL: **The saccharification of corn stover by cellulase from *Penicillium-funiculosum*.** *Bioresour Technol* 1991, **35**:73-80.

410. Lerouxel O, Choo TS, Seveno M, Usadel B, Faye L, Lerouge P, Pauly M: **Rapid structural phenotyping of plant cell wall mutants by enzymatic oligosaccharide fingerprinting.** *Plant Physiol* 2002, **130**:1754-1763.

411. Miller GL: **Use of dinitrosalicylic acid reagent for determination of reducing sugar.** *Anal Chem* 1959, **31**:426-428.

412. Somogyi M: **Notes on sugar determination.** *J Biol Chem* 1952, **195**:19-23.

413. Green F, Clausen CA, Highley TA: **Adaptation of the Nelson-Somogyi reducing-sugar assay to a microassay using microtiter plates.** *Anal Biochem* 1989, **182**:197-199.

414. Zhang Y-HP, Lynd LR: **Determination of the number-average degree of polymerization of cellodextrins and cellulose with application to enzymatic hydrolysis.** *Biomacromolecules* 2005, **6**:1510-1515.

415. Roe JH: **The determination of sugar in blood and spinal fluid with anthrone reagent.** *J Biol Chem* 1955, **212**:335-343.

416. Sengupta S, Jana ML, Sengupta D, Naskar AK: **A note on the estimation of microbial glycosidase activities by dinitrosalicylic acid reagent.** *Applied Microbiology and Biotechnology* 2000, **53**:732-735.

417. Schwald W, Chan M, Breuil C, Saddler JD: **Comparison of HPLC and colorimetric methods for measuring cellulolytic activity.** *Appl Microbiol Biotechnol* 1988, **28**:398-403.

418. Rivers D, Gracheck S, Woodford L: **Limitations of the DNS assay for reducing sugars from saccharified lignocellulosic.** *Biotechnol Bioeng* 1984, **26**:800-802.

419. Jørgensen H, Kutter J, Olsson L: **Separation and quantification of cellulases and hemicellulases by capillary electrophoresis.** *Anal Biochem* 2003, **317**:85–93.

420. Kolbe J, Kubicek C: **Quantification and identification of the main components of the Trichoderma cellulase complex with monoclonal antibodies using an enzyme-linked immunosorbent assay (ELISA).** *Appl Microbiol Biotechnol* 1990, **34**:26–30.

421. Vinzant T, Adney W, Decker S, Baker J, Kinther M, Sherman N, Fox J, Himmel M: **Fingerprinting Trichoderma reesei hydrolases in a commercial cellulase preparation.** *Appl Biochem Biotechnol* 2001, **91-93**:99–107.

422. Markov A, Gusakov A, Kondratyeva E, Okunev O, Bekkarevich A, Sinitsyn A: **New Effective Method for Analysis of the Component Composition of Enzyme Complexes from Trichoderma reesei.** *Biochemistry (Moscow)* 2005, **70**:657-663.

423. Lipton MS, Pasa-Tolic L, Gordon AA, Anderson DJ, Auberry DL, Battista JR, Daly MJ, Fredrickson J, Hixson KK, Kostandarithes H, et al.: **Global Analysis of the Deinococcus radiodurans Proteome by Using Accurate Mass Tags.** *Proceedings of the National Academy of Sciences of the United States of America* 2002, **99**:11049-11054.

424. Steen H, Mann M: **The ABC's (and XYZ's) of peptide sequencing.** *Nature Reviews Molecular Cell Biology* 2004, **5**:699-711.

425. Nesvizhskii A, Vitek O, Aebersold R: **Analysis and validation of proteomic data generated by tandem mass spectrometry.** *Nature Methods* 2007, **4**:787-797.

426. Ong S, Mann M: **Mass-spectrometry based proteomics turns quantitative.** *Nature Chemical Biology* 2005, **1**:252-262.

427. Liu H, Sadygov RG, Yates JR: **A Model for Random Sampling and Estimation of Relative Protein Abundance in Shotgun Proteomics.** *Analytical Chemistry* 2004, **76**:4193-4201.

428. Gao J, Opiteck GJ, Friedrichs MS, Dongre AR, Hefta SA: **Changes in the Protein Expression of Yeast as a Function of Carbon Source.** *Journal of Proteome Research* 2003, **2**:643-649.

429. Pang JX, Ginanni N, Dongre AR, Hefta SA, Opiteck GJ: **Biomarker Discovery in Urine by Proteomics.** *Journal of Proteome Research* 2002, **1**:161-169.

430. Nagendran S, Hallen-Adams HE, Paper JM, Aslam N, Walton JD: **Reduced genomic potential for secreted plant cell-wall-degrading enzymes in the ectomycorrhizal fungus Amanita bisporigera, based on the secretome of Trichoderma reesei.** *Fungal Genetics and Biology* 2009, **46**:427-435.

431. Berlin A, Gilkes N, Kilburn D, Bura R, Markov A, Skomarovsky A, Okunev O, Gusakov A, Maximenko V, Gregg D, et al.: **Evaluation of novel fungal cellulase preparations for ability to hydrolyze softwood substrates - evidence for the role of accessory enzymes.** *Enzyme and Microbial Technology* 2005, **37**:175-184.

432. Berlin A, Gilkes N, Kilburn D, Maximenko V, Bura R, Markov M, Skomarovsky A, Gusakov A, Sinitsyn A, Okunev O, et al.: **Evaluation of cellulase preparations for hydrolysis of hardwood substrates.** *Appl Biochem Biotechnol* 2006, **130** 528-545.

433. Boisset C, Petrequin C, Chanzy H, Henrissat B, Schulein M: **Optimized mixtures of recombinant Humicola insolens cellulases for the biodegradation of crystalline cellulose.** *Biotech Bioeng* 2001, **72**:339-345.

434. Saloheimo A, Ilmen M, Aro N, Margolles-Clark E, Penttila M: **Regulatory mechanisms involved in the expression of extracellular hydrolytic enzymes from Trichoderma.** In *Carbohydrases from Trichoderma reesei and other microorganisms – Structure, biochemistry, genetics and applications: Proceedings of Tricel 1997 meeting*;

Cambridge, UK,Edited by Claeyssens M, Nerinckx W, Piens K: The Royal Soceity of Chemistry: 1998:267-273.

435. Thomas S, Laymon R, Chou Y, Tucker M, Vinzant T, William S, Baker J, Mielenz J, Himmel M: *Initial approaches to artificial cellulase systems for conversion of biomass to ethanol*, vol 618. Edited by Saddler J, Penner M. Washington, DC: American Chemical Society; 1995.

436. Lynd LR, Weimer PJ, van Zyl WH, Pretorius IS: **Microbial Cellulose Utilization: Fundamentals and Biotechnology**. *Microbiol. Mol. Biol. Rev.* 2002, **66**:506-577.

437. Lynd LR, Zyl WHv, McBride JE, Laser M: **Consolidated bioprocessing of cellulosic biomass: an update**. *Current Opinion in Biotechnology* 2005, **16**:577-583.

438. Scheffé H: **The Simplex-Centroid Design for Experiments with Mixtures**. *J Royal Stat Soc Ser B (Methodological)* 1963, **25**:235-263.

439. Kim E, Irwin D, Walker L, Wilson D: **Factorial optimization of a six-cellulase mixture**. *Biotechnology and Bioengineering* 1998, **58**:494-501.

440. Buchert J, Ranua M, Kantelinen A, Viikari L: **The role of two Trichoderma reesei xylanases in the bleaching of kraft pulp**. *Appl Microb Biotechnol* 1992, **37**:825-829.

441. Tabka M, Herpoel-Gimbert I, Monod F, Asther M, Sigoillot J: **Enzymatic saccharification of wheat straw for bioethanol production by a combined cellulase, xylanase and feruloyl esterase treatment**. *Enzyme and microbial technology* 2006, **39**:897-902.

442. Hespell RB, O'Bryan PJ, Moniruzzaman M, Bothast RJ: **Hydrolysis by commercial enzyme mixtures of AFEX-treated corn fiber and isolated xylans**. *Appl Biochem Biotech* 1997, **62** 87-97.

443. Dien B, Ximenes E, O'Bryan P, Moniruzzaman M, Li X, Balan V, Dale B, Cotta M: **Enzyme characterization for hydrolysis of AFEX and liquid hot-water pretreated distillers' grains and their conversion to ethanol**. *Bioresour Technol* 2008, **99**:5216-5225.

444. Eun J, Beauchemin K, Hong S, Bauer M: **Exogenous enzymes added to untreated or ammoniated rice straw: Effects on in vitro fermentation characteristics and degradability**. *Anim Feed Sci Technol* 2006, **131**:86-101.

445. Sapan CV, Lundblad RL, Price NC: **Colorimetric protein assay techniques**. *Biotechnology and Applied Biochemistry* 1999, **29**:99-108.

446. Lovrien R, Matulis D: **Appendix 3A: Assays for Total Protein**. *Current Protocols in Protein Science* 1995, **3**:1-24.

447. Compton SJ, Jones CG: **Mechanism of dye response and interference in the Bradford protein assay.** *Anal Biochem* 1985, **151**:369-374.

448. Peterson GL: **A simplification of the protein assay method of Lowry et al. which is more generally applicable.** *Anal Biochem* 1977, **83**:346-356.

449. Eng J, Mccormack A, Yates J: **An approach to correlate tandem mass-spectral data of peptides with amino-acid-sequences in a protein database.** *J Am Soc Mass Spectrom* 1994, **5**:976–989.

450. Qian W, Liu T, Monroe M, Strittmatter E, Jacobs J, Kangas L, Petritis K, Camp D, Smith R: **Probability-based evaluation of peptide and protein identifications from tandem mass spectrometry and SEQUEST analysis: the human proteome.** *J Proteome Res* 2005, **4**:53–62.

451. Elias JE, Gygi SP: **Target-decoy search strategy for increased confidence in large-scale protein identifications by mass spectrometry.** *Nat Meth* 2007, **4**:207-214.

452. Henrissat B, Teeri T, Warren R: **A scheme for designating enzymes that hydrolyze the polysaccharides in the cell walls of plants.** *FEBS Letters* 1991, **425**:352-354.

453. Gao D, Chundawat SPS, Krishnan C, Balan V, Dale BE: **Mixture optimization of six core glycosyl hydrolases for maximizing saccharification of ammonia fiber expansion (AFEX) pretreated corn stover.** *Bioresource Technology* 2009, **Manuscript In Press (DOI: 10.1016/j.biortech.2009.10.056)**.

454. Box GEP, Hunter WG, Hunter JS: *Statistics for Experimenters*. New York: Wiley; 1978.

455. Derringer G, Suich R: **Simultaneous Optimization of Several Response Variables.** *Journal of Quality Technology* 1980, **12**:214-219.

456. Kumar R, Wyman CE: **Effects of cellulase and xylanase enzymes on the deconstruction of solids from pretreatment of poplar by leading technologies.** *Biotechnology Progress* 2009, **25**:302-314.

457. Kumar R, Wyman CE: **Effect of enzyme supplementation at moderate cellulase loadings on initial glucose and xylose release from corn stover solids pretreated by leading technologies.** *Biotechnology and Bioengineering* 2009, **102**:457-467.

458. Selig M, Knoshaug E, Adney W, Himmel M, Decker S: **Synergistic enhancement of cellobiohydrolase performance on pretreated corn stover by addition of xylanase and esterase activities.** *Bioresour Technol* 2008, **99**:4997-5005.

459. Xiao Z, Zhang X, Gregg DJ, Saddler JN: **Effects of sugar inhibition on cellulases and beta-glucosidase during enzymatic hydrolysis of softwood substrates.** *Applied Biochemistry and Biotechnology* 2004, **115**:1115-1126.

460. Bronnenmeier K: **Separation of the cellulolytic and xylanolytic enzymes of Clostridium stercorarium.** *J Chrom* 1990, **521**:301-310.

461. Jin Z, Yong-Hong W, Ju C, Ying-Ping Z, Si-Liang Z, Peng Y: **Identification and purification of the main components of cellulases from a mutant strain of Trichoderma viride T 100-14.** *Biores Technol* 2008, **99**:6826-6833.

462. Sangseethong K, Penner M: **p-Aminophenyl-β-cellobioside as an affinity ligand for exo-type cellulases.** *Carbohydr Res* 1998, **314**:245-250.

463. Lee S, Shin H, Ryu D: **Adsorption of Cellulase on Cellulose: Effect of Physicochemical Properties of Cellulose on Adsoprtion and Rate of Hydrolysis.** *Biotechnol Bioeng* 1982, **24**:2137-2153.

464. Jeoh T, Ishizawa CI, Davis MF, Himmel ME, Adney WS, Johnson DK: **Cellulase digestibility of pretreated biomass is limited by cellulose accessibility.** *Biotechnology and Bioengineering* 2007, **98**:112-122.

465. Jeoh T, Wilson D, Walker L: **Effect of Cellulase Mole Fraction and Cellulose Recalcitrance on Synergism in Cellulose Hydrolysis and Binding.** *Biotechnol Prog* 2006, **22**:270-277.

466. Baker J, Ehrman C, Adney W, Thomas S, Himmel M: **Hydrolysis of cellulose using ternary mixtures of purified cellulases.** *Appl Biochem Biotechnol* 1998, **70-72**:395-403.

467. Nidetzky B, Sterner W, Hayn M, Claeyssens M: **Cellulose hydrolysis by the cellulase from Trichoderma reesei: a new model for synergistic interaction.** *Biochem J* 1994, **298**:705-710.

468. Nidetzky B, Steiner W, Claeyssens M: **Cellulose hydrolysis by the cellulases from Trichoderma reesei: absorptions of the two cellobiohydrolases, two endoglucanases and their core proteins on filter paper and their relation to hydrolysis.** *Biochem J* 1994, **303**:817-823.

469. Ramos L, Filho A, Deschamps F, Saddler J: **The effect of Trichoderma cellulases on the fine structure of a bleached softwood kraft pulp.** *Enzyme Microb Technol* 1999, **24**:371-380.

470. Kyriacou A, Mackenzie C, Neufeld R: **Detection and characterization of the specific and nonspecific endoglucanases of Trichoderma reesei: evidence demonstrating endoglucanase activity by cellobiohydrolase II.** *Enzyme Microb Technol* 1987, **9**:25-32.

471. Gusakov A, Salanovich T, Antonov A, Ustinov B, Okunev O, Burlingame R, Emalfarb M, Baez M, Sinitsyn A: **Design of highly efficient cellulase mixtures for enzymatic hydrolysis of cellulose.** *Biotechnology and Bioengineering* 2007, **97**:1028-1038.

472. Palonen H, Tjerneld F, Zacchi G, Tenkanen M: **Adsorption of Trichoderma reesei CBH I and EG II and their catalytic domains on steam pretreated softwood and isolated lignin.** *J Biotechnol* 2004, **107**:65-72.

473. Karlsson J, Siika-aho M, Tenkanen M, Tjerneld F: **Enzymatic properties of the low molecular mass endoglucanases Cel12A (EG III) and Cel45A (EG V) of Trichoderma reesei.** *J Biotechnol* 2002, **99**:63-78.

474. Lawoko M, Nutt A, Henriksson H, Gellerstedt G, Henriksson G: **Hemicellulase activity of aerobic fungal cellulases.** *Holzforschung* 2000, **54**:497-500.

475. Neville A: *Biology of fibrous composites: Development beyond the cell membrane.* Cambridge: The University Press; 1993.

476. Zandomeni K, Schopfer P: **Reorientation of microtubules at the outer epidermal wall of maize coleoptiles by phytochrome, blue-light photoreceptor and auxin.** *Protoplasma* 1993, **173**:103-112.

477. Selig M, Knoshaug E, Decker S, Baker J, Himmel M, Adney W: **Heterologous expression of Aspergillus niger β-D-xylosidase (XlnD): Characterization on lignocellulosic substrates.** *Appl Biochem Biotechnol* 2008, **146**:57-68.

478. Korte H, Offermann W, Puls J: *Holzforschung* 1991, **45**:419.

479. Knoshaug E, Selig M, Baker J, Decker S, Himmel M, Adney W: **Heterologous Expression of Two Ferulic Acid Esterases from Penicillium funiculosum.** *Appl Biochem Biotechnol* 2008, **146**:79–87.

480. Mellerowicz E, Immerzeel P, Hayashi T: **Xyloglucan: The Molecular Muscle of Trees.** *Annals of Botany* 2008, **(doi:10.1093/aob/mcn170)**.

481. Zsuzsa B, Matti S, Liisa V, Kati R: **Evaluation of the role of xyloglucanase in the enzymatic hydrolysis of lignocellulosic substrates.** *Enzyme Microb Technol* 2008, **43**:109–114.

482. Vincken J, Beldman G, Voragen A: **Substrate specificity of endoglucanases: what determines xyloglucanase activity?** *Carbohydr Res* 1997, **298**:299-310.

483. Piyachomkwan K, Gable KP, Penner MH: **p-Aminophenyl 1-thio-beta-D-cellobioside: Synthesis and application in affinity chromatography of exo-type cellulases.** *Carbohydrate Research* 1997, **303**:255-259.

484. Piyachomkwan K, Penner MH: **Aryl Thioglycoside-Based Affinity Purification of Exo-Acting Cellulases.** *Analytical Biochemistry* 1998, **255**:223-235.

485. Bradshaw TC, Alizadeh H, Teymouri F, Balan V, Dale BE: **Ammonia fiber expansion pretreatment and enzymatic hydrolysis on two different growth stages of reed canarygrass.** *Applied Biochemistry and Biotechnology* 2007, **137**:395-405.

486. Bals B, Dale BE, Balan V: **Enzymatic hydrolysis of distiller's dry grain and solubles (DDGS) using ammonia fiber expansion pretreatment.** *Energy & Fuels* 2006, **20**:2732-2736.

487. Ayed A, Rabhi I, Dellagi K, Kallel H: **High level production and purification of human interferon alpha-2b in high cell density culture of Pichia pastoris.** *Enzyme and Microbial Technology* 2008, **42**:173-180.

488. Brunel L, Neugnot V, Landucci L, Boze WN, Moulin G, Bigey F, Dubreucq E: **High-level expression of Candida parapsilosis lipase/acyltransferase in Pichia pastoris.** *Journal of Biotechnology* 2004, **111**:41-50.

489. Bauer S, Vasu P, Persson S, Mort A, Somerville C: **Development and application of a suite of polysaccharide-degrading enzymes for analyzing plant cell walls.** *Proc Natl Acad Sci USA* 2006, **103**:11417–11422.

490. Gruno M, Väljamäe P, Pettersson G, Johansson G: **Inhibition of the *Trichoderma reesei* cellulases by cellobiose is strongly dependent on the nature of the substrate.** *Biotechnology and Bioengineering* 2004, **86**:503-511.

491. Medve J, Stahlberg J, Tjerneld F: **Adsorption and Synergism of Cellobiohydrolase I and II of *Trichoderma reesei* during Hydrolysis of Microcrystalline Cellulose.** *Biotechnology and Bioengineering* 1994, **44**:1064-1073.

492. Chundawat SPS, Donohoe BS, Sousa L, Sharma L, Elder T, Askeland P, Vismeh R, Agarwal U, Humpula J, Garlock R, et al.: **Ultra-structural and physicochemical modifications within ammonia pretreated lignocellulosic cell walls that influence enzyme accessibility.** In *31st Symposium on Biotechnology for Fuels and Chemicals (3-6 May); Oral Presentation (Paper #9530) Session 3 (#05) - Biomass Pretreatment and Fractionation*; *San Fransisco, California*: 2009:50.

493. Fengel D: **Ideas on the ultrastructural organization of the cell wall components.** *Journal of Polymer Science Part C: Polymer Symposia* 1971, **36**:383-392.

494. Beukes N, Chan H, Doi RH, Pletschke BI: **Synergistic associations between Clostridium cellulovorans enzymes XynA, ManA and EngE against sugarcane bagasse.** *Enzyme and Microbial Technology* 2008, **42**:492-498.

495. Benko Z, Siika-aho M, Viikari L, Reczey K: **Evaluation of the role of xyloglucanase in the enzymatic hydrolysis of lignocellulosic substrates.** *Enzyme Microb Technol* 2008, **43**:109–114.

496. Mastronarde DN: **Dual-Axis Tomography: An Approach with Alignment Methods That Preserve Resolution.** *Journal of Structural Biology* 1997, **120**:343-352.

497. Schell DJ, Farmer J, Newman M, McMillan JD: **Dilute-sulfuric acid pretreatment of corn stover in pilot-scale reactor: Investigation of yields, kinetics, and enzymatic digestibilities of solids.** *Applied Biochemistry and Biotechnology* 2003, **105**:69-85.

498. Hames BR, Thomas SR, Sluiter AD, Roth CJ, Templeton DW: **Rapid Biomass Analysis: New Tools for Compositional Analysis of Corn Stover Feedstocks and Process Intermediates from Ethanol Production**. *Applied Biochemistry and Biotechnology* 2003, **105-108**:5-16.

499. Wright WR, Rainwater JC, Tolle LD: **Glucose Assay Systems: Evaluation of a Colorimetric Hexokinase Procedure**. *Clin Chem* 1971, **17**:1010-1015.

MICHIGAN STATE UNIVERSITY LIBRARIES
3 1293 03063 4673